Using Remote Sensing to Explore the Spectral and Spatial Characteristics of Wetland Vegetation

By

Cróna Judith O'Shea

Submitted to

The Faculty of Natural Sciences, University of Stirling

November 2005

For the degree of

Doctor of Philosophy

This research was undertaken at the School of Biological and Environmental Sciences, University of Stirling, Stirling.

ProQuest LLC.
789 East Eisenhower Parkway
P.O. Box 1346
Ann Arbor, MI 48106 – 1346

STATEMENT OF ORIGINALITY

I hereby confirm that this is an original study conducted independently by the undersigned and the work contained herein has not been submitted for any other degree. All research material has been duly acknowledged and cited.

Signature of candidate:

Date: 2nd May '06

ABSTRACT

Wetlands play an important role as ecotones between terrestrial and aquatic habitats and, as a result, represent an environment of high biodiversity and important hydrological function. Ecological understanding in these environments is hampered by difficult terrain and the dynamic and heterogeneous nature of the vegetation. Remote sensing can provide large amounts of contemporaneous data quickly, objectively and over large areas. This study utilises remote sensing data in conjunction with field data and habitat maps derived from traditional ecological surveys to investigate the use of remote sensing as a tool to aid the ecological understanding and monitoring of wetland environments.

This study investigated three main objectives; the first two involved the use of field spectrometry from six habitat types in a freshwater wetland in the north of Scotland. Multivariate analyses demonstrated the possibility of distinguishing between these habitat types using field spectra alone. Detailed vegetation datasets were also collected and the relationship between these and variation in the associated spectra was investigated. Significant relationships were established between ordination axes and spectral bands in the green and NIR regions of the spectrum. Results also demonstrated the potential for remote sensing data to characterise the nature of habitat boundaries. The third objective involved the use of airborne imagery to classify remote sensing data into ecologically meaningful classes. Classification accuracies of over 70% were obtained.

Work over the last decade has seen a bridging of the relationship between remote sensing and ecology although it is widely acknowledged that our ecological understanding of the remote sensing-vegetation relationship is still limited at many scales and in many ecosystems, not least the wetland environment. This study provides a much needed basis to research in this cross-disciplinary field and identifies further areas that would benefit from future work.

ACKNOWLEDGEMENTS

Firstly, I would like to thank my supervisors Dr. Sandy Winterbottom and Dr. Nigel Willby for their continued support and advice throughout this project. Financial support was provided through a University of Sitrling Studentship awarded by the Faculty of Natural Sciences and, also, from the Royal Society for the Protection of Birds; I am very grateful for both.

Many people have been involved in this project over the last three years in various roles and to various degrees and I would like to take this opportunity to thank them for their help, they are: Rob McMorron-field work enthusiast extraordinaire, the RSPB staff and volunteers at Insh Marshes and the technical staff at the School of Biological and Environmental Sciences at University of Stirling including Carl Mitchell, Pete Moore, Stuart Bradley, John McArthur, Scott Jackson and Bill Jamieson.

There are too many names to list in order to thank all those people who have helped to get me through this rollercoaster of a ride that is a PhD. Whether it was by making sure I was fed, dragging me out on the bike or up the hills, having a good blether or just making me smile, I appreciate you all. In particular, I would like to mention Jon and Helen, Andy and Pauly, Becca, Linda and of course, Scott and Loretta. I must also thank my office mates Rich and Pete for all of the laughs we've had-some days I only came in for the banter!

Lastly, to my consistently supportive parents, Liam and Judy O'Shea, thanks for always believing in me.

TABLE OF CONTENTS

Statement of Originality i

Abstract ii

Acknowledgements iii

Table of Contents iv

List of Figures vii

List of Tables xiii

1 Introduction 1

1.1 Rationale 1

1.2 Aims and Objectives 3

1.3 Thesis Structure 4

2 Background and Literature Review 6

2.1 The Global Interest in Wetlands 6

2.2 Wetland Characteristics 8

2.3 Vegetation as Environmental Predictors 10

2.3.1 Site-condition Monitoring 11

2.4 Remote Sensing for Natural Vegetation Mapping 12

2.4.1 Habitat Boundaries 13

2.5 Techniques for Discriminating between Natural Vegetation Types 15

2.5.1 Field Spectrometry 15

2.5.2 Spectral Discrimination between Habitat Types 16

2.5.3 Spectral Characteristics of Vegetation 17

2.5.4 Using Multivariate and Multitemporal Datasets to Explore the Relationship between Vegetation and Spectral Patterns 25

2.5.5 Using Remote Sensing Imagery to Map Vegetation 28

2.6 Study Site: Insh Marshes 33

2.6.1 History and Site Characteristics 35

2.6.2 Conservation and Habitat Types 36

2.6.3 Management Issues 42

2.6.4 Previous Work 43

2.7 Summary 45

3 Data Collection and Preparation 48

3.1 Introduction 48

3.2 Sampling Design 50

3.2.1 Introduction 50

3.2.2 Location of Study Plots and Transects 50

3.2.3 Sampling Stages 52

3.3 Collecting Spectra in the Field 55

3.3.1 Collecting Spectra 55

3.3.2 Data Management and Construction of Spectral Bands 57

3.3.3 Sampling 59
3.4 Vegetation Datasets 61
3.4.1 Location of Sample Points 61
3.4.2 Equipment 61
3.4.3 Species Composition, Structural and Environmental Variables 63
3.5 Airborne Imagery 65
3.5.1 Introduction 65
3.5.2 Instrumentation and Flightlines 65
3.5.3 Data Preprocessing 68
3.6 Meteorological Dataset 75
3.7 Summary 79

4 Hyperspectral Dissimilarities between Wetland Habitat Types 80
4.1 Introduction 80
4.2 Aims and Objectives 80
4.3 Methods and Analyses 81
4.3.1 Datasets and Methods Overview 81
4.3.2 Spectra Collected at Study Plots 82
4.3.3 Spectra by Habitat Type 82
4.3.4 Principal Components Analysis 83
4.3.5 Multiple Discriminant Analysis 84
4.3.6 Spectral Indices 84
4.3.7 Geostatistics 89
4.4 Results 91
4.4.1 Objective a) Differences in spectral patterns between habitat types 91
4.4.2 Objective b) Inter-habitat variation using Multiple Discriminant Analysis 102
4.4.3 Objective c) Within-habitat variation 104
4.4.4 Objective d) Between-habitat variation 111
4.4.5 Objective e) Spectral indices 117
4.5 Discussion and Conclusions 141
4.5.1 Objective a) Differences in spectral pattern between habitat type 141
4.5.2 Objective b) Inter-habitat variation using Multiple Discriminant Analysis 146
4.5.3 Objective c) Within-habitat variation 147
4.5.4 Objective d) Between-habitat variation 149
4.5.5 Objective e) Spectral indices 150
4.6 Summary 156

5 Exploring the Spectral Characteristics of Environmental Datasets 159
5.1 Introduction 159
5.1.1 Aims and Objectives 159
5.2 Methods and Analyses 160
5.2.1 Datasets and Methods Overview 160
5.2.2 Vegetation Datasets and Two Way INdicator SPecies ANalysis 162
5.2.3 Multiple Discriminant Analysis 163
5.2.4 Multivariate Analysis of Ecological Data 163
5.3 Results 170
5.3.1 Objective a) Vegetation datasets and Two Way INdicator SPecies ANalysis. 170
5.3.2 Objective b) Multiple Discriminant Analysis 177
5.3.3 Objective c) Covariation between Spectra and Meteorological Data 178
5.3.4 Objective d) Detrended Correspondence Analysis 179
5.3.5 Objective e) Canonical Correspondence and Redundancy Analyses 187
5.4 Discussion and Conclusions 208
5.4.1 Objective a) Vegetation datasets and Two Way INdicator SPecies ANanlysis208

5.4.2 Objective b) Multiple Discriminant Analysis 209
5.4.3 Objective c) Covariation between Spectra and Meteorological Data 211
5.4.4 Objective d) Detrended Correspondence Analysis 213
5.4.5 Objective e) Canonical Correspondence and Redundancy Analyses 215
5.5 Summary 223

6 Airborne Imagery and Wetland Habitat Classification 226
6.1 Introduction 226
6.1.1 Aims and Objectives 226
6.2 Methods 227
6.2.1 Datasets and Methods Overview 227
6.2.2 Imagery and Habitat Types 228
6.2.3 Classification Methods and Analyses 232
6.2.4 Transects: DCA and CCA 244
6.3 Results 247
6.3.1 Objective a) Spectral endmembers 247
6.3.2 Objective b) Unsupervised Classification 255
6.3.3 Objective c) Supervised Classification 263
6.3.4 Objective d) Variation across habitat boundaries 283
6.4 Discussion and Conclusions 290
6.4.1 Objective a) Spectral endmembers 290
6.4.2 Objective b) Unsupervised Classification 291
6.4.3 Objective c) Supervised Classification 293
6.4.4 Objective d) Variation across habitat boundaries 298
6.5 Summary 299

7 Conclusions 302
7.1 Introduction 302
7.2 Spectral Discrimination of Habitat Types using Field Data 303
7.2.1 Field Spectrometry 303
7.2.2 Multivariate analyses 303
7.2.3 Future Work 305
7.3 Application of Airborne Imagery 306
7.3.1 Determining Ecological Meaningful Classes 306
7.3.2 Airborne Remote Sensing as a Management Tool 307
7.3.3 Future Work 307
7.4 Main Contributions 309
7.4.1 Contributions to the Remote Sensing of Wetlands 309
7.4.2 Contributions to Wetland Ecology and Management 309
7.5 Final Conclusions and Recommendations 310

Reference List 313

A. Appendix 333

B. Appendix 346

C. Appendix 391

D. Appendix 420

LIST OF FIGURES

Figure 2:1 Location of Insh Marshes, Speyside and SSSI Boundary 34
Figure 2:2 Insh marshes-looking NW from Insh village 34
Figure 2:3 Habitats at Insh Marshes (Maier & Cowie 2002) 41
Figure 2:4 Schematic diagram of water inflows and outflows within the Insh Marshes (taken from Grieve *et al.* 1995) 44
Figure 3:1 Habitat types at Insh Marshes (Maier & Cowie 2002) (Area shown in Figure 2.3 is outlined) 53
Figure 3:2 Area of Insh Marshes covered by airborne imagery 54
Figure 3:3 Location of study plots (1-16) and transects ('a'-'c') (1=EF1, 2=LS1, 3=LS2, 4=LS3, 5=MC1, 6=MC2, 7=MC3, 8=MC4, 9=MG1, 10=MG2, 11=MS1, 12=MS2, 13=MS3, 14=RP1, 15=RP2, 16=RP3) 54
Figure 3:4 Within-plot sampling for collection of spectral measurements (sample points marked with an 'X') 59
Figure 3:5 Within-plot sampling for vegetation datasets: Points illustrated in red indicated paired sampling points 62
Figure 3:6 0.5 x 0.5 m quadrat with 25 0.1 x 0.1 m compartments using for vegetation sampling 62
Figure 3:7 Dornier 228-101 NERC Aircraft used to collect airborne imagery 66
Figure 3:8 Location of flightlines employed by NERC ARSF over Insh Marshes, 17th September, 2003 (Yellow-'CASI 91'; Blue-'CASI 101') 67
Figure 3:9 CASI 91 prepared for cross-track correction 71
Figure 3:10 CASI 101 prepared for cross-track correction 71
Figure 3:11 CASI 91-Average radiance across lines 72
Figure 3:12 CASI 91-Average radiance across lines (offset for clarity) 72
Figure 3:13 CASI 101-Average radiance across lines without cross-track correction 73
Figure 3:14 CASI 101-Average radiance across lines without cross-track correction (offset for clarity) 73
Figure 3:15 CASI 91-polynomials (2nd order) applied to correct for cross-track variance 74
Figure 3:16 CASI 91-resultant radiance patterns across image after cross-track correction (offset for clarity) 74
Figure 4:1 Typical spectral reflectance of vegetation (black) and first derivative (red) in the visible and near infrared 86
Figure 4:2 Calculating Continuum Removed Reflectance 88
Figure 4:3 The semivariogram with model type and nugget, sill and range indicated 90
Figure 4:4 Mean spectra (and +/- 1 standard deviations) per study plot (EF1, LS1 and LS2) at each sampling stage a) July b) August c) September 92
Figure 4:5 Mean spectra (and +/- 1 standard deviations) per study plot (LS3, MC1 and MC2) at each sampling stage a) July b) August c) September 93
Figure 4:6 Mean spectra (and +/- 1 standard deviations) per study plot (MC3, MC4 and MG1) at each sampling stage a) July b) August c) September 94
Figure 4:7 Mean spectra (and +/- 1 standard deviations) per study plot (MG2, MS1 and MS2) at each sampling stage a) July b) August c) September 95
Figure 4:8 Mean spectra (and +/- 1 standard deviations) per study plot (MS3, RP1 and RP2) at each sampling stage a) July b) August c) September 96
Figure 4:9 Mean spectra (and +/- 1 standard deviations) from RP3 at each sampling stage a) July b) August c) September 97
Figure 4:10 Mean spectra by habitat type a) July b) August c) September (EF=*Equisetum fluviatile*; LS=Species-rich low sedge; MC=*Molinia caerulea*-sedge mire; MG=*Molinia caerulea-Myrica gale* mire; MS=Mixed sedge; RP=Rush pasture/Grassland) 98

Figure 4:11 Mean spectra by habitat type (500 – 700 nm) a) July b) August c) September (EF=*Equisetum fluviatile*; LS=Species-rich low sedge; MC=*Molinia caerulea*-sedge mire; MG=*Molinia caerulea-Myrica gale* mire; MS=Mixed sedge; RP=Rush pasture/Grassland) 99

Figure 4:12 July Dataset: Study Plots-PCA using AVS 1-42 spectra (mean and +/- 1 SD) (eigenvalue Axis 1: 0.97; eigenvalue Axis 2: 0.02) 100

Figure 4:13 July Dataset: Study Plots-PCA using CASI bandwidths (mean and +/- 1 SD) (eigenvalue Axis 1: 0.97; eigenvalue Axis 2: 0.02) 100

Figure 4:14 August Dataset: Study Plots-PCA using AVS 1-42 spectra (mean and +/- 1 SD) (eigenvalue Axis 1: 0.93; eigenvalue Axis 2: 0.05) 101

Figure 4:15 September Dataset: Study Plots-PCA using AVS 1-42 spectra (mean and +/- 1 SD) (eigenvalue Axis 1: 0.95; eigenvalue Axis 2: 0.03) 101

Figure 4:16 Mean spectra grouped by habitat type collected in July 2003 (EF1 shown as 'EF' for illustrative purposes) EF=*Equisetum fluviatile*; LS=Species-rich low sedge; MC=*Molinia caerulea*-sedge mire; MG=*Molinia caerulea-Myrica gale* mire; MS=Mixed sedge; RP=Rush pasture/Grassland 105

Figure 4:17 Mean spectra grouped by habitat type collected in August 2003 (EF1 shown as 'EF' for illustrative purposes) EF=*Equisetum fluviatile*; LS=Species-rich low sedge; MC=*Molinia caerulea*-sedge mire; MG=*Molinia caerulea-Myrica gale* mire; MS=Mixed sedge; RP=Rush pasture/grassland 106

Figure 4:18 Mean spectra grouped by habitat type collected in September 2003 (EF1 shown as 'EF' for illustrative purposes) EF=*Equisetum fluviatile*; LS=Species-rich low sedge; MC=*Molinia caerulea*-sedge mire; MG=*Molinia caerulea-Myrica gale* mire; MS=Mixed sedge; RP=Rush pasture/grassland 107

Figure 4:19 July Dataset: PCA results grouped by Habitat Type (mean and +/- 1 SD) (eigenvalue Axis 1: 0.97; eigenvalue Axis 2: 0.02) (EF=*Equisetum fluviatile*; LS=Species-rich low sedge; MC=Molinia *caerulea*-sedge mire; MG=*Molinia caerulea-Myrica gale* mire; MS=Mixed sedge; RP=Rush pasture/grassland) 108

Figure 4:20 August Dataset: PCA results grouped by Habitat Type (mean and +/- 1 SD) (eigenvalue Axis 1: 0.93; eigenvalue Axis 2: 0.05) (EF=*Equisetum fluviatile*; LS=Species-rich low sedge; MC=*Molinia caerulea*-sedge mire; MG=*Molinia caerulea-Myrica gale* mire; MS=Mixed sedge; RP=Rush pasture/grassland) 108

Figure 4:21 September Dataset: PCA results grouped by Habitat Type (mean and +/- 1 SD) (Eigenvalue Axis 1: 0.95; eigenvalue Axis 2: 0.03) (EF=*Equisetum fluviatile*; LS=Species-rich low sedge; MC=*Molinia caerulea*-sedge mire; MG=*Molinia caerulea-Myrica gale* mire; MS=Mixed sedge; RP=Rush pasture/grassland) 109

Figure 4:22 Mean spectra from the six study plots analysed using Mann Whitney statistical test a) July b) August c) September (EF=*Equisetum fluviatile*; LS=Species-rich low sedge; MC=*Molinia caerulea*-sedge mire; MG=*Molinia caerulea-Myrica gale* mire; MS=Mixed sedge; RP=Rush pasture/grassland) 112

Figure 4:23 July Dataset: Mean, minimum and maximum spectra from RP1 and EF1-significantly different (95% Significance Level) at all wavelengths (greyed area) 116

Figure 4:24 August Dataset: Mean, minimum and maximum spectra from RP1 and EF1-Significantly different (95% Significance Level) at wavelengths highlighted in grey 116

Figure 4:25 September Dataset: Mean, minimum and maximum spectra from RP1 and EF1-Significantly different (95% Significance Level) at wavelengths highlighted in grey 117

Figure 4:26 Box and whisker plots of NDVI values calculated at each study plot - a) July, b) August and c) September 119

Figure 4:27 Box and whisker plots of NDVI values grouped by habitat type - a) July, b) August and c) September 120

Figure 4:28 1st derivative slopes for the July spectra (data grouped by habitat type) along full length of the spectrum (graphs labelled with '1') and between 650 nm and 790 nm (graphs labelled with '2') (a = *Equisetum fluviatile;* b = Species-rich low sedge mire; c = *Molinia caerulea*-sedge mire; d = *Molinia caerulea-Myrica gale* mire; e = Mixed sedge; f = Rush pasture/grassland) (Mean = — ; +1SD= - - - - ; -1SD= - -- -) 123

Figure 4:29 1st derivative slopes for the August spectra (data grouped by habitat type) along full length of the spectrum (graphs labelled with '1') and between 650 nm and 790 nm (graphs labelled with '2') (a = *Equisetum fluviatile*; b = Species-rich low sedge mire; c = *Molinia caerulea*-sedge mire; d = *Molinia caerulea-Myrica gale* mire; e = Mixed sedge; f = Rush pasture/grassland) (Mean = — ; +1SD= - - - - ; -1SD= - -- -) 124

Figure 4:30 1st derivative slopes for the September spectra (data grouped by habitat type) along full length of the spectrum (graphs labelled with '1') and between 650 nm and 790 nm (graphs labelled with '2') (a = *Equisetum fluviatile*; b = Species-rich low sedge mire; c = *Molinia caerulea*-sedge mire; d = *Molinia caerulea-Myrica gale* mire; e = Mixed sedge; f = Rush pasture/grassland) (Mean = — ; +1SD= - - - - ; -1SD= - -- -) 125

Figure 4:31 REIPs for *Equisetum fluviatile* study plots throughout the sampling period (a = July, b = August, c = September) 127

Figure 4:32 REIPs for Species-rich low sedge mire study plots throughout the sampling period (a = July, b = August, c = September) 128

Figure 4:33 REIPs for *Molinia caerulea*-sedge mire study plots throughout the sampling period (a = July, b = August, c = September) 129

Figure 4:34 REIPs for *Molinia caerulea-Myrica gale* mire study plots throughout the sampling period (a = July, b = August, c = September) 130

Figure 4:35 REIPs for Mixed sedge study plots throughout the sampling period (a = July, b = August, c = September) 131

Figure 4:36 REIPs for Rush pasture/grassland study plots throughout the sampling period (a = July, b = August, c = September) 132

Figure 4:37 Indices derived from continuum removal analyses in the blue region (a = Band Depth, b = Continuum Removed Derivative Reflectance, c = Band Depth Ratio and d = Normalized Band Depth Ratio) 133

Figure 4:38 Indices derived from continuum removal analyses in the red region (a = Band Depth, b = Continuum Removed Derivative Reflectance, c = Band Depth Ratio and d = Normalized Band Depth Ratio) 134

Figure 4:39 Semivariograms calculated using NDVI values at plots EF1, LS2 and MC1 in July ('a'), August ('b') and September ('c') 137

Figure 4:40 Semivariograms calculated using NDVI values at plots MG2, MS3 and RP1 in July ('a'), August ('b') and September ('c') 138

Figure 4:41 Semivariograms calculated using REIPs at plots EF1, LS2 and MC1 in July ('a'), August ('b') and September ('c') 139

Figure 4:42 Semivariograms calculated using REIPs at plots MG2, MS3 and RP1 in July ('a'), August ('b') and September ('c') 140

Figure 4:43 PCA performed on Meteorological Data for August field spec data collection days (Study plots means plotted) 144

Figure 4:44 All REIPs calculated using each sample spectrum from July, August and September hyperspectral datasets 153

Figure 5:1 DCA species-samples biplot (triangles and circles respectively) for vegetation-species composition dataset in July (some species have been omitted for clarity) (axis I eigenvalue: 0.7, axis II eigenvalue: 0.5) 182

Figure 5:2 DCA species-samples biplot (triangles and circles respectively) for vegetation-species composition dataset in September 185

Figure 5:3 Vegetation and spectra (AVS1-42 and CASI) sample scores along each transect (a-c) using July ('1') and September ('2') datasets (Vertical Line = Position of boundary line on *a priori* habitat map: a = 30 m, b = 40 m, c = NA) 186

Figure 5:4 CCA triplot for AVS1-42 July analyses and species composition vegetation dataset (some species names omitted for clarity and only significant predictors labelled) (eigenvalue axis I: 0.616; eigenvalue axis II: 0.531) 192

Figure 5:5 CCA triplot for CASI July spectra and species composition vegetation dataset (some species names omitted for clarity and only significant predictors labelled) (eigenvalue axis I: 0.528; eigenvalue axis II: 0.324) 193

Figure 5:6 CCA triplot for AVS1-42 September analyses and species composition vegetation dataset (some species names omitted for clarity and only significant predictors labelled) (eigenvalue axis I: 0.617; eigenvalue axis II: 0.568) 202
Figure 5:7 CCA triplot for CASI September analyses and species composition vegetation dataset (some species names omitted for clarity and only significant predictors labelled) (eigenvalue axis I: 0.465; eigenvalue axis II: 0.386) 203
Figure 5:8 Stepwise MDA on altitude, azimuth and meteorological data to illustrate the different conditions under which the spectra were collected-July 2003 212
Figure 5:9 Stepwise MDA on altitude, azimuth and meteorological data to illustrate the different conditions under which the spectra were collected-September 2003 212
Figure 5:10 Attribute plots showing spread in species richness across ordination diagram (larger sample symbols correspond to greater species richness) 220
Figure 5:11 Attribute plots showing spread in species diversity across ordination diagram (larger sample symbols correspond to greater species diversity) 221
Figure 6:1 CASI flightlines (Yellow: CASI 91; Blue: CASI 101) 229
Figure 6:2 Habitat types covered by both images (x25 in total but this includes *Sphagnum* flush at eastern margin of the marsh which is not shown) 230
Figure 6:3 Habitats of special ecological interest (Rare and invasive species) 231
Figure 6:4 CASI 91: Red absorption feature (Continuum removed) -All habitat types 242
Figure 6:5 CASI91: Red absorption feature (Continuum removed) –Grouped habitat types 243
Figure 6:6 Location of transects analysed using spectral data collected from CASI imagery 244
Figure 6:7 Habitats along transects analysed using spectral data collected from CASI imagery 245
Figure 6:8 Habitat changes along transects a-e (Start positions circled) (a Transect 4.2: Balavil Q; b Transect 4.6: Balavil C; c Transect 8.3: Insh G; d Transect 8.4: Insh I; e Transect 9.2: Coull Q) 246
Figure 6:9 CASI 91: All habitat classes 248
Figure 6:10 Mean spectra collected from habitat polygons-CASI 91 249
Figure 6:11 CASI 101:All habitat classes 250
Figure 6:12 Mean spectra collected from habitat polygons-CASI 101 251
Figure 6:13 CASI 91-Grouped habitat types 253
Figure 6:14 Spectral 'Endmembers' from Grouped Habitat Types-CASI 91 253
Figure 6:15 CASI I01-Grouped habitat types 254
Figure 6:16 Spectra 'Endmembers' from Grouped Habitat Types-CASI 101 254
Figure 6:17 CASI 91 K-Means Classifications and water features and habitat boundaries overlays a) 6 classes b) 11 habitats c) 22 habitats. 259
Figure 6:18 CASI 101 K-Means Classifications and water features and habitat boundaries overlays a) 6 classes b) 11 habitats c) 22 habitats. 260
Figure 6:19 CASI 91: NDVI values a) Raw Results (bright pixels=higher NDVI) b) Results grouped via K-Means Classification into 15 classes c) Results grouped via K-Means Classification into 5 classes (White-Red = Low-High NDVI) (NB b) and c) overlay: All habitat type boundaries) 260
Figure 6:20 CASI 101: NDVI values a) Raw Results (bright pixels=higher NDVI) b) Results grouped via K-Means Classification into 15 classes c) Results grouped via K-Means Classification into 5 classes (White-Red = Low-High NDVI) (NB b) and c) overlay: All habitat type boundaries) 261
Figure 6:21 Position of red edge calculated for CASI 91 a) Raw Results b) Results grouped via K-Means Classification into 10 classes 262
Figure 6:22 Position of red edge calculated for CASI 101 a) Raw Results b) Results grouped via K-Means Classification into 15 classes 262
Figure 6:23 CASI 91: *A priori* habitats (x22) above and results from supervised classification-below (Stratified Random Training samples (Overall Accuracy: 67.5%)) 264

Figure 6:24 CASI 101: *A priori* habitats (x22) above and results from supervised classification below (Stratified Random Training samples (Overall Accuracy: 74.1%)) 267
Figure 6:25 CASI 91 (a) and CASI 101 (b) Uncertainty maps showing producer's accuracy (%) of classes produced by Maximum Likelihood Classifications using all 22 *a priori* habitat types 270
Figure 6:26 CASI 91: Supervised Classification - Grouped Habitat Types (x11) (Equalized Random Training samples (Overall Accuracy: 72.2%)) 272
Figure 6:27 CASI 101: Supervised Classification - Grouped Habitat Types (x11) (Stratified Random Training samples (Overall Accuracy: 76.7%)) 274
Figure 6:28 CASI91 (a) and CASI101 (b) Uncertainty maps showing producer's accuracy (%) of classes produced by Maximum Likelihood Classifications using all 22 a priori habitat types 276
Figure 6:29 Probability maps of sensitive habitats (CASI 91) (Dark pixels=Low probability; Lighter pixels=greater probabilities; red pixels=greatest probabilities..... 279
Figure 6:30a Probability maps of sensitive habitats (CASI 101) (Dark pixels=Low probability; Lighter pixels=greater probabilities; red pixels=greatest probabilities) 281
Figure 6:31 Analyses along Transect 4.2: a) habitat type change along transect; b) DCA results showing sample scores at quadrat survey points along transect and DN values derived from imagery; c) illustates the DCA Sample Scores at all pixels along the transect; recorded changes in vegetation cover are indicated by vertical bars; d) illustrates the patterns of NDVI and REIP values along the transect..... 284
Figure 6:32 Analyses along Transect 4.6: a) habitat type change along transect; b) DCA results showing sample scores at quadrat survey points along transect and DN values derived from imagery; c) illustates the DCA Sample Scores at all pixels along the transect; recorded changes in vegetation cover are indicated by vertical bars; d) illustrates the patterns of NDVI and REIP values along the transect..... 285
Figure 6:33 Analyses along Transect 8.3: a) habitat type change along transect; b) DCA results showing sample scores at quadrat survey points along transect and DN values derived from imagery; c) illustates the DCA Sample Scores at all pixels along the transect; recorded changes in vegetation cover are indicated by vertical bars; d) illustrates the patterns of NDVI and REIP values along the transect..... 286
Figure 6:34 Analyses along Transect 8.4: a) habitat type change along transect; b) DCA results showing sample scores at quadrat survey points along transect and DN values derived from imagery; c) illustates the DCA Sample Scores at all pixels along the transect; recorded changes in vegetation cover are indicated by vertical bars; d) illustrates the patterns of NDVI and REIP values along the transect..... 287
Figure 6:35 Analyses along Transect 9.2: a) habitat type change along transect; b) DCA results showing sample scores at quadrat survey points along transect and DN values derived from imagery; c) illustates the DCA Sample Scores at all pixels along the transect; recorded changes in vegetation cover are indicated by vertical bars; d) illustrates the patterns of NDVI and REIP values along the transect..... 288
Figure 6:36 Fitted Line Plots and regression results (-Predictor-DN Sample Scores, Response-Vegetation Sample Scores) a) Transect 4.2 b) Transect 4.6 c) Transect 8.3 d) Transect 8.4 e) Transect 9.2 289

Appendices

Figure B:1 Equisetum fluviatile (EF1) All spectra (July: top; August: middle; Sept: bottom) 347
Figure B:2 Species rich low sedge mire (LS1) All spectra (July: top; August: middle; Sept: bottom) 348
Figure B:3 Species rich low sedge mire (LS2) All spectra (July: top; August: middle; Sept: bottom) 349
Figure B:4 Species rich low sedge mire (LS3) All spectra (July: top; August: middle; Sept: bottom) 350
Figure B:5 Molinia caerulea-sedge mire (MC1) All spectra (July: top; August: middle; Sept: bottom) 351

Figure B:6 Molinia caerulea-sedge mire (MC2) All spectra (July: top; August: middle; Sept: bottom) 352
Figure B:7 Molinia caerulea-sedge mire (MC3) All spectra (July: top; August: middle; Sept: bottom) 353
Figure B:8 Molinia caerulea-sedge mire (MC4) All spectra (July: top; August: middle; Sept: bottom)..... 354
Figure B:9 Myrica gale-Molinia caerulea-sedge mire (MG1) All spectra (July: top; August: middle; Sept: bottom) 355
Figure B:10 Myrica gale-Molinia caerulea-sedge mire (MG2) All spectra (July: top; August: middle; Sept: bottom) 356
Figure B:11 Mixed sedge (MS1) All spectra (July: top; August: middle; Sept: bottom)..... 357
Figure B:12 Mixed sedge (MS2) All spectra (July: top; August: middle; Sept: bottom)..... 358
Figure B:13 Mixed sedge (MS3) All spectra (July: top; August: middle; Sept: bottom)..... 359
Figure B:14 Rush pasture/Grassland (RP1) All spectra (July: top; August: middle; Sept: bottom) 360
Figure B:15 Rush pasture/Grassland (RP2) All spectra (July: top; August: middle; Sept: bottom) 361
Figure B:16 Rush pasture/Grassland (RP3) All spectra (July: top; August: middle; Sept: bottom) 362
Figure C:1 Regression results on vegetation and spectra (AVS1-42- '1' and CASI- '2' datasets) sample scores from data collected at Transects a-c in July..... 404
Figure C:2 Regression results on vegetation and spectra (AVS1-42- '1' and CASI- '2' datasets) sample scores from data collected at Transects a-c in September..... 405
Figure C:3 Environmental variables graph from all four CCA analyses-July 2003 (species composition data with AVS1-42 spectra: top left, species composition data with CASI: top right, species and structure dataset with AVS1-42: bottom left, species and structure dataset with AVS1-42: bottom left, species and structure dataset with CASI: bottom right) 414
Figure C:4 Environmental variables graph from all four CCA analyses-September 2003 (species composition data with AVS1-42 spectra: top left, species composition data with CASI: top right, species and structure dataset with AVS1-42: bottom left, species and structure dataset with CASI: bottom right) 415
Figure C:5 CCA triplot for AVS1-42 July analyses and species composition with structural and environmental variables vegetation dataset (some species names omitted for clarity and only significant predictors labelled) (eigenvalue axis I: 0.874; eigenvalue axis II: 0.931) (see ordination diagrams above for predictor variables labels) (some species omitted for clarity)..... 416
Figure C:6 CCA triplot for CASI July analyses and species composition with structural and environmental variables vegetation dataset (some species names omitted for clarity) (eigenvalue axis I: 0.764; eigenvalue axis II: 0.689) 417
Figure C:7 CCA triplot for AVS1-42 Sept analyses and species composition with structural and environmental variables vegetation dataset (some species names omitted for clarity and only significant predictors labelled) (eigenvalue axis I:0.305; eigenvalue axis II: 0.193) (see ordination diagrams above for predictor variables labels) 418
Figure C:8 CCA triplot for CASI Sept analyses and species composition with structural and environmental variables vegetation dataset (some species names omitted for clarity and only significant predictors labelled) (eigenvalue axis I: 0.196; eigenvalue axis II: 0.108) (some species omitted for clarity) 419

LIST OF TABLES

Table 2:1 Environmental factors that define wetland type (from Heathwaite *et al.* 1993).....8
Table 2:2 Hydrochemical groupings of wetland types (from Hughes & Heathwaite 1995).....8
Table 2:3 Major British wetlands (adapted from Hughes & Heathwaite 1995) 9
Table 2:4 Factors to consider in order to employ good field practice during field spectrometry 16
Table 2:5 Flora and fauna species and vegetation assemblages of notable interest at Insh Marshes (adapted from RSPB 2000) 37
Table 2:6 RSNC/NCC and equivalent NVC codes at Insh marshes (taken from RSPB 2000)39
Table 2:7 Simple habitat types and respective area (ha) recorded in the floodplain of Insh Marshes (taken from Maier & Cowie 2002).....40
Table 3:1 Habitat types and respective plot codes with first and second most dominant species determined from field survey 51
Table 3:2 Dates during the sampling period.....56
Table 3:3 Instrument specifications for the ASD FieldSpec™ 56
Table 3:4 Table showing the wavelength range of the spectrometer channels that represent the CASI Default Vegetation bandset (taken from Armitage *et al.* 2000).....57
Table 3:5 Table showing the wavelength range of the spectrometer channels that represent each of the hyperspectral bands (AV1-42).....58
Table 3:6 Codes applied to survey species presence and abundance.....64
Table 3:7 Structural variables recorded at each quadrat 64
Table 3:8 CASI-Veg band centres and half band widths 66
Table 3:9 Meteorological Data collected at Aviemore, 17th September, 2003 (provided by the Meterological Office) and local solar azimuth and altitude (as calculated at http://aa.usno.navy.mil/data/docs/AltAz.html) 68
Table 3:10 Header information for CASI 91 & CASI 101 68
Table 3:11 Monthly meteorological data variables (provided for July, August and September 2003 by Met. Office) 75
Table 3:12 Daily meteorological data at Aviemore (provided for each day during the spectral sampling period by Met. Office).....76
Table 4:1 Geostatistics: Terms used in the description of the semivariogram (Adapted from Curran & Atkinson 1998) 90
Table 4:2 Results from Multiple Discriminant Analysis on the sample spectra grouped by habitat for all three sampling stages (EF=*Equisetum fluviatile*; LS=Species-rich low sedge; MC=*Molinia caerulea*-sedge mire; MG=*Molinia caerulea-Myrica gale* mire; MS=Mixed sedge; RP=Rush pasture/grassland; A=AVS1-42; C=CASI) 102
Table 4:3 MDA results: Significant wavebands determined by MDA stepwise model (highlighted in bold) 103
Table 4:4 MDA results: Significant wavebands-CASI (highlighted in bold)..... 104
Table 4:5 Results from Kruskal Wallis H test (July) (highlighted: P=<0.05) ('C'=CASI band; EF=*Equisetum fluviatile*; LS=Species-rich low sedge; MC=*Molinia caerulea*-sedge mire; MG=*Molinia caerulea-Myrica gale* mire; MS=Mixed sedge; RP=Rush pasture/grassland) 110
Table 4:6 Results from Kruskal Wallis H test (August) (highlighted: P=<0.05) ('C'=CASI band; EF=*Equisetum fluviatile*; LS=Species-rich low sedge; MC=*Molinia caerulea*-sedge mire; MG=*Molinia caerulea-Myrica gale* mire; MS=Mixed sedge; RP=Rush pasture/grassland) 110
Table 4:7 Results from Kruskal Wallis H test (September) (highlighted: P=<0.05) ('C'=CASI band; EF=*Equisetum fluviatile*; LS=Species-rich low sedge; MC=*Molinia caerulea*-sedge mire; MG=*Molinia caerulea-Myrica gale* mire; MS=Mixed sedge; RP=Rush pasture/grassland)..... 110
Table 4:8 Mann Whitney Results: July (Highlighted cells are significant at P<0.005) 113

Table 4:9 Mann Whitney Results: August (Highlighted cells are significant at P<0.005) 114
Table 4:10 Mann Whitney Results: September (Highlighted cells are significant at P<0.005) 115
Table 4:11 Results from Kruskal Wallis Analysis using NDVI values calculated from two or more study plots within each habitat type 121
Table 4:12 Results from Mann Whitney calculations using NDVI values from study plots EF1, LS2, MC1, MG2, MS3, RP3 (highlighted cells are significant at P<0.05) 121
Table 4:13 Geostatistics carried out on NDVIs calculated at plots EF1 (*Equisetum fluviatile*), LS2 (Species-rich low sedge mire), MC1 (*Molinia caerulea*), MG2 (*Molinia caerulea-Myrica gale* mire), MS3 (Mixed sedge) and RP1 (Rush pasture/grassland) over the sampling period 135
Table 4:14 Geostatistics carried out on REIPs calculated at plots EF1 (*Equisetum fluviatile*), LS2 (Species-rich low sedge mire), MC1 (*Molinia caerulea*), MG2 (*Molinia caerulea-Myrica gale* mire), MS3 (Mixed sedge) and RP1 (Rush pasture/grassland) over the sampling period 136
Table 4:15 Management within each study plot (Maier & Cowie 2002) 145
Table 4:16 First eight most significant predictors identified in Multiple Discriminant Analyses for each sampling stage (listed in rank order starting with highest) 147
Table 5:1 Species composition data compiled from all study plots and grouped by habitat type (data collected in late June/early July 2003) 171
Table 5:2 Species composition data compiled from all study plots and grouped by habitat type (data collected in September 2003) 172
Table 5:3 Structural and environmental data compiled from all study plots and grouped by habitat type (data collected in late June/early July 2003) 173
Table 5:4 Structural and environmental data compiled from all study plots and grouped by habitat type (data collected in September 2003) 173
Table 5:5 Species composition data compiled from all study plots and grouped by TWINSPAN clusters (data collected in late June/early July 2003) 174
Table 5:6 Species composition data compiled from all study plots and grouped by TWINSPAN clusters (data collected in September 2003) 175
Table 5:7 Structural and environmental data compiled from all study plots and grouped by TWINSPAN clusters (data collected in late June/early July 2003) 176
Table 5:8 Structural and environmental data compiled from all study plots and grouped by TWINSPAN clusters (data collected in September 2003) 176
Table 5:9 Multiple Discriminant Analysis results (percentage correct per habitat type and overall) using paired spectral datasets only and grouped by habitat type (1=EF, 2=LS, 3=MC, 4=MG, 5=MS, 6=RP; results from using a random group labelling system in brackets) 177
Table 5:10 Multiple Discriminant Analysis results using paired spectral datasets only and grouped by TWINSPAN; Groups 1-6 for September datasets and 1-7 for July datasets (percentage correct per habitat type and overall) (Results from using a random group labelling system in brackets) 177
Table 5:11 The significance of the canonical axes when covariation is removed 178
Table 5:12 DCA output-July 2003 180
Table 5:13 DCA output-September 2003 183
Table 5:14 Regression results (R^2Adj) between vegetation and spectra sample scores using DCA along transects 'a', 'b' and 'c' (both AVS1-42 and CASI datasets) (Graphs in Appendix C) 186
Table 5:15 Summary of permutation test (x499) results: Monte Carlo tests carried out during the CCA of July datasets 187
Table 5:16 Summary of CCA results on July spectra: (all combinations of species and environmental variables). 188

Table 5:17 The performance of each AVS 1-42 waveband used to predict variation in the species dataset (canon eigen: 3.207; total inertia 7.732) and the species/structure dataset (canon eigen: 1.228; total inertia 2.712)-output by forward selection (Conditional effects)-July 2003 (FVE: Fraction of Variance Explained) *Italicized results are not significant model variables* 189
Table 5:18 The performance of each CASI waveband (conditional effects) used to predict variation in the species dataset (canon eigen: 1.667; total intertia 7.732) and the species/structure dataset (canon eigen: 0.649; total inertia 2.712)-output by forward selection (Conditional effects)-July 2003 (FVE: Fraction of Variance Explained)..... 190
Table 5:19 RDA results: Tests on all first canonical axes-July 2003 194
Table 5:20 RDA outputs July 2003-all analyses..... 195
Table 5:21 First twenty species listed in output (conditional effects) from RDA on July AVS1-42 and species (canon eigen: 0.570) and species/structure datasets (canon eigen: 0.589) (FVE: Fraction of Variance Explained) (*Italicized and greyed out variables are not significant model variables* 196
Table 5:22 First twenty species listed in output from RDA on July CASI and species (canon eigen: 0.499) and species/structure datasets (canon eigen: 0.570) (FVE: Fraction of Variance Explained) (*Italicized and greyed out variables are not significant model variables* 197
Table 5:23 Summary of permutation test (x499) results: monte carlo tests carried out during the CCA of September datasets..... 198
Table 5:24 Summary of CCA results on September spectra: both spectral bandsets and both combinations of vegetation data..... 199
Table 5:25 The performance of each AVS 1-42 wavebands used to predict variation in the species dataset (canon eigen: 3.206; total inertia 7.293) and the species/structure dataset-(canon eigen: 1.013; total inertia 2.126) output by forward selection (Conditional effects)-September 2003 (FVE: Fraction of Variance Explained) *Italicized results are not significant model variables* 200
Table 5:26 The performance of each CASI waveband used to predict variation in the species dataset (canon eigen: 1.498; total inertia 7.293) and the species/structure dataset (canon eigen: 0.469; total inertia 2.126)-output by forward selection (Conditional effects)-September 2003 (FVE: Fraction of Variance Explained) 201
Table 5:27 RDA results: Tests on all first canonical axes-September 2003 204
Table 5:28 RDA outputs September 2003-all analyses 205
Table 5:29 First twenty species listed in forward stepwise output from RDA on September AVS1-42 dataset using species composition as species variables (canon eigen: 0.549) and species and structure data (canon eigen: 0.571) as species variables (FVE: Fraction of Variance Explained) (*Italicized and greyed out variables are not significant model variables* 206
Table 5:30 First twenty species listed in forward stepwise output from RDA on September CASI dataset using species composition as species variables (canon eigen: 0.583) and species and structure data (canon eigen: 0.604) as species variables (FVE: Fraction of Variance Explained) (*Italicized and greyed out variables are not significant model variables* 207
Table 6:1 CASI bands used in Guyot-Baret Red Edge Model 235
Table 6:2 Training Samples-CASI 91-Main Habitat Types (x22) 238
Table 6:3 Samples-CASI 101-Main Habitat Types (x22) 239
Table 6:4 Training Samples-CASI 91-Grouped Habitat Types (x11)..... 239
Table 6:5 Training Samples-CASI 101-Grouped Habitat Types (x11)..... 240
Table 6:6 Codes used in confusion matrices (Special habitats in bold)..... 241
Table 6:7 CASI band centres and band widths 242
Table 6:8 Grouped Habitat Types (x11) and Area-CASI 91 and CASI 101 252
Table 6:9a Unsupervised clustering CASI 91 (35 clusters) (first 27 clusters)..... 256
Table 6:10 Unsupervised clustering CASI 101 (35 clusters)..... 258

Table 6:11 Overall Accuracy Results from Maximum Likelihood Classification-All Habitat Types (x22) 263
Table 6:12a Information extracted from confusion matrix produced from most successful supervised classification on CASI 91 (First 12 classes) 265
Table 6:13a Information extracted from confusion matrix produced from most successful supervised classification on CASI 101 (First 11 classes) 268
Table 6:14 Overall Accuracy Results from Maximum Likelihood Classification-Grouped Habitat Types (x11) 271
Table 6:15 Information extracted from confusion matrix produced from most successful supervised classification on CASI 91 (Grouped habitat types) 273
Table 6:16 Information extracted from confusion matrix produced from most successful supervised classification on CASI 101 (Grouped habitat types) 275
Table 6:17 Confusion Matrix to highlight habitats of particular interest (CASI 91 MaxLike Classification: Overall accuracy-67.5%; Kappa 0.58) 277
Table 6:18 Confusion Matrix to highlight habitats of particular interest (CASI 101 MaxLike Classification: Overall accuracy-74.1%; Kappa 0.66) 278
Table 6:19 CASI 91 and CASI 101-Overall Accuracy Results from Spectral Feature Fitting (Blue region absorption feature and red region absorption feature):-All Habitat Types (x22) and Grouped Habitat Types (x11) (using ground truth images as test data) 283
Table 6:20 Habitat ordering in the NIR (Band 9) for both images (highest to lowest values of reflectance) 291

Appendices

Table A:1 CASI 91-Ground Control Points and associated RMS error 334
Table A:2 CASI 101- Ground Control Pointss and associated RMS error 335
Table A:3 Meteorological data and solar altitude and azimuth at paired sampling points -July 2003 336
Table A:4 Meteorological data and solar altitude and azimuth at paired sampling points –Sept 2003 339
Table A:5 Daily meteorological averages for July 2003 (sampling days highlighted) 343
Table A:6 Daily meteorological averages for August 2003 (sampling days highlighted) 344
Table A:7 Daily meteorological averages for September 2003 (sampling days highlighted) 345
Table B:1 Normality tests (Anderson-Darling) on spectra from each CASI band and NDVI(CASI) results at all study plots in July 2003 363
Table B:2 Normality tests (Anderson-Darling) on spectra from each CASI band and NDVI(CASI) results at all study plots in August 2003 364
Table B:3 Normality tests (Anderson-Darling) on spectra from each CASI band and NDVI(CASI) results at all study plots in September 2003 365
Table B:4 Kruskal Wallis H test results: LS habitat, July 366
Table B:5 Kruskal Wallis H test results: MC habitat, July 367
Table B:6 Kruskal Wallis H test results: MG habitat, July 368
Table B:7 Kruskal Wallis H test results: MS habitat, July 369
Table B:8 Kruskal Wallis H test results: RP habitat, July 370
Table B:9 Kruskal Wallis H test results: LS habitat, August 371
Table B:10 Kruskal Wallis H test results: MC habitat, August 372
Table B:11 Kruskal Wallis H test results: MG habitat, August 373
Table B:12 Kruskal Wallis H test results: MS habitat, August 374

Table B:13 Kruskal Wallis H test results: RP habitat, August..... 375
Table B:14 Kruskal Wallis H test results: LS habitat, September..... 376
Table B:15 Kruskal Wallis H test results: MC habitat, September..... 377
Table B:16 Kruskal Wallis H test results: MG habitat, September..... 378
Table B:17 Kruskal Wallis H test results: MS habitat, September..... 379
Table B:18 Kruskal Wallis H test results: RP habitat, September..... 380
Table B:19 MDA stepwise model output (groups by habitat type-See Chapter 4 for Group labels) July-AVS1-42..... 381
Table B:20 MDA stepwise model output (groups by habitat type-See Chapter 4 for Group labels) July-CASI..... 382
Table B:21 MDA stepwise model output (groups by habitat type-See Chapter 4 for Group labels) Aug-AVS1-42..... 383
Table B:22 MDA stepwise model output (groups by habitat type-See Chapter 4 for Group labels) Aug-CASI..... 384
Table B:23 MDA stepwise model output (groups by habitat type-See Chapter 4 for Group labels) Sept-AVS1-42..... 385
Table B:24 MDA stepwise model output (groups by habitat type-See Chapter 4 for Group labels) Sept-CASI..... 386
Table B:25 All results from Kruskal Wallis analyses on CASI derived NDVI values (greyed out cells=statistically significant at P<0.05)..... 387
Table B:26 Frequency table to show REIP at each study plot using spectra collected in July 2003..... 388
Table B:27 Frequency table to show REIP at each study plot using spectra collected in August 2003..... 389
Table B:28 Frequency table to show REIP at each study plot using spectra collected in September 2003..... 390
Table C:1 July-AVS1-42 spectra grouped using a priori habitat types..... 392
Table C:2 July-CASI spectra grouped using a priori habitat types..... 393
Table C:3 September-AVS1-42 spectra grouped using a priori habitat types..... 394
Table C:4 Sept-CASI spectra grouped using a priori habitat types..... 395
Table C:5 July-AVS1-42 spectra grouped using TWINSPAN cluster groups (species composition datasets only)..... 396
Table C:6 July-CASI spectra grouped using TWINSPAN cluster groups (species composition datasets only)..... 397
Table C:7 Sept-AVS1-42 spectra grouped using TWINSPAN cluster groups (species composition datasets only)..... 398
Table C:8 Sept-CASI spectra grouped using TWINSPAN cluster groups (species composition datasets only)..... 399
Table C:9 July AVS1-42 spectra grouped using TWINSPAN cluster groups (species with structure and environmental variables datasets only)..... 400
Table C:10 CASI spectra grouped using TWINSPAN cluster groups (species with structure and environmental variables datasets only)..... 401
Table C:11 Sept AVS1-42 spectra grouped using TWINSPAN cluster groups (species with structure and environmental variables datasets only)..... 402
Table C:12 July CASI spectra grouped using TWINSPAN cluster groups (species with structure and environmental variables datasets only)..... 403
Table C:13 Marginal effects results from CCA with AVS1-42 spectral dataset (predictors) and both vegetation datasets (independents)-July..... 406
Table C:14 Marginal effects results from CCA with CASI spectral dataset (predictors) and both vegetation datasets (independents)-July..... 407
Table C:15 Marginal effects results from CCA with AVS1-42 spectral dataset (predictors) and both vegetation datasets (independents)-Sept..... 408
Table C:16 Marginal effects results from CCA with CASI spectral dataset (predictor) and both vegetation datasets (independents)-Sept..... 409
Table C:17 Marginal effects results from RDA with AVS1-42 spectral dataset (independent) and both vegetation datasets (predictors)-July..... 410

Table C:18 Marginal effects results from RDA with CASI spectral dataset (independent) and both vegetation datasets (predictors)-July..... 411
Table C:19 Marginal effects results from RDA with AVS1-42 spectral dataset (independent) and both vegetation datasets (predictors)-Sept..... 412
Table C:20 Marginal effects results from RDA with CASI spectral dataset (independent) and both vegetation datasets (predictors)-Sept..... 413
Table D:1 Habitat Areas (x22)-CASI 91. 421
Table D:2 Habitat Areas (x22) –CASI 101..... 421
Table D:3 Transect 4.2 (Balavil) –start NH 80261, 02445..... 422
Table D:4 Transect 4.6 (Balavil) –start NH 79538, 01801..... 423
Table D:5 Transect 8.3 (Insh) –start NH 80300, 02389..... 425
Table D:6 Transect 8.4 (Insh) –start NH 80604, 02428..... 425
Table D:7 Transect 9.2 (Coull) –start NH 80987, 03148..... 426

1 INTRODUCTION

1.1 Rationale

Wetlands are regarded as areas of increasingly important ecological function, biodiversity and economic resources particularly as greater demands and pressures are placed on decision-makers of land use practice and policy from local to global scales. As population, demand for housing, agricultural expansion and pressures on water as a resource increase worldwide, wetlands, both directly and indirectly, have significantly diminished in area as a consequence. However, the hydrological, ecological and economic value of wetlands has received an increasing degree of attention from the scientific community, conservation organisations and political parties since the establishment of the Ramsar Convention on Wetlands of International Importance in 1971.

Wetlands play an important role as ecotones between terrestrial and aquatic habitats and, as a result, represent an environment of high biodiversity and essential hydrological function within the catchment. It is, therefore, not uncommon for wetland sites to contain rare flora and fauna and the habitats of protected species. Consequently, wetlands are hot-spots for ecological, hydrological and hydrochemical research driven by the needs to understand these different components and interactions within these important and complex natural environments. As legislative demands on national governments and wetland managers increase and conflicts of interests between end-user groups heighten, there is a growing need to fully understand how the management and use of these sites affects the ecological and hydrological stability of the wetland as a system that functions on a variety of temporal and spatial scales.

Wetland vegetation can be used as an environmental indicator in terms of representing any change in the system through changes in the species composition and structure within wetland habitats. However, spatial variation is inherent, to a degree, to the wetland habitat itself and

depending on the scale of interest can also vary naturally over time. It is, therefore, an important management objective to accurately document the spatial patterns of vegetation before it is possible to understand any changes over space and time.

The process of categorising species assemblages into generic wetland habitat types itself is very difficult and common classification systems are inappropriate for the continuous and intergrading nature of semi-natural wetland environments. The nature of the boundaries between recognized wetland vegetation assemblages can offer a wealth of information to ecologists as these areas have been identified as important environmental indicators. These areas are referred to in the literature as ecotones or ecoclines depending on the scale of the transition although the terminology often overlaps. Methods that can serve as effective ways in which to characterise the nature of these of these boundary areas are heavily sought after.

The use of airborne photography has been widely applied to accurately map the spatial pattern of wetland vegetation. Similarly, applications that use airborne imagery containing spectral information in many parts of the electromagnetic spectrum to identify and classify various land uses have greatly increased over the last couple of decades. The processing and analysis of remotely sensed data has become less costly in terms of time and resources as desktop technology develops. Many classification techniques have been developed by the remote sensing scientific community to successfully map vegetation type and characteristics, although, applications at fine ecological scales remain underexploited. Difficulties arise when the classes identified using the spectral data do not marry well with ecologically meaningful reference data.

This project uses *in situ* spectral information gathered from temperate wetland habitats to demonstrate the separability of habitat type using spectral response in the visible and near infrared parts of the electromagnetic spectrum. As a result, the potential of airborne remote sensing missions to successfully classify spectral data into ecologically meaningful information can also be demonstrated. In addition, by analysing spectral patterns in relation to vegetation datasets at different times during the growing season can provide certain insights

into vegetation characteristics and these are also presented here. Airborne imagery was provided and various classification methods were explored with the aim to interpret the data based on a habitat map developed in an *a priori* vegetation survey. The use of airborne imagery to confidently map classes with an associated ecological meaning is an attractive tool for use by wetland managers due to the ease of repeatability and the objectivity that is involved. The potential that remotely sensed datasets have to offer in the decision-making processes of wetland site managers, conservation bodies and policy makers is demonstrated in this study.

1.2 Aims

This research aims to determine whether or not remote sensing is a worthwhile tool for the effective management of wetland environments. The three main aims of the project are listed below.

1. Determine the extent to which wetland habitats are spectrally distinct.

2. Determine how well species composition relates to spectral response between habitat types and across habitat boundaries.

3. Assess the potential of high spatial resolution multispectral airborne imagery for classifying and characterising wetland habitats.

1.3 Thesis Structure

The thesis is split into six parts not including this introductory chapter. Chapters include a literature review chapter, a methodology and a conclusions chapter as well as three chapters that investigate three main aims of the research as listed above. The latter are split into introduction, aims and objectives, methods, results, discussion and conclusions sub sections. Within each of these chapters the overall aim being investigated is split further into five chapter-specific objectives. Summaries are given at the end of each chapter.

A literature review of remote sensing vegetation studies is presented Chapter 2. A background to the remote sensing principles employed in this study, both for field spectrometry and airborne applications is also included. The research is placed into a global and UK context as a background on the conservation of global wetlands is given, as well as the related management issues at hand. The field study site employed throughout this study is introduced and described and present and past management practices and concerns are described.

Chapter 3 describes the sampling design, fieldwork and datasets employed for this study. The equipment used and methods employed in the field are described. Technical information on the imagery provided by the Natural Environment Research Council (NERC) and the instrument used is also presented here as well as the results from the preprocessing techniques applied before analysis of the imagery as presented in a later chapter (Chapter 6).

Chapter 4 presents the statistical and analytical techniques employed to explore the spectral response of the habitat types under study. The datasets used here are those which were collected using field spectrometry only. Chapter 5 analyses the relationships between data collected in the field with detailed vegetation datasets.

The application of the results from Chapters 4 and 5 to airborne imagery of the site is explored in Chapter 6 as well as other classification techniques. The overall success of classifying airborne imagery of such heterogeneous sites is assessed in terms of the ecological meaning of the results obtained. Remote sensing and GIS (geographical information system)

software programmes are used to analyse and display results in geographical space. The discussion and conclusions section of this chapter provides a review of the potential for the use of airborne remote sensing data as an ecological tool with benefits specific to site management for conservation purposes.

The results of this research are discussed and summarized in Chapter 7 and the applicability of remote sensing as an aid to environmental managers is discussed. The main contributions of this research to both remote sensing wetlands and to wetland management are summarized here and further work is recommended. Conclusions relating to the three main aims of this research are also listed in Chapter 7.

2 BACKGROUND AND LITERATURE REVIEW

This chapter introduces natural wetlands and the issues involved with mapping wetland vegetation using remote sensing data. It also places into context the research carried out in this project and outlines the need for tools that will aid wetland managers to effectively map and monitor the patterns of wetland vegetation over time. The study site employed in this project, the Insh Marshes, is described and discussed in terms of management needs and the role that remote sensing could play. Published work on the use of remote sensing for vegetation mapping and, in particular wetland vegetation is discussed and major knowledge gaps are highlighted.

2.1 The Global Interest in Wetlands

Wetlands provide a transition zone between the terrestrial environment and a lacustrine, riverine or an estuarine environment. These transition zones are often under pressure from activities on adjacent land surfaces and direct impacts such as drainage. The rarity and uniqueness of wetlands in terms of their associated flora and fauna has resulted in international efforts to protect the biodiversity thet they support (Agostinho *et al.* 2005; Janssen *et al.* 2005; Revenga *et al.* 2005). The Ramsar Convention on Wetlands of International Importance was established in 1971 and is an intergovernmental treaty that provides a framework for national action and international cooperation for the conservation and wise use of wetlands and their resources. The UK is a Contracting Party to the Ramsar Convention and, as well as this, has implemented the UK Biodiversity Action Plan, in response to the 1992 Rio Earth Summit and the Convention of Biological Diversity.

Wetlands have featured highly in international conventions not only due to the rich biodiversity that they support, but also in view of their hydrochemical functions. These functions include the immobilisation of environmental contaminants such as heavy metals, pesticides and industrial wastes, the provision of nutrient sinks and sources (Fisher &

Acreman 2004; Kao *et al.* 2003). In terms of a nutrient source for example, spring-fed or groundwater-dominated wetlands are capable of nutrient export when water tables and rates of throughflow are high (Hillbricht-Ilkowska 2002). Wetlands serve as important nutrient sinks in the phosphorus, nitrogen and the carbon cycles (Whigham & Jordan 2003; Mitsch *et al.* 2005). Reducing nitrate and phosphate export to adjacent freshwaters has important implications in terms of public health and water quality, and the associated environmental issues associated with this (Koskiaho & Puustinen 2005). The role of wetlands in the carbon cycle has a global significance in light of current concerns over climate change (Wang *et al.* 2003; Moore 2002; Turner *et al.* 2004) as the maintenance of wetland ecosystem stability can avoid the release of stored carbon back into the atmosphere. Wetlands are also recognised for an ability to store floodwaters, protect shorelines, recharge groundwater aquifers (Acharya 2000) and as their resources associated with recreation and aesthetics (Othman *et al.* 2004; Mitsch & Gosselink 2000a).

2.2 *Wetland Characteristics*

There are many types of wetlands which has given rise to a complex terminology. An excellent overview of British wetlands is given by Hughes and Heathwaite (1995). Wetlands in Britain have developed largely due to the relatively retentive soils and humid climate of the country as well as local hydrology, geology and topography. The terms applied in the study of wetlands are summarized in Table 2:3. In general, wetlands can be effectively subdivided by substrate. Peatlands (or 'mires'), for example, have an organic substrate and marshes, swamps and meadows have, predominantly, a mineral substrate. Morphology is then an effective way to further subdivide (see Table 2:3). Several different methods of classification can be applied to British wetlands on the basis of vegetation, chemistry, hydrology, or conservation status. However, there are a number of methods that may be employed. Rodwell (1991) produced 38 different types based on an analysis of UK-wide vegetation samples. Heathwaite *et al.* (1993) classify wetlands using a small number of environmental factors (see Table 2:1); Table 2:2 lists these three main hydrochemical groupings of wetlands.

Table 2:1 Environmental factors that define wetland type (from Heathwaite *et al.* 1993)

Environmental factor	**Classes**
Water status	Very wet Wet Fluctuating wet/dry cycle
Source of water and water movement	River flow Springs Surface runoff
Water chemistry	Eutrophic: high nutrient and calcium content Mesotrophic: medium nutrient and calcium content Oligotrophic: low nutrient and calcium content Dystrophic: high humic acid content

Table 2:2 Hydrochemical groupings of wetland types (from Hughes & Heathwaite 1995)

Hydrochemical grouping	**Notes**
Minerotrophic	Fens (Often high nutrient status)
Ombro-minerogenic	Transitional wetlands
Ombrotrophic	Raised bogs and blanket bogs (Poor nutrient status)

Table 2:3 Major British wetlands (adapted from Hughes & Heathwaite 1995)

Umbrella terms and description	Major types	Description of major types
MIRE/BOG/FENS Mire: Peat soils and stagnant or slow moving water; Bog: acid or almost entirely organic, peat developing rapidly, limited species type; Fen: Either/both inorganic and organic, peat developing slowly; Treeless: grass or herb rich; Carr: dominated by *Alnus glutinosa* (alder)	SOLIGENOUS MIRES	Small in extent (normally <5 ha), occupy springs, flushes and slope hollows and channels, slow/limited peat development
	BASIN MIRES	Formed in topographic hollows (e.g. kettle holes) and often isolated from groundwater
	VALLEY MIRES	In river valleys with wide range of base status
	FLOODPLAIN MIRES	In alluvium and with wide range of nutrient status
	RAISED MIRES	Developed from basin mires, isolated from groundwater, nutrient poor
	BLANKET MIRES	Cover large area and nutrient poor
MARSHES and MEADOWS Predominantly mineral substrate, not accumulating peat, regular inundation with surface water (riverine and/or lacustrine) and are vegetation grass or herb-rich	MARSHES	Sedge and herb communities, traditionally used as rough grazing
	WASHLANDS	In East Anglia, largely drained
	WATER MEADOWS	Artificially created and mainly confined to chalk streams of southern England
	FLOOD MEADOWS	Periodic inundation, traditionally used for hay production
OTHER	WET HEATH	Mineral based, acidophilous vegetation. Mainly associated with the sandstones on southern and eastern England
	RECREATED/ RESTORED	Often small in extent. Increasing in number and degree of success globally but difficulties arise in establishing high levels of biodiversity associated with natural wetlands
	COASTAL	Estuarine environments often associated with significant numbers of important waders. Coastal realignment projects have recently been implemented in the UK and deemed a successful method of increasing the extent of this wetland type

2.3 Vegetation as Environmental Predictors

In light of the importance of wetlands, the interrelationships between hydrology, hydrochemistry and vegetation composition are areas where a comprehensive scientific understanding of wetland ecosystem function is needed (Malcolm & Soulsby 2001; Keddy 2000). The structure and function of wetland ecosystems are a direct and indirect reflection of the hydrology of the wetland and the catchment (Heathwaite 1995; Ross 1995; Hughes & Johnes 1995), which in turn influences the chemical and physical properties such as pH, sediment characteristics, nutrient status, substrate and water salinity, and substrate anoxia (Hughes & Johnes 1995). Alteration of the hydrological and physico-chemical environment of a wetland system, whether by natural or artificial means, can therefore influence the biota within the ecosystem by, for example, altering the distribution of vegetation communities (Willby *et al.* 1997; Grieve *et al.* 1995; Tremolieres *et al.* 1998; Gilvear & Bradley 2000). Comprehensive and effective monitoring is needed to allow for informed management decisions and to further the scientific understanding of species-environment relationships and responses to change.

The goal of understanding vegetation patterns in a wetland ecosystem is a difficult one as vegetation change is a natural phenomenon. There is, therefore, a need for rigorous and long-term monitoring that can be repeatable and as objective as possible and these are two of the biggest strengths of remote sensing data for ecological applications (Aplin 2005; Ozesmi & Bauer 2002; Schuman & Ambrose 2003; Gilvear & Bradley 2000). Remote sensing is explored in this project as a tool by which wetland vegetation can be mapped and monitored and to enhance the knowledge base used to direct effective management of these globally important sites. However, remote sensing can also be used to detect vegetation change if baseline data is at first well established and archived and it is how well spectral data can represent what is understood on the ground that is explored in this project.

2.3.1 Site-condition Monitoring

In 1998, a new UK-wide programme of monitoring the condition of nature conservation sites began, known as the Common Standards Monitoring and Reporting framework (also referred to 'Site Condition Monitoring'). SSSIs, Natura 2000 sites and Ramsar sites were all targeted for the scheme within the UK. The nature conservation agencies (including SNH) have all been tasked with implementing the basic standards and the programme is currently being trialled and refined in light of operational experiences (Ramsar 2004).

The aim of Site Condition Monitoring is to monitor the condition status of interest features at conservation sites to establish whether or not the site is in 'favourable condition'. Conservation Objectives are prepared as part of the management planning process for each interest feature and these will describe the attributes and targets used to determine whether or not the desired condition of the site is being achieved. The site monitoring programme operates on a six yearly cycle to take account of the scale of monitoring required, the likely rates of changes and the national and international reporting requirements (Ramsar 2004). Site Condition Monitoring will support the identification of wetlands in need for restoration as well as efforts to determine actions for rehabilitation, to monitor changes through time and to assess the management of these sites in light of the wise-use guidelines set out by the Ramsar Convention. The remote sensing of wetlands is presently under-utilised in providing baseline information for Site Condition Monitoring despite the attractions of rapid data capture over large, often featureless, sites in which access is often difficult. The ability to identify habitat types and the characteristics of wetland vegetation from spectral data is explored in this project.

2.4 Remote Sensing for Natural Vegetation Mapping

As mentioned above, a confident scientific understanding of the significant processes and components of the wetland ecosystem is an integral and necessary component of successful wetland management (Smith 1997; Willby *et al.* 1997; Gilvear & Bradley 2000). Integral to this is a record of the spatial pattern of vegetation at a site so that the effects of management can be monitored and any natural fluctuations in vegetation pattern can be monitored. Vegetation mapping is traditionally a labour-intensive and time-consuming process which involves the manual construction of boundaries between vegetation types. There is ongoing debate between ecologists as to the most appropriate ways to classify vegetation (Clements 1916; Gleason 1926; Gleason 1939; Whittaker 1962; Pignatti *et al.* 1995; Mucina 1997; Witte 2002; Witte & Van der Meijden 2000; Biondi *et al.* 2004). It is widely recognised that there are practical and conceptual difficulties involved with the often subjective nature of vegetation classification and mapping (Cherrill & McClean 1995; Steven *et al.* 2004). This may obscure patterns of long term change and responses to management that, in turn, constrain effective conservation of wetlands and understanding of the effects of management to vegetation patterns.

In addition to the more traditional methods of vegetation ground surveys, methods that exploit the spatial dimension using Geographical Information Systems (GIS), and airborne and satellite imagery are being increasingly employed (Gilvear & Watson 1995; Cingolani 2004; Fensham & Fairfax 2002; Ekebom & Erkkila 2003; Schmidt *et al.* 2004; Goodwin *et al.* 2005). These methods offer a significant amount of information to the general scientific community as well as to those managing these complex environments, in terms of the spatial and temporal dynamics of vegetation from a non-taxonomic perspective. In addition, related applications in conservation science are increasing (Turner *et al.* 2001; Schweik & Thomas 2002; Oindo *et al.* 2003).

Classifications of land cover based upon spectral data collected from remote sensing must relate with those classes familiar to practical conservationists working in the field (Cherrill *et al.* 1995; Fuller *et al.* 1998) and methodologies must be consistent enough to allow for comparative datasets (Comber *et al.* 2004). Emphasis has often been placed on the spectral properties and separability of classes rather than on any botanically or ecologically accepted criteria (Roughgarden *et al.* 1991; Lewis 1994) and there still exists uncertainty as to the benefits of remote sensing to wetland habitat identification (Harvey & Hill 2001; Shuman & Ambrose 2003).

2.4.1 Habitat Boundaries

The pixel based nature of remote sensing imagery has proven an advantage in the study of boundaries or 'ecotones' between vegetation classes (Fortin *et al.* 2000; Trodd 1993; Trodd 1996). However, many of the traditional cartographic constraints of vegetation mapping have been carried over into classification schemes derived from remote sensing data. The end-product in many cases is a vectorised model with hard line boundaries between vegetation categories. It is these types of maps that ecologists and site managers are most familiar with. They present information in a way that is easy to understand and conceptualise and the data becomes easily functional within spatially referenced databases and GIS. However, this is not an accurate representation of semi-natural vegetation where boundaries between vegetation types are often poorly defined and non-static (Kent *et al.* 1997; Metzger & Muller 1996).

Boundary areas between classification categories are particularly interesting in ecological studies as these ecotonal areas are often sensitive to environmental change and may thus serve as effective environmental indicators (Trodd 1993; Spanglet *et al.* 1998). The information potential to the ecologist regarding ecotone characteristics in comparison to the more traditional methods of recording point and transect data is therefore great, particularly, if it is possible to accurately record their characteristics in easily interpretable map formats. As Adams (1999) points out, gradients and mosaics are the rule in natural vegetation and not the

exception (Whittaker 1967), and so the use of raster data and suitable classification methods eliminate the necessity for sharp boundaries between vegetation categories and so offer great potential as a tool for ecologists. Many image processing techniques known as 'soft classification methods' have been developed to combat the difficulties involved in identifying and interpreting the spectral properties of fuzzy boundaries. These include the use of support vector machines (Cortes & Vapnik 1995) and fuzzy classification algorithms and research is currently widespread in this area (Carpenter *et al.* 1999a; Carpenter *et al.* 1999b; Townsend 2001; Townsend & Walsh 2001; Ricotta 2004; Zhang *et al.* 2004).

2.5 Techniques for Discriminating between Natural Vegetation Types

2.5.1 Field Spectrometry

Field spectrometry is the process by which spectra are collected in the field using a portable device that is often hand-held or mounted on a pole of tripod. The device used is a battery powered spectroradiometer (or 'spectrometer') and the process involves the quantitative measurement of radiance, irradiance, reflectance or transmission of the target. Field spectrometry is a useful method for extracting spectral information from vegetation thereby obtaining a 'true to life' spectral pattern that can then be related to spectral imagery and can contribute to the understanding of the vegetation-spectra relationship. It is particularly advantageous to use this method of data collection here as the target area covered by the spectrometer relates to the scale at which ecological survey is applied and spectral datasets can, therefore, be directly compared with vegetation datasets collected using these methods. The nature of field spectrometry is also such that large amounts of data can be collected in relatively short periods of time.

In relation to laboratory studies, field spectrometry is subject to the complexities of the natural environment and vegetation structure. The spectral response is a mixture of canopy structure, 'background components' such as the soil type and vegetation characteristics as well as the natural illumination conditions at the time of data acquisition (Goel & Qin 1994). Many of the techniques introduced in this section involve the use of data collected using field spectrometry. Before these are detailed, a summary of good field practice is therefore required.

Good field practice

One of the biggest limitations to accurate data acquisition using field spectrometry is the dynamic nature of the atmosphere through which the incident radiation must be transmitted. Potential transformations to the incoming solar radiation include absorption by water vapour

or scattering by atmospheric gases. Atmospheric conditions vary in space and time and at a variety of temporal scales and as they do so, there may be significant consequences for the successful acquisition of field spectra measurements. As a result, there are some common field practices employed to minimise sampling variance caused by atmospheric fluctuations at various scales as well as changes in sun-sensor-target geometry (Curran 1981; Milton 1987). Points to note are listed in Table 2:4.

Table 2:4 Factors to consider in order to employ good field practice during field spectrometry

Factor to consider	Notes
Sun-sensor-target geometry	The use of fixed tripods or masts would help to ensure this as would care to position the face of the spectrometer at a constant angle with relation to the angle of direct solar flux. A fixed geometry between the spectrometer and the standard panel as well as the operator should also be maintained.
Time of data acquisition	The position of the sun changes in relation to the horizon (known as 'solar zenith') and also as solar azimuth (position in relation to due north) also varies throughout the year. Variation will increase linearly either side of local solar noon and so good practice is to perform spectral measurements as close to local solar noon as possible (Curran 1980; Curran 1981).
Position of spectrometer	'Field of view' is determined by the height at which the spectrometer is positioned above the target, this should remain constant between spectral measurements and height at which it is held should be at least 1 m (and preferably 2 m) above the upper surface of the target (Milton 1987).
Clothes and location of vehicles	Operator should wear white (Kimes *et al.* 1983) and vehicles should be located at least 3 m from sampling (Milton 1987).
Local weather conditions	Moisture on the vegetation will vary from day to day depending on local climate as will the local wind condition. Wind has been identified as a potential source of variability within field spectra datasets (Wright 1986; Lord *et al.* 1985).

2.5.2 Spectral Discrimination between Habitat Types

Habitat types consist of a unique combination of vegetation types and/or structure with a unique blend of biochemical and physical properties. These properties include photosynthesis, respiration, evapotranspiration, decomposition, concentration of chlorophyll and other

chemical components. As work on leaf spectra has identified features within the resultant spectra that correspond with these properties (Kokaly & Clark 1999; Curran *et al.* 1992b; Jago *et al.* 1999) it follows that spectra obtained from differing habitat types will integrate spectral features identifiable and unique to that habitat type (Blackburn & Steele 1999; Schmidt & Skidmore 2003). Difficulty arises, however, when differentiating between the spectral variation caused by within-habitat variability in both structure and species composition and spectral variation that is directly attributable to the characteristics of habitat type.

2.5.3 Spectral Characteristics of Vegetation

The major spectral absorption features of vegetation spectra can be attributed to plant pigments such as chlorophylls, xanthophylls and carotenoids (Penuelas *et* al. 1997; Evain *et* al. 2004). Other minor spectral features present in a plant canopy are the result of chemical components such as lignin, tannin (Soukupova *et al.* 2002; Sims & Gamon 2002) proteins, starches, sugars and cellulose (Campbell 2002). The major spectral features occur in the blue (450 nm), green (550 nm) and red (680 nm) parts of the visible spectrum. The nature of these absorption features has been related to the biochemical components of the vegetation and modelling of the relationships involved is ongoing (Dawson *et al.* 1998; Jacquemond *et al.* 1995; Curran *et al.* 2001).

Beyond the visible wavelengths (greater than 700 nm) vegetation spectra show a steep rise in reflectance and then plateau off in the near infrared (NIR) part of the spectrum (750 – 1300 nm) (Steven *et al.* 1995). The slope and position of this sharp rise in reflectance between the visible and near-infrared have been directly correlated with leaf chlorophyll concentrations (Horler *et al.* 1983; Rock *et al.* 1986; Murphy *et al.* 2005; Baranoski & Rokne 2005; Dash & Curran 2004), giving rise to approaches known as 'red edge' or derivative analyses. Where chlorophyll concentrations and the associated positions of the red edge differ between habitat

types which are otherwise spectrally similar they may provide a method for discriminating between habitat types.

The high reflectance of vegetation spectra in the NIR is due to the physical properties of the plant cell wall, which acts to change the index of refraction and causes an increase in the amount of scattering. Aspects of the internal leaf structure, such as the number and configuration of air spaces, also plays a role in determining the spectral response (Campbell 2002; Danson 1995). Radiation passes through the upper surfaces of the leaf cell (the cuticle and epidermis) and enters the spongy mesophyll. Here it is strongly scattered amongst the mesophyll tissue and the air spaces where up to 60 % is scattered either upward ('reflected') or transmitted downward (Campbell 2002). As well as these structural properties, there is also an absence of absorption by plant pigments at these wavelengths. It is an intrinsic property of vegetation that irradiance at the NIR is prevented from being absorbed as the nature of this radiation would increase the core temperature of the plant and cause serious damage to cell tissue.

The physical components of vegetation make important contributions to the spectral response under natural field conditions. These include the size and orientation of the leaves and the shape or vertical structure of the canopy (Curran 1980; Curran 1983; Spanglet *et al.* 1998) and the coverage of the ground surface. Spanglet *et al.* (1998) found that vertical leaf structures (e.g. *Typha, Scirpus, Juncus*) have a very small cross-sectional area when viewed from above giving them very low reflectance levels whereas plants with a horizontal canopy structure tend to have the highest reflectance. Species with spherical canopies (e.g. sedge dominated habitat types) have a very high variance in reflectance spectra as most of the incoming radiation (irradiance) strikes non-horizontal surfaces and is scattered away (Spanglet *et al.* 1998). Canopy architecture also affects the amount of non-vegetated background that is exposed through the canopy, such as bare soil or water, and the amount of shadowing that is present which in turn can have significant effects on the spectral response (Verhoef 1985; Goel 1988; Spanglet *et al.* 1998).

Stronger absorption in the blue part of the spectrum and stronger reflection values in the red part of the spectrum are indicative of dead or senescing vegetation (Campbell 2002). The strong water absorption features present in live vegetation spectra are no longer present in that of dead vegetation and absorption features otherwise concealed become evident. These features are present at wavelengths 1730 nm, 2100 nm and 2300 nm and are due to organic bonds in plant biochemicals such as proteins, lignin and cellulose (Campbell 2002; Kokaly *et al.* 2003). As a plant senesces or is subject to stress induced, for example, by disease or moisture deficiency, the internal structure and chemical composition of the plant is altered and consequently, the spectral response will change. Studies of the spectral response of vegetation can therefore point towards alterations in plant vigour (Davids & Tyler 2003; Lovelock & Robinson 2002; Smith *et al.* 2004) and if differences exist between habitat types in terms of vigour and phytophenological change then spectral data may afford sufficient discrimination even when there is comparatively little change in species composition (Anderson *et al.* 1996; Lloyd 1990; Skidmore 2002).

As spectral response and certain indices using various parts of the spectrum have been found to be sensitive to leaf area and vegetation abundance or harvested biomass (Curran *et* al. 1992a; Ramsey *et al.* 1995; Hurcom and Harrison 1998; Jensen 1980; Lorenzen & Jensen 1988; Qi *et al.* 1994), the study of various spectral indices has been used to identify relative vegetation growth and vigour (Gamon *et al.* 1995; Penuelas *et al.* 1993; Davids & Tyler 2003; Smith *et al.* 2004). Following on from this, the use of such indices can then be applied to vegetation spectra from different habitat types that may otherwise be spectrally very similar, in order to tease out differences between the habitat types, represented within the spectra. This presumes that there are differences between habitat types in the parameters associated with the spectral indices and is an area explored within this research in a purely inductive manner.

Methods of Spectral Analysis

A number of methods have been developed to analyse the spectral characteristics of vegetation and their relationships with the target vegetation and these vary depending on the

datasets available. The methods reviewed below have been selected because of their suitability for use with hyperspectral datasets such as those collected using field spectrometry.

Continuum Removal

Continuum Removal (CR) is a method that has been used more frequently in the past in the geological and mineralogy sciences (Clark & Roush 1984) but features increasingly in the remote sensing literature concerning the understanding of vegetation biochemistry and spectral response (Kokaly & Clark 1999; Curran *et al.* 2001; Kokaly *et al.* 2003; Mutanga & Skidmore 2003; Mutanga *et al.* 2004; Huang *et al.* 2004). CR isolates the absorption features of a spectral dataset and effectively normalises the data, thereby reducing the effects of varying illumination conditions. This is a particularly useful method when using field spectra to account for the subtle effects caused by rapidly varying illumination conditions at the time of data acquisition on the spectral measurements. CR has been identified as an effective method of separating out the spectral responses of different vegetation types using data collected from field spectrometry at a coastal wetland (Schmidt & Skidmore 2003; Underwood *et al.* 2003). It has also been used in conjunction with remote sensing imagery in a forested environment using a spectral feature fitting classification method (Kokaly *et al.* 2003). CR will be explored here as a way of differentiating between inland wetland habitat types as this has yet to be demonstrated in the remote sensing literature.

Red edge and derivative analyses

The position of the 'red edge' (also termed the 'Red Edge Inflection Point' (REIP)) is the steepest point between the red and NIR regions of the reflectance spectra. This has been found to correlate with concentrations of chlorophyll (Baranoski & Rokne 2005; Pinar & Curran 1996; Dash & Curran 2004; Dawson & Curran 1998). The REIP is identified using the first derivative which is a calculation that transforms the spectral response dataset to a set of numbers that represent the slope of the spectrum (Tsai & Philpot 1998). Variations in the REIP and first derivative curves have been linked with chlorophyll concentrations and plant

physiological function as a response to stress factors and nutritional status, both of which may well vary between wetland habitat types (Anderson *et al.* 1996; Filella & Penuelas 1994; Trenholm *et al.* 2000; Carter 1993; Blackburn & Steele 1999; Blackburn 1999).

Curran *et al.* (1995) measured the reflectance spectra of slash pine (*Pinus elliottii*) both *in situ* and under laboratory conditions. A relationship between REIP and chlorophyll concentration was established and an R^2 of 0.82 was recorded. It was concluded that red edge was an effective indicator of chlorophyll concentration of detached needles. This and, other research at the leaf scale, has demonstrated with impressive accuracy the strong relationship between chlorophyll content and REIP (Liu *et al.* 2004). However, the biological processes involved are still not fully understood (Campbell 2002; Lamb *et al.* 2002; Zarco-Tejada 2003; Mutanga & Skidmore 2004). Munden *et al.* (1994) studied REIP at the canopy scale and although the study was largely successful in terms of the effectiveness of REIP in predicting yield, it was noted that the use of REIP to estimate yield is dependent upon a well-understood relationship between chlorophyll concentration and yield and a poorly understood relationship between red edge and chlorophyll concentration. Research in this area continues, particularly as scales of spatial and spectral resolution change with the onset of more advanced technology (Clevers *et al.* 2001; Clevers *et al.* 2002).

The study of REIP is particularly well suited to field spectrometry studies at the canopy scale as the method used to derive the REIP is not affected by varying illumination conditions and is insensitive to leaf structure variation (Sims & Gamon 2002). The use of the REIP as a method of discriminating between habitat types is under represented in the literature and debate continues as to what the REIP and patterns in the first derivative of spectral reflectance in the red region of the spectrum actually represent in phytological terms (Lamb *et al.* 2002; Le Maire *et al.* 2004; Silvestri *et al.* 2002; Zarco-Tejada *et al.* 2003).

Spectral Indices: Normalized Difference Vegetation Index

The Normalized Difference Vegetation Index (NDVI) is the most widely used vegetation index in vegetation remote sensing studies and was developed because of the positive and negative correlations of green and red reflectance respectively, with the amount of green vegetation matter (Rouse *et al.* 1974; Tucker 1979). A great deal of research has since been published that discusses the close correlation between NDVI and various vegetation attributes such as biomass and leaf area (Curran 1981; Christensen & Goudriaan 1993; Thenkabail *et al.* 2004; Thenkabail *et al.* 2000; Hansen & Schjoerring 2003). Although there have been many successful applications, the use of NDVI has been criticised in some circumstances because of its sensitivity to atmospheric conditions and its asymptotic behaviour with vegetation biomass beyond certain thresholds. Many studies investigating the NDVI-biomass relationship have also been carried out within relatively homogenous agricultural environments and make use of broad spectral bands and coarse spatial resolutions. This limits the understanding of the NDVI-biomass relationships within semi-natural vegetation types as vegetation is largely heterogenous at relatively fine scales.

There have been many studies that confirm the general vegetation index-biomass relationship in wetlands but mainly in the context of coastal environments (Bartlett & Klemas 1980; Phinn *et al.* 1999; Hardisky *et al.* 1986, Gross *et al.* 1993; Penuelas 1993; Ramsey & Jensen 1996) though, this relationship is still not fully understood. Studies have shown that different vegetation indices correlate most strongly with biomass depending on the wetland vegetation species or types. These indices include the simple Vegetation Index (VI), the Atmospherically Resistant Vegetation Index (ARVI), the Soil Adjusted Vegetation Index (SAVI), Soil Adjusted and Atmospherically Resistant Vegetation Index (SARVI) and the Global Environment Monitoring Index (GEMI) (Zhang *et al.* 1997; Spanglet *et al.* 1998). Canopy architecture also plays a role in the spectral reflectance-biomass relationship, although Spanglet *et al.* (1998) only examined one species type per canopy architecture type. Further work on the relationship between spectral reflectance and the biomass of various wetland

vegetation types is required to establish the nature of this relationship and the extent to which spectral indices can be utilised to confidently predict biomass within wetland environments.

The work of Spanglet *et al.* (1998) also involved the use of hyperspectral data that had been processed to simulate the broad bands of Landsat Thematic Mapper. These bands average out the reflectance in broad areas of the spectrum which may then result in information loss that would otherwise have served to tease out spectral differences between samples (Thenkabail *et al.* 2004). Mutanga and Skidmore (2004) carried out crop biomass estimations using NDVI constructed using narrow bandwidths and achieved notable improvements (R^2 0.77 vs. R^2 0.26). From work on a pine canopy however, Elvidge and Chen (1995) compared broad and narrowband vegetation indices and concluded that narrow bands were only slightly better than their broad band counterparts. The value of narrowband indices in terms of biomass prediction in wetland environments has yet to be evaluated in the scientific literature.

Foody and Cutler (2003) tested the ability of Landsat Thematic Mapper (TM) data to predict biodiversity indices in a tropical rain forest and concluded that remote sensing data may be used as a source of information at the landscape scale regarding biodiversity, with obvious implications for conservation science and management. Wetland biomass has been shown to correlate with species richness and this is a statistic that is of great ecological interest (Keddy 2000; Grime 1973; Wheeler & Giller 1982; Wheeler & Shaw 1991; Gough *et al.* 1994; Williams 1996; Bhattarai *et al.* 2004) although debate continues in the ecological literature as to its functional significance (Weiher *et al.* 2004; Schaffers 2002). The relationship between NDVI, an assumed surrogate for wetland biomass, and species richness will be explored here using the red and NIR band centres of the CASI instrument (Griffiths *et al.* 2000; Kerr & Ostrovsky 2003). This represents a novel and unexploited method that warrants further work in the literature as the expansive nature of remote sensing data offers a wealth of potential ecological information at scales directly beneficial to wetland conservation managers (Aplin 2005; Ozesmi & Bauer 2002).

Rundquist (2002) notes that few researchers have examined these relationships empirically for vegetation canopies that contain complex mixes of optical elements and this is certainly the case for wetland environments. There is a great deal of scope for the ecological applications of a spectral index such as the NDVI to predict wetland vegetation biomass in a non destructive way and over large areas which are ecologically sensitive and otherwise very difficult to sample.

Geostatistics

Scales of spatial variation can be characterised using geostatistics and the variogram which is used to design optimum sampling strategies and to evaluate the effect of spatial resolution (Curran 1988; Atkinson 1993; Atkinson & Curran 1995, 1997; Wang *et al.* 2001; Phinn *et al.* 1996). The variogram has also been used to incorporate spatial information into image classification (Atkinson & Lewis 2000; Curran 2001) The spatial resolution of remote sensing imagery in terms of the pixel size becomes crucial especially when detecting transition areas. Too large a pixel will average out and over-simplify the subtle changes in vegetation and mask the transition zones. Too small a pixel will mean that small-scale variations in plant density and background influences will result in high reflectance variability thus obscuring any spatial patterning. The variogram is, therefore, considered a useful technique to examine the spatial variation within various wetland habitat types and thus determine the most appropriate spatial scale of imagery (Atkinson & Curran 1995; Atkinson & Curran 1997).

As habitat types differ in terms of species composition and structure, it follows that spectrally determined spatial variation may also vary between classes and these differences can then be exploited to distinguish between plant community types (Wallace *et al.* 2000). Components of the variogram constructed in a study by Phinn *et al.* (1996) effectively quantified the vegetation patterns in imagery from a semi-arid environment using NDVI values relying on the relationship between NDVI and biomass. The application of this approach to wetland environments is novel and has yet to be explored in the literature as a means of distinguishing between habitat types.

2.5.4 Using Multivariate and Multitemporal Datasets to Explore the Relationship between Vegetation and Spectral Patterns

Underpinning most of the environmental applications of remote sensing is the derivation of maps that accurately document land use (Laba *et al.* 1997; Vogelmann *et al.* 1998; Mucher *et al.* 2000) and vegetation or habitat types (Basham May *et al.* 1997; Millington & Alexander 2000; Hirata *et al.* 2001). Remote sensing has been applied successfully for these purposes on a variety of scales including global and continental (e.g. Stone *et al.* 1994; Townshend & Tucker 1984; Justice *et al.* 1985; Yates *et al.* 1986) and regional (e.g. Tucker *et al.* 1985a; Tucker *et al.* 1985b; Spanglet *et al.* 1998). Few studies have worked at the local or species scale and, relative to homogenous and single species stands, little work has been carried out on species mixtures and semi-natural environments. Field spectrometry is a useful tool in such applications as the physical area from which spectral information is gathered can equal that from which vegetation information is gathered and so, the relationship between the two can be effectively explored. Research regarding how well spectra relates to vegetation datasets at the species composition scale can input useful *a priori* information for image classification and the derivation of maps, however, the relationship is reportedly complex.

Armitage *et al.* (2004) investigated the nature of the relationship between spectral response and species composition and structure within an upland environment in the UK (Armitage *et al.* 2004). Using detailed vegetation datasets paired with hyperspectral data obtained using field spectrometry, the data was analysed using multivariate techniques such as Canonical Correspondence Analysis (CCA), to establish how well the spectra predicted variation within the species composition datasets. Results identified a different pattern of spectral response with different combinations and abundance of species and consequently showed some promise in identifying a pattern between vegetation composition from an upland semi-natural environment and spectral response using field spectrometry. The results though somewhat inconclusive do suggest promise in the application of CCA and, similar multivariate techniques commonly used in ecological analyses, to spectral datasets (Brook and Kenkel

2002; Thomas *et al.* 2002). Although this method was novel in its application for use with upland vegetation datasets, it remains unexplored with datasets collected from wetland vegetation.

CASI bands will be simulated in this study in order to explore the relationship between detailed wetland vegetation data collected and these spectral bands. A direct comparison between the results from work by Armitage *et al.* (2004) and, therefore, upland vegetation datasets, could then be made. Advances in airborne and spaceborne technologies are such that sensors capable of fine spectral resolution are likely to become readily available at spatial scales more amenable to ecological studies (Sawaya *et al.* 2003; Mehner *et al.* 2005; Klemas 2001; Phinn 1999). As such, a hyperspectral dataset will also be constructed for applications in this study. Work has been carried out by Becker *et al.* (2005) to identify spectral bands that appear to have enhanced information content regarding coastal wetland species and therefore are most useful as predictors for these vegetation types. No such study has been carried out for inland wetland vegetation and this is explored here using multivariate analyses. Schmidt and Skidmore (2003) did investigate the regions of the spectrum where canopy reflectances from various saltmarsh communities were significantly different using non-parametric statistics and this was also carried out on a sample of the spectra collected from a freshwater marsh in this study.

It has often been speculated that with finer spatial resolution will come greater classification accuracies (Skidmore 2002; St-Onge & Cavayas 1997; Wulder *et al.* 2000). Vegetation change can often involve large changes in spatial pattern but small changes in the spectral response of individual pixels (Hobbs 1990) and so finer spatial datasets may present the ability to detect these differences assuming the spectral resolution is also high enough. However, Muller (1997) notes that many authors have suggested that finer spatial resolution will not necessarily improve per-pixel classification of vegetation (Irons *et al.* 1985; Green *et al.* 1993). As such, a dataset made up of 42 spectral bands approximately 10 nm in width, is constructed to be used in multivariate analyses similar to those used by Armitage *et al.*

(2004). This is a novel approach that may support the need for hyperspectral datasets in order to fully understand the relationships between spectral and detailed vegetation datasets using multivariate methods (Basham May *et al.* 1997).

Multitemporal datasets

Vegetation varies in structure and composition at a variety of spatial and temporal scales (Hobbs 1990); seasonal variation, for example, causes habitat types to differ to varying degrees over the year depending on the characteristics of the vegetation. These changes are due to the influence of temporal variations in environmental conditions such as day-length, air temperature and water availability on the timing of plant development stages (or 'phenophases'), including germination, flowering and senescence and research into these changes is termed 'phytophenological studies'. These changes can have a direct influence on the spectral response of vegetation (Warren & Hutchinson 1984; Blackburn & Milton 1995), as plant communities have distinct seasonal peaks of growth and flowering activity (Mooney *et al.* 1986; Mackey 1990). It follows, therefore, that unique annual patterns in spectral response may be attributable to habitat types and assist in the classification of vegetation that exhibit similar spectral responses at many times of the year (Hobbs 1990; Millington *et al.* 1994; Kokaly *et al.* 2001; Townsend & Walsh 2001; Key *et al.* 2001).

Habitat boundaries

Trodd (1993) investigated the capability of remotely sensed data to characterise habitat boundaries in lowland heath in southern England (Townsend & Walsh 2001; Trodd 1996) and demonstrated the application of multivariate analyses to this research question. Vegetation datasets, derived NDVI and ordination analyses were applied to highlight the structure of the datasets in an attempt to relate the variation in the spectral information across the transects with that of the species composition dataset. The results illustrated the potential of multispectral data to characterise vegetation continua and ecotones. There has, however, been little work in the literature carrying on from this direction of research.

2.5.5 Using Remote Sensing Imagery to Map Vegetation

Mapping vegetation rather than relying on ground sampling has the advantage of providing data that can be used to ask specific questions about the location of areas of interest by those charged with the management of these areas (Congalton *et al.* 2002; Foody & Cutler 2003). The coverage of specific areas of interest and their location, as well as the associated condition of these areas, are critical information that can assist in developing effective management practices. The cumulative effects of different land use practices and management strategies can then be assessed over time as baseline maps can assist in the study of environmental change in time and space (Levin 1992; Franklin 1995; Millington & Alexander 2000; Skidmore 2002; Reed *et* al. 1994). Nevertheless, it is still widely accepted that accurate land cover classification methods using remote sensing techniques still present scientific and technical challenges as a result of the many spectral and spatial variables influencing surface reflectance, coupled with the constraints imposed by the spectral and spatial characteristics of the remote sensing instrumentation (Zarco-Tejada & Miller 1999; Johnston & Barson 1993).

Aerial photography

Aerial photography has been utilised extensively in the classification of wetland areas (Ozesmi & Bauer 2002; Rutchey & Vilchek 1999; Doren *et al.* 1999; Welch *et al.* 1999) and has been an effective alternative to traditional methods that often involve high costs, subjectivity, and low spatial and temporal coverage. Schmidt *et al.* (2004), however, report that the process of vegetation mapping in the salt marshes of the Netherlands is a time consuming and expensive process with low classification accuracies (43%). Digital photography is being increasingly utilized in the environmental sciences and this may be a considerable growth area in the future (Gourmelon 2002; Murphy *et* al. 2004). Although aerial photography is generally preferred in place of remote sensing imagery (Pitt *et al.* 1997; Miyamoto *et al.* 2004), the use of remote sensing imagery coupled with more detailed mapping of vegetation and aerial photography can provide a greater source of ecological

information to the end-users which are often those charged with the monitoring and management of such sites (Pavri & Aber 2004; Ustin *et al.* 2004; Gamon *et al.* 2004; Phillips *et al.* 2005).

Airborne and satellite imagery for ecological applications

Some of the benefits of using airborne and satellite remote sensing imagery include the extensive coverage that they supply and the repeatability and objective nature of the data collection (Haack 1996). A review of literature on the remote sensing of wetlands by Ozesmi and Bauer (2002) focuses on satellite platforms and concludes that classifications using satellite imagery, although difficult, is a promising and useful research area (Lunetta & Balogh 1999; Jensen *et al.* 1984; Harvey & Hill 2001; Franklin *et al.* 1994). Congalton *et al.* (2002) however, explored the use of Landsat TM satellite imagery in the classification of riparian vegetation and concluded that this type of data was inadequate for use in policy decisions and the identification of structural characteristics of the vegetation. Dechka *et al.* (2002) utilised IKONOS satellite imagery which represents fine spatial resolution coupled with coarse spectral resolution to classify a number of wetland habitat classes and communities in the southern Saskatchewan in Canada; classification accuracies of only 47% were attained in broad wetland habitat classes. It is the coarse spectral and spatial resolutions of much of the satellite data currently available that make this type of data unsuitable for vegetation classification at fine scales and, as such, has kept much of the ecological community at bay.

Airborne remote sensing in wetland environments

Lee and Lunetta (1995) discuss wetland airborne remote sensing missions in their review on wetland monitoring using remote sensing. The studies reviewed, including some involving satellite data, reported high classification accuracies but involved the classification of broad wetland communities (such as reedswamp or sedge meadows) and made use of the broad spectral and spatial resolutions from instruments available at the time (May 1986; Jensen *et al*

1984; Jensen *et al.* 1986). Recent advances in technology have resulted in increased spectral and spatial resolutions whereby satellite imagery is now available at spatial resolutions similar to those obtained using airborne platforms thereby increasing the scope for remote sensing and ecological applications (Aplin 2005).

At present, airborne imagery is a suitable compromise in terms of spatial and spectral resolutions with multispectral and hyperspectral remote sensing instruments and fine spatial resolution at scales comparable to most ecological studies (<10 m^2). Airborne imagery has been used successfully to map vegetation in terms of ecological condition (Jago *et al.* 1999) and work in a coastal wetland in southern California by Shuman and Ambrose (2003) identified the use of low altitude, high resolution colour and NIR photographs as an accurate and efficient means of sampling vegetation cover (Phinn *et al.* 1999) and classifying simple habitats, although individual species could not be identified. This may be attributable to the low spectral resolution dataset that was used as Underwood *et al.* (2003) successfully applied hyperspectral airborne imagery to predict the spatial pattern of certain invasive coastal wetland species in California. Although, Schmidt *et al.* (2004) achieved accuracies of only 40% when classifying coastal vegetation in the Netherlands using hyperspectral airborne remote sensing; variation in the terrain was accounted for using an expert classification system which then resulted in an improvement in accuracy up to 66%.

Classification methods: Supervised and Unsupervised

Ejrnaes *et al.* (2004) describe the use of supervised methods for classifying grassland vegetation and conclude that supervised methods deserve more attention in vegetation science. Their direct connection with ecologically meaningful information is conceptually attractive and methods such as Maximum Likelihood Classification (MLC) (Lewis 1998; Munyati 2000; Lee *et al.* 1992; Gould 2000) involve the production of probability maps which can have direct ecological application in, for example, vegetation prediction models and ecological modelling (Guisan & Zimmermann 2000; Franklin 1995; Foody *et al.* 1992; Doren *et al.* 1999). There have been mixed results in studies classifying wetland vegetation

types involving low classification accuracies (Dechka *et al.* (2002) with successful studies applying only broad vegetation classifications (Munyati 2000) or utilising coarse resolution datasets (Gould 2000).

Unsupervised classification techniques are a way of assessing the spectral clusters within a dataset and determining specific areas that may overlap spectrally with others (Bachmann *et al.* 2002). These methods of classification have been applied to accurately represent land cover types but this is largely in areas of broad land cover types (Mackey 1990; Wulder *et al.* 2004b) and at spatial scales that are of limited value for habitat scale management and ecological applications. Gourmelon (2002), however, has demonstrated that the use of digitized infrared and colour aerial photographs coupled with a Digital Elevation Model (DEM) can be successfully applied to the large-scale mapping of terrestrial plants using unsupervised classification methods in a coastal environment averaging accuracies of 70%. These results are promising although it is likely that topography has a greater influence on vegetation patterns in a coastal environment than inland freshwater wetlands (Schmidt *et al.* 2004); this method of classification has not been adequately discussed in literature concerning the remote sensing of wetlands.

Spectral information has been found to correlate with various plant pigments, as well as biochemical and biophysical components (Penuelas *et al.* 1993; Matson *et al.* 1994; Johnson *et al.* 1994) and so, airborne imagery may then be applied in indirect ecological interpretations (Aplin 2005; Svoray & Shoshany 2003). Sampson *et al* (2003) used CASI imagery to remotely detect vegetation stress using chlorophyll content as an environmental proxy (Coops *et al.* 2003). It was concluded that this capability could be readily applied to classifying forest condition based on chlorophyll content and the usefulness of this technique in change analysis studies was also acknowledged. In a similar study, Zarco-Tejada and Miller (1999) obtained high classification accuracies using red edge parameters as a feasible and robust method which successfully outperformed other classification methods. They noted the potential use of systematic differences in canopy pigment or chemistry by cover type as a

basis for land cover classification. This approach has yet to be explored in a wetland environment in relation to habitat types.

Temporal datasets of NDVI have been used to classify large scale land cover types at the continental and global level using unsupervised classification (Defries & Townshend 1994; Moody & Strahler 1994). Many studies have explored the application of NDVI imagery and unsupervised classification to landscape studies that may contribute to conservation management (Van Wagtendonk & Root 2003; Chust *et al* 1999). Other work utilises NDVI maps in the understanding of the spatial distribution of species richness and fauna and the potential of this within wetland environments is explored here (Seto *et al.* 2004; Mittelbach *et al.* 2001; Engstrom *et al* 2002). In particular, work by Gould *et al.* (2000) establishes a strong relationship between imagery derived NDVI vales and ground based measures of species richness in the Arctic but, this is at at the landscape level and, there is little work published that assesses the relationship between NDVI and species richness at the local level.

2.6 Study Site: Insh Marshes

Insh Marshes is located near Aviemore on Speyside in the Southern Highlands of Scotland (See Figure 2:1 and Figure 2:2) at an elevation of 220 m above sea level. The site represents an expansive area of natural wetland vegetation and associated habitat types and covers more than 9 km^2, representing the largest single tract of northern poor fen in Britain. The site was suitable for data collection as large areas of discrete habitat types are identifiiable and the location of sample plots for spectral collection could, therefore, be easily located. A contemporary habitat classification map was also available to assist in data collection which was developed using traditional survey methods and aerial photography. A long history of research at the site also added to the value of working at Insh Marshes as did the structure of the ditch system as it criss-crosses the marshes, providing a number of easily identifiable ground control points for the geocorrection of airborne imagery.

The River Spey flows through Insh Marshes and rises around 30 km to the west of Newtonmore in the Monadhliath Mountain range and flows in a north-easterly direction towards the Moray Firth near Inverness. The marshes are located in the middle reaches of the valley with the Cairngorms mountain range to the south and east. Three major tributaries flow through the marshes and into the River Spey, these are the Gynack, Tromie and Raitts; there are also several small streams that drain from the surrounding valley sides into the marsh itself. On the south side of the marsh, a large drainage ditch and a series of internal parallel and perpendicular interconnected drainage ditches criss-cross the marsh and empty into Loch Insh via a culvert at Coull (Willby *et al.* 1997).

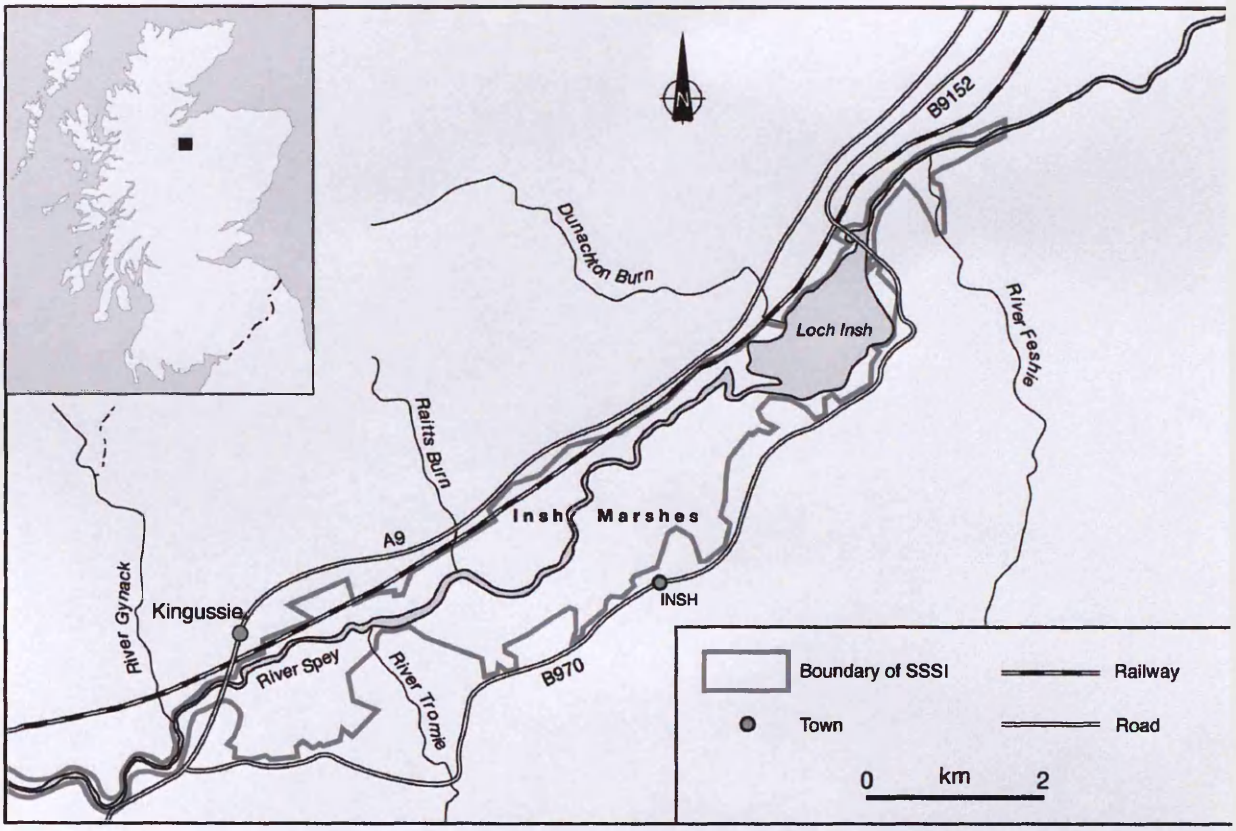

Figure 2:1 Location of Insh Marshes, Speyside and SSSI Boundary

Figure 2:2 Insh marshes-looking NW from Insh village

2.6.1 History and Site Characteristics

Floodplain mire systems similar to that at Insh, were once common in Britain and so extensive that they created impassable valleys. Many have been drained due to agricultural and industrial demands for land and urban development and, subsequently, soft and hard engineering has been put in place to control flow regimes. At present, there is no hydrological management and the marshes are left to flood naturally, creating a floodplain fen that Fojt *et al.* (1987) describes as 'the type of site by which others in Britain are judged'.

A good review of the history of management at Insh Marshes is presented by Beaumont *et al.* (1998). Grazing was the most prevalent form of management throughout history. However, some attempts were made to improve the land for agriculture and, as a result, flood banks and drainage channels were constructed in the late eighteenth and early nineteenth centuries. Grazing declined to its lowest levels in the 1970s and willow scrub encroached. Reprofiling and 'cleaning out' of overgrown and silted up ditches was carried out periodically and several pools, scrapes and ditches were created on the site (Beaumont *et al.* 1998). Since this time, the naturalness of the geomorphology and the intact hydrosphere and hence the importance of conserving this site have been acknowledged and, consequently, these activities have been halted.

At present, Insh Marshes forms a major part of the River Spey/Insh Marshes Site of Special Scientific Interest (SSSI) (1176 ha) and, in addition to this, part of the reserve lies within the Cairngorms National Scenic Area and the Proposed Cairngorms National Park. Other conservation designations include National Nature Reserve (NNR), Special Protection Area (SPA) and Special Area of Conservation (SAC). Scottish Natural Heritage (SNH) is the key statutory agency in Scotland for advising the Government and acting as the Government's agent in the delivery of conservation designations in Scotland. In addition, SNH is also responsible for the outworking of the UK Biodiversity Action Plan in Scotland which is the UK response to the 1992 Earth Summit at Rio de Janeiro. As such, a number of Local

Biodiversity Action Plans have been put into place and Insh Marshes falls within the Cairngorms Local Biodiversity Action Plan Area.

Due to the EC Habitat Directive (the Conservation of Natural Habitats and of Wild Fauna and Flora: 92/43/EEC) a network of protected areas across the European Union was created known as 'Natura 2000' sites. These are recognised as wildlife sites of international importance that are under pressure from increasing demands made on the environment. Insh Marshes has been designated a Natura 2000 site and has also been recognised as a Ramsar site since February 1997. Other important legislation and directives that apply to the management of Insh Marshes include the Wildlife and Countryside Act (1981), EU Water Framework Directive (2000/60/EC) and the Directive on the Conservation of Wild Birds (79/409/EEC).

2.6.2 Conservation and Habitat Types

Flora and fauna

The RSPB have kept a comprehensive record of the results from surveys at Insh Marshes (RSPB 2000) which also includes lists of significant species of plants and their communities, invertebrates and wildlife at the site (Wood 1989; Maier & Cowie 2002). Only some of these plus important fauna are listed in Table 2:5.

Table 2:5 Flora and fauna species and vegetation assemblages of notable interest at Insh Marshes (adapted from RSPB 2000)

Species/Vegetation assemblages	Notes
Phragmites australis-sub-community: *Menyanthes trifoliate*	UK Nationally rare
Carex vesicaria	UK Nationally uncommon
Carex vesicaria-sub-community: *Carex rostrata*	UK Nationally uncommon
Deschampsia caespitose	Support many species of invertebrates, provide roosting sites for hen harriers and hunting grounds for short eared owls and kestrels
Carex chordorrhiza	(String sedge) Red Data Book: Vulnerable Insh marshes holds largest and most vigorous stand of this species in Britain.
Calamagrostis purpurea	(Scandinavian small reed) Red Data Book: vulnerable
Carex aquatilis	(Water sedge) Insh marshes holds 25 % of the Scottish population of this sedge
Juniperus communis	(Juniper) UK Biodiversity Action Plan Priority Species
Pilularia globulifera	(Pillwort) Nationally Scarce and UK Biodiversity Action Plan Priority Species
Bryophytes	110 species identified in a recent survey by Rothero (1998)
Leskea polycarpa	(Moss) Idenitifed by Rothero (1998) as only known site in country and occurs in 'remarkable abundance'
Orthotrichium obtusifolium	(Moss) UK Biodiversity Action Plan Priority Species Idenitifed by Rothero (1998), only currently known at one other site in Britain
100+ species of lichens	Low atmospheric pollution and humid climate of area provide ideal growing conditions for lichens. List of species in preparation at present for the RSPB
Homalocephala albitarsis	Red Data Book 1: Endangered Insect found in at least one aspen stand
Hammerschmidtia ferruginea	(Hoverfly) Red Data Book 1: Endangered Insect found in at least one aspen stand

Such a large extent of natural and often scarce vegetation types inevitably provides an abundance of habitat for important wildlife at the site. About 134 species of birds occur annually at the site of which about 69 breed annually, including some 10 species of breeding waders. About one thousand pairs of waders nest on the floodplain at Insh Marshes plus some of the rarest breeding birds in the UK, such as, goldeneye, osprey, spotted crake and wood sandpiper. The reserve holds over 50 % of the UK breeding goldeneye population as well as four pairs of osprey that regularly feed at the site. Insh is just one of five nesting attempts in Britain by bluethroat (RSPB 2000) and other rare, irregular breeders at the site include

wryneck, redwing, whooper swan plus the largest roost of hen harriers in Britain. The site provides over-wintering habitat for significant wildfowl including whooper swan and greylag geese, the former of which occur in nationally important numbers in Great Britain (averaging 160 between 1993-1998). Twenty-seven species of mammal have been identified at Insh Marshes including otter, wildcat, pine marten, badger, red squirrel and various species of bats (Beaumont *et al.* 1998).

Invertebrate recording at Insh Marshes SSSI, although reportedly incomplete (Beaumonet *et al.* 1998), has confirmed over 500 species, including 30 Red Data Book species (rare) and 48 Nationally Notable species. Nine species of dragonflies and damselflies have been recorded and 112 species of beetles, including two Red Data Book species and 16 Nationally Notable ones (Beaumont *et al.* 1998; Smith *et al.* 1994; Baines 1992). Beaumont *et al.* (1998) also notes that 19 species of butterfly have been recorded which includes the pearl-bordered fritillary (*Boloria euphrosyne*), a species that has undergone rapid decline in Britain. In addition, 208 species of macro-moth have been noted as present on the site and these include three Red Data Book 3 species and 30 Nationally Notable species.

Vegetation surveys

A number of vegetation surveys have been carried out at Insh Marshes in the past and the following National Vegetation Classification (NVC) vegetation types have been identified (see Table 2:6). The vegetation communities present are typical of a floodplain mire and represent many stages of hydroseral succession with open water communities, herb rich fen, sedge communities, tall reed beds, *Sphagnum* moss communities and fen carr, with stands of semi-natural woodland at the drier edges.

Table 2:6 RSNC/NCC and equivalent NVC codes at Insh marshes (taken from RSPB 2000)

RSNC/NCC Habitat type	Area in ha	NVC code
Broadleaved, semi-natural woodland	62.2	W4†, W11, W17
Coniferous, semi natural woodland	0.5	
Coniferous, plantation woodland	4.5	W18†
Scrub	25.0	W3, W19†*, W23
Acidic, upland grassland	67.6	U4, U5
Improved/reseeded Grassland	44.9	CG10†*, U4
Marsh/marshy grassland	189.6	M23, M25, M26**
Bracken		U20
Dry upland heathland*	4.5	H10*, H12, H16*
Wet upland heathland*	0.4	M3†, M15, M18†, M19
Basin mire	0.5	M1*, M4, M18
Flushes	4.0	M6, M10
Swamp-Transition mires and quaking bog*	3.0	S8, S9, S10, S11
Tall fen	351.7	S4, S9, S10
Marginal, inundation	2.0	
Open water, standing	68.7	S14, S19, S22
Open water, running	7.5	
Arable	5.0	
Spoil	2.4	
Total area	844	
* = EC Habitats Directive habitat		

*Uncommon or local in the UK
**Threatened and of limited extent, only occur in widely dispersed small stands in the UK
†European Habitats Directive

The use of the National Vegetation Classification (NVC) (Rodwell *et al.* 1991a; Rodwell *et al.* 1991b; Rodwell *et al.*1993; Rodwell *et al.* 1995; Rodwell *et al.* 2000), a phytosociological classification of terrestrial and freshwater vegetation, has been valuable to ecological surveys in the UK providing the basis for vegetation mapping and recording. The NVC has been officially adopted to implement key aspects of national or international legislation, in particular, in the selection of biological SSSIs and in the interpretation of Annex I of the EC Habitats Directive. However, there are recognised limitations in its applications and particularly so for the dynamic and heterogeneous vegetation of minerotrophic wetlands and their regional variations. The NVC has been applied at Insh Marshes in past studies (Table 2:6). However, more recently, a site specific vegetation classification scheme was developed for Insh Marshes that incorporated species abundance with vegetation structure. This produced vegetation types which better reflected the vegetation assemblages at the site rather than being constrained by larger scale classifications that were sometimes of limited relevance

or too coarse to reflect significant local variations in community composition (Maier & Cowie 2002) (Table 2:7 and Figure 2:3).

Table 2:7 Simple habitat types and respective area (ha) recorded in the floodplain of Insh Marshes (taken from Maier & Cowie 2002)

Simple Habitat Type	Total Area (ha)
Tall species-poor sedge (*Carex aquatilis*)	40.30
Tall species-poor sedge (*Carex vesicaria*)	4.49
Carex rostrata-Equisetum fluviatile swamp	63.01
Carex lasiocarpa swamp	5.62
Carex rostrata-Glyceria fluitans swamp	11.64
Mixed sedge swamp	61.84
Species-rich low sedge mire	14.31
Sphagnum lawn	8.07
Molinia caerulea-Myrica gale mire	14.55
Molinia caerulea-sedge mire	55.12
Reedbed	40.03
Phalaris arundinacea	0.52
Dry grassland	17.97
Rush pasture/wet grassland	94.74
Dense *Deschampsia cespitosa*	6.76
Fen meadow	3.07
Willow scrub	29.43
Pine plantation	2.33
Sphagnum flush	6.24
Deep water swamp	1.60
Open water	9.75
Ruderal	0.37
Carex rostrata-Equisetum fluviatile/Carex rostrata-Glyceria fluitans swamp mosaic	7.40
Carex rostrata-Equisetum fluviatile/Carex lasiocarpa swamp mosaic	0.58
Mixed sedge swamp/*Molinia caerulaea*-sedge mire mosaic	0.57
Rush pasture/grassland/mixed sedge swamp mosaic	0.64
Rush pasture/grassland/Tall spp-poor sedge (*Carex aquatilis*) mosaic	2.73
Tall species-poor sedge (*Carex aquatilis*) /mixed sedge swamp mosaic	7.72
Species-rich low sedge mire/rush pasture/grassland mosaic	3.61
Species-rich low sedge mire/Tall species-poor sedge (*Carex vesicaria*) swamp mosaic	6.40
Sphagnum lawn/Mixed sedge swamp mosaic	4.97
Total	523.38

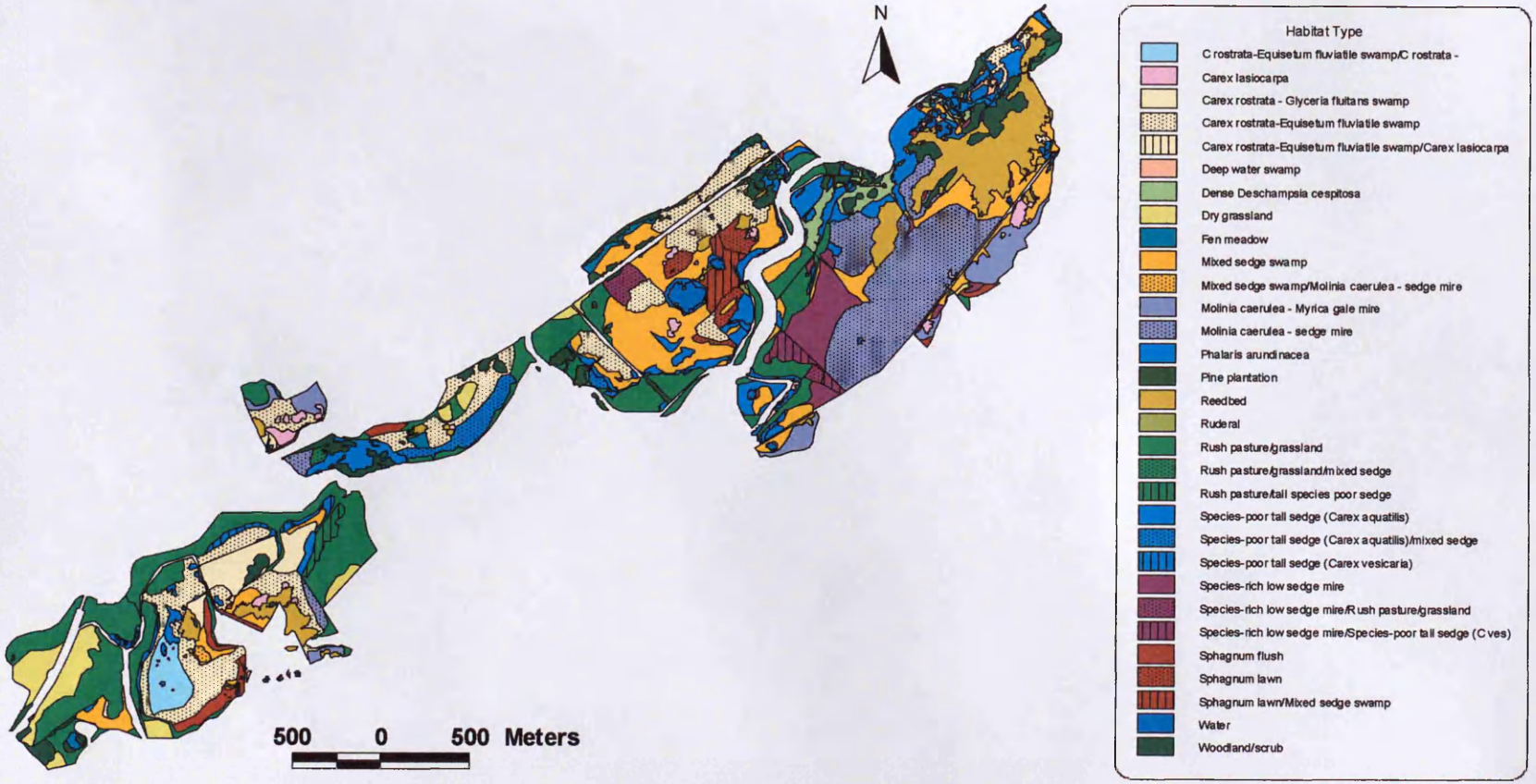

Figure 2:3 Habitats at Insh Marshes (Maier & Cowie 2002)

2.6.3 Management Issues

Sward management allows less competitive plants to thrive and a variety of habitats for invertebrates and wildlife to develop. Breeding waders at Insh Marshes such as lapwing, redshank, curlew and snipe directly benefit from sward management. All four of these species are recently reported to have undergone significant declines in the UK; curlew and snipe are now Amber Species of Conservation Concern in the UK. Beaumont *et al.* (1998) reports that Insh Marshes is one of the top five sites in the UK in terms of the densities and variety of these Amber species and other breeding waders and, therefore, management to promote the retention of habitat for these species is an important objective.

Sheep and cattle grazing are the predominant sward management tools employed at Insh Marshes, and involve important partnerships with local farmers. The main purpose of these management activities are to prevent the establishment of tall and rank vegetation that may result in large areas of scrub and a reduction in vegetation diversity and wildlife habitat loss at the site. Topping (mowing) was initiated at the site by the RSPB in 1991 and aims to convert the rank and tussocky vegetation into a more open and diverse sward, thereby improving the attractiveness of the sward to the graziers and breeding waders.

Willow scrub clearance began in 1995 at Insh Marshes and is undertaken by RSPB staff and volunteers. The aims are to clear areas that have been invaded over the last 30 years and return the area of scrub cover to that recorded in aerial photographs from 1965-1970. The extent of willow (*Salix cinerea*) scrub has historically been restricted by grazing but as this declined the rate of willow encroachment increased strongly especially between 1964-1975 (Hodge 1993). This increase has reportedly continued up to present day though at a variable rate. A reduction in scrub is important for the maintenance of the vegetation mosaic and also benefits breeding waders which require nest sites with open vistas that are unlikely to harbour predators. Some taller, rank, vegetation is left both ungrazed and untopped as this directly benefits the roosting harriers. The objective and repeatable collection of data on the spatial

extent of vegetation types such as those mentioned above is required to assess performance relative to certain management targets and this is an area where airborne remote sensing surveys may be of direct benefit.

2.6.4 Previous Work

Water input to Insh Marshes is from four different sources, two of which are drainage from surface waters and the upwelling of groundwater (Grieve *et al.* 1995). Drainage of surface waters from the valley sides is acid and base-poor but enriched in dissolved organic carbon (DOC), complexed Al, and ions such as Na and Cl from rainfall. Upwelling of ground water supplies the central part of the marshes with water relatively enriched in bases with high pH, conductivity and concentrations of Ca and Mg. A third source of water input to the Insh marshes is from the River Spey. The chemical composition of this river would be similar to that of the runoff from the hillsides but with higher pH and smaller levels of DOC. Lastly, rainwater inputs to the marshes have variable pH and high concentrations of sea-salt ions such as Na and Cl. Grieve *et al.* (1995) conclude that the overall control of the shallow groundwater chemistry of the site is a balance of three major sources, groundwater inputs, surface water inputs from the valley sides and inundation and drainage from the river (See Figure 2:4).

It is well known in wetland ecology that hydrology and hydrochemistry play significant roles in ecosystem function and management (Mitsch & Gosselink 1993; Mitsch & Gosselink 2000b; Naiman & Décamps 1990) and Hughes and Johnes (1995) discuss the two-way interrelationships between the hydrology and hydrochemistry of wetlands and their ecology and management (Malcolm & Soulsby 2001; Bragazza & Gerdol 1999). The differences in the shallow groundwater chemistry at the site are sufficiently large to have a potential effect on the vegetation communities (Grieve *et al.* 1995; Tremolieres *et al.* 1998; Willby *et al.* 1997; Ross *et al.* 1998) and so a comprehensive monitoring scheme that includes information on vegetation mosaics and change at the site is a necessary component of any management

plan. The research outlined here highlights the significant role that local variation in hydrochemical regime plays in driving variation in plant communities and dependent species. A comprehensive monitoring scheme covering the spatial and temporal variation in vegetation structure and composition in relation to environmental variables and management is, therefore, a necessary component of any management plan.

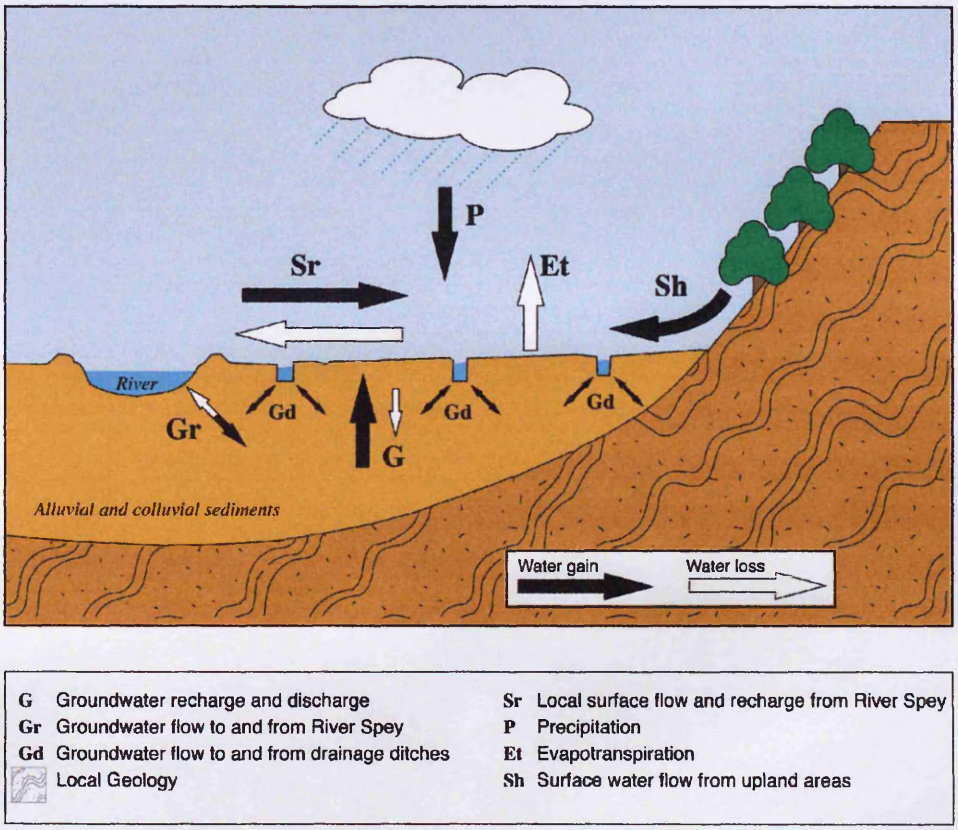

Figure 2:4 Schematic diagram of water inflows and outflows within the Insh Marshes (taken from Grieve *et al.* 1995)

2.7 Summary

Aplin (2005) writes that the relationship between remote sensing and ecology remains ill-defined and underexploited. This is despite calls from Roughgarden *et al.* (1991) for scientists who specialize in remote sensing and those who study ecology to bridge the gap between their disciplines and to combine skills and pursue shared research objectives. Instead it appears that the remote sensing community has continued in its pursuit of technological prowess and understanding and ecologists have focussed on tried and tested techniques in the understanding of complex environmental problems without much consideration to the potential benefits offered by remote sensing. However, this has not been without valid reason as much of the data available to ecologists from the remote sensing community is at scales that are insufficient for meaningful ecological investigation (Turner *et al.* 2003). This is of course prior to the new generation of fine spatial resolution satellite sensors with resolutions comparable to field measurements carried out in ecological research. However, these sensors are still limited to coarse spectral resolutions which are inappropriate for certain applications in vegetation science (Thenkabail *et al.* 2004). Despite these limitations there have been some recent papers in the ecological journals championing the benefits and future potential of remote sensing applications in the ecological sciences (Kerr & Ostrovsky 2003; Gould 2000; Cohen & Goward 2004; Wulder *et al.* 2004b).

Research in the area of remote sensing applications in wetland environments is dwarfed by projects in forested and grassland environments given their significance in global climate and productivity issues respectively. The importance of wetlands in conservation science is well understood and an increase in research that explores the benefits of remote sensing to monitoring and understanding the complex interactions of wetlands is clearly lacking in comparison with other terrestrial and marine applications of remote sensing (Aplin 2005). This research aims to fill some of the gaps concerning the questions still unanswered in the literature regarding the spectral properties of inland freshwater wetland vegetation. These are

related to the objectives outlined in the Introduction (Chapter 1) and are listed again here with some details concerning the gaps in the literature that these objectives address.

1. Determine the extent to which wetland habitats are spectrally distinct.

Studies that explore the extent to which wetland habitats differ using remote sensing data have focussed on salt marsh vegetation and statistical analyses have largely been successful in discriminating between vegetation types using hyperspectral data. This study applies and discusses the use of these analysis techniques to a selection of freshwater wetland habitat types.

2. Determine how well species composition relates to spectral response between habitat types and across habitat boundaries.

The application of standard multivariate analysis techniques to remote sensing data is still relatively novel and their application in a wetland environment for the understanding of the species-spectra relationship is at present unreported. This study draws on work carried out on upland vegetation in the UK and applies a multivariate statistical approach to explore the relationship between spectral response at the ground level with detailed ecological information regarding vegetation parameters. Boundary ecology is identified here as an important area of ecological research and, as such, there have been very few studies that explore the potential applications of spectral data to this research at the local scale and the benefits to vegetation monitoring that this may then offer.

3. Assess the potential of high spatial resolution multispectral airborne imagery for classifying and characterising wetland habitats.

The majority of literature presented in this review regarding airborne classification of wetland environments is limited to coastal areas using broad ecological classifications. Photographic imagery interpretation is still prevalent in ecological studies concerning wetland classification but the direct and indirect applications of remote sensing data is still considered more powerful provided a relationship exists between ecologically meaningful classes and spectral

information. This relationship remains unclear and, in particular, studies that examine the habitat classification of inland freshwater wetlands at local scales are lacking in the scientific literature.

3 DATA COLLECTION AND PREPARATION

3.1 Introduction

This chapter describes the methods used to meet the objectives outlined in Chapter 1. A summary is provided at the end of the chapter. A field spectrometry approach was adopted during the summer 2003 and multispectral imagery at a fine spatial resolution was provided from September 2003. Preliminary field visits were carried out to identify the most practical options available for fieldwork and discussions were had with the site managers with regards to site access issues, wader breeding season and livestock movement. Due to the ecological sensitivity of the site in terms of wader activity, commencement of data collection on the site was June 2003 and continued up until the end of September 2003.

The overall aim of this research is to assess whether remote sensing is a useful tool for understanding the spatial distribution and characteristics of naturally heterogeneous wetland vegetation. This is explored at the local level and, in particular, with the view to using remote sensing imagery at spatial scales amenable to ecological studies and management. Before the potential of remote sensing for mapping natural wetland vegetation at these scales can be determined, research must explore the spectral characteristics of vegetation classes using appropriate statistical analyses of field data (Brook & Kenkel 2002). Field spectrometry data was gathered from a selection of habitat types at Insh Marshes to explore Objectives 1-3 as listed in Chapter 1. Data were gathered from transects and fixed plots at three different sampling stages during summer 2003 in order to assess the effect of temporal variation on the spectra-vegetation relationship. Analyses included Principal Components Analyses (PCA) (Bell & Baranoski 2004) and Multiple Discriminant Analyses (MDA) which were performed to examine the spectral properties of the habitat types and to determine the statistical significance of the vegetation classes in spectral space.

In order to meet objectives 2 and 3, vegetation data, which were paired with spectral samples, were collected in order to carry out the statistical analyses required. Multivariate analyses such as Canonical Correspondence were then employed to explore the relationship between the two datasets (Armitage *et al.* 2004). Habitat boundaries were analysed using the digital data provided by the imagery as well as the field samples. This was in order to build upon the analyses carried out using the field data and to explore their applicability to analyses using airborne imagery.

The airborne imagery collected at the site was used to produce habitat classification maps and assess the extent to which spectral clustering methods and classification techniques correspond with the pattern of habitat types as determined by traditional methods of ecological survey and vegetation classification. Techniques employed to explore the structure of the field spectra are applied to the imagery to explore their wider applicability with an increased number of habitat types. All of these analyses were carried out in order to meet Objective 4 as outlined in Chapter 1.

3.2 Sampling Design

3.2.1 Introduction

A map of the habitat types at Insh Marshes was provided by the RSPB (Maier & Cowie 2002) in ESRI's shapefile format (Figure 3:1). Data used to produce these maps were gathered over the summers of 2000 and 2001 using traditional ecological survey methods and intensive field surveys as well as aerial photography. Six of the thirty habitat types mapped by Maier & Cowie (2002) were identified for this study and permanent plots (20 x 20 m) were established, within which, sample points were located from June to September 2003. Data collection was split into three sampling stages over the summer.

3.2.2 Location of Study Plots and Transects

A balance had to be struck between collecting enough sample spectra from one habitat type to determine the nature of habitat specific spectra and collecting samples from a big enough range of habitat types to identify any significant spectral differences between habitats. An area within Insh Marshes with access to a suitable selection of habitat types was identified and illustrated in Figure 3:2. It was also preferable that habitat types of similar species composition and structure were also included in the study in order to determine the degree of spectral dissimilarity inherent in physically similar habitat types. As such, six habitats were chosen and the number of study plots located within each was determined largely by the area represented by that habitat type and limitations imposed by access to the habitats. As this study also aimed to investigate spectral changes across habitat boundaries, three transects were also established on the marshes. Two of these transects crossed over two habitat types and one transect was contained within one habitat type beginning at the habitat boundary; each transect was approximately 50 m in length.

Study Plots

The six habitats studied are listed in Table 3:1 and illustrated in Figure 3:3. The plot codes applied throughout this study for the respective habitat types are also listed in Table 3:1.

Table 3:1 Habitat types and respective plot codes with first and second most dominant species determined from field survey

Habitat Type	Plot Code	Dominant species*- Jun/Jul 2003	Dominant species*- Sept 2003
Carex rostrata-Equisetum fluviatile swamp	EF1	Carex rostrata Equisetum fluviatile	*Carex rostrata* *Equisetum fluviatile*
Species-rich low sedge mire	LS1, LS2 and LS3	Carex curta *Carex nigra*	*Juncus effusus* *Carex nigra*
Molinia caerulea sedge mire	MC1, MC2, MC3, MC4	*Carex echinata* *Molinia caerulea*	*Eriophorum angustifolium* *Molinia caerulea*
Molinia caerulea-Myrica gale mire	MG1, MG2	*Myrica gale* *Eriophorum angustifolium*	*Myrica gale* *Eriophorum angustifolium*
Mixed sedge swamp	MS1,MS 2 and MS3	*Carex aquatilis* *Carex vesicaria*	*Carex nigra* *Molinia caerulea*
Rush pasture/grassland	RP1, RP2 and RP3	*Carex nigra* *Deschampsia cespitosa*	*Deschampsia cespitosa* *Nardus stricta*

*Most abundant species as recorded in vegetation survey from this study only, followed by second most abundant species

The locations of the plots were determined using a random points generator extension in ESRI Arcview (3.2) GIS software. An area of 20 x 20 m in size was considered suitably large to collect 30 spectral measurements in a systematic manner in order to avoid trampling the vegetation over the length of the study period. Thirty samples were collected as this is the number considered acceptable for classical statistical analyses. The plots were all marked by bamboo poles at the corners so that they could be easily returned to over the course of the study and a GPS reference point was also made at each corner and the coordinates recorded using a Leica Geosystem 300 DGPS (used with SR9500 GPS receivers and AT302 antennae; base station position fixed using OSGB active network data and processed through SKI software; realtime relative base/rover with accuracy approx. 2cm). A corner of the plot was noted as the starting position and the GPS coordinates were recorded in the field notes. The

method employed to locate sample points within the study plots is outlined in Sections 3.3.1 and 3.4.1 for spectra and vegetation data respectively.

Transects

Three transects (a-c) were located within the study area (Figure 3:3). Two of these cross habitat boundaries and the third covers an area within one habitat type (See Figure 3:3). Transect 'a' ('T1') was 44.5 m in length and crossed from Rush pasture/grassland habitat (corner of study plot RP1) into Mixed sedge swamp habitat (corner of study plot MS1). Transect 'b' ('T2') was 62.5 m in length and crossed from Species-rich low sedge mire (corner of study plot LS1) into rush pasture/grassland habitat (corner of study plot RP3). Transect 'c' ('T3') was 61 m in length and is largely located within Species-rich low sedge mire.

3.2.3 Sampling Stages

Three periods of spectral sampling were carried out over the summer 2003 in order to gather data which can be used to determine the temporal change in the spectral reflectance of the habitat types studied. The sampling period was limited by access to the site and also the environmental conditions suitable for field spectrometry. As such sampling commenced in July 2003; continued in August and concluded in September. Each sampling period lasted approximately two weeks so that sampling occurred under the same illumination conditions, at the same time of day and in as short a time period as possible (See Section 3.3.1) (Milton 1987; Steven 1987). Vegetation data were collected at the start and end of the sampling period at sample sites paired with a selection of spectral samples.

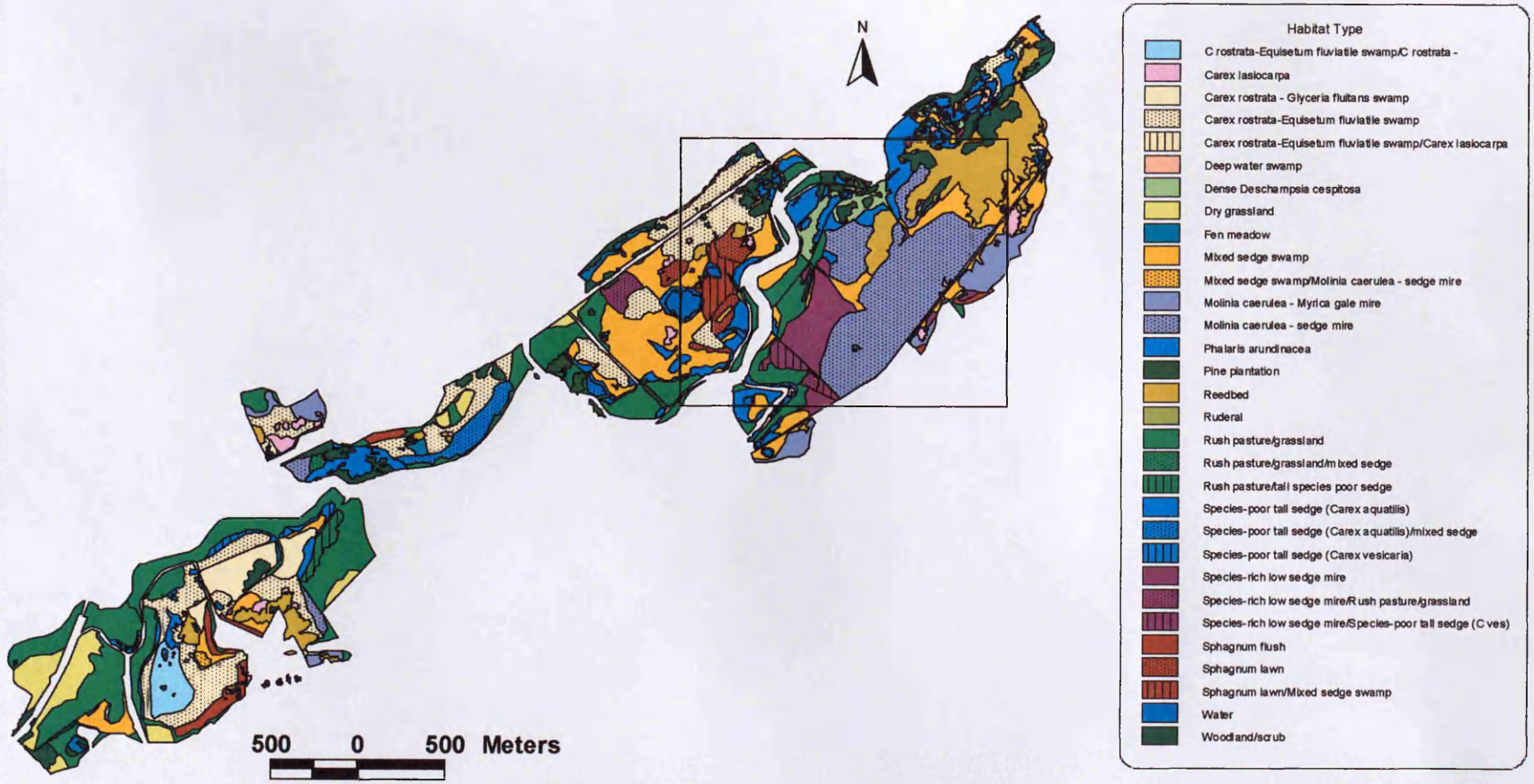

Figure 3:1 Habitat types at Insh Marshes (Maier & Cowie 2002) (Area shown in Figure 3.2 is outlined)

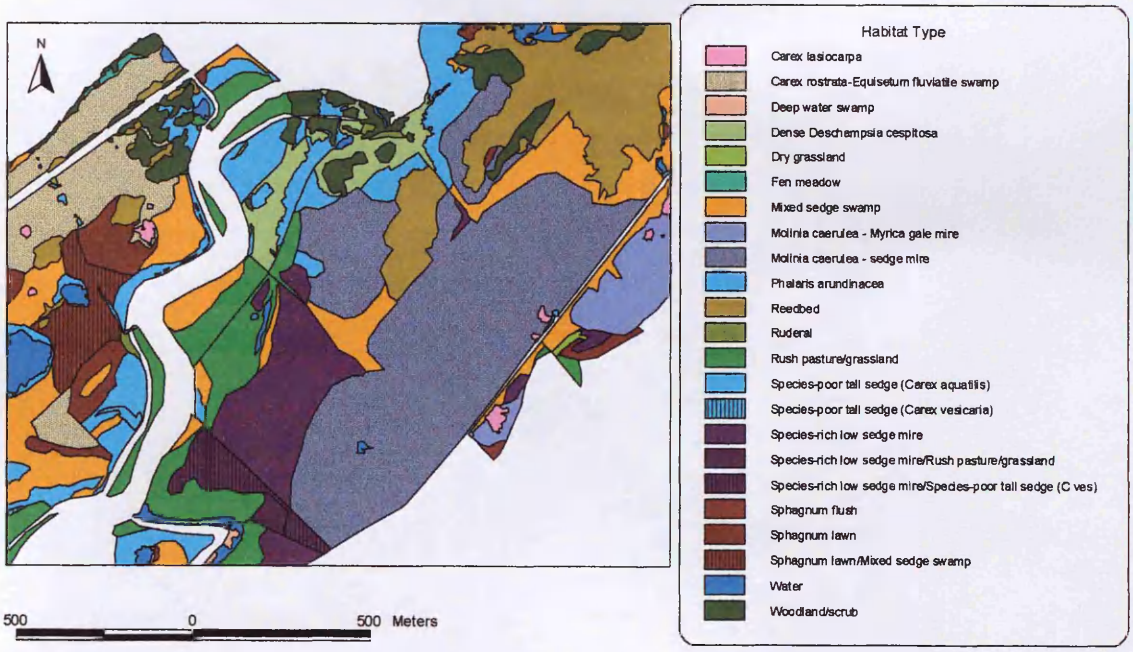

Figure 3:2 Area of Insh Marshes outlined in Figure 3.1

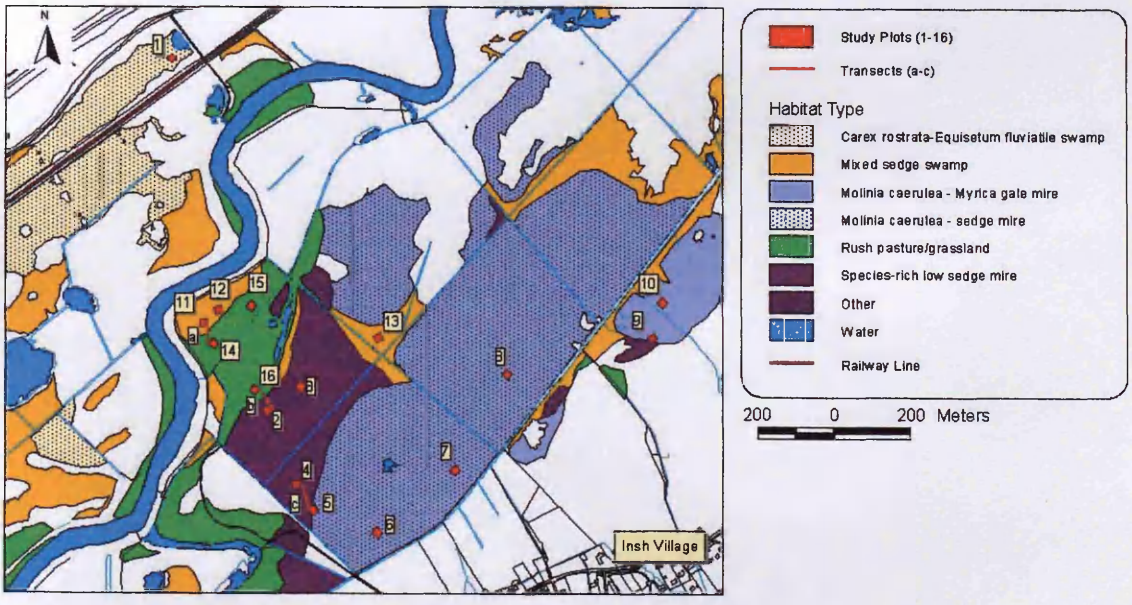

Figure 3:3 Location of study plots (1-16) and transects ('a'-'c') (1=EF1, 2=LS1, 3=LS2, 4=LS3, 5=MC1, 6=MC2, 7=MC3, 8=MC4, 9=MG1, 10=MG2, 11=MS1, 12=MS2, 13=MS3, 14=RP1, 15=RP2, 16=RP3)

3.3 Collecting Spectra in the Field

3.3.1 Collecting Spectra

Spectral reflectance was recorded at each sample point using an ASD FiedSpec™ HandHeld spectrometer (Table 3:3) mounted on a pole and calibrated to a Spectralon® panel every five measurements. The dark current reference was also made before each spectral measurement. All *in situ* measurements were taken using a 25° optic. Measurements were taken at the same height above ground surface at each plot at approximately 1.5 m in height (Milton 1987). Care was taken to ensure that the face of the spectrometer was pointing towards the position of the sun (Rundquist *et al.* 2004). As well as this, the target-sensor geometry remained consistent throughout the study so that all spectral measurements were made at nadir to the target.

Spectral measurements were taken at each of the plots as close to each other in time as possible to reduce variations in solar azimuth between the spectral responses. Field notes were made to record the local weather conditions at the time of sampling. Measurements were taken between 10.30am and 3pm to maximise the number of measurements that could be made during a day with suitable weather conditions for field spectrometry. Sampling was therefore limited a great deal by the weather conditions and approximately two-week periods were required for each of the three sampling stages largely due to the time taken to travel between plots within the marsh. The dates on which spectral sampling took place for each plot and transect are shown below in Table 3:2.

Table 3:2 Data collection dates during the sampling period

Plot	Jul	Aug	Sept
EF1	22	24	25
LS1	16	23	24
LS2	16	23	24
LS3	17	21	24
MC1	18	23	25
MC2	11	28	25
MC3	10	18	25
MC4	18	24	25
MG1	21	24	24
MG2	21	24	24
MS1	15	20	19
MS2	15	20	19
MS3	15	28	19
RP1	15	20	18
RP2	15	15	18
RP3	16	20	18
T'a'	16	-	26
T'b'	16	-	26
T'c'	17	-	26

Table 3:3 Instrument specifications for the ASD FieldSpec™

Spectral Range	325 - 1075 nm
Spectral Resolution	3.5 nm @ 700 nm
Sampling Interval	1.6 nm @ 325 - 1075 nm
Typical data collection rate (solar illumination)	0.7 spectra/second
Detector	One 512 element Si photodiode array 325 - 1075 nm
Input	Fixed 25° field of view. Optional fiber optic and foreoptics available
Calibration	Wavelength, reflectance, radiance*, irradiance*. All calibrations are NIST traceable (*radiometric calibrations are optional)
Noise Equivalent Radiance (NeDL)	UV/VNIR 5.0 x 10 -9 W/cm 2 /nm/sr @ 700 nm

3.3.2 Data Management and Construction of Spectral Bands

The hyperspectral data obtained using the handheld spectrometer in the field were used to simulate the bands of Compact Airborne Spectrographic Imager (CASI) data (Armitage *et al.* 2000). Table 3:4 shows the exact wavelengths of the bands employed in this study as determined by the ASD FieldSpec™.

In addition to the study of the default vegetation bands of the CASI instrument, a spectral dataset was constructed with wavebands approximately 10 – 15 nm in width and is referred to as 'AVS1- 42' (Table 3:5). This dataset was utilised in various statistical analyses so that information on parts of the spectrum that are not represented by the CASI dataset can be extracted and assessed. This was also necessary for the reduction of the dataset collected using the field spectrometer to avoid overfitting in some of the multivariate analyses that were employed. The data at the noisy ends of the spectrum were not incorporated in the AVS1-42 dataset; these were spectra below approximately 350 nm and above 1010 nm.

Table 3:4 Table showing the wavelength range of the spectrometer channels that represent the CASI Default Vegetation bandset (taken from Armitage *et al.* 2000)

CASI Channel	CASI range (nm)	Wavelength (nm)
1	441-461	441.4633-461.9591
2	548-557	548.6721-556.5551
3	666-674	666.917-674.8
4	694-703	693.7192-703.1788
5	705-711	704.7554-711.0618
6	736-744	736.2874-744.1704
7	746-753	745.7469-753.63
8	775-784	775.7024-783.5853
9	815-824	815.1174-824.577
10	860-870	860.8387-870.2983

Table 3:5 Table showing the wavelength range of the spectrometer channels that represent each of the hyperspectral bands (AV1-42)

AV band	Wavelength (nm)
1	348.444-362.6334
2	364.21-378.3994
3	379.976-394.1653
4	395.7419-409.9313
5	411.5079-425.6973
6	427.2739-441.4633
7	443.0399-457.2293
8	458.8059-472.9953
9	474.5719-488.7613
10	490.3379-504.5273
11	506.1039-520.2933
12	521.8699-536.0593
13	537.6359-551.8253
14	553.4019-567.5913
15	569.1678-583.3573
16	584.9338-599.1233
17	600.6998-614.8893
18	616.4658-630.6553
19	632.2318-646.4213
20	647.9978-662.1873
21	663.7638-677.9532
22	679.5298-693.7192
23	695.2958-709.4852
24	711.0618-725.2512
25	726.8278-741.0172
26	742.5938-756.7832
27	758.3597-772.5492
28	774.1257-788.3152
29	789.8917-804.0812
30	805.6578-819.8472
31	821.4238-835.6132
32	837.1898-851.3792
33	852.9557-867.1451
34	868.7217-882.9111
35	884.4877-898.6771
36	900.2537-914.4431
37	916.0197-930.2091
38	931.7857-945.9751
39	947.5517-961.7411
40	963.3177-977.5071
41	979.0837-993.2731
42	994.8497-1009.039

3.3.3 Sampling

Location of Sample Points within Study Plots

Thirty sample points were located within each of the sixteen study plots using a systematic design (See Figure 3:4). This method of sampling would ensure that the same sample points could be returned to over the sampling period. It was also necessary to employ a systematic method of sample design within the study plots in order to avoid problems of damaging the structure of the target sample point. Samples were made 2 m from the corner of each plot and then at 4 m intervals for five points along each of the sides. Samples were then made down the diagonal of the plot at ten points at 2 m intervals beginning at a point 4 m in from the corner of the plot.

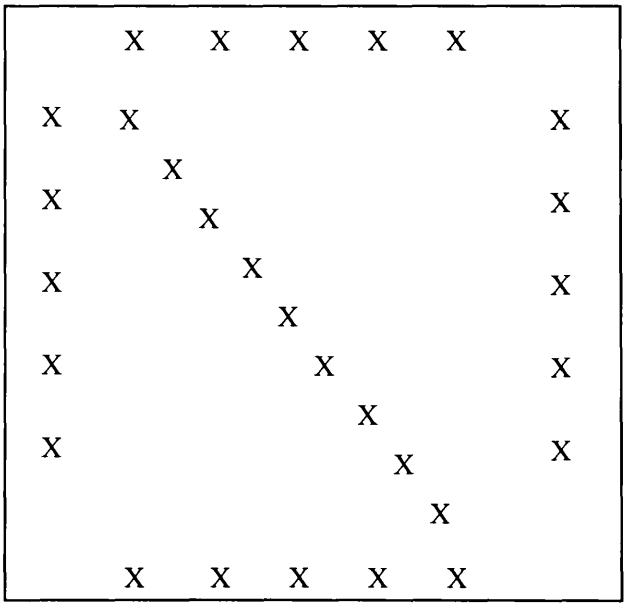

Figure 3:4 Within-plot sampling for collection of spectral measurements (sample points marked with an 'X')

Sampling along transects

Spectral measurements were taken along each of the three transects at 2 m intervals. Bamboo poles marked the start and finish of each transect and direction of travel was always in a northerly direction. Care was taken in the sampling of spectra as outlined in 3.3.1. Vegetation

sampling quadrats were also located at these points along the transects (See 3.4.3 below). Sample points were located 1 m to the south of the transect line to sample over areas that were undisturbed from trampling. Each transect was sampled in July and September so that the difference in the vegetation-spectra relationship over the sampling period could be explored.

3.4 Vegetation Datasets

3.4.1 Location of Sample Points

Ten vegetation sampling points were coupled with spectra sampling points at each of the sixteen plots. A systematic approach was adopted so that sampling could take place at points paired with spectral measurements where disturbance by trampling was minimal. The locations of the vegetation sample points within the plots have been highlighted in red in Figure 3:5. Vegetation sampling along transect, as mentioned above, was at 2 m intervals and 1 m to the south of the transect line at points that were undisturbed from trampling between the start and finish points of each transect.

3.4.2 Equipment

A 0.5 x 0.5 m quadrat sectioned into 25 compartments (Figure 3:6) was used to collect vegetation composition and structural data. Each compartment measured 0.1 x 0.1 m in area. A measuring pole was also used to measure height and was 2 m in length with minor intervals marked at 0.02 m distances and major intervals marked at 0.01 m distances along the length of the pole.

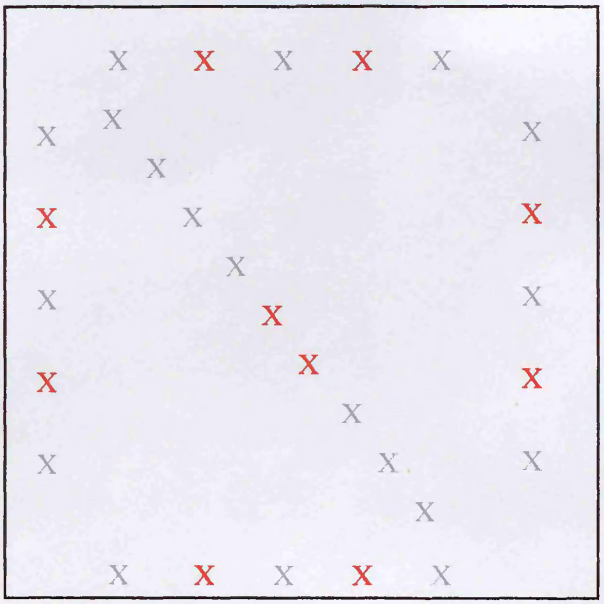

Figure 3:5 Within-plot sampling for vegetation datasets: Points illustrated in red indicated paired sampling points

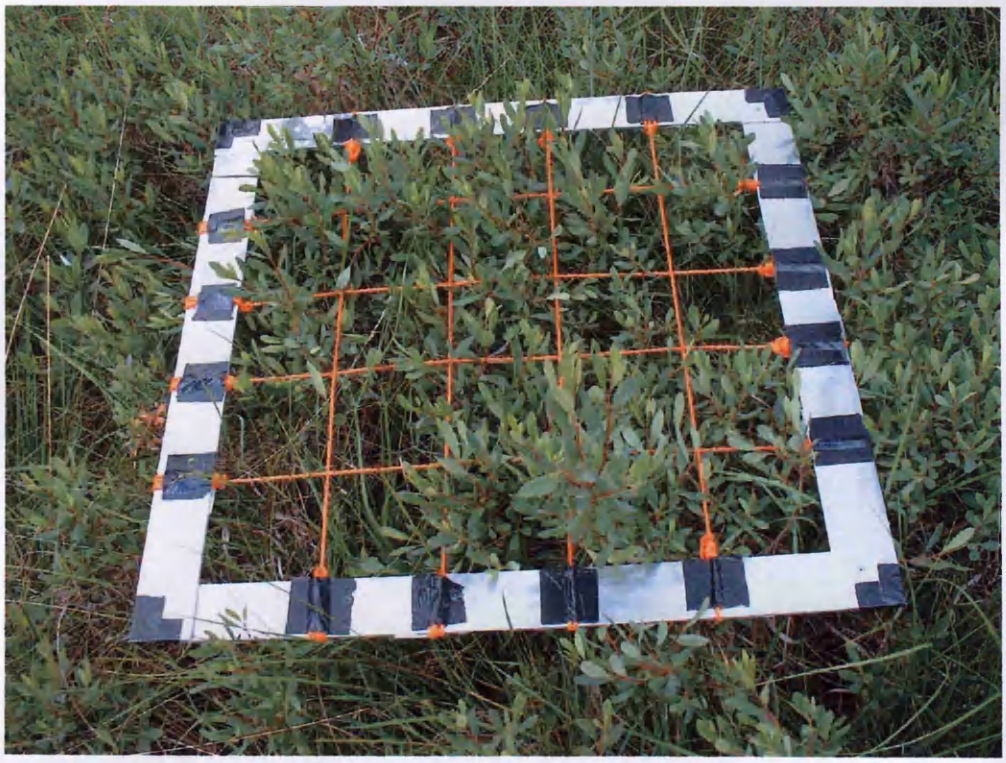

Figure 3:6 0.5 x 0.5 m quadrat with 25 0.1 x 0.1 m compartments using for vegetation sampling

3.4.3 Species Composition, Structural and Environmental Variables

The species present within each sample quadrat were identified and the number of compartments that they were present in were counted and recorded (Table 3:6). This is an efficient measure of species abundance that can be compared with the Domin scale method often employed by vegetation scientists (Armitage *et al.* 2000).

The structure and environmental variables that were measured at each quadrat are listed in Table 3:7. Vegetation height variables were measured from the centre 0.1 x 0.1 m compartment. The method described by Maier & Cowie (2002) was employed using a measuring pole that was held at the same distance away and observed from the same height at each sample point. Maximum height was determined using vegetation in the centre 0.1 x 0.1 m compartment. Vegetation was held up to the pole at full length and the maximum height was recorded. The height at which the vegetation touched the pole without being disturbed was recorded as the Partially Obscured Height (POH). A measurement was also taken from the maximum height at which the pole was totally obscured by the vegetation (Totally Obscured Height 'TOH'). Stem density was recorded by determining the number of stems present within the centre 0.1 x 0.1 m compartment. The presence or absence of tussocks was recorded with a 1 or 0 respectively and water depth was measured using the measuring pole and recording the maximum water level with the pole resting on a firm surface. Other variables were recorded using a percentage cover value determined by eye.

Table 3:6 Codes applied to survey species presence and abundance

Code	% Cover	Domin scale equiv.
1	4%	3
2	8%	4
3	12%	5
4	16%	5
5	20%	5
6	24%	5
7	28%	6
8	32%	6
9	36%	7
10	40%	7
11	44%	7
12	48%	7
13	52%	8
14	56%	8
15	60%	8
16	64%	8
17	68%	8
18	72%	8
19	76%	9
20	80%	9
21	84%	9
22	88%	9
23	92%	10
24	96%	10
25	100%	10

Table 3:7 Structural variables recorded at each quadrat

Variable (units)
Maximum vegetation height (cm)
Partially Obscured Height POH) (cm)
Totally Obscured Height (TOH) (cm)
Stem density (# stems per 100 cm^3)
Tussocks (presence'1'/absence'0')
Water depth (cm)
Evidence of grazing/topping (% cover)
Animal droppings (% cover)
Leaf litter (% cover)
Woody stems (% cover)
Bare peat (% cover)

3.5 Airborne Imagery

3.5.1 Introduction

In order to explore the objectives outlined under Objective 4 as listed in Chapter 1 high spatial resolution airborne imagery was obtained at Insh Marshes. This imagery was obtained at a spatial scale amenable to ecological surveys and the spectral bandsets were those used for vegetation classification studies (Haboudane *et al.* 2004; Armitage *et al.* 2004; Thomson *et al.* 2003; Shanmugam *et al.* 2003).

3.5.2 Instrumentation and Flightlines

The instrument used by NERC Airborne Research and Survey Facility onboard their Dornier 228-101 aircraft (Figure 3:7) to collect data for this project was the Compact Airborne Spectrographic Imager (CASI) (ARSF 2005). This multispectral sensor has the ability to detect a vast array of narrow spectral bands in the visible and infrared wavelengths, using along-track scanning. The spectral range covered by the 288 channels is between 405 and 945 nm. While spatial resolution depends on the altitude of the aircraft, the spectral bands measured and the bandwidths used are all programmable to meet the user's specifications and requirements. The bands utilised in this study were the Vegetation Default Bandset and Table 3:8 lists the band centres and half band widths provided by this imagery. Pixels were 2.5 x 2.5 m in size.

Figure 3:7 Dornier 228-101 NERC Aircraft used to collect airborne imagery

Table 3:8 CASI-Veg band centres and half band widths

Band	Band centre	Band half-width
1	449.96	10.41
2	490.13	11.41
3	552.23	5.82
4	608.12	6.80
5	651.9	6.82
6	671.93	3.96
7	700.59	5.88
8	711.11	4.93
9	739.83	6.85
10	750.37	3.97
11	762.83	3.02
12	780.09	6.85
13	819.42	5.89
14	865.48	5.90
15	942.16	5.89

CASI imagery was collected by NERC ARSF on 17th September 2003 (Julian day-260) (see Figure 3:8) at an altitude of approximately 1500 m at around 12.30pm (GMT). Weather conditions during the time of flight as recorded at a nearby weather station are presented

below in Table 3:9 (See Section 3.6). Conditions recorded by NERC and provided in the flight details are noted as 'light haze, moderate turbulence'.

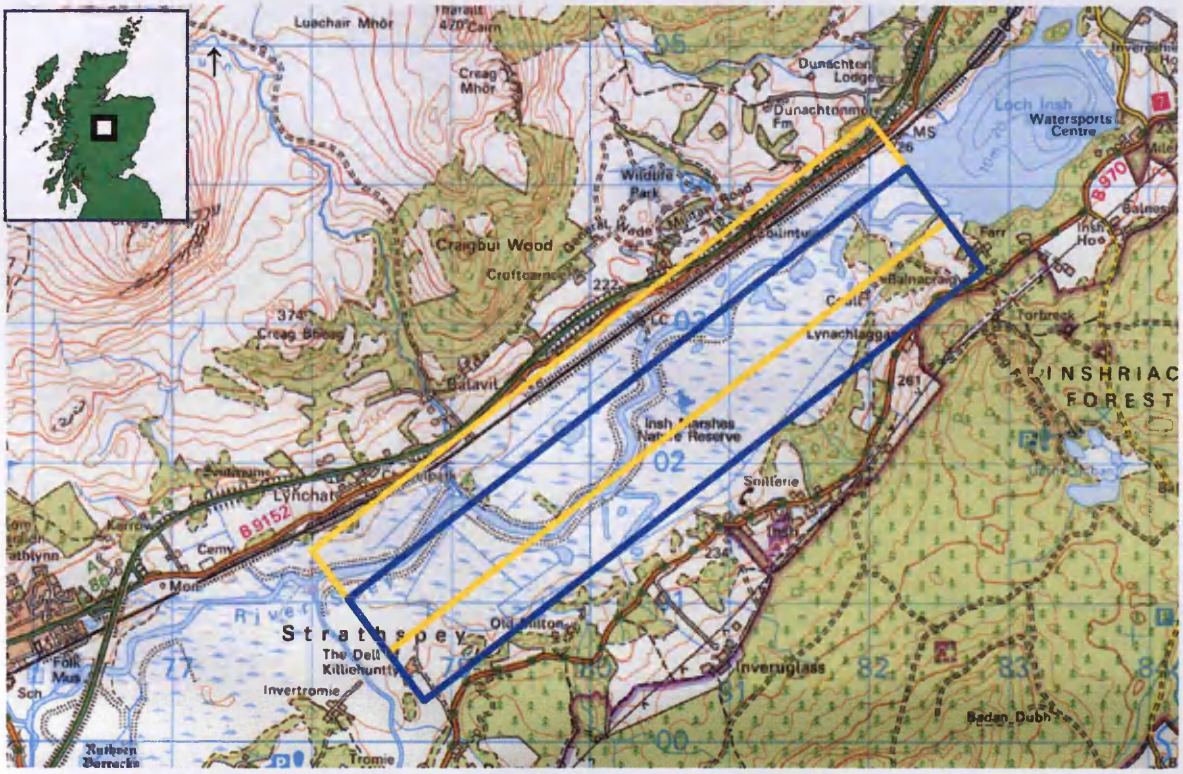

Figure 3:8 Location of flightlines employed by NERC ARSF over Insh Marshes, 17th September, 2003 (Yellow-'CASI 91'; Blue-'CASI 101')

Table 3:9 Meteorological Data collected at Aviemore, 17th September, 2003 (provided by the Meterological Office) and local solar azimuth and altitude (as calculated at http://aa.usno.navy.mil/data/docs/AltAz.html)

Variable	Time	
	12:00	13:00
Wind - Mean Direction	210	200
Wind - Mean Speed (kn)	16	18
Cloud - Total Amount (oktas)	1	0
Temp - Dry Bulb (°C)	21.7	22
Relative Humidity	42.7	41.1
Pressure at Mean Sea Level (hPa)	1008	1007.2
Rain - Amount (mm)	0	0
Radiation - Global (KJ/sq m)	2003	1935
Altitude at 12.30	Approx. 34°	
Azimuth at 12.30	Approx. 187°	

Table 3:10 Header information for CASI 91 & CASI 101

	CASI 91	CASI 101
Date Flown	17/09/03	17/09/03
Altitude	4596 ft	4540 ft
Speed	134 knots	131 knots
View angle: Port	-26.3117	-26.3117
View angle: Star	26.7592	26.7592
OS Reference Start	NH 8349506	NH 8349506
OS Reference End	NH 7886152	NH 7886152
Total Number of Lines	512	512
Total number of Samples	2821	2821
Total number of bands	15	15
Output Pixel Size	2.5 m x 2.5 m	2.5 m x 2.5 m
Flightline Grid Azimuth	-232.7	-234.9
Direction Flightline	West	West

3.5.3 Data Preprocessing

Two sets of imagery have been used in analyses that seek to explore the objectives outlined in Objective 4 in Chapter 1. These are referred to as CASI 91 and CASI 101 and cover the northern and southern half of the marshes respectively (Figure 3:8). Both images were gathered from flights flown in a westerly direction at a flight azimuth of approximately 233° (Table 3:10). Navigation equipment on board the flight records the GPS coordinates of the

data collected. Atmospheric correction of the imagery was considered to be unnecessary for the purposes of this study as the analyses performed on the distribution of the vegetation during the time when the images were recorded only and not over time (Cingolani *et al.* 2004; Song *et al.* 2001; Mertes *et al.* 1995). The imagery was imported into RSI ENVI 4.1 and geocorrected in order to derive the lowest possible Root Mean Square Error (RMSE).

Geo-correction

The imagery must relate to the UK Ordnance Survey National Grid (OSNG) in order to proceed with analyses using remote sensing software. An RMSE of around two pixels was the best that was achieved given the environment that the imagery covers and the lack of distinguishable discrete features that could be incorporated into the geocorrection. The Ground Control Points (GCPs) used to geocorrect this imagery are listed in Appendix A. Each has an error associated with it in both the x and y directions. The model used to warp the image was a first order polynomial re-sampled using the Nearest Neighbour default method. The resultant warped images have associated RMSEs which relate to the average of the squared errors in the x direction summed with the average of the squared errors in the y direction and square-rooted. The overall RMSE for CASI 91 is 4.76 m (average error squared in the x: 2.9 m and y: 2.6 m) and for CASI 101 this figure was slightly higher than that obtained for CASI 91 at 5.57 m (average error squared in the x: 2.9 m and y: 3.5 m).

Cross-track Correction

In order to classify habitats based on differences in the spectral characteristics of certain areas within remote sensing imagery, systematic variations caused by solar illumination, sensor geometry and systematic atmospheric variation during data acquisition must first be identified and removed from the imagery. This problem is particularly apparent within airborne imagery if the flightline runs perpendicular to the direction of solar illumination which is therefore east to west or *vice versa* in the northern hemisphere. Local shadowing effects can cause within pixel shadowing of varying degrees depending on pixel location with respect to solar

illumination and the sensor. Other factors that influence systematic variations in radiance across the flight path are caused by variations in the path lengths of radiation from source (the sun in this case) to sensor and the differing effects of atmospheric variables along this path. The atmosphere can alter the amount of radiance reaching the sensor through both absorption and scattering of the radiation itself due to physical processes.

The cross-track correction function in ENVI works by averaging radiance from each band for each row of pixels (i.e. total number of samples) running along the length of the image for each 'line' of data. This is then plotted against the width of the image ('line' or 'row number'). It is then up to the user to identify whether or not there is a trend present that needs to be removed i.e. if the pattern of radiance across the width of the image does not oscillate around a mean. If the latter is identified, a mathematical function can be applied to the entire image and to each band that will then ensure the removal of any non-normal trend which is presumed to be caused by atmospheric effects.

In order to determine whether or not systematic variation in the illumination of the imagery was apparent, the images were rotated to lie horizontally so that the cross-track algorithm could be applied. The CASI 91 image therefore, was rotated by 37.3° and the CASI 101 image by 35.1°. The images were also spatially subsetted so that there were no areas of 'No Data' values that would then affect the cross-track algorithm. As Loch Insh was present in both images and was not required in the analyses applied to this study, the area covered by the loch on the imagery was also masked out. The resultant images prior to cross-track analysis are presented in Figure 3:9 and Figure 3:10.

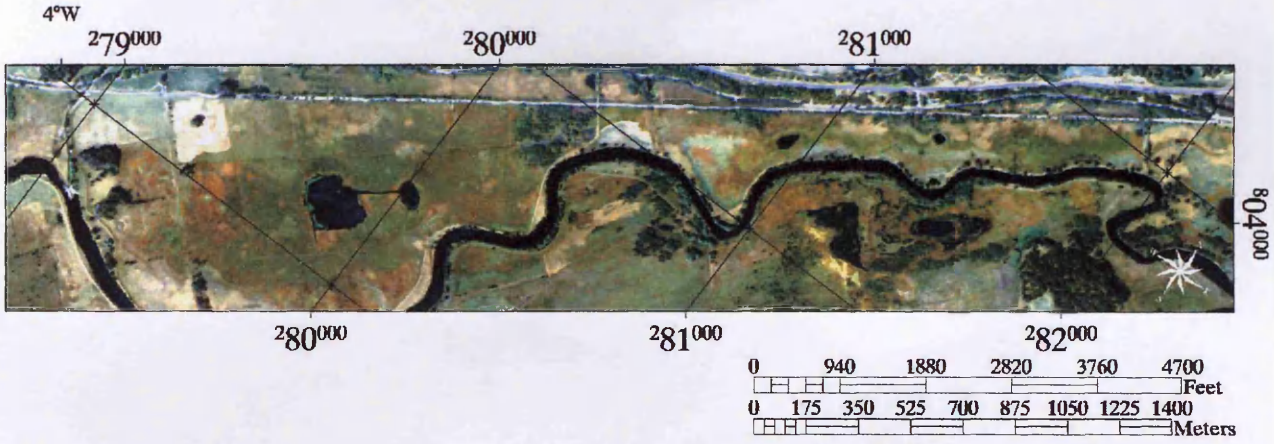

Figure 3:9 CASI 91 prepared for cross-track correction

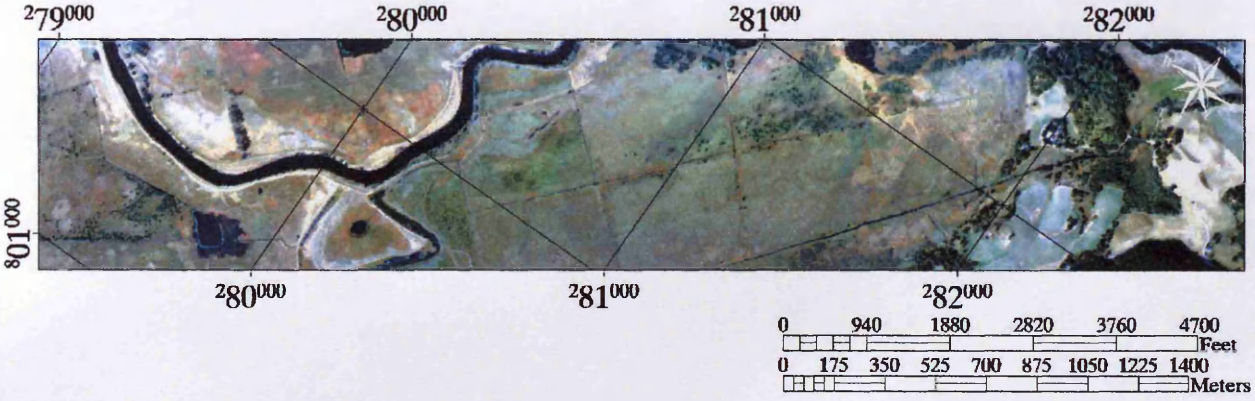

Figure 3:10 CASI 101 prepared for cross-track correction

Prior to performing any transformation to the imagery, the average radiance across the imagery was plotted for CASI 91 and CASI 101 respectively. These are illustrated in Figure 3:11 (Figure 3:12 offset for clarity) and Figure 3:13 (Figure 3:14 offset for clarity) respectively.

CASI 91 showed a clear systematic trend running from the northerly line of the image towards the south however this was not apparent with the CASI 101 imagery. As such, this trend was corrected for using cross-track correction on the CASI 91 imagery only. Although it is difficult to determine the exact cause of the trend it is clear that it is not one that is a result of the land cover and therefore must be removed.

The polynomial curve associated with the trend across the CASI 91 image are illustrated in Figure 3:15. These algorithms were then applied to the respective bands in CASI 91 within the ENVI software. The pixels with the resultant image therefore have had this systematic trend removed and now exhibit a pattern of radiance across the image as illustrated in Figure 3:16.

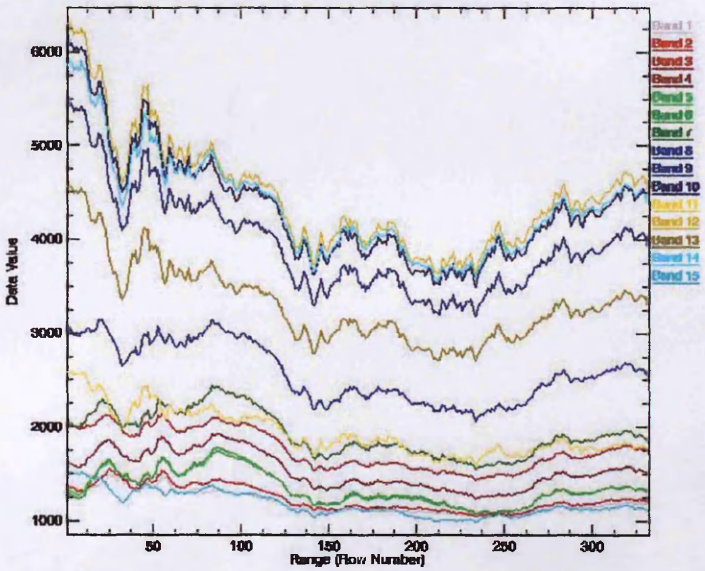

Figure 3:11 CASI 91-Average radiance across lines

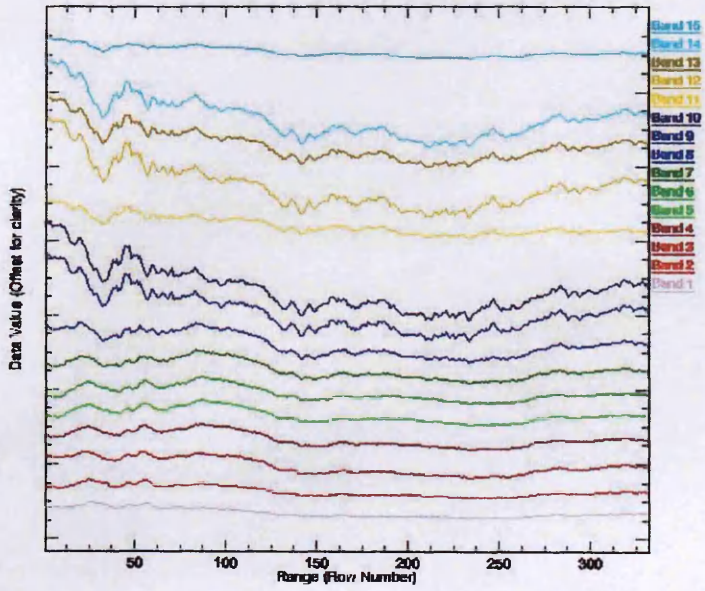

Figure 3:12 CASI 91-Average radiance across lines (offset for clarity)

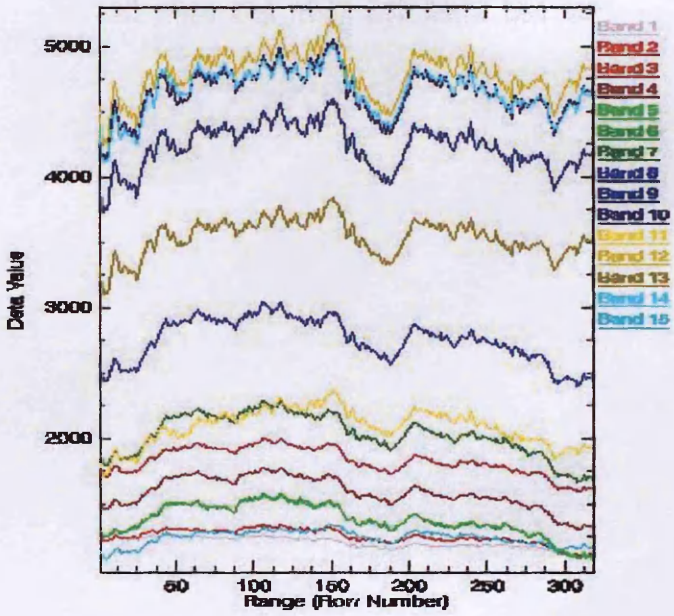

Figure 3:13 CASI 101-Average radiance across lines without cross-track correction

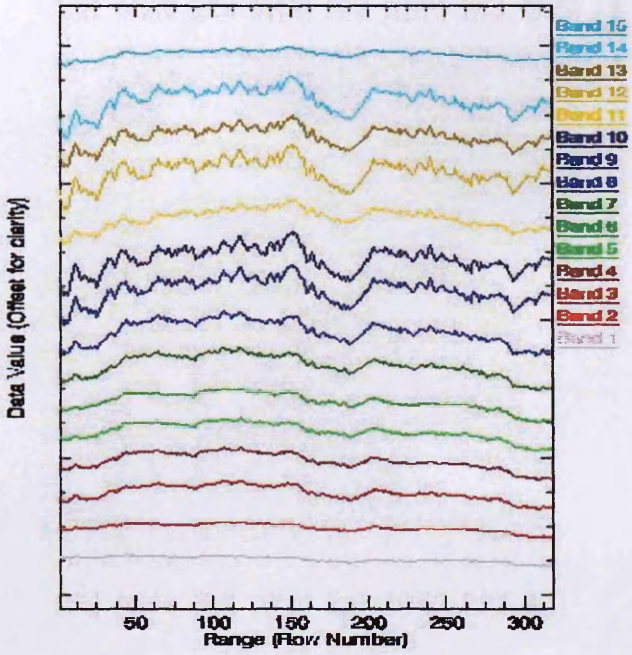

Figure 3:14 CASI 101-Average radiance across lines without cross-track correction (offset for clarity)

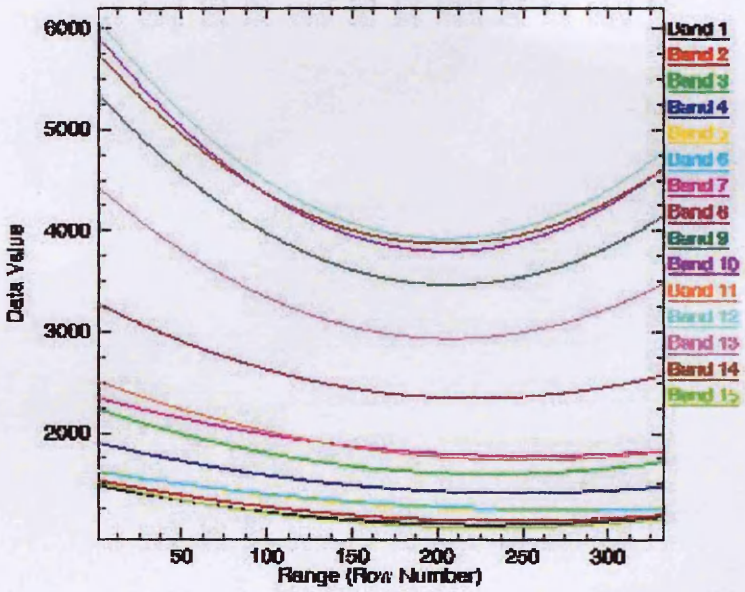

Figure 3:15 CASI 91-polynomials (2nd order) applied to correct for cross-track variance

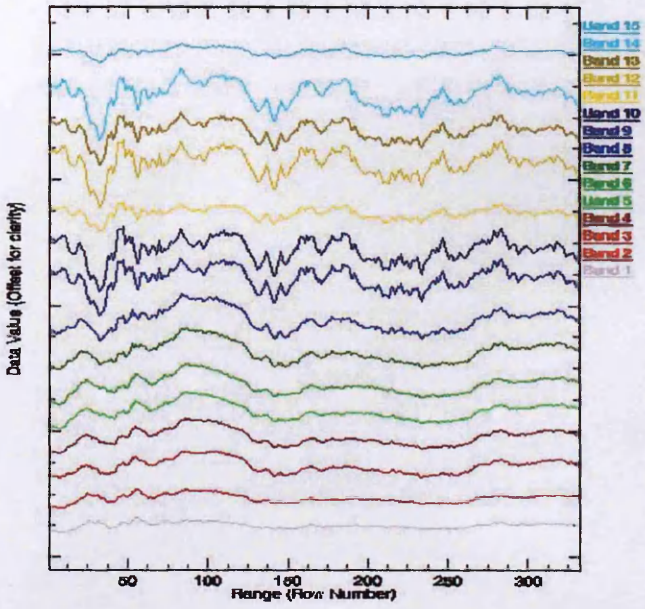

Figure 3:16 CASI 91-resultant radiance patterns across image after cross-track correction (offset for clarity)

3.6 Meteorological Dataset

Field spectrometry is made difficult in variable weather conditions some of which are visibly unnoticeable (ASD 2001). As the nature of the sampling environment throughout this study was such that it took time to move between sampling plots and on occasion the weather deteriorated cutting short sampling days, the covariation in the spectral dataset with the pattern in weather conditions during the sampling stages, should be considered. Meteorological data for the field season was provided by the Meteorological Office. This data was recorded at Aviemore weather station at 228 m above sea level National Grid Reference: 289600 E and 814300 N (Latitude 57 21' N Longitude 03 83' W). Monthly data for July, August and September consisted of information on the variables listed in Table 3:11. Daily average readings recorded for each variable was provided. Data for the days on which sampling took place are highlighted in Appendix A.

Table 3:11 Monthly meteorological data variables (provided for July, August and September 2003 by Met. Office)

Variable	Unit/Annotation	Notes
Max. temp.	°C	Maximum temperature in the 24 hours from 0900 GMT
Min. temp.	°C	Minimum temperature in the 24 hours to 0900 GMT
Rain	mm	Rainfall in millimetres in the 24 hours from 0900 GMT
Sun	hours	Sunshine amount in the 24 hours from 0000 GMT
Grass Min.	°C	Grass minimum temperature in the 24 hours from 0900 GMT
Wind Speed	knots	Mean wind speed in the 24 hours from 0000 GMT
Wind direction	(degrees)	Wind direction at 0900 GMT
Gust	(knots)	Maximum gust in the 24 hours from 0000 GMT
Weather	s, x, h, t, f, g	s: snow or sleet fell in the 24 hours from 0000 GMT
		x: snow lying at 0900 GMT (over half the ground representative of the site was covered with snow)
		h: hail fell in the 24 hours from 0000 GMT
		t: thunder was heard in the 24 hours from 0000 GMT
		f: fog at 0900 GMT (horizontal visibility less than 1000m)
		g: gale occurred in the 24 hours from 0000 GMT (mean wind speed reached 34 knots or more)

As well as the monthly datasets, data were also provided for each of the days that spectral sampling was carried out. The daily datasets contained information on the variables listed in Table 3:12 recorded hourly. Data for the July and September sampling at the paired sampling points are listed in Appendix A.

From the time at which each spectrum was recorded (saved within the Header Information file output from the ASD FieldSpec™), it was possible to determine the solar altitude and azimuth at the time of sample collection. This data was utilized in Chapter 5 as covariable data in multivariate analyses and was calculated using a service provided by the U.S. Naval Observatory website: www.aa.usno.navy.mil/data/docs/AltAz.html. By inputting the longitude and latitude and date, solar altitude and azimuth values are provided in ten minute intervals.

Table 3:12 Daily meteorological data at Aviemore (provided for each day during the spectral sampling period by Met. Office)

Variable	Unit
Wind Direction	degrees
Wind Speed	knots
Cloud	oktas
Temperature-Dry bulb	°C
Relative Humidity	%
Pressure at mean sea level	hPa
Rain	mm
Radiation	KJ/sq m

On occasion, there was data missing from the datasets provided by the Meteorological Office. When this was the case, regression equations were calculated using the remaining data that was present. Radiation values for MG2 on 21st July 2003 for example were missing from the dataset. To compensate for this the available meteorological data from the other study plots was used to create a regression equation in Minitab (v. 14) with an R^2 (Adj.) value of 90.6 % (Equation 3:1).

$$Radiation = 452265 + 6.3Altitude - 11.6Azimuth - 6.44WindDirection + 64WindSpeed - 175CloudCover + 63.7emperature - 40.4\,\mathrm{Re}lativeHumidity - 441\,\mathrm{Pr}essure + 10273Rain$$ **Equation 3:1**

The study plot EF1 was also missing information for all variables from the July dataset (22nd July 2003 13:00 and 14:00) apart from information on cloud cover. To compensate for this a number of different measures were taken. To obtain a value for mean wind direction and mean wind speed an average was calculated from data that was available for that day and applied, thereby assuming variation throughout the day was minimal. A regression equation for temperature (dry bulb) using only cloud cover, wind speed and wind direction was then calculated using the available dataset and an R^2 (Adj.) 66.1% was attained (Equation 3:2). This was considered high enough to then apply to the now available data for EF1 to obtain values for temperature. The same method was then applied to calculate values for relative humidity. An R^2 (Adj.) value of 83.8% was obtained from the available data and applied (Equation 3:3). An acceptable model to derive values for pressure could not be derived from the available data (R^2 values of 0.0) so values of 'No Data' were replaced with values recorded at the relevant times on 21st July 2003. Radiation was calculated based on the regression equation in Equation 3:1.

$$Temperature = 16.1 - 0.00728WindDirection + 0.492WindSpeed - 0.232CloudCover$$ **Equation 3:2**

$$\mathrm{Re}lativeHumidity = 132 - 0.0114WindDirection - 0.533WindSpeed + 0.149CloudCover - 2.76Temperature$$ **Equation 3:3**

In the September meteorological dataset, wind speed and wind direction values were missing for four plots. An acceptable model was derived for wind speed from the available data (Equation 3:4) (R^2 Adj. 86.3%). As only some wind direction values were missing for one of the plots (11:00) the missing values were replaced with the values that were available (12:00). The wind direction values missing for the plots sampled on the 18th September 2003 were

replaced with an average derived from the daily values recorded five days either side of the 18th September.

$$\text{Wind Speed} = -1117 + 0.675\text{Cloud} + 2.08\text{Temp} - 0.111\text{Relative Humidity} + 1.0\text{Pressure} + 0.00257\text{Radition}$$ **Equation 3:4**

The resultant dataset was then complete and available to use in further analyses regarding the influence of local weather conditions on the variation in the spectral dataset (Chapter 5).

3.7 Summary

This chapter describes the methods employed to collate and prepare the data required to carry out the research aims of this project as outlined in Chapter 1. The main points are listed below.

- Data were collected at six habitat types within Insh Marshes from June to September 2003.

- Permanent plots were set up within each habitat type. This ranged from 1 to 4 plots within a single habitat type and plots totalled 16. Three transects were also established on the marsh.

- Spectral sampling took place at three stages over the sampling period.

- Vegetation sampling was paired with spectral sampling at the start and end of the sampling period.

- CASI-Veg imagery was provided for analyses. This was geocorrected and checked for anomalies caused by cross-track illumination. Correction was performed on CASI 91.

- Meteorological data and information regarding solar altitude and azimuth were collated for incorporation into future analyses.

4 HYPERSPECTRAL DISSIMILARITIES BETWEEN WETLAND HABITAT TYPES

4.1 Introduction

The overall aim for this chapter and the objective that this relates to with regard to the project as a whole is stated again below. This can be split into a number of objectives that are specific to this chapter and those are also listed below.

4.2 Aims and Objectives

Chapter 4: Overall Aim (Project Objective 1)

Determine the extent to which wetland habitats are spectrally distinct.

This aim can be split into the following objectives and an outline of how these are addressed in this chapter is summarized.

Chapter 4: Objectives

a) *Determine the degree to which spectral reflectance pattern varies between habitat types in the visible and near infrared (NIR) regions of the spectrum.*

b) *Assess the degree to which spectra grouped by habitat type are spectrally distinct using multivariate statistical analyses.*

c) *Explore the within habitat spectral variation using data collected from two or more study plots within each habitat type.*

d) *Explore the between habitat variation at different wavelengths using study plots from each habitat type.*

e) *Determine the between habitat variation as demonstrated by spectral indices and geostatistics.*

4.3 Methods and Analyses

This section details the methods applied in this chapter beginning with a brief overview of the datasets used to achieve each of the objectives outlined above ('a)' to 'e)').

4.3.1 Datasets and Methods Overview

The methods employed to collect the data used in this chapter have been outlined in Chapter 3. Subsets of the entire dataset were selected to perform certain analyses and these are specified here in relation to the Chapter Objectives 'a)' to 'e)'.

a) The hyperspectral data collected using the field spectrometer are used to illustrate the mean spectral response as collected at each study plot (data in 1-2 nm bands between 400 and 850 nm). These were also pared down to a smaller dataset ('AVS1-42') (band widths 10 - 15 nm) (Chapter 3) and used to carry out Principal Components Analyses (PCA).

b) The AVS1-42 data were used in the Multiple Discriminant Analyses (MDA) as were the simulated CASI data (Chapter 3).

c) To explore intra (or 'within') habitat variation, the mean spectra collected from each habitat type from two or more study plots were calculated along with the standard deviations. PCA was carried out on the simulated CASI datasets per habitat type for each sampling period. Classical statistics were performed on each simulated CASI waveband to assess the degree of within habitat variation.

d) To explore inter habitat variation at different wavelengths over the sampling period, one plot from each habitat type was selected (EF1, LS2, MC1, MG2, MS3 and RP1) and the spectral dissimilarity between plots located at each simulated CASI waveband was explored. Two of these plots were selected to perform the same statistical tests using the AVS1-42 dataset over the three sampling periods (RP1 and EF1).

e) The NDVI results were derived using spectra from the simulated CASI datasets. The REIPs were derived from 1st derivative analyses on the raw spectra collected at each sample point. Continuum removal was carried out on two regions of the spectrum, 480 – 520 nm and 585 – 750 nm. Continuum removed indices were calculated for three habitat types using the August dataset. These were EF1, MG2 and MC4. The NDVI and REIP datasets were paired with their x and y OS coordinate (derived using ArcView 3.2 GIS software) and used to calculate geostatistics associated with each study plot.

4.3.2 Spectra Collected at Study Plots

The mean spectral response and standard deviations of each study plot were calculated for each sampling period (July, August and September) using the hyperspectral field data in Microsoft Excel (raw spectra per study plot are illustrated in Appendix B). This dataset was also used to derive Red Edge Inflection Points (REIPs) for each sample spectra (see below). CASI wavebands were simulated using the hyperspectral data (Chapter 3) and analysed further using Principal Components Analysis (see below). The simulated CASI data were used to calculate the Normalized Difference Vegetation Index at each sample point within each study plot and, along with the REIP results, each plot was analysed using geostatistical techniques.

4.3.3 Spectra by Habitat Type

Sample spectra collected from two or more study plots from the same habitat type were grouped together and the mean and standard deviations derived in Microsoft Excel. The simulated CASI datasets from these plots were also grouped by habitat type and entered into Principal Components Analyses.

Two or more study plots were located in five of the habitat types sampled and the statistical differences between plots from within the same habitat type was assessed at each CASI band.

The data was tested for normality and found to be non-normal on occasion; because of this the non parametric Kruskal Wallis test was chosen to assess the statistical significance of the variability within the habitat types (equivalent to the parametric ANOVA test). When using a statistical test such as the Kruskal Wallis, the test statistic calculated is interpreted using the 'P-value'. A P-value of less than 0.05 (all statistical tests will be assessed at the 95% significance level) enables the null hypothesis to be rejected. The null hypothesis always states that the samples are from the same population.

One plot from each habitat type was selected to test the statistical significance of the difference in the spectral response at each CASI waveband between each combination of habitat types and to determine how this varied over the sampling period. The study plots that were selected are EF1, LS2, MC1, MG2, MS3 and RP1. These were chosen due to the fact that the samples collected at these plots illustrated a normal distribution at most wavelengths over most of the sampling period compared with the rest of the dataset (Appendix B). Due to the non-normal distribution in the spectral response at certain wavebands for some of the data however, the non-parametric Mann Whitney Two Sample Test was selected for the analyses (equivalent to the non-parametric Two Sample T-Test). As in the Kruskal-Wallis analyses, the null hypothesis states that samples are from the same population and this will be tested at the 95% significance level. Mann Whitney tests were also carried out for each of the 42 wavebands in the AVS1-42 dataset for two of the study plots RP1 and EF1.

4.3.4 Principal Components Analysis

Principal Components Analysis (PCA) was carried out on the simulated CASI spectra using data from each sampling stage, both per plot and, per habitat type. All PCAs were calculated using CANOCO for Windows (v. 4.5). PCA is a descriptive method of decomposing the variation among a set of original objects and illustrating respective positions within a cartesian coordinate system defined by an n x n matrix of dissimilarities (Brook & Kenkel 2002). The mean values and respective standard deviations per plot and habitat type for

sample scores along the first two components for each of the samples were calculated in Microsoft Excel. This information was then plotted in cartesian space.

4.3.5 Multiple Discriminant Analysis

Multiple Discriminant Analysis (MDA) was performed on the AVS1-42 and CASI datasets using habitat types as the discriminant categories in SPSS 12.0.1. The habitat types were labelled 1-6 and these numbers correspond respectively to the following habitat types: 1 = *Carex rostrata-Equisetum fluviatile* ('EF'), 2 = Species-rich low sedge mire ('LS'), 3 = *Molinia caerulea*-Sedge mire ('MC'), 4 = *Molinia caerulea-Myrica gale* mire ('MG'), 5 = Mixed sedge ('MS') and 6 = Rush pasture/grassland ('RP'). MDA is a multivariate statistical technique whereby the ability to predict category type using a number of variables is assessed with the ability to cross-validate the predictions (Ustin *et al.* 1986; Pando *et al.* 1992; Brook & Kenkel 2002). MDA is applied here to assess the predictive capabilities of the information contained within 42 bands for each sample to determine the habitat type that labels the spectrum. The percentage of correct predictions obtained for each class type over the sampling period is presented for each habitat type in the output and the results from the three datasets over the sampling period are discussed. A random list of categorical labels (1-6) was produced in Minitab 14 and used to label the spectra. An additional MDA was then carried out using the randomized labelling to compare these results with those obtained from the correctly labelled datasets.

4.3.6 Spectral Indices

Normalized Difference Vegetation Index

The Normalized Difference Vegetation Index (NDVI) is calculated using the red and near infrared (NIR) bands of the simulated CASI datasets for samples within each plot at all three

sampling stages (Equation 4:1). The CASI bands used are Bands 3 and 8 of the simulated dataset which correspond to mean spectra over 666-674 nm and 775-784 nm respectively.

$$\frac{(NIR - \mathrm{Re}\,d)}{(NIR + \mathrm{Re}\,d)}$$ **Equation 4:1**

Box and whisker plots were produced within Minitab 14 to display the results. Normality tests are also carried out on the data and Kruskal Wallis tests were carried out on data from each habitat type to determine the within habitat variability in derived NDVI values. Mann Whitney tests were used to determine the statistical difference in NDVI values between the six study plots as chosen above, they are EF1, LS2, MC1, MG2, MS3 and RP1. All tests were carried out to the 95% significance level.

Red Edge

The location of the steepest part of a reflectance spectrum in the red region is termed the Red Edge Inflection Point (REIP) (Figure 4:1) and this was calculated using the first derivative or slope values calculated for each sample spectra. The first derivative datasets were calculated in Microsoft Excel using Equation 4:2:

$$\left.\frac{ds}{d\lambda}\right|_i \approx \frac{s(\lambda_i) - s(\lambda_j)}{\Delta\lambda}$$ **Equation 4:2**

-where $\Delta\lambda$ is the separation between adjacent bands, $\Delta\lambda=\lambda i-\lambda j$ and $\lambda i>\lambda j$ and the interval between bands is assumed to be constant. The interval between bands applied here was approximately 2 nm (every waveband covered by the field spectrometer) between 350 nm and 1000nm.

This technique is sensitive to residual effects caused by noise in the data (Curran *et al.* 1992b; Kumar & Skidmore 1998), and so, a simple mean filter was applied to smooth the original reflectance spectra before the first derivative was calculated (Schmidt & Skidmore 2004; Tsai & Philpot 1998). The mean and standard deviations of the first derivative curve are calculated using Microsoft Excel for each study plot, as well as, for each habitat type.

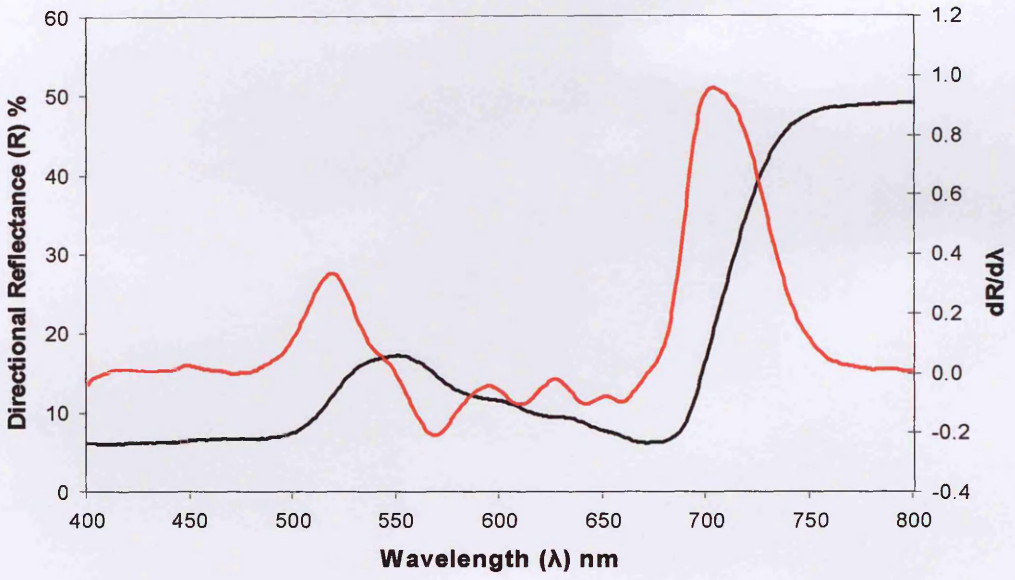

Figure 4:1 Typical spectral reflectance of vegetation (black) and first derivative (red) in the visible and near infrared

The mean filter smoothes data within a predetermined smoothing window and does not involve any polynomial curve-fitting or least-mean-square procedures. Data processing times and simplicity of approach are important considerations and as such the mean filter method was chosen here (Schmidt & Skidmore 2004). However, the choice of window size received due consideration as successful data smoothing is always a balance between noise reduction and the ability to resolve fine spectral features; the larger the size of the smoothing window, the smoother the resulting spectra. The spectral features that should be retained are the wavelength positions of the local minima and maxima and the inflection points (position along the spectrum at which the curvature changes from convex to concave). A suitable compromise for this dataset was a window size of five. The method involved taking the mean spectral value of all points within the specified window as the new value of the middle point of the window (Equation 4:3).

$$\hat{s}(\lambda_j) \frac{\Sigma s(\lambda_{i-k})}{n}$$ **Equation 4:3**

-where n is the number of sampling points (i.e. window or filter size) and j is the index of the middle point of the filter.

Continuum Removal

Continuum removed indices were calculated for spectra collected at three study plots, each a different habitat type, using spectra from the August dataset. The continuum is essentially a convex hull fitted over the top of the reflectance spectrum with straight lines connecting each of the segment maxima that do not cross the spectrum itself. Once the position of the convex hull is determined, the continuum is removed and the resultant values can be used to calculate a number of indices that may then illustrate differences in the structure of the absorption features represented by each of the study plots.

The study plots that were used in this analysis were EF1, MC4 and MG2. These plots were chosen as spectra were collected at these plots on the same day (24th August 2003) and very close to each other in time given their location within the marsh. Two regions of spectral absorption were analysed ('Feature (a)' and 'Feature (b)'). Feature (a) is located between 482 nm and 519 nm and Feature (b) between 585 nm and 750 nm. Band Depth (BD) of the continuum curve, Band Depth Ratio (BDR), Continuum Removed Derivative Reflectance (CRDR) and a Normalized Band Depth Index (NBDI) were calculated for each spectra collected at these plots (Equation 4:5 to Equation 4:8).

The continuum removed reflectance values are derived by first determining the number of increment steps between the two maxima of interest. Using the data obtained through field spectrometry in this study, the number of increment steps (n_{i-j}) for one of the absorption features studied (e.g between 482 nm (λ_a) and 519 nm (λ_b) -3 s.f.) is calculated as 23 (Figure 4:2 'a'). The difference in reflectance between λ_b and λ_a ($R\lambda_{b(j)} - R\lambda_{a(i)}$) is divided by the number of increment steps to create the continuum line (Figure 4:2 'b'). Continuum Removed Reflectance (CRR) is then calculated by dividing reflectance along the continuum line by original reflectance (R_{i-j}). Band depth is calculated by subtracting the CRR from 1 (Figure 4:2 'c') (Equation 4:4). (The process was the same for Feature B).

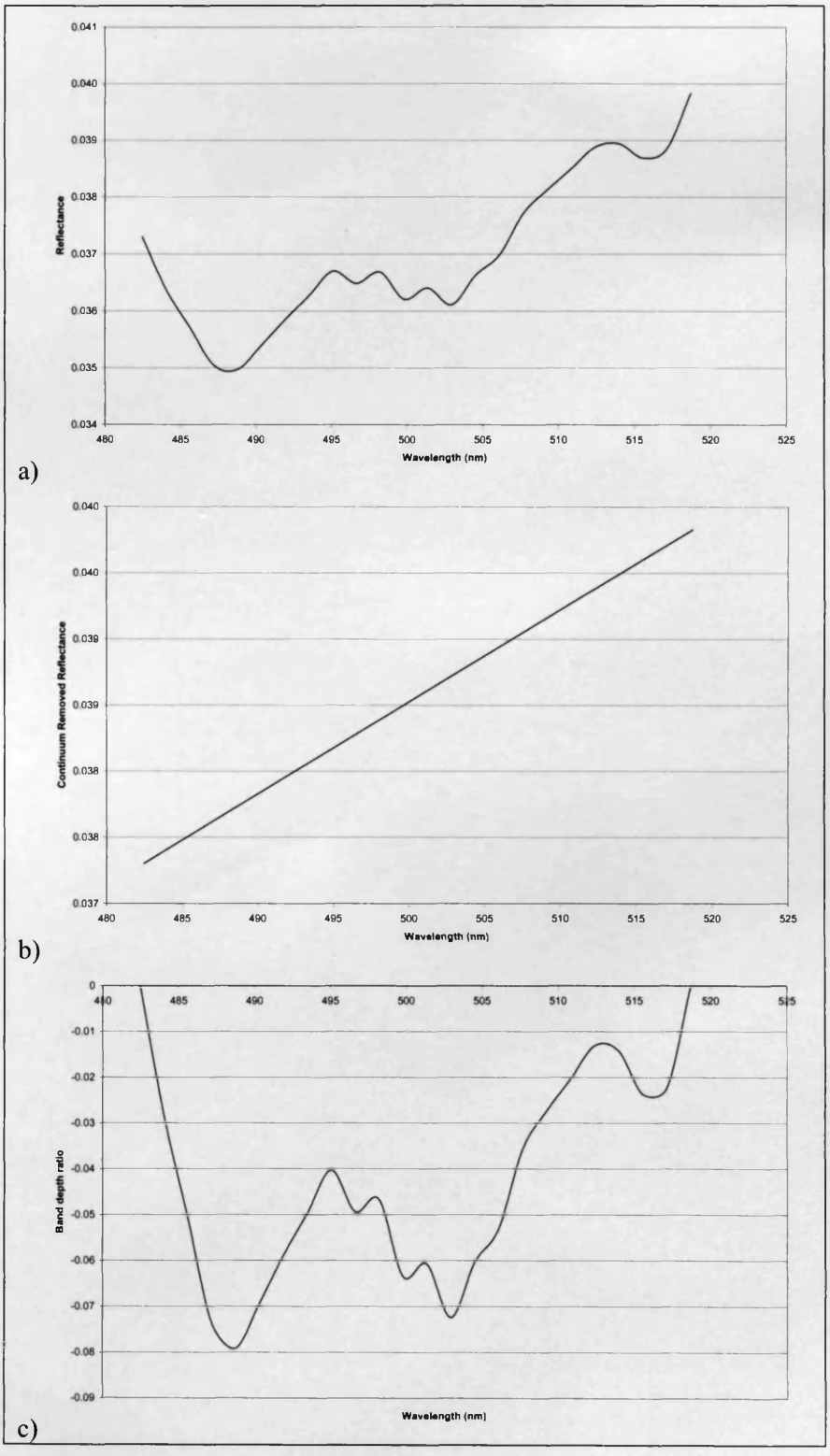

Figure 4:2 Calculating Continuum Removed Reflectance

CRR $$\frac{R\lambda_{b(j)} - R\lambda_{a(i)} / N_{i-j}}{R_{i-j}}$$ **Equation 4:4**

BD $1-(CRR)$ **Equation 4:5**

BDR $1-(CRR_i / CRR_{MAX(i)-(j)})$ **Equation 4:6**

CRDR $(CRR_i + CRR_{i+1})/((i+1)-i)$ **Equation 4:7**

NBDI $1(CRR_i - CRR_{MAXi-j})/(CRR_i + CRR_{MAXi-j})$ **Equation 4:8**

(See text for notation)

4.3.7 Geostatistics

The x and y coordinates of the sample points within each study plot was determined using ArcView 3.2 and data collected using a DGPS (Section 1.2.2 Chapter 3). This information was then paired with NDVI measurements and REIP values (z) for each point (x) and analysed within GS+ v. 7 geostatistical software. The semivariogram for each study plot was calculated for the July, August and September datasets (Equation 4:9) where '$\gamma(h)$' = the semivariance for interval class 'h'

$$\gamma(h) = \frac{1}{2}\Sigma[Z(x) - Z(x+h)]^2 \qquad \textbf{Equation 4:9}$$

The interval class is the separation distance and is divided into intervals (or 'lag classes'). The semivariogram is computed as the mean of the summed semivariances at each lag interval. All possible pairs of sample points in the study plot are assigned to an interval class in GS+ (the lag class distance interval was 4). In order to maximise the number of lag classes used to produce the semivariogram, the maximum active lag distance was applied (~18 m). The variance between all of the combinations of sample points that fall within each interval class (0-4 m, 4-8 m and so on up to the maximum active lag distance) are calculated (and halved when plotted on the semivariogram). A number of statistics were derived for each study plot, these include the nugget, the sill, the range, the residual sum of squares, the r^2 and proportion (Table 4:1); a note of the best model was also made.

Figure 4:3 illustrates an example semivariogram. Each box represents an interval class and the mean variance within the class, halved, is plotted. The range is probably the most interesting statistic in remote sensing studies as this indicates the distance beyond which spatial variance within the sample dataset does not increase i.e. sample points are not statistically related. This will have important implications for optimum spatial sampling campaigns for remote sensing projects (Atkinson & Curran 1997; Atkinson & Curran 1995) as well as implications for classification (Lark 1996; Dejong & Burrough 1995).

Table 4:1 Geostatistics: Terms used in the description of the semivariogram (Adapted from Curran & Atkinson 1998)

Statistic	Description
Lag (h)	Distance (and direction in two or more dimensions) between sampling pairs.
Nugget variance (C_0)	The point where $\gamma(h)$ model intercepts the y axis. This represents the component of the variation within the dataset that is not spatially correlated.
Sill ($C_0 + C$)	Model asymptote i.e. maximum value of $\gamma(h)$.
Effective Range (A)	The separation distance over which spatial dependence is apparent i.e point on x axis where $\gamma(h)$ model reaches maximum.
Structured variance (C)	Sill minus nugget variance.
Residual sum of squares (RSS)	Provides an exact measure of how well the model fits the variogram data.
r^2	Provides an indication as to how well the model fits the variogram data-not as sensitive or robust as RSS value for best-fit calculations.
Proportion ($C/(C_0 + C)$	Provides a measure of the proportion of sample variance (C_0 + C) that is explained by spatially structured variance C.

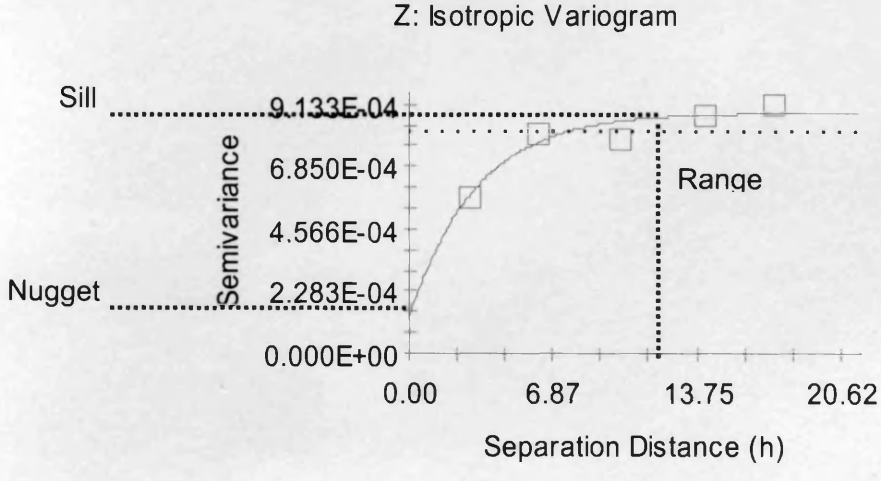

Figure 4:3 The semivariogram with model type and nugget, sill and range indicated

4.4 Results

4.4.1 Objective a) Differences in spectral patterns between habitat types

Determine the degree to which spectral reflectance pattern varies between habitat types in the visible and near infrared (NIR) regions of the spectrum.

The means and standard deviations of the data collected at each of the study plots are illustrated here (Figure 4:4 to Figure 4:9). (The raw spectra collected at each point within the study plots are presented in Appendix B). Figure 4:10 shows the mean spectra of each habitat type from the July, August and September datasets ('a', 'b' and 'c' respectively) when study plots are grouped together by habitat type. Figure 4:11 illustrates this information in the 500 – 700 nm region.

The results from Principal Components Analyses (PCA) are also shown in this section for data by study plot (Figure 4:12 to Figure 4:15) at each stage of data collection. PCA using the simulated CASI bandsets and the larger AVS1-42 dataset was carried out and the results shown to be comparable (Figure 4:12 and Figure 4:13). Figure 4:14 and Figure 4:15 show the PCA results for the August and September AVS1-42 datatsets respectively. The ovals represent the position of the mean x and y coordinates of the first and second components of the spectra at each study plot respectively. The size of the ovals represents the degree of variance present in the values of the first and second components in their respective directions. The position of these ovals in feature space gives an indication of the separability of the spectra from each study plot in relation to the overall degree of dimensionality present

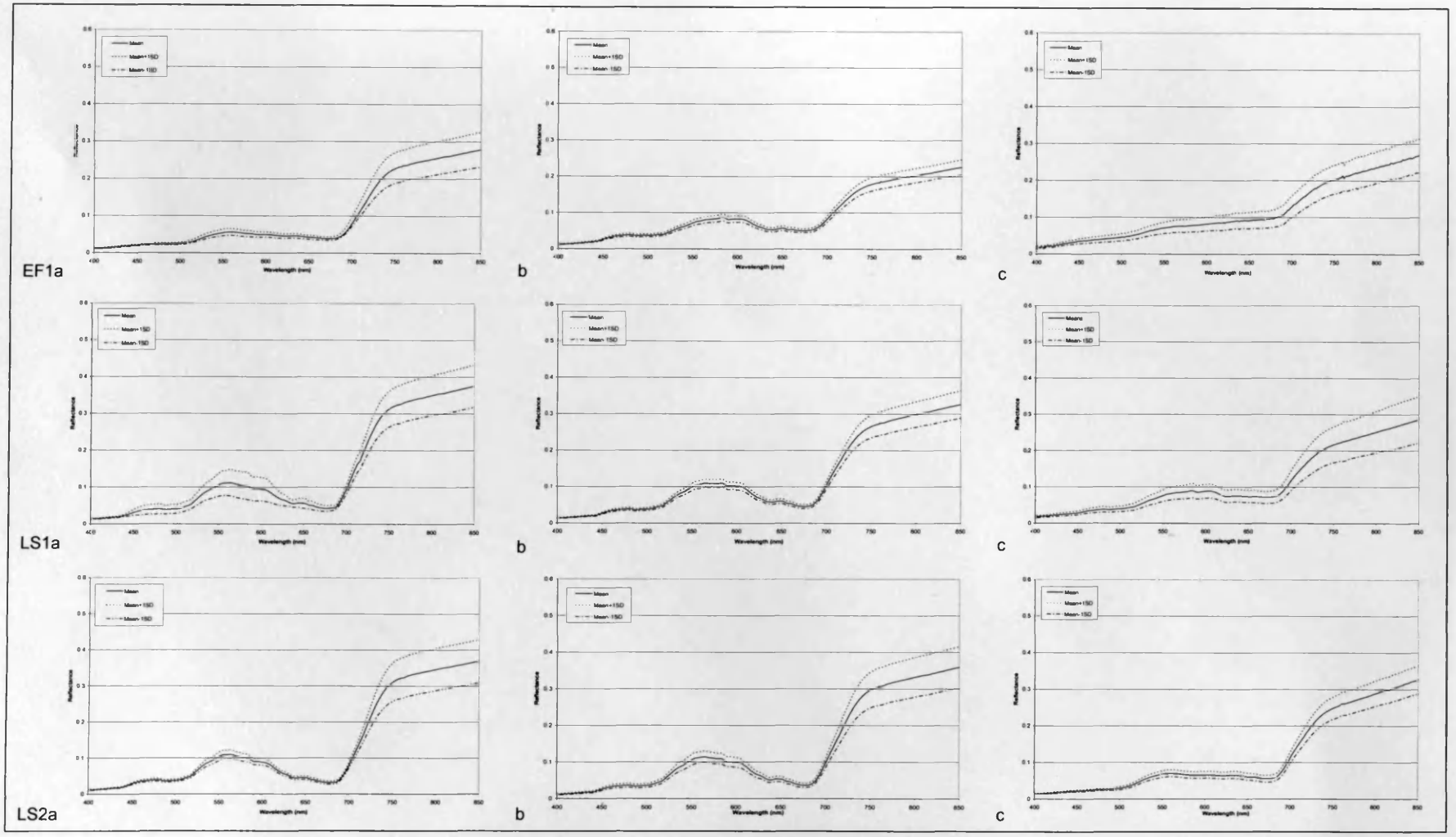

Figure 4:4 Mean spectra (and +/- 1 standard deviations) per study plot (EF1, LS1 and LS2) at each sampling stage a) July b) August c) September

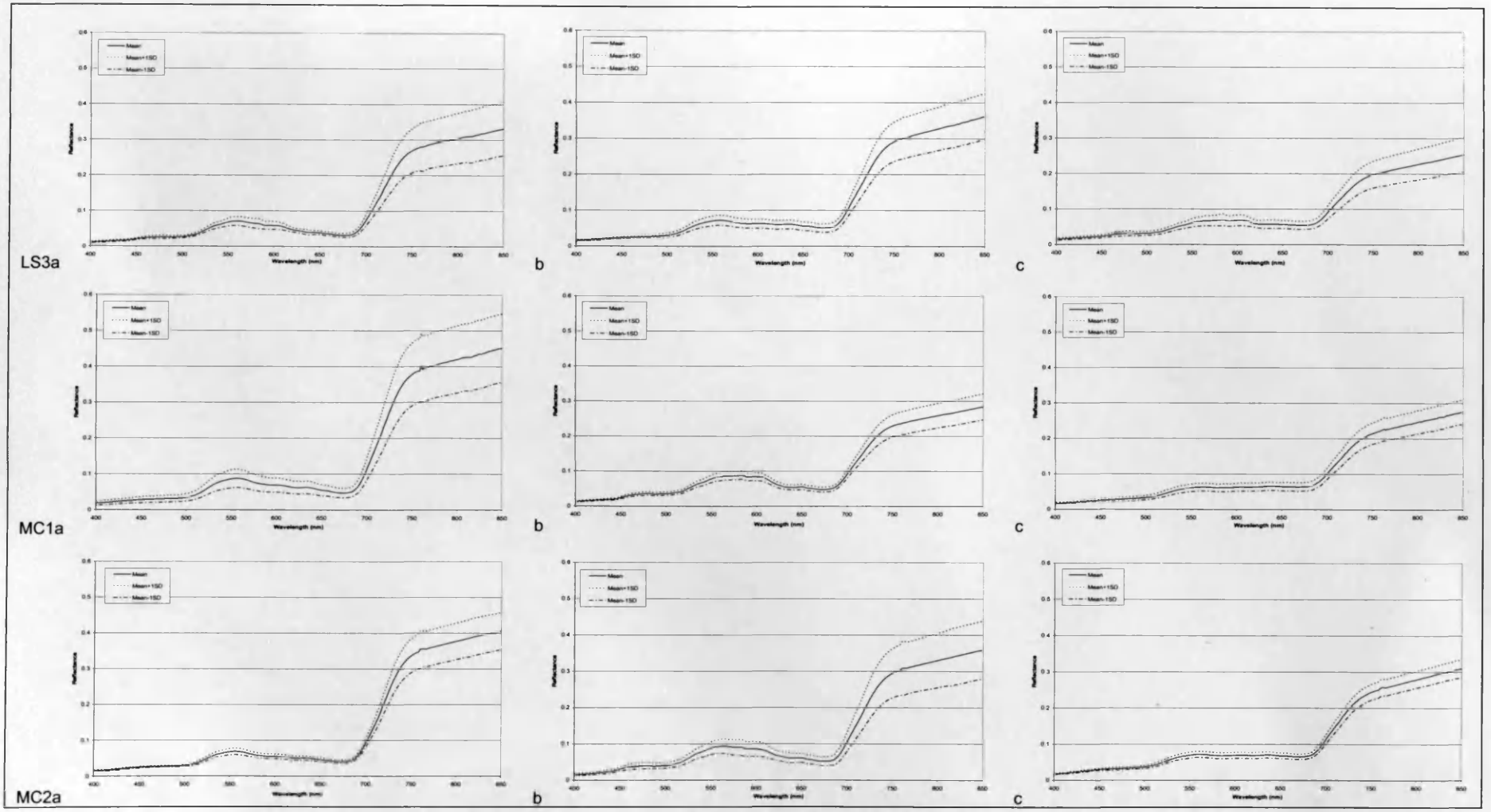

Figure 4:5 Mean spectra (and +/- 1 standard deviations) per study plot (LS3, MC1 and MC2) at each sampling stage a) July b) August c) September

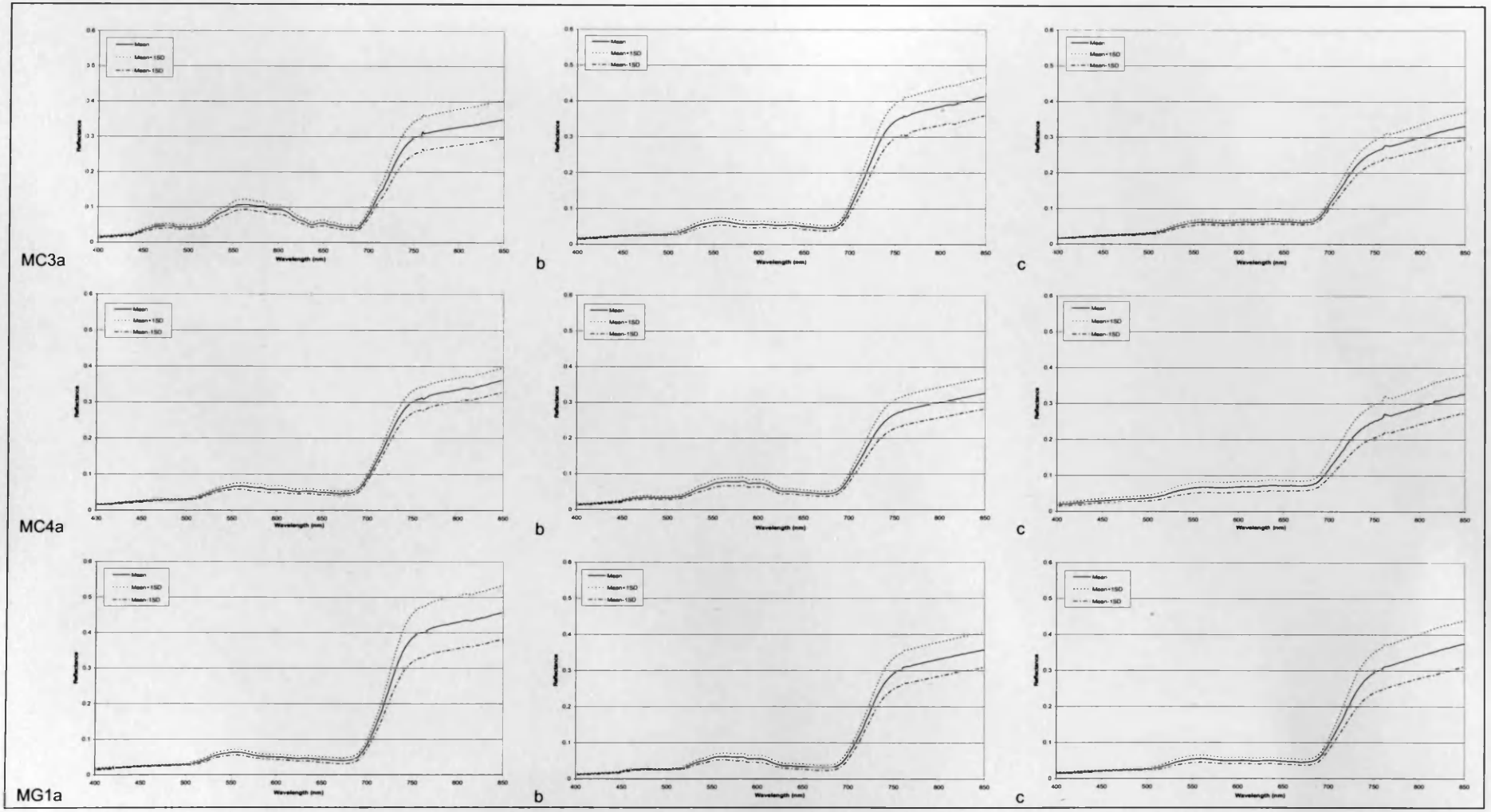

Figure 4:6 Mean spectra (and +/- 1 standard deviations) per study plot (MC3, MC4 and MG1) at each sampling stage a) July b) August c) September

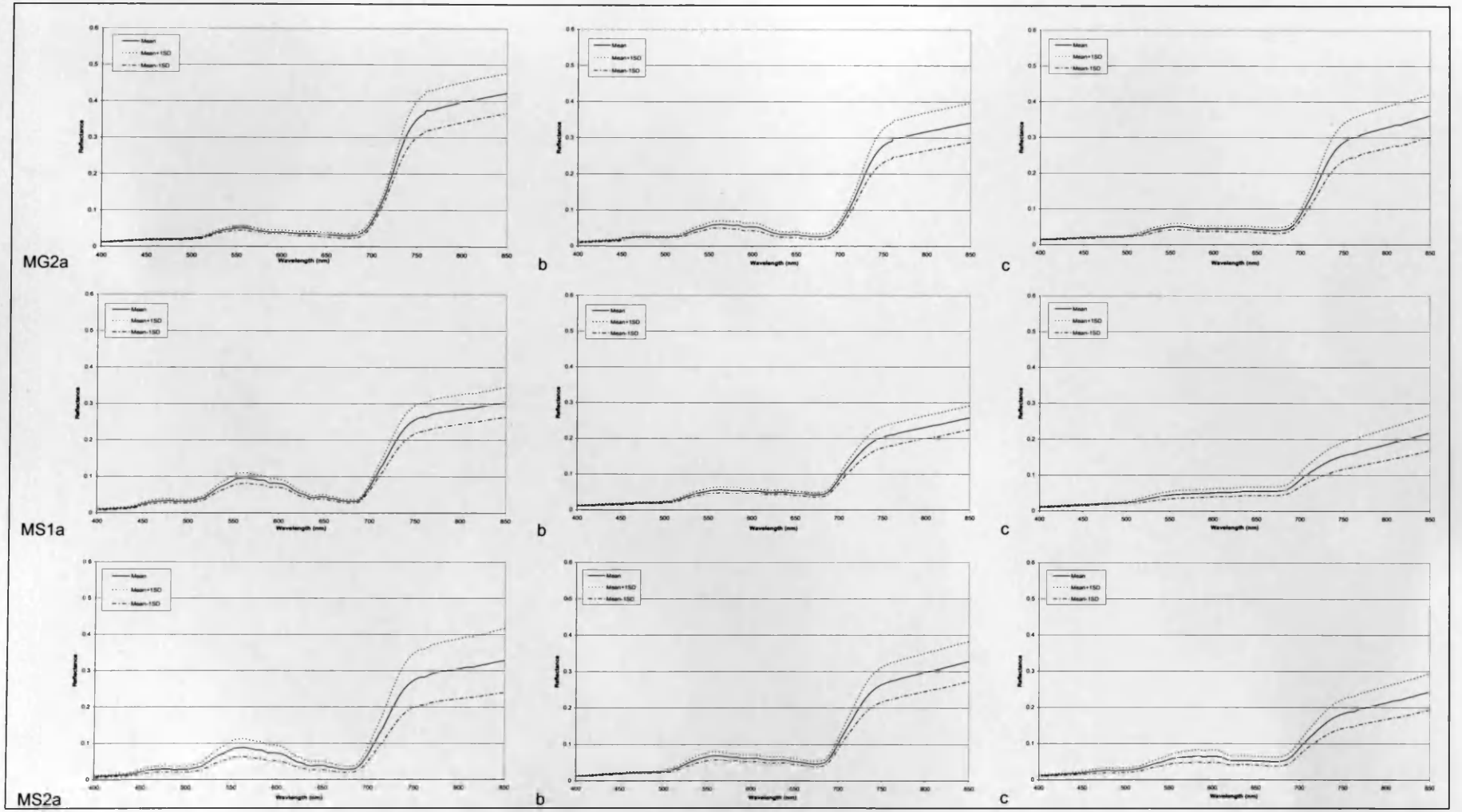

Figure 4:7 Mean spectra (and +/- 1 standard deviations) per study plot (MG2, MS1 and MS2) at each sampling stage a) July b) August c) September

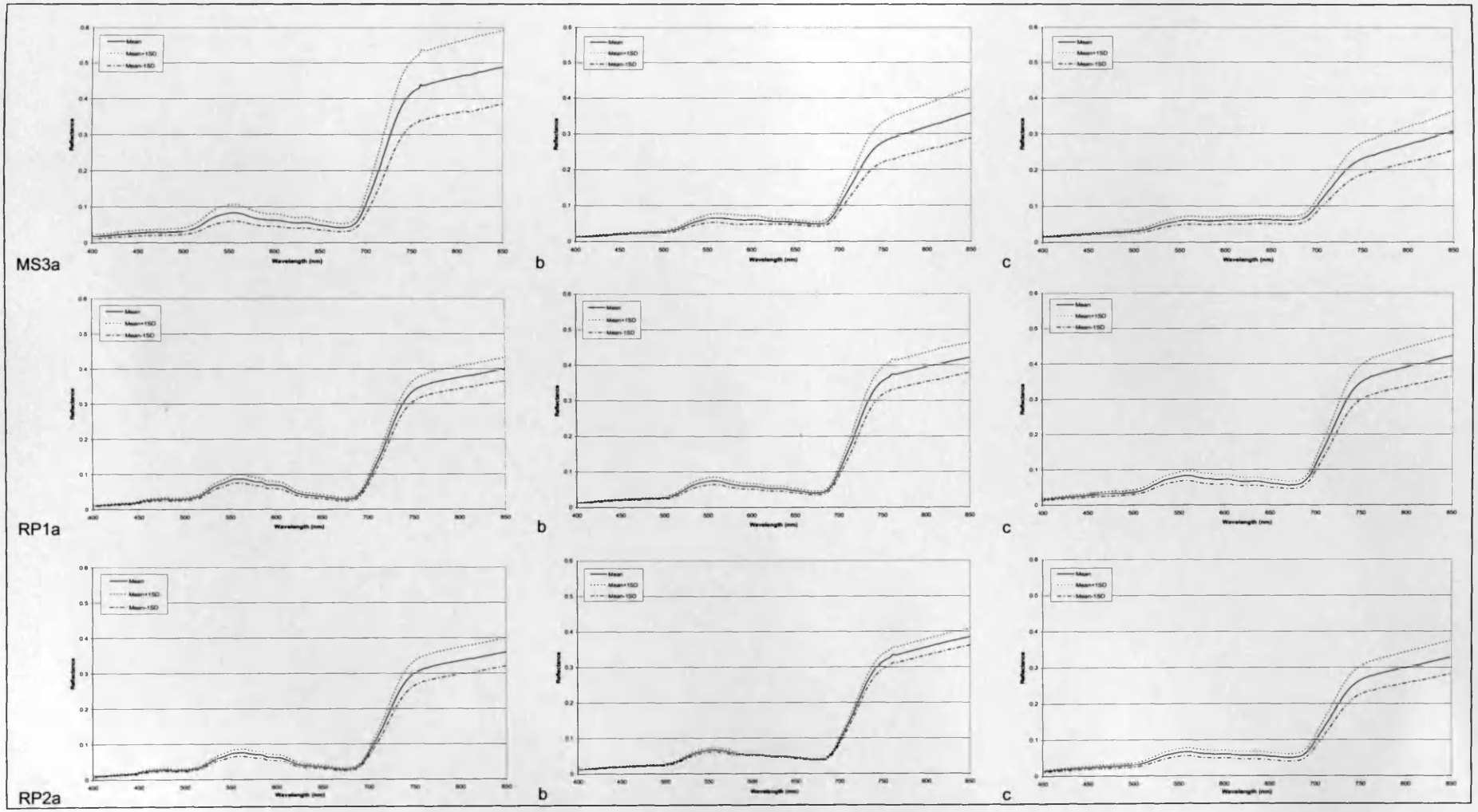

Figure 4:8 Mean spectra (and +/- 1 standard deviations) per study plot (MS3, RP1 and RP2) at each sampling stage a) July b) August c) September

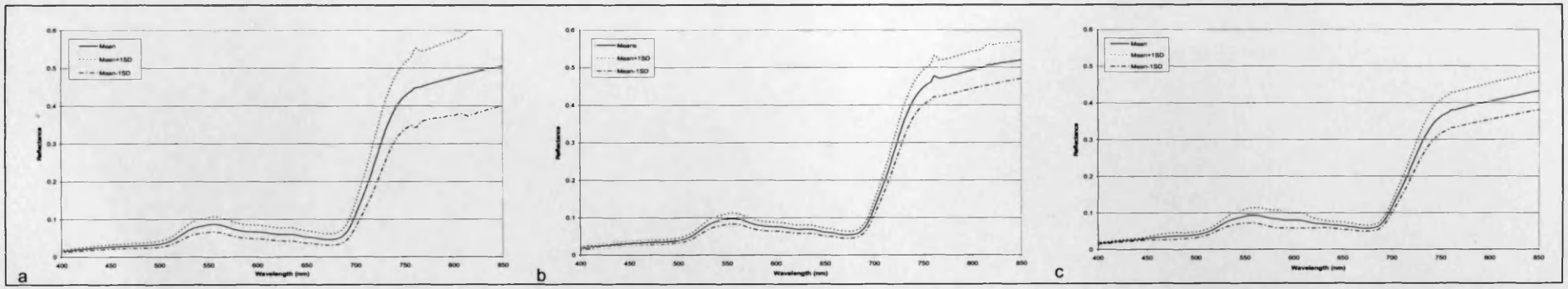

Figure 4:9 Mean spectra (and +/- 1 standard deviations) from RP3 at each sampling stage a) July b) August c) September

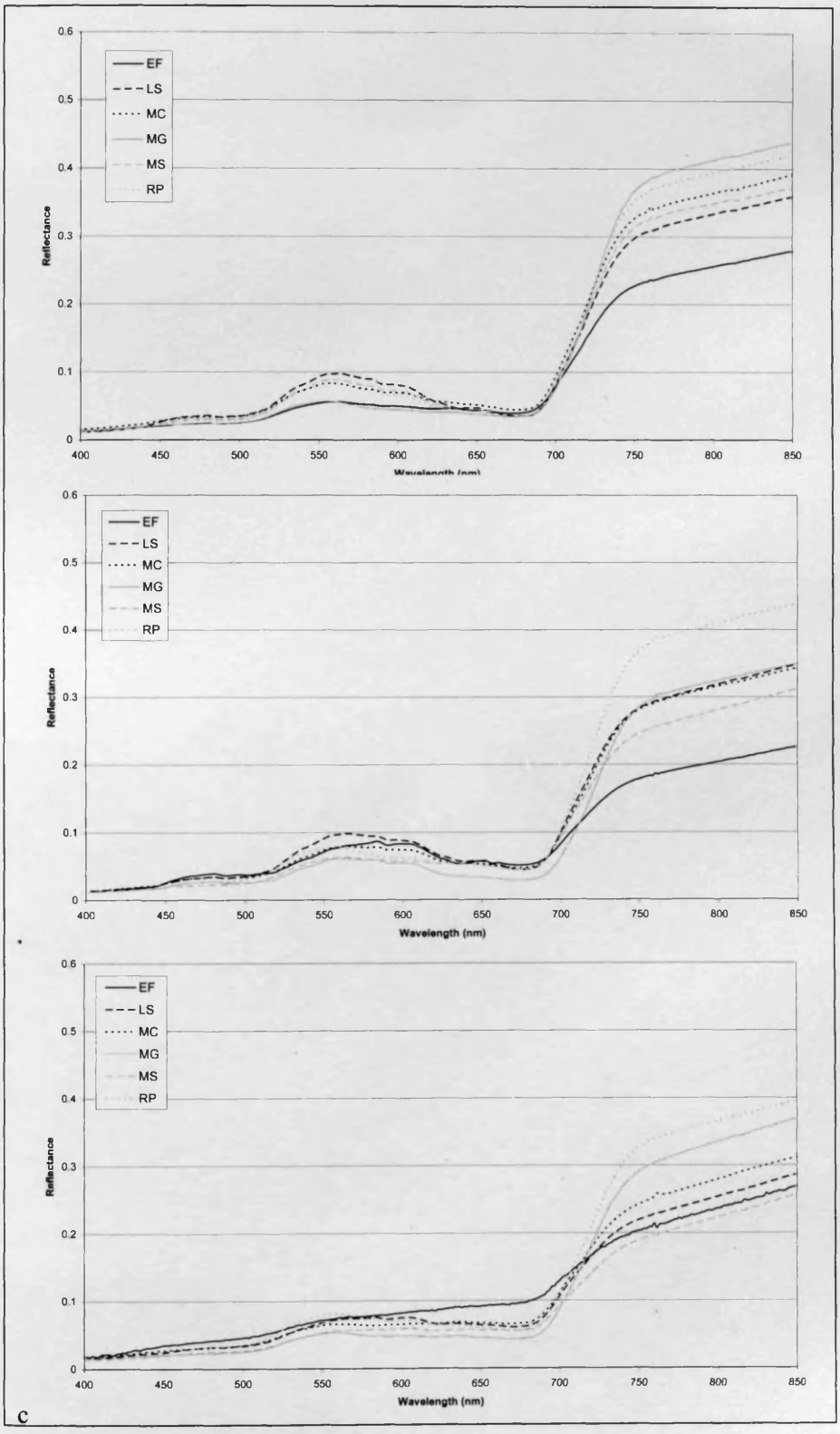

Figure 4:10 Mean spectra by habitat type a) July b) August c) September (EF=*Equisetum fluviatile*; LS=Species-rich low sedge; MC=*Molinia caerulea*-sedge mire; MG=*Molinia caerulea-Myrica gale* mire; MS=Mixed sedge; RP=Rush pasture/Grassland)

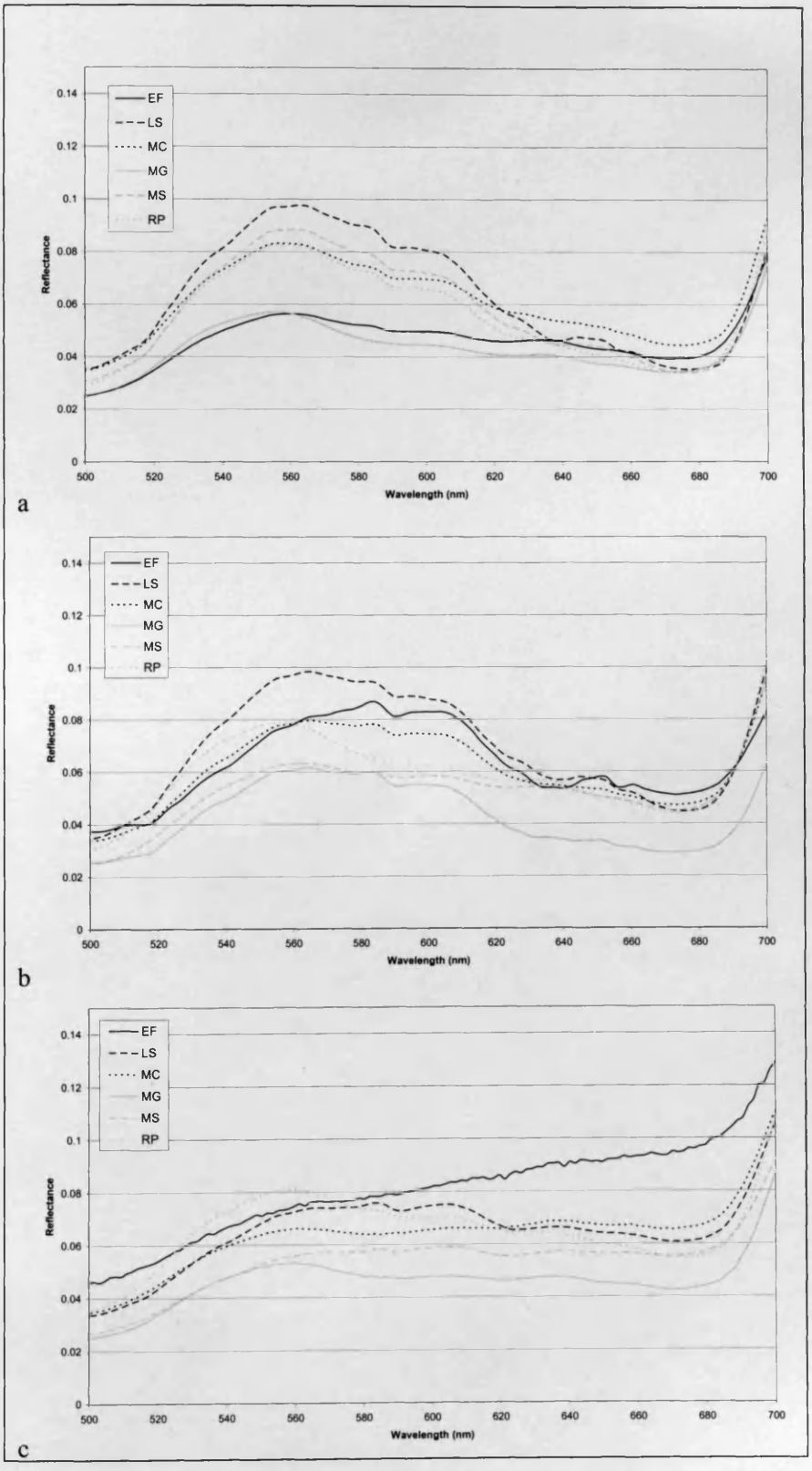

Figure 4:11 Mean spectra by habitat type (500 – 700 nm) a) July b) August c) September (EF=*Equisetum fluviatile*; LS=Species-rich low sedge; MC=*Molinia caerulea*-sedge mire; MG=*Molinia caerulea-Myrica gale* mire; MS=Mixed sedge; RP=Rush pasture/Grassland)

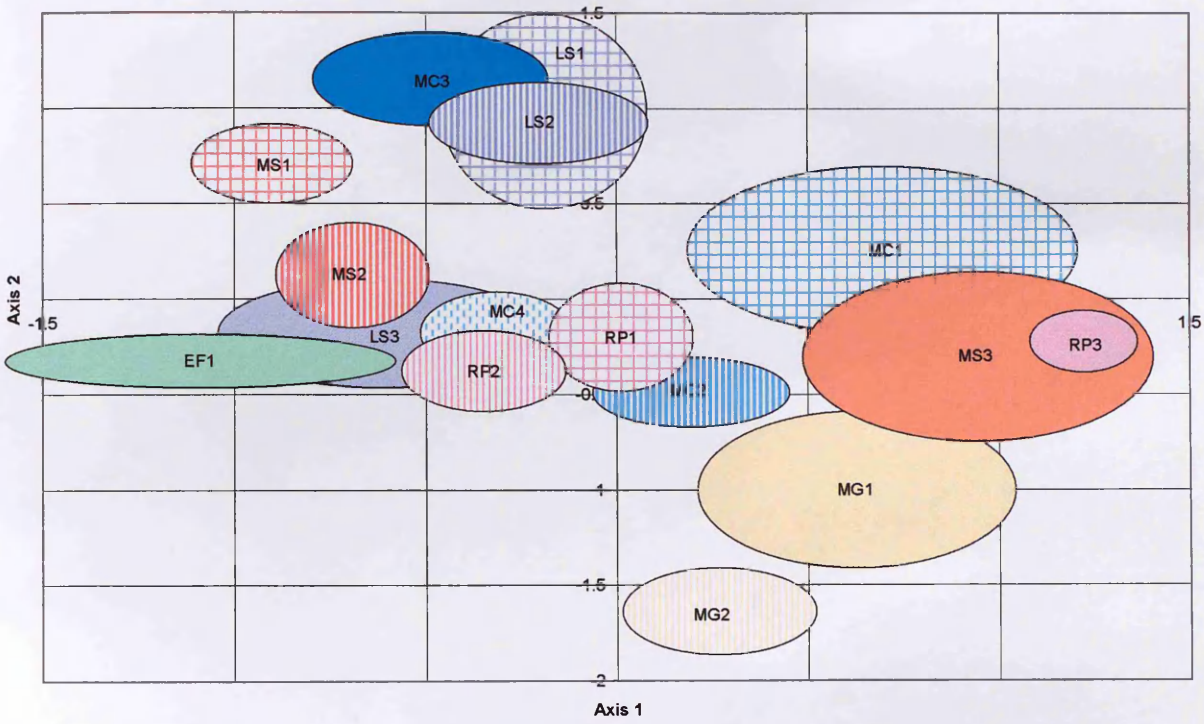

Figure 4:12 July Dataset: Study Plots-PCA using AVS 1-42 spectra (mean and +/- 1 SD) (eigenvalue Axis 1: 0.97; eigenvalue Axis 2: 0.02)

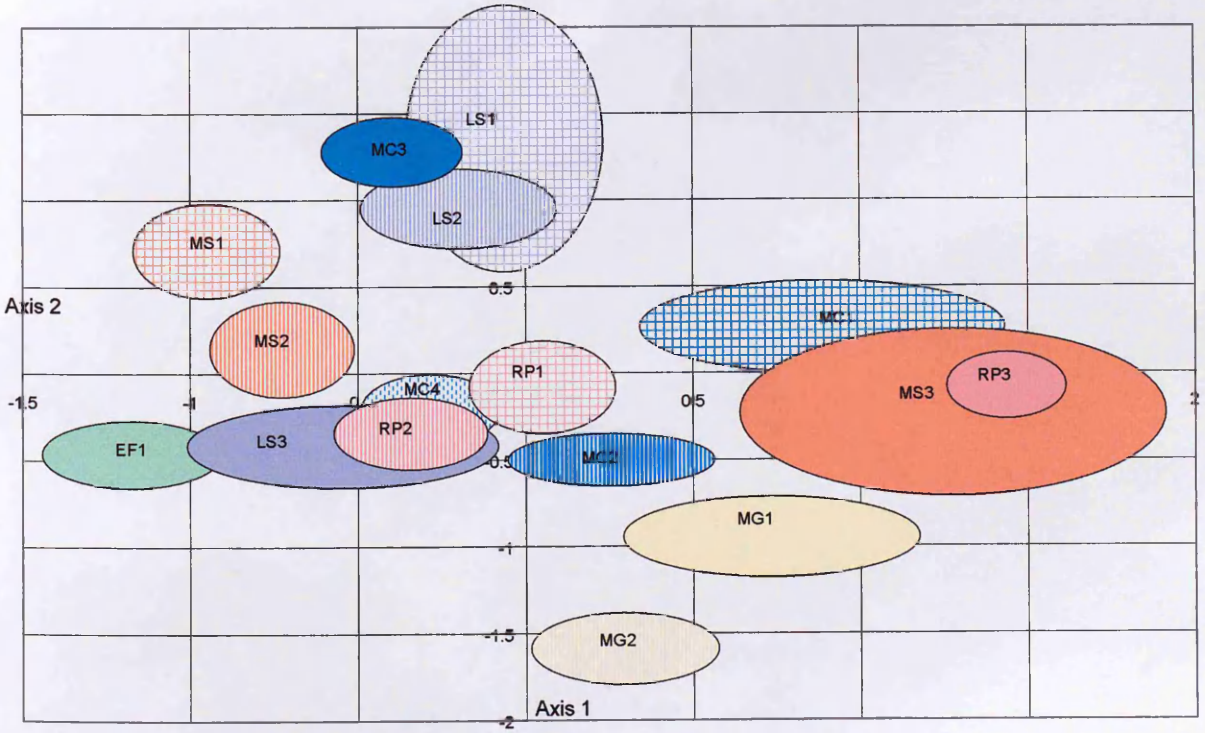

Figure 4:13 July Dataset: Study Plots-PCA using CASI bandwidths (mean and +/- 1 SD) (eigenvalue Axis 1: 0.97; eigenvalue Axis 2: 0.02)

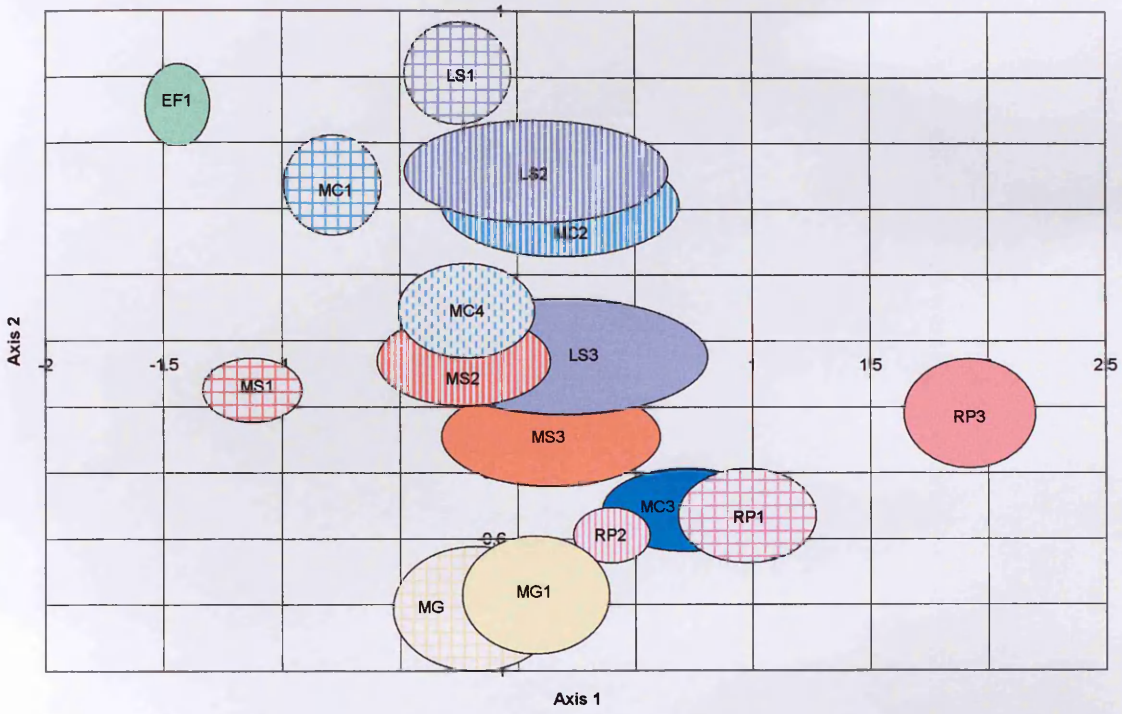

Figure 4:14 August Dataset: Study Plots-PCA using AVS 1-42 spectra (mean and +/- 1 SD) (eigenvalue Axis 1: 0.93; eigenvalue Axis 2: 0.05)

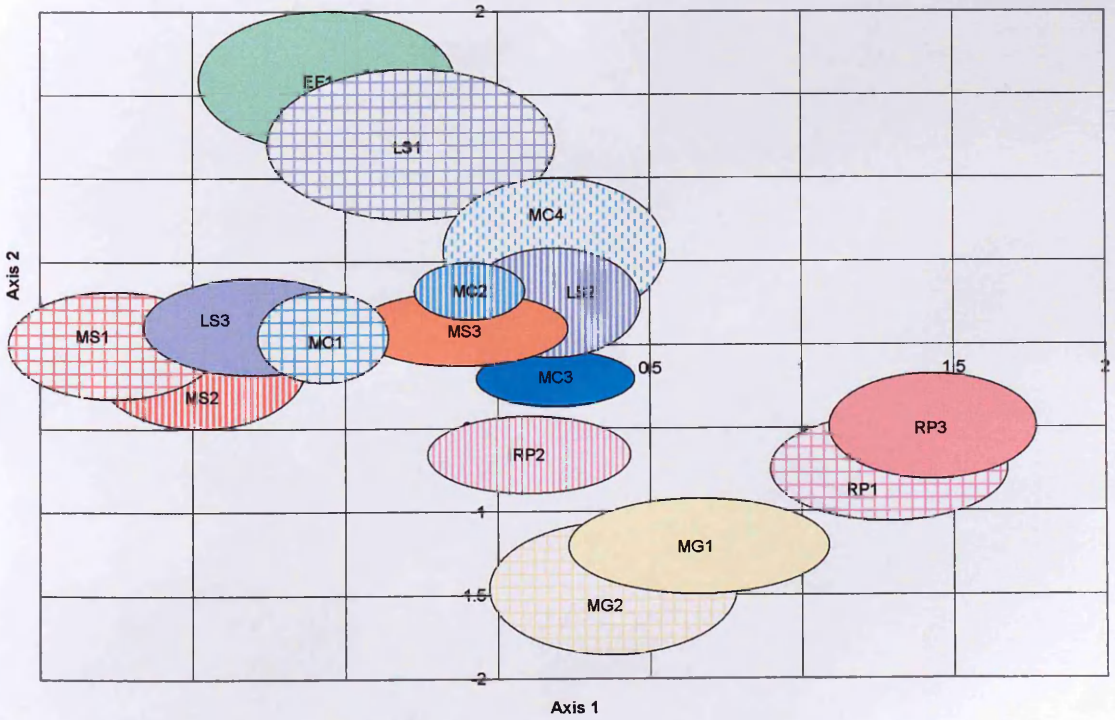

Figure 4:15 September Dataset: Study Plots-PCA using AVS 1-42 spectra (mean and +/- 1 SD) (eigenvalue Axis 1: 0.95; eigenvalue Axis 2: 0.03)

4.4.2 Objective b) Inter-habitat variation using Multiple Discriminant Analysis

Assess the degree to which spectra grouped by habitat are spectrally distinct using multivariate statistical analyses.

The output from MDA on the AVS1-42 and CASI datasets is presented in Appendix B. These results have been summarized and presented below in Table 4:2. The MDA output in SPSS provides a list of significant variables when a stepwise model is selected and these are listed for each analysis in Table 4:3 and Table 4:4 for the AVS1-42 and CASI datasets respectively.

Table 4:2 Results from Multiple Discriminant Analysis on the sample spectra grouped by habitat for all three sampling stages (EF=*Equisetum fluviatile*; LS=Species-rich low sedge; MC=*Molinia caerulea*-sedge mire; MG=*Molinia caerulea-Myrica gale* mire; MS=Mixed sedge; RP=Rush pasture/grassland; A=AVS1-42; C=CASI)

Dataset		Group 1 (EF)	2 (LS)	3 (MC)	4 (MG)	5 (MS)	6 (RP)	Overall accuracy (%) (Random*)
July	A	96.7	87.4	72.7	86.7	81.3	97.8	85.3 (14.7)
	C	96.7	72.4	77.3	86.7	51.6	78.9	74.1 (14.7)
Aug	A	96.7	94.4	94.4	91.7	96.4	100.0	95.6 (14.2)
	C	100.0	66.7	64.5	88.3	91.7	91.5	80.4 (15.0)
Sept	A	83.3	76.5	86.6	88.3	77.8	92.1	84.1 (14.2)
	C	90.0	74.1	88.3	90.0	72.2	88.8	83.1 (18.8)

*Results in brackets determined from randomizing group labels and performing MDA

Table 4:3 MDA results: Significant wavebands determined by MDA stepwise model (highlighted in bold)

	July			Aug			Sept		
AV1	348	-	363	**348**	**-**	**363**	**348**	**-**	**363**
AV2	364	-	378	364	-	378	364	-	378
AV3	**380**	**-**	**394**	**380**	**-**	**394**	**380**	**-**	**394**
AV4	**396**	**-**	**410**	**396**	**-**	**410**	**396**	**-**	**410**
AV5	**412**	**-**	**426**	**412**	**-**	**426**	**412**	**-**	**426**
AV6	**427**	**-**	**441**	**427**	**-**	**441**	427	-	441
AV7	**443**	**-**	**457**	**443**	**-**	**457**	**443**	**-**	**457**
AV8	**459**	**-**	**473**	**459**	**-**	**473**	**459**	**-**	**473**
AV9	475	-	489	475	-	489	475	-	489
AV10	490	-	505	**490**	**-**	**505**	**490**	**-**	**505**
AV11	**506**	**-**	**520**	506	-	520	**506**	**-**	**520**
AV12	522	-	536	**522**	**-**	**536**	522	-	536
AV13	538	-	552	**538**	**-**	**552**	**538**	**-**	**552**
AV14	553	-	568	553	-	568	553	-	568
AV15	**569**	**-**	**583**	569	-	583	569	-	583
AV16	**585**	**-**	**599**	585	-	599	585	-	599
AV17	601	-	615	601	-	615	601	-	615
AV18	616	-	631	**616**	**-**	**631**	616	-	631
AV19	632	-	646	**632**	**-**	**646**	**632**	**-**	**646**
AV20	648	-	662	**648**	**-**	**662**	648	-	662
AV21	664	-	678	664	-	678	664	-	678
AV22	680	-	694	**680**	**-**	**694**	**680**	**-**	**694**
AV23	695	-	709	695	-	709	**695**	**-**	**709**
AV24	**711**	**-**	**725**	**711**	**-**	**725**	711	-	725
AV25	727	-	741	727	-	741	727	-	741
AV26	743	-	757	743	-	757	743	-	757
AV27	758	-	773	**758**	**-**	**773**	**758**	**-**	**773**
AV28	**774**	**-**	**788**	774	-	788	774	-	788
AV29	790	-	804	790	-	804	**790**	**-**	**804**
AV30	806	-	820	806	-	820	806	-	820
AV31	821	-	836	**821**	**-**	**836**	821	-	836
AV32	837	-	851	837	-	851	837	-	851
AV33	853	-	867	853	-	867	853	-	867
AV34	**869**	**-**	**883**	869	-	883	869	-	883
AV35	884	-	899	884	-	899	884	-	899
AV36	900	-	914	900	-	914	900	-	914
AV37	916	-	930	916	-	930	916	-	930
AV38	**932**	**-**	**946**	**932**	**-**	**946**	932	-	946
AV39	948	-	962	948	-	962	948	-	962
AV40	963	-	978	963	-	978	963	-	978
AV41	979	-	993	979	-	993	979	-	993
AV42	**995**	**-**	**1009**	995	-	1009	995	-	1009

Table 4:4 MDA results: Significant wavebands-CASI (highlighted in bold)

	July			Aug			Sept		
CASI1	**441**	-	***461**	**441**	-	***461**	**441**	-	**461**
CASI2	**548**	-	***557**	**548**	-	**557**	**548**	-	**557**
CASI3	**666**	-	**674**	666	-	674	**666**	-	**674**
CASI4	**694**	-	**703**	694	-	703	**694**	-	***703**
CASI5	**705**	-	**711**	**705**	-	***711**	**705**	-	***711**
CASI6	736	-	744	736	-	744	736	-	744
CASI7	746	-	753	**746**	-	**753**	**746**	-	***753**
CASI8	**775**	-	***784**	**775**	-	***784**	775	-	784
CASI9	**815**	-	**824**	815	-	824	**815**	-	**824**
CASI10	**860**	-	**870**	860	-	870	**860**	-	**870**

*top three

4.4.3 Objective c) Within-habitat variation

Explore the within habitat spectral variation using data collected from two or more study plots within each habitat type.

Figure 4:16 to Figure 4:18 illustrate the mean spectra grouped by habitat type with the respective standard deviations in July, August and September respectively. These provide some indication as to the spread of the data when spectra from two or more study plots are grouped together to represent the habitat type. Principal Components Analysis (Figure 4:19 to Figure 4:21) also illustrates the structure of the dataset in terms of the separability between the samples when grouped by habitat type.

These datasets were analysed using formal statistics in order to determine the significance of the variation in the spectral response at each CASI waveband present within the dataset. Prior to analysis, tests for normality were carried out on the data collected at each waveband for each point within every study plot. The results are presented in Appendix B and indicate that there are some non-normal distributions in certain wavebands and the extent differs amongst the samples. The non-parametric test Kruskal Wallis was applied and the results presented in Table 4:5 to Table 4:7 (full statistical outputs are presented in Appendix B).

There appears to be statistically significant variance within the chosen habitats using the data collected at the respective study plots. It was therefore inappropriate to group the data before

analyzing the spectral separability between the habitats themselves (Objective c)) and as such, only one plot from each habitat type was selected to then explore the spectral dissimilarity between these particular plots over the sampling period (Figure 4:22).

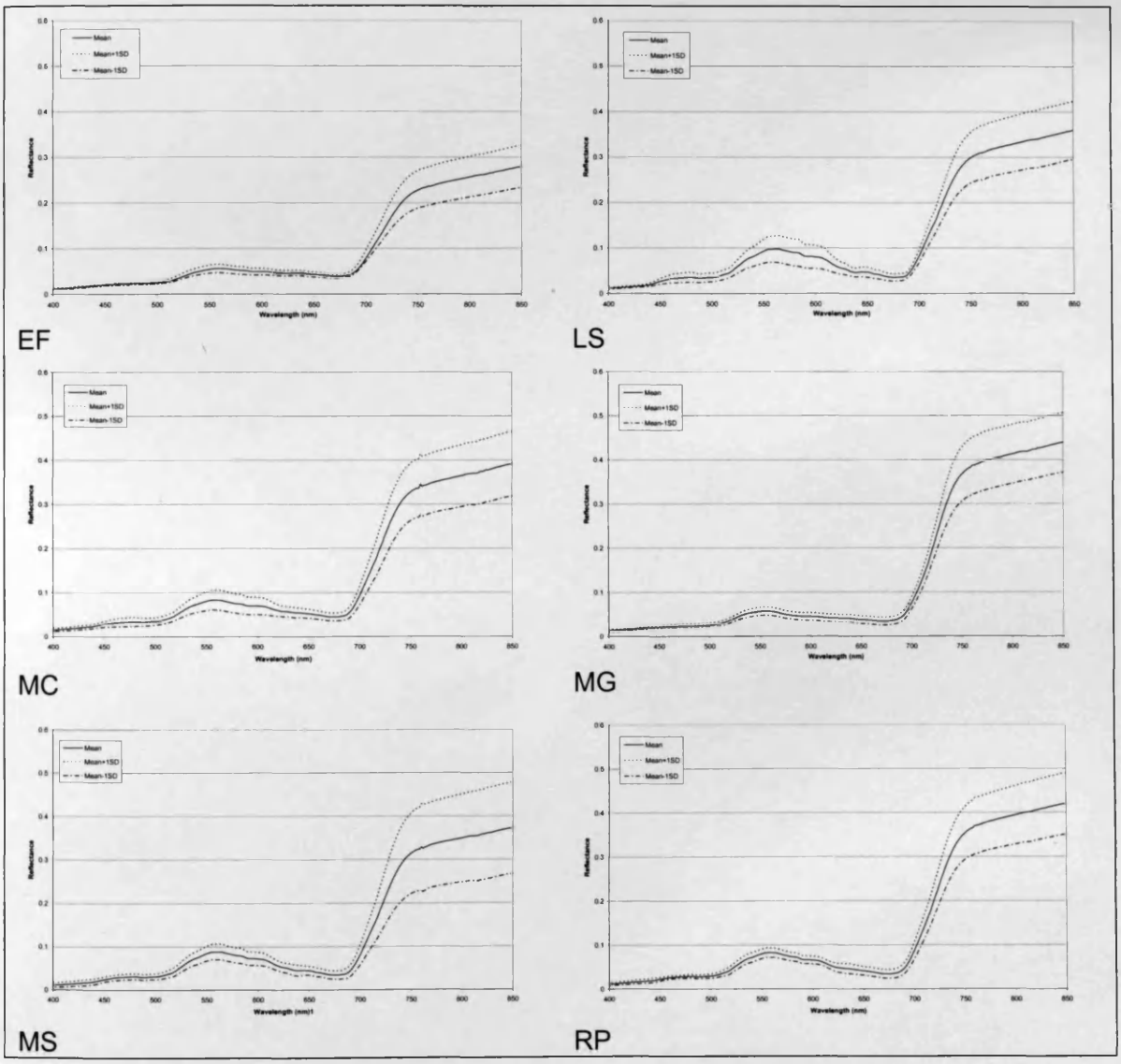

Figure 4:16 Mean spectra grouped by habitat type collected in July 2003 (EF1 shown as 'EF' for illustrative purposes) EF=*Equisetum fluviatile*; LS=Species-rich low sedge; MC=*Molinia caerulea*-sedge mire; MG=*Molinia caerulea-Myrica gale* mire; MS=Mixed sedge; RP=Rush pasture/Grassland

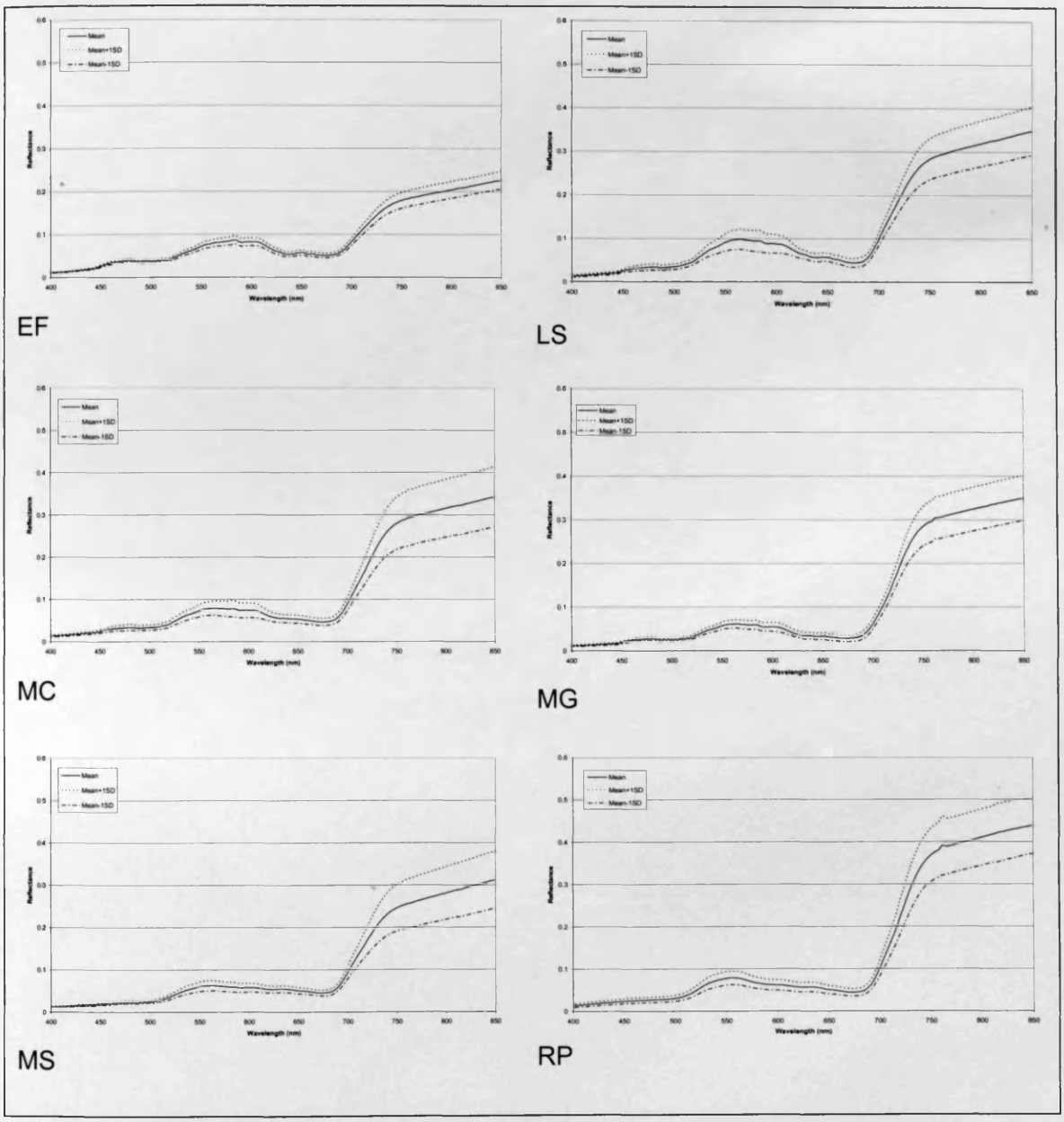

Figure 4:17 Mean spectra grouped by habitat type collected in August 2003 (EF1 shown as 'EF' for illustrative purposes) EF=*Equisetum fluviatile*; LS=Species-rich low sedge; MC=*Molinia caerulea*-sedge mire; MG=*Molinia caerulea-Myrica gale* mire; MS=Mixed sedge; RP=Rush pasture/grassland

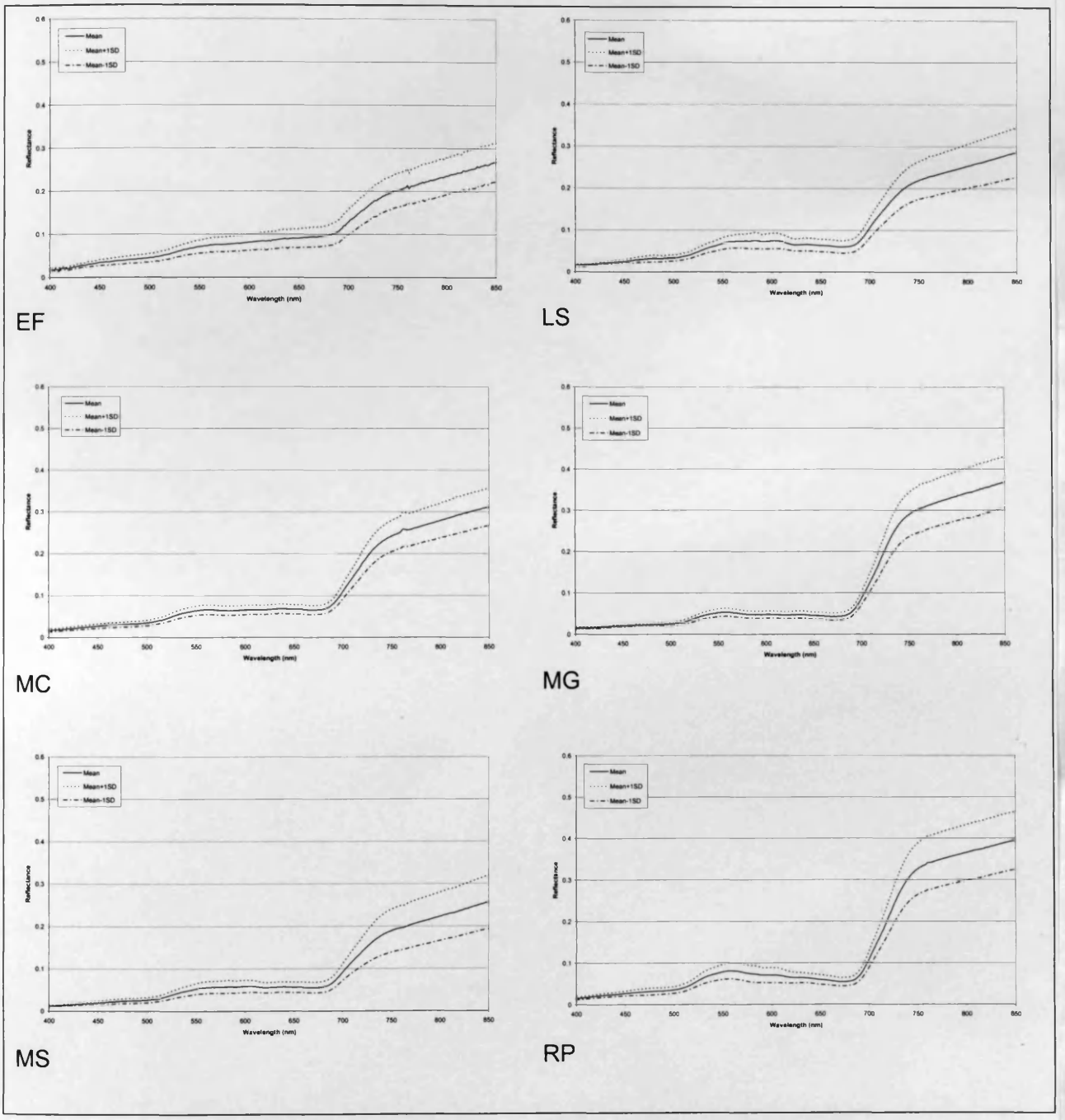

Figure 4:18 Mean spectra grouped by habitat type collected in September 2003 (EF1 shown as 'EF' for illustrative purposes) EF=*Equisetum fluviatile*; LS=Species-rich low sedge; MC=*Molinia caerulea*-sedge mire; MG=*Molinia caerulea-Myrica gale* mire; MS=Mixed sedge; RP=Rush pasture/grassland

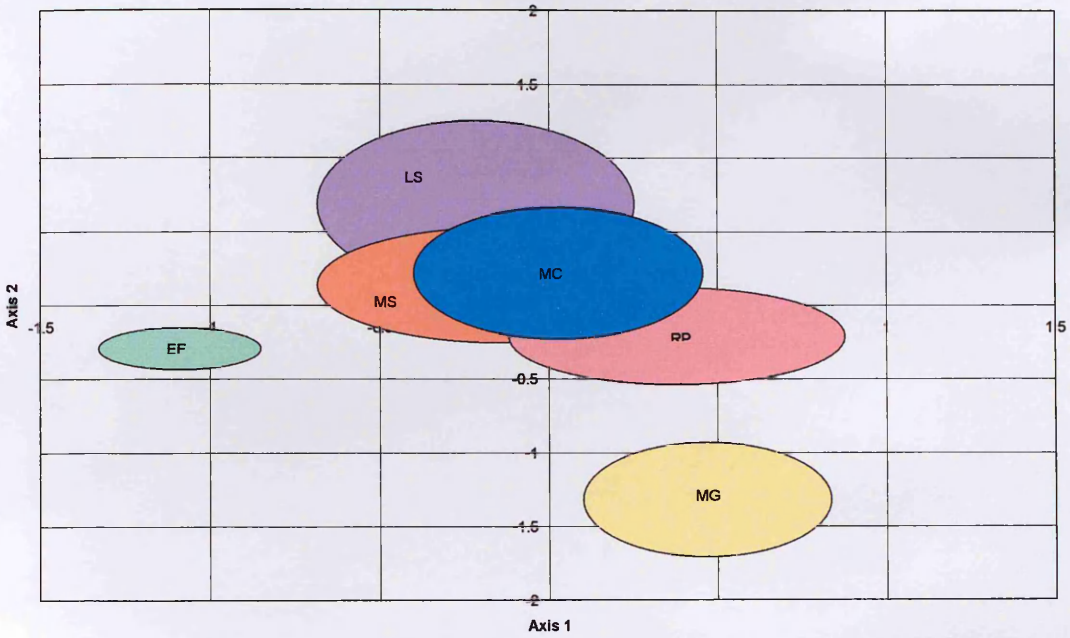

Figure 4:19 July Dataset: PCA results grouped by Habitat Type (mean and +/- 1 SD) (eigenvalue Axis 1: 0.97; eigenvalue Axis 2: 0.02) (EF=*Equisetum fluviatile*; LS=Species-rich low sedge; MC=Molinia *caerulea*-sedge mire; MG=*Molinia caerulea-Myrica gale* mire; MS=Mixed sedge; RP=Rush pasture/grassland)

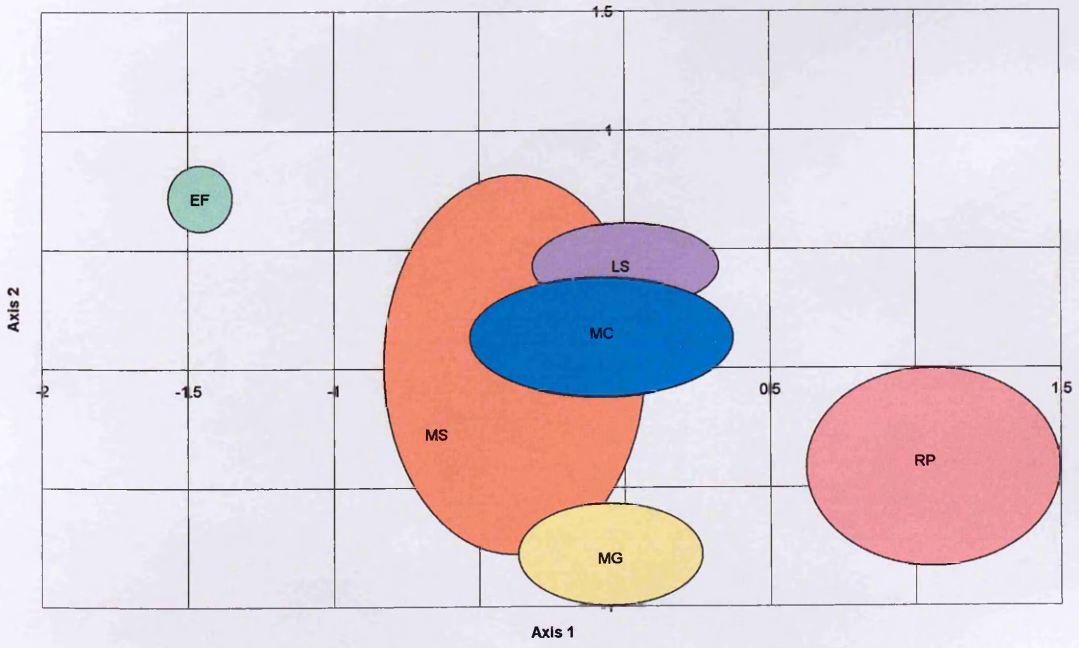

Figure 4:20 August Dataset: PCA results grouped by Habitat Type (mean and +/- 1 SD) (eigenvalue Axis 1: 0.93; eigenvalue Axis 2: 0.05) (EF=*Equisetum fluviatile*; LS=Species-rich low sedge; MC=*Molinia caerulea*-sedge mire; MG=*Molinia caerulea-Myrica gale* mire; MS=Mixed sedge; RP=Rush pasture/grassland)

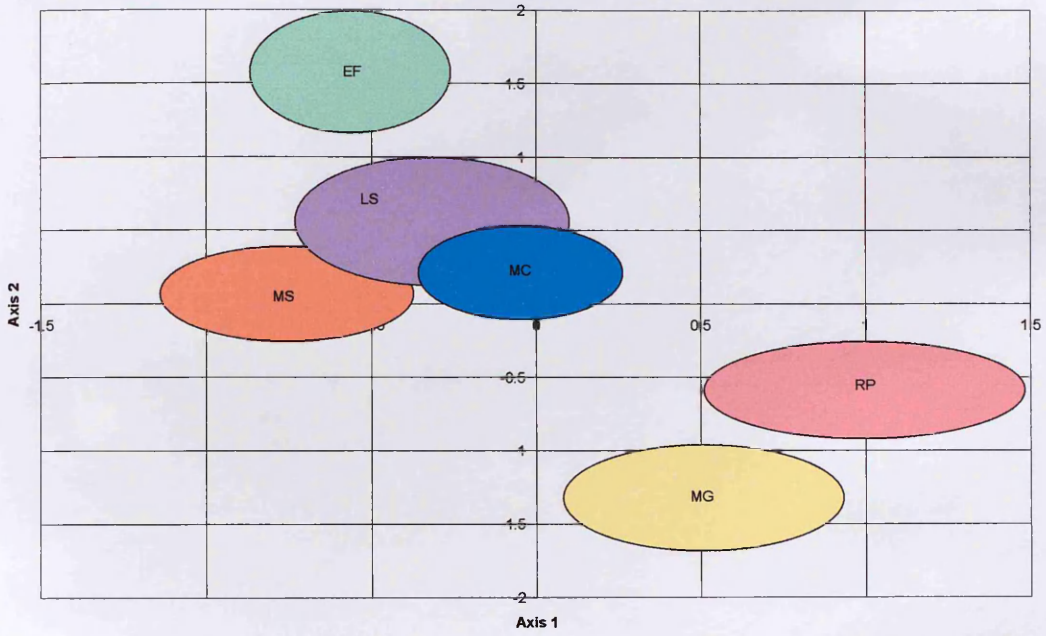

Figure 4:21 September Dataset: PCA results grouped by Habitat Type (mean and +/- 1 SD) (Eigenvalue Axis 1: 0.95; eigenvalue Axis 2: 0.03) (EF=*Equisetum fluviatile*; LS=Species-rich low sedge; MC=*Molinia caerulea*-sedge mire; MG=*Molinia caerulea-Myrica gale* mire; MS=Mixed sedge; RP=Rush pasture/grassland)

Table 4:5 Results from Kruskal Wallis H test (July) (highlighted: P=<0.05) ('C'=CASI band; EF=*Equisetum fluviatile*; LS=Species-rich low sedge; MC=*Molinia caerulea*-sedge mire; MG=*Molinia caerulea-Myrica gale* mire; MS=Mixed sedge; RP=Rush pasture/grassland)

	C-1	C-2	C-3	C-4	C-5	C-6	C-7	C-8	C-9	C-10
LS	0.000	0.000	0.000	0.000	0.000	0.006	0.009	0.012	0.011	0.023
MC	0.000	0.000	0.033	0.000	0.000	0.000	0.000	0.000	0.000	0.000
MG	0.000	0.000	0.000	0.000	0.000	0.002	0.006	0.014	0.030	0.016
MS	0.001	0.048	0.000	0.000	0.000	0.000	0.000	0.000	0.000	0.000
RP	0.000	0.000	0.000	0.000	0.000	0.000	0.000	0.000	0.000	0.000

Table 4:6 Results from Kruskal Wallis H test (August) (highlighted: P=<0.05) ('C'=CASI band; EF=*Equisetum fluviatile*; LS=Species-rich low sedge; MC=*Molinia caerulea*-sedge mire; MG=*Molinia caerulea-Myrica gale* mire; MS=Mixed sedge; RP=Rush pasture/grassland)

	C-1	C-2	C-3	C-4	C-5	C-6	C-7	C-8	C-9	C-10
LS	0.001	0.000	0.419	0.800	0.723	0.072	0.054	0.044	0.039	0.017
MC	0.000	0.000	0.060	0.028	0.000	0.000	0.000	0.000	0.000	0.000
MG	0.249	0.564	0.086	0.062	0.033	0.231	0.337	0.367	0.359	0.308
MS	0.000	0.000	0.005	0.000	0.000	0.000	0.000	0.000	0.000	0.000
RP	0.000	0.000	0.000	0.000	0.000	0.000	0.000	0.000	0.000	0.000

Table 4:7 Results from Kruskal Wallis H test (September) (highlighted: P=<0.05) ('C'=CASI band; EF=*Equisetum fluviatile*; LS=Species-rich low sedge; MC=*Molinia caerulea*-sedge mire; MG=*Molinia caerulea-Myrica gale* mire; MS=Mixed sedge; RP=Rush pasture/grassland)

	C-1	C-2	C-3	C-4	C-5	C-6	C-7	C-8	C-9	C-10
LS	0.000	0.000	0.000	0.000	0.000	0.000	0.000	0.000	0.000	0.000
MC	0.000	0.001	0.008	0.008	0.001	0.000	0.000	0.000	0.000	0.000
MG	0.22	0.243	0.076	0.022	0.035	0.535	0.647	0.636	0.451	0.515
MS	0.000	0.000	0.013	0.004	0.000	0.000	0.000	0.000	0.000	0.000
RP	0.000	0.000	0.007	0.000	0.000	0.000	0.000	0.000	0.000	0.000

4.4.4 Objective d) Between-habitat variation

Explore the between habitat variation at different wavelengths using study plots from each habitat type.

Figure 4:22 illustrates the mean spectra collected from each of the study plots used to meet the objective outlined above. The Mann Whitney test (equivalent to the parametric Two-sample T-test) was applied (at each CASI band) and the results are presented in Table 4:8 to Table 4:10. Figure 4:23 to Figure 4:25 show the mean, maximum and minimum spectra obtained from the spectral responses at each sample point from the RP1 (Rush pasture/grassland) study plot and the EF1 (*Equisetum fluviatile*) study plots in July, August and September respectively. Areas of the graphs in grey represent wavelengths (using the AVS1-42 datasets) at which a significant difference (at the 95% significance level) was determined between the two datasets.

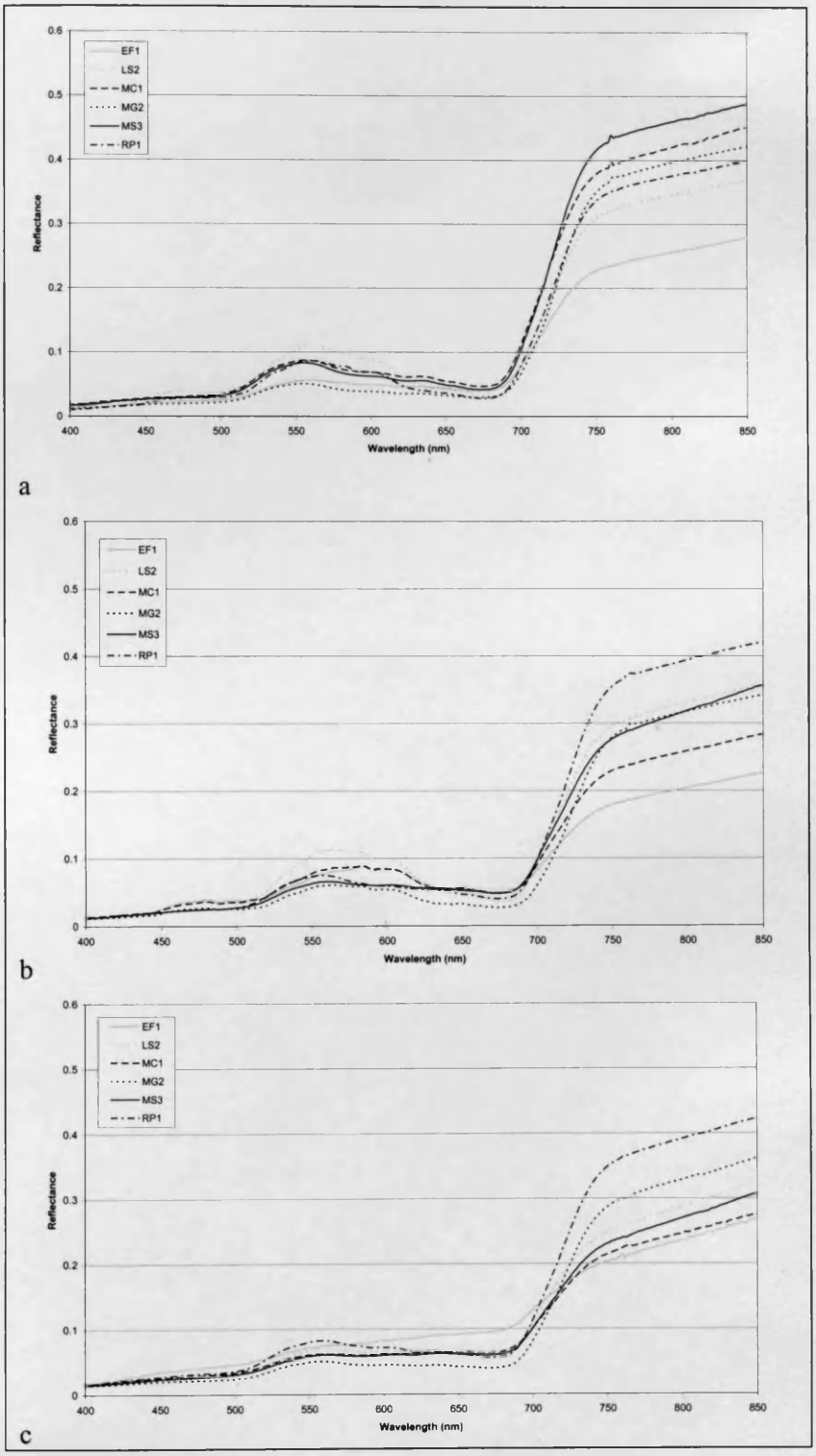

Figure 4:22 Mean spectra from the six study plots analysed using Mann Whitney statistical test a) July b) August c) September (EF=*Equisetum fluviatile*; LS=Species-rich low sedge; MC=*Molinia caerulea*-sedge mire; MG=*Molinia caerulea-Myrica gale* mire; MS=Mixed sedge; RP=Rush pasture/grassland)

Table 4:8 Mann Whitney Results: July (Highlighted cells are significant at P<0.005)

Plots		CASI1	CASI2	CASI3	CASI4	CASI5	CASI6	CASI7	CASI8	CASI9	CASI10	NDVI	Total*
EF1	LS2	0.0000	0.0000	0.0000	0.9117	0.0008	0.0000	0.0000	0.0000	0.0000	0.0000	0.0000	10
EF1	MC1	0.0006	0.0000	0.0251	0.0000	0.0000	0.0000	0.0000	0.0000	0.0000	0.0000	0.0000	11
EF1	MG2	0.0016	0.0163	0.0000	0.0000	0.4918	0.0000	0.0000	0.0000	0.0000	0.0000	0.0000	10
EF1	MS3	0.0004	0.0000	0.2226	0.0001	0.0000	0.0000	0.0000	0.0000	0.0000	0.0000	0.0000	10
EF1	RP1	0.0969	0.0000	0.0000	0.9940	0.0001	0.0000	0.0000	0.0000	0.0000	0.0000	0.0000	9
LS2	MC1	0.2116	0.0016	0.0000	0.0000	0.0000	0.0015	0.0022	0.0019	0.0018	0.0007	0.0519	9
LS2	MG2	0.0000	0.0000	0.0044	0.0000	0.0000	0.0351	0.0112	0.0040	0.0037	0.0037	0.0006	11
LS2	MS3	0.0484	0.0000	0.0001	0.0000	0.0000	0.0000	0.0000	0.0000	0.0000	0.0000	0.1297	10
LS2	RP1	0.0000	0.0000	0.0018	0.9215	0.5696	0.0514	0.0414	0.0285	0.0399	0.0514	0.0009	7
MC1	MG2	0.0000	0.0000	0.0000	0.0000	0.0000	0.2009	0.3953	0.6100	0.6309	0.4035	0.0000	6
MC1	MS3	0.6952	0.6520	0.1809	0.4290	0.6520	0.2458	0.1453	0.1224	0.1907	0.2581	0.0000	1
MC1	RP1	0.0071	0.8142	0.0000	0.0000	0.0002	0.1796	0.2717	0.2990	0.2783	0.1276	0.0000	5
MG2	MS3	0.0000	0.0000	0.0000	0.0000	0.0000	0.0004	0.0012	0.0026	0.0024	0.0021	0.0010	11
MG2	RP1	0.0003	0.0000	0.6767	0.0001	0.0000	0.8378	0.4439	0.2223	0.1202	0.0909	0.3511	4
MS3	RP1	0.0047	0.4621	0.0000	0.0000	0.0001	0.0001	0.0001	0.0001	0.0000	0.0000	0.0004	10
	Total*	12	12	12	12	12	10	11	11	11	10	12	

*Significant at P<0.005

Table 4:9 Mann Whitney Results: August (Highlighted cells are significant at P<0.005)

Plots		CASI1	CASI2	CASI3	CASI4	CASI5	CASI6	CASI7	CASI8	CASI9	CASI10	NDVI	Total*
EF1	LS2	0.5997	0.0000	0.0042	0.0000	0.0000	0.0000	0.0000	0.0000	0.0000	0.0000	0.0000	10
EF1	MC1	0.0138	0.0679	0.0150	0.0392	0.0001	0.0000	0.0000	0.0000	0.0000	0.0000	0.0000	9
EF1	MG2	0.0000	0.0000	0.0000	0.0000	0.0006	0.0000	0.0000	0.0000	0.0000	0.0000	0.0000	11
EF1	MS3	0.0000	0.0014	0.0434	0.0016	0.0000	0.0000	0.0000	0.0000	0.0000	0.0000	0.0000	11
EF1	RP1	0.0000	0.2707	0.0000	0.0000	0.0000	0.0000	0.0000	0.0000	0.0000	0.0000	0.0000	10
LS2	MC1	0.0056	0.0000	0.7394	0.0002	0.0000	0.0000	0.0000	0.0001	0.0000	0.0001	0.0001	10
LS2	MG2	0.0000	0.0000	0.0000	0.0000	0.0000	0.9470	0.3255	0.1260	0.1809	0.3632	0.0000	6
LS2	MS3	0.0000	0.0000	0.6664	0.0862	0.0926	0.9798	0.7933	0.5595	0.3840	0.1484	0.7417	2
LS2	RP1	0.0000	0.0000	0.0003	0.2226	0.0877	0.0000	0.0000	0.0000	0.0000	0.0000	0.0000	9
MC1	MG2	0.0000	0.0000	0.0000	0.0000	0.0000	0.0004	0.0000	0.0000	0.0000	0.0000	0.0000	11
MC1	MS3	0.0003	0.0000	0.9798	0.1437	0.0384	0.0016	0.0010	0.0005	0.0001	0.0000	0.0000	9
MC1	RP1	0.0011	0.2973	0.0001	0.0122	0.0000	0.0000	0.0000	0.0000	0.0000	0.0000	0.0000	10
MG2	MS3	0.1960	0.0802	0.0000	0.0000	0.0000	0.8724	0.6912	0.6062	1.0000	0.4519	0.0000	4
MG2	RP1	0.0083	0.0000	0.0000	0.0000	0.0000	0.0000	0.0000	0.0000	0.0000	0.0000	0.0019	11
MS3	RP1	0.2831	0.0004	0.0002	0.5828	0.0110	0.0000	0.0000	0.0000	0.0000	0.0003	0.0000	9
	Total*	13	11	12	10	13	12	12	12	12	12	14	

*Significant at P<0.005

Table 4:10 Mann Whitney Results: September (Highlighted cells are significant at P<0.005)

Plots		CASI1	CASI2	CASI3	CASI4	CASI5	CASI6	CASI7	CASI8	CASI9	CASI10	NDVI	Total*
EF1	LS2	0.0000	0.5373	0.0000	0.0049	1.0000	0.0003	0.0001	0.0001	0.0001	0.0000	0.0000	9
EF1	MC1	0.0000	0.0138	0.0000	0.0000	0.0191	0.3953	0.2905	0.2905	0.4119	0.4643	0.0000	6
EF1	MG2	0.0000	0.0000	0.0000	0.0000	0.0011	0.0000	0.0000	0.0000	0.0000	0.0000	0.0000	11
EF1	MS3	0.0000	0.0014	0.0000	0.0000	0.0451	0.0351	0.0215	0.0150	0.0108	0.0037	0.0000	11
EF1	RP1	0.0001	0.0251	0.0000	0.0070	0.1335	0.0000	0.0000	0.0000	0.0000	0.0000	0.0000	10
LS2	MC1	0.0026	0.0210	0.0060	0.0959	0.0022	0.0003	0.0004	0.0002	0.0001	0.0000	0.0000	10
LS2	MG2	0.0773	0.0000	0.0000	0.0000	0.0000	0.0400	0.0133	0.0110	0.0274	0.0572	0.0000	9
LS2	MS3	0.1790	0.0023	0.1179	0.0509	0.0146	0.0595	0.0759	0.0862	0.0926	0.1261	0.0000	3
LS2	RP1	0.0000	0.0003	0.8724	0.9125	0.0368	0.0000	0.0000	0.0000	0.0000	0.0000	0.0000	9
MC1	MG2	0.0002	0.0004	0.0000	0.0001	0.1297	0.0000	0.0000	0.0000	0.0000	0.0000	0.0000	10
MC1	MS3	0.1055	0.4119	0.2340	0.9470	0.5895	0.1958	0.1858	0.0933	0.0451	0.0108	0.0002	3
MC1	RP1	0.0701	0.0000	0.0053	0.0327	0.0000	0.0000	0.0000	0.0000	0.0000	0.0000	0.0000	10
MG2	MS3	0.0058	0.0018	0.0000	0.0001	0.1055	0.0012	0.0005	0.0005	0.0017	0.0051	0.0000	10
MG2	RP1	0.0000	0.0000	0.0000	0.0000	0.0000	0.0000	0.0000	0.0001	0.0001	0.0003	0.0232	11
MS3	RP1	0.0042	0.0000	0.1297	0.0555	0.0000	0.0000	0.0000	0.0000	0.0000	0.0000	0.0000	9
	Total*	11	13	11	10	10	12	12	12	13	12	15	

*Significant at P<0.005

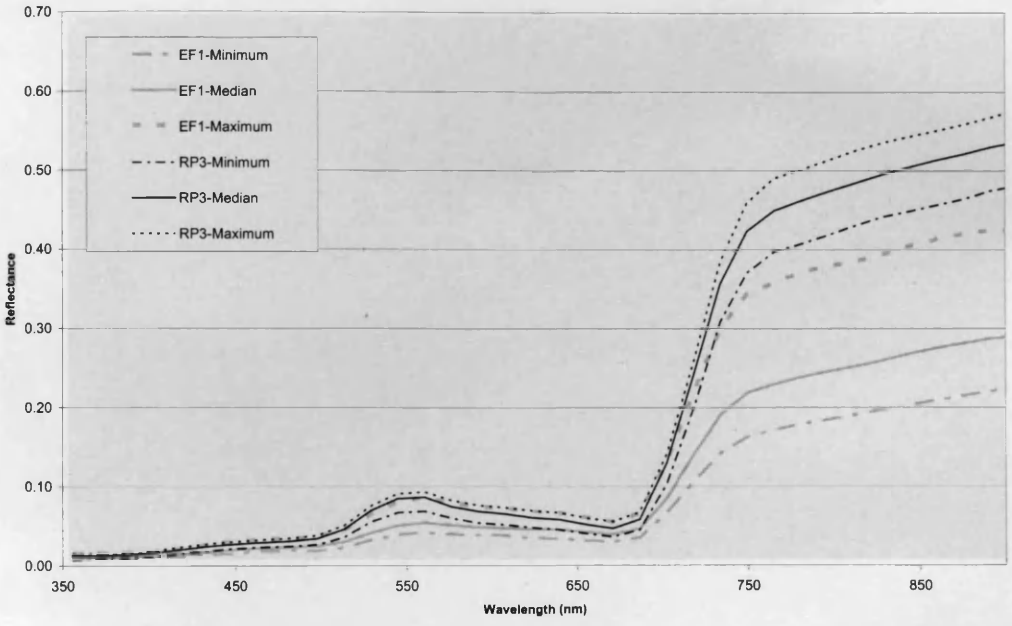

Figure 4:23 July Dataset: Mean, minimum and maximum spectra from RP1 and EF1-significantly different (95% Significance Level) at all wavelengths (greyed area)

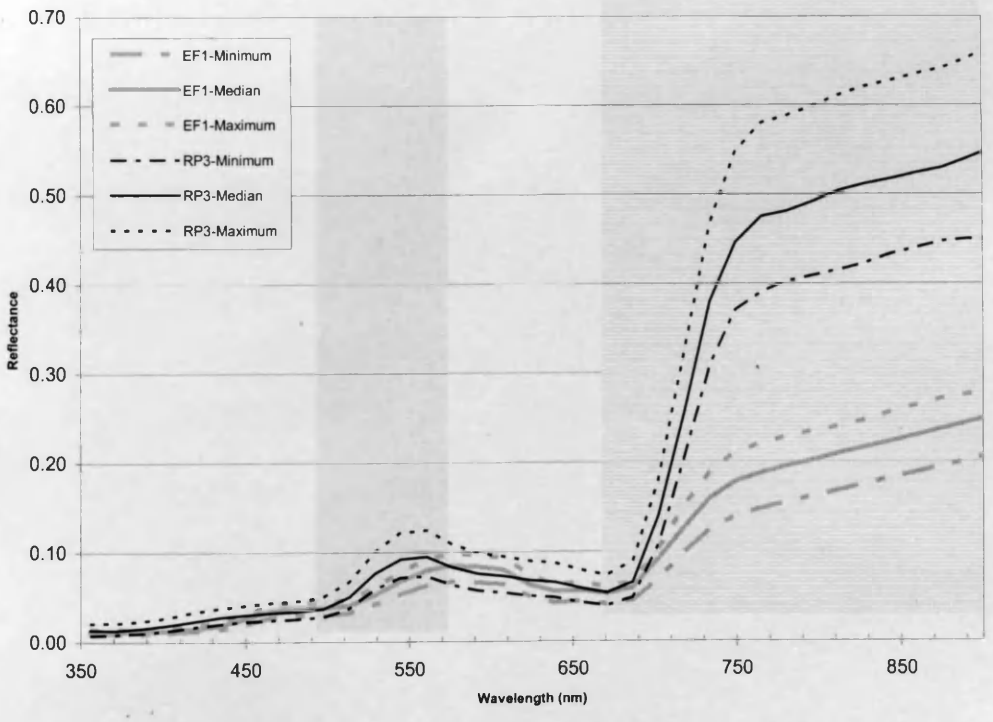

Figure 4:24 August Dataset: Mean, minimum and maximum spectra from RP1 and EF1-Significantly different (95% Significance Level) at wavelengths highlighted in grey

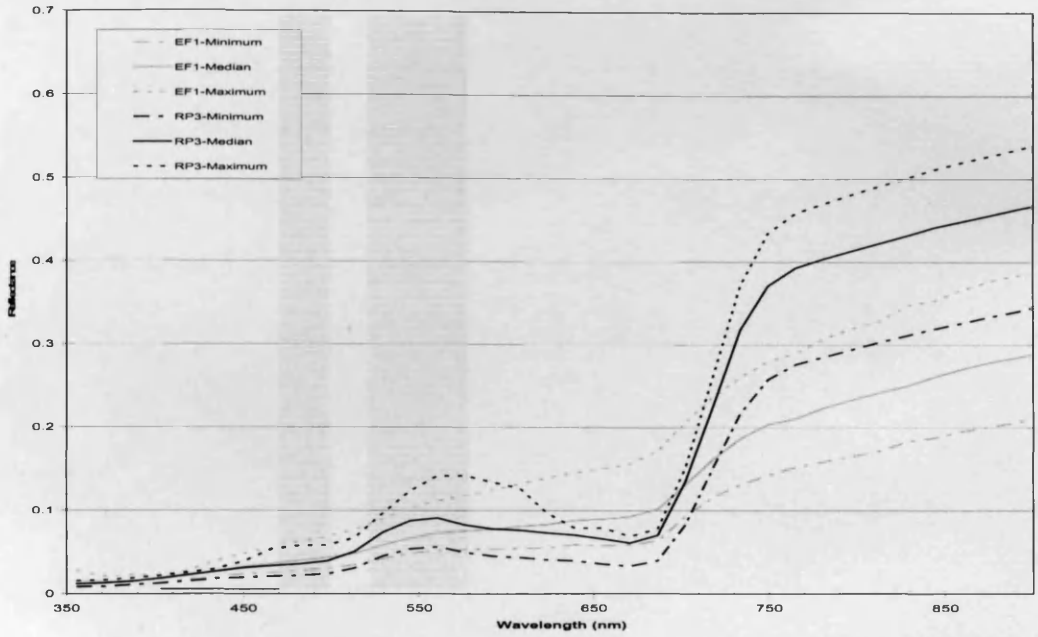

Figure 4:25 September Dataset: Mean, minimum and maximum spectra from RP1 and EF1-Significantly different (95% Significance Level) at wavelengths highlighted in grey

4.4.5 Objective e) Spectral indices

Determine the between habitat variation as illustrated by spectral indices and geostatistics.

Normalized Difference Vegetation Index (NDVI)

Box and whisker plots are an effective method of visualising the spread of values within a dataset and their distribution about the median. It is also quick and easy to then compare between groups. Figure 4:26 illustrates the NDVI values calculated per study plot (results from normality tests shown in Appendix B) and Figure 4:27 shows these as samples grouped by habitat type. Grouping the data by habitat type and testing the separability between habitat types using ANOVA or Kruskal Wallis tests is only feasible if it can be established that the samples from two or more study plots in the same habitat type are from the same population. Normality tests on the data grouped by habitat type are not carried out therefore as the within habitat variation between NDVI values at different study plots is first determined. The Kruskal Wallis method was used as some non-normal distributions in NDVIs were calculated at the study plots (Table 4:11 – full statistical output Appendix B).

Table 4:12 displays the results from Mann Whitney analyses on study plots representing each of the six habitat types. Although the results from the Kruskal Wallis analyses suggest that these particular study plots are not necessarily representative of the habitat type (or 'population') themselves, the results in Table 4:12 do provide some indication as to how the dissimilarity in NDVI between the habitat types does vary temporally. They also highlight the habitat types, as represented by these study plots, which may be problematic to distinguish between at certain times over the summer period.

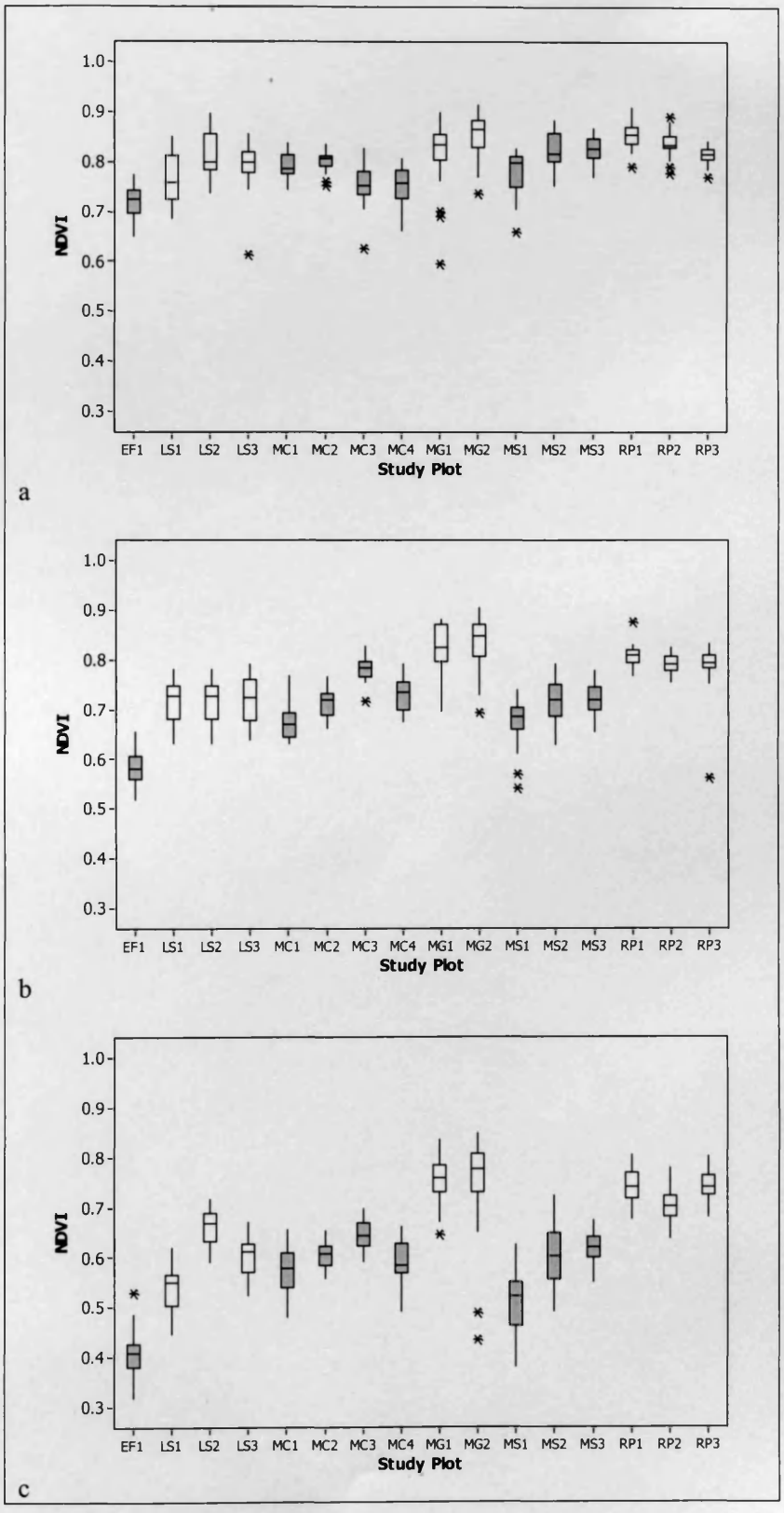

Figure 4:26 Box and whisker plots of NDVI values calculated at each study plot - a) July, b) August and c) September (asterisks = outliers)

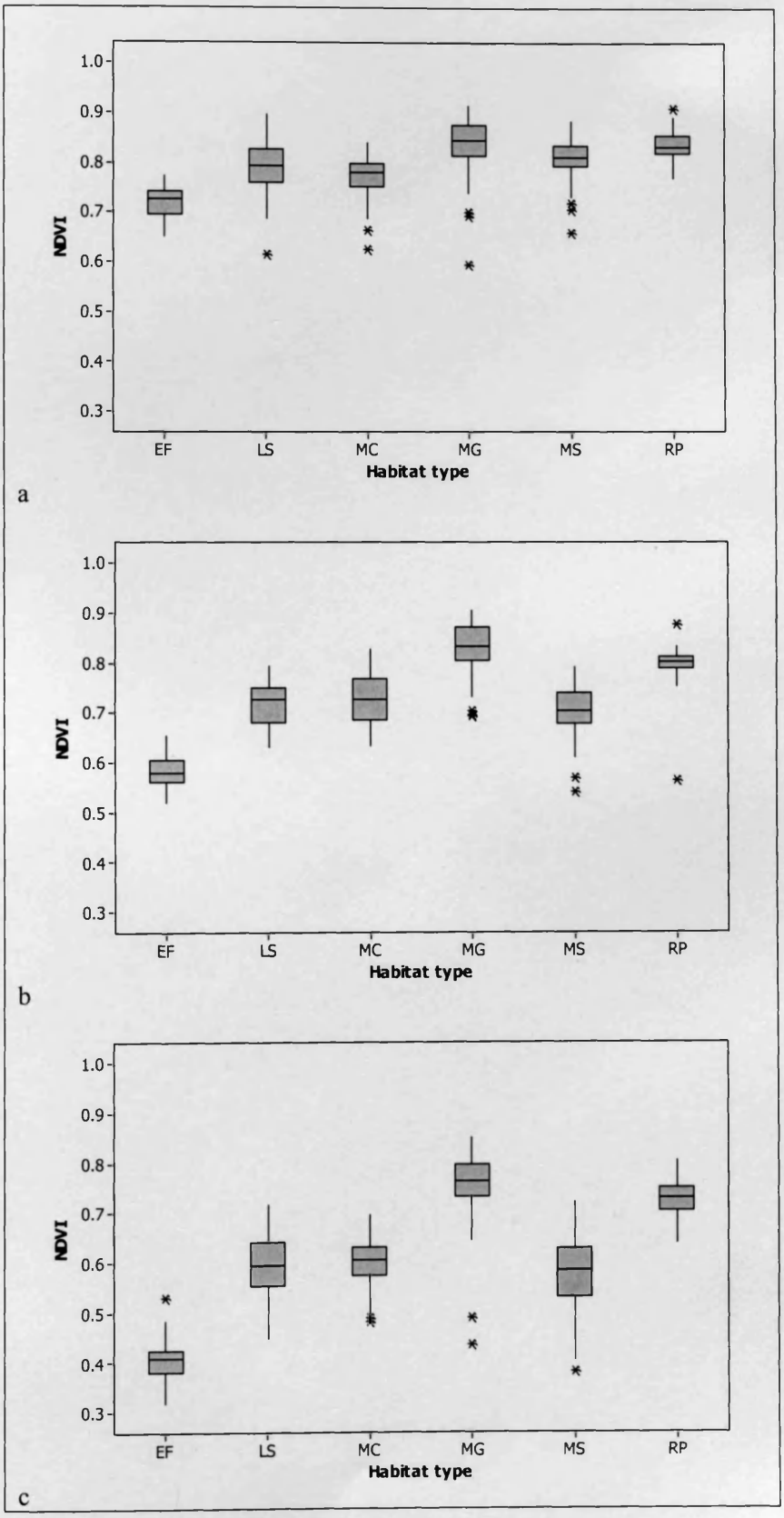

Figure 4:27 Box and whisker plots of NDVI values grouped by habitat type - a) July, b) August and c) September (asterisks = outliers)

Table 4:11 Results from Kruskal Wallis Analysis using NDVI values calculated from two or more study plots within each habitat type (highlighted cells are significant at P<0.05)

Habitat	July	Aug	Sept
LS	0.001	0.954	0.000
MC	0.000	0.000	0.000
MG	0.000	0.344	0.214
MS	0.000	0.000	0.000
RP	0.000	0.015	0.000

Table 4:12 Results from Mann Whitney calculations using NDVI values from study plots EF1, LS2, MC1, MG2, MS3, RP3 (highlighted cells are significant at P<0.05)

Plots		July	Aug	Sept
EF1	LS2	0.0000	0.0000	0.0000
EF1	MC1	0.0000	0.0000	0.0000
EF1	MG2	0.0000	0.0000	0.0000
EF1	MS3	0.0000	0.0000	0.0000
EF1	RP1	0.0000	0.0000	0.0000
LS2	MC1	0.0519	0.0001	0.0000
LS2	MG2	0.0006	0.0000	0.0000
LS2	MS3	0.1297	0.7417	0.0000
LS2	RP1	0.0009	0.0000	0.0000
MC1	MG2	0.0000	0.0000	0.0000
MC1	MS3	0.0000	0.0000	0.0002
MC1	RP1	0.0000	0.0000	0.0000
MG2	MS3	0.0010	0.0000	0.0000
MG2	RP1	0.3511	0.0019	0.0232
MS3	RP1	0.0004	0.0000	0.0000
	Total*	13	14	15

*Significant at P<0.005

1st Derivatives

The 1st derivative values of each sample spectrum within each study plot and at every sampling stage was calculated and from this the REIP was derived. These results are presented here grouped by habitat type in order to identify any inherent differences in the

pattern of the 1st derivative. Standard deviations across habitat means are also shown. Next to each of the 1st derivative slopes shown in Figure 4:28 to Figure 4:29 are graphs to show the shape of the first derivative slope in respective habitat types in the region between 650 nm and 790 nm.

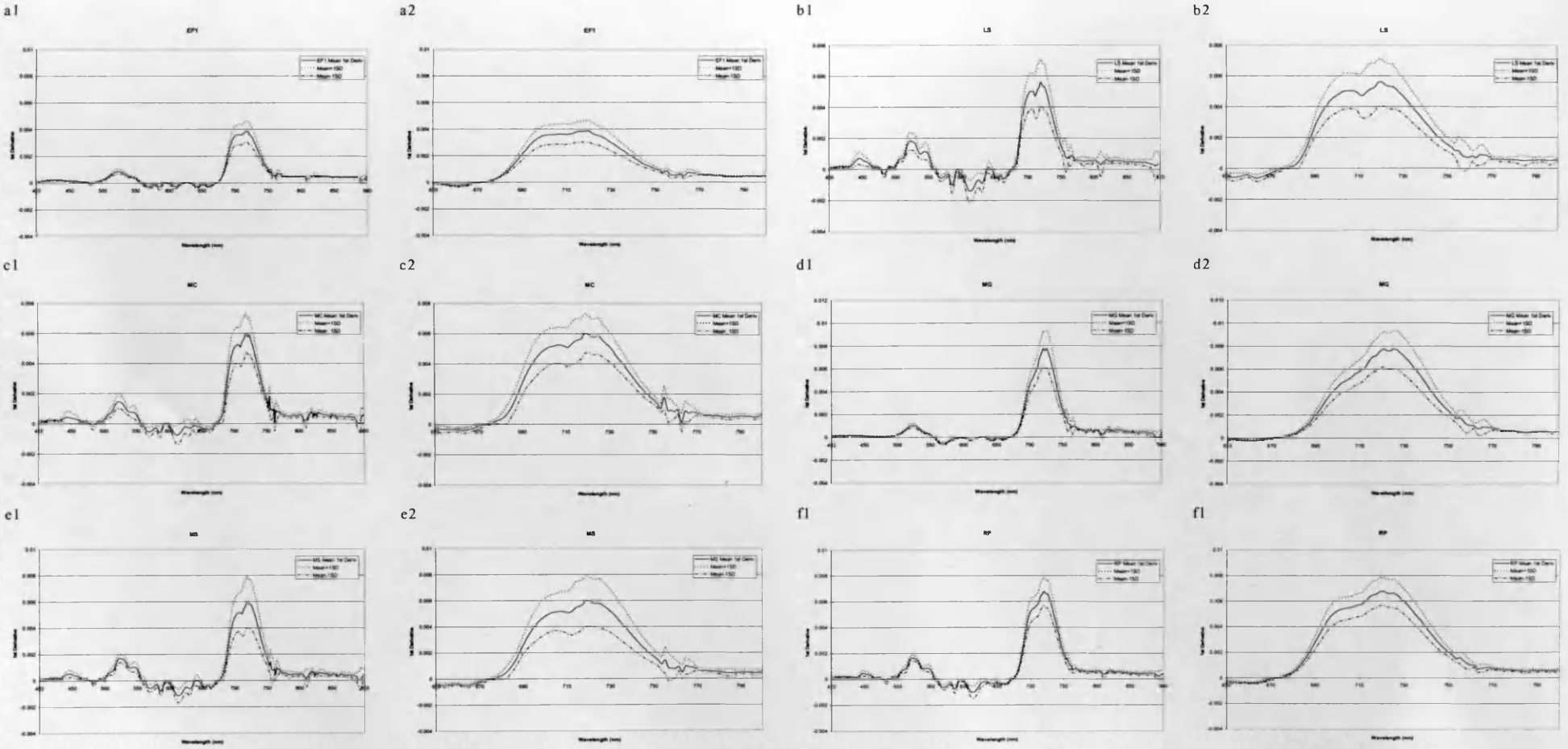

Figure 4:28 1st derivative slopes for the July spectra (data grouped by habitat type) along full length of the spectrum (graphs labelled with '1') and between 650 nm and 790 nm (graphs labelled with '2') (a = *Equisetum fluviatile;* b = Species-rich low sedge mire; c = *Molinia caerulea*-sedge mire; d = *Molinia caerulea-Myrica gale* mire; e = Mixed sedge; f = Rush pasture/grassland) (Mean = —— ; +1SD= - - - - ; -1SD= - -- -)

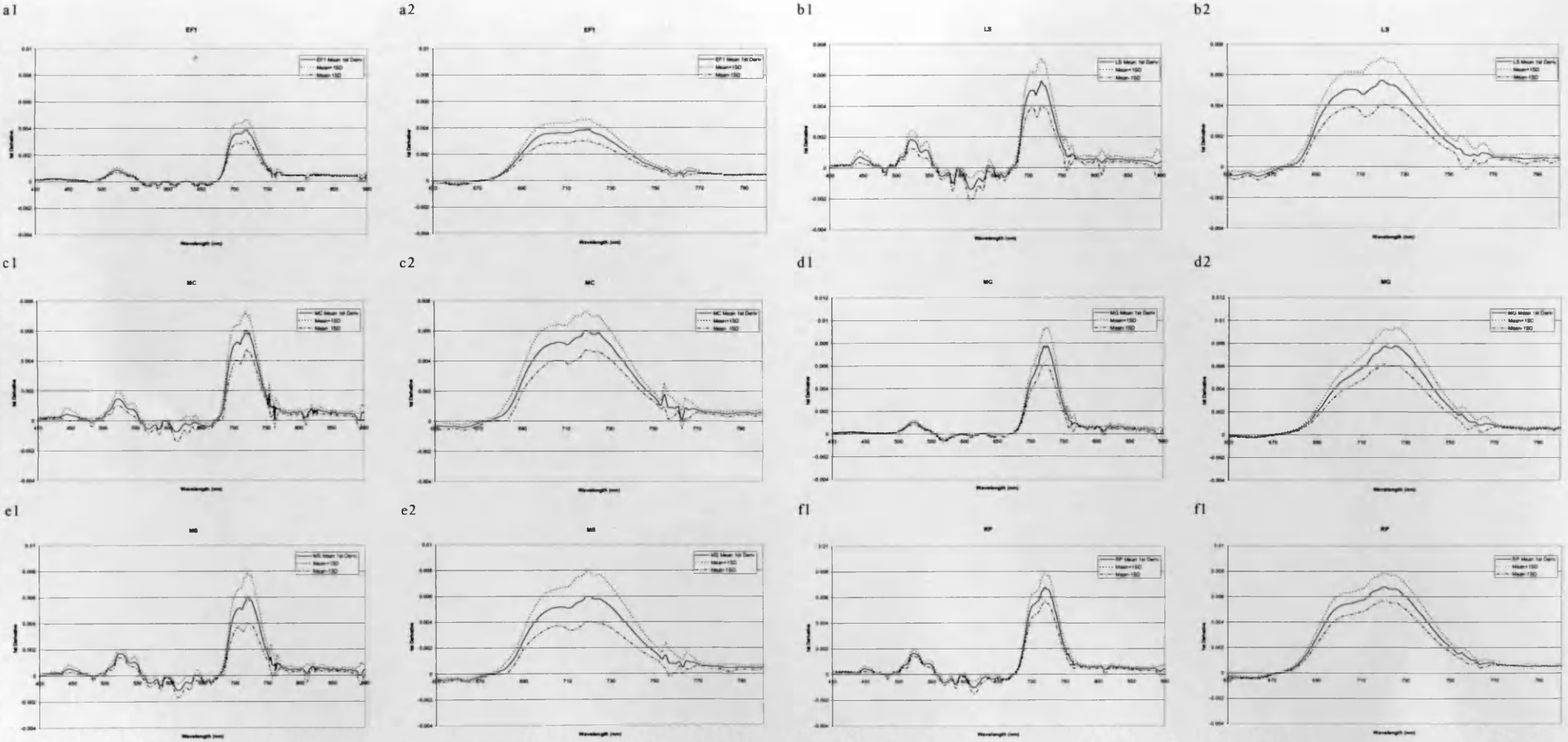

Figure 4:29 1st derivative slopes for the August spectra (data grouped by habitat type) along full length of the spectrum (graphs labelled with '1') and between 650 nm and 790 nm (graphs labelled with '2') (a = *Equisetum fluviatile*; b = Species-rich low sedge mire; c = *Molinia caerulea*-sedge mire; d = *Molinia caerulea-Myrica gale* mire; e = Mixed sedge; f = Rush pasture/grassland) (Mean = —; +1SD= - - - - ; -1SD= - -- -)

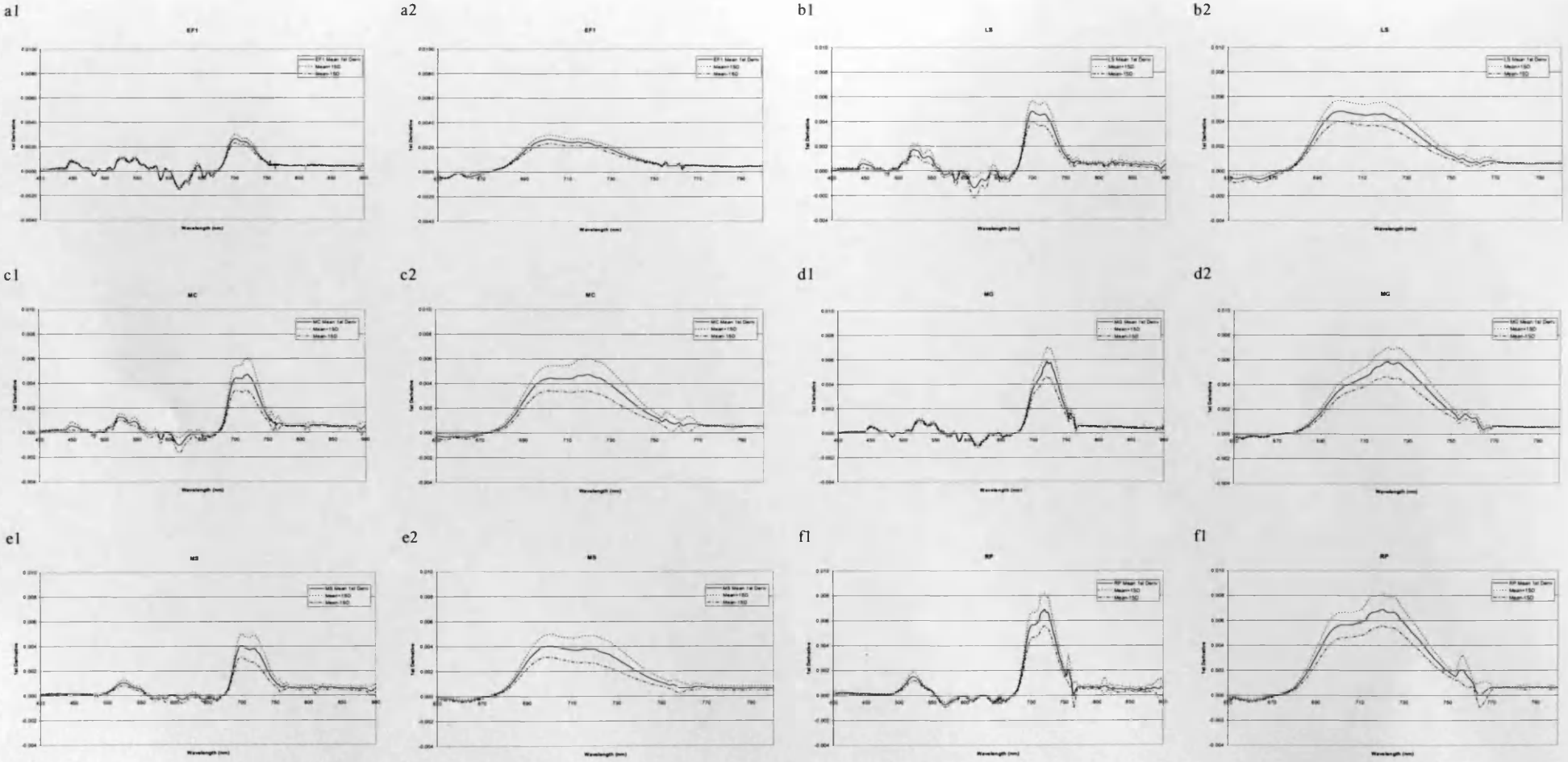

Figure 4:30 1st derivative slopes for the September spectra (data grouped by habitat type) along full length of the spectrum (graphs labelled with '1') and between 650 nm and 790 nm (graphs labelled with '2') (a = *Equisetum fluviatile*; b = Species-rich low sedge mire; c = *Molinia caerulea*-sedge mire; d = *Molinia caerulea-Myrica gale* mire; e = Mixed sedge; f = Rush pasture/grassland) (Mean = —— ; +1SD= - - - - ; -1SD= - -- -)

Position of Red Edge Inflection Point

The position of the steepest slope (Red Edge Inflection Point-'REIP') in the region between 690 nm and 730 nm was determined using the first derivative calculations. This region was split into 2 nm wide bands and the number of times an REIP was calculated as being a value within one of these bands was determined. The frequency tables to display these data at each sampling stage are shown in Appendix B and Figure 4:31 to Figure 4:36 illustrate these results in the form of frequency charts.

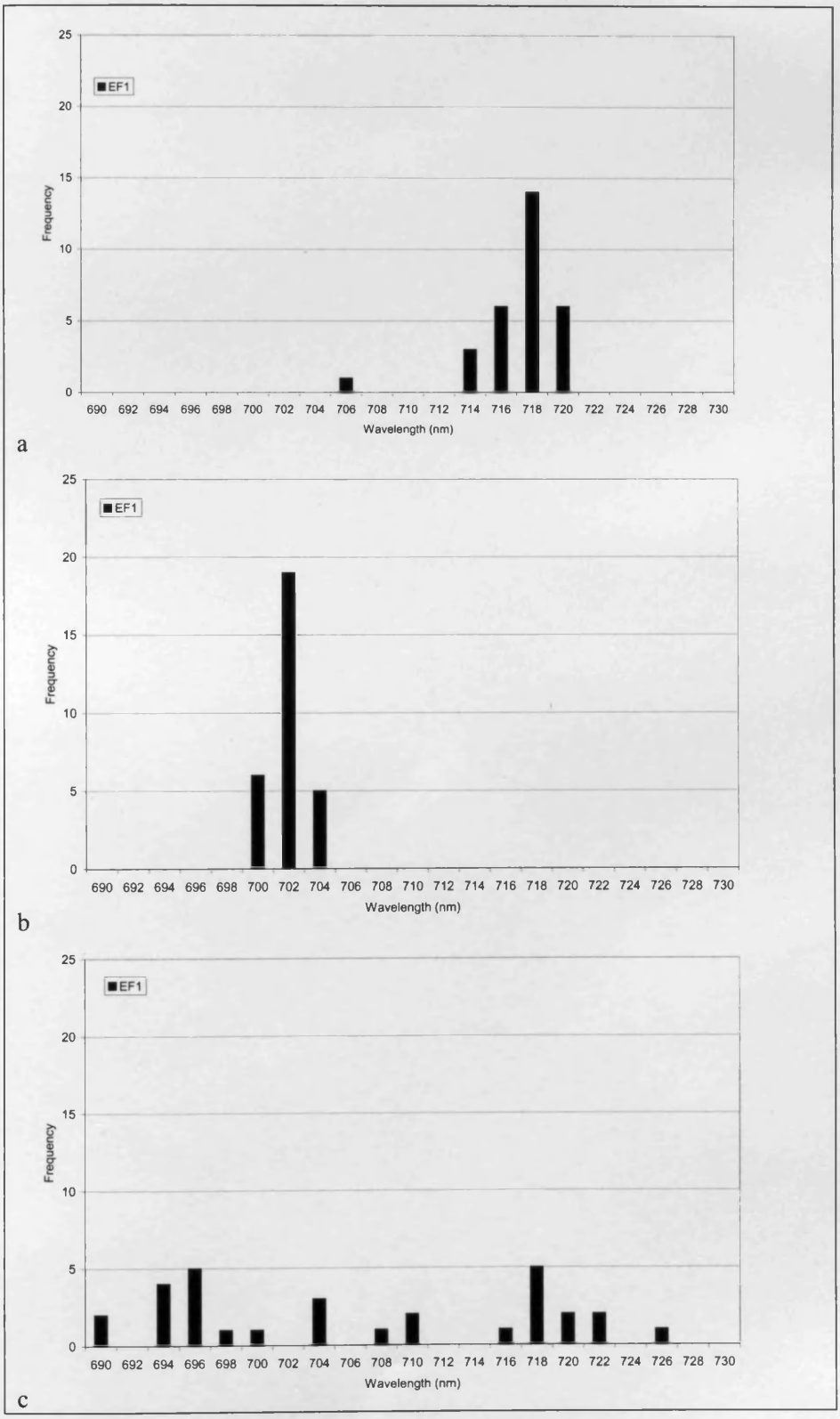

Figure 4:31 REIPs for *Equisetum fluviatile* study plots throughout the sampling period (a = July, b = August, c = September)

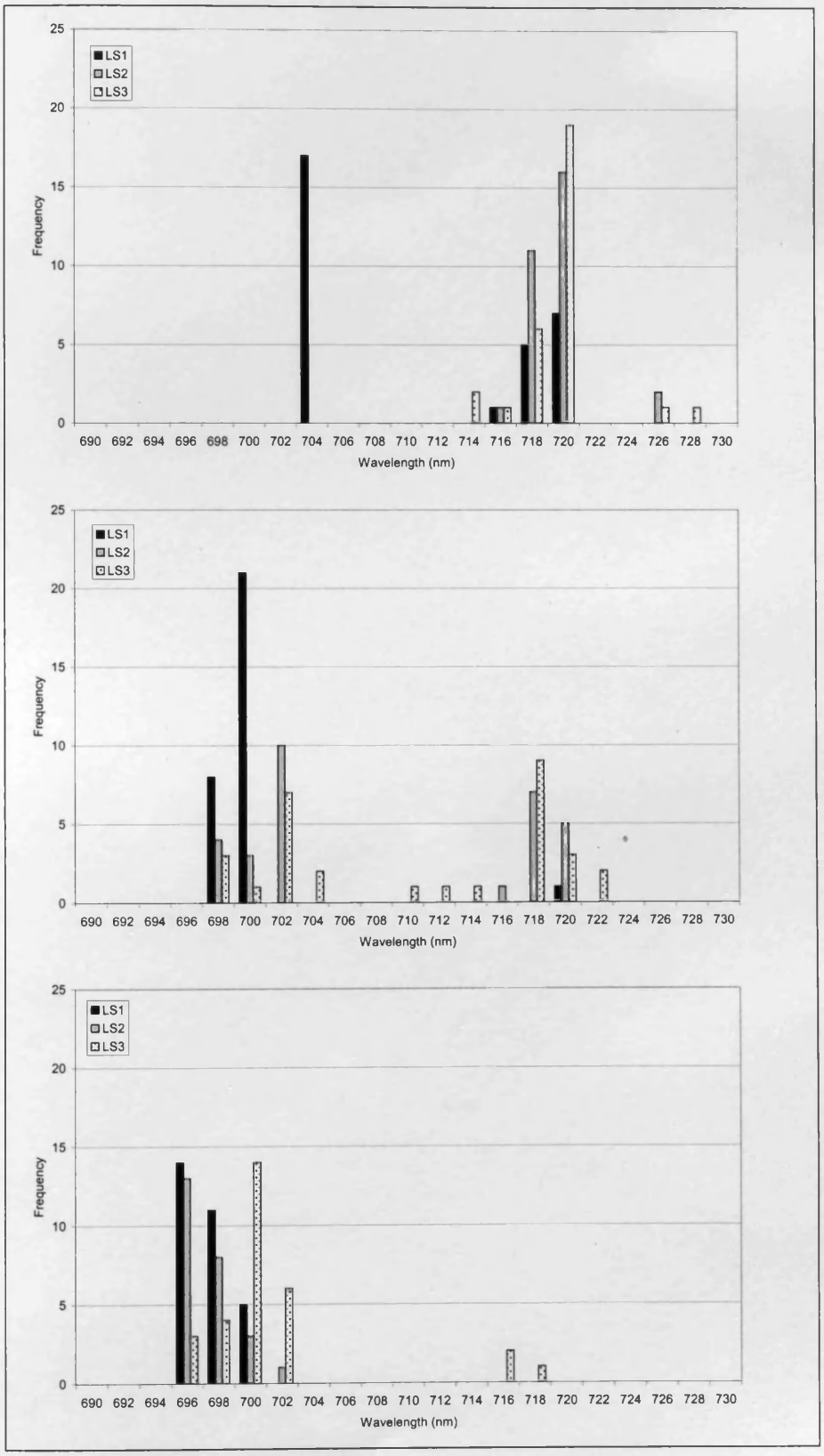

Figure 4:32 REIPs for Species-rich low sedge mire study plots throughout the sampling period (a = July, b = August, c = September)

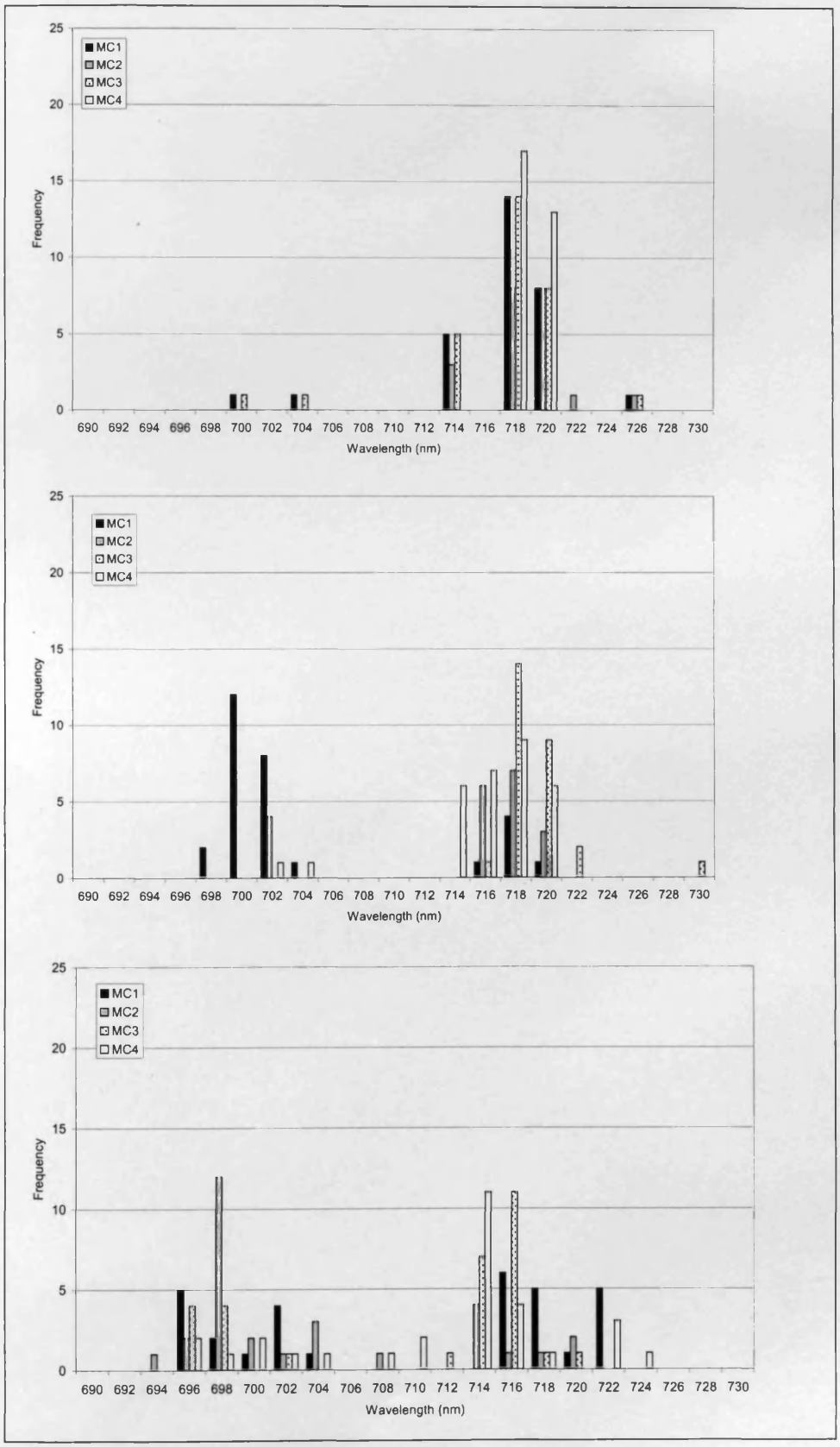

Figure 4:33 REIPs for *Molinia caerulea*-sedge mire study plots throughout the sampling period (a = July, b = August, c = September)

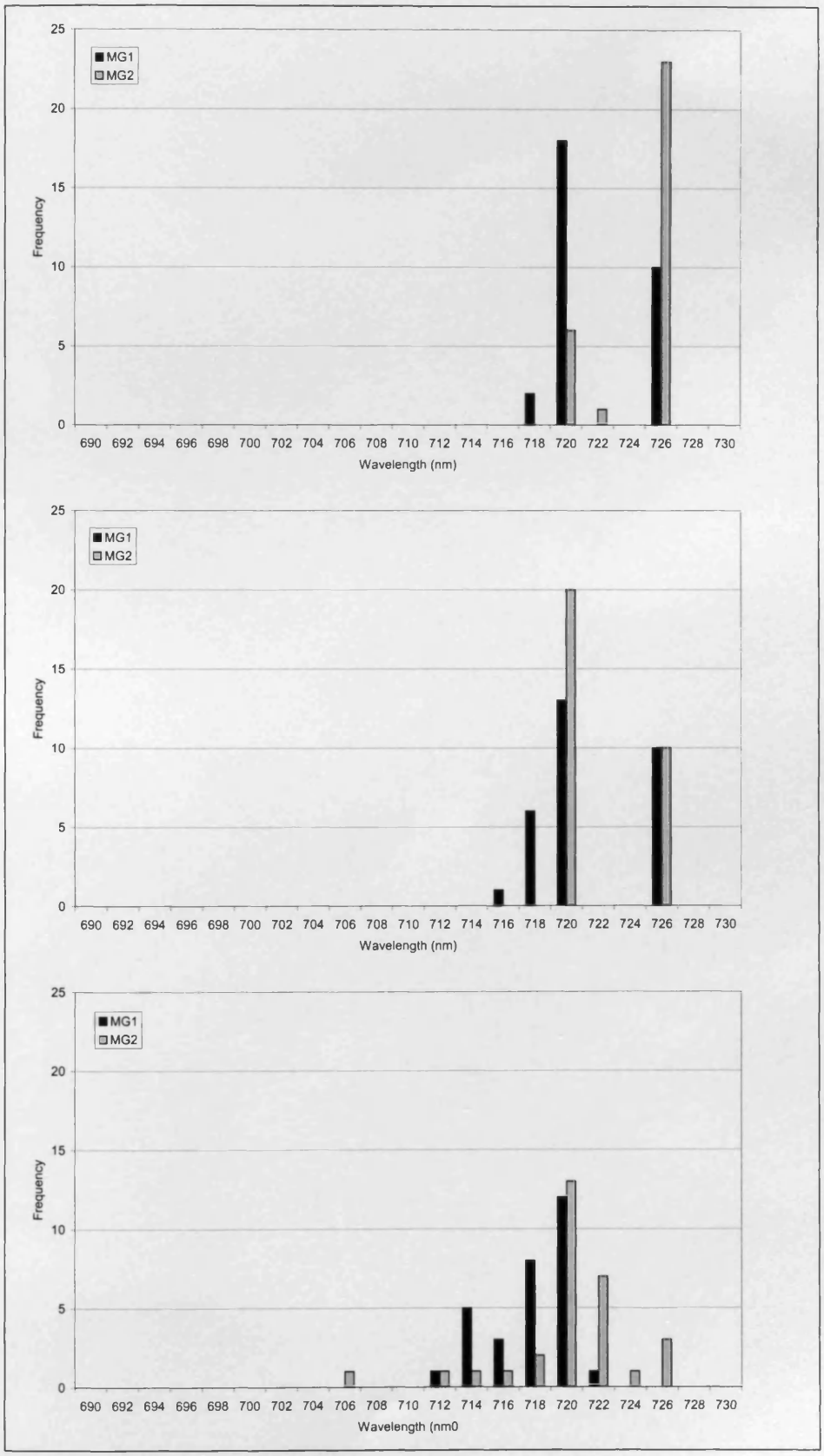

Figure 4:34 REIPs for *Molinia caerulea-Myrica gale* mire study plots throughout the sampling period (a = July, b = August, c = September)

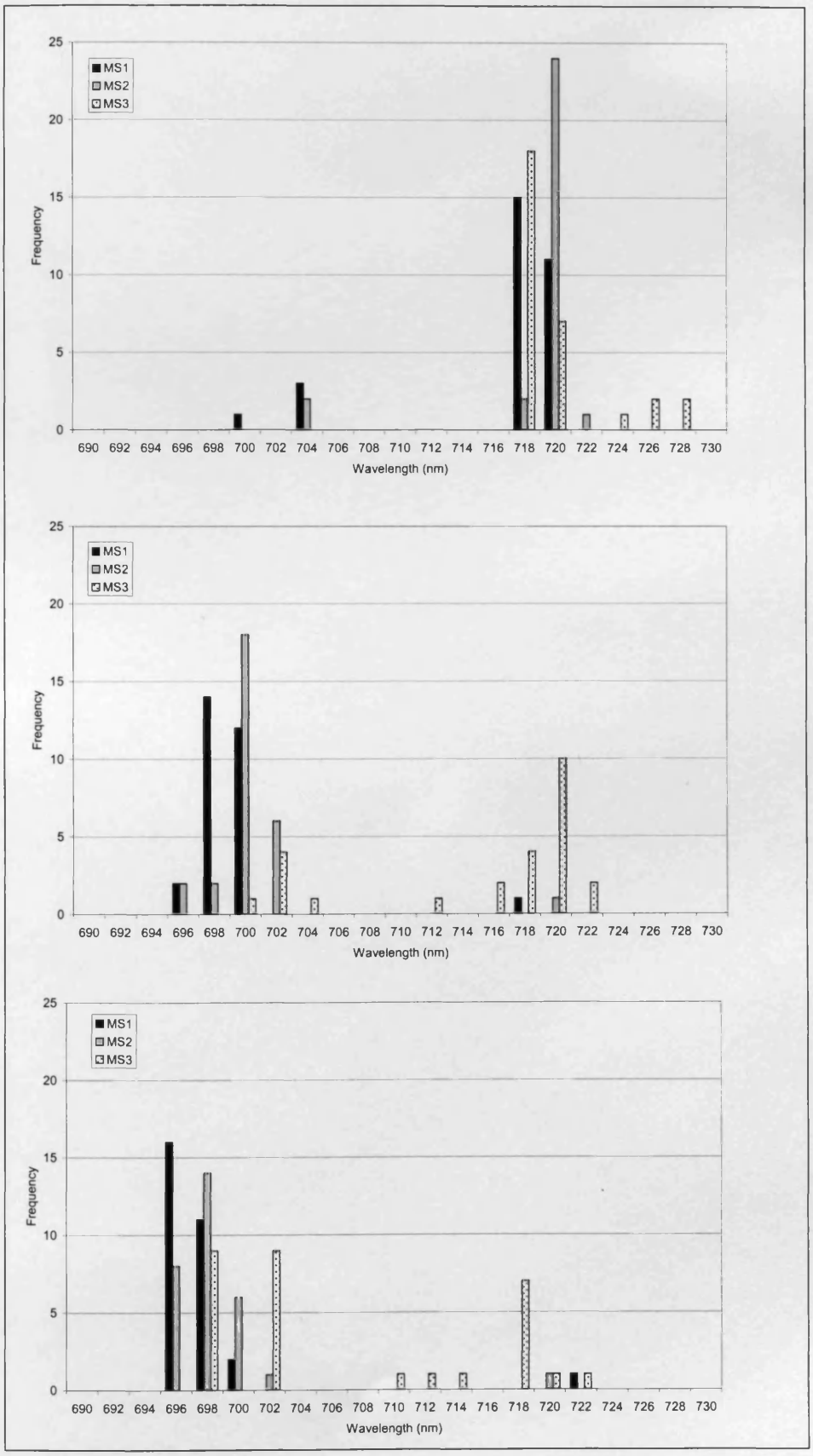

Figure 4:35 REIPs for Mixed sedge study plots throughout the sampling period (a = July, b = August, c = September)

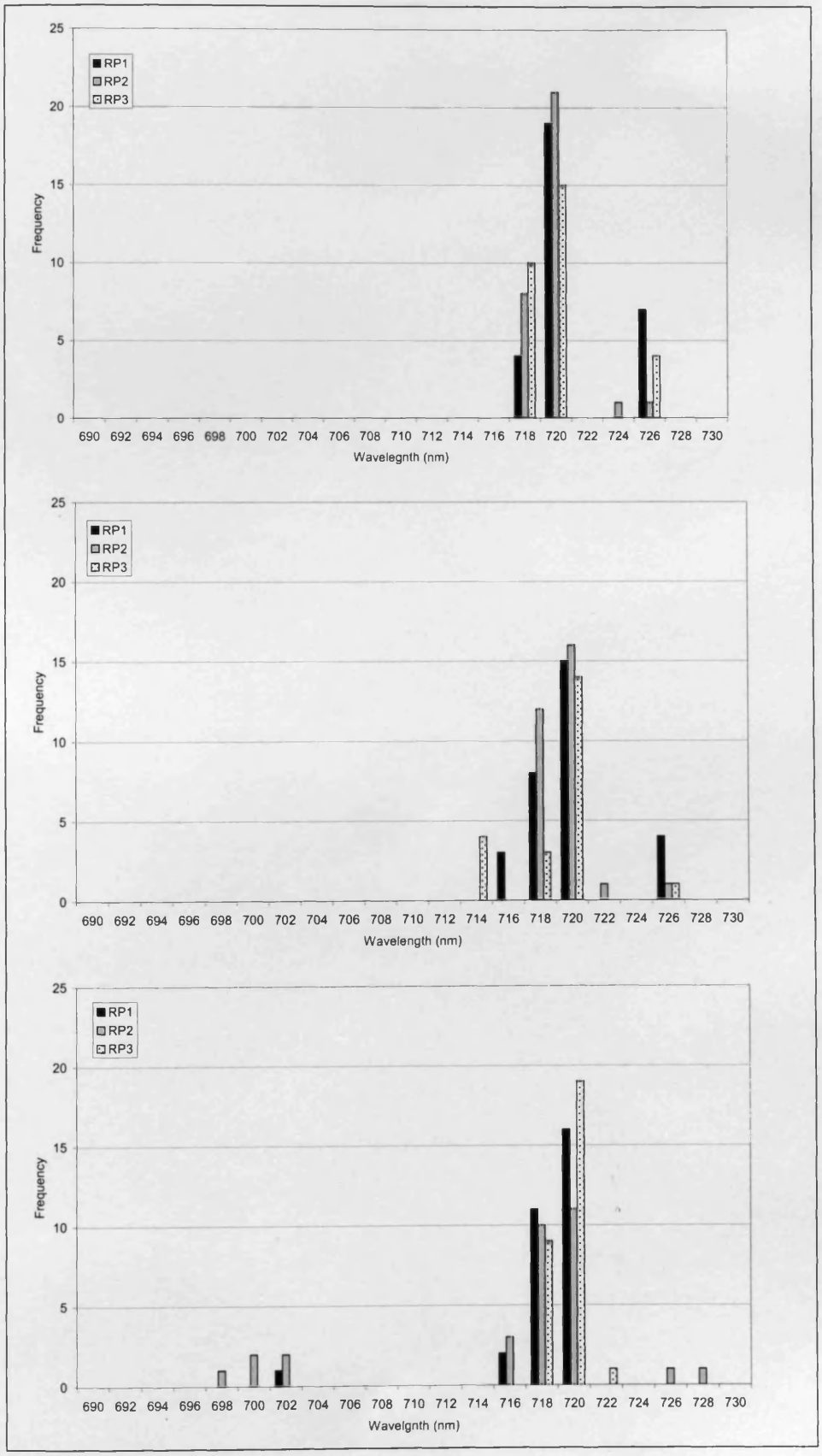

Figure 4:36 REIPs for Rush pasture/grassland study plots throughout the sampling period (a = July, b = August, c = September)

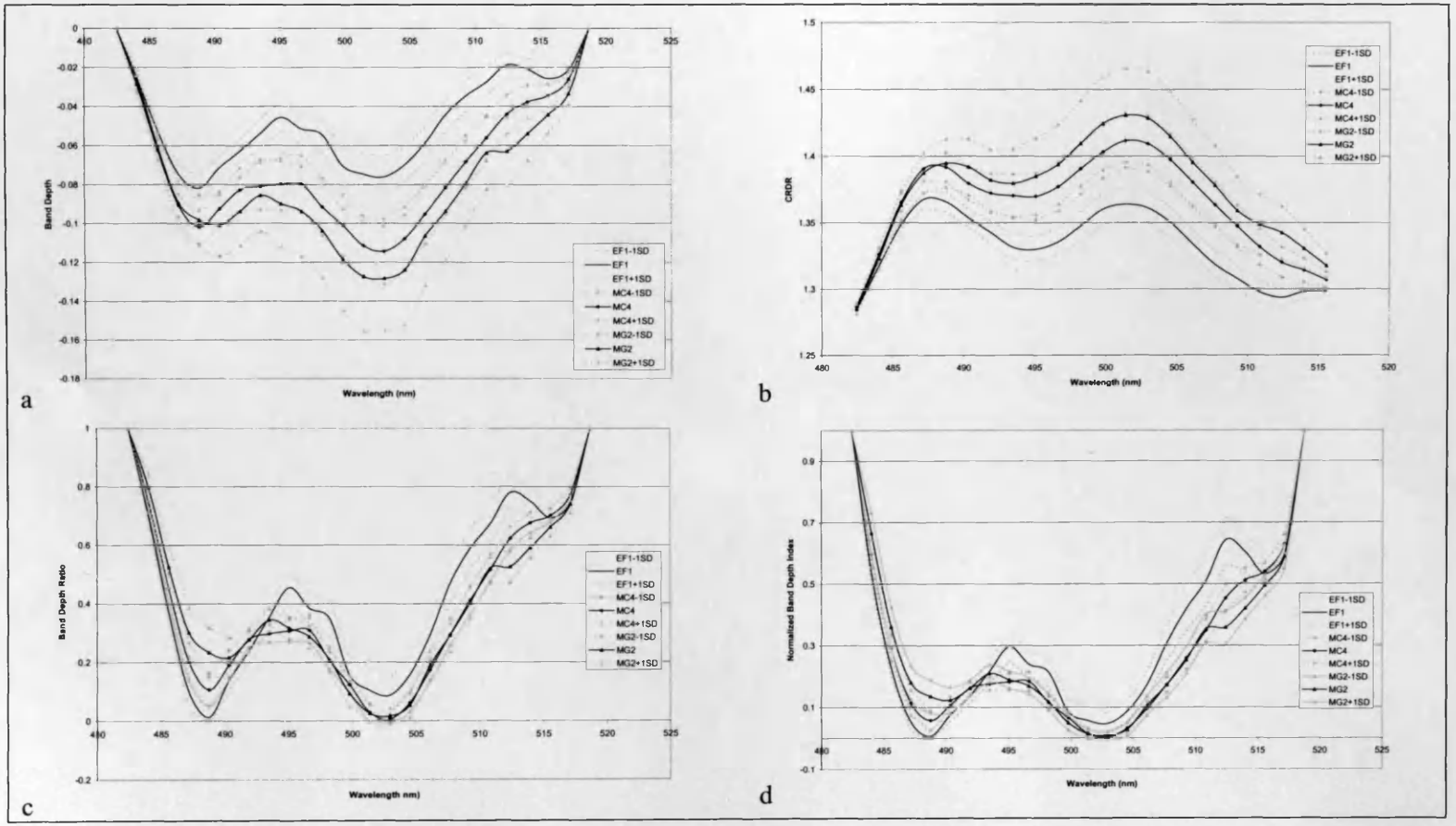

Figure 4:37 Indices derived from continuum removal analyses in the blue region (a = Band Depth, b = Continuum Removed Derivative Reflectance, c = Band Depth Ratio and d = Normalized Band Depth Ratio)

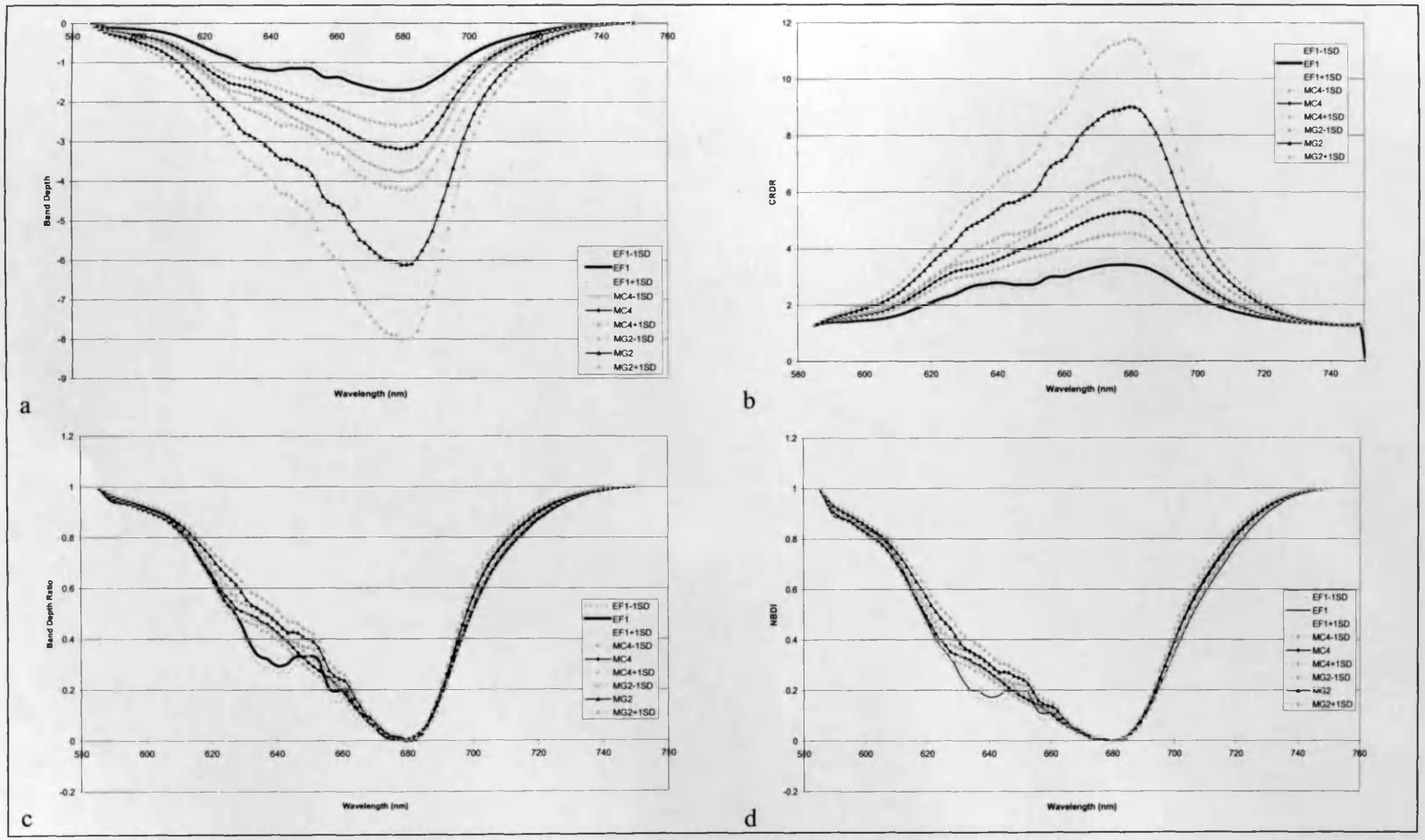

Figure 4:38 Indices derived from continuum removal analyses in the red region (a = Band Depth, b = Continuum Removed Derivative Reflectance, c = Band Depth Ratio and d = Normalized Band Depth Ratio)

Geostatistics

Geostatistics was carried out using spectra collected at each of the six study plots selected for previous analyses, these are EF1, LS2, MC1, MG2, MS3 and RP1. Table 4:13 and Table 4:14 list the geostatistics calculated at each of these plots and Figure 4:39 to Figure 4:42 illustrate the semivariograms calculated using NDVIs and REIPs at respective study plots.

Table 4:13 Geostatistics carried out on NDVIs calculated at plots EF1 (*Equisetum fluviatile*), LS2 (Species-rich low sedge mire), MC1 (*Molinia caerulea*), MG2 (*Molinia caerulea-Myrica gale* mire), MS3 (Mixed sedge) and RP1 (Rush pasture/grassland) over the sampling period

Plot	Sampling stage	Model	Nugget (6 d.p.)	Sill (6 d.p.)	Range	Residual sum of squares (4.d.p.)	R^2	Pro-portion
EF1	July	Gaussian	0.000296	0.001562	27.4357	0.0000	0.984	0.810
	August	Spherical	0.000003	0.000727	4.4200	0.0000	0.462	0.996
	Sept	Spherical	0.000015	0.001460	6.1700	0.0000	0.188	0.990
LS2	July	Spherical	0.000446	0.003542	46.0300	0.0000	0.770	0.874
	August	Gaussian	0.000485	0.002750	44.0461	0.0000	0.963	0.824
	Sept	Gaussian	0.000001	0.000781	6.7896	0.0000	0.680	0.990
MC1	July	Gaussian	0.000001	0.000615	5.6638	0.0000	0.449	0.998
	August	Spherical	0.000001	0.000792	3.4800	0.0000	0.002	0.999
	Sept	Gaussian	0.000063	0.001376	4.0357	0.0000	0.060	0.954
MG2	July	Gaussian	0.000692	0.001494	15.2420	0.0000	0.989	0.537
	August	Exponential	0.000184	0.001998	2.4000	0.0000	0.010	0.908
	Sept	Gaussian	0.002580	0.009730	27.8167	0.0000	0.813	0.735
MS3	July	Spherical	0.000009	0.000676	4.5500	0.0000	0.848	0.987
	August	Spherical	0.000001	0.000829	6.4000	0.0000	0.671	0.999
	Sept	Exponential	0.000106	0.000787	8.6100	0.0000	0.354	0.865
RP1	July	Spherical	0.000001	0.000504	3.9000	0.0000	0.016	0.998
	August	Spherical	0.000001	0.000373	6.4200	0.0000	0.143	0.997
	Sept	Exponential	0.000069	0.000908	0.2100	0.0000	0.000	0.924

Table 4:14 Geostatistics carried out on REIPs calculated at plots EF1 (*Equisetum fluviatile*), LS2 (Species-rich low sedge mire), MC1 (*Molinia caerulea*), MG2 (*Molinia caerulea-Myrica gale* mire), MS3 (Mixed sedge) and RP1 (Rush pasture/grassland) over the sampling period

Plot	Sampling stage	Model	Nugget (6 d.p.)	Sill (6 d.p.)	Range	Residual sum of squares (4.d.p.)	R^2	Pro portion
EF1	July	Gaussian	4.910000	10.880000	15.7963	0.601	0.970	0.549
	August	Spherical	0.022000	0.960000	5.4900	0.0394	0.645	0.977
	Sept	Exponential	94.700000	340.900000	123.0000	2431	0.555	0.722
LS2	July	Exponential	2.090000	7.189000	144.5700	2.44	0.447	0.709
	August	Spherical	22.000000	96.500000	8.5500	351	0.745	0.772
	Sept	Linear	2.033106	2.033106	21.5258	2.45	0.667	0.000
MC1	July	Linear	24.697341	24.697341	21.6517	346	0.045	0.000
	August	Linear	52.980206	52.980206	21.6517	1440	0.352	0.000
	Sept	Spherical	0.100000	106.100000	3.5500	852	0.046	0.999
MG2	July	Linear	4.579984	4.936821	17.4711	2.54	0.022	0.072
	August	Linear	8.136539	8.136539	17.4711	4.34	0.252	0.000
	Sept	Linear	8.866266	18.835133	17.4711	53.4	0.415	0.529
MS3	July	Gaussian	0.010000	8.570000	6.5472	2.05	0.907	0.999
	August	Gaussian	8.700000	66.850000	5.1442	45.2	0.879	0.870
	Sept	Gaussian	38.500000	93.650000	12.6959	98.2	0.942	0.589
RP1	July	Spherical	0.240000	6.039000	3.6900	0.573	0.186	0.960
	August	Spherical	0.320000	7.551000	5.8500	14.8	0.234	0.958
	Sept	Linear	10.600782	10.600782	21.1153	593	0.325	0.000

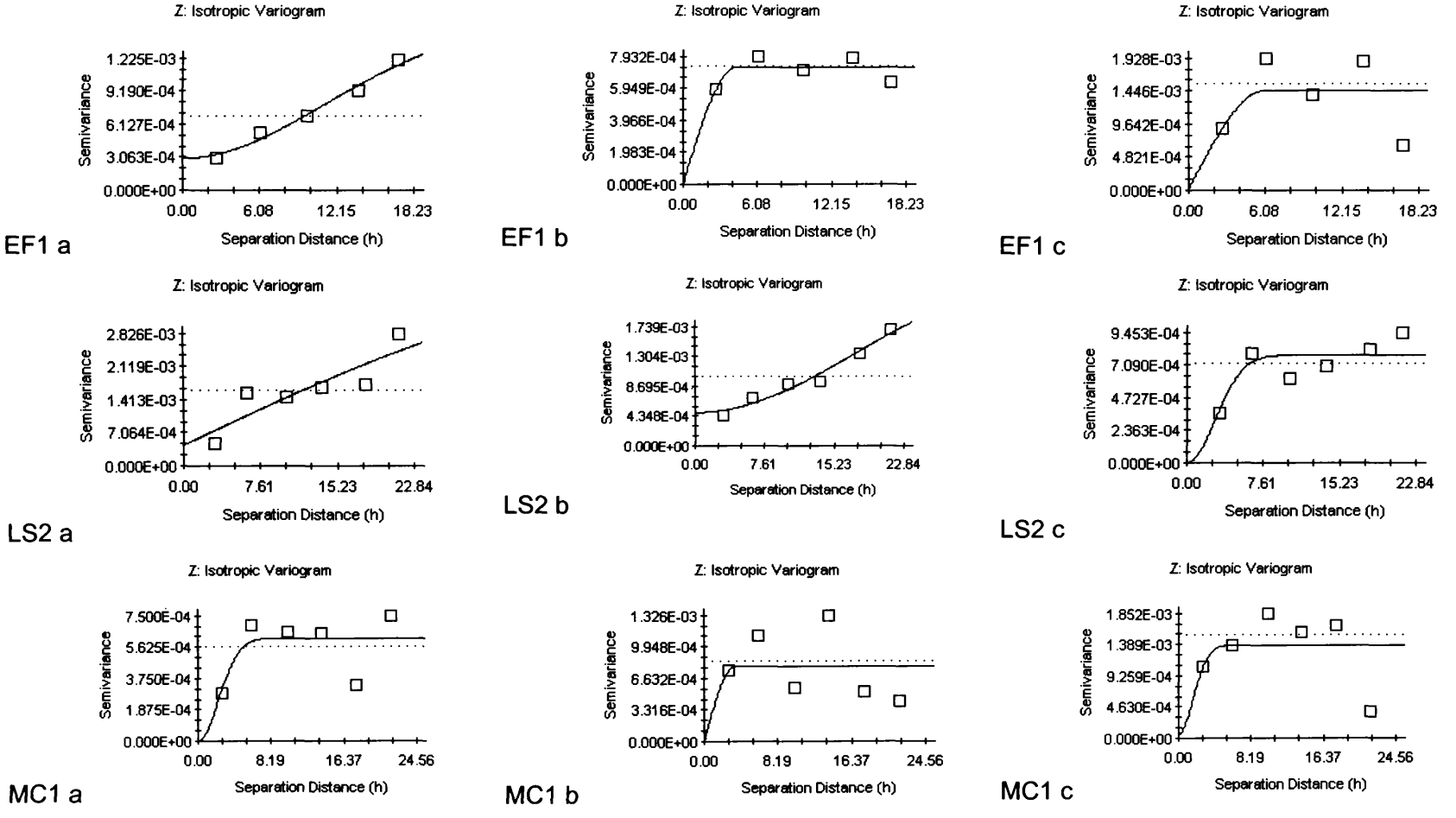

Figure 4:39 Semivariograms calculated using NDVI values at plots EF1, LS2 and MC1 in July ('a'), August ('b') and September ('c')

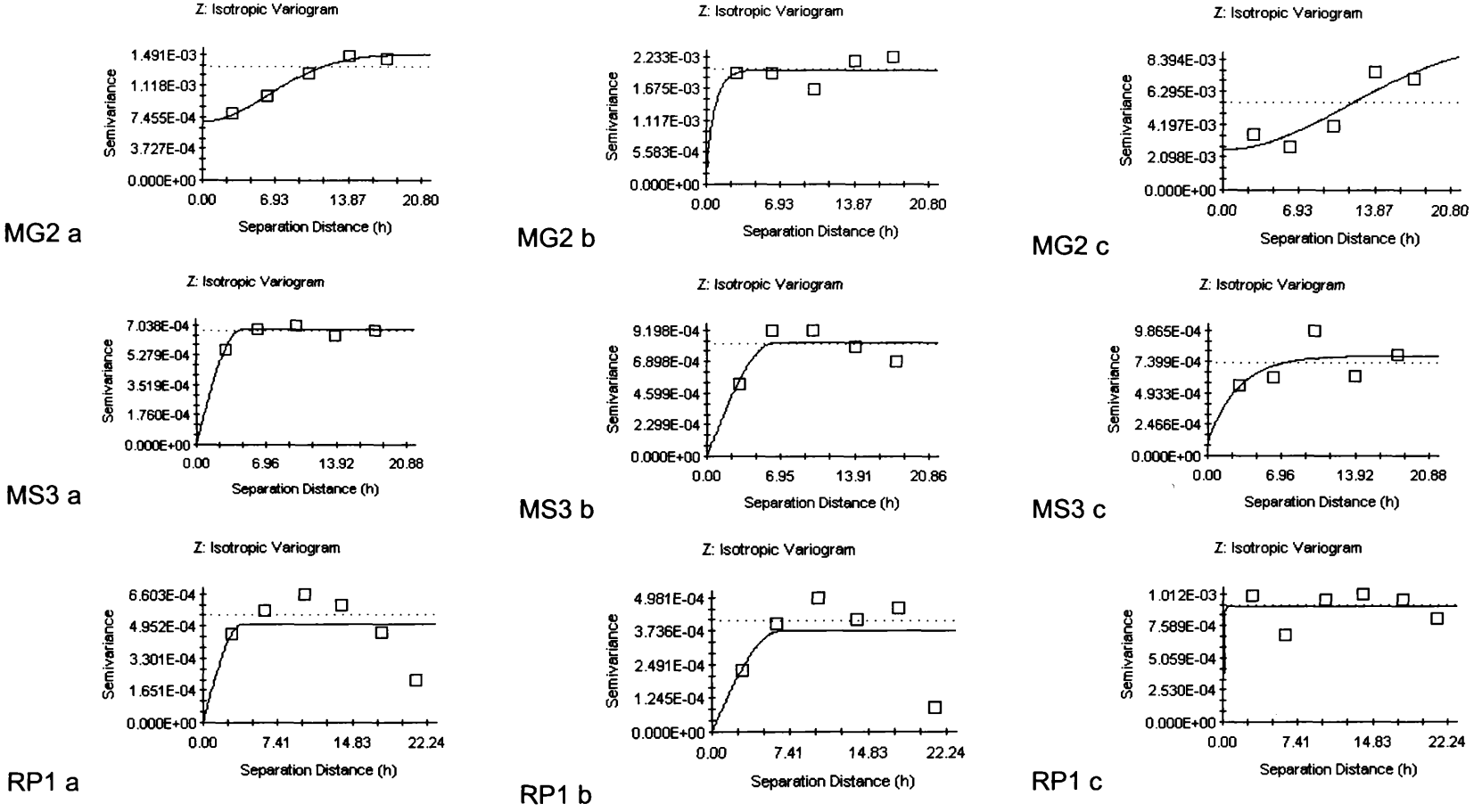

Figure 4:40 Semivariograms calculated using NDVI values at plots MG2, MS3 and RP1 in July ('a'), August ('b') and September ('c')

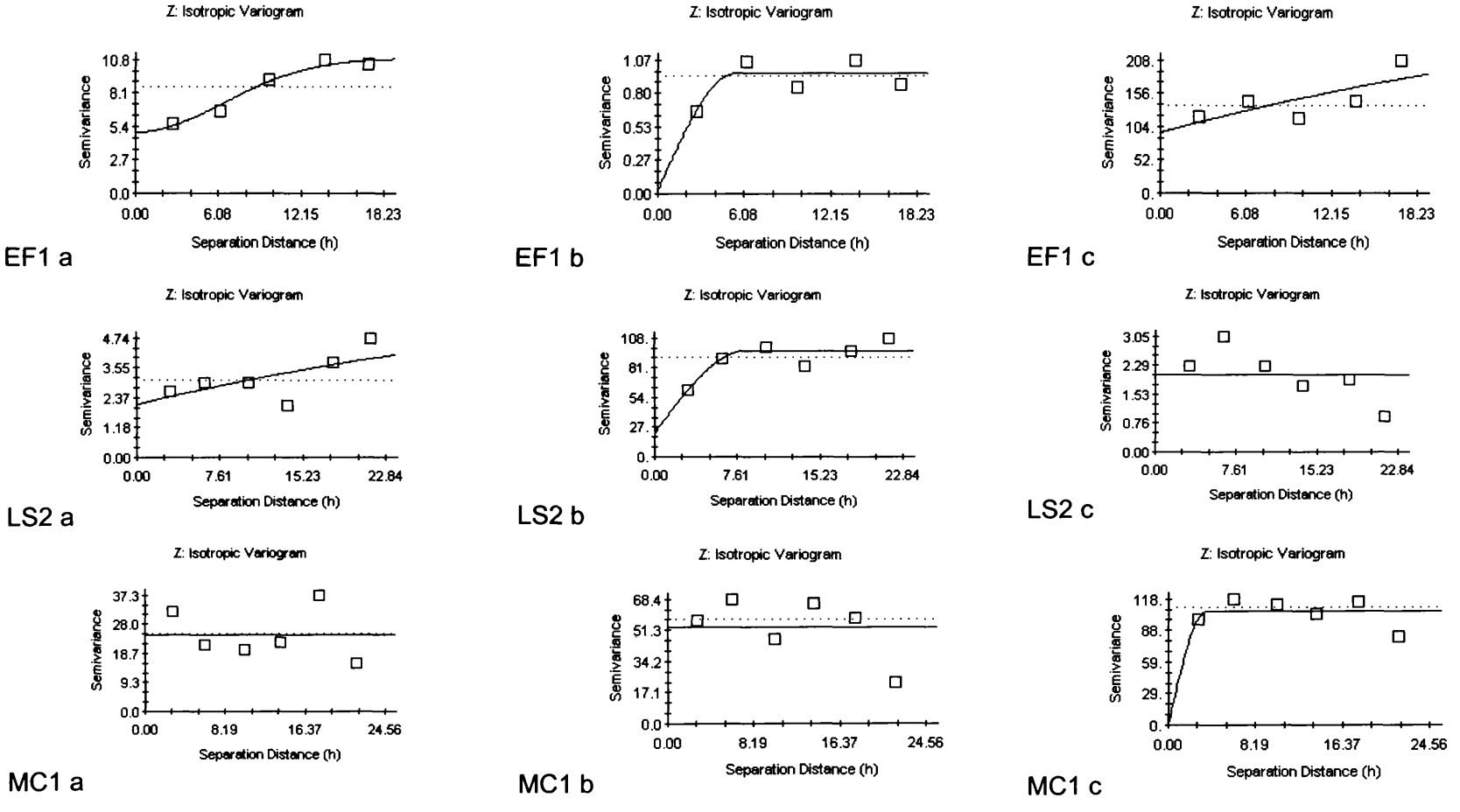

Figure 4:41 Semivariograms calculated using REIPs at plots EF1, LS2 and MC1 in July ('a'), August ('b') and September ('c')

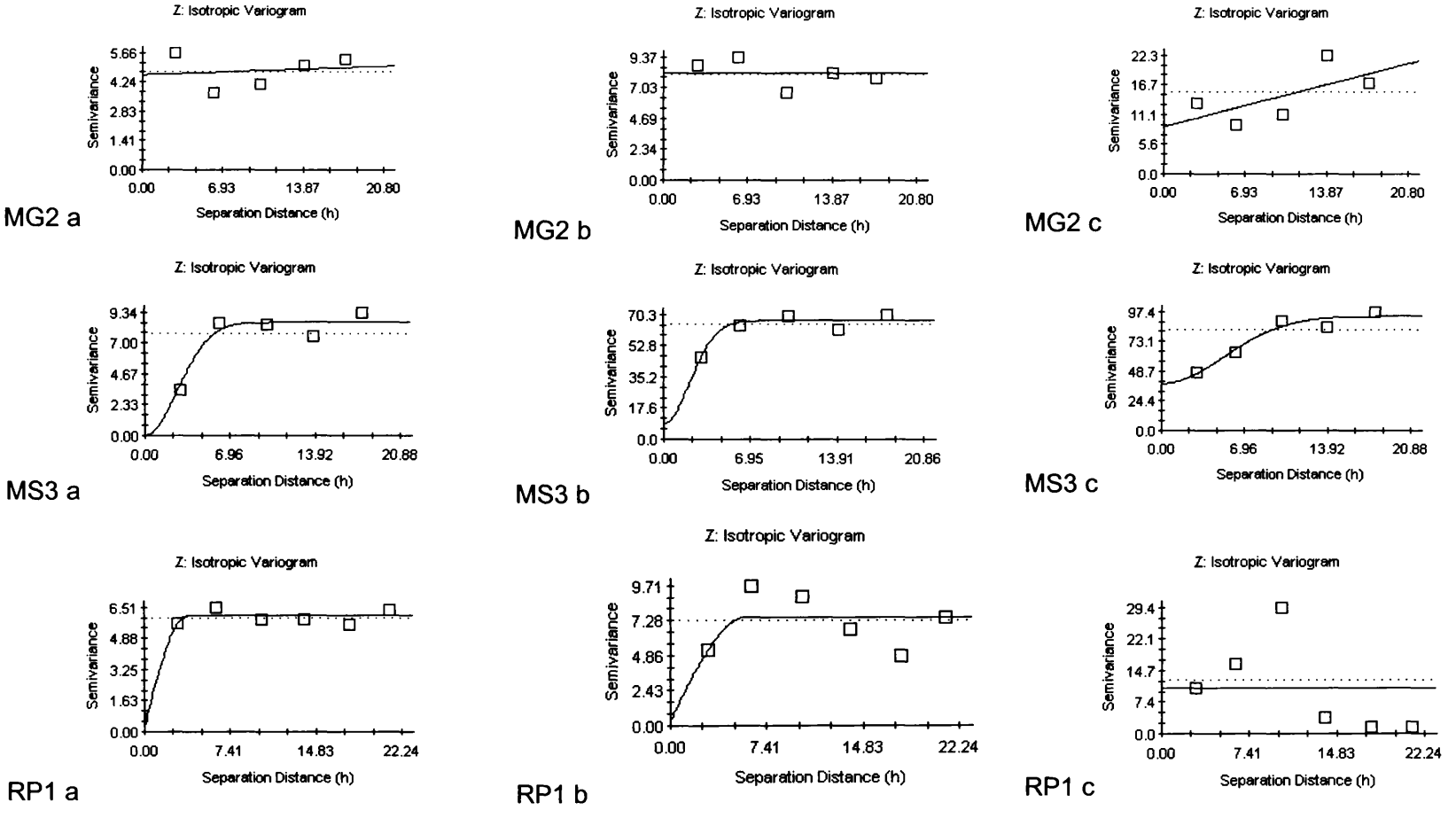

Figure 4:42 Semivariograms calculated using REIPs at plots MG2, MS3 and RP1 in July ('a'), August ('b') and September ('c')

4.5 Discussion and Conclusions

4.5.1 Objective a) Differences in spectral pattern between habitat type

Determine the degree to which spectral reflectance pattern varies between habitat types in the visible and near infrared (NIR) regions of the spectrum.

Spectra

The graphs of the mean spectra collected at each study plot (Figure 4:4 to Figure 4:9) illustrate only subtle differences between the spectral responses at study plots from different habitat types. Most spectra exhibit a typical pattern found in vegetation spectra namely a distinctive reflectance feature in the green region followed by an absorption feature in the red region and a marked increase in the NIR resulting in a red edge shoulder between the two regions. Similar patterns of change over the sampling period show strong similarity between study plots of different habitat types whereby reflectance in the red region increases as vegetation senesces and reflectance in the NIR decreases steadily (Skidmore 2002; Price 1994; Schmidt & Skidmore 2003).

Notable differences are evident in the green region of the spectra where the rush pasture/grassland and mixed sedge habitats for example exhibit high reflectance when compared with most of the other habitat types. The reflectance in the green region of two of the low sedge study plots is also relatively high. Study plot LS3 exhibits a visibly lesser reflectance in the green region which may be attributable to the differences in the location of this study plot outwith the same compartment as the others. The compartment where LS3 is located is managed differently and as such contains tussocky vegetation and a relatively greater proportion of tall grasses all of which may contribute to a greater degree of scattering amongst the spectral samples. In addition, whereas some study plots differ greatly between reflectance in the green region, they do not necessarily differ to the same extent in the NIR region. This is the case for LS2 and MC2 or RP3 and MG1 in the July datasets. These results

are similar to Cochrane (2000) where reflectance along the spectrum was compared between various tree species and differences in the green region did not necessarily carry over into other parts of the spectrum.

Standard deviations are greatest in the NIR region of the spectra right across the study plots and over the sampling period. This is unsurprising as radiation at these wavelengths is scattered to a greater extent in vegetation spectra due to variations in canopy structure (Schmidt & Skidmore 2003; Spanglet *et al.* 1998). Diffuse skylight can contribute as much as 5-10% of the total illumination however (and at shorter wavelengths this value can be even greater at 20-25% of the total illumination) and tends to fill in shadows and reduce the contrast between surfaces with dissimilar surface textures. Spectra in this study were often collected in conditions of partial cloud cover and therefore diffuse skylight may well have contributed to the reflectance patterns although this is a difficult problem to avoid. The use of the Spectralon® panel and white reference spectra would have kept the effects of subtly varying illumination conditions to a minimum.

Spectra were recorded on days when wind was considered to be a non-contributing factor although no measurements of local wind speed were made. Wind can affect the structure of vegetation and therefore the amount of shadowing present within the Field of View (FOV). This in turn can affect the within-habitat spectral variation and lessen the ability to discriminate between habitat types. In addition to caution being taken on the choice of sample days, the ASD FieldSpec™ employed in this study is a rapid scanner thereby minimizing any very short term variations in canopy spectra affecting the spectral pattern.

Figure 4:10 and Figure 4:11 illustrate the mean spectral patterns between habitat types when the data from the study plots are grouped together. The differences in the green region are highlighted in Figure 4:11 and do provide some indication that spectral signature does vary between habitat type. Similar results in this region were identified by Schmidt and Skidmore (2003) using field spectra collected for salt marsh vegetation types. The relative patterns between habitat spectra do not appear to be consistent, however, and this may highlight the

importance of time of data collection on the spectral separability between habitat types. The within habitat variation in spectral response is not illustrated in these graphs but is discussed further under work presented for Objective c).

PCA

Each dataset was gathered over a number of days and study plots close in proximity to each other were often sampled on the same days. This therefore leads to a degree of spatial and temporal autocorrelation within the dataset which is difficult to identify and extract (Atkinson & Emery 1999; Cliff & Ord 1973; Fortin *et al.* 1989). A principal components analysis of the meteorological data that applied to each study plot during the August sampling stage was assessed in order to investigate this potential problem further. The August dataset was the only meteorological dataset wholly intact for all of the sampling days and so was deemed the most suitable for this analysis. The results of this analysis are shown in Figure 4:43 and the relative locations of the study plots in feature space do appear to correspond with the order applied in data collection. Figure 4:43 is considered in relation with the PCA on the spectra collected at each study plot in August (Figure 4:14) and although there is a very slight correlation between the sample scores along Axis 1 for both results (Pearson Correlation Coefficient 0.376, P-value 0.000) the patterns between the relative locations of the study plots in feature space do differ.

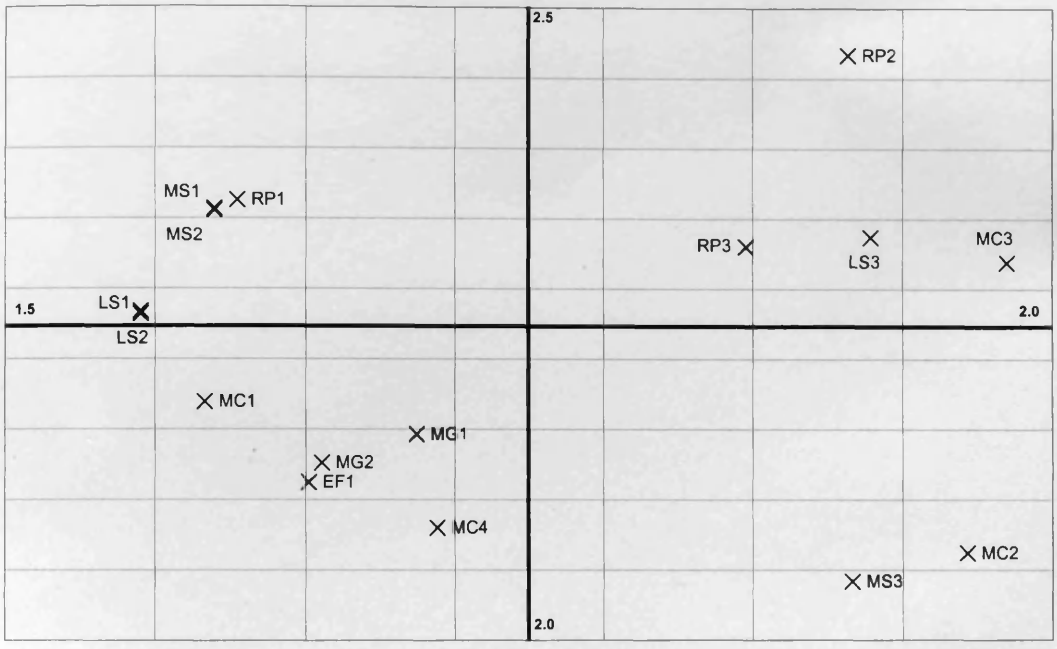

Figure 4:43 PCA performed on Meteorological Data for August field spec data collection days (Study plots means plotted)

Principal Components Analysis (PCA) was carried out on both the AVS1-42 dataset and the simulated CASI dataset using spectra collected in July (Figure 4:12 and Figure 4:13). The similarity evident between these diagrams is partly unsurprising, however, it is a good example of how a dataset with fewer spectral bands can retain the same structure and class separability as a dataset with a much larger number of spectral bands. It therefore suggests that there is a threshold of spectral information that will result in class separability that is not improved upon with larger datasets. The precise relationship between class separability and scale of spectral resolution in this sense is not explored further in this study though it is an area that does warrant further research.

Insh Marshes is split into compartments that are managed differently whether by varying the intensity of grazing within the compartment, topping or scrub clearance programmes. As such habitats that fall within different compartments may be subject to different management which results in within-habitat variation in terms of canopy structure and possibly species composition. This in turn, may result in a greater range of spectral patterns associated with one habitat type. As the PCA results show relatively large differences between study plots

from the same habitat type, the possibility of vegetation structure differences within each habitat type due to different management techniques was considered. The following table lists the management associated with each study plot as identified in Maier & Cowie (2002).

Table 4:15 Management within each study plot (Maier & Cowie 2002)

Study Plot	Management
EF1	No stock access
LS1	Sheep high grazing; Topping
LS2	Sheep high grazing; Topping
LS3	Sheep low grazing; Scrub Clearance
MC1	Sheep medium grazing
MC2	Sheep medium grazing
MC3	Sheep medium grazing
MC4	Sheep low grazing; Scrub clearance
MG1	Sheep medium grazing
MG2	Sheep medium grazing
MS1	Sheep high grazing; Topping
MS2	Sheep high grazing; Topping
MS3	Sheep low grazing; Scrub clearance
RP1	Sheep high grazing; Topping
RP2	Sheep high grazing; Topping
RP3	Sheep high grazing; Topping

The study plots to consider in terms of within habitat management practices are the 'LS' study plots (Species-rich low sedge), 'MC' (*Molinia* caerulea sedge mire) and 'MS' (Mixed sedge). A glance at the patterns between the study plots located within these habitat types (see Figure 4:12, Figure 4:14 and Figure 4:15) often highlight a strong similarity between study plots located within the same management compartment. In addition, those habitat types that share the same management practices also display a large degree of dissimilarity between the study plots, such as 'RP' for example (Rush pasture/grassland).

Although PCA is presented here as an effective method to assess the spectral dissimilarity between classes of spectral data the results remain difficult to interpret. The effect of the spatial and temporal autocorrelation cannot be quantified and can therefore not be discounted although the results presented in Figure 4:43 suggest that this had a minimal effect. It is neither possible to identify consistent trends along the axes nor to explain with great detail the nature of the clustering amongst the classes. Also, the data is presented using only the

standard deviations of sample scores in axis 1 and axis 2 and so, in reality, the overlap and spread is even greater. The results illustrate the degree to which spectral separability between classes may change over just three months and that there may therefore be optimal times to classify between habitat types. The results for the mixed sedge samples for example, illustrate that July may be a less profitable time of the year to separate this particular habitat type from others as spectral overlap with other habitat types is shown to be greatest at this time of the year (Figure 4:13). In contrast however, the *Equisetum fluviatile* samples are most distinct in the August dataset as are data collected in the *Myrica gale* habitat type.

4.5.2 Objective b) Inter-habitat variation using Multiple Discriminant Analysis

Assess the degree to which spectra grouped by habitat are spectrally distinct using multivariate statistical analyses.

Results from the Multiple Discriminant Analyses (MDA) displayed high proportions of correct predictions ranging from 74.1% – 95.6% in overall accuracy. This varied only slightly between the dataset used and in some cases, the smaller dataset performed more successfully for some habitat types than the other larger dataset. Hyperspectral datasets may not therefore be necessary in order to identify spectral disimilarity between wetland habitat types. This compares favourably to work by Becker *et al.* (2005) where eight bands were identified as containing the most important information regarding coastal wetland species in the Great Lakes Region. The bands identified by Becker *et al.* (2005) were 515 nm, 560 nm, 686 nm, 732 nm, 812 nm, 824 nm, 836 nm and 940 nm. To compare with the results presented here, the first eight bands identified in the stepwise MDAs were identified and are listed below in Table 4:16. The same regions of the spectrum that Becker *et al.* (2005) identified also featured highly in the MDA results here though other important regions, which were amongst the first eight predictors on at least two of the three sampling dates, are 380 – 394 nm, 443 – 457 nm, 459 – 473 nm, 711 – 725 nm and 758 – 773 nm.

Table 4:16 First eight most significant predictors identified in Multiple Discriminant Analyses for each sampling stage (listed in rank order starting with highest)

July		August		September	
AVS band	Wavelengths	AVS band	Wavelengths	AVS band	Wavelengths
15	569-583 nm	27	758-773 nm	27	758-773 nm
8	459-473 nm	24	711-725 nm	23	695-709 nm
28	774-788 nm	8	459-473 nm	29	790-804 nm
24	711-725 nm	12	522-536 nm	22	680-694 nm
42	995-1009 nm	13	538-552 nm	3	380-394 nm
16	585-599 nm	3	380-394 nm	13	538-552 nm
7	443-457 nm	31	821-836 nm	7	443-457 nm
11	506-520 nm	19	632-646 nm	5	412-426 nm

The results from the PCA illustrated a good degree of overlap in the 1st and 2nd component scores between study plots from different habitat types. The results from the MDA illustrate a good degree of separability between the spectra in terms of habitat type when all spectral information is considered and this is the case for each of the three sampling stages. This illustrates that between July and September the time of data acquisition does not affect the degree to which spectral data can be used to successfully discriminate between these six habitat types. Table 4:3 and Table 4:4 map the regions of the spectrum that were identified as being significant predictors in the models developed by the MDAs. The variation between the results presented from these sampling stages is likely to be indicative of structural change or variation in plant vigour or species composition over the sampling period. Understanding the complex relationship between reflectance along the spectrum and detailed vegetation datasets is explored in Chapter 5. This is an area worthy of further research in order to further our understanding regarding the wavebands that are more likely to identify specific changes in vegetation from wetland environments.

4.5.3 Objective c) Within-habitat variation

Explore the within habitat spectral variation using data collected from two or more study plots within each habitat type.

In order to carry out statistical analyses between the habitat types, the degree of intra- or within-habitat variation first had to be established. If this was found to be significant, then

formal statistical analyses on grouped data from study plots of the same habitat type would be inappropriate. The purpose of Figure 4:16 to Figure 4:21 is to illustrate the variability within the datasets when grouped by habitat type using standard deviation and overlap in a PCA. Results from each of the sampling stages are comparable for the habitat types. The *Equisetum fluviatile* habitat type exhibited the lowest amount of within habitat variation when the standard deviation of reflectance along the spectrum is considered. This may be largely due to the fact that this dataset only consisted of samples collected at one study plot. At all other habitat types, sample spectra were made up of data from two or more study plots. The species-rich low sedge habitat type exhibited the highest standard deviations in spectral reflectance along the spectrum and this may be in relation to the variability in species composition present within this habitat type.

The five habitats with two or more study plots were tested for within-habitat variation at each of the CASI wavebands using the Kruskal Wallis H test. Most of the results show significant within-habitat variation between the study plots of the same habitat type suggesting that study plots 20 x 20 m in size do not encompass all of the variation present within the habitats studied. It is thought that the significance in the differences between plots of the same habitat may be due to proximity to habitat boundaries and the nature of intergrading vegetation. This, in particular, may be the case for LS3 and MC1. As noted earlier, MS3 is located within a compartment that is under different management than MS2 and MS1 and so, differences are apparent within this habitat type. Future studies should consider a more subjective choice of sampling strategy rather than that of the random method employed here, thereby avoiding areas close to habitat boundaries where vegetation types overlap.

4.5.4 Objective d) Between-habitat variation

Explore the between habitat variation at different wavelengths using study plots from each habitat type.

Table 4:8 to Table 4:10 show the results from comparing a study plot from each habitat type at each of the CASI wavebands (the mean spectra of the study plots used here are shown in Figure 4:22). All pairs of study plots are listed and if spectra were found to be statistically different they are highlighted in the tables. This method was similar to that applied by Schmidt and Skidmore (2003) in that classical statistics were used to identify which parts of the spectrum exhibited statistically different results between vegetation type pairs. Schmidt and Skidmore (2003) did not, however, present information on individual vegetation type pairs, but rather frequency plots of statistically significant differences between pairs along the spectrum. The number of calculations presented in this study are considerably less and so detailed information on results from each habitat type pair is presented. This allows for a greater amount of information to be extracted regarding each habitat type which may then provide an insight into the spectral separability of particularly sensitive habitat types.

The results show very little in the way of pattern along the spectrum of wavelengths where reflectance between plots is consistently statistically different. Instead, this varies between plots and indicates that some wavebands are more appropriate than others for discriminating between different habitat types. The study plot pairs that indicate the most spectral similarity are largely those that include the mixed sedge study plot. Study plot pairings that include *Equisetum fluviatile*, rush pasture/grassland and *Molinia caerulea-Myrica gale* mire plots all exhibit a greater number of statistically different results. Overall, these results illustrate how some habitat types (namely the latter three listed here) may be spectrally more distinct and therefore predicted with greater accuracy in habitat maps. Others such as mixed sedge habitat may well be susceptible to errors of commission and omission (Chapter 6).

The results from a study of the statistical difference along the spectrum between two habitat types in particular, are presented in Figure 4:23 to Figure 4:25. Here, the Mann Whitney test was carried out on each of the 42 spectral bands in the AVS1-42 dataset between spectra from study plot EF1 (*Equisetum fluviatile-Carex rostrata* swamp) and RP3 (Rush pasture/grassland). These diagrams illustrate the increase in areas of the spectrum that do not show significant difference in spectral response between these two study plots, over the course of the summer. Despite the substantial difference in the nature of these two plots (in terms of species structure and composition) these results demonstrate that reflectance in certain areas of the spectrum is such that it is difficult to differentiate between the two habitat types. These results show that data collected in July demonstrates significant differences in the reflectance at all wavelengths for these two habitat types. Conversely, overlap occurs in data collected in September between 400 – 470 nm, 500 – 520 nm, 580 – 610 nm and at 700 nm. Table 4:8 to Table 4:10 do not indicate an overall trend toward spectral similarity between habitat types over the sampling period and it is clear that habitat types differ, in terms of their spectral similarity with others, depending on the time of data collection. It then follows that there are optimum times of the year to discriminate between habitat types and this should be investigated further for sensitive habitat types and, in particular, those that form intergrading boundaries with others where the goal is to identify habitat edges and area.

4.5.5 Objective e) Spectral indices

Determine the between habitat variation as illustrated by spectral indices and geostatistics.

Normalized Difference Vegetation Index

The Normalized Difference Vegetation Index (NDVI) has been used widely to predict biomass in marsh communities (Jensen 1980; Lorenzen & Jensen 1988; Spanglet *et al.* 1998; Gross *et al.* 1988). The nature of the relationship between NDVI and biomass is compounded by canopy structure, primary productivity and leaf-area index (LAI-one-sided leaf area divided by subtending ground area) and further research into this within wetland

environments is still warranted (Gamon *et al.* 1995; Posse & Cingolani 2004; Phinn *et al.* 1999). NDVI data has been used to classify vegetation types using decision tree analyses (Lloyd 1990) and in particular when this information is available between seasons. NDVI was investigated here as a potential tool to assist in the classification of wetland vegetation at the habitat scale and the results presented in Figure 4:26 and Figure 4:27 (Anderson & Perry 1996).

Figure 4:26 illustrates the within habitat variation in NDVI and how this varies over the sampling period. Within-habitat variation is particularly pronounced in the September dataset. When grouped together (Figure 4:27) it becomes clear that NDVI values overlap for the grass and sedge habitat types which is largely unsurprising given their similarities in canopy structure and biomass.

Red-edge and Derivative analysis

Cochrane (2000) considered red-edge analysis as a superior tool for vegetation discrimination and given that the position of the red edge may highlight differences between habitat types that are related to internal leaf structure and pigment concentrations, the differences in the position of the red edge between habitat types was investigated here. First derivative analysis was conducted on the data in order to locate the position of the red edge and prior to this the data had to be smoothed. As the mean-filter is straightforward and computationally efficient it was the preferred method of smoothing the raw spectra before calculating the position of the red edge. However, other methods could have been employed and the different effects of these methods on the end result could be investigated in a future study (Savitzky & Golay 1964; Kawata & Minami 1984).

If just the position of the red edge was reported or too great a smoothing function was applied to the spectra, small features that could contain important information on the nature of the vegetation may be removed. Notably, several researchers have reported that the area of the red edge peak revealed by derivative analysis is actually composed of two or more features

(Horler *et al.* 1983; Boochs *et al.* 1990; Llewellyn & Curran 2005). The results of the first derivative analyses in this study are presented in Figure 4:28 to Figure 4:30 grouped by habitat type (mean and +/-1SDs) and illustrate quite clearly the shape of this double-peak and how this might vary between the habitat types. The shape of the first derivative 'double-peak' area is thought to be related with chlorophyll fluorescence, pigment characteristics and canopy structure (Zarco-Tejada *et al.* 2003; Lichtenthaler & Miehe 1997; Liu *et al.* 2005; Smith *et al.* 2004; Zarco-Tejada *et al.* 2000a; Zarco-Tejada *et al.* 2000b; Llewellyn & Curran 2005; Dobrowski *et al.* 2005). No attempt is made here to explain the nature of the double-peak, although it is recognised that it may well represent characteristics of the vegetation representative of habitat types.

No formal test is made of the significance of the differences between the curves shown in Figure 4:28 to Figure 4:30 and this is an area that could be studied in much greater depth than is presented here. Instead, it is possible to identify by eye, the differences or similarities between the habitat types and to trace this relationship over the three sampling stages. The three habitat types that have proven difficult to separate using other methods introduced up to this point are species rich low sedge mire, *Molinia caerulea*-sedge mire and mixed sedge (these are graphs 'b', 'c' and 'e' in Figure 4:28 to Figure 4:30 respectively). The species rich low sedge mire graphs exhibit a greater separation between the two peaks than the other two sedge habitat types during July and August. The other two habitats are visibly very similar in July and August. However, in September the prominent peak in the mixed sedge first derivative graph shifts to the lower wavelength. These graphs are made up of spectra collected within the study plots employed throughout this study. It has been shown previously that grouping the data from these study plots may not be an ideal method of comparing spectra and first derivative data between the habitat types and so further work using this information should be carried out using a slightly different sampling strategy. These results illustrate that this is an area of research that would benefit wetland habitat classification whilst research into the exact explanatory variables involved continues.

Some researchers have identified the location of these two peaks, although the exact values appear to vary between vegetation and study. Boochs *et al.* (1990) identified peaks in winter wheat at 703 and 735 nm, Lamb *et al.* (2002) identified peaks at 705 and 725 nm in leaves of ryegrass and Zarco-Tejada *et al* (2002) identified peaks in the first derivative reflectance spectrum of sugar maple at 705 and 722 nm. The locations of these peaks seem to shift over the summer between a mode of around 700 and 720 nm as illustrated in Figure 4:31 to Figure 4:36 and presented in a summary graph below. The pattern in the shift between these two wavelengths and the prominence and nature of the double-peak areas, may be exclusive to each habitat type (Figure 4:31 to Figure 4:36) and this warrants further investigation in the future.

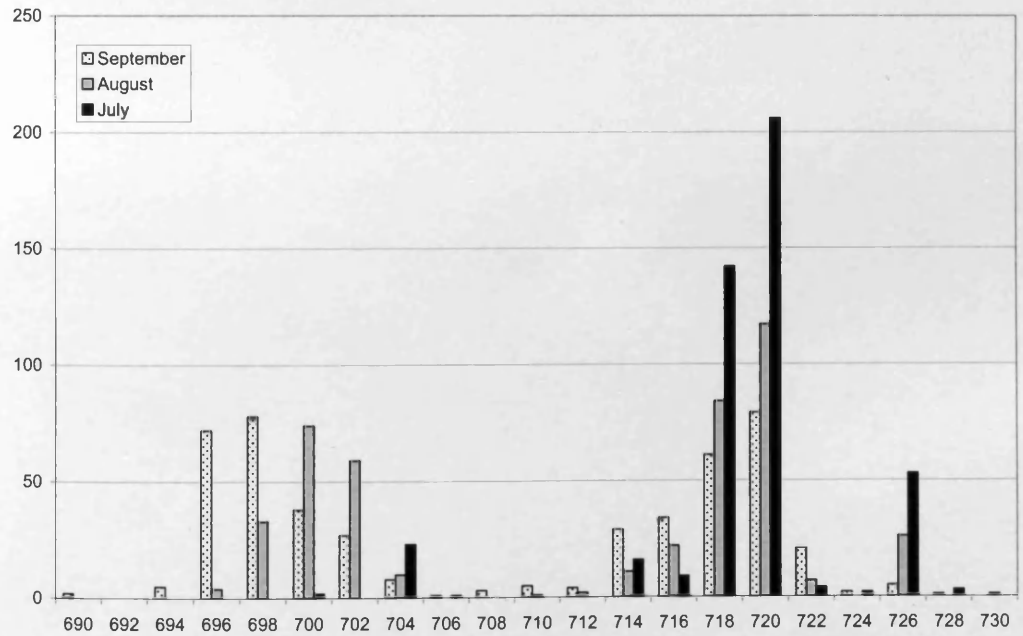

Figure 4:44 All REIPs calculated using each sample spectrum from July, August and September hyperspectral datasets

Continuum Removal

The use of Continuum Removal (CR) has been shown to improve the separability between vegetation types that have varying biochemical content but similar soil conditions and canopy structure (Schmidt & Skidmore 2003; Clark & Roush 1984). This was investigated here on a

small subset of the data to demonstrate the effectiveness of continuum removed reflectance curves and indices to highlight the differences between the absorption features inherent within the spectra of wetland habitat. Research has linked leaf biochemistry features with continuum removed indices and has been scaled up to the landscape scale to predict vegetation quality (Mutanga & Skidmore 2003; Mutanga & Skidmore 2004). Kokaly *et al.* (2003) applied this kind of spectral feature analysis in vegetation mapping in Yellowstone National Park and Schmidt and Skidmore (2003) found continuum removal analyses to increase separability between types of saltmarsh vegetation. In light of the above and the differences illustrated in Figure 4:37 and Figure 4:38 between the various CR reflectance indices of three different habitat types, CR shows promise in the area of habitat discrimination in wetland vegetation.

The results shown in Figure 4:37 and Figure 4:38 indicate that very little difference in terms of group separability exists between Band Depth and the Normalized Band Depth Ratio datasets. These graphs also demonstrate the potential use of field spectra derived CR data to identify locations along the spectrum from which to develop further CR indices that may aid in spectral discrimination between wetland habitat types. The manual construction of the algorithms involved in these graphs is time consuming and labour intensive unless suitable macros or mathematical software is available.

Geostatistics

As with other sections that have dealt with only one study plot from each of the habitats studied, further work should be done to obtain a dataset per habitat type that is formally representative of that area. As such, no formal comparisons between the results of the geostatistics presented here were made. In light of the two variables that were analysed, the nature of the distributions of REIP values within the plots is characterized by relatively high nugget values in comparison with the NDVI results as shown in Table 4:13 and Table 4:14 (<0.00 and 0.01-94.7 respectively). This suggests a much greater degree of random variation within the study plots in terms of REIP values amongst the sample points in relation to NDVI values. This may be due to the non-continuous nature of the position of the red edge, or the

most prominent peak in the first derivative of the samples. Also, in terms of model fit, the R^2 values do appear to fluctuate widely for the NDVI results though the Residual Sum of Squares is a more sensitive and robust statistic to consider. These values are very small for the NDVI results (0.0000 to 4 d.p.) thereby justifying the interpretation of the semivariograms produced for this variable.

The graphs presented in Figure 4:39 and Figure 4:40 illustrate the nature of the semivariograms produced for these plots over the three sampling stages. Interestingly, the range across the habitats was usually found to be around 6 or 7 m, although this did vary slightly within habitats depending on the time of data collection (Wang *et al.* 2001; Atkinson & Curran 1997). These results are significant in that they suggest that spatial datasets collected by remote sensing with a pixel size of at least 6 m x 6 m should effectively identify the variation within the habitat types. This work focused on six habitat types only and further work should include an assessment of other habitat types, in particular, those that may be more important in terms of ecology and wetland management.

4.6 Summary

The overall aim of this chapter was to determine the extent to which wetland habitats are spectrally distinct. Using a hyperspectral dataset and simulated CASI bands, various analyses and indices were explored using data collected from six wetland habitat types at Insh Marshes at three separate times during the growing season. A number of objectives as outlined at the start of this chapter were met and these are listed again below. For each objective, a brief summary of the results obtained is included.

a) Determine the degree to which spectral reflectance pattern varies between habitat types in the visible and near infrared (NIR) regions of the spectrum.

- All habitat types displayed spectral signatures that contained comparable reflectance and absorption features and tended towards increased reflectance in the red region in September.
- Spectral variation within the study plots was consistently high in the NIR region of the spectrum.
- Differing management practices result in spectral variation between study plots from the same habitat type.

b) Assess the degree to which spectra grouped by habitat type are spectrally distinct using multivariate statistical analyses

- MDA demonstrated that when using complete spectral datasets discrimination between the six habitat types that were sampled was possible.
- The smaller spectral dataset from the simulated CASI wavebands proved to be just as effective (and sometimes more effective) at discriminating between habitat types.

- Significant wavebands that were identified by at least two of the three MDA stepwise models are as follows: 380 – 394 nm, 443 – 457 nm, 459 – 473 nm, 711 – 725 nm and 758 – 773 nm.

c) *Explore the within habitat spectral variation using data collected from two or more study plots within each habitat type*

- Significant differences in spectral response between study plots of the same habitat type were found for each of the five habitat types studied at each of the CASI wavebands in the July dataset.
- Study plots from species-rich low sedge mire and *Molinia caerulea-Myrica gale* mire showed significant differences in five or fewer of the CASI wavebands in August and September.
- Study plot location in relation to proximity with habitat boundaries and habitat management are important considerations for spectral discrimination between habitat types.

d) *Explore the between habitat variation at different wavelengths using study plots from each habitat type.*

- Statistically significant differences are fewer between all habitat types and the mixed sedge habitat at each of the simulated CASI dataset.
- Spectral separability is best demonstrated by habitat pairings that include *Equisetum fluviatile*, rush pasture/grassland and *Molinia caerulea-Myrica gale* datasets.

e) *Determine the between habitat variation as demonstrated by spectral indices and geostatistics.*

- Variation in NDVI values between sample plots is much greater in September compared with results from July.
- Variation in NDVI between habitat types is greater in September.
- The position of the red edge shifts between approximately 720 nm and 700 nm over the summer period.
- Differences in the shape of the double peak in the 1st derivatives are identifiable between samples from species rich low sedge mire, *Molinia caerulea*-sedge mire and mixed sedge habitat types.

5 EXPLORING THE SPECTRAL CHARACTERISTICS OF ENVIRONMENTAL DATASETS

5.1 Introduction

The overall aim of this chapter is to determine how well field spectra correlate with detailed vegetation datasets collected at the ground. This relates specifically to Objective 2 as outlined in Chapter 1. Multivariate analysis techniques were employed as well as traditional descriptive methods that are often used within the ecological sciences, to explore the spectra-vegetation relationship. The nature of this relationship was compared between six habitat types at the study site using a dataset collected in July and one collected in September 2003. The specific objectives that will be used to meet the aim of this chapter are listed below.

5.1.1 Aims and Objectives

Chapter 5: Overall Aim (Project Objective 2)

Determine how well vegetation datasets relate to spectral response between habitat types and across habitat boundaries.

The main objectives used to achieve the overall aim of this project as outlined above are listed below.

Chapter 5: Objectives

a) *Describe vegetation datasets grouped by a priori habitat mapping as well as clustering methods.*

b) *Use Multiple Discriminant Analysis to assess how well the habitat class is predicted from the spectral dataset using* a priori *classifications and groups derived from clustering methods.*

c) *Assess the significance of Canonical Correspondence Analyses (CCA) after removal of any existing covariation between the spectra and local weather conditions at time of sampling.*

d) *Assess the spatial turnover (beta diversity) within the vegetation dataset and explore the relationship between this and the beta diversity inherent within the spectral data at paired sample points along the transects.*

e) *Explore the relationship between spectral response and vegetation datasets using multivariate techniques.*

5.2 Methods and Analyses

This section details the methods applied in this chapter beginning with listing the datasets used to achieve each of the objectives outlined above (a) to d)).

5.2.1 Datasets and Methods Overview

The methods and datasets used in order to meet the objectives outlined above are described here in brief. In order to clarify which datasets were used to meet each of these objectives, they are presented here to correspond with the Chapter Objectives a) to e).

a) Vegetation datasets were collected at ten sampling points at each of the 16 study plots in both July 2003 and September 2003. These data were then grouped by habitat type as specified in an *a priori* habitat map. The vegetation samples were also clustered using TWINSPAN. Clusters were constructed by an iterative process and using a rule of no less than six samples per cluster.

b) Two vegetation datasets were compiled from vegetation sampling at each stage of data collection. These included a dataset made up of species names only and one with species names plus structural and environmental variables recorded at each transect (referred to in

the text as 'species and structure' dataset). At each sample point, the field derived spectral data was then converted to both the AVS1-42 spectral dataset and the simulated CASI bands. Each sample point was assigned a 'Group' label, this was either the habitat type (as specified in the *a priori* habitat map) or the cluster name that the sample was assigned using TWINSPAN. Data from the July and September sampling stages were analysed using Multiple Discriminant Analysis (MDA).

c) The meteorological data as described in Chapter 3 were assigned to each paired sample point. This dataset was then entered into CANOCO as covariable data and CCA analyses were carried out on all datasets collected in July and September. Both vegetation datasets were entered as the 'dependent' data and these were the species composition and the species and structural (and environmental) variables. The predictors were the AVS1-42 spectral dataset and the simulated CASI bands. Using data collected in July and September this therefore involved eight different analyses. Each analysis provided an indication of the significance of the first canonical axis and all canonical axes.

d) Detrended Correspondence Analysis (DCA) was performed on both vegetation datasets (i.e. species composition only and species and structure (and environmental) datasets) collected in both July and September. The respective AVS1-42 and CASI datasets were used as supplementary variables. DCA extracts out the maximum variability within the vegetation datasets. Sample scores at paired sample points along transects are used to explore the relationship between beta diversity within both datasets across habitat boundaries.

e) Canonical Correspondence Analysis (CCA) and Redundancy Analysis (RDA) were carried out using both vegetation and spectral datasets (as above in 'd)') for the July and September sampling stages. For CCA, the spectra were the 'predictors' datasets and in RDA they were the 'dependents'. Tests on the significance of the canonical axes were carried out, as were stepwise analyses to determine the most significant predictors at each analysis.

5.2.2 Vegetation Datasets and Two Way INdicator SPecies ANalysis

Results from the collection of vegetation data were tabulated with the frequency of species occurrence recorded (I-V) followed by the range in brackets. The frequency values were calculated by noting the number of quadrats from each habitat or cluster type that each species was present in and calculating this as a percentage of the total number of quadrats recorded within that habitat or cluster type. Results corresponding to the structure and environmental variables that were measured at each sample point (Chapter 3) are also listed, as well as a species richness value for each class. Species richness was calculated for each quadrat within a habitat type or cluster class and then a mean species richness for that class was calculated.

A cluster analysis of the raw vegetation data (species composition) was carried out using the Two Way INdicator SPecies ANalysis (TWINSPAN) method (Hill 1979; Hill *et al.* 1975; Southall *et al.* 2003; Tsuyuzaki *et al.* 2004). The samples within each cluster were identified and the associated structural and environmental data was then incorporated into the cluster. TWINSPAN is popular amongst community ecologists and is based on the use of indicator species to define vegetation types. The method is therefore qualitative and introduces the concept of pseudo-species cut levels whereby a single species is represented by a number of pseudo-species depending how its cover or abundance is partitioned. Quantitative data is therefore transformed into presence-absence data (ones and zeros) upon which a correspondence analysis is carried out. A dichotomy is constructed on the basis of the ordination and the aim of the algorithm used is to get a polarized ordination, that is, an ordination where most of the samples are not positioned close to the centre of gravity, or 'centroid', of the dataset. The cut levels applied in this analysis were 1.1, 3.1, 6.1, 12.1 and 18.1 resulting in six pseudo-species categories, the categories therefore being equivalent to frequency of occurrence within quadrat cells of <5%, 5-10%, 10-25%, 25-50%, 50-75% or above 75%. Further explanation of this method is given by Lepŝ & Ŝmilauer (2003).

5.2.3 Multiple Discriminant Analysis

Multiple Discriminant Analysis (MDA) was performed on the paired vegetation-spectral datasets. Therefore, only spectra collected at the same sample point as a quadrat was used. Analyses were performed using the AVS 1-42 dataset and the simulated CASI datasets with habitat types and TWINSPAN cluster was used to group the classes. MDA is a statistical technique whereby the ability to predict category membership using a set number of variables, in this case habitat type or cluster and spectral response respectively, is assessed via the ability to cross-validate the predictions (Pando *et al.* 1992). The percentage of correct predictions obtained for each class type over the sampling period is presented for each habitat type or vegetation cluster in the output as is the ability to explore incorrect results with the vegetation dataset paired with it.

5.2.4 Multivariate Analysis of Ecological Data

Ordination: An Introduction

An excellent description and discussion of ordination methods of data analysis and applications in ecological science is given in Lepŝ and Ŝmilauer (2003) as well as Kent and Coker (1992) and only a brief outline of the methods used and their related methods of interpretation is given here (Hill 1974; Hill *et al.* 1975). There are two types of ordination methods, constrained and unconstrained and both are used here. For both, an eigenvalue for each of the axes extracted provides a measure of the explanatory power of that axis. As each axis is constructed so that it explains as much variability as possible and independent of the previous axes, the eigenvalues decrease with the order of the axes.

Unconstrained ordination, otherwise referred to as indirect gradient analysis, finds a configuration of samples in feature space so that the distance between samples corresponds with the dissimilarities between samples in terms of their species composition. Principal Components Analysis (PCA) and Correspondence Analysis (CA) are examples of

unconstrained ordination. In the computer programme CANOCO 4.5, 'latent' variables (i.e. the ordination axes) are established that represent the best predictors for the values of all species. The axes correspond to the direction of the greatest variability within the dataset. Constrained ordination, otherwise referred to as direct gradient analysis or canonical ordination, calculates ordination axes that are weighted sums of the environmental variables. Canonical Correspondence Analysis (CCA) and Redundancy Analysis (RDA) are examples of constrained ordination methods. Similar to multiple regression, the fitted values, or site scores, are linear combinations of the environmental variables. The constrained ordination axes correspond to the directions of the greatest data set variability that can be explained by the environmental variables and their number cannot be greater than the number of environmental variables.

Presenting results

The results of ordinations are most often presented graphically as diagrams with data spread over two axes. The data displayed within these diagrams and the form that they take is dependent on the analysis performed. For the results presented in this study, samples (sample points at which data were derived in the field) are represented by points (symbols-circles). In weighted averaging methods of ordination, such as Correspondence Analysis (CA) or Canonical Correspondence Analysis (CCA) species are also represented by points (symbols-triangles). Quantitative environmental variables are represented by arrows and the direction of these corresponds to the value or importance of the environmental variable. The origin of the diagram represents the centroid of the arrows assigned to the environmental variables that are present.

CANOCO produces a log output table with a number of statistics associated with the analysis performed. All types of analyses produce an eigenvalue for each axis, as well as a species-environment correlation, percentage variance explained in the species dataset and of the species-environment relationship. The sum of all eigenvalues and all canonical eigenvalues are also given. In a Detrended Correspondence Analysis (DCA), the lengths of gradients are

also given for each axis. These results provide an indication as to the proportion of the total variation in the species dataset that can be explained by the environmental data and the relative suitability of linear (e.g. PCA or RDA) versus unimodal analyses (e.g. DCA or CCA). The total inertia (or sum of eigenvalues) represents the variance in the dataset and the canonical eigenvalue represents the proportion of that variance that is explained by the environmental variables. Forward stepwise analysis produces a lambdaA statistic for each of the environmental variables and, if this value is divided by the canonical eigenvalue produced for the respective analysis, a 'Fraction of Variance Explained' (FVE) statistic can be attained.

Interpreting ordination diagrams

Ordination diagrams are an effective method of visualising complex structural relationships both within and between datasets. The species data table, the matrix of distances between individual samples, and the matrix of correlations or dissimilarities between individual species, can all be illustrated. In analyses that include environmental variables, the contents of the environmental data table, the relationship between the species and the environmental variables and the correlations amongst environmental variables can also all be represented. In general, the absolute values of the coordinates in ordination space do not have any true meaning and only relative distances, relative directions and relative ordering of projection points are used when interpreting ordination diagrams.

The biplot rule applies to the interpretation of the diagrams presented in this study. This is where, for example, sample points present within the diagram are projected perpendicular to the species' arrow and then correspond to an approximate ordering of the values of the species relative to these samples. A sample point that lies at the origin of the coordinate system (i.e. perpendicular to the direction of the species arrow) is predicted to have an average value of that species. A point further along in the arrow's direction corresponds to increasing abundances and vice versa. The species are assumed to have an optimum position along each of the ordination axes with their abundances decreasing symmetrically in all

directions from that point. The positions of these species are weighted averages of the sample positions with weights related to respective species' abundances.

Detrended Correspondence Analysis

Detrended Correspondence Analysis (DCA) is the detrended version of correspondence analysis, which is a weighted averaging method of unconstrained ordination and effectively extracts out the maximum variation in species composition (Hill & Gauch 1980; Southall *et al.* 2003). No data transformation is needed because the ordinal transformation has a logarithmic nature with respect to cover and provides reasonable weighting of species dominance. DCA is an effective analytical technique for exploring the structure, in particular, the beta diversity within the dataset (i.e. the spatial turnover between samples).

DCA was carried out in CANOCO for Windows (v. 4.5) on the vegetation datasets collected at the study plots as well as along each of the transects (on both vegetation and spectral datasets). The environmental datasets (i.e. spectra) were also included in the analysis (as 'supplementary variables') although in this type of analysis, they do not influence the species and samples orientation and are merely projected onto the ordination diagrams after the analysis. The sample scores for the sample points derived from the DCA on the vegetation recorded along each transect were then compared with the sample scores for the paired spectral data. Regression analyses were performed in SPSS for Windows (v. 12.0.1) and a value of R^2 Adj. was recorded to assess the degree to which variation in the vegetation dataset along the transect is correlated with variation in spectral response.

Canonical Correspondence Analysis

Canonical Correspondence Analysis (CCA) is a method of constrained ordination and was run here using CANOCO for Windows (v. 4.5) (ter Braak 1994; ter Braak & Šmilauer 2002; Lepŝ & Šmilauer 2003) and applied to all vegetation datasets paired with spectral measurements (AVS1-42 and simulated CASI bands). CCA is a multivariate statistical technique that is often used when the objective is to determine the capabilities of environmental variables to

predict vegetation assemblages or species composition datasets (Tsuyuzaki *et al.* 2004; Frederiksen & Lawesson 1992). Constrained ordination techniques allow for the variability in the species data to be explored in direct relation to the variability in the environmental data. The environmental variables employed here were the spectral bands and the spectral response at each of the sample points. These were used to determine how well the spectra could explain the variation in the species composition dataset. Separate analyses were carried out using the spectral dataset coupled with the combined species composition and structural datasets. Analyses were carried out using the hyperspectral dataset as well as the simulated CASI datasets from the first and last sampling stages, (i.e. both the July and September datasets).

Monte Carlo Permutations and the *F*-statistic

Forward stepwise analysis was carried out in CANOCO 4.5 as part of the CCAs using Monte Carlo tests (499 permutations). These tests relate to the general null hypothesis that the species data are independent of the values of the explanatory variables (in this case, the spectral response). The test is carried out by reshuffling (permuting) the explanatory dataset whilst keeping the species dataset intact. If the null hypothesis were true, then any of the reshuffled combinations of environmental and species data are as probable as the original combination. For each permuted dataset, a constrained ordination model is constructed and a test statistic (*F*-statistic) is produced. If it is highly improbable that the 'data-derived' *F*-statistic comes from the distribution of these 'artificial' *F*-statistics then the null hypothesis is rejected.

The variation in the species dataset as described by the environmental dataset is such that it can be expressed by more than one axis in constrained ordination. An *F*-statistic for either all axes or just one can be calculated using the mathematics described in the equations below. Equation 5:1 shows the mathematics used to derive an *F*-statistic for the first canonical axis. Here, λ represents the variance that is explained by the first canonical axis and the residual sum of squares (RSS) term corresponds to the difference between the total variance in the species data and the amount of variability explained by this axis (and also the covariables if

present). The number of covariables is q, the number of independent environmental variables is p (i.e. the total number of canonical axes) and the number of ordination axes is represented by n. Equation 5:2 shows the mathematics used to derive an F-statistic regarding the overall effect of all explanatory variables (p) on the total variance in the species data. The RSS in this equation corresponds to the difference between the total variability in the species data and the sum of the eigenvalues of all canonical axes (adjusted for covariables if applicable). The explanations outlined above for permutation tests and the F-statistic are expanded upon in Lepŝ & Ŝmilauer (2003).

$$F_1 = \frac{\lambda_1}{RSS/(n-p-q)} \qquad \textbf{Equation 5:1}$$

$$F_{trace} = \frac{\sum_{i=1}^{p} \lambda_i / p}{RSS/(n-p-q)} \qquad \textbf{Equation 5:2}$$

Removing the effects of covariation

Covariables can influence the response variable. In this research, meteorological data is regarded as a covariable with the spectral data when the 'response' is the vegetation dataset. It was important to determine whether or not the spectra still had a significant relationship with the vegetation dataset when the influence of the local weather conditions at the time of data collection was considered. It is possible to remove the covariation between two environmental datasets using CANOCO 4.5 before formally assessing the relationship between the explanatory variables and the species dataset. A formal test on the significance of the first ordination axes as well as the combination of all respective ordination axes was performed for all datasets with which CCA was carried out.

Redundancy Analysis

Redundancy analysis (RDA) is a constrained linear method of ordination. This was carried out in CANOCO for Windows (v. 4.5) using the vegetation datasets as the environmental variables or 'predictors' and the spectral dataset as the 'species' (Brook & Kenkel 2002). This

approach is therefore the reverse of that described above and as such, it seeks to identify the species and structural or environmental variables that contribute most strongly to the spectral response. This is based on the assumption that the spectral response is to some extent the product of the structural and pigment characteristics of the component species in the vegetation sample.

RDA finds values of a new variable that represents the 'best' predictor for the values of the response variables, which are in this case, the spectra. In contrast to PCA, RDA is constrained so that the sample scores are a linear combination of the true species as explanatory variables (in this instance, the plant species or structural and environmental variables). Further details on the mathematics behind this ordination are detailed in Lepŝ and Ŝmilauer (2003). Monte Carlo tests were also performed during the RDA in order to test the significance of the first axis and the output consisted of the best predictors (i.e. vegetation species) listed in order of significance. The methods of interpretation of the output from RDA are the same as those applied to CCA above.

5.3 Results

5.3.1 Objective a) Vegetation datasets and Two Way INdicator SPecies ANalysis

Description of the vegetation datasets grouped by a priori *habitat mapping as well as clustering methods.*

Four tables are presented in this section and each contain information on the species composition (including abundance and range) and a summary of the structural and environmental measurements collected at each habitat type (Table 5:1 to Table 5:4). Each quadrat was assigned to a cluster group by TWINSPAN and the species, structural and environmental data were sorted accordingly (Table 5:5 to Table 5:8). Habitat types are coded as follows: EF = *Equisetum fluviatile-Carex rostrata* swamp; LS = species-rich low sedge mire; MC = *Molinia caerulea* – sedge mire; MG = *Molinia-caerulea – Myrica gale* mire; MS = mixed sedge swamp; RP = rush pasture/grassland.

Table 5:1 Species composition data compiled from all study plots and grouped by habitat type (data collected in late June/early July 2003)

	EF	LS	MC	MG	MS	RP
Agrostis sp.		III(1-8)	II(1-8)	**I(11-11)**	II(1-9)	**III(1-20)**
Anthoxanthum odoratum						II(2-6)
Betula pendula				I(1-6)		
Caltha palustris		*	I(1-8)	I(1-1)	I(7-7)	**III(1-14)**
Cardamine pratensis		II(1-3)	*		I(1-2)	I(1-2)
Carex aquatilis		I(1-3)	I(2-4)		**III(2-25)**	*
Carex curta		III(3-18)	I(2-2)	I(1-1)	I(2-3)	I(9-9)
Carex demissa			I(3-3)	II(4-14)		
Carex echinata		II(1-12)	IV(1-19)	**I(2-9)**	*	I(16-20)
Carex hostiana			I(1-3)	I(7-8)		III(3-22)
Carex nigra	**I(7-18)**	IV(2-22)	II(2-18)	I(12-12)	**II(2-12)**	*
Carex ovalis		I(6-6)	I(2-2)	I(3-8)		
Carex panicea		II(1-4)	II(3-14)	**III(1-16)**	II(3-8)	I(1-6)
Carex pauciflora			I(3-5)	I(2-8)		
Carex rostrata	V(3-16)	II(2-14)	II(2-6)	*	II(4-23)	
Carex vesicaria					II(4-23)	I(13-21)
Deschamsia cespitosa		I(1-1)	I(1-2)		*	IV(1-25)
Epilobium palustre		I(1-4)			*	
Equisetum fluviatile	V(14-23)	**III(1-6)**	I(1-2)		III(1-3)	
Equisetum palustre		II(1-11)				
Erica cinerea			I(2-13)	II(1-10)		
Eriophorum angustifolium		I(1-6)	IV(1-12)	III(1-17)	II(3-10)	I(1-4)
Filipendula ulmaria		II(1-6)	I(3-3)		I(1-11)	I(1-1)
Fungi						*
Galium palustre		V(2-11)	II(1-20)	I(1-1)	**V(1-13)**	II(1-20)
Glyceria fluitans		*	*			
Holcus lanatus			I(2-2)	I(7-7)		II(1-4)
Juncus effusus		II(2-14)	II(2-20)	*	II(1-8)	II(1-23)
Juncus sp.		*	*		*	
Menyanthes trifoliata	**V(3-20)**		I(2-3)	II(2-13)		
Molinia caerulea			V(1-23)	IV(1-24)	I(1-7)	
Myrica gale			I(2-2)	**III(1-24)**		
Nardus stricta		I(3-3)	I(2-5)			**II(2-13)**
Narthecium ossifragum				I(1-6)		
Phalaris arundinacea					I(1-8)	
Phragmites australis					*	
Poa pratensis		I(2-2)				II(1-4)
Potamogeton polygonifolius	V(5-14)			I(1-4)		
Potentilla erecta			I(2-2)	I(1-3)		I(1-5)
Potentilla palustris		IV(1-9)	II(1-3)	I(1-9)	IV(1-11)	I(2-6)
Ranunculus flammula		IV(1-6)	**III(1-8)**		I(2-3)	I(1-5)
Ranunculus repens		I(1-1)	I(2-2)		I(2-2)	I(1-4)
Rumex acetosa		*				**I(2-2)**
Salix sp.					*	
Sphagnum sp.	*	II(3-17)	I(2-10)	I(1-12)	III(2-18)	III(4-23)
Trifolium repens		*				II(2-24)
Utricularia intermedia agg	II(3-4)		*			
Veronica scutellata					I(2-2)	
Viola palustris		II(1-6)	I(1-1)		I(2-5)	III(1-14)

(A value of 'I' = presence; 'II' = presence but frequency <20%, 'II' = 20 to 39%, 'III' = 40 to 59%, 'IV' if between 60 and 79% and 'V' if between 80 and 100%; numbers in brackets = 'the range' = # compartments present within in any one quadrat belonging to the class type or cluster (min.-max.); bold font = change of two or more frequency classes between sample stages and '*' = absent but present in September sample set)

Table 5:2 Species composition data compiled from all study plots and grouped by habitat type (data collected in September 2003)

	EF	LS	MC	MG	MS	RP
Agrostis sp.		III(2-8)	I(2-2)	**III(1-12)**	II(2-8)	**I(3-4)**
Anthoxanthum odoratum						I(3-3)
Betula pendula				II(1-3)		
Caltha palustris		I(1-2)	I(1-2)	I(1-1)	I(1-1)	**I(2-2)**
Cardamine pratensis		II(1-2)	I(1-1)		II(1-5)	I(1-1)
Carex aquatilis		I(3-4)	*		**I(3-20)**	I(5-10)
Carex curta		III(2-12)	I(2-6)	*	I(3-5)	*
Carex demissa			I(5-5)	*		
Carex echinata		I(3-4)	III(3-17)	**III(1-14)**	I(4-4)	*
Carex hostiana			I(3-4)	I(3-3)		*
Carex nigra	**III(5-10)**	V(2-22)	II(3-16)	*	**IV(3-24)**	I(1-5)
Carex ovalis		I(4-4)	I(4-4)	*		
Carex panicea		I(3-12)	II(2-8)	I(3-4)	III(3-10)	*
Carex pauciflora				*	*	
Carex rostrata	V(12-25)	II(2-14)	II(2-18)	I(2-8)	II(2-12)	
Carex vesicaria					I(2-10)	*
Deschamsia cespitosa		I(4-6)	I(3-20)		I(7-7)	IV(2-17)
Epilobium palustre		**I(1-2)**			I(2-2)	
Equisetum fluviatile	V(12-24)	I(2-6)	I(1-4)		II(1-7)	
Equisetum palustre		II(1-15)				
Erica cinerea			II(1-22)	*		
Eriophorum angustifolium		II(2-7)	IV(2-22)	IV(3-24)	II(2-10)	I(2-2)
Filipendula ulmaria		I(1-2)	I(1-1)		II(1-5)	I(3-3)
Fungi						I(1-1)
Galium palustre		IV(1-12)	I(2-17)	I(2-2)	**II(1-4)**	II(1-5)
Glyceria fluitans		I(6-6)	I(2-8)			
Holcus lanatus			*	*		II(2-7)
Juncus effusus		II(5-23)	II(1-24)	I(1-5)	I(8-18)	II(1-16)
Juncus sp.		I(2-4)	I(1-7)			
Menyanthes trifoliata	**III(1-5)**		*	*		
Molinia caerulea			IV(3-23)	III(3-18)	II(3-12)	
Myrica gale			I(12-12)	**V(1-22)**		
Nardus stricta		II(2-9)	I(5-9)			**V(3-22)**
Narthecium ossifragum				I(8-8)		
Phalaris arundinacea					I(1-6)	
Phragmites australis					I(1-2)	
Poa pratensis		I(1-8)				I(7-7)
Potamogeton polygonifolius	V(6-17)			*		
Potentilla erecta			II(1-5)	I(1-2)		I(2-3)
Potentilla palustris		IV(2-9)	I(1-4)	I(1-4)	III(1-8)	I(1-5)
Ranunculus flammula		III(1-7)	**I(1-2)**		I(1-2)	I(1-1)
Ranunculus repens		I(1-2)	I(1-1)		I(2-2)	I(1-3)
Rumex acetosa		I(1-4)				**III(2-8)**
Salix sp.					I(2-2)	
Sphagnum sp.	I(1-1)	II(1-5)	I(1-15)	I(2-5)	II(3-7)	III(1-15)
Trifolium repens		I(1-9)				I(1-20)
Utricularia intermedia agg	I(2-2)		I(4-9)			
Veronica scutellata					*	
Viola palustris		I(1-7)	II(1-5)		I(2-3)	III(1-18)

(A value of 'I' = presence; 'II' = presence but frequency <20%, 'II' = 20 to 39%, 'III' = 40 to 59%, 'IV' if between 60 and 79% and 'V' if between 80 and 100%; numbers in brackets = 'the range' = # compartments present within in any one quadrat belonging to the class type or cluster (min.-max.); bold font = change of two or more frequency classes between sample stages and '*' = absent but present in July sample set)

Table 5:3 Structural and environmental data compiled from all study plots and grouped by habitat type (data collected in late June/early July 2003)

	EF	LS	MC	MG	MS	RP
Number quadrats	10	30	40	20	30	30
Total Number of Species	6	24	30	23	22	25
Mean quadrat species richness	4.3	8.0	6.6	5.1	6.1	7.1
Totally Obscured Height (cm) (TOH)	5.30	6.23	10.65	16.80	7.57	2.65
Partially Obscured Height (cm) (POH)	19.10	21.67	24.15	31.00	33.20	8.97
Maximum Height (cm)	44.50	39.73	50.18	52.35	52.20	20.13
Stem density (per 100cm^2)	8.80	21.03	22.50	13.00	16.00	38.33
Grazed/Topped (% cover)	0.00	13.10	0.00	0.00	1.47	65.37
Tussocks (Mean presence)	0.00	0.33	0.63	0.25	0.33	0.23
Water depth (cm)	3.60	0.02	0.00	0.30	0.00	0.00
Bare peat (% cover)	19.00	1.80	0.00	1.85	5.47	0.40
Droppings (% cover)	0.00	0.00	0.35	0.00	0.00	0.93
Leaf litter (% cover)	3.50	3.17	11.30	6.00	7.37	3.00
Woody stems (% cover)	0.00	0.00	0.00	1.80	0.00	0.00

Table 5:4 Structural and environmental data compiled from all study plots and grouped by habitat type (data collected in September 2003)

	EF	LS	MC	MG	MS	RP
Number quadrats	10	30	40	20	30	30
Total Number of Species	7	29	30	16	26	23
Mean quadrat species richness	4.2	8.1	6.1	4.9	5.7	5.6
Totally Obscured Height (cm) (TOH)	2.00	10.60	6.88	14.10	10.80	1.73
Partially Obscured Height (cm) (POH)	15.30	21.97	19.68	30.30	26.93	5.83
Maximum Height (cm)	41.10	47.23	50.80	57.40	61.67	15.13
Stem density (per 100 cm^2)	11.70	32.00	33.85	21.05	27.17	30.50
Grazed/Topped (% cover)	0.00	16.53	39.03	2.00	14.07	73.10
Tussocks (Mean presence)	0.00	0.00	0.73	0.45	0.23	0.00
Water depth (cm)	0.00	0.00	0.00	0.00	0.00	0.00
Bare peat (% cover)	10.10	0.53	0.33	0.45	1.40	0.07
Droppings (% cover)	0.00	0.00	0.10	0.00	0.00	1.20
Leaf litter (% cover)	75.50	28.03	26.78	18.20	47.00	15.93
Woody stems (% cover)	0.00	0.00	0.00	2.65	0.00	0.00

Table 5:5 Species composition data compiled from all study plots and grouped by TWINSPAN clusters (data collected in late June/early July 2003)

	Cluster 1	Cluster 2	Cluster 3	Cluster 4	Cluster 5	Cluster 6	Cluster 7
Agrostis sp.	IV(1-20)		III(1-9)	III(1-8)	II(1-11)		
Anthoxanthum odoratum	III(2-6)						
Betula pendula					I(1-1)	I(6-6)	
Caltha palustris	IV(1-14)			II(1-8)			I(1-1)
Cardamine pratensis	I(1-2)	I(2-2)	II(1-3)	I(1-1)			
Carex aquatilis		V(2-25)	II(1-8)	I(2-4)	I(2-2)		
Carex curta			IV(3-18)	I(2-10)	I(2-2)	I(1-1)	
Carex demissa					I(3-3)	IV(4-13)	I(14-14)
Carex echinata	I(16-20)		I(2-2)	III(1-12)	III(5-19)	I(2-2)	
Carex hostiana	IV(3-22)	I(6-6)		I(7-11)	I(1-3)	II(7-8)	
Carex nigra			IV(2-22)	IV(2-14)	I(2-18)		I(7-18)
Carex ovalis				I(6-6)	I(2-2)	I(8-8)	I(3-3)
Carex panicea	II(1-6)		II(1-6)	II(1-6)	III(2-16)	II(1-6)	
Carex pauciflora					I(3-5)	II(2-8)	
Carex rostrata		II(4-23)	II(2-20)	I(2-14)	II(2-6)		V(3-16)
Carex vesicaria	I(16-20)	IV(4-23)	I(20-21)				
Deschamsia cespitosa	III(1-18)	I(2-2)	I(1-1)	II(1-25)	I(1-1)		
Epilobium palustre			I(1-4)				
Equisetum fluviatile		II(1-3)	III(1-6)	I(1-2)	I(1-2)		V(14-23)
Equisetum palustre			II(1-11)				
Erica cinerea					I(1-13)	III(1-10)	
Eriophorum angustifolium	I(1-4)		II(2-10)	II(1-6)	V(1-17)		
Filipendula ulmaria	I(1-1)		II(1-6)	I(1-4)	I(6-11)		
Galium palustre	I(10-12)	V(1-8)	V(1-13)	V(2-20)	II(1-3)		
Holcus lanatus	II(1-4)			I(2-2)			I(7-7)
Juncus effusus	II(1-9)	II(1-6)		IV(2-23)	I(2-9)		
Menyanthes trifoliata					I(2-3)	IV(2-13)	V(3-20)
Molinia caerulea			I(1-1)	II(1-7)	V(1-23)	V(1-24)	I(6-6)
Myrica gale			I(11-11)		II(1-24)		
Nardus stricta	III(2-13)			I(3-3)	I(2-5)		
Narthecium ossifragum					I(1-6)		
Phalaris arundinacea			I(5-8)	I(1-8)	I(1-1)		
Poa pratensis	III(1-4)		I(2-2)				
Potamogeton polygonifolius						II(1-2)	V(4-14)
Potentilla erecta	II(1-5)				I(1-2)	II(3-3)	
Potentilla palustris	I(2-5)	IV(1-11)	V(1-9)	III(1-7)	II(1-9)		
Ranunculus flammula	I(1-1)	I(3-3)	IV(1-6)	IV(1-8)	II(1-4)		
Ranunculus repens	I(1-4)		I(1-1)	I(1-1)	I(2-2)		
Rumex acetosa	I(2-2)						
Sphagnum sp.	IV(4-23)	V(4-18)	II(2-17)		I(1-10)		
Trifolium repens	II(2-24)			I(2-2)			
Utricularia intermedia agg							II(3-4)
Veronica scutellata			I(2-2)				
Viola palustris	III(1-14)		II(1-4)	III(1-6)	I(1-2)		

(A value of 'I' = presence; 'II' = presence but frequency <20%, 'II' = 20 to 39%, 'III' = 40 to 59%, 'IV' if between 60 and 79% and 'V' if between 80 and 100%; numbers in brackets = 'the range' = # compartments present within in any one quadrat belonging to the class type or cluster (min.-max.)

Table 5:6 Species composition data compiled from all study plots and grouped by TWINSPAN clusters (data collected in September 2003)

	Cluster 1	Cluster 2	Cluster 3	Cluster 4	Cluster 5	Cluster 6
Agrostis sp.	V(3-12)	II(1-3)	II(2-8)	II(2-8)	I(3-4)	
Anthoxanthum odoratum				I(3-3)		
Betula pendula		II(1-3)	I(1-1)			
Caltha palustris		I(1-1)	I(1-2)	I(1-2)	I(1-2)	
Cardamine pratensis				II(1-5)	I(1-1)	II(1-5)
Carex aquatilis				I(3-12)	I(5-10)	I(6-20)
Carex curta		I(3-3)	I(3-6)	II(2-12)		
Carex demissa			I(5-5)			
Carex echinata	III(5-8)	III(1-12)	III(3-17)	I(3-4)		
Carex hostiana		I(3-3)	I(3-4)			
Carex nigra			III(3-16)	IV(2-24)	I(1-4)	III(4-12)
Carex ovalis			I(4-4)	I(4-4)		
Carex panicea			IV(2-10)	II(3-12)		I(6-6)
Carex rostrata	I(8-8)	II(2-18)	I(3-8)	II(2-14)	I(9-9)	V(4-25)
Carex vesicaria				I(2-2)		I(8-10)
Deschamsia cespitosa			I(7-7)	II(3-20)	IV(2-20)	
Epilobium palustre			I(2-2)	I(1-2)		
Equisetum fluviatile		I(1-2)	I(1-4)	I(1-6)		IV(2-24)
Equisetum palustre				I(1-15)		
Erica cinerea			II(5-22)			
Eriophorum angustifolium	III(4-8)	V(3-24)	V(2-20)	II(2-15)	I(2-2)	
Filipendula ulmaria			II(1-5)	I(1-2)	I(1-3)	
Fungi					I(1-1)	
Galium palustre			II(1-6)	III(1-17)	II(1-3)	I(1-1)
Glyceria fluitans			I(2-8)	I(6-6)		
Holcus lanatus					III(2-7)	
Juncus effusus		I(1-5)	I(1-14)	III(5-24)	II(1-24)	
Juncus sp.		I(1-1)	I(5-7)	I(2-4)		
Menyanthes trifoliata						II(1-5)
Molinia caerulea	I(3-3)	IV(4-22)	V(3-23)	I(3-5)		
Myrica gale	V(2-22)	IV(2-17)	I(1-1)			
Nardus stricta			I(5-5)	II(2-9)	V(3-22)	
Narthecium ossifragum	I(8-8)					
Phalaris arundinacea			I(1-6)			
Phragmites australis			I(1-2)			
Poa pratensis				I(1-8)	I(7-7)	
Potamogeton polygonifolius						III(6-17)
Potentilla erecta	I(2-2)	I(1-1)	III(1-5)		I(2-3)	
Potentilla palustris	II(1-2)	II(1-4)	II(1-8)	III(1-9)	I(1-5)	I(2-5)
Ranunculus flammula		I(1-1)	I(1-2)	II(1-7)	I(2-2)	
Ranunculus repens			I(1-2)	I(1-2)	I(1-3)	
Rumex acetosa				I(1-2)	IV(2-8)	
Salix sp.			I(2-2)			
Sphagnum sp.	I(3-3)	II(2-7)	I(1-15)	II(1-7)	III(1-15)	II(1-3)
Trifolium repens				I(1-9)	II(1-20)	
Utricularia intermedia agg		I(5-5)	I(4-9)			I(2-2)
Viola palustris		I(1-2)	II(1-5)	I(1-7)	III(1-18)	

(A value of 'I' = presence; 'II' = presence but frequency <20%, 'II' = 20 to 39%, 'III' = 40 to 59%, 'IV' if between 60 and 79% and 'V' if between 80 and 100%; numbers in brackets = 'the range' = # compartments present within in any one quadrat belonging to the class type or cluster (min.-max.)

Table 5:7 Structural and environmental data compiled from all study plots and grouped by TWINSPAN clusters (data collected in late June/early July 2003)

	Cluster 1	Cluster 2	Cluster 3	Cluster 4	Cluster 5	Cluster 6	Cluster 7
Number quadrats	23	18	28	28	44	8	11
Total Number of Species	24	12	26	26	31	13	11
Mean quadrat species richness	7.6	4.9	7.9	7.5	6	4.9	4.5
Totally Obscured Height (cm) (TOH)	2.46	7.22	5.61	8.50	11.14	20.13	6.91
Partially Obscured Height (cm) (POH)	7.48	33.17	22.36	26.11	23.73	37.75	20.00
Maximum Height (cm)	15.91	52.11	41.57	44.25	49.34	60.38	45.45
Stem density (per 100 cm^2)	41.96	8.33	20.29	27.07	19.09	15.63	9.36
Grazed/Topped (% cover)	75.30	7.61	14.89	4.00	0.00	0.00	0.00
Tussocks (Mean presence)	0.13	0.22	0.32	0.39	0.64	0.13	0.09
Water depth (cm)	0.00	0.00	0.02	0.00	0.14	0.00	3.27
Bare peat (% cover)	0.17	7.72	2.18	0.93	0.48	2.00	17.27
Droppings (% cover)	1.13	0.00	0.00	0.07	0.32	0.00	0.00
Leaf litter (% cover)	3.43	10.00	3.14	2.54	12.07	3.50	3.27
Woody stems (% cover)	0.00	0.00	0.00	0.00	0.45	1.75	0.18

Table 5:8 Structural and environmental data compiled from all study plots and grouped by TWINSPAN clusters (data collected in September 2003)

	Cluster 1	Cluster 2	Cluster 3	Cluster 4	Cluster 5	Cluster 6
Number quadrats	7	19	33	56	28	17
Total Number of Species	10	18	32	30	21	13
Mean quadrat species richness	3.9	4.8	7.7	6.5	5.7	4.1
Totally Obscured Height (cm) (TOH)	19.43	10.00	8.64	9.20	1.54	6.00
Partially Obscured Height (cm) (POH)	40.57	22.47	18.58	23.79	5.89	21.59
Maximum Height (cm)	69.57	49.26	49.45	53.38	15.93	48.35
Stem density (per 100 cm^2)	15.14	31.84	37.18	27.54	30.71	14.24
Grazed/Topped (% cover)	0.00	23.16	32.09	17.68	77.61	2.94
Tussocks (Mean presence)	0.43	0.53	0.91	0.04	0.00	0.00
Water depth (cm)	0.00	0.00	0.00	0.00	0.00	0.00
Bare peat (% cover)	0.71	0.26	0.36	0.75	0.50	6.18
Droppings (% cover)	0.00	0.21	0.00	0.07	1.14	0.00
Leaf litter (% cover)	10.43	30.32	21.36	35.61	17.36	63.82
Woody stems (% cover)	3.57	1.37	0.06	0.00	0.00	0.00

5.3.2 Objective b) Multiple Discriminant Analysis

Use Multiple Discriminant Analysis to assess how well the habitat class is predicted from the spectral dataset using a priori *classifications and groups derived from clustering methods.*

Table 5:9 Multiple Discriminant Analysis results (percentage correct per habitat type and overall) using paired spectral datasets only and grouped by habitat type (1=EF, 2=LS, 3=MC, 4=MG, 5=MS, 6=RP; results from using a random group labelling system in brackets*)

Dataset		Group 1	2	3	4	5	6	Overall accuracy (%) (Random*)
July	AVs1-42	90.0	71.4	92.1	30.0	76.7	70.0	73.1 (13.9)
	CASI	100.0	75.0	65.8	90.0	60.0	56.7	69.9 (11.4)
Sept	AVs1-42	90.0	76.7	90.0	90.0	80.0	86.7	85.0 (15.6)
	CASI	80.0	73.3	85.0	90.0	73.3	90.0	81.9 (17.5)

The table above displays the results of Multiple Discriminant Analysis (MDA) in terms of classification success where spectra are used to predict group membership (See Appendix C for full model outputs). The last column displays the overall accuracy results and in brackets, the results produced using randomized group labeling for comparison purposes. Results for the AVS1-42 and CASI datasets are very similar despite the large reduction in number of predictors in the CASI dataset.

Table 5:10 Multiple Discriminant Analysis results using paired spectral datasets only and grouped by TWINSPAN; Groups 1-6 for September datasets and 1-7 for July datasets (percentage correct per habitat type and overall) (Results from using a random group labelling system in brackets*)

Dataset		Group (Cluster) 1	2	3	4	5	6	7	Overall accuracy (%) (Random*)
July	AVs1-42	47.8	72.2	10.7	14.3	83.3	25.0	72.7	48.1 (17.1)
	CASI	52.2	61.1	46.4	46.4	42.9	87.5	90.9	53.2 (19.0)
Sept	AVs1-42	85.7	63.2	69.7	73.2	39.3	76.5	N/A	66.3(18.1)
	CASI	85.7	47.4	57.6	55.4	21.4	70.6	N/A	51.9 (20.6)

A direct comparison between the July results in Table 5:9 with those in Table 5:10 is difficult to make as the number of groups used to predict the group membership of each sample spectra are different. Seven clusters were produced using TWINSPAN for the July vegetation datasets and six for the September data using the cut levels and group rules applied in the

method. Compared with results in Table 5:9, the results of the MDA on the TWINSPAN groups are lower than those achieved using the *a priori* habitat type groups.

5.3.3 Objective c) Covariation between Spectra and Meteorological Data

Assess the significance of Canonical Correspondence Analyses (CCA) after removal of any existing covariation between the spectra and local weather conditions at time of sampling.

The results from the analyses on the effects of covariation between spectral response at the sample points and the local weather conditions on species datasets are displayed in Table 5:11. From the P-values it is apparent that a significant relationship between the environmental and species variables remained for all combinations of datasets (to 99.9% significance level).

Table 5:11 The significance of the canonical axes when covariation is removed

Dataset ('Dependent':'Predictor')	Test of significance of first canonical axis: Eigenvalue	F-ratio	P-value
July			
Species:AVS1-42	0.278	7.391	0.0020
Species:CASI	0.231	6.628	0.0020
Spp.&Structure:AVS1-42	0.113	8.949	0.0020
Spp.&Structure:CASI	0.082	6.872	0.0020
September			
Species:AVS1-42	0.232	5.125	0.0020
Species:CASI	0.128	3.585	0.0040
Spp.&Structure:AVS1-42	0.101	8.271	0.0020
Spp.&Structure:CASI	0.038	3.904	0.0040
Dataset ('Dependent':'Predictor')	**Test of significance of all canonical axes Trace**	**F-ratio**	**P-value**
July			
Species:AVS1-42	1.205	1.900	0.0020
Species:CASI	0.618	1.928	0.0020
Spp.&Structure:AVS1-42	0.439	2.171	0.0020
Spp.&Structure:CASI	0.211	2.134	0.0020
Sept			
Species:AVS1-42	1.624	1.196	0.0080
Species:CASI	0.509	1.547	0.0020
Spp.&Structure:AVS1-42	0.474	1.291	0.0020
Spp.&Structure:CASI	0.140	1.531	0.0020

5.3.4 Objective d) Detrended Correspondence Analysis

Assess the spatial turnover (beta diversity) within the vegetation dataset and explore the relationship between this and the beta diversity inherent within the spectral data at paired sample points along the transects.

DCA was performed in CANOCO for each vegetation dataset (species only and species with structural and environmental variables) with both AVS1-42 and CASI spectral datasets used as supplementary data. Corresponding output tables for these analyses are presented below for both the July and September datasets. The results obtained using the July and September species composition datasets only are presented here in graphical form (Figure 5:1 and Figure 5:2) as these are only slightly different from results obtained using the species with structural and environmental variables.

DCA was also performed on the paired vegetation and spectral datasets along each transect. The respective samples scores are illustrated in Figure 5:3 and the results from regression analyses between spectral sample scores (both AVS1-42 and CASI datasets) with the species composition datasets from July and September are shown in Table 5:14.

Table 5:12 DCA output-July 2003

		Axis I	Axis II	Axis III	Axis IV
Vegetation-Species(AVS1-42 as sup. env. data)					
Sum of all eigenvalues (sum of all canonical eigenvalues) 7.732 (3.207)					
Eigenvalues		0.723	0.506	0.361	0.291
Lengths of gradient		5.131	4.467	4.222	3.354
Species-env correlations		0.830	0.770	0.608	0.590
Cumulative % variance	-of species data	9.4	15.9	20.6	24.3
	-of species-env relation	15.1	24.9	0.0	0.0
Vegetation-Species(CASI as sup. env. data)					
Sum of all eigenvalues (sum of all canonical eigenvalues) 7.732 (1.667)					
Eigenvalues		0.723	0.506	0.361	0.291
Lengths of gradient		5.131	4.467	4.222	3.354
Species-env correlations		0.646	0.646	0.422	0.338
Cumulative % variance	-of species data	9.4	15.9	20.6	24.3
	-of species-env relation	17.9	31.2	0	0
Vegetation-Species and Structure(AVS1-42 as sup. env. data)					
Sum of all eigenvalues (sum of all canonical eigenvalues) 2.712 (1.228)					
Eigenvalues		0.502	0.176	0.105	0.092
Lengths of gradient		3.127	1.952	1.485	1.461
Species-env correlations		0.871	0.749	0.674	0.655
Cumulative % variance	-of species data	18.5	25.0	28.9	32.3
	-of species-env relation	27.7	36.2	0.0	0.0
Vegetation-Species and Structure(CASI as sup. env. data)					
Sum of all eigenvalues (sum of all canonical eigenvalues) 2.712 (0.649)					
Eigenvalues		0.502	0.176	0.105	0.092
Lengths of gradient		3.127	1.952	1.485	1.461
Species-env correlations		0.691	0.680	0.389	0.405
Cumulative % variance	-of species data	18.5	25.0	28.9	32.3
	-of species-env relation	33.2	46.5	0.0	0.0

The results of the DCA on the species only dataset exhibit high eigenvalues and, correspondingly, a relatively high degree of total inertia within the dataset when compared with results from the species and structural variables dataset. The first gradient is the longest at 0.723, explaining 9.4% of the total species variability. The second and third gradients are also long and explain 6.5% and 4.7% of the total species variability respectively. The first axis is very well correlated with the environmental data when this is the AVS1-42 dataset (r = 0.830) but less so for the CASI dataset (r = 0.646). The correlations for the other three axes for both analyses tend to decrease as axis number increases. However, for the CASI dataset

the species-environment correlation is the same for axis I and axis II. On the whole these are higher for the AVS1-42 dataset. The cumulative percentage variance of the species-environment relation is higher for the CASI dataset at 31.2% and this is 24.9% for the AVS1-42 dataset.

The lengths of the gradients for the species and structure dataset are relatively small with the biggest being axis I: 3.099 explaining 18.2% of the species variability. This is a good deal higher than the equivalent axis from the species only dataset. The species-environment correlations are high for the AVS1-42 dataset starting at 0.871 for axis I, the equivalent for the CASI dataset is still reasonably good at 0.690. The total percentage variance for the CASI dataset was again higher than that for the AVS1-42 dataset at 46% compared with 35.3%. These are both higher than the equivalent results from the species only analyses.

The ordination diagram shown in Figure 5:1 shows the quadrats from the six different habitat types grouped together in feature space and the position of associated species. Overlap is apparent though between samples from LS and MC and samples from MS and MG. The pattern in the location of species triangles in the DCA of the species composition dataset is such that three groupings of species are apparent. One of these is to the far left of the ordination diagram where species that are characteristic of very wet mires are located such as *Utricularia, Potamogeton polygonifolius* and *Menyanthes trifoliata.* These species are located close to the cluster of EF sample points. To the far right of the diagram where sample points from RP are located, is a cluster of species that would be observed in a fairly dry, acid grassland environment such as *Rumex acetosa*, *Nardus stricta* and *Poa pratensis.*

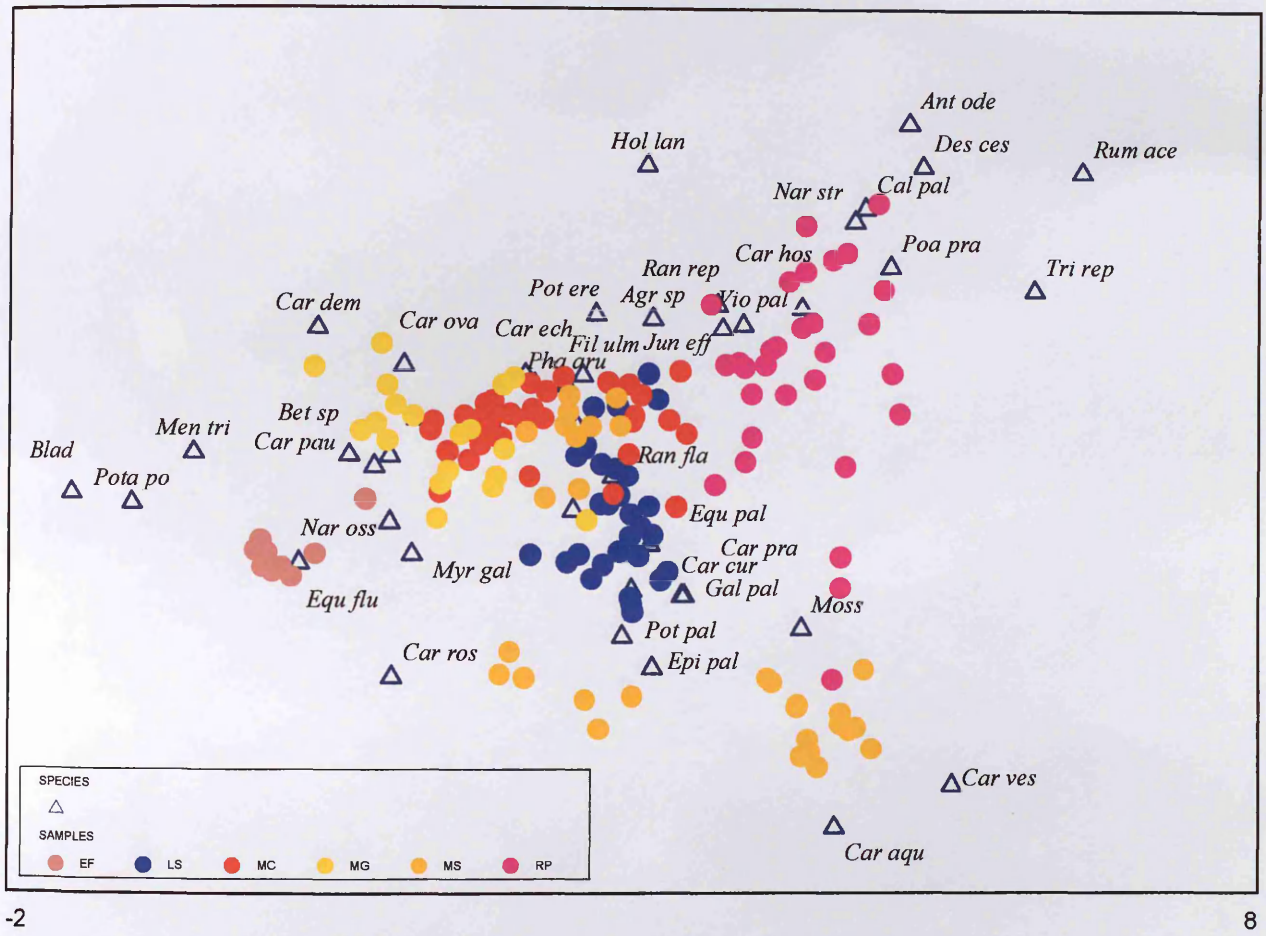

Figure 5:1 DCA species-samples biplot (triangles and circles respectively) for vegetation-species composition dataset in July (some species have been omitted for clarity) (axis I eigenvalue: 0.7, axis II eigenvalue: 0.5) (species labels: *Agr sp-Agrostis sp.; Ant ode-Anthoxanthum odoratum; Bet sp-Betula pendula; Blad-Utricularia intermedia agg; Cal pal-Caltha palustris; Car pra-Cardamine pratensis; Car aqu-Carex aquatilis; Car cur-Carex curta; Car dem-Carex demissa; Car ech-Carex echinata; Car hos-Carex hostiana; Car nig-Carex nigra; Car ova-Carex ovalis; Car pan-Carex panacea; Car pau-Carex pauciflora; Car ros-Carex rostrata; Car ves-Carex vesicaria; Des ces-Deschamsia cespitosa; Epi pal-Epilobium palustre; Equ flu-Equisetum fluviatile; Equ pal-Equisetum palustre; Eri cin-Erica cinerea; Eri ang-Eriophorum angustifolium; Fil ulm-Filipendula ulmaria; Gal pal-Galium palustre; Hol lan-Holcus lanatus; Jun eff-Juncus effusus; Men tri-Menyanthes trifoliata; Mol cae-Molinia caerulea; Moss-Sphagnum sp.; Myr gal-Myrica gale; Nar str-Nardus stricta; Nar oss-Narthecium ossifragum; Pha aru-Phalaris arundinacea; Poa pra-Poa pratensis; Pota po-Potamogeton polygonifolius; Pot ere-Potentilla erecta; Pot pal-Potentilla palustris; Ran fla-Ranunculus flammula; Ran rep-Ranunculus repens; Rum ace-Rumex acetosa; Tri rep-Trifolium repens; Ver scu-Veronica scutellata; Vio pal-Viola palustris*)

September DCA: Study Plots

Table 5:13 DCA output-September 2003

		Axis I	Axis II	Axis III	Axis IV
Vegetation-Species(AVS1-42 as sup. env. data)					
Sum of all eigenvalues (sum of all canonical eigenvalues) 7.293 (3.206)					
Eigenvalues		0.725	0.512	0.347	0.302
Lengths of gradient		5.307	4.712	3.575	2.869
Species-env correlations		0.879	0.890	0.736	0.691
Cumulative % variance	-of species data	9.9	17.0	21.7	25.9
	-of species-env relation	17.4	32.5	0.0	0.0
Vegetation-Species(CASI as sup. env. data)					
Sum of all eigenvalues (sum of all canonical eigenvalues) 7.293 (1.498)					
Eigenvalues		0.725	0.512	0.347	0.302
Lengths of gradient		5.307	4.712	3.575	2.869
Species-env correlations		0.684	0.702	0.406	0.425
Cumulative % variance	-of species data	9.9	17.0	21.7	25.9
	-of species-env relation	23.3	43.4	0.0	0.0
Vegetation-Species and Structure(AVS1-42 as sup. env. data)					
Sum of all eigenvalues (sum of all canonical eigenvalues) 2.126 (1.013)					
Eigenvalues		0.409	0.172	0.079	0.053
Lengths of gradient		2.723	2.176	1.545	1.642
Species-env correlations		0.837	0.852	0.716	0.734
Cumulative % variance	-of species data	19.3	27.4	31.1	33.5
	-of species-env relation	25.3	40.5	0.0	0.0
Vegetation-Species and Structure(CASI as sup. env. data)					
Sum of all eigenvalues (sum of all canonical eigenvalues) 2.126 (0.469)					
Eigenvalues		0.409	0.172	0.079	0.053
Lengths of gradient		2.723	2.176	1.545	1.642
Species-env correlations		0.603	0.629	0.348	0.559
Cumulative % variance	-of species data	19.3	27.4	31.1	33.5
	-of species-env relation	28.2	46.2	0.0	0.0

The results of the DCA on the species only dataset from September (Table 5:13) exhibit high eigenvalues and correspondingly a relatively high degree of total inertia within the dataset when compared with results from the species and structural variables dataset. This was the same pattern found in Table 5:12 for the July datasets. The first gradient is the longest at 0.725, explaining 9.9% of the total species variability. The second and third gradients are also long and explain 7.1% and 4.7% of the total species variability respectively. The first axis is very well correlated with the environmental data when this is the AVS1-42 dataset (r = 0.879) but less so for the CASI dataset (r=0.684). Axes III and IV species-environment correlations

are also high for the AVS1-42 analyses suggesting that variation along these axes may also correspond significantly to predictor variables.

The results from a DCA on the species data collected in September (Figure 5:2) show the sample quadrats to be distributed between three main distinctive zones and a zone in the centre. The distribution of species triangles illustrates a grouping of species that are characteristic of relatively wet swampy environments located to the bottom left of the ordination diagram, close to the EF cluster of sample points. Also in this area of the diagram are the sedges *Carex aquatilis* and *Carex vesicaria* and these, along with *Carex rostrata* and *Cardamine pratensis* are closely associated with a small cluster of MS sample points. The species *Narthecium ossifragum*, *Myrica gale* and *Betula pendula* are all to the far right of the ordination diagram and as such are closely associated with the MG sample points. *Holcus lanatus*, *Rumex acetosa, Nardus stricta* and *Deschamsia cespitosa* are all species that are located to the top left of the diagram and these are often characteristic of well drained grassland that is subject to inundation. Patterns in the location of species within the central area of the diagram are difficult to interpret.

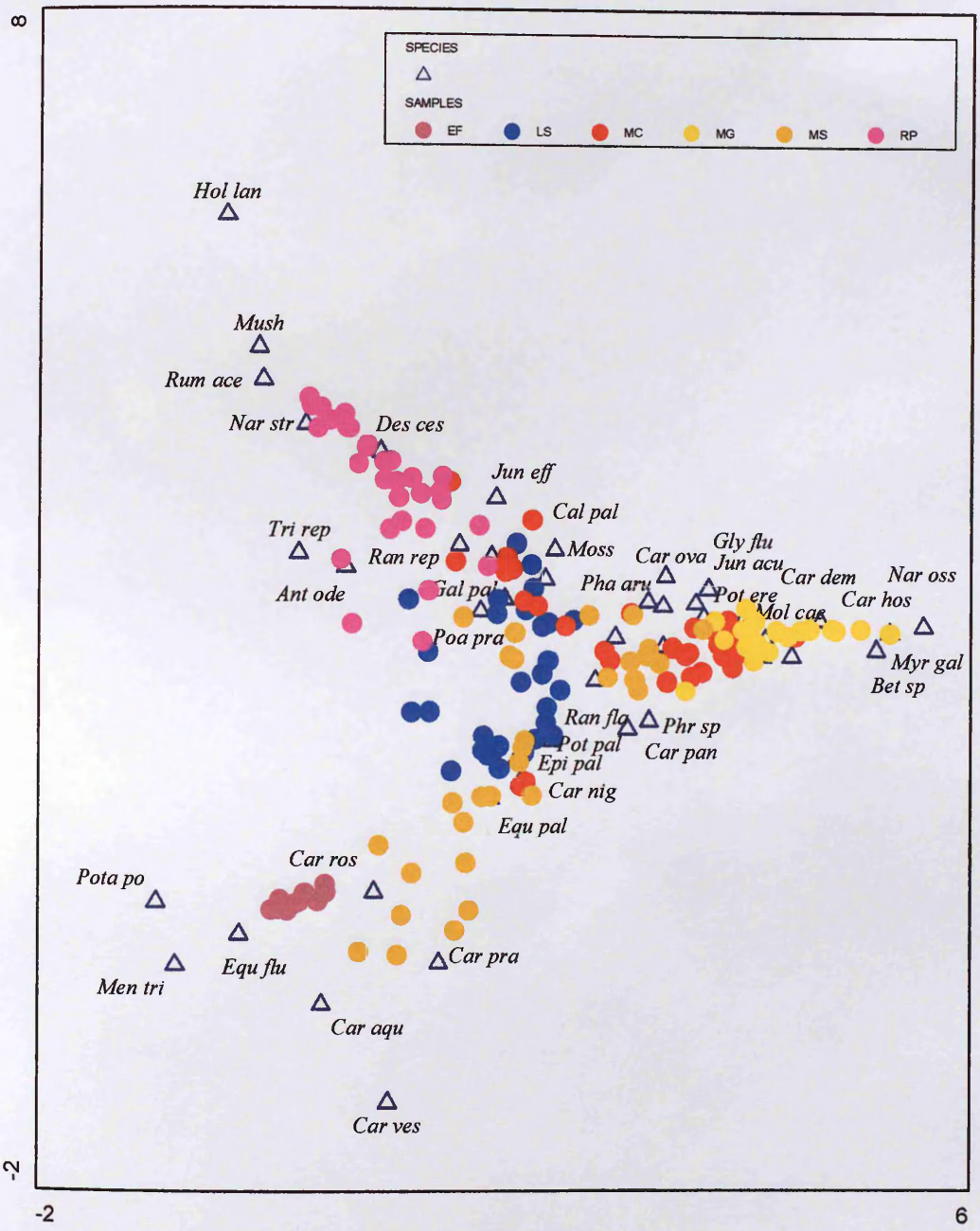

Figure 5:2 DCA species-samples biplot (triangles and circles respectively) for vegetation-species composition dataset in September (some species have been omitted for clarity) (axis I eigenvalue: 0.7, axis II eigenvalue: 0.5) (species labels: *Agr sp-Agrostis sp.; Ant ode-Anthoxanthum odoratum; Bet sp-Betula pendula; Blad-Utricularia intermedia agg; Cal pal-Caltha palustris; Car pra-Cardamine pratensis; Car aqu-Carex aquatilis; Car cur-Carex curta; Car dem-Carex demissa; Car ech-Carex echinata; Car hos-Carex hostiana; Car nig-Carex nigra; Car ova-Carex ovalis; Car pan-Carex panacea; Car ros-Carex rostrata; Car ves-Carex vesicaria; Des ces-Deschamsia cespitosa; Epi pal-Epilobium palustre; Equ flu-Equisetum fluviatile; Equ pal-Equisetum palustre; Eri cin-Erica cinerea; Eri ang-Eriophorum angustifolium; Fil ulm-Filipendula ulmaria; Gal pal-Galium palustre; Gly flu-Glyceria fluitans; Hol lan-Holcus lanatus; Jun eff-Juncus effusus; Jun acu-Juncus sp.; Men tri-Menyanthes trifoliata; Mol cae-Molinia caerulea; Moss-Sphagnum sp.; Mush-Fungi; Myr gal-Myrica gale; Nar str-Nardus stricta; Nar oss-Narthecium ossifragum; Pha aru-Phalaris arundinacea; Phrag-Phragmites australis; Poa pra-Poa pratensis; Pota po-Potamogeton polygonifolius; Pot ere-Potentilla erecta; Pot pal-Potentilla palustris; Ran fla-Ranunculus flammula; Ran rep-Ranunculus repens; Rum ace-Rumex acetosa; Sal sp.-Salix sp.;Tri rep-Trifolium repens; Vio pal-Viola palustris*)

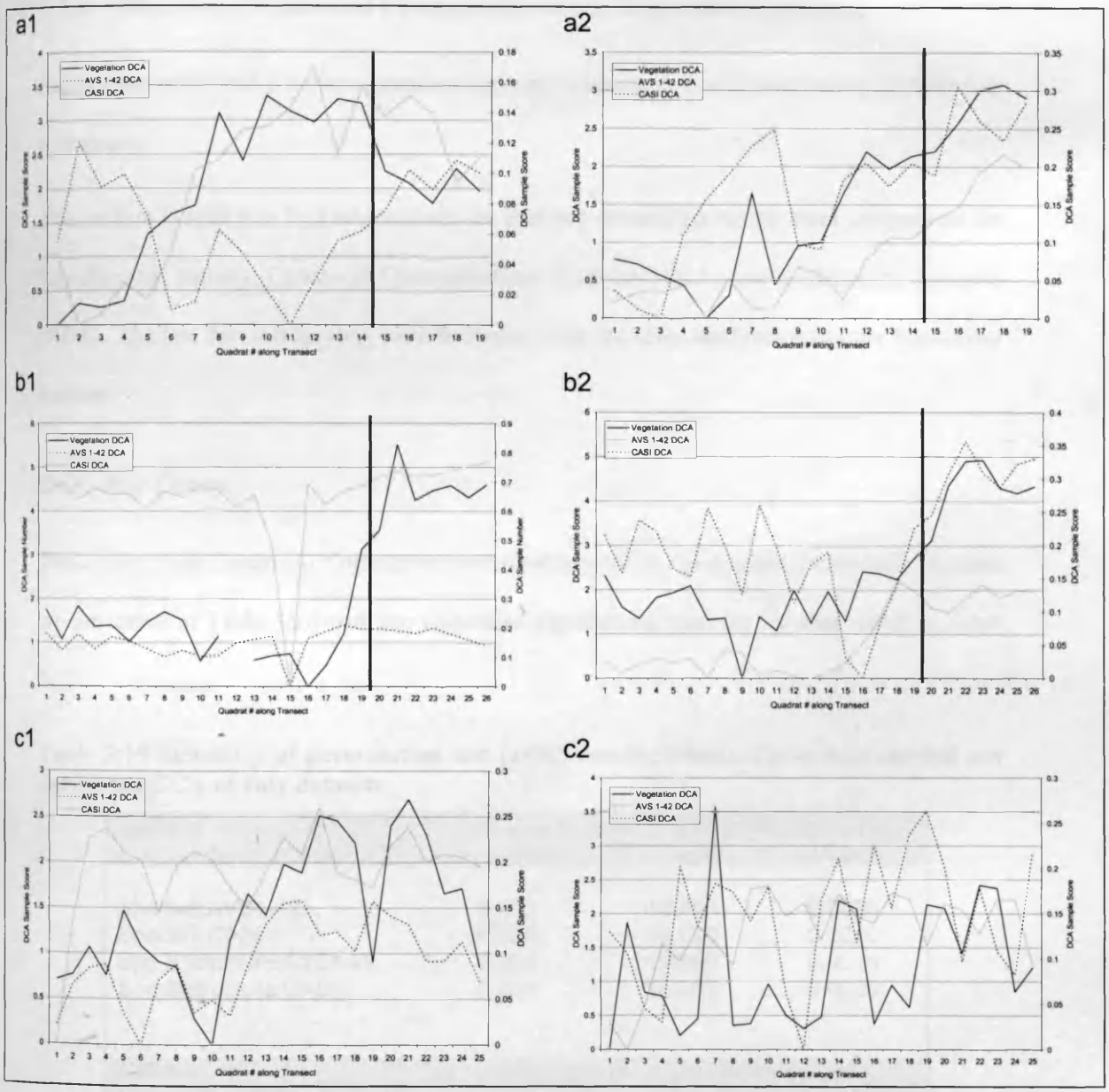

Figure 5:3 Vegetation and spectra (AVS1-42 and CASI) sample scores along each transect (a-c) using July ('1') and September ('2') datasets (Vertical Line = Position of boundary line on *a priori* habitat map: a = 30 m, b = 40 m, c = NA)

Table 5:14 Regression results (R^2Adj) between vegetation and spectra sample scores using DCA along transects 'a', 'b' and 'c' (both AVS1-42 and CASI datasets) (Graphs in Appendix C)

July	AVS1-42	CASI	Sept	AVS1-42	CASI
a1	15.5	66.1	a2	75.6	39.3
b1	11.2	13.7	b2	61.2	38.0
c1	33.7	8.1	c2	0.0	1.2

5.3.5 Objective e) Canonical Correspondence and Redundancy Analyses

Explore the relationship between spectral response and vegetation datasets using multivariate techniques.

This section is split into four subsections; the first two contain the results from analyses on the July datasets, namely, Canonical Correspondence Analysis (CCA) and Redundancy Analysis (RDA). The last two subsections include results from the same analyses using the September datasets.

CCA: July Dataset

The output from Canonical Correspondence Analyses (CCA) performed on the July datasets are presented in Table 5:16 with the respective significance tests on the axes listed in Table 5:15.

Table 5:15 Summary of permutation test (x499) results: Monte Carlo tests carried out during the CCA of July datasets

Dataset ('Dependent':'Predictor')	Test of significance of first canonical axis: Eigenvalue	F-ratio	P-value
Species:AVS1-42	0.616	10.813	0.0020
Species:CASI	0.528	10.780	0.0020
Spp.&Structure:AVS1-42	0.369	19.860	0.0020
Spp.&Structure:CASI	0.260	15.665	0.0020
Dataset ('Dependent':'Predictor')	**Test of significance of all canonical axes: Trace**	**F-ratio**	**P-value**
Species:AVS1-42	3.207	2.768	0.0020
Species:CASI	1.667	4.040	0.0020
Spp.&Structure:AVS1-42	1.228	3.363	0.0020
Spp.&Structure:CASI	0.649	4.628	0.0020

All results show that at 95% significance level, all first axes and all axes together explain a significant amount of variation in the respective dependents datasets. Forward selection is a method that enables a simpler model of environmental variables to be constructed which can still sufficiently explain the species composition patterns. These are the 'conditional effects' and are presented in Table 5:17 and Table 5:18 for analyses involving the AVS1-42 and CASI

datasets respectively. The 'marginal effects' results tables provide information on the significance of each variable independent of the others and these are listed in Appendix C.

Table 5:16 Summary of CCA results on July spectra: (all combinations of species and environmental variables).

		Axis I	Axis II	Axis III	Axis IV
Vegetation (AVS1-42 as predictors)					
Sum of all eigenvalues (canonical eigenvalues) 7.732 (3.207)					
% Explained Variation 41.48					
Eigenvalues		0.616	0.531	0.332	0.319
Species-env correlations		0.939	0.899	0.811	0.798
Cumulative % variance	-of species data	8.0	14.8	19.1	23.3
	-of species-env relation	19.2	35.7	46.1	56.1
Vegetation (CASI as predictors)					
Sum of all eigenvalues (canonical eigenvalues) 7.732 (1.667)					
% Explained Variation 21.56					
Eigenvalues		0.528	0.324	0.280	0.202
Species-env correlations		0.883	0.800	0.683	0.677
Cumulative % variance	-of species data	6.8	11.0	14.6	17..3
	-of species-env relation	31.7	51.2	67.9	80.0
Vegetation and Structure (AVS1-42 as predictors)					
Sum of all eigenvalues (canonical eigenvalues) 2.712 (1.228)					
% Explained Variation 45.28					
Eigenvalues		0.369	0.249	0.107	0.087
Species-env correlations		0.874	0.931	0.820	0.748
Cumulative % variance	-of species data	13.6	22.8	26.8	30.0
	-of species-env relation	30.1	50.4	59.1	66.1
Vegetation and Structure (CASI as predictors)					
Sum of all eigenvalues (canonical eigenvalues) 2.712 (0.649)					
% Explained Variation 23.93					
Eigenvalues		0.261	0.117	0.100	0.061
Species-env correlations		0.764	0.689	0.713	0.692
Cumulative % variance	-of species data	9.6	13.9	17.6	19.8
	-of species-env relation	40.2	58.2	73.5	82.9

Table 5:17 The performance of each AVS1-42 waveband used to predict variation in the species dataset (canon. eigen: 3.207; total inertia 7.732) and the species/structure dataset (canon eigen: 1.228; total inertia 2.712)-output by forward selection (Conditional effects)-July 2003 (FVE: Fraction of Variance Explained) ***Italicized and greyed out results are not significant model variables***

Species composition dataset				Species composition and structure dataset			
Band	LambdaA	P	FVE	Variable	LambdaA	P	FVE
AV14*	0.26	0.002	0.08	AV26	0.1	0.002	0.08
AV13*	0.3	0.002	0.09	AV14	0.13	0.002	0.11
AV23*	0.18	0.002	0.06	AV15	0.1	0.002	0.08
AV42*	0.12	0.002	0.04	AV28	0.1	0.002	0.08
AV37	0.21	0.002	0.07	AV16	0.09	0.002	0.07
AV24*	0.14	0.002	0.04	AV19	0.08	0.002	0.07
AV15*	0.18	0.002	0.06	AV17	0.05	0.002	0.04
AV16*	0.24	0.002	0.08	AV13	0.04	0.002	0.03
AV10*	0.1	0.002	0.03	AV22	0.04	0.002	0.03
AV18*	0.13	0.002	0.04	AV20	0.04	0.002	0.03
AV25	0.08	0.006	0.03	AV27	0.03	0.002	0.02
AV29*	0.09	0.002	0.03	AV42	0.04	0.002	0.03
AV19*	0.09	0.002	0.03	AV29	0.02	0.002	0.02
AV1	0.07	0.042	0.02	AV31	0.03	0.002	0.02
AV17*	0.07	0.006	0.02	AV7	0.03	0.006	0.02
AV9	0.06	0.032	0.02	AV23	0.03	0.002	0.02
AV8	*0.06*	*0.052*	*0.02*	AV12	0.03	0.004	0.02
AV3	*0.08*	*0.002*	*0.03*	AV11	0.03	0.004	0.02
AV7	*0.08*	*0.004*	*0.03*	AV38	0.03	0.002	0.02
AV41	*0.05*	*0.048*	*0.02*	AV33	0.03	0.002	0.02
AV36	*0.06*	*0.046*	*0.02*	AV4	0.02	0.012	0.02
AV20	*0.06*	*0.066*	*0.02*	AV24*	0.02	0.002	0.02
AV22	*0.07*	*0.008*	*0.02*	AV21	0.02	0.012	0.02
AV21	*0.07*	*0.002*	*0.02*	AV41	0.02	0.014	0.02
AV27	*0.05*	*0.078*	*0.02*	AV10*	0.02	0.022	0.02
AV33	*0.06*	*0.024*	*0.02*	AV8	0.02	0.03	0.02
AV39	*0.06*	*0.022*	*0.02*	AV18*	0.02	0.086	0.02
AV32	*0.06*	*0.04*	*0.02*	*AV39*	*0.02*	*0.044*	*0.02*
AV11	*0.04*	*0.11*	*0.01*	*AV1*	*0.01*	*0.12*	*0.01*
AV12	*0.06*	*0.068*	*0.02*	*AV9*	*0.02*	*0.184*	*0.02*
AV30	*0.04*	*0.222*	*0.01*	*AV2*	*0.01*	*0.202*	*0.01*
AV4	*0.04*	*0.338*	*0.01*	*AV35*	*0.01*	*0.228*	*0.01*
AV35	*0.04*	*0.336*	*0.01*	*AV3*	*0.02*	*0.382*	*0.02*
AV5	*0.04*	*0.238*	*0.01*	*AV5*	*0.01*	*0.436*	*0.01*
AV6	*0.04*	*0.254*	*0.01*	*AV36*	*0.01*	*0.166*	*0.01*
AV38	*0.04*	*0.292*	*0.01*	*AV37*	*0.01*	*0.556*	*0.01*
AV2	*0.04*	*0.388*	*0.01*	*AV6*	*0.01*	*0.532*	*0.01*
AV40	*0.03*	*0.428*	*0.01*	*AV40*	*0.01*	*0.752*	*0.01*
AV34	*0.03*	*0.95*	*0.01*	*AV34*	*0.01*	*0.998*	*0.01*
AV28	*0.01*	*0.996*	*0.00*	*AV32*	*0*	*1*	*0.00*
AV26	*0.02*	*1*	*0.01*	*AV25*	*0.01*	*0.998*	*0.01*
AV31	*0*	*1*	*0.00*	*AV30*	*0*	*1*	*0.00*

*Wavebands that are significant in both models

Table 5:18 The performance of each CASI waveband (conditional effects) used to predict variation in the species dataset (canon eigen: 1.667; total intertia 7.732) and the species/structure dataset (canon. eigen: 0.649; total inertia 2.712)-output by forward selection (Conditional effects)-July 2003 (FVE: Fraction of Variance Explained)

Species composition dataset				Species composition and structure dataset			
Variable	LambdaA	P	FVE	Variable	LambdaA	P	FVE
CASI 8	0.22	0.002	0.13	CASI 8	0.09	0.002	0.14
CASI 2	0.24	0.002	0.14	CASI 2	0.07	0.002	0.11
CASI 1	0.29	0.002	0.17	CASI 1	0.11	0.002	0.17
CASI 5	0.21	0.002	0.13	CASI 5	0.07	0.002	0.11
CASI 3	0.12	0.002	0.07	CASI 3	0.04	0.002	0.06
CASI 6	0.18	0.002	0.11	CASI 4	0.09	0.002	0.14
CASI 10	0.12	0.002	0.07	CASI 6	0.04	0.004	0.06
CASI 7	0.12	0.002	0.07	CASI 10	0.05	0.002	0.08
CASI 9	0.1	0.002	0.06	CASI 7	0.05	0.002	0.08
CASI 4	0.07	0.03	0.04	CASI 9	0.04	0.002	0.06

Table 5:18 lists the order of the wavebands entered into the model derived by CCA on both vegetation datasets sets using the CASI data as the predictors. All ten CASI bands are significant predictors. In relation to the AVS1-42 dataset, the inclusion of the structure and environmental data in the independents datasets does not reflect a change in the order of CASI predictors used in the model. Sixteen and twenty-seven wavebands are listed as significant in Table 5:17 for the species composition and the species with structure and environmental variables datasets respectively. Table 5:17 illustrates a marked difference between the order of the results using the two predictors datasets although most of the significant wavebands identified in CANOCO are shared between the two sets of results (asterisked wavebands). The areas of the spectrum identified as significant in predicting variation in both vegetation datasets are AVS13-19 (544-639 nm) AVS23-25 (702-734 nm) AV10 (497 nm) and AV29 (797 nm).

Ordination Diagrams

Ordination diagrams of the predictor datasets from the CCAs are presented in Appendix C. These show the direction of variation for each predictor, their relative significance in the model and their correlation with the canonical axes and other variables. Figure 5:4 and Figure 5:5 show the ordination triplots from CCA on the AVS1-42 and CASI datasets respectively with the species composition datasets (see Appendix C for species with structural and environmental datasets triplots). These diagrams provide information on the relationships between the direction of variation in the predictors with the location of the samples and associated species in feature space. Species are positioned near to the samples in which they have the highest relative abundance and similarly, the positions of the samples (circles coloured by habitat type) are near the species that tend to occur in those samples. Hence, for example, *Carex rostrata* and *Equisetum fluviatile* species are located near all of the 'EF' habitat sample points. As both axes in both diagrams have comparable eigenvalues, the distance between sample points approximates the chi-square distances between samples (as biplot scaling was used) and the same is true for the species points (as focus was on species distances).

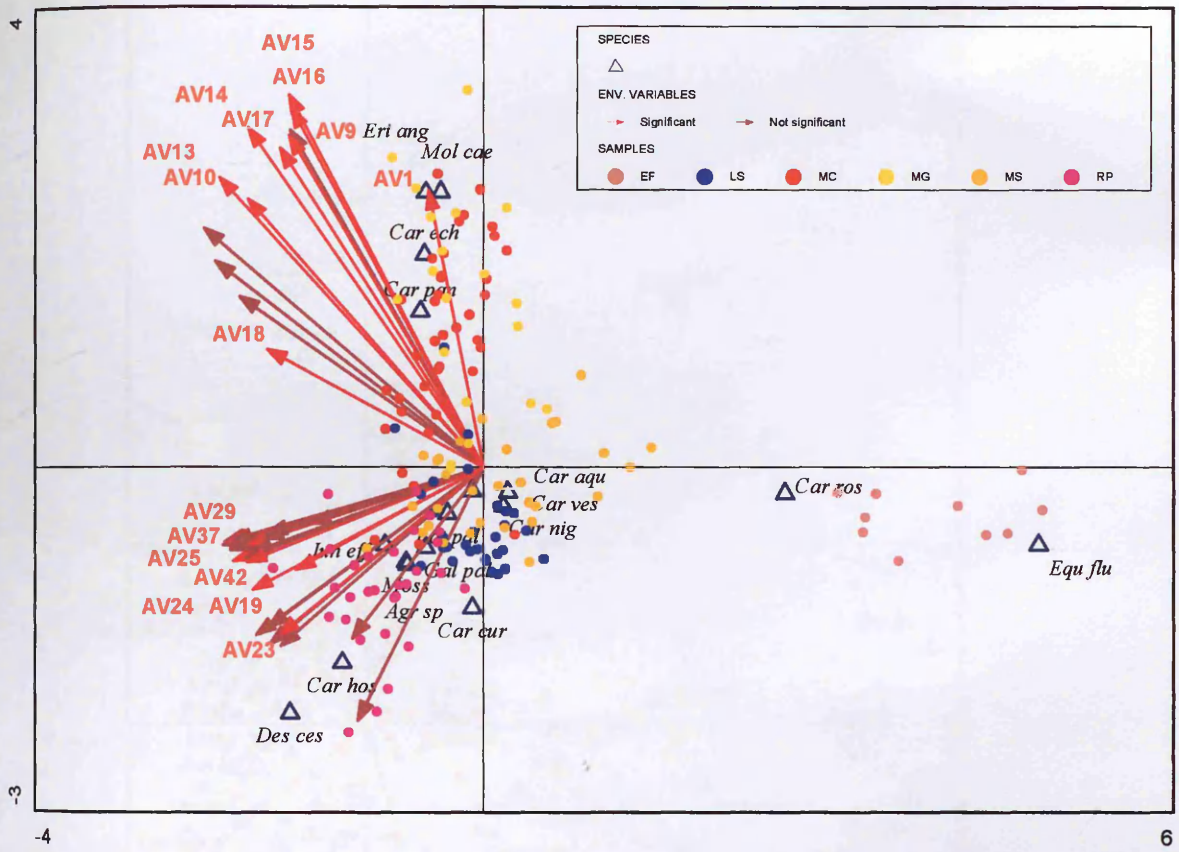

Figure 5:4 CCA triplot for AVS1-42 July analyses and species composition vegetation dataset (some species names omitted for clarity and only significant predictors labelled) (eigenvalue axis I: 0.616; eigenvalue axis II: 0.531) (species labels: *Agr sp-Agrostis sp.; Cal pal-Caltha palustris; Car aqu-Carex aquatilis; Car cur-Carex curta; Car ech-Carex echinata; Car hos-Carex hostiana; Car nig-Carex nigra; Car pau-Carex pauciflora; Car ros-Carex rostrata; Car ves-Carex vesicaria; Des ces-Deschamsia cespitosa; Equ flu-Equisetum fluviatile; Eri ang-Eriophorum angustifolium; Gal pal-Galium palustre; Jun eff-Juncus effusus; Mol cae-Molinia caerulea; Moss-Sphagnum sp.*)

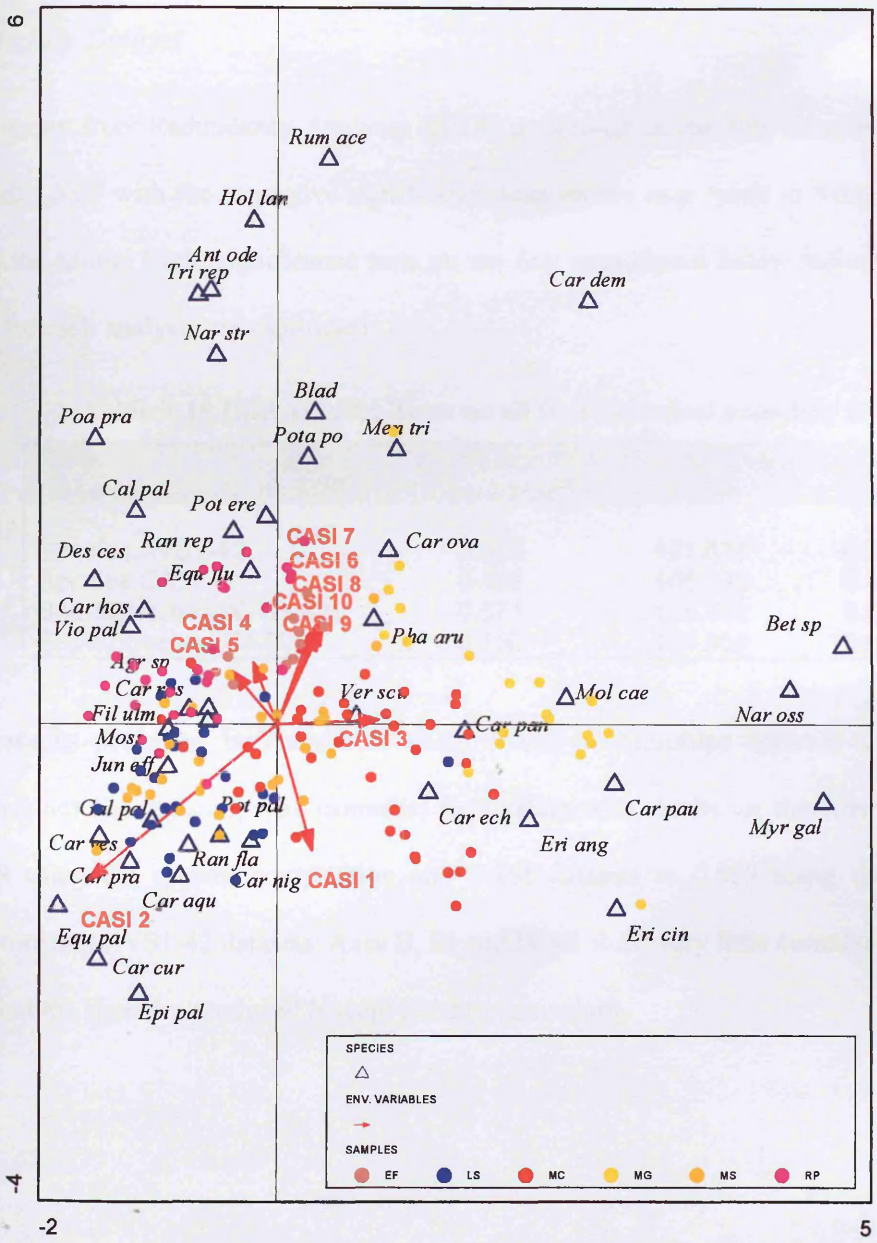

Figure 5:5 CCA triplot for CASI July spectra and species composition vegetation dataset (some species names omitted for clarity and only significant predictors labelled) (eigenvalue axis I: 0.528; eigenvalue axis II: 0.324) (species labels: *Agr sp-Agrostis sp.; Ant ode-Anthoxanthum odoratum; Bet sp-Betula pendula; Blad-Utricularia intermedia agg; Cal pal-Caltha palustris; Car pra-Cardamine pratensis; Car aqu-Carex aquatilis; Car cur-Carex curta; Car dem-Carex demissa; Car ech-Carex echinata; Car hos-Carex hostiana; Car nig-Carex nigra; Car ova-Carex ovalis; Car pan-Carex panacea; Car pau-Carex pauciflora; Car ros-Carex rostrata; Car ves-Carex vesicaria; Des ces-Deschamsia cespitosa; Epi pal-Epilobium palustre; Equ flu-Equisetum fluviatile; Equ pal-Equisetum palustre; Eri cin-Erica cinerea; Eri ang-Eriophorum angustifolium; Fil ulm-Filipendula ulmaria; Gal pal-Galium palustre; Hol lan-Holcus lanatus; Jun eff-Juncus effusus; Men tri-Menyanthes trifoliata; Mol cae-Molinia caerulea; Moss-Sphagnum sp.; Myr gal-Myrica gale; Nar str-Nardus stricta; Nar oss-Narthecium ossifragum; Pha aru-Phalaris arundinacea; Poa pra-Poa pratensis; Pota po-Potamogeton polygonifolius; Pot ere-Potentilla erecta; Pot pal-Potentilla palustris; Ran fla-Ranunculus flammula; Ran rep-Ranunculus repens; Rum ace-Rumex acetosa; Tri rep-Trifolium repens; Ver scu-Veronica scutellata; Vio pal-Viola palustris*)

RDA: July Dataset

The output from Redundancy Analyses (RDA) performed on the July datasets are presented in Table 5:20 with the respective significance tests on the axes listed in Table 5:19. Results from the Monte Carlo significance tests on the first axes shown below indicate that all first axes for each analysis are significant.

Table 5:19 RDA results: Tests on all first canonical axes-July 2003

Dataset ('Dependent':'Predictor')	Test of significance of first canonical axis: Eigenvalue	F-ratio	P-value
Species:AVS1-42	0.519	121.876	0.0020
Species:CASI	0.482	105.293	0.0040
Spp.&Structure:AVS1-42	0.571	135.492	0.0020
Spp.&Structure:CASI	0.550	124.838	0.0020

The results presented in Table 5:20 show similar relationships between the sum of all eigenvalues and the sum of all canonical eigenvalues with results for the latter ranging from 0.499 using the species composition and CASI datasets to 0.589 using the species and structure and AVS1-42 datasets. Axes II, III and IV all show very little cumulative differences in all of the statistics produced (except for the eigenvalue).

Table 5:20 RDA outputs July 2003-all analyses

		Axis I	Axis II	Axis III	Axis IV
AVS1-42 (Vegetation as predictors)					
Sum of all eigenvalues (canonical eigenvalues) 1.000 (0.536)					
Eigenvalues		0.519	0.013	0.003	0.001
Species-env correlations		0.733	0.784	0.559	0.504
Cumulative % variance	-of species data	51.9	53.1	53.4	53.5
	-of species-env relation	96.8	99.2	99.7	99.9
CASI (Vegetation as predictors)					
Sum of all eigenvalues 1.000 (canonical eigenvalues) 1.000 (0.0.499)					
Eigenvalues		0.482	0.013	0.004	0.000
Species-env correlations		0.706	0.730	0.708	0.716
Cumulative % variance	-of species data	48.2	49.4	49.8	49.8
	-of species-env relation	96.5	99.1	99.8	99.9
AVS1-42 (Vegetation and Structure as predictors)					
Sum of all eigenvalues 1.000 (canonical eigenvalues) 1.000 (0.589)					
Eigenvalues		0.569	0.014	0.004	0.002
Species-env correlations		0.768	0.812	0.644	0.687
Cumulative % variance	-of species data	56.9	58.3	58.6	58.8
	-of species-env relation	96.7	99	99.6	99.9
CASI (Vegetation and Structure as predictors)					
Sum of all eigenvalues 1.000 (canonical eigenvalues) 1.000 (0.570)					
Eigenvalues		0.550	0.014	0.004	0.001
Species-env correlations		0.755	0.786	0.763	0.597
Cumulative % variance	-of species data	55.0	56.5	56.9	57.0
	-of species-env relation	96.5	99.0	99.8	99.9

The first twenty species listed by forward stepwise selection during RDA on the July AVS1-42 dataset and CASI dataset are presented in Table 5:21 and Table 5:22 respectively. Marginal effects are presented in Appendix C.

Table 5:21 First twenty species listed in output (conditional effects) from RDA on July AVS1-42 and species (canon. eigen: 0.570) and species/structure datasets (canon eigen: 0.589) (FVE: Fraction of Variance Explained) (*Italicized and greyed out variables are not significant model variables*)

Species composition dataset				Species composition and structure dataset			
Variable	LambdaA	P	FVE	Variable	LambdaA	P	FVE
Poa pra*	0.11	0.002	0.21	Poa pra*	0.11	0.002	0.19
Car cur*	0.09	0.004	0.17	Car cur *	0.09	0.004	0.15
Des ces*	0.05	0.004	0.09	Des ces*	0.05	0.004	0.08
Mol cae*	0.05	0.006	0.09	Mol cae*	0.05	0.004	0.08
Car hos*	0.03	0.008	0.06	Car hos*	0.03	0.008	0.05
Car ova*	0.02	0.024	0.04	Car ova*	0.02	0.026	0.03
Car pau*	0.02	0.018	0.04	Car pau*	0.02	0.02	0.03
Cal pal	*0.02*	*0.056*	*0.04*	*Cal pal*	*0.02*	*0.056*	*0.03*
Fil ulm	*0.01*	*0.042*	*0.02*	*Fil ulm*	*0.01*	*0.046*	*0.02*
Equ pal	*0.02*	*0.052*	*0.04*	*wd stms*	*0.02*	*0.048*	*0.03*
Ant ode	*0.01*	*0.102*	*0.02*	*Myr gal*	*0.02*	*0.07*	*0.03*
Vio pal	*0.01*	*0.116*	*0.02*	*Equ pal*	*0.01*	*0.052*	*0.02*
Equ flu	*0.01*	*0.108*	*0.02*	*Equ flu*	*0.01*	*0.094*	*0.02*
Men tri	*0.01*	*0.058*	*0.02*	*Ant ode*	*0.01*	*0.078*	*0.02*
Bet sp	*0.01*	*0.152*	*0.02*	*Vio pal*	*0.01*	*0.1*	*0.02*
Nar oss	*0*	*0.144*	*0.00*	*POH*	*0.01*	*0.17*	*0.02*
Tri rep	*0.01*	*0.146*	*0.02*	*Men tri*	*0.01*	*0.142*	*0.02*
Pota po	*0.01*	*0.226*	*0.02*	*Nar oss*	*0*	*0.114*	*0.00*
Car pra	*0*	*0.284*	*0.00*	*drops*	*0.01*	*0.192*	*0.02*
Pha aru	*0.01*	*0.172*	*0.02*	*Pot ere*	*0.01*	*0.19*	*0.02*

*Variable significant in both models

Table 5:22 First twenty species listed in output from RDA on July CASI and species (canon eigen: 0.499) and species/structure datasets (canon eigen: 0.570) (FVE: Fraction of Variance Explained) (*Italicized and greyed out variables are not significant model variables*)

Species composition dataset				Species composition and structure dataset			
Variable	LambdaA	P	FVE	Variable	LambdaA	P	FVE
Ant ode*	0.09	0.004	0.18	bar pt	0.12	0.002	0.21
Car aqu	0.06	0.006	0.12	Ant ode *	0.06	0.002	0.00
Equ flu	0.06	0.004	0.12	Pha aru*	0.04	0.014	0.00
Pha aru*	0.04	0.014	0.08	Ran fla *	0.04	0.006	0.02
Ran fla*	0.03	0.01	0.06	Pot pal*	0.03	0.018	0.01
Myr gal	0.03	0.044	0.06	*Myr gal*	*0.02*	*0.05*	*0.03*
Pot pal*	0.02	0.014	0.04	*wd stms*	*0.02*	*0.026*	*0.04*
Car ves	0.02	0.038	0.04	*Car dem*	*0.02*	*0.034*	*0.05*
Cal pal	*0.01*	*0.054*	*0.02*	*Agr sp*	*0.02*	*0.042*	*0.06*
Car dem	*0.02*	*0.058*	*0.04*	*Tri rep*	*0.01*	*0.042*	*0.07*
Men tri	*0.01*	*0.032*	*0.02*	*Ver scu*	*0.02*	*0.066*	*0.07*
Eri cin	*0.01*	*0.11*	*0.02*	*Car pra*	*0.01*	*0.058*	*0.12*
Bet sp	*0.02*	*0.078*	*0.04*	*Blad*	*0.01*	*0.092*	*0.10*
Ver scu	*0.01*	*0.084*	*0.02*	*Car aqu*	*0.01*	*0.168*	*0.16*
Tri rep	*0*	*0.15*	*0.00*	*Eri cin*	*0.01*	*0.144*	*0.29*
Car pra	*0.01*	*0.168*	*0.02*	*Bet sp*	*0.01*	*0.126*	*0.25*
Agr sp	*0.01*	*0.16*	*0.02*	*Car ves*	*0*	*0.166*	*0.22*
Eri ang	*0*	*0.228*	*0.00*	*Men tri*	*0.01*	*0.116*	*0.29*
Blad	*0.01*	*0.302*	*0.02*	*Cal pal*	*0.01*	*0.232*	*0.20*
Fil ulm	*0*	*0.406*	*0.00*	*drops*	*0.01*	*0.118*	*0.41*

*Variable significant in both models

CCA: September Dataset

The outputs from Canonical Correspondence Analyses carried out on the September datasets are presented in Table 5:24.

Table 5:23 Summary of permutation test (x499) results: monte carlo tests carried out during the CCA of September datasets

Dataset ('Dependent':'Predictor')	Test of significance of first canonical axis: Eigenvalue	F-ratio	P-value
Species:AVS1-42	0.617	10.810	0.0020
Species:CASI	0.465	10.151	0.0020
Spp.&Structure:AVS1-42	0.305	19.595	0.0020
Spp.&Structure:CASI	0.196	15.095	0.0020
Dataset ('Dependent':'Predictor')	**Test of significance of all canonical axes Trace**	**F-ratio**	**P-value**
Species:AVS1-42	3.206	2.185	0.0020
Species:CASI	1.498	3.851	0.0020
Spp.&Structure:AVS1-42	1.013	2.536	0.0020
Spp.&Structure:CASI	0.469	4.214	0.0020

Table 5:23 shows the results of the tests on the significance of the first axes of the September CCAs and significance of the all axes involved in each analysis. All results show that at a 95% significance level, all first axes and all axes together in each CCA explains a significant amount of variation in the respective species dataset (P-values are all 0.0020). The results of forward selection (conditional effects) are presented in Table 5:25 and Table 5:26. As with the July results, there is some overlap in the wavebands identified as being significant between the two AVS1-42 models but not in the order of entry into the stepwise model. The wavebands found to be significant (in both models) are AVS7 (450 nm), AVS12 (529 nm), AVS16-19 (592 to 639 nm) and AVS21 (670 nm).

Table 5:24 Summary of CCA results on September spectra: both spectral bandsets and both combinations of vegetation data.

		Axis I	Axis II	Axis III	Axis IV
Vegetation (AVS1-42 as predictors)					
Sum of all eigenvalues (canonical eigenvalues) 7.293 (3.206)					
% Explained Variation 43.96					
Eigenvalues		0.617	0.568	0.403	0.306
Species-env correlations		0.948	0.893	0.906	0.808
Cumulative % variance	-of species data	8.5	16.2	21.8	0.808
	-of species-env relation	19.2	36.9	49.5	59.0
Vegetation (CASI as predictors)					
Sum of all eigenvalues (canonical eigenvalues) 7.293 (1.498)					
% Explained Variation 24.65					
Eigenvalues		0.465	0.386	0.283	0.109
Species-env correlations		0.845	0.762	0.765	0.537
Cumulative % variance	-of species data	6.4	11.7	15.5	17.0
	-of species-env relation	31.1	56.8	75.7	82.9
Vegetation and Structure (AVS1-42 as predictors)					
Sum of all eigenvalues (canonical eigenvalues) 2.126 (1.013)					
% Explained Variation 47.65					
Eigenvalues		0.305	0.193	0.115	0.075
Species-env correlations		0.874	0.890	0.842	0.779
Cumulative % variance	-of species data	14.3	23.4	28.9	32.4
	-of species-env relation	30.1	49.2	60.6	67.9
Vegetation and Structure (CASI)					
Sum of all eigenvalues (canonical eigenvalues) 2.126 (0.469)					
% Explained Variation 22.06					
Eigenvalues		0.196	0.108	0.070	0.036
Species-env correlations		0.729	0.696	0.697	0.525
Cumulative % variance	-of species data	9.2	14.3	17.6	19.3
	-of species-env relation	41.7	64.8	79.8	87.5

Table 5:25 The performance of each AVS 1-42 wavebands used to predict variation in the species dataset (canon. eigen: 3.206; total inertia 7.293) and the species/structure dataset-(canon eigen: 1.013; total inertia 2.126) output by forward selection (Conditional effects)-September 2003 (FVE: Fraction of Variance Explained) ***Italicized results are not significant model variables***

Species composition dataset				Species composition and structure dataset			
Variable	LambdaA	P	FVE	Variable	LambdaA	P	FVE
AV-21*	0.31	0.002	0.10	AV-26	0.11	0.002	0.11
AV-12*	0.36	0.002	0.11	AV-21*	0.09	0.002	0.09
AV-25	0.23	0.002	0.07	AV-12*	0.12	0.002	0.12
AV-7*	0.19	0.002	0.06	AV-17*	0.06	0.002	0.06
AV-18*	0.21	0.002	0.07	AV-3	0.05	0.002	0.05
AV-4	0.19	0.002	0.06	AV-7*	0.06	0.002	0.06
AV-11	0.13	0.002	0.04	AV-18*	0.04	0.002	0.04
AV-16*	0.1	0.002	0.03	AV-9	0.03	0.002	0.03
AV-19*	0.1	0.002	0.03	AV-8	0.04	0.002	0.04
AV-32	0.08	0.002	0.02	AV-5	0.02	0.004	0.02
AV-10	0.08	0.006	0.02	AV-42	0.02	0.004	0.02
AV-22	0.07	0.006	0.02	AV-16*	0.02	0.006	0.02
AV-17*	0.06	0.034	0.02	AV-31	0.02	0.024	0.02
AV-30	0.06	0.01	0.02	AV-19*	0.02	0.016	0.02
AV-8	*0.05*	*0.068*	*0.02*	AV-20	0.01	0.032	0.01
AV-9	*0.05*	*0.062*	*0.02*	*AV-41*	*0.02*	*0.058*	*0.02*
AV-40	*0.05*	*0.104*	*0.02*	*AV-23*	*0.01*	*0.058*	*0.01*
AV-34	*0.07*	*0.004*	*0.02*	*AV-27*	*0.02*	*0.142*	*0.02*
AV-15	*0.04*	*0.152*	*0.01*	*AV-10*	*0.01*	*0.172*	*0.01*
AV-2	*0.04*	*0.296*	*0.01*	*AV-11*	*0.01*	*0.132*	*0.01*
AV-27	*0.04*	*0.238*	*0.01*	*AV-32*	*0.01*	*0.162*	*0.01*
AV-29	*0.04*	*0.342*	*0.01*	*AV-34*	*0.02*	*0.012*	*0.02*
AV-13	*0.04*	*0.402*	*0.01*	*AV-25*	*0.01*	*0.08*	*0.01*
AV-24	*0.03*	*0.442*	*0.01*	*AV-2*	*0.01*	*0.198*	*0.01*
AV-6	*0.04*	*0.554*	*0.01*	*AV-38*	*0.02*	*0.056*	*0.02*
AV-41	*0.03*	*0.508*	*0.01*	*AV-24*	*0.01*	*0.16*	*0.01*
AV-42	*0.04*	*0.272*	*0.01*	*AV-29*	*0.01*	*0.146*	*0.01*
AV-14	*0.03*	*0.562*	*0.01*	*AV-37*	*0.02*	*0.092*	*0.02*
AV-37	*0.04*	*0.428*	*0.01*	*AV-15*	*0.01*	*0.206*	*0.01*
AV-31	*0.03*	*0.404*	*0.01*	*AV-6*	*0.01*	*0.134*	*0.01*
AV-3	*0.04*	*0.484*	*0.01*	*AV-13*	*0.01*	*0.51*	*0.01*
AV-1	*0.03*	*0.53*	*0.01*	*AV-14*	*0.01*	*0.334*	*0.01*
AV-20	*0.03*	*0.626*	*0.01*	*AV-22*	*0.01*	*0.526*	*0.01*
AV-5	*0.04*	*0.39*	*0.01*	*AV-4*	*0.01*	*0.634*	*0.01*
AV-36	*0.03*	*0.56*	*0.01*	*AV-35*	*0*	*0.604*	*0.00*
AV-35	*0.03*	*0.36*	*0.01*	*AV-36*	*0.02*	*0.126*	*0.02*
AV-38	*0.04*	*0.394*	*0.01*	*AV-40*	*0.01*	*0.37*	*0.01*
AV-26	*0.03*	*0.564*	*0.01*	*AV-33*	*0*	*0.678*	*0.00*
AV-33	*0.03*	*0.632*	*0.01*	*AV-1*	*0.01*	*0.834*	*0.01*
AV-28	*0.03*	*0.688*	*0.01*	*AV-28*	*0.01*	*0.752*	*0.01*
AV-23	*0.03*	*0.88*	*0.01*	*AV-30*	*0.01*	*0.738*	*0.01*
AV-39	*0.02*	*0.98*	*0.01*	*AV-39*	*0*	*0.92*	*0.00*

*Variable significant in both models

Table 5:26 The performance of each CASI waveband used to predict variation in the species dataset (canon. eigen: 1.498; total inertia 7.293) and the species/structure dataset (canon eigen: 0.469; total inertia 2.126)-output by forward selection (Conditional effects)-September 2003 (FVE: Fraction of Variance Explained)

Species composition dataset				Species composition and structure dataset			
Variable	LambdaA	P	FVE	Variable	LambdaA	P	FVE
CASI-3*	0.29	0.002	0.19	CASI-7*	0.1	0.002	0.21
CASI-2*	0.32	0.002	0.21	CASI-3*	0.1	0.002	0.21
CASI-7*	0.25	0.002	0.17	CASI-2*	0.08	0.002	0.17
CASI-10*	0.16	0.002	0.11	CASI-10*	0.05	0.002	0.11
CASI-1*	0.16	0.002	0.11	CASI-1*	0.03	0.004	0.06
CASI-4*	0.11	0.002	0.07	CASI-4*	0.03	0.004	0.06
CASI-6	*0.06*	*0.05*	*0.04*	CASI-6	0.03	0.016	0.06
CASI-9	*0.06*	*0.054*	*0.04*	CASI-8	0.01	0.044	0.02
CASI-8	*0.05*	*0.22*	*0.03*	CASI-9	0.02	0.042	0.04
CASI-5	*0.04*	*0.358*	*0.03*	*CASI-5*	*0.02*	*0.204*	*0.04*

*Variable significant in both models

Table 5:26 lists the order of the wavebands entered into the model derived by CCA on both species datasets sets using the CASI wavebands as the predictors in September 2003. The first seven wavebands listed from both analyses are the same, with CASI 3, 2 and 7 being the first three for both. Not all variables have P-values <0.05 this time whereas in July all variables were found to be significant for both analyses. There are six and nine wavebands found to be significant for the species analyses and species and structure analyses respectively.

Ordination Diagrams

Ordination diagrams from the CCAs illustrating the relationships between the significant predictors and the samples (with some or all of the species) from the September datasets are presented in Figure 5:6 and Figure 5:7 These show the direction of variation for each predictor, their relative significance in the model and their correlation with the canonical axes and other variables. The analyses using the species composition vegetation datasets only are shown in these diagrams. Figure C5 to Figure C8 in Appendix C show the equivalent diagrams from the species with structure and environmental variables datasets. Results from analyses using the AVS1-42 and CASI spectral datasets as predictors are shown in Figure 5:6 and Figure 5:7 respectively.

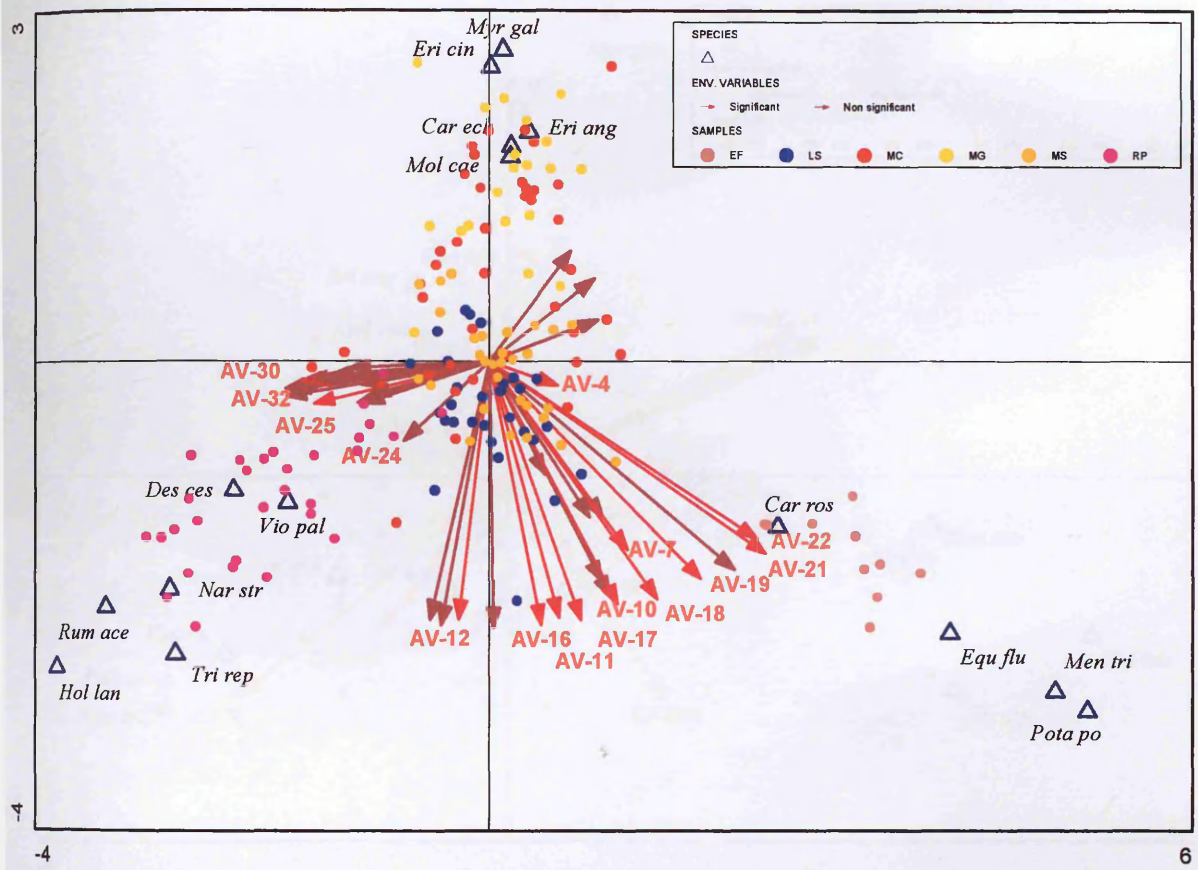

Figure 5:6 CCA triplot for AVS1-42 September analyses and species composition vegetation dataset (some species names omitted for clarity and only significant predictors labelled) (eigenvalue axis I: 0.617; eigenvalue axis II: 0.568) (species labels: *Car ech-Carex echinata; Car ros-Carex rostrata; Des ces-Deschamsia cespitosa; Equ flu-Equisetum fluviatile; Eri cin-Erica cinerea; Eri ang-Eriophorum angustifolium; Hol lan-Holcus lanatus; Men tri-Menyanthes trifoliata; Mol cae-Molinia caerulea; Myr gal-Myrica gale; Nar str-Nardus stricta; Pota po-Potamogeton polygonifolius; Rum ace-Rumex acetosa; Tri rep-Trifolium repens; Vio pal-Viola palustris*)

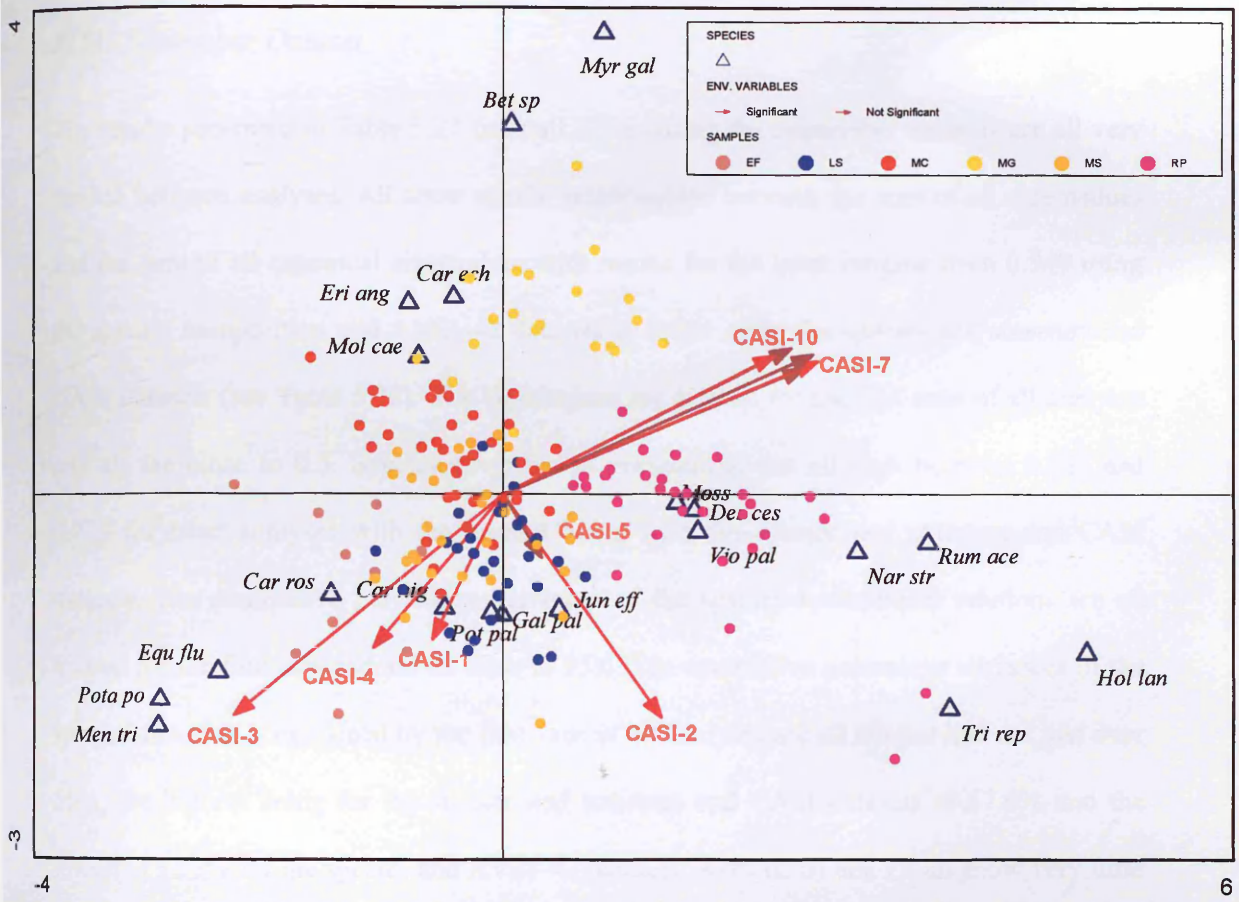

Figure 5:7 CCA triplot for CASI September analyses and species composition vegetation dataset (some species names omitted for clarity and only significant predictors labelled) (eigenvalue axis I: 0.465; eigenvalue axis II: 0.386) (species labels: *Bet sp-Betula pendula; Car ech-Carex echinata; Car nig-Carex nigra; Car ros-Carex rostrata; Des ces-Deschamsia cespitosa; Equ flu-Equisetum fluviatile; Eri ang-Eriophorum angustifolium; Gal pal-Galium palustre; Hol lan-Holcus lanatus; Jun eff-Juncus effusus; Men tri-Menyanthes trifoliata; Mol cae-Molinia caerulea; Moss-Sphagnum sp; Myr gal-Myrica gale; Nar str-Nardus stricta; Pota po-Potamogeton polygonifolius; Pot pal-Potentilla palustris; Rum ace-Rumex acetosa;Tri rep-Trifolium repens;; Vio pal-Viola palustris*)

RDA: September Dataset

The results presented in Table 5:27 from all RDAs using the September datasets are all very similar between analyses. All show similar relationships between the sum of all eigenvalues and the sum of all canonical eigenvalues with results for the latter ranging from 0.549 using the species composition and AVS1-42 datasets to 0.604 using the species and structure and CASI datasets (see Table 5.28). The eigenvalues are highest for the first axes of all analyses and all are close to 0.5. Species-environment correlations are all high between 0.744 and 0.779 for most analyses with the highest being with the species and structure and CASI datasets. The cumulative percentage variances of the species-environment relations are all highest for the first axis and are all close to 95%. The cumulative percentage variances of the species data that is explained by the first axes of all analyses are all similar and are just over 50%, the highest being for the species and structure and CASI datasets at 57.6% and the lowest at 52.2% for the species and AVS1-42 datasets. Axes II, III and IV all show very little change to Axis I in all of the statistics produced (except value for eigenvalue). Results from Monte Carlo significance tests on the first axes are presented in Table 5:27 and all are shown to be significant at the 95% significance level.

Table 5:27 RDA results: Tests on all first canonical axes-September 2003

	Test of significance of first canonical axis:		
('Dependent':'Predictor')	Eigenvalue	F-ratio	P-value
Species:AVS1-42	0.523	122.963	0.0020
Species:CASI	0.560	142.677	0.0020
Spp.&Structure:AVS1-42	0.543	121.161	0.0020
Spp.&Structure:CASI	0.577	139.373	0.0020

Table 5:28 RDA outputs September 2003-all analyses

		Axis I	Axis II	Axis III	Axis IV
AVS1-42 (Vegetation as predictors)					
Sum of all eigenvalues (canonical eigenvalues) 1.000 (0.549)					
Eigenvalues		0.522	0.018	0.007	0.002
Species-env correlations		0.744	0.718	0.679	0.733
Cumulative % variance	-of species data	52.2	54.0	54.7	54.7
	-of species-env relation	95.1	98.3	99.5	99.8
CASI (Vegetation as predictors)					
Sum of all eigenvalues (canonical eigenvalues) 1.000 (0.583)					
Eigenvalues		0.558	0.021	0.002	0.001
Species-env correlations		0.767	0.705	0.736	0.690
Cumulative % variance	-of species data	55.8	58.0	58.2	58.36
	-of species-env relation	95.7	99.4	99.8	99.9
AVS1-42 (Vegetation and Structure as predictors)					
Sum of all eigenvalues (canonical eigenvalues) 1.000 (0.571)					
Eigenvalues		0.542	0.019	0.007	0.002
Species-env correlations		0.758	0.746	0.681	0.744
Cumulative % variance	-of species data	54.2	56.1	56.8	56.9
	-of species-env relation	95.0	98.3	99.5	99.7
CASI (Vegetation and Structure as predictors)					
Sum of all eigenvalues (canonical eigenvalues) 1.000 (0.604)					
Eigenvalues		0.576	0.024	0.002	0.001
Species-env correlations		0.779	0.748	0.755	0.692
Cumulative % variance	-of species data	57.6	60.0	60.2	60.3
	-of species-env relation	95.4	99.4	99.8	99.9

For analyses using the AVS1-42 dataset, *Filipendula ulmaria* is once again a significant predictor. However none of the other species that were found to be significant predictors using the July dataset were found to be significant predictors with the September dataset. Instead, these included *Nardus stricta*, *Myrica gale*, *Carex echinata* and *Rumex acetosa.* The results using the species composition data with the structural data are similar but include bare peat ('bar-pt') as a significant predictor. Of these species only *Myrica gale* and *Carex echinata* are found to have relatively high quadrat abundances (Table 5:2) but this is true for the former only within a small number of plots. Species that were found to be significant but exhibit very low abundances relatively are *Filipendula ulmaria*, *Rumex acetosa* and *Nardus stricta*. Bare peat is indicated to be a significant predictor when the species and structure dataset is used as the environmental variables. The same five species listed above are presented in Table 5:30 as significant predictors when the CASI dataset is the 'species

variables'. Other significant species include *Carex panicea*, *Equisetum fluviatile* and *Carex rostrata*.

Table 5:29 First twenty species listed in forward stepwise output from RDA on September AVS1-42 dataset using species composition as species variables (canon eigen: 0.549) and species and structure data (canon. eigen: 0.571) as species variables (FVE: Fraction of Variance Explained) (*Italicized and greyed out variables are not significant model variables*)

Species composition dataset				Species composition and structure dataset			
Variable	LambdaA	P	FVE	Variable	LambdaA	P	FVE
Nar str*	0.23	0.002	0.42	Nar str*	0.23	0.002	0.40
Myr gal*	0.09	0.002	0.16	Myr gal*	0.09	0.002	0.16
Fil ulm*	0.06	0.002	0.11	Fil ulm*	0.06	0.002	0.11
Car ech*	0.02	0.014	0.04	Car ech*	0.02	0.014	0.04
Rum ace*	0.01	0.04	0.02	Rum ace*	0.01	0.04	0.02
Car ros*	0.01	0.05	0.02	Car ros*	0.01	0.05	0.02
Equ flu	*0.01*	*0.086*	*0.02*	bar pt	0.02	0.038	0.04
Bet sp	*0.01*	*0.12*	*0.02*	*Bet sp*	*0.01*	*0.114*	*0.02*
Nar oss	*0.01*	*0.074*	*0.02*	*Nar oss*	*0.01*	*0.06*	*0.02*
Car aqu	*0.01*	*0.106*	*0.02*	*Car aqu*	*0.01*	*0.114*	*0.02*
Cal pal	*0.01*	*0.138*	*0.02*	*Car pan*	*0.01*	*0.12*	*0.02*
Jun eff	*0.01*	*0.138*	*0.02*	*Car ves*	*0*	*0.12*	*0.00*
Car pan	*0.01*	*0.126*	*0.02*	*Moss*	*0.01*	*0.146*	*0.02*
Pot pal	*0*	*0.152*	*0.00*	*Cal pal*	*0.01*	*0.27*	*0.02*
Car ves	*0.01*	*0.252*	*0.02*	*Gal pal*	*0*	*0.21*	*0.00*
Eri cin	*0*	*0.254*	*0.00*	*Ran fla*	*0.01*	*0.176*	*0.02*
Ran fla	*0.01*	*0.216*	*0.02*	*Eri cin*	*0*	*0.278*	*0.00*
Tri rep	*0*	*0.264*	*0.00*	*Epi pal*	*0.01*	*0.312*	*0.02*
Eri ang	*0*	*0.292*	*0.00*	*Jun eff*	*0*	*0.322*	*0.00*
Mol cae	*0.01*	*0.166*	*0.02*	*Phr sp*	*0*	*0.226*	*0.00*

*Variable significant in both models

Table 5:30 First twenty species listed in forward stepwise output from RDA on September CASI dataset using species composition as species variables (canon eigen: 0.583) and species and structure data (canon eigen: 0.604) as species variables (FVE: Fraction of Variance Explained) (*Italicized and greyed out variables are not significant model variables*)

Species composition dataset				Species composition and structure dataset			
Variable	LambdaA	P	FVE	Variable	LambdaA	P	FVE
Nar str*	0.24	0.002	0.41	Nar str*	0.24	0.002	0.40
Myr gal*	0.1	0.002	0.17	Myr gal*	0.1	0.002	0.17
Fil ulm*	0.06	0.002	0.10	Fil ulm*	0.06	0.002	0.10
Car ech*	0.02	0.014	0.03	Car ech*	0.02	0.014	0.03
Car pan*	0.02	0.028	0.03	Car pan*	0.02	0.028	0.03
Rum ace*	0.01	0.026	0.02	Rum ace*	0.01	0.026	0.02
Car ros	*0.02*	*0.076*	*0.03*	*bar pt*	*0.02*	*0.062*	*0.03*
Equ flu	*0.01*	*0.048*	*0.02*	*Car ros*	*0.02*	*0.026*	*0.03*
Eri ang	*0.01*	*0.086*	*0.02*	*Eri ang*	*0.01*	*0.09*	*0.02*
Bet sp	*0.01*	*0.074*	*0.02*	*Bet sp*	*0.01*	*0.08*	*0.02*
Car aqu	*0.01*	*0.134*	*0.02*	*Nar oss*	*0*	*0.086*	*0.00*
Nar oss	*0.01*	*0.136*	*0.02*	*Car ves*	*0.01*	*0.098*	*0.02*
Car ves	*0*	*0.166*	*0.00*	*Epi pal*	*0.01*	*0.146*	*0.02*
Cal pal	*0.01*	*0.188*	*0.02*	*Moss*	*0.01*	*0.114*	*0.02*
Hol lan	*0*	*0.142*	*0.00*	*Car aqu*	*0*	*0.212*	*0.00*
Eri cin	*0.01*	*0.14*	*0.02*	*Phr sp*	*0.01*	*0.208*	*0.02*
Mol cae	*0.01*	*0.218*	*0.02*	*Cal pal*	*0*	*0.286*	*0.00*
Gal pal	*0*	*0.248*	*0.00*	*Eri cin*	*0*	*0.23*	*0.00*
Phr sp	*.0*	*0.272*	*0.00*	*Hol lan*	*0.01*	*0.234*	*0.02*
Epi pal	*0.01*	*0.304*	*0.02*	*Mol cae*	*0*	*0.206*	*0.00*

*Variable significant in both models

5.4 *Discussion and Conclusions*

5.4.1 Objective a) Vegetation datasets and Two Way INdicator SPecies ANanlysis

Description of the vegetation datasets grouped by a priori *habitat mapping as well as clustering methods.*

Table 5:1 to Table 5:4 present a summary of the species composition data collected over the sampling period as well as the environmental data collected at each habitat and grouped by cluster. Simple statistics are also presented concerning the number of quadrats and species included in the class or cluster as well as the mean quadrat species richness. The results show a good deal of species overlap between the quadrats collected in five of the six habitats with the *Equisetum fluviatile* habitat exhibiting the most distinctive set of species. Ssegawa *et al.* (2004) studied the distribution of sedges in wetlands surrounding Lake Victoria in Uganda and reported that several sedges were found to be broadly distributed but never abundant, or narrowly distributed and abundant or neither broadly distributed nor abundant where they were found. This was sometimes the case with species reported here such as *Carex panicea*, *Carex aquatilis,* and *Carex pauciflora* respectively. Others such as *Carex echinata* and *Carex rostrata,* however, did show a broad distribution and relative abundance in one particular habitat type. To what extent this might influence the spectral separability of these habitat types is explored below.

Change in the data sets between the two sampling stages is indicated and this is largely due to the dominant species becoming more abundant over the growing season and sub-canopy species becoming less visible from above. This is most evident in the *Myrica gale* habitat where Table 5:3 and Table 5:4 show an apparent decrease in number of species. Increases of ~50% in stem density occurs for most of the habitats over the summer although Rush pasture/grassland remains high for both sample sets. No other significant changes occur in the structural and environmental variables recorded other than leaf litter. An increase in leaf litter

in the September dataset is apparent from Table 5:3 and Table 5:4 and this is unsurprising as plants begin to senesce with the close of the growing season.

The results from the TWINSPAN analyses cannot be directly compared between the sample stages as the clusters were constructed using different datasets. Some of the clusters are comparable with the *a priori* habitats as described above. The *Equisetum fluviatile* habitat seems to correspond with Cluster 7 and Cluster 6 in July and September respectively and the *Molinia* habitat can be associated with Clusters 5 and 3 respectively. The high frequency of *Molinia* and low species richness associated with Cluster 6 and Cluster 2 in July and September suggest that these clusters may be associated with the *Myrica gale* quadrats as described above. However, Cluster 1 in September also exhibits a high frequency of *Myrica gale*. A cluster that corresponds with the Rush pasture/grassland habitat can also be identified in each of the TWINSPAN results tables. These are Cluster 1 in July and Cluster 5 in September. Overall, therefore, the clusters demonstrate that in terms of species composition, samples collected from Rush pasture/grassland and *Equisetum fluviatile* quadrats cluster well together. The next best are the *Myrica gale* samples and the others then overlap so that no easy comparison with the *a priori* habitat types can be made. This is not surprising as the patterns in species composition and associated structural and environmental variables in the quadrats from mixed sedge and species-rich low sedge habitats overlap a great deal. There is similar overlap with the *Molinia* quadrats.

5.4.2 Objective b) Multiple Discriminant Analysis

Use Multiple Discriminant Analysis to assess how well the habitat class is predicted from the spectral dataset using a priori *classifications and groups derived from clustering methods.*

Multiple Discriminant Analysis (MDA) was performed on the spectra associated with each qaudrat sample point and labelled by the *a priori* habitat types and Clusters (Table 5:9 and Table 5:10). There was little consistent difference between the use of the larger AVS1-42 dataset and the simulated CASI datasets and the success of the MDA at predicting between

habitats or groups. On occasion, the smaller spectral dataset outperformed the results of the AVS1-42 dataset. The results in Table 5:9 were not as high as those presented in the previous chapter and this is probably because there were fewer samples per Group in this analysis. However, overall accuracies are around 30% higher than those in Table 5:10. As the Groups in Table 5:6 are made up of quadrats of similar species composition and associated structural and environmental variables, it was expected that the results would out-perform those obtained for the *a priori* groupings. Quadrats from one habitat type composed of unusual combinations of variables for that habitat type and more similar to another habitat type would no longer influence the spectral signature of that habitat type used in the MDA. The MDA for the TWINSPAN Groups did perform very well in relation to the random group labelling test though exactly why results are lower than those presented in Table 5:9 needs consideration.

A closer look at the individual Group results presented in Table 5:10 shows that some of the groups perform as well and some even better than the Group results in Table 5:9. These are the groups that are most associated with *Molinia* and *Equisetum* habitats in July (Cluster 5 and 7) and in September (Cluster 3 and 6). The cluster associated with *Myrica* performs well in September but not in July and, surprisingly, those clusters made up of species related to the rush pasture/grassland habitat do not perform well. It is clear from these results that the relationship between spectral reflectance and species composition and structure is particularly complex in environments composed of communities that intergrade to any extent. The nature in which TWINSPAN clustered the datasets may be a significant factor in these results as the division of the clusters may have been more influenced by variables that have little influence on the spectral reflectance. The illumination conditions during data collection may also have influenced the spectral datasets to a small degree and the extent of this is difficult to determine.

5.4.3 Objective c) Covariation between Spectra and Meteorological Data

Assess the significance of Canonical Correspondence Analyses (CCA) with any existing covariation between the spectra and local weather conditions at time of sampling removed.

In order to visualise the differences between habitat types and the conditions under which field sampling took place, an MDA was performed for both July and September using the Meteorological data (including solar altitude and azimuths). This was provided by the Meteorological Office although some gaps existed in the dataset and regression equations were using to replace these in order to work with a full dataset (Chapter 3).

The scatterplots of the discriminant functions from the MDA analyses are illustrated here in Figure 5:8 and Figure 5:9. From these it is clear that there exists a significant difference between the habitat types in terms of the weather conditions under which data from the respective study plots were collected. This was due to the nature of the data collection and the practicalities involved in getting from one area of the marsh to another. Spectra from the same habitat type were then more likely to be sampled close in time to each other and were, therefore, more likely to be influenced in the same way by local weather conditions. As such, a degree of autocorrelation may be present within the datasets. The extent to which this may have had a co-varying effect on the spectral measurements was explored using Canonical Correspondence Analysis. The results presented in Table 5:11 demonstrate the significance of the relationship between the spectra and vegetation datasets even when any covariation that may exist between the spectra and meteorological data is removed.

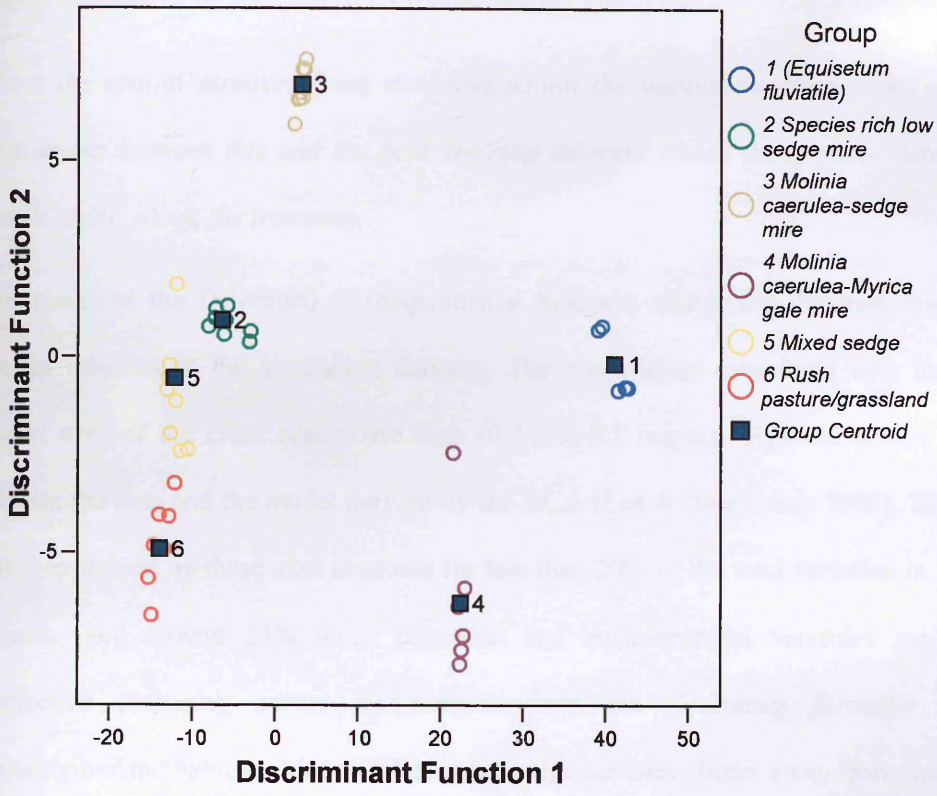

Figure 5:8 Stepwise MDA on altitude, azimuth and meteorological data to illustrate the different conditions under which the spectra were collected-July 2003

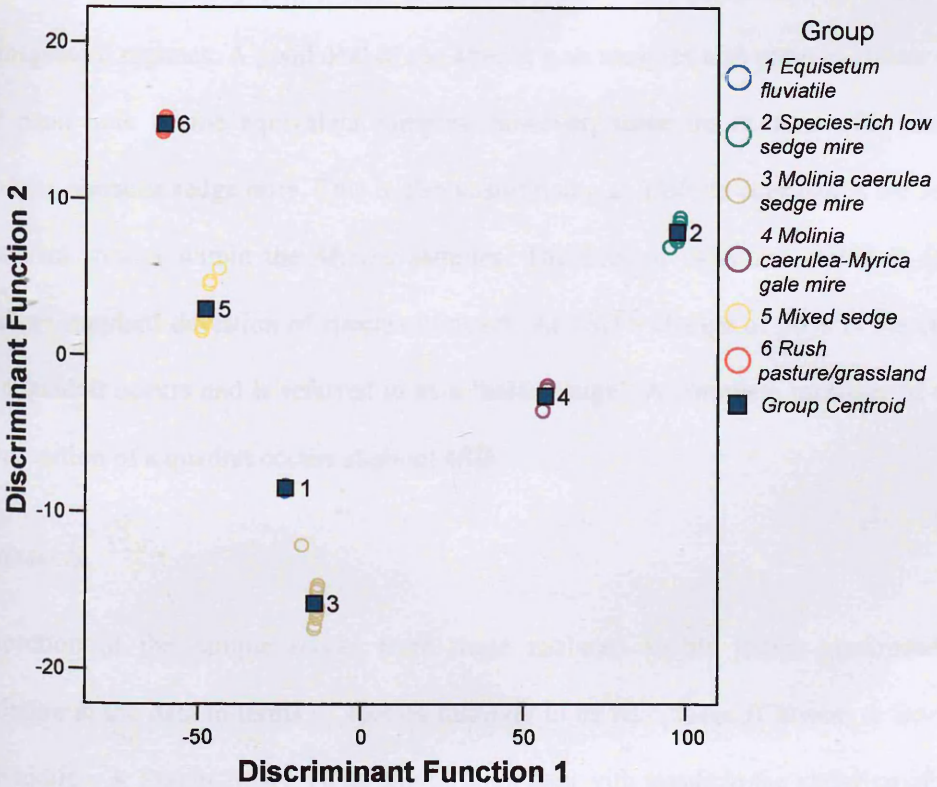

Figure 5:9 Stepwise MDA on altitude, azimuth and meteorological data to illustrate the different conditions under which the spectra were collected-September 2003

5.4.4 Objective d) Detrended Correspondence Analysis

Assess the spatial turnover (beta diversity) within the vegetation dataset and explore the relationship between this and the beta diversity inherent within the spectral data at paired sample points along the transects.

The results of the Detrended Correspondence Analyses effectively illustrate the degree of overlap inherent in the vegetation datasets. The eigenvalues associated with the first and second axes of the DCA results are high (0.7 and 0.5 respectively) and denote a good fit between the data and the model derived by the DCA (Lee & Rotenberry 2005). The variation that is explained by these axes accounts for less than 20% of the total variation in the species datasets (and around 25% when structural and environmental variables are included). Distinctive clustering occurs for samples from the *Equisetum fluviatile* and Rush pasture/grassland habitats. Many of the mixed sedge samples cluster away from the main bulk of mixed sedge samples in both sets of results and this can be explained by the nature of the data collection whereby plots were sampled across compartments that received contrasting management regimes. A good deal of the *Myrica gale* samples also seem to cluster away from the main bulk of the equivalent samples, however, some do overlap with samples from *Molinia caerulea* sedge mire. This is also unsurprising as *Molinia caerulea* is the second most abundant species within the *Myrica* samples. The axes in DCA are scaled in units of the average standard deviation of species turnover. At 1SD a change of 50% in the composition of a quadrat occurs and is referred to as a 'half-change'. A complete turnover of the species composition of a quadrat occurs at about 4SD.

Transects

Inspection of the sample scores from these analyses enable trends associated with the variation in the data in terms of species turnover to be recognised (Choesin & Boerner 2002; Schmidtlein & Sassin 2004). These can be compared with trends in the variation of other data, namely in this case, the spectral reflectance at each sample point. The nature of the

relationship between these two datatsets can then be explored. This concept was applied to obtain the results shown in Figure 5:3 for paired data along the three transects sampled in this study. An indication of the point at which the habitat boundaries are located along transects 'a' and 'b' is given (as determined in an *a priori* habitat survey, Maier & Cowie 2002). Transect 'c' does not cross a habitat boundary and acts as a control with which to compare the other results.

As would be expected, the regression results between spectra and vegetation samples scores along transect 'c' are shown to be the lowest of the three in Table 5:14. This transect falls within one habitat type and as such little 'trend' in species turnover would be expected and therefore the DCA sample scores from the two datasets would not necessarily show a strong relationship. Despite this, there does appear to be an indication that sample scores are increasing along the transect in the July data. Although the relationships between the datasets are weak (regression with AVS1-42 dataset R^2 Adj. = 33.7 and CASI R^2 Adj. = 8.1) a possible trend in the samples could be attributed to a gradual change in the datasets as sample points extend along the transect away from a habitat boundary (Chapter 3). This is not the case in the September data for this transect where greater intra-habitat variation may have contributed to noisier datasets.

The results for transects 'a' and 'b' indicate that both the vegetation datasets and the spectra exhibited similar trends in terms of change along an axis of variation for the September data. This was less apparent in the July datasets suggesting that, at different points in the growing season, substantial changes in vegetation datasets may not be enough to reflect a substantial change in the overall canopy reflectance. This is an interesting point as, it then follows that, there may be limits to the types of change which spectra can be used to identify. Further work should focus on what these limits are and at what stages in the growing season spectra can best be used as a tool in this area. In this dataset, September appears to be a better time of year to use change in spectra as a surrogate for change in vegetation datasets. Further work should explore how this applies to other habitat types and, in addition, investigate the use of DCA

using spectra from high spatial resolution imagery, with vegetation data collected along transects on the ground. Further groundwork would need to be done before spectra could be used in this way to confidently identify habitat boundaries. This concept is explored again in the next chapter.

Habitat boundaries along the transects were identified on the graphs in Figure 5:3 using a habitat map produced for the RSPB, immediately prior to the commencement of this study (Maier & Cowie 2002). DCA has been used successfully to detect vegetation changes at the community scale so was considered suitable for habitat boundary detection (Choesin & Boerner 2002; Goodchild 1994). The July dataset of transect 'b' shows a steep increase in species turnover at a roughly equal area either side of the boundary marker. This is not reflected in the DCA of the spectra. It is difficult to use most of these results to identify clear changes in the vegetation DCA results at the points where these habitat boundaries were mapped. This is illustrative of the problems associated with drawing hardline boundaries on habitat maps of semi-natural environments (Kent *et al.* 1997; Trodd 1993; Millington & Alexander 2000). Boundary characteristics may spread over a large area before characteristics unique to each habitat type bordering the boundary become more evident (van der Maarel 1990). This would vary between habitat types and so further work on using DCA of vegetation and spectral datasets is required over longer transects and using more habitat types.

5.4.5 Objective e) Canonical Correspondence and Redundancy Analyses

Explore the relationship between spectral response and vegetation datasets using multivariate techniques.

Redundancy Analysis (RDA)

Results from the RDA show that different species will be significant predictors of the variation in the spectra, depending on date of data collection. Understanding how this relationship varies throughout the growing season would add to the understanding of the

species-spectra relationship and further work should include this area of research. There are also notable differences between which species are significant predictors of the variation in the AVS1-42 dataset and the simulated CASI dataset for the July results but not the September results. The effect of spectral resolution on the species-spectra relationship is therefore another important factor to consider in further work.

The results from all analyses (Table 5:21, Table 5:22, Table 5:29 and Table 5:30) highlight the relative importance of many understorey species such as *Ranunculus flammula, Rumex acetosa* and *Potentilla palustris*. Species such as *Poa pratensis, Nardus stricta* and *Carex hostiana* which represent a very small proportion of the samples were also included in the significant predictors. These plants are largely erectophile and cover a relatively small area of the target canopy. The independent influence on the reflectance spectra of relatively rare, erectophile, and understorey plants would be expected to be minimal. These are species that are associated with samples that have a significant relationship with the spectral data and, therefore, do not themselves necessarily *cause* that significant relationship. To what extent this is the case is difficult to determine from these results; *Myrica gale*, for example, is a species that exhibits both a relatively unique spectral signature and is located in a habitat with a distinct canopy structure and background components. Analyses using Canonical Correspondence Analysis allow for further insight into these relationships.

Canonical Correspondence Analyses (CCA)

Data collected in July 2003 and September 2003 were analysed using Canonical Correspondence Analysis (CCA) and definite patterns emerged in the relationship between the variation in the spectra and that in the vegetation as illustrated previously by Ssegawa *et al.* (2004) and Southall *et al.* (2003). The AVS1-42 datasets performed with greater success than the CASI dataset (by a factor of around 2 in most cases) in terms of the amount of variation in the vegetation datasets explained by the spectra. The spectra also predicted the variation in the vegetation datasets with greater success when structural and environmental variables were included. Lewis (1994) reported a greater degree of success than previous

studies at relating botanically-derived groups to spectral data by quantifying both species composition, non-vegetative ground cover and considering structural variables. This is complimented by the results presented here, although which variables (measured or not in this instance) might serve to further improve the relationship should be investigated in further studies. Brook and Kenkel (2002) conclude in a similar study, that a large amount of variation in floristic composition remains unaccounted for as spectral reflectance is largely a function of the structural, rather than the floristic, properties of vegetation (Muller 1997; Schmidtlein & Sassin 2004).

The success of the larger spectral datasets is partly due to the greater number of predictors in the AVS1-42 dataset. Correlation between predictors is accounted for in the analyses and so this highlights the potential importance of larger spectral datasets that encompass regions of the spectrum which are not available in the simulated CASI dataset. This suggests that were this technique ever transferred to interpret imagery in terms of vegetation composition on the ground, hyperspectral datasets would offer more interpretive potential than multispectral datasets. The detailed pattern in the relationship between these two datasets should, however, be explored further in order to understand the interaction between species distribution and reflectance in different spectral bands. This is the basis behind the work presented here, although it is acknowledged that this is a limited dataset and only the first of its kind on wetland vegetation in the UK. There is, therefore, a considerable need for further work applying these methods of analysis to these kinds of data.

Tests on the first canonical axes and the predictive power of all axes combined were carried out for each analysis and results were all significant (Table 5:15 and Table 5:23). The spectral datasets (AVS1-42 and simulated CASI bands) did not perform better relative to themselves between the July and September analyses (Table 5:16 and Table 5:24). This is interesting as even though the vegetation datasets do change slightly between the sample dates the predictive capabilities of the spectral datasets remain the same. The extent to which this is the case when substantial changes in the vegetation dataset occur remains unexplored in this

study. There are difficulties when using field spectrometry at high latitudes in the winter months and these issues would need to be addressed before such work was undertaken.

The ordination plots of the CCA results using the AVS1-42 datasets and the CASI datasets all illustrate that some spectral bands correlate strongly with the axes. The length of the arrows in these diagrams relate to their significance as predictors and the angle of the arrow in relation to each axis indicates how well correlated the predictor is with that axis. The ordination graphs using the AVS1-42 dataset illustrate the importance of reflectance in wavebands in the green and red regions and NIR shoulder particularly at around 600 nm, 725 nm and 820 nm in terms of predicting the variation in the vegetation datasets. These results are comparable to those published by Armitage *et al.* (2004) who reported that a sequence of individual species changes along axis I was related to simulated CASI bands covering the 736 nm to 870 nm region of the spectrum. The significant bands shown here correlate strongly with axes I and II in the September analyses compared with the July analyses, as is also reflected in the results for the CASI bands. The spectra do perform better in terms of overall variation in the vegetation datasets explained using the September data and, therefore, the influence of the time of the year and data collection on results from these kinds of analyses are important considerations.

The results of the CCA analyses using the simulated CASI data are presented in Figure 5:5 and Figure 5:7. The axes can be associated with variation in the red-edge shoulder and NIR regions of the spectrum (axis II in July, axis I in September) and the green region (axis II in September). The CASI 2 band in Figure 5:5 (550 nm – green region) is the most significant predictor although it is only slightly more correlated with axis I than with axis II. These results all compare well to previous studies where axes I and II were correlated with either reflectance in the NIR or in the green regions of the spectrum (Trodd 1996; Armitage *et al.* 2004) but Armitage *et al.* (2000) report little correlation between any spectral bands and axis II using data collected in late June/July. How these relationships relate to the vegetation datasets in terms of species composition is difficult to interpret in terms of habitat type and

habitat clusters as there is so much inherent species overlap in the samples. By considering simply species richness and sample diversity across the ordination a relationship with the predictors may be established.

The relationship between species richness (simply the number of species within each sample) within the samples and their subsequent ordering along the axes was explored upon observing the ordination patterns produced by the CCA (Figure 5:10). The spread in species richness across the two axes for each analysis was explored using Generalised Linear Modelling (GLM) in CanoDraw. This provides a P-value which can be interpreted in the usual manner. The results are illustrated below and were found to be significant for the July analyses at a 95% significance level. Diversity was also considered (also looks at number of species but takes into account relative species abundance in the entire dataset) and all GLM results indicated that the relationship between sample diversity and ordering along axes I and II were significant at a 95% significant level or greater (Figure 5:11). The relationships between species richness and diversity and their interaction with spectra have not been explored in the literature in this manner but these results clearly warrant further work (Southall *et al.* 2003; Carter *et al.* 2005).

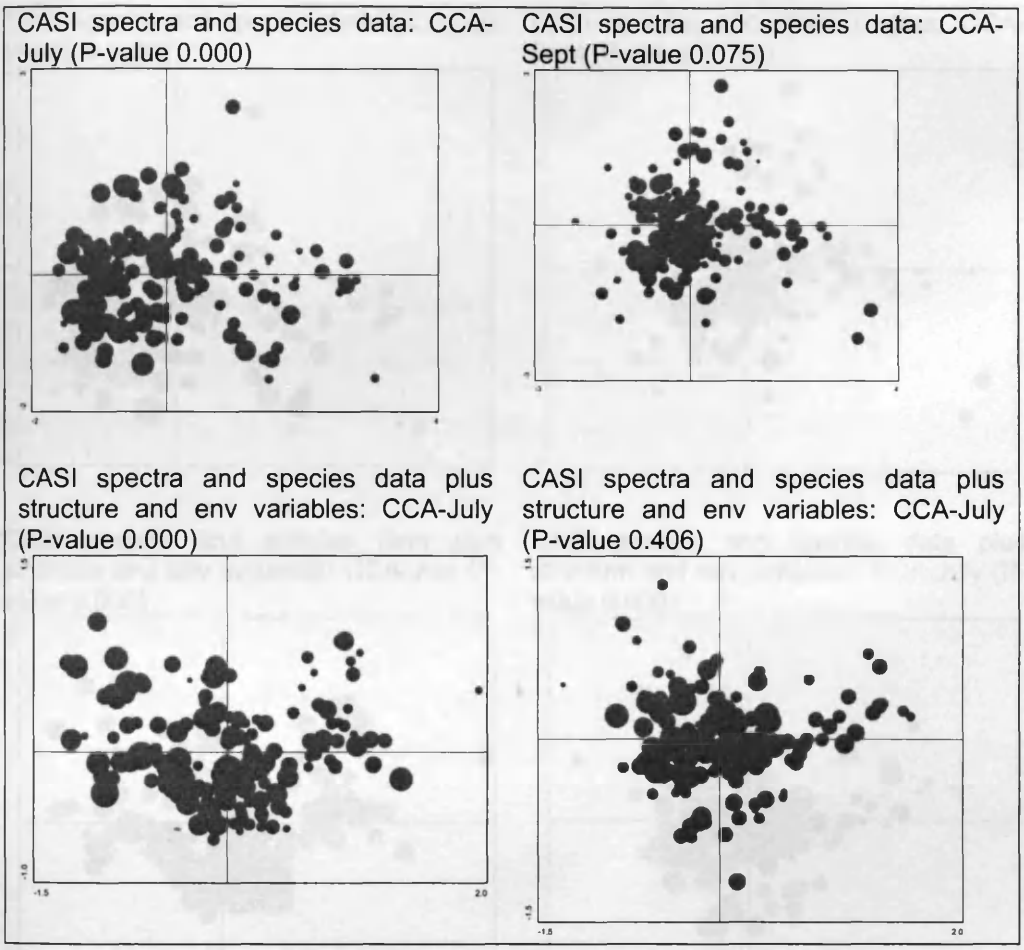

Figure 5:10 Attribute plots showing spread in species richness across ordination diagram (larger sample symbols correspond to greater species richness)

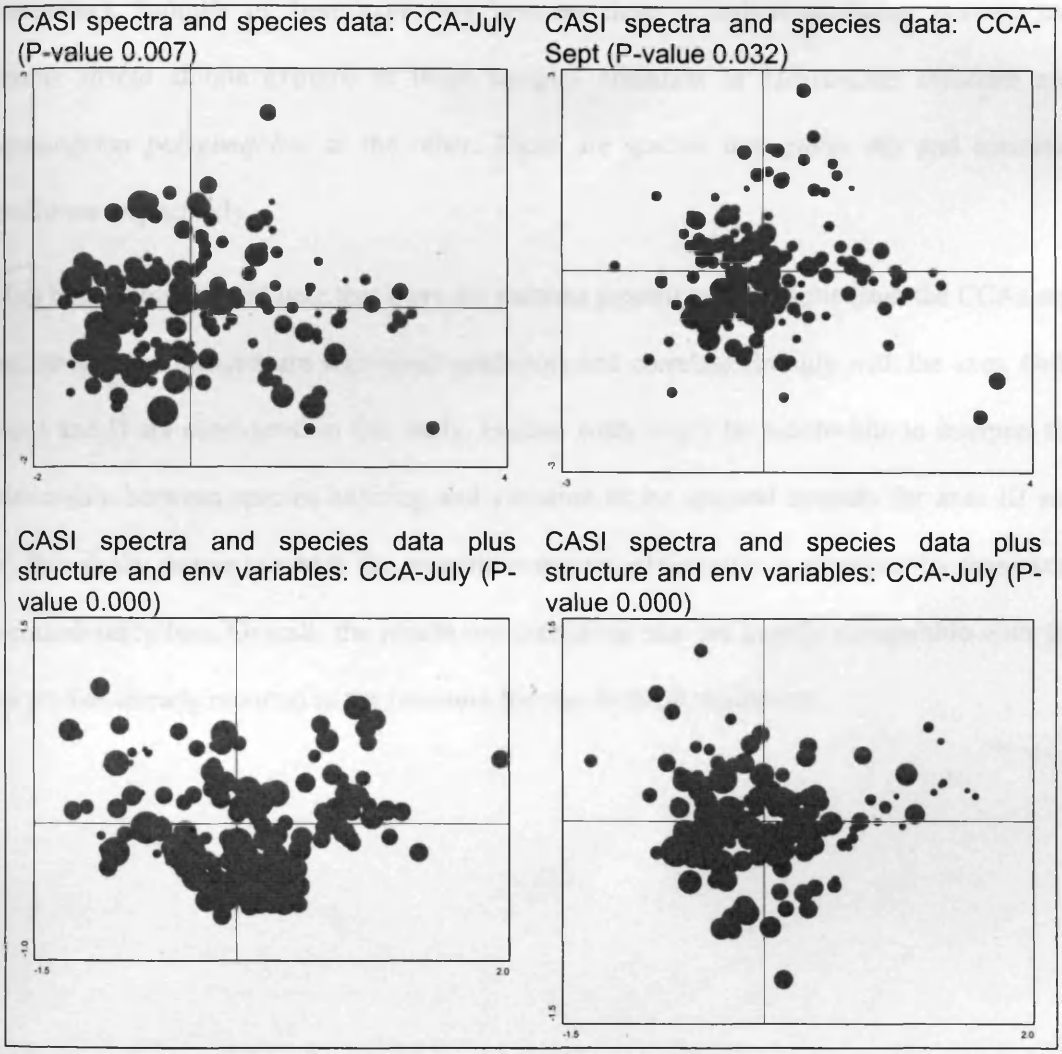

Figure 5:11 Attribute plots showing spread in species diversity across ordination diagram (larger sample symbols correspond to greater species diversity)

The ordering of the samples in the ordinations was also considered in terms of physiognomy (Muller 1997). The samples seem to be ordered according to factors such as relative leaf area or stem density. Axis I in July, for example, and axis II in September have samples abundant in *Myrica gale* at one extreme and samples collected in habitats made up of fine, dense vegetation types such as those in rush pasture/grassland and species-rich low sedge mire at the other extreme (cf. Armitage *et al.* 2000). Canopy structure has influenced the ordering of the samples along these axes to some extent as the *Myrica* and *Molinia* habitats are more spherical in comparison to the erectophile structure of the sedge habitats (Spanglet *et al.* 1998). Environmental factors such as dryness and wetness of the sample also seem to play a

part in the ordering of samples in the CCA results in the alternate axes (axis II July and axis I September). Samples in these axes vary between those abundant in *Rumex acetosa* and *Nardus stricta* at one extreme to those samples abundant in *Menyanthes trifoliata* and *Potamogeton polygonifolius* at the other. These are species that prefer dry and saturated conditions respectively.

It has been demonstrated here that there are patterns present in the results from the CCAs and that the spectral datasets are significant predictors and correlate strongly with the axes. Only axes I and II are considered in this study. Further work might be worthwhile to interpret the relationship between species ordering and variation in the spectral datasets for axes III and IV, though the degree to which the vegetation-spectra relationship is explained by these axes is considerably less. Overall, the results are promising and are largely comparable with the few studies already reported in the literature for non-wetland vegetation.

5.5 *Summary*

The interactions between detailed vegetation composition and structural datasets with reflectance in the optical region of the spectrum are explored in this chapter using multivariate analytical techniques. The overall aim was to determine how well vegetation datasets relate to spectral response between habitat types and across boundaries. The results of the vegetation survey highlight the difficulties associated with using spectra in semi-natural environments to classify between habitat types composed of similar vegetation types yet many of the results presented here are promising and demonstrate the effectiveness of these methods of analysis to further our understanding of these relationships. Although it has been recognized that further work is necessary, the present study is an important first step for work regarding remote sensing wetland vegetation. It is also notable that studies using spectral data and these types of ecological analyses are sparse in the current literature and this work is therefore an important addition to this area of research. Each of the objectives related to this chapter is listed below with a brief summary of the conclusions drawn from the respective analyses.

a) *Describe vegetation datasets grouped by* a priori *habitat mapping as well as clustering methods.*

- A large degree of overlap in species composition and structure was evident within the vegetation datasets from the *Molinia* and sedge habitat types.

b) *Use Multiple Discriminant Analysis to assess how well the habitat class is predicted from the spectral dataset using* a priori *classifications and groups derived from clustering methods.*

- Overall accuracies ranged from 69.9 % to 85.0 % and were slightly higher using the September datasets compared with results from July.
- Results from the CASI datasets were often as good and, sometimes better, than those obtained using the larger AVS1-42 dataset.

c) *Assess the significance of Canonical Correspondence Analyses (CCA) after removal of any existing covariation between the spectra and local weather conditions at time of sampling.*

- With the covariation between local weather conditions and spectral response removed, spectra were still significant predictors of the variation in the vegetation datasets.

d) *Assess the spatial turnover (beta diversity) within the vegetation dataset and explore the relationship between this and the beta diversity inherent within the spectral data at paired sample points along the transects.*

- Using sample scores derived from DCAs, the nature of habitat boundary characteristics as represented by the vegetation datasets was strongly related to the spectral datasets in the September analyses.
- The relationship between the two datasets was strongest when the AVS1-42 dataset was used (R^2 Adj. ranged from 61.2–75.6) compared with the simulated CASI dataset (R^2 Adj. ranged from 38.0–39.3)

e) *Explore the relationship between spectral response and vegetation datasets using multivariate techniques.*

- The variation in the distribution of understorey species such as *Ranunculus flammula, Rumex acetosa* and *Potentilla palustris* and erectophile plants such as *Poa pratensis* and *Nardus stricta* was strongly associated with the variation in the spectral datasets using RDA.
- The AVS1-42 dataset proved consistently more effective at explaining the variation in the vegetation datasets using CCA by around a factor of 2; though correlation between the AVS1-42 variables was very high.
- Although the CASI dataset explained less of the variation in the vegetation datasets, the relationship between the spectra and the vegetation datasets in the CCA output

was easily observed and patterns in the ordination of the data were much more visible.

- Axis I was strongly related to variation in the red edge shoulder and NIR regions of the spectrum in the September datasets. In the July results, Axis II was strongly related to these parts of the spectrum. Axis II in the September results was strongly related to variation in the green region of the spectrum.
- Species richness and diversity were found to be strongly related to the pattern of the sample ordinations produced in the CCAs.

6 AIRBORNE IMAGERY AND WETLAND HABITAT CLASSIFICATION

6.1 Introduction

It is widely accepted that there is a clear need for accurate vegetation mapping. However, the conventional field techniques that are employed to map the spatial distribution of vegetation or monitor responses to management are time consuming, labour-intensive, expensive and limited in their spatial accuracy and coverage. Alternatively, remote sensing provides synoptic data that is repeatable and objectively acquired. It can provide information regarding vegetation change over time and space, the effects of management, the health and vigour of vegetation as well as longer term variation. This chapter explores methods by which the understanding of spatial patterns in vegetation can be enhanced using spectral information in the form of airborne imagery.

6.1.1 Aims and Objectives

Chapter 6: Overall Aim (Project Objective 3)

Assess the potential of high spatial resolution multispectral airborne imagery for classifying and characterising wetland habitats.

This chapter seeks to meet Project Objective 3 as outlined in Chapter 1. The main objectives used to achieve this are listed below. The results achieved will be considered in light of the overall aim above, and due consideration will be given to their potential as an ecological tool for wetland management.

a) *Identify spectral endmembers of* a priori *and grouped habitat types.*

b) *Explore the spectral variation within the available imagery using unsupervised classifications and various spectral indices.*

c) *Assess the potential for supervised classification to correctly classify habitat types derived from field based* a priori *habitat maps.*

d) *Explore the relationships between spectral variability derived from airborne imagery and detailed vegetation datasets along transects.*

6.2 Methods

This section details the methods applied in this chapter beginning with listing the datasets used to achieve each of the objectives outlined above (in 'a)' to 'd)').

6.2.1 Datasets and Methods Overview

a) Endmember spectra for each habitat type, as defined in an *a priori* habitat map (Maier & Cowie 2002), were derived within ENVI v. 4.1 using both available images (CASI 91 and CASI 101-see Chapter 3). In addition, habitat types were grouped into broader vegetation classifications and endmember spectra were derived for these new grouped classes.

b) Unsupervised classification was applied to each image utilizing the data in each of the available fifteen CASI bands. This was also applied to imagery derived values of NDVI and REIP.

c) Supervised classification was carried out on each image (CASI 91 and CASI 101) using equalized random training samples (x 100) from each *a priori* habitat type as well as grouped habitat types. A stratified random approach was also used to generate random samples from 5% of the total areas of each habitat type or group. Probability maps were

derived for sensitive habitat types using the rule images produced as part of the MLC process performed on each image. Spectral subsets of the data using blue, red, green and NIR wavebands were also analysed. Spectral feature fitting was carried out on the blue and red absorption features associated with each image and used in the supervised classification of the *a priori* habitat types and the grouped habitat types.

d) Five transects were analysed using the *a priori* vegetation datasets (Maier & Cowie 2002). Start and end locations were identified on the imagery and values at each waveband were obtained at a point 2.5 m along each transect. Values were derived for NDVI and REIP along each transect. Analyses were carried out using bands 1-15 for each transect and the paired sample points.

6.2.2 Imagery and Habitat Types

Two CASI images were provided by NERC ARSF and these were analysed in RSI ENVI v 4.1. The areas of Insh Marshes that these images covered are shown in Figure 6:1. Chapter 3 details how these images were geocorrected and preprocessed prior to the analyses described in this chapter. Figure 6:2 shows the habitat types within the Insh Marshes SSSI covered by the available imagery. Each CASI image covers 22 of the total number of habitat types (24). Vector files of the habitat types were provided by RSPB in ArcView shapefile format and imported into ENVI. These were then overlaid as vectors onto the images and subsequently converted into ENVI Vector Files (.evf) from which class images were derived.

A number of areas within the marsh were identified in a survey carried out for RSPB as areas containing species associated with a particular conservation concern as they are either rare or invasive (Maier & Cowie 2002). These are illustrated in Figure 6:3.

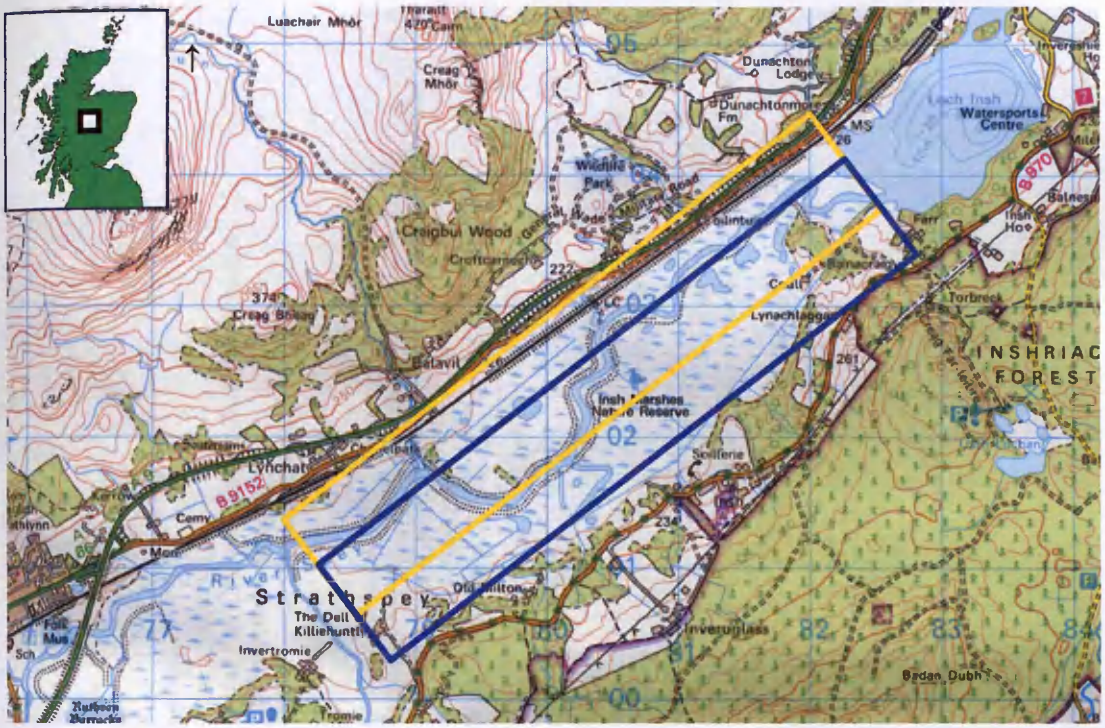

1:50:000 OS Landranger Series # 35 Crown copyright © Ordnance Survey

Figure 6:1 CASI flightlines (Yellow: CASI 91; Blue: CASI 101)

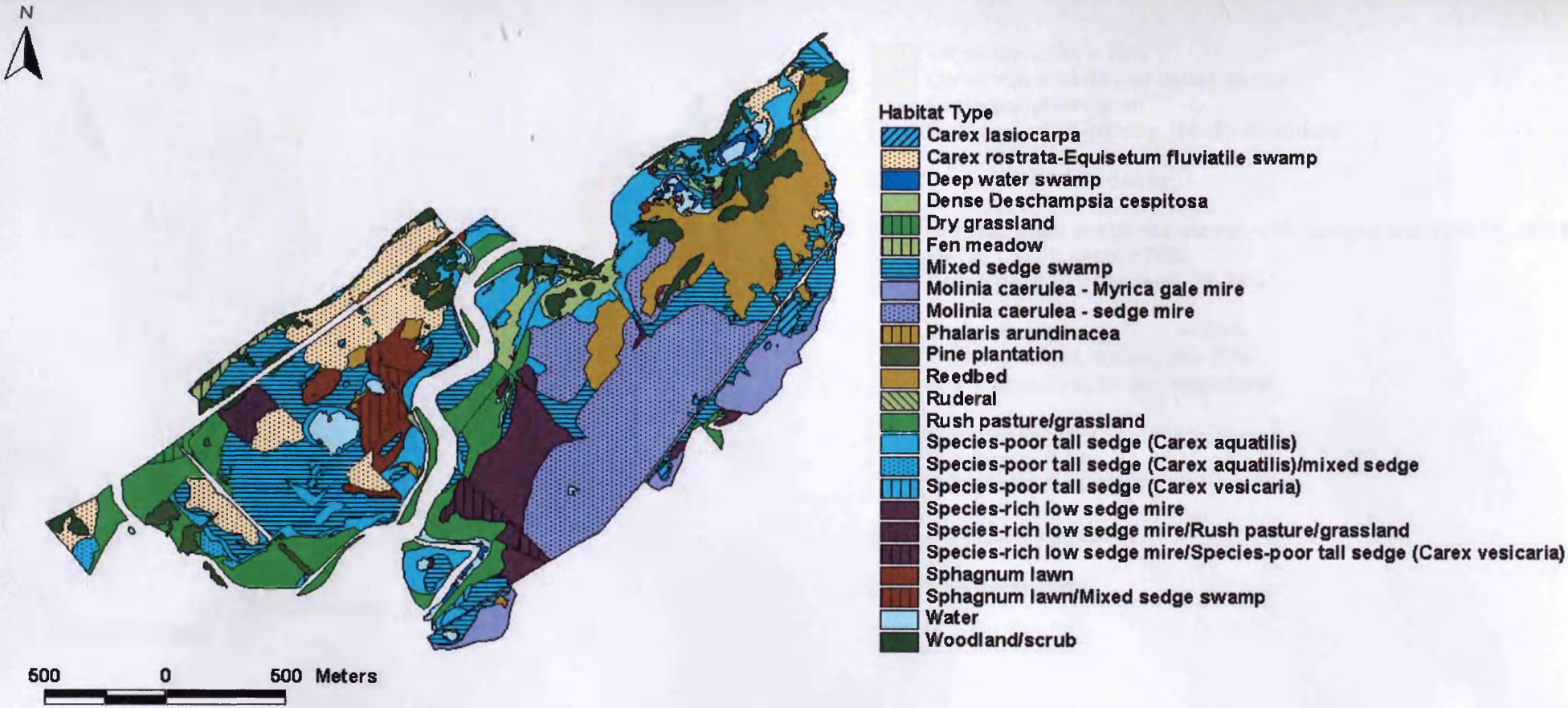

Figure 6:2 Habitat types covered by both images (x25 in total but this includes *Sphagnum* flush at eastern margin of the marsh which is not shown)

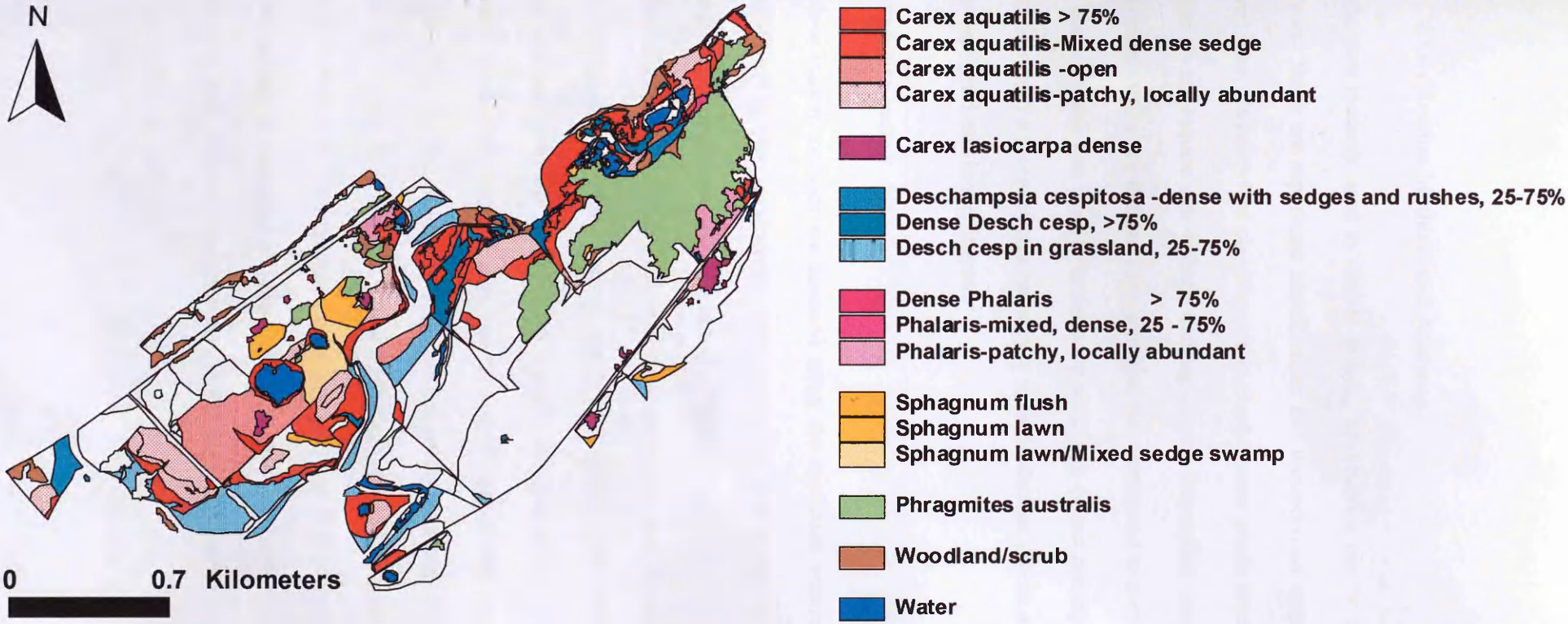

Figure 6:3 Habitats of special ecological interest (Rare and invasive species)

6.2.3 Classification Methods and Analyses

Classification methods used in remote sensing applications can be divided into two main categories. These are supervised classification and unsupervised classification and both are explored here. Unsupervised classification methods cluster pixels together based on statistics only and do not require user-defined training classes. Supervised classification assigns class type to pixels using pre-defined class statistics that correspond to user-defined training areas. In all cases a mask was used to exclude the areas that do not correspond with the available information from a recent vegetation survey at Insh Marshes. These areas are blacked out in all the maps produced in this chapter.

The confusion matrix

The classification methods are assessed using the confusion matrix (Basham May 1997; Goodchild 1994). This is calculated using the ground truth image (or class image) provided by the *a priori* habitat survey. The confusion matrix is calculated by comparing the location and class of each ground truth pixel with the location and class of the corresponding pixel in the classification image. Each column represents a ground truth class and the values in the column correspond to the classification image's labeling of the ground truth pixels. The number of pixels that were classified into the correct ground truth class are located down the diagonal of the confusion matrix. The statistics produced along with the confusion matrix include the overall accuracy, the kappa coefficient, producer accuracy, user accuracy and errors of commission and omission (Story & Congalton 1986; Goodchild 1994). Confusion matrices provide a great deal of information, but only a selection of complete matrices are presented in this chapter; on other occasions, only a summary of the results from the confusion matrix is provided.

Overall Accuracy

The overall accuracy is calculated by summing the number of pixels that have been classified correctly and dividing this by the total number of pixels which is the sum of all the pixels in the ground truth classes. The ground truth image or the ground truth ROIs define the true class of the pixels. This can be expressed in number of pixels or as a percentage.

Kappa Coefficient

Along with the overall accuracy, the kappa coefficient (κ) is a further measure of the classification accuracy. This is calculated as laid out in Equation 6:1 where N is the total number of pixels in all the ground truth classes, x_{kk} represent the confusion matrix diagonals and $x_{k\Sigma}x_{\Sigma k}$ represent the ground truth pixels in a class multiplied by the sum of the classified pixels in that class summed over all classes. The Kappa statistic is considered by some to be superior to the overall accuracy statistic (Fitzgerald & Lees 1994) as it allows for correct classifications that have occurred by chance (NB also known as Cohen's statistic or K_{hat}). Kappa is defined as follows and ranges from 0 in the case of the most confused classification to 1 in the case of the most accurate (Goodchild 1994).

$$\kappa = \frac{N\sum_{k} x_{kk} - \sum_{k} x_{k\Sigma}x_{\Sigma k}}{N^2 - \sum_{k} x_{k\Sigma}x_{\Sigma k}}$$

Equation 6:1

Producer Accuracy

The producer accuracy is a measure indicating the probability that the classifier has labeled the pixels representing each class in the classification image as the respective classes in the ground truth image or ROIs. This provides an indication therefore of how the classification performed regarding each habitat class within the ground truth data. This is presented below as a percentage of the overall areas of each habitat type of the ground truth image.

User Accuracy

The user accuracy is a measure indicating the probability that pixels within each class of the classified image are labelled with the respective class from the ground truth image or ROI. This provides an indication of how confident the user can be that the class labels correspond to the ground truth data. This is presented below as a percentage of the overall area of each habitat type in the classified image.

Errors of Commission

The errors of commission are shown along the rows of the confusion matrix. These represent the number of pixels that belong to another class but are labeled as the class of interest. It is the ratio of the number of pixels classified incorrectly by the total number of pixels in the ground truth class that forms the error of commission. This is expressed as a percentage.

Errors of Omission

The errors of omission are shown along the columns of the confusion matrix. These represent the number of pixels that belong to the class of interest but are labeled as another class. It is the ratio of the number of pixels classified incorrectly by the total number of pixels in the ground truth class that forms the error of omission. This is expressed as a percentage.

Unsupervised classification

The K-Means method of unsupervised classification was carried out on the imagery. This works by calculating initial class means evenly distributed in the data feature space and then clusters the pixels into the nearest class using a minimum distance technique in an iterative manner. Each iteration recalculates class means and subsequently reclassifies pixels with respect to the new means. This continues until a maximum number of iterations is reached. The classes produced, using this classification method, are then interpreted in light of the ground truth information.

K-Means Classification is carried out using all 15 of the CASI bands using 35 cluster classes. These are then analysed in ArcView 3.2 to determine which of the *a priori* habitat types fall into which cluster class. The results of the first and second most abundant habitat type located within each class are presented here. Images of the unsupervised classifications were generated using 22, 11 and 6 cluster classes in order to visualise the patterns produced by the clustering with respect to the outline of the *a priori* habitat types. In addition, the spatial pattern across the images with respect to the Normalised Difference Vegetation Index (NDVI) and Red Edge Inflection Point (REIP) is assessed using this clustering technique. Images of NDVI and REIP are first calculated (See Equation 6:2 to Equation 6:4 below). (The bands used to calculate these indices are listed below in Table 6:1).

The position of the REIP was calculated using the Guyot-Baret Model (Clevers *et al.* 2001; Clevers *et al.* 2002; Dawson & Curran 1998) (Equation 6:3 and Equation 6:4). This method was chosen because of the simplicity of the approach and the ease of applicability within the available software. The Guyot-Baret model was also considered the most appropriate method given that hyperspectral imagery was not available and this model still effectively calculated relative trends in this index between habitat types and over the marsh.

Table 6:1 CASI bands used in Guyot-Baret Red Edge Model

Wavelength	CASI Band	Band Centre (nm)
670	6 (Red)	672
700	7	701
740	9 (NIR)	740
780	12	780

$$NDVI = \frac{(NIR - \mathrm{Red})}{(NIR + \mathrm{Red})}$$ **Equation 6:2**

$$R_{REIP} = (R_{670} + R_{780})/2$$ **Equation 6:3**

Where 'R_{REIP}' = Reflectance at REIP, R_λ = Reflectance at λ (nm)

$$\lambda_{REIP} = 700 + [40((R_{REIP} - R_{700})/(R_{740} - R_{700}))]$$ **Equation 6:4**

Where λ_{REIP} = wavelength (nm) at R_{REIP}

Supervised classification

Maximum Likelihood Classification (MLC) is one of the most commonly applied methods of supervised classification. It is a 'hard' method of classification whereby the output consists of a per pixel classification, with pixels labeled as the most likely class, based on rules derived from the training data. MLC therefore assumes that all pixels are spectrally pure and belong to one of the classes defined. Another assumption is that each class has a distinct spectral response. This method does not cope well with mixed pixels and in some cases it is required to 'unmix' the pixels into component parts. These are termed 'soft' methods of classification and include methods such as Fuzzy C-Means classification, mixture modelling and Artificial Neural Networks (ANNs) (Foody 1996b). An important assumption of MLC is that the frequency distribution of the spectral response of each class is Gaussian or 'normal' in nature.

MLC is a relatively user-friendly method that requires little in the way of computational resources or 'black box' computations. An added advantage with MLC is the potential to utilise the 'rules' calculated for each class during the process to derive 'probability maps' for use in the field (Wood & Foody 1989; Foody *et al.* 1992; Foody 1996a). The production of a class image made up of hardline boundaries between class types may be considered a limitation of this method. However, this is a method of mapping that is commonly used in semi-natural environments and is therefore familiar to those involved in ecological survey and management. At this spatial resolution (2.5 x 2.5 m pixel) a pixel is unlikely to consist of two distinct habitat types. In semi-natural vegetation, habitat types can grade into one another over large areas and these 'fuzzy' boundary areas may then contain a spectral pattern that is

distinct to them. This may create a problem for the application of remote sensing to vegetation classification in semi-natural environments when the aim is to characterize these areas. Creating hardline boundaries is a common bi-product of mapping complex environments and is a concept that is widely accepted and applied in ecology and conservation science.

MLC was carried out on both CASI imagery (CASI 91 and CASI 101) utilising all fifteen spectral bands. In addition, spectral subsets of both images were created utilising the blue (441-461 nm), green (548-557 nm), red (666-674 nm) and NIR (736-744 nm) bands. Analyses were carried out using all 22 *a priori* habitat classes as well as the 11 grouped classes (see Table 6:8). The training classes that were applied were based on the *a priori* habitat types determined by a vegetation survey carried out on Insh Marshes, close to the start of this project, using field techniques and aerial photography analysis (Maier & Cowie 2002). The habitat classes derived from this survey were provided in ArcView shapefile format and imported into the ENVI environment. Within ENVI the information was converted into a class image (or 'ground truth image') that can then be utilised in the classification procedures. One hundred training samples from each habitat type in the class image were generated (see Table 6:2 and Table 6:3) (Mehner *et al.* 2004). Classifications were also carried out using Stratifed Random Sample sets using a proportionate sampling method (a 5% total class area was used as the minimum sample size) (see Table 6:4 and Table 6:5).

The only post-classification procedure employed prior to the production of the confusion matrix was Majority Analysis. This is an effective method employed to change pixels from one class into another depending on the majority of the surrounding pixels. A kernel size of 5 x 5 pixels representing an area on the ground of 12.5 m x 12.5 m was used, where the centre pixel is replaced with the class value or name associated with the majority of the pixels within the kernel. This method was considered an appropriate way of 'cleaning up' the classification images as areas smaller than 10 m x 10 m were not considered during the data collection for the *a priori* habitat map.

Table 6:2 Training Samples-CASI 91-Main Habitat Types (x22)

Habitat (CASI 91)	Total # of pixels	Equalized Random (x100 pixels) % of tot area (2d.p.)	Stratified Random (5% total area) (2d.p.) # pixels*
Carex lasiocarpa	1843	5.43	92.15
Carex rostrata-Equisetum fluviatile swamp	41668	0.24	2083.4
Deep Water Swamp	1918	5.21	95.90
Dense *Deschampsia cespitosa*	10898	0.92	544.90
Dry grassland	1847	5.41	92.35
Fen meadow	971	10.30	48.55
Mixed sedge swamp	55190	0.18	2759.50
Molinia caerulea - sedge mire	10331	0.968	516.55
Phalaris arundinacea	600	16.67	30.00
Pine plantation	3496	2.86	174.80
Reedbed	25704	0.39	1285.20
Ruderal	608	16.45	30.40
Rush pasture/grassland	38426	0.26	1921.30
Species-poor tall sedge (*Carex aquatilis*)	43315	0.23	2165.75
Species-poor tall sedge (*Carex aquatilis*)/mixed sedge	2128	4.70	106.40
Species-poor tall sedge (*Carex vesicaria*)	764	13.09	38.20
Species-rich low sedge mire	1893	5.28	94.65
Species-rich low sedge mire/Rush pasture/grassland	4696	2.13	234.80
Sphagnum lawn	10784	0.93	539.20
Sphagnum lawn/Mixed sedge swamp	7969	1.25	398.45
Water	10706	0.93	535.30
Woodland/scrub	30654	0.33	1532.70

Table 6:3 Samples-CASI 101-Main Habitat Types (x22)

Habitat (CASI 101)	Total # of pixels	Equalized Random (x100 pixels) % of tot area (2d.p.)	Stratified Random (5% total area) (2d.p.) # pixels*
Carex lasiocarpa	3026	3.30	151.30
Carex rostrata-Equisetum fluviatile swamp	5752	1.74	287.60
Deep Water Swamp	912	10.96	45.60
Dense *Deschampsia cespitosa*	7823	1.28	391.15
Dry grassland	50640	0.20	2532.00
Fen meadow	6340	1.58	317.00
Mixed sedge swamp	71671	0.14	3583.55
Molinia caerulea - sedge mire	782	12.79	39.10
Phalaris arundinacea	1261	7.93	63.05
Pine plantation	45178	0.22	2258.90
Reedbed	610	16.39	30.50
Ruderal	33779	0.30	1688.95
Rush pasture/grassland	26381	0.38	1319.05
Species-poor tall sedge (*Carex aquatilis*)	1721	5.81	86.05
Species-poor tall sedge (*Carex aquatilis*)/mixed sedge	896	11.16	44.80
Species-poor tall sedge (*Carex vesicaria*)	19384	0.52	969.20
Species-rich low sedge mire	1056	9.47	52.80
Species-rich low sedge mire/Rush pasture/grassland	4453	2.25	222.65
Sphagnum lawn	4177	2.39	208.85
Sphagnum lawn/Mixed sedge swamp	3583	2.79	179.15
Water	6427	1.56	321.35
Woodland/scrub	14719	0.68	735.95

Table 6:4 Training Samples-CASI 91-Grouped Habitat Types (x11)

Grouped Habitat	Total # of pixels	Equalized Random (x100 pixels) % of tot area (2d.p.)	Stratified Random (5% total area) (2d.p.) # pixels*
Deep Water Swamp	1918	5.21	95.90
Carex rostrata-Equiesetum fluviatile swamp	41668	0.24	2083.40
Grass1	12477	0.80	623.85
Grass2	40273	0.25	2013.65
Grass3	10331	0.97	516.55
Reed-Phal	26304	0.38	1315.20
Sp-poor	103240	0.10	5162.00
Sp-rich	6589	1.52	329.45
Sphag	18753	0.53	937.65
Trees-Scrub	34150	0.29	1707.50
Water	10706	0.93	535.30

Table 6:5 Training Samples-CASI 101-Grouped Habitat Types (x11)

Grouped Habitat	Total # of pixels	Equalized Random (x100 pixels) % of tot area (2d.p.)	Stratified Random (5% total area) (2d.p.) # pixels*
Deep Water Swamp	912	10.96	45.60
Carex rostrata-Equisetum fluviatile swamp	5752	1.74	287.60
Grass1	8433	1.19	421.65
Grass2	33779	0.30	1688.95
Grass3	78011	0.13	3900.55
Reed-Phal	45960	0.22	2298.00
Sp-poor	82664	0.12	4133.20
Sp-rich	24893	0.40	1244.65
Sphag	7760	1.29	388.00
Trees-Scrub	15980	0.63	799.00
Water	6427	1.56	321.35

Rule images and probability mapping

The process of Maximum Likelihood Classification produces rule images, one per class, which contain a maximum likelihood discriminant function with a modified Chi Squared probability distribution (ENVI 2003). Higher values of pixel brightness in a rule image correspond to high probabilities of pixels belonging to the class that the rule image represents. Probability maps for each of the special habitat types (see Figure 6:3) were derived using the rule images that were produced from the supervised classifications of each image which resulted in the highest overall accuracies. The band statistics were calculated and from these the range of values in each of the rule images was attained. This information was used to create Regions Of Interest (ROIs) that represented the highest (= < 1%) of the total range of values.

Probability mapping was applied to the habitats that are of particular interest to conservation management as illustrated in Figure 6:3. Confusion matrices were produced for those classifications that produced the best overall accuracy results for each image using all 22 habitats. The statistics generated for the confusion matrices are described in Section 6.2.3 and the codes per habitat type are listed below in Table 6:6.

Table 6:6 Codes used in confusion matrices (Special habitats in bold)

Class	Code
Unclassified	Uncl.
Carex lasiocarpa	**Cl**
Carex rostrata-Equisetum fluviatile swamp	Cr-Ef
Deep Water Swamp	DWS
Dense *Deschampsia cespitosa*:	**DDc**
Dry grassland	Dg'land
Fen meadow	Fen med
Mixed sedge	MS
Molinia caerulea-Myrica gale mire	Mc-Mg
Molinia caerulea-sedge mire	Mc-sedge
Phalaris arundinacea	**Pa**
Pine plantation	Pine
Reedbed	**Reed**
Ruderal	Rud
Rush pasture/Grassland	Rp/g'land
Species-poor tall sedge (*Carex aquatilis*)	**Sp-poor1**
Species-poor tall sedge (*C. aqua*)/Mixed sedge	Sp-poor2
Species-poor tall sedge (*C. vesicaria*)	Sp-poor3
Species-rich low sedge mire	Sp-rich1
Species-rich low sedge mire/Rush pasture/grassland	Sp-rich2
Species-rich low sedge mire/Species-poor tall sedge (*C. vesic.*)	Sp-rich3
***Sphagnum* lawn**	**Sphag1**
***Sphagnum* lawn/Mixed sedge swamp**	**Sphag2**
Water	**Water**
Woodland/scrub	**W/s**

Spectral Feature Fitting

Spectral Feature Fitting (SFF) is used to compare the fit of image spectra to selected reference spectral features; in this way it is comparable to continuum removal (Chapter 4). The method uses a least-squares technique and is based on information regarding the absorption features within both the reference and image spectra. Using 'Multi Range' SFF options (in RSI ENVI 4.1), multiple absorption features can be used. The spectral subsets applied here include the absorption feature in the blue region and that in the red region (CASI Bands 1-3 and 3-10 respectively). The header files were edited accordingly so that each Band Number was converted into wavelength (nm) (See Table 6:7). This method was applied to both images (CASI 91 and CASI 101) using spectral features derived from *a priori* habitat types and grouped habitat types (see Figure 6:4 and Figure 6:5 respectively) (Maier & Cowie 2002). An

output classification-like image was produced for each of these analyses and, in the same way as for the Maximum Likelihood analyses, overall classification accuracies were obtained.

Table 6:7 CASI band centres and band widths

CASI Band Number	Band Centre (nm)	Band Width (from centre) (nm)
1	449.96	10.41
2	490.13	11.41
3	552.23	5.82
4	608.12	6.80
5	651.9	6.82
6	671.93	3.96
7	700.59	5.88
8	711.11	4.93
9	739.83	6.85
10	750.37	3.97
11	762.83	3.02
12	780.09	6.85
13	819.42	5.90
14	865.48	5.90
15	942.16	5.89

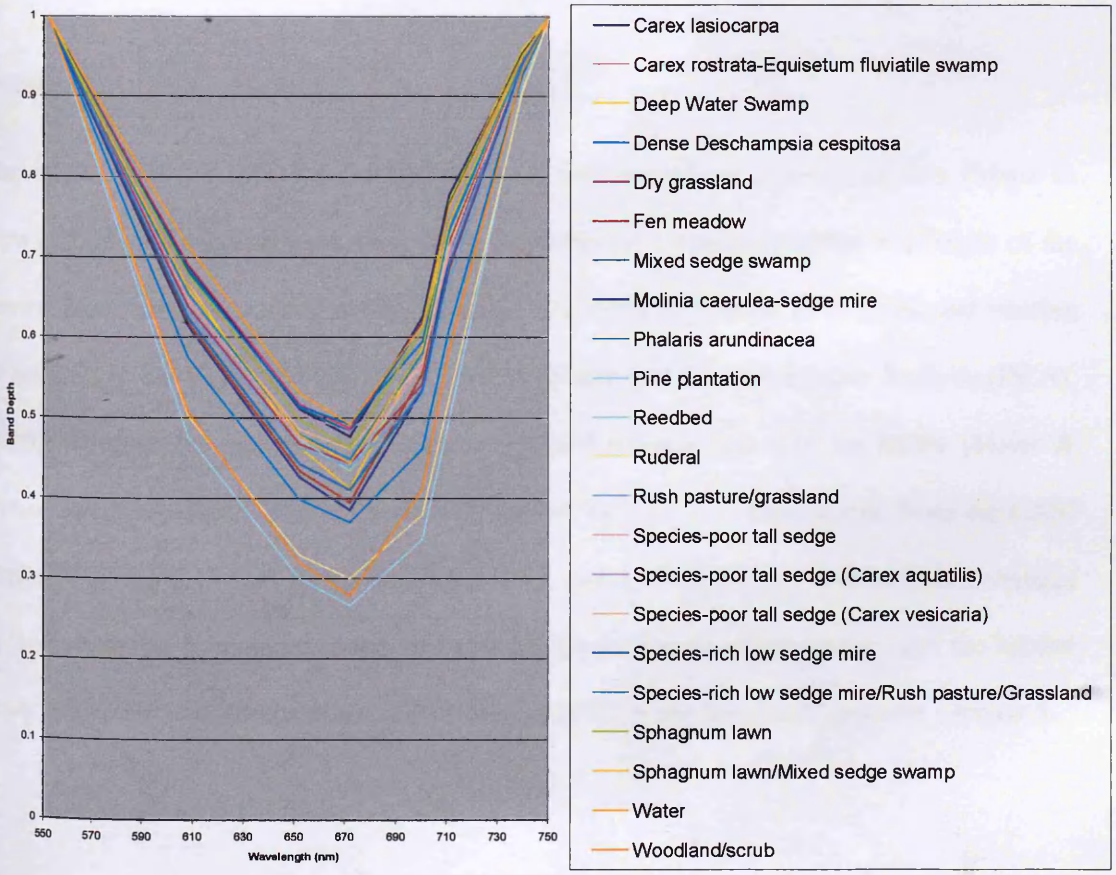

Figure 6:4 CASI 91: Red absorption feature (Continuum removed) -All habitat types

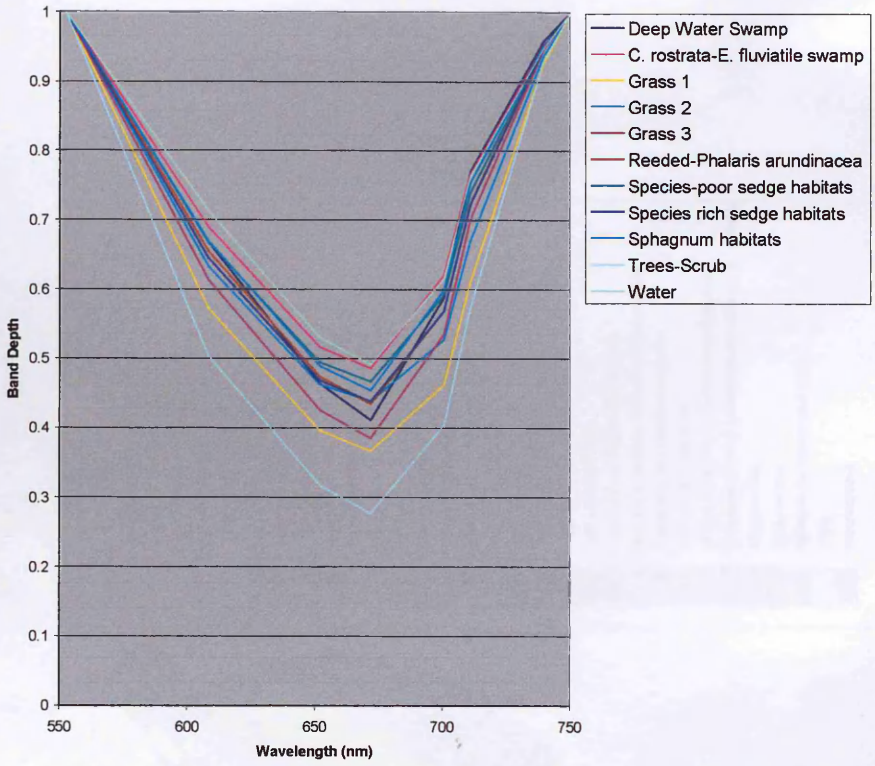

Figure 6:5 CASI91: Red absorption feature (Continuum removed) – Grouped habitat types

Transects

The information gathered for the vegetation survey carried out at Insh Marshes (Maier & Cowie 2002) included detailed work along a number of transects spanning the length of the marsh. Five transects that fell within the study area were chosen for their length and number of quadrats to carry out the multivariate analysis Detrended Correspondence Analysis (DCA). Detailed vegetation survey data (species composition) were provided by RSPB (Maier & Cowie 2002) and these sample points were paired with spectral data derived from the CASI imagery. Tables D3 to D7 in Appendix D list the points along the transects at which changes in the vegetation cover were noted and also details the nature of the change and the habitat types associated with the samples. The principles of DCA are described further in Chapter 5.

6.2.4 Transects: DCA and CCA

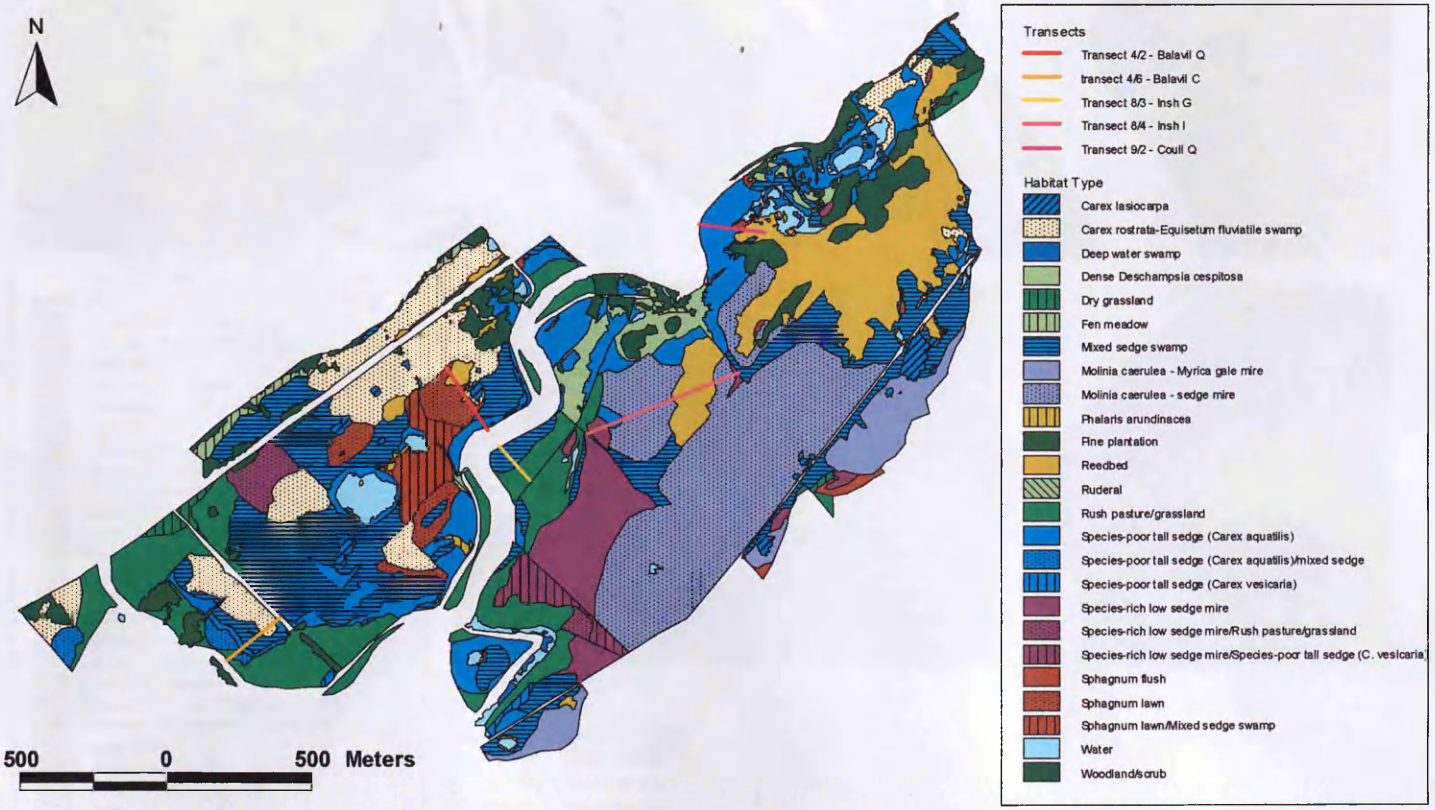

Figure 6:6 Location of transects analysed using spectral data collected from CASI imagery

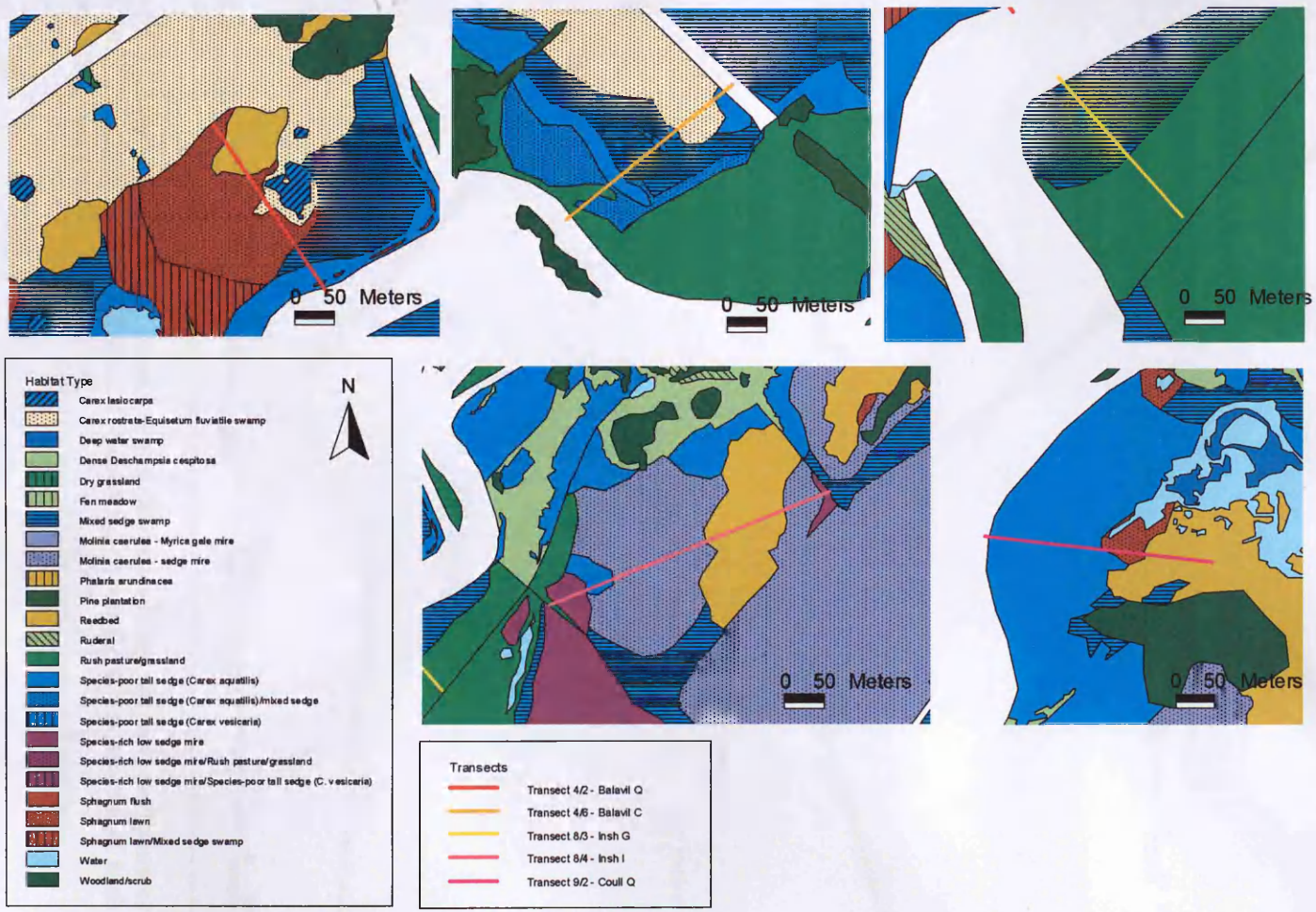

Figure 6:7 Habitats along transects analysed using spectral data collected from CASI imagery

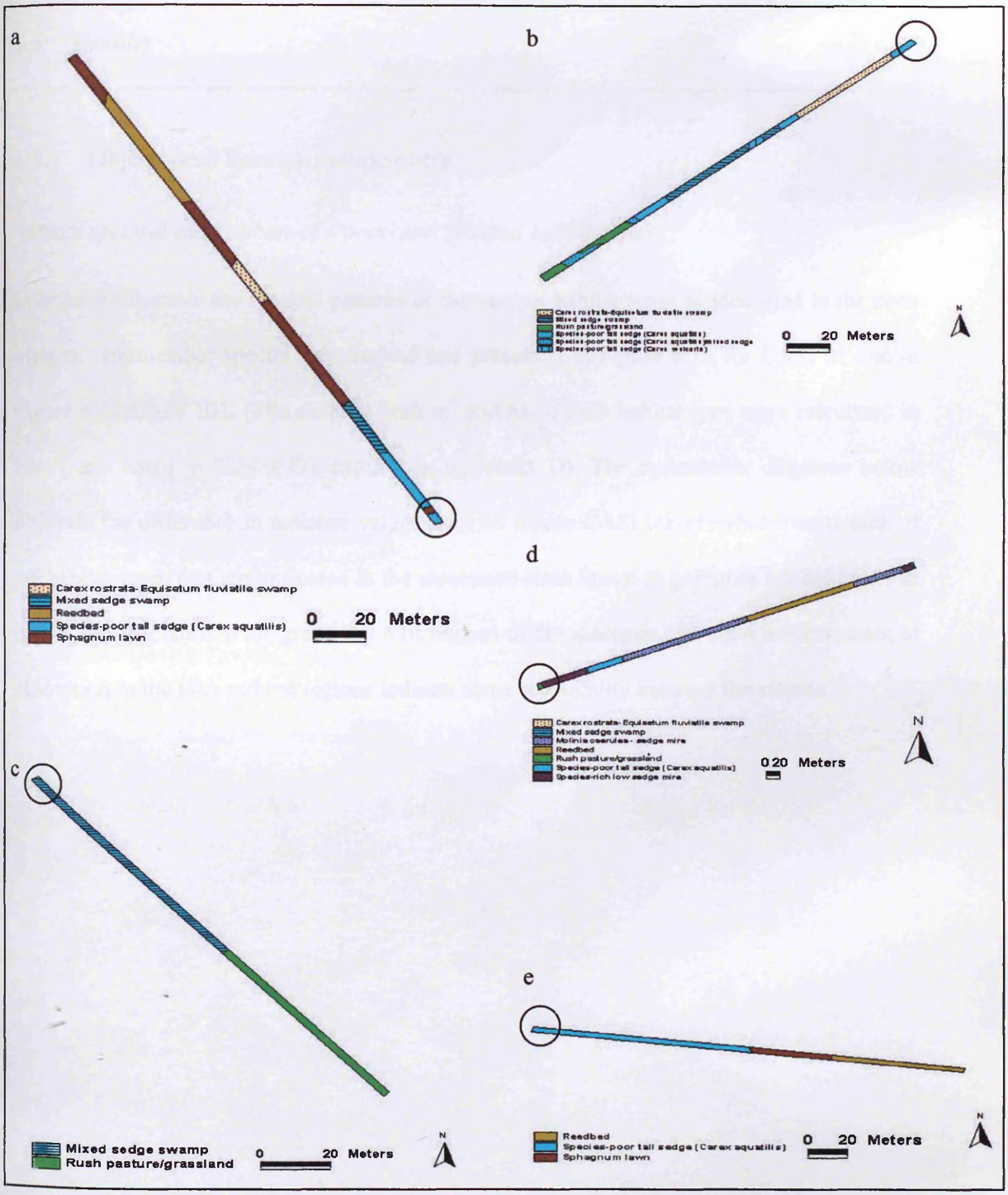

Figure 6:8 Habitat changes along transects a-e (Start positions circled) (a Transect 4.2: Balavil Q; b Transect 4.6: Balavil C; c Transect 8.3: Insh G; d Transect 8.4: Insh I; e Transect 9.2: Coull Q)

6.3.1 Objective a) Spectral endmembers

Identify spectral endmembers of a priori *and grouped habitat types.*

In order to illustrate the spectral patterns of the various habitat types as identified in the class images, 'endmember spectra' are derived and presented in Figure 6:10 for CASI 91 and in Figure 6:12 CASI 101. (The areas in both m^2 and ha of each habitat type were calculated in ENVI and listed in Tables D1 and D2 in Appendix D). The endmember diagrams below illustrate the difference in radiance values from all fifteen CASI wavebands between each of the habitat types that are presented in the associated class image (e.g. Figure 6:9 below). The degree of reflectance in the green and NIR regions of the spectrum and the relative amount of absorption in the blue and red regions indicate some separability between the classes.

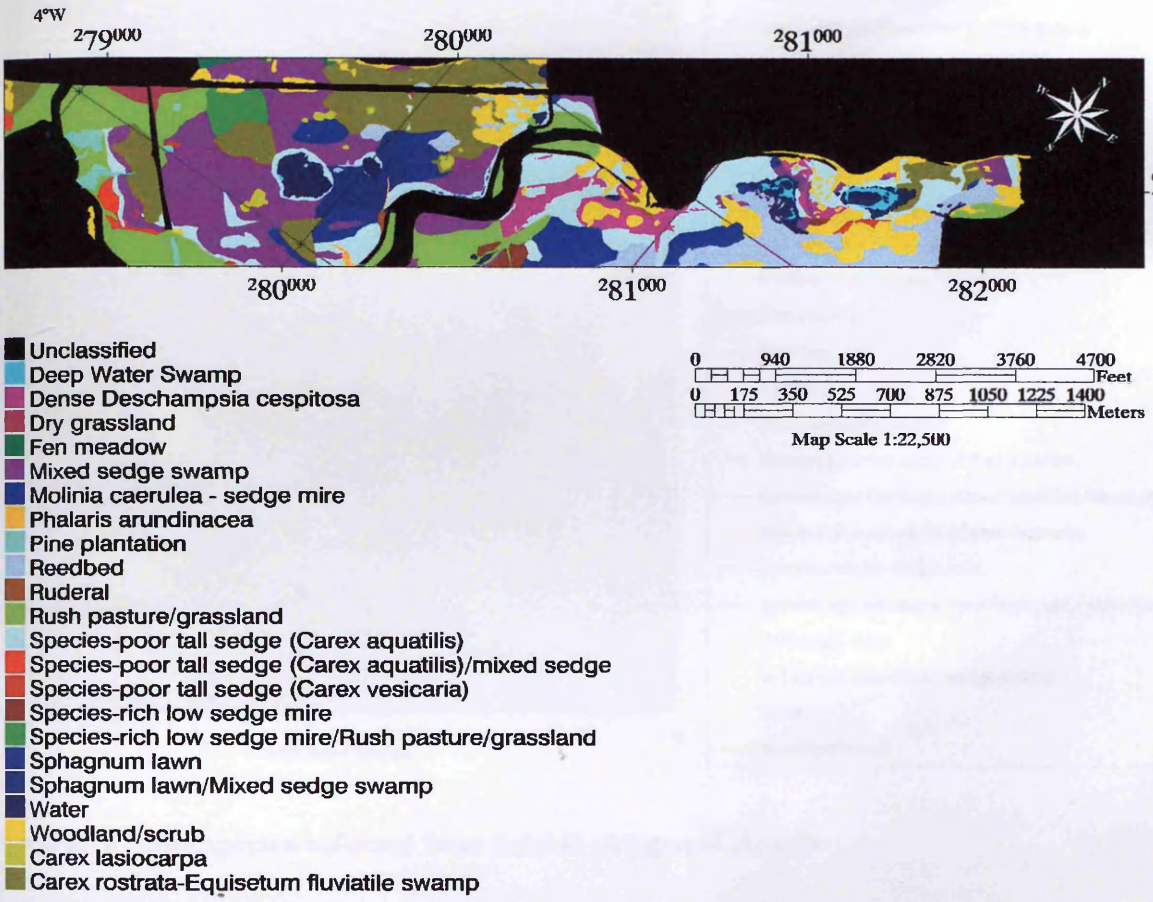

Figure 6:9 CASI 91: All habitat classes

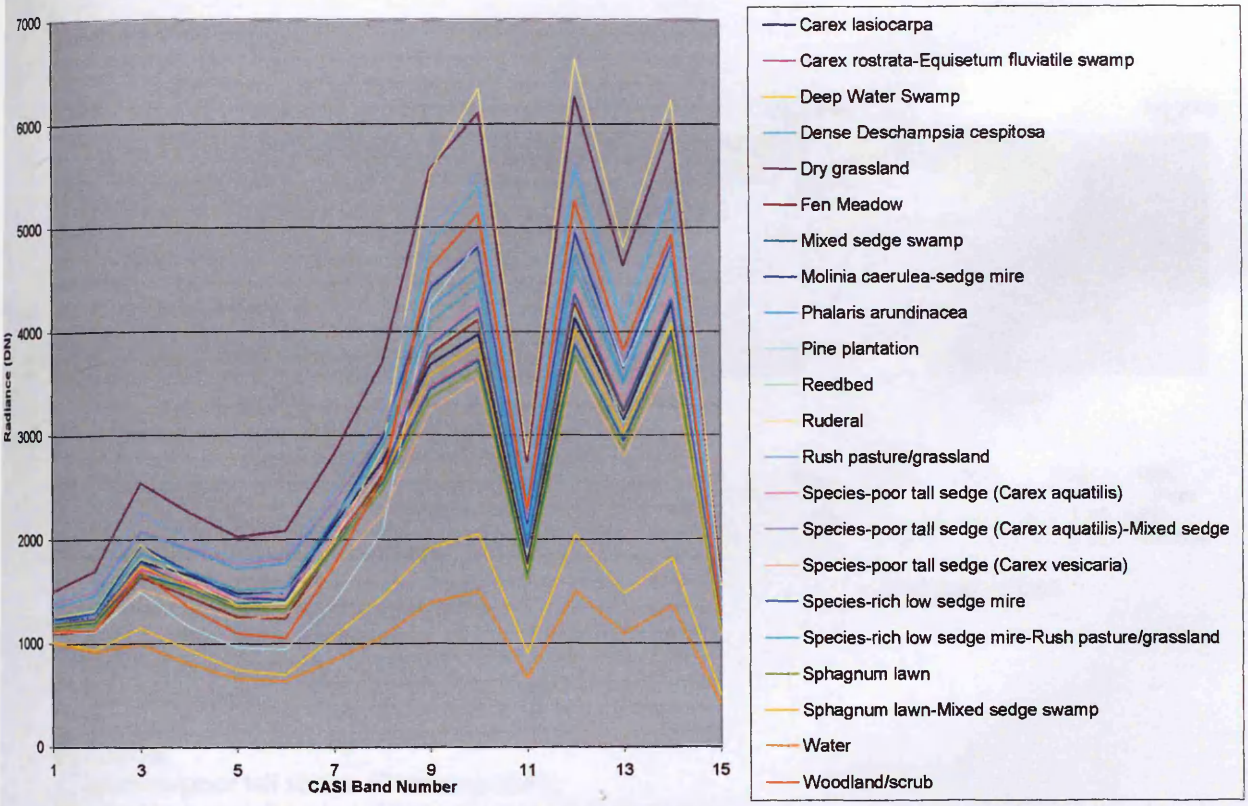

Figure 6:10 Mean spectra collected from habitat polygons-CASI 91

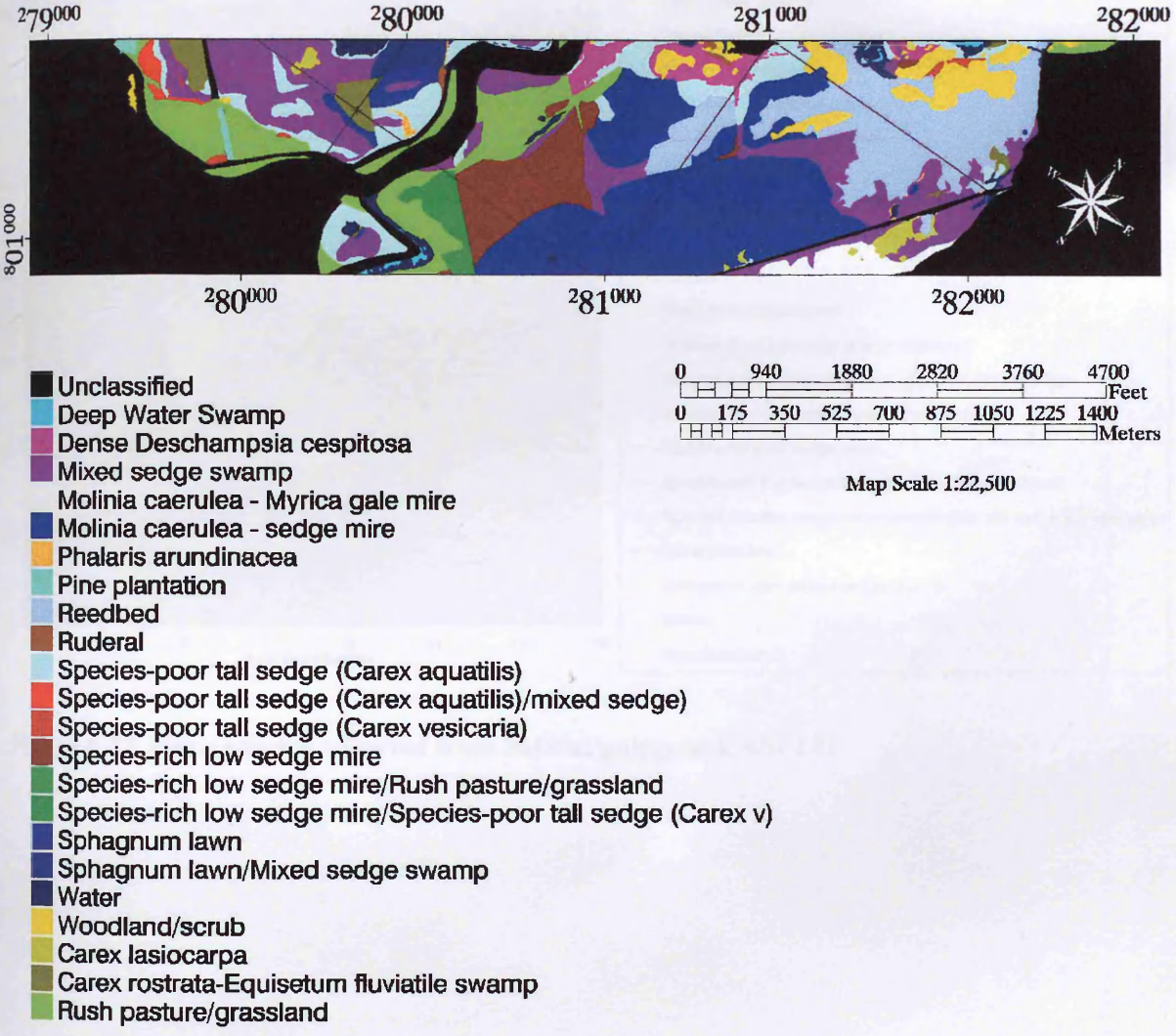

Figure 6:11 CASI 101:All habitat classes

Images were derived to create grouped habitat types based on species composition and functionality of the *a priori* habitat types and classifications were also carried out on these. This reduced the number of classes in each image from 22 to 11. The group names and habitats that they are made up of are listed below in Table 6:8 along with the respective areas within both images. Figure 6:13 and Figure 6:15 show the respective areas of Insh Marshes that represent the newly grouped habitat types. In addition, the endmember spectra associated with each newly grouped habitat type from both images are illustrated in Figure 6:14 and (CASI 91) and Figure 6:16 (CASI 101).

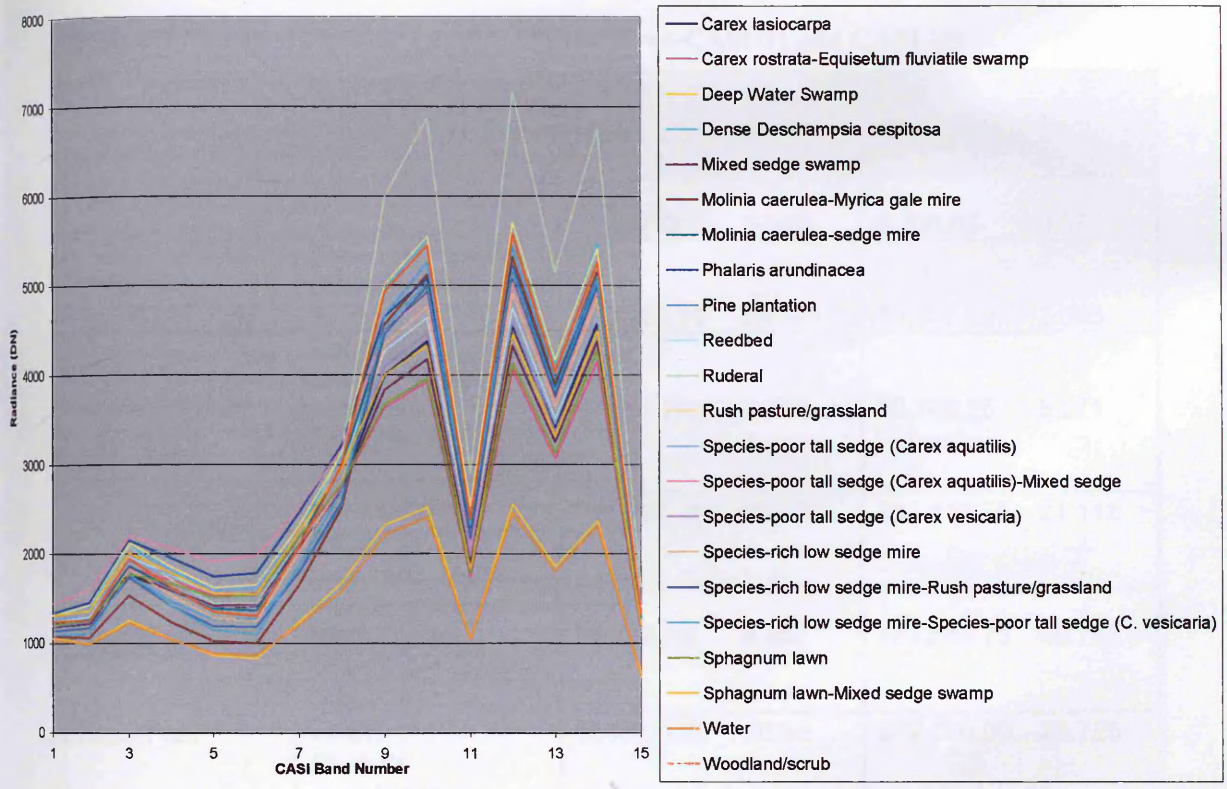

Figure 6:12 Mean spectra collected from habitat polygons-CASI 101

Table 6:8 Grouped Habitat Types (x11) and Area-CASI 91 and CASI 101

GroupedHabitat Type	Original Habitat Types	CASI91		CASI101	
		Meters²	Hectares	Meters²	Hectares
Deep Water Swamp	Deep Water Swamp	11,987.50	1.199	5,700.00	0.57
Carex rostrata-Equiesetum fluviatile swamp	*Carex rostrata-Equiesetum fluviatile* swamp	260,425.00	26.043	35,950.00	3.595
Grass1	Dense *Deschampsia cespitosa* Fen meadow Ruderal	77,981.25	7.798	52,706.25	5.271
Grass2	Dry Grassland Rush pasture/Grassland	251,706.25	25.171	211,118.75	21.112
Grass3	*Molinia caerulea-Myrica gale* *Molinia caerulea*-sedge mire	64,568.75	6.457	487,568.75	48.757
Reed-Phal	Reedbed *Phalaris arundinacea*	164,400.00	16.44	287,250.00	28.725
Sp-poor	Species-poor tall sedge (*Carex aquatilis*) Species-poor tall sedge (*Carex aquatilis*)/mixed sedge Species-poor tall sedge (*Carex vesicaria*) *Carex lasiocarpa* Mixed Sedge	645,250.00	64.525	516,650.00	51.665
Sp-rich	Species-rich low sedge mire Species-rich low sedge mire/Rush pasture/grassland Species-rich low sedge mire/Species-poor tall sedge (*Carex vesicaria*)	41,181.25	4.118	155,581.25	15.558
Sphag	Sphagnum lawn Sphagnum lawn/Mixed sedge swamp	117,206.25	11.721	48,500.00	4.85
Trees-Scrub	Woodland/scrub Pine plantation	213,437.50	21.344	99,875.00	9.988
Water	Water	66,912.50	6.691	40,168.75	4.017

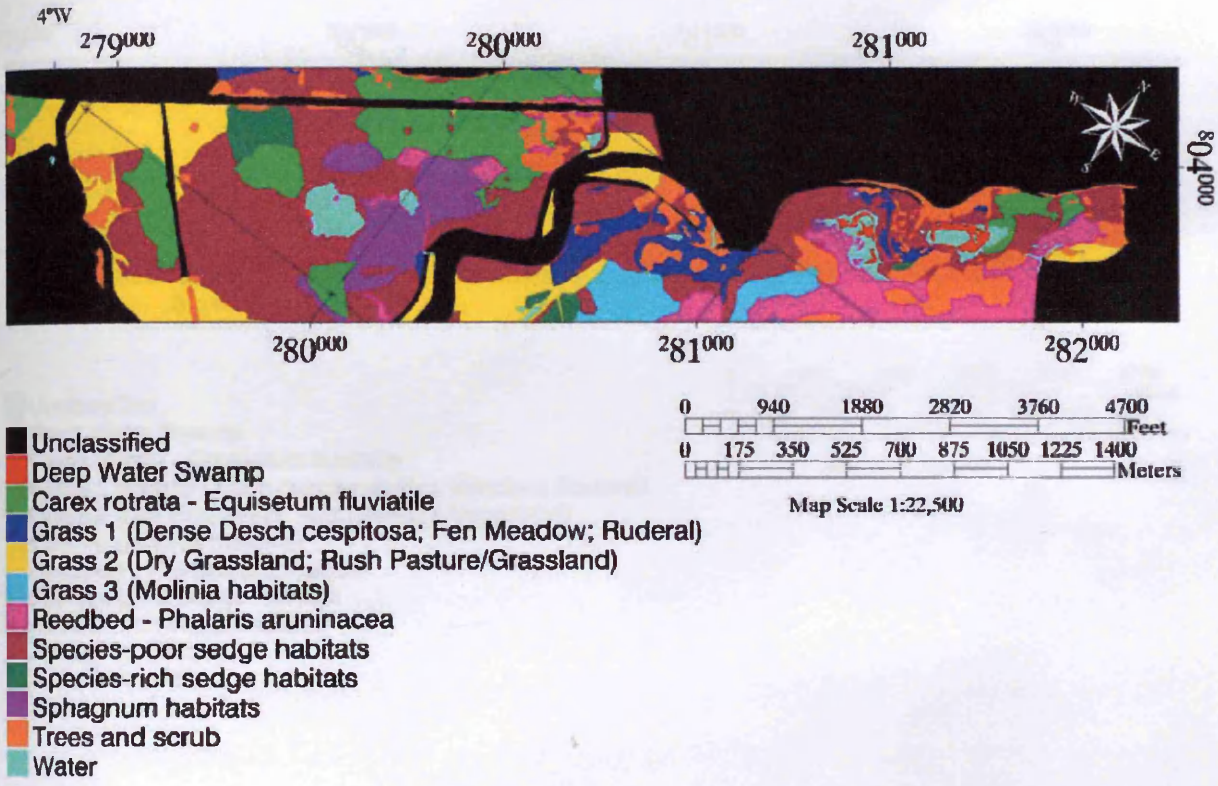

Figure 6:13 CASI 91-Grouped habitat types

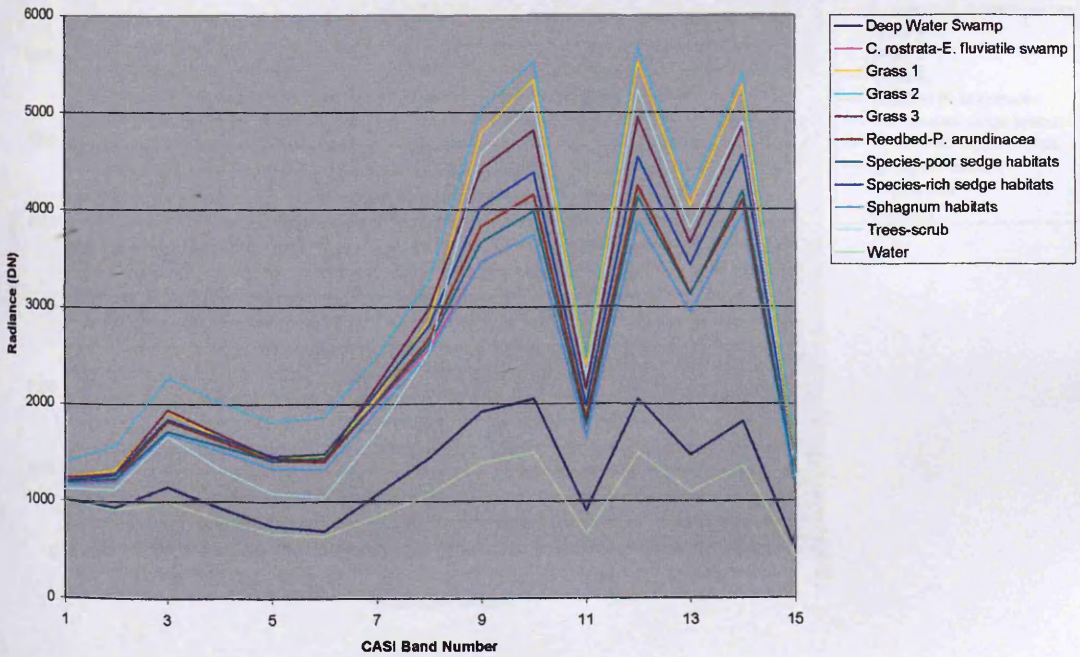

Figure 6:14 Spectral 'Endmembers' from Grouped Habitat Types-CASI 91

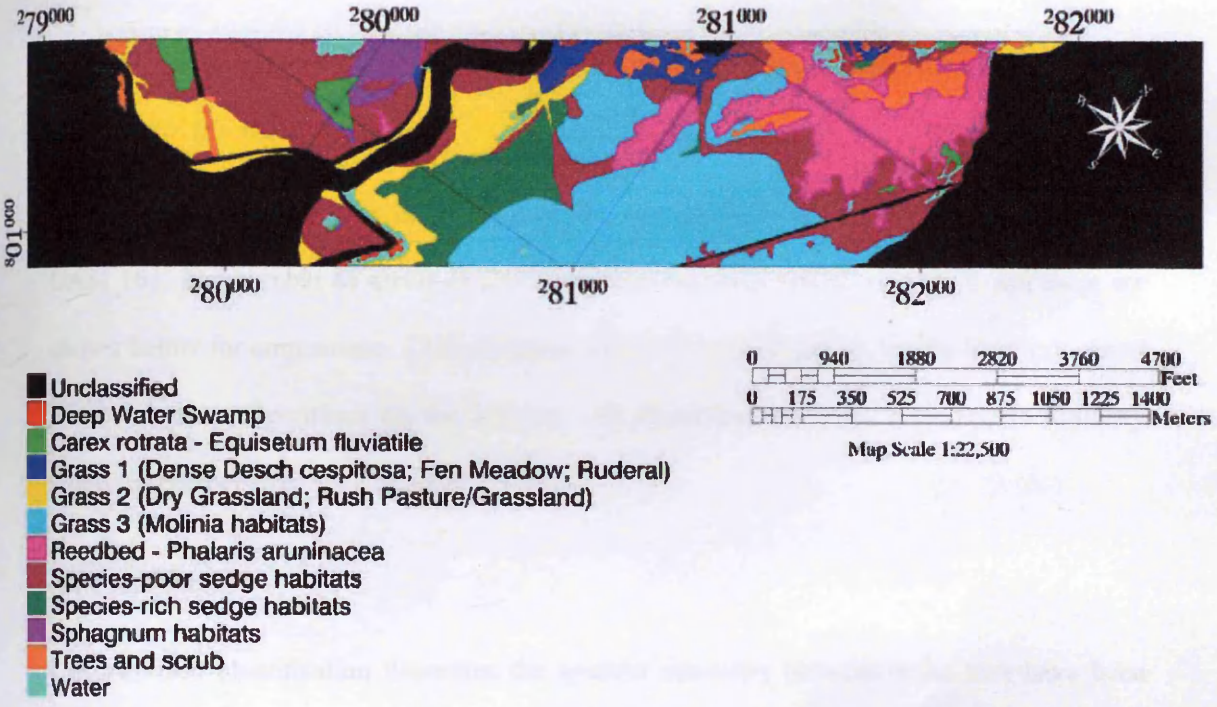

Figure 6:15 CASI I01-Grouped habitat types

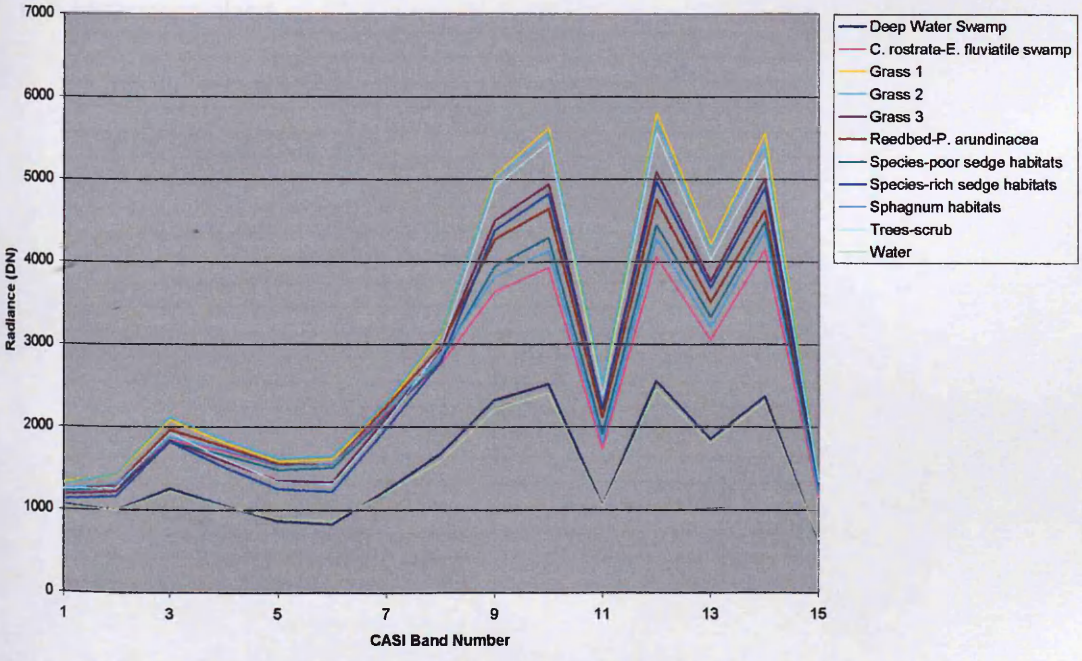

Figure 6:16 Spectra 'Endmembers' from Grouped Habitat Types-CASI 101

6.3.2 Objective b) Unsupervised Classification

Explore the spectral variation within the available imagery using unsupervised classifications and various spectral indices.

K-Means Classification was carried out on the raw spectral images for both CASI 91 and CASI 101. The number of specified classes for each analysis was 6, 11 and 22 and these are shown below for comparison. Classifications were also carried out on results from calculated spectral indices algorithms on the imagery. All classifications were subjected to Majority Analyses (kernel size: 5 x 5 pixels).

All CASI bands

Unsupervised classification illustrates the spectral similarity between areas that have been identified as different habitat types using traditional survey methods as well as within-habitat type heterogeneity. The results shown in Table 6:9 and Table 6:10 for CASI 91 and CASI 101 respectively suggest that two distinctly spectral regions are identifiable; these are water and rush pasture/grassland.

Table 6:9a Unsupervised clustering CASI 91 (35 clusters) (first 27 clusters)

Cluster class	Proportion of total area (%)	Most abundant habitat type	Second most abundant habitat type
1	9.31	Water	Carex rostrata-Equisetum fluviatile swamp
2	1.11	Mixed sedge swamp	Carex rostrata-Equisetum fluviatile swamp
3	1.50	Mixed sedge swamp	Carex rostrata-Equisetum fluviatile swamp
4	1.58	Mixed sedge swamp	Carex rostrata-Equisetum fluviatile swamp
5	1.97	Mixed sedge swamp	Carex rostrata-Equisetum fluviatile swamp
6	2.61	Mixed sedge swamp	Carex rostrata-Equisetum fluviatile swamp
7	2.53	Mixed sedge swamp	Carex rostrata-Equisetum fluviatile swamp
8	3.15	Mixed sedge swamp	Carex rostrata-Equisetum fluviatile swamp
9	3.21	Mixed sedge swamp	Carex rostrata-Equisetum fluviatile swamp
10	3.12	Mixed sedge swamp	Carex rostrata-Equisetum fluviatile swamp
11	3.71	Mixed sedge swamp	Carex rostrata-Equisetum fluviatile swamp
12	3.26	Mixed sedge swamp	Carex rostrata-Equisetum fluviatile swamp
13	3.05	Mixed sedge swamp	Species-poor tall sedge (Carex aquatilis)
14	3.22	Mixed sedge swamp	Carex rostrata-Equisetum fluviatile swamp
15	2.98	Mixed sedge swamp	Carex rostrata-Equisetum fluviatile swamp
16	2.84	Mixed sedge swamp	Carex rostrata-Equisetum fluviatile swamp
17	2.38	Mixed sedge swamp	Carex rostrata-Equisetum fluviatile swamp
18	2.97	Mixed sedge swamp	Carex rostrata-Equisetum fluviatile swamp
19	2.57	Mixed sedge swamp	Species-poor tall sedge (Carex aquatilis)
20	2.67	Species-poor tall sedge (Carex aquatilis)	Mixed sedge swamp
21	2.36	Species-poor tall sedge (Carex aquatilis)	Mixed sedge swamp
22	2.46	Species-poor tall sedge (Carex aquatilis)	Reedbed
23	2.23	Species-poor tall sedge (Carex aquatilis)	Reedbed
24	2.12	Carex rostrata-Equisetum fluviatile swamp	Species-poor tall sedge (Carex aquatilis)
25	2.10	Species-poor tall sedge (Carex aquatilis)	Reedbed
26	1.93	Woodland/scrub	Species-poor tall sedge (Carex aquatilis)

Table 6.9b Unsupervised clustering CASI 91 (35 clusters) (cont.)

Cluster class	Proportion of total area (%)	Most abundant habitat type	Second most abundant habitat type
27	1.87	Woodland/scrub	Rush pasture/grassland
28	1.65	Woodland/scrub	Species-poor tall sedge (Carex aquatilis)
29	1.73	Woodland/scrub	Species-poor tall sedge (Carex aquatilis)
30	1.64	Species-poor tall sedge (Carex aquatilis)	Woodland/scrub
31	1.63	Rush pasture/grassland	Woodland/scrub
32	1.46	Rush pasture/grassland	Species-poor tall sedge (Carex aquatilis)
33	1.36	Rush pasture/grassland	Species-poor tall sedge (Carex aquatilis)
34	1.28	Rush pasture/grassland	Species-poor tall sedge (Carex aquatilis)
35	14.46	Rush pasture/grassland	Woodland/scrub

The CASI 91 results show the spectral dissimilarity of a class that is best interpreted as the location of water and deep water swamp at the site and classified in red in Figure 6:17 a), b) and c). There are exceptions to this however, most notably, the pine plantation area to the west of the site. Another class that appears to be clearly distinct is best interpreted as habitat types with high spectral responses in the green and NIR parts of the spectrum; these include the rush pasture and dry grassland habitats along with the trees and scrub areas (highlighted in pink). Wet habitat types such as the *Sphagnum*, *Carex aquatilis* and *Equisetum* dominated habitats appear to be associated with each other but this is illustrated more clearly in Figure 6:17 a) where bright green and blue areas are highlighted. Other classes in this map are highlighted in turquoise and yellow and these areas are mostly associated with *Molinia* dominated habitat types although this interpretation is more ambiguous to the far east of the site.

Table 6:10 Unsupervised clustering CASI 101 (35 clusters)

Cluster class	Proportion of total area (%)	Most abundant habitat type	Second most abundant habitat type
1	10.97	Mixed sedge swamp	Water
2	1.36	Mixed sedge swamp	Species-poor tall sedge (Carex aquatilis)
3	1.54	Mixed sedge swamp	Species-poor tall sedge (Carex aquatilis)
4	1.55	Mixed sedge swamp	Species-poor tall sedge (Carex aquatilis)
5	1.52	Mixed sedge swamp	Reedbed
6	1.59	Mixed sedge swamp	Reedbed
7	1.75	Mixed sedge swamp	Reedbed
8	1.72	Mixed sedge swamp	Reedbed
9	2.13	Mixed sedge swamp	Molinia caerulea - sedge mire
10	2.13	Molinia caerulea - sedge mire	Mixed sedge swamp
11	2.15	Mixed sedge swamp	Reedbed
12	2.67	Molinia caerulea - sedge mire	Mixed sedge swamp
13	2.67	Molinia caerulea - sedge mire	Mixed sedge swamp
14	2.93	Molinia caerulea - sedge mire	Mixed sedge swamp
15	2.93	Molinia caerulea - sedge mire	Mixed sedge swamp
16	3.16	Molinia caerulea - sedge mire	Reedbed
17	3.57	Molinia caerulea - sedge mire	Reedbed
18	3.57	Molinia caerulea - sedge mire	Mixed sedge swamp
19	3.24	Molinia caerulea - sedge mire	Reedbed
20	3.15	Molinia caerulea - sedge mire	Reedbed
21	3.32	Molinia caerulea - sedge mire	Reedbed
22	3.29	Molinia caerulea - sedge mire	Reedbed
23	2.94	Molinia caerulea - sedge mire	Reedbed
24	2.83	Molinia caerulea - sedge mire	Reedbed
25	2.64	Molinia caerulea - sedge mire	Reedbed
26	2.23	Molinia caerulea - sedge mire	Reedbed
27	2.22	Molinia caerulea - sedge mire	Reedbed
28	1.97	Molinia caerulea - sedge mire	Reedbed
29	1.86	Molinia caerulea - sedge mire	Reedbed
30	1.93	Molinia caerulea - sedge mire	Reedbed
31	1.71	Molinia caerulea - sedge mire	Reedbed
32	1.48	Molinia caerulea - sedge mire	Rush pasture/grassland
33	1.36	Molinia caerulea - sedge mire	Rush pasture/grassland
34	1.33	Molinia caerulea - sedge mire	Rush pasture/grassland
35	12.60	Rush pasture/grassland	Woodland/scrub

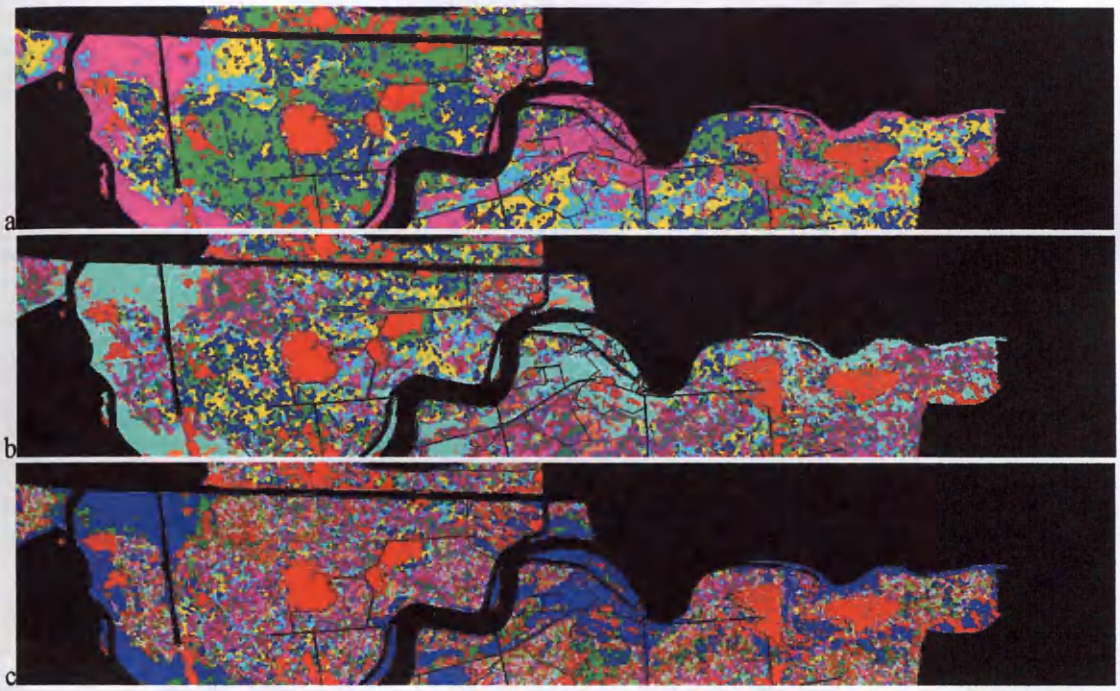

Figure 6:17 CASI 91 K-Means Classifications and water features and habitat boundaries overlays a) 6 classes b) 11 habitats c) 22 habitats.

Unsupervised classification on the CASI 101 image produced results that could be interpreted in a similar way as those produced for CASI 91. Figure 6:18 a) illustrates six classes where once again the pink class is best interpreted as the rush pasture and woodland/scrub dominated areas with the turquoise areas being highly associated. The wetter, *Sphagnum* and *Carex aquatilis* dominated areas are highlighted in red although there is also a high degree of association between these areas and those highlighted in green. The remaining classes, highlighted in blue and yellow appear to be associated with *Molinia* dominated habitats.

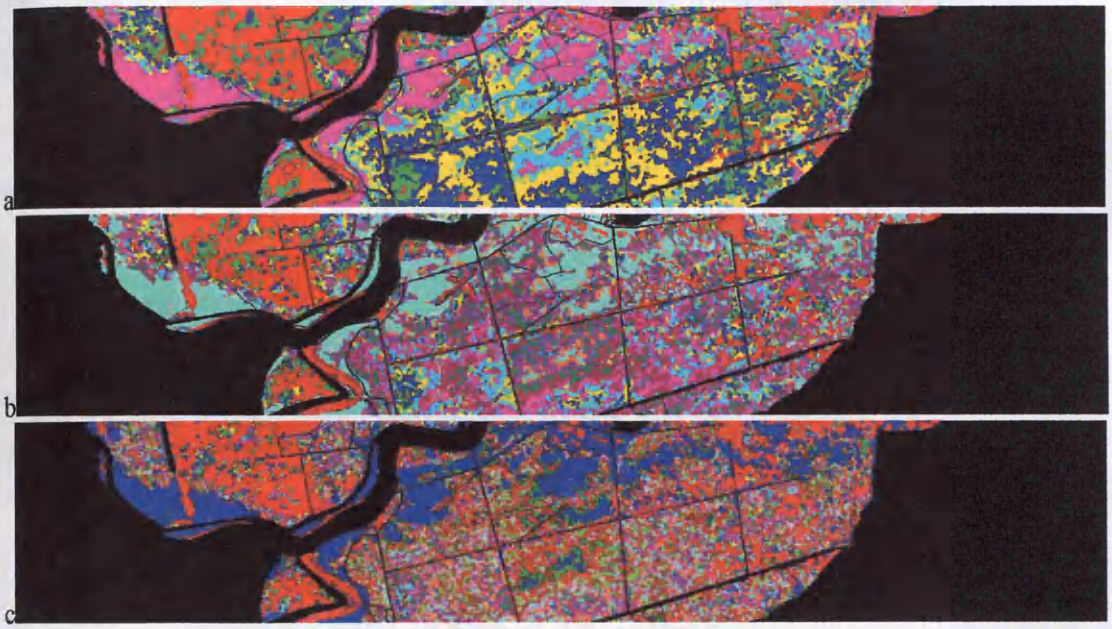

Figure 6:18 CASI 101 K-Means Classifications and water features and habitat boundaries overlays a) 6 classes b) 11 habitats c) 22 habitats.

NDVI

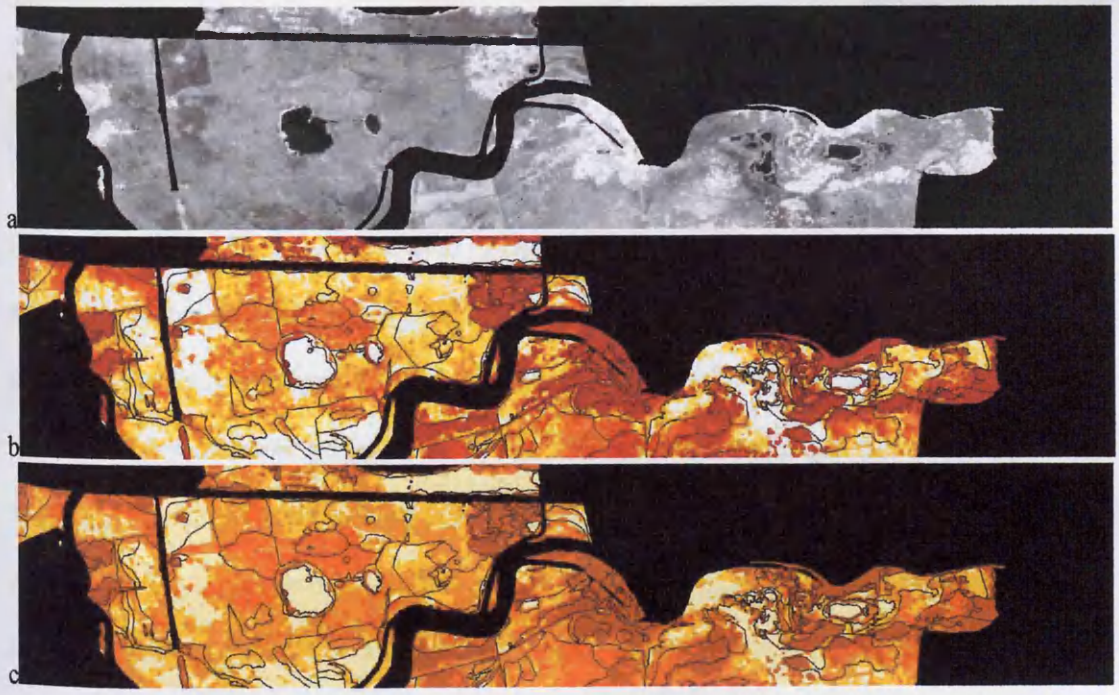

Figure 6:19 CASI 91: NDVI values a) Raw Results (bright pixels=higher NDVI) b) Results grouped via K-Means Classification into 15 classes c) Results grouped via K-Means Classification into 5 classes (White-Red = Low-High NDVI) (NB b) and c) overlay: All habitat type boundaries)

Figure 6:19 and Figure 6:20 illustrate the pattern of NDVI across the site and how this pattern relates with habitat boundaries. Areas highlighted by bright pixels (Figure 6:19 a) and Figure 6:20 a)) or red (Figure 6:19 b) and c) and Figure 6:20 b) and c)) represent areas with the greatest values of NDVI.

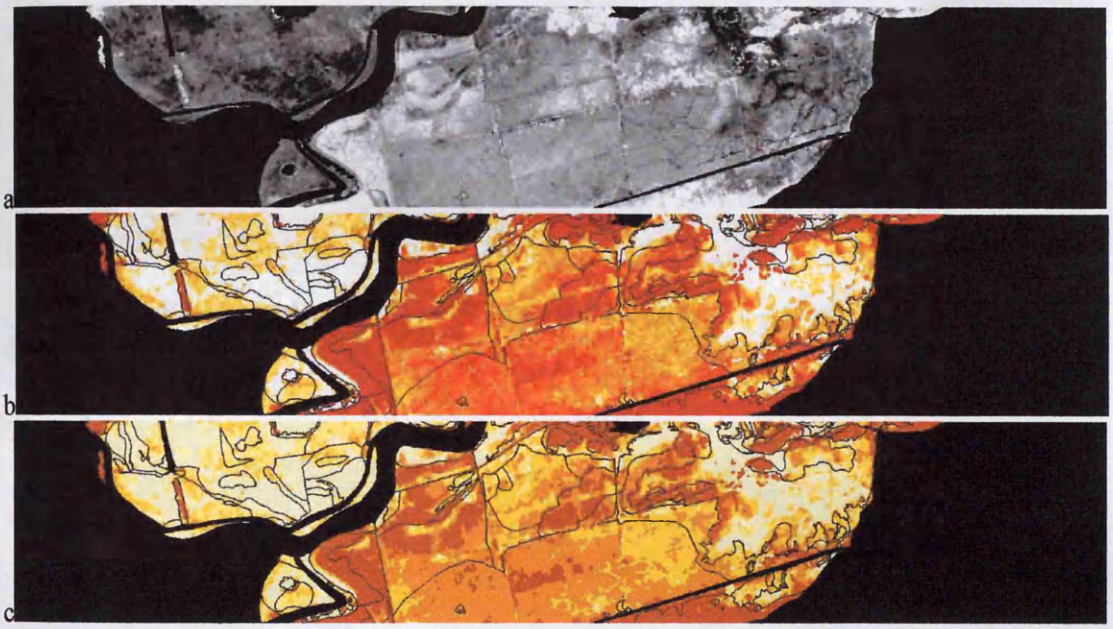

Figure 6:20 CASI 101: NDVI values a) Raw Results (bright pixels=higher NDVI) b) Results grouped via K-Means Classification into 15 classes c) Results grouped via K-Means Classification into 5 classes (White-Red = Low-High NDVI) (NB b) and c) overlay: All habitat type boundaries)

NDVI results for CASI 91 illustrate quite clearly the effectiveness of this method for classifying woodland using an image collected in September, particularly, when 15 classes are applied to the analysis (Figure 6:19 b)). A large range of NDVI values are represented by rush pasture and dry grassland polygons as well as the reedbed polygon and, there also appears to be a large amount of heterogeneity associated with many habitat polygons. This is also the case for the CASI 101 imagery, however, this also effectively illustrates variation within a habitat type across management compartments (e.g. species rich low sedge mire).

Figure 6:21 Position of red edge calculated for CASI 91 a) Raw Results b) Results grouped via K-Means Classification into 10 classes

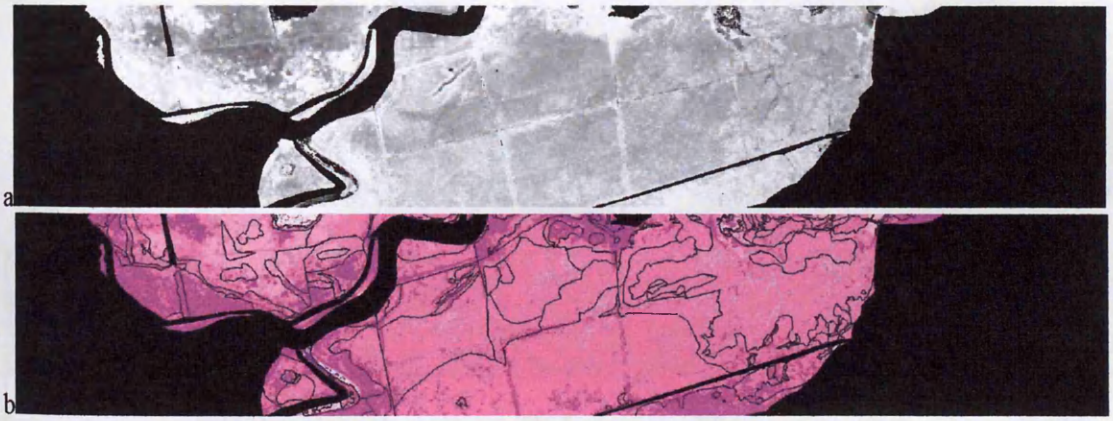

Figure 6:22 Position of red edge calculated for CASI 101 a) Raw Results b) Results grouped via K-Means Classification into 15 classes

The values of REIPs illustrated in Figure 6:21 and Figure 6:22 range from 710 nm to 730 nm. Woodland areas near the top and centre of the image are related to higher REIPs. This follows the same pattern of NDVI but there are some exceptions, such as the rush pasture at the top left of the image which shows high REIP values but low NDVI values.

6.3.3 Objective c) Supervised Classification

Assess the potential for supervised classification to correctly classify habitat types derived from field based a priori *habitat maps*

Maximum Likelihood Classification using all habitat classes (x22)

Overall accuracy results from supervised classification on both CASI 91 and CASI 101 are shown in Table 6:11. These range from 66.1% to 74.1% when all 22 habitats on each image are utilised in the training process. The best results for each image are attained when a stratified random method of identifying training sites is used although this improves overall accuracy by only a small percent in each case. When a spectral subset is applied and used in the classification process the best results attained are 55.6% and 61.6% for CASI 91 and CASI 101 respectively. These results are significantly less when compared with those achieved using all spectral bands.

Table 6:11 Overall Accuracy Results from Maximum Likelihood Classification-All Habitat Types (x22)

Image	Training Samples	All 15 CASI bands		Spectral Subset (Bands 1, 3, 6 and 12)	
		Overall Accuracy	Kappa coefficient	Overall Accuracy	Kappa coefficient
CASI 91	Equalized Random-x100 per Habitat Class	66.1	0.57	55.6	0.44
	Stratified Random-5% Total Habitat Class Area	67.5	0.58	54.9	0.43
CASI 101	Equalized Random-x100 per Habitat Class	71.2	0.63	58.4	0.47
	Stratified Random-5% Total Habitat Class Area	74.1	0.66	61.6	0.51

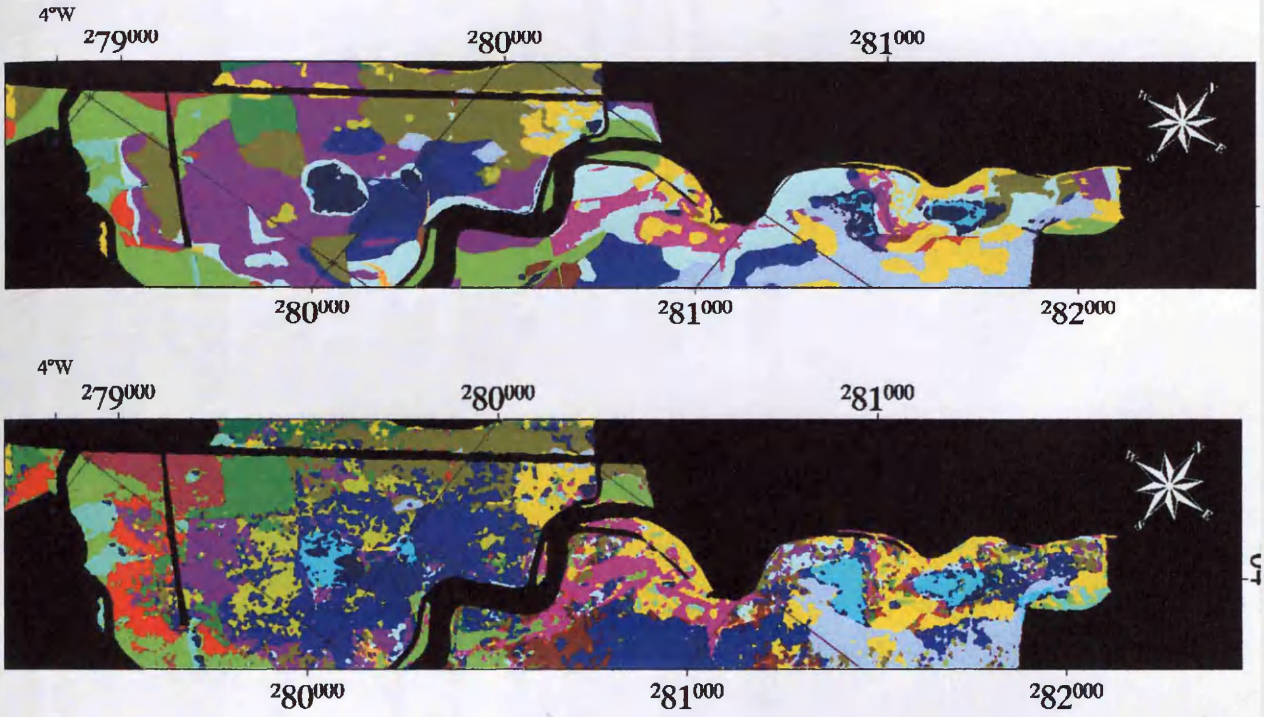

- Unclassified
- Deep Water Swamp
- Dense Deschampsia cespitosa
- Dry grassland
- Fen meadow
- Mixed sedge swamp
- Molinia caerulea - sedge mire
- Phalaris arundinacea
- Pine plantation
- Reedbed
- Ruderal
- Rush pasture/grassland
- Species-poor tall sedge (Carex aquatilis)
- Species-poor tall sedge (Carex aquatilis)/mixed sedge
- Species-poor tall sedge (Carex vesicaria)
- Species-rich low sedge mire
- Species-rich low sedge mire/Rush pasture/grassland
- Sphagnum lawn
- Sphagnum lawn/Mixed sedge swamp
- Water
- Woodland/scrub
- Carex lasiocarpa
- Carex rostrata-Equisetum fluviatile swamp

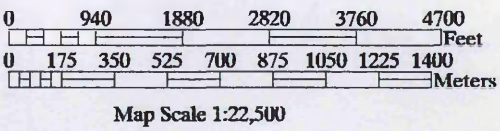

Map Scale 1:22,500

Figure 6:23 CASI 91: *A priori* habitats (x22) above and results from supervised classification-below (Stratified Random Training samples (Overall Accuracy: 67.5%))

Table 6:12a Information extracted from confusion matrix produced from most successful supervised classification on CASI 91 (First 12 classes)

Habitat	Producer Accuracy (%)	User Accuracy (%)	Error of Commission (%)			Error of Omission (%)		
			Overall (%)	Greatest indiv. Habitat (%)	Habitat	Overall (%)	Greatest indiv. Habitat (%)	Habitat
Unclassified	100	98.39	1.61	5.01	Dry grassland	0	0	-
Deep Water Swamp	82.43	16.33	83.67	57.51	Water	17.57	13.73	Water
Dense *Deschampsia cespitosa*	55.39	44.54	55.46	43	Ruderal	44.61	14.13	Woodland/scrub
Dry grassland	90.7	19.17	80.83	15.6	Rush pasture/Grassland	9.3	5.01	Unclassified
Fen meadow	71.13	14.02	85.98	4.44	Mixed sedge	28.87	8.89	Woodland/scrub
Mixed sedge	20.95	58.42	41.58	12.87	Species-poor tall sedge (*C. vesicaria*)	79.05	21.73	*Sphagnum* lawn
Molinia caerulea-sedge mire	82.9	38.42	61.58	11.29	Species-rich low sedge mire	17.1	11	Species-rich low sedge mire
Phalaris arundinacea	32.05	12.81	87.19	1.38	Species-poor tall sedge (*C. aquatilis*)	67.95	27.35	Rush pasture/Grassland
Pine plantation	93.06	40.94	59.06	7.67	Ruderal	6.94	2.45	Rush pasture/Grassland
Reedbed	53.56	75.72	24.28	11.45	Woodland/scrub	46.44	10.37	*Molinia caerulea*-sedge mire
Ruderal	7.17	20.19	79.81	0.97	Dense *Deschampsia cespitosa*	92.83	43	Dense *Deschampsia cespitosa*:
Rush pasture/Grassland	44.36	81.57	18.43	27.35	*Phalaris arundinacea*	55.64	15.6	Dry grassland

Table 12b Information extracted from confusion matrix produced from most successful supervised classification on CASI 91 (Last 11 classes)

Habitat	Producer Accuracy (%)	User Accuracy (%)	Error of Commission (%)			Error of Omission (%)		
			Overall (%)	Greatest indiv. Habitat (%)	Habitat	Overall (%)	Greatest indiv. Habitat (%)	Habitat
Species-poor tall sedge (*C. aquatilis*)	13.41	68.93	31.07	5.2	*Phalaris arundinacea*	86.59	11.31	Mixed sedge
Species-poor tall sedge (*C. aquatilis*)/Mixed sedge	73.59	14.39	85.61	11.84	Rush pasture/Grassland	26.41	6.11	Species-rich low sedge mire/Rush pasture/grassland
Species-poor tall sedge (*C. vesicaria*)	30.83	8.38	91.62	2.62	Species-poor tall sedge (*C. aquatilis*)	69.17	19.84	Woodland/scrub
Species-rich low sedge mire	65.24	14.54	85.46	11	*Molinia caerulea*-sedge mire	34.76	11.29	*Molinia caerulea*-sedge mire
Species-rich low sedge mire/Rush pasture/grassland	97.21	33.95	66.05	9.22	*Carex rostrata-Equisetum fluviatile* swamp	2.79	1.9	*Carex rostrata-Equisetum fluviatile* swamp
Sphagnum lawn	67.14	21.5	78.5	21.73	Mixed sedge	32.86	9.27	*Sphagnum* lawn/Mixed sedge swamp
Sphagnum lawn/Mixed sedge swamp	58.79	31.94	68.06	15.6	*Phalaris arundinacea*	41.21	18.74	*Sphagnum* lawn
Water	30.62	53.49	46.51	13.73	Deep Water Swamp	69.38	57.51	Deep Water Swamp
Woodland/scrub	58.84	59.09	40.91	19.84	Species-poor tall sedge (*C. vesicaria*)	41.16	11.45	Reedbed
Carex lasiocarpa	75.07	7.82	92.18	16.47	Mixed sedge	24.93	14.68	*Sphagnum* lawn
Carex rostrata-Equisetum fluviatile swamp	36.57	54.01	45.99	12.09	Mixed sedge	63.43	20.11	*Sphagnum* lawn

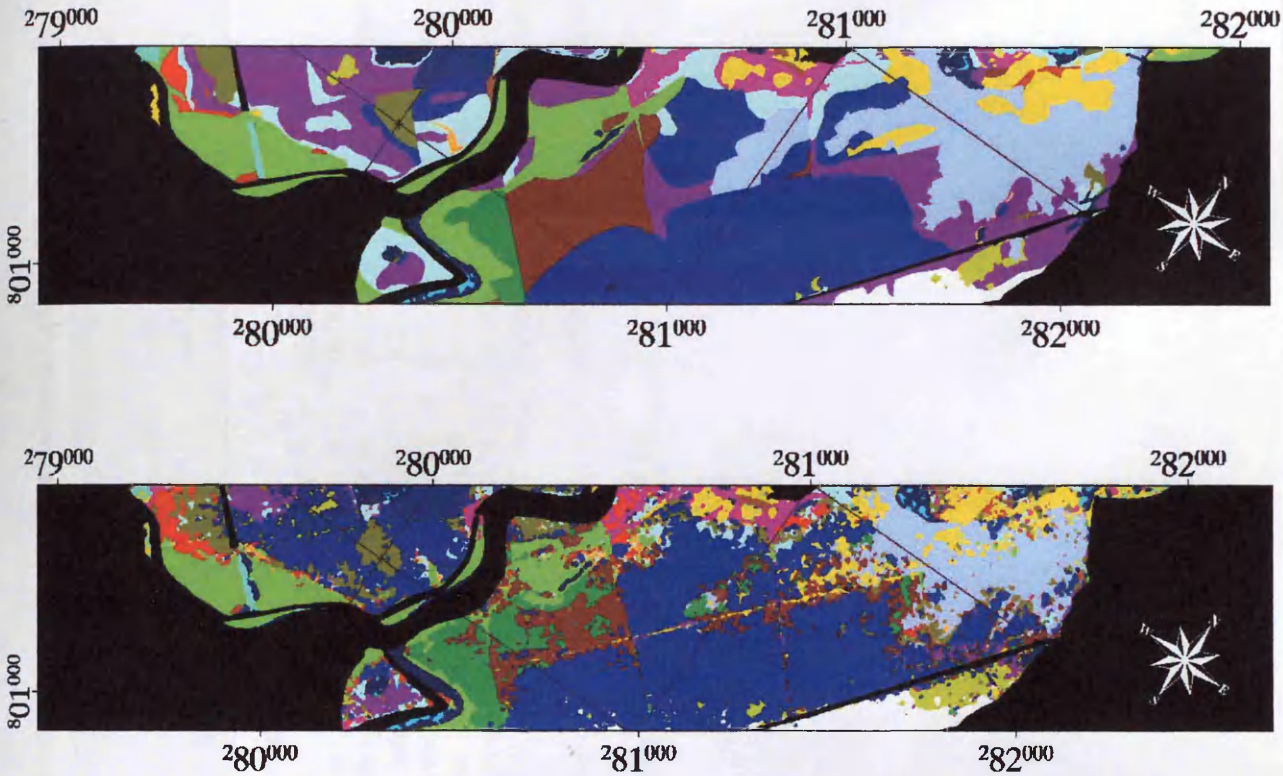

Figure 6:24 CASI 101: *A priori* habitats (x22) above and results from supervised classification below (Stratified Random Training samples (Overall Accuracy: 74.1%))

Table 6:13a Information extracted from confusion matrix produced from most successful supervised classification on CASI 101 (First 11 classes)

Habitat	Producer Accuracy (%)	User Accuracy (%)	Error of Commission (%)			Error of Omission (%)		
			Overall (%)	Greatest indiv. Habitat (%)	Habitat	Overall (%)	Greatest indiv. Habitat (%)	Habitat
Unclassified	100	98.79	1.21	7.09	Deep Water Swamp	0	0	-
Deep Water Swamp	42.29	24.7	75.3	10.29	Water	57.71	38.63	Water
Dense *Deschampsia cespitosa*:	42.72	49.34	50.66	32.45	Ruderal	57.28	16.09	Woodland/scrub
Mixed sedge	12.21	75.36	24.64	5.24	*Phalaris arundinacea*	87.79	19.22	*Molinia caerulea*-sedge mire
Molinia caerulea-Myrica gale mire	95.39	68.45	31.55	8.76	*Carex lasiocarpa*	4.61	2.34	*Carex lasiocarpa*
Molinia caerulea-sedge mire	87.87	73.15	26.85	19.22	Mixed sedge	12.13	3.82	Species-rich low sedge mire
Phalaris arundinacea	10.35	3.02	96.98	3.49	Ruderal	89.65	31.32	Rush pasture/Grassland
Pine plantation	69.16	45.67	54.33	2.11	Rush pasture/Grassland	30.84	10.95	Rush pasture/Grassland
Reedbed	52.82	81.13	18.87	24.02	Woodland/scrub	47.18	14.31	*Molinia caerulea*-sedge mire
Ruderal	33.61	29.79	70.21	3.61	Dense *Deschampsia cespitosa*:	66.39	32.45	Dense *Deschampsia cespitosa*
Species-poor tall sedge (*C. aquatilis*)	18.62	52.18	47.82	10.62	*Phalaris arundinacea*	81.38	21.51	*Sphagnum* lawn

Table 13b Information extracted from confusion matrix produced from most successful supervised classification on CASI 101 (Last 12 classes)

Habitat	Producer Accuracy (%)	User Accuracy (%)	Error of Commission (%)			Error of Omission (%)		
			Overall (%)	Greatest indiv. Habitat (%)	Habitat	Overall (%)	Greatest indiv. Habitat (%)	Habitat
Species-poor tall sedge (*C. aqua.*)/Mixed sedge	78.01	23.22	76.78	13.04	Dense *Deschampsia cespitosa*:	21.99	11.58	*Carex rostrata-Equisetum fluviatile* swamp
Species-poor tall sedge (*C. vesicaria*)	20.21	8.01	91.99	2.36	*Phalaris arundinacea*	79.79	28.42	Woodland/ scrub
Species-rich low sedge mire	48.35	39.44	60.56	13.89	Species-rich low sedge mire/Species-poor tall sedge (*C. vesicaria.*)	51.65	24.31	Species-rich low sedge mire/Species-poor tall sedge (*C. vesic.*)
Species-rich low sedge mire/Rush pasture/grassland	74.09	56.81	43.19	2.86	Species-rich low sedge mire/Species-poor tall sedge (*C. vesicaria*)	25.91	10.46	Species-rich low sedge mire/Species-poor tall sedge (*C. vesic.*)
Species-rich low sedge mire/Species-poor tall sedge (*C. vesicaria*)	78.13	22.68	77.32	24.31	Species-rich low sedge mire	21.87	13.89	Species-rich low sedge mire
Sphagnum lawn	62.4	14.39	85.61	21.51	Species-poor tall sedge (*C. aquatilis*)	37.6	13.07	*Carex rostrata-Equisetum fluviatile* swamp
Sphagnum lawn/Mixed sedge swamp	88.84	28.15	71.85	12.62	*Carex lasiocarpa*	11.16	3.96	Sphagnum lawn
Water	64.16	44.75	55.25	38.63	Deep Water Swamp	35.84	10.29	Deep Water Swamp
Woodland/scrub	53.54	46.44	53.56	28.42	Species-poor tall sedge (*C. vesicaria*)	46.46	24.02	Reedbed
Carex lasiocarpa	60.08	28.95	71.05	5.3	Mixed sedge	39.92	12.62	Sphagnum lawn/Mixed sedge swamp
Carex rostrata-Equisetum fluviatile swamp	63.47	21.16	78.84	13.58	Species-poor tall sedge (*C. vesicaria*)	36.53	10.8	*Sphagnum* lawn
Rush pasture/Grassland	57.65	80.56	19.44	31.32	*Phalaris arundinacea*	42.35	11.87	Species-rich low sedge mire/Species-poor tall sedge (C. vesic.)

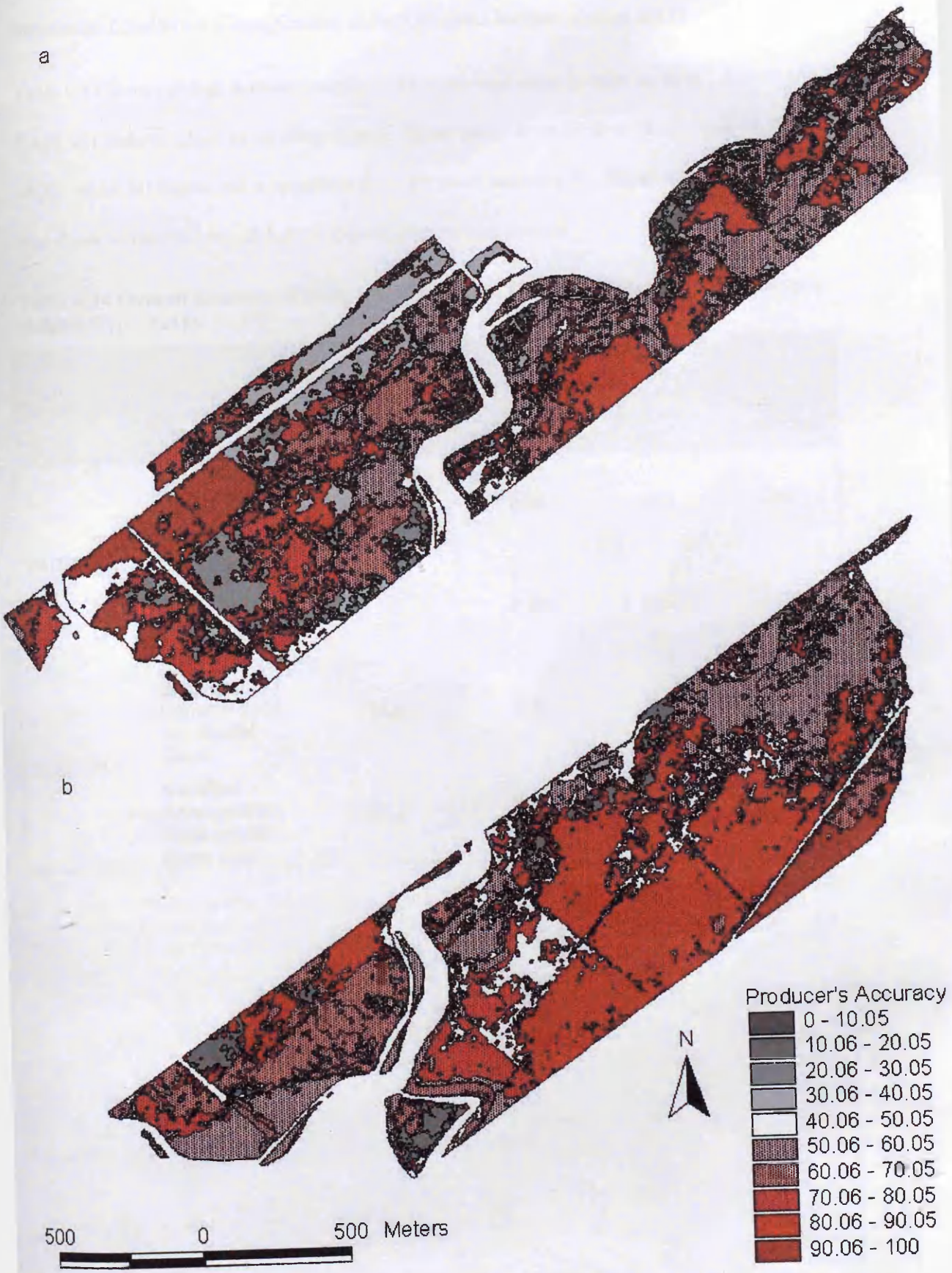

Figure 6:25 CASI 91 (a) and CASI 101 (b) Uncertainty maps showing producer's accuracy (%) of classes produced by Maximum Likelihood Classifications using all 22 *a priori* habitat types

Maximum Likelihood Classification using Grouped habitat classes (x11)

Table 6:14 shows overall accuracy results from supervised classification on both CASI 91 and CASI 101 habitat types as training classes. These range from 71.2 to 76.7% and 65.1% to 68.3% when all bands and a spectral subset are used respectively. These results are greater than those achieved using all habitat types in the training process.

Table 6:14 Overall Accuracy Results from Maximum Likelihood Classification-Grouped Habitat Types (x11)

Image	Training Samples	All 15 CASI bands		Spectral Subset (Bands 1, 3, 6 and 12)	
		Overall Accuracy (%)	Kappa coefficient	Overall Accuracy (%)	Kappa coefficient
CASI 91	Equalized Random-x100 per Habitat Class	72.2	0.64	65.1	0.55
	Stratified Random-5% Total Habitat Class Area	71.2	0.63	66.0	0.56
CASI 101	Equalized Random-x100 per Habitat Class	74.0	0.66	65.4	0.55
	Stratified Random-5% Total Habitat Class Area	76.7	0.69	68.3	0.58

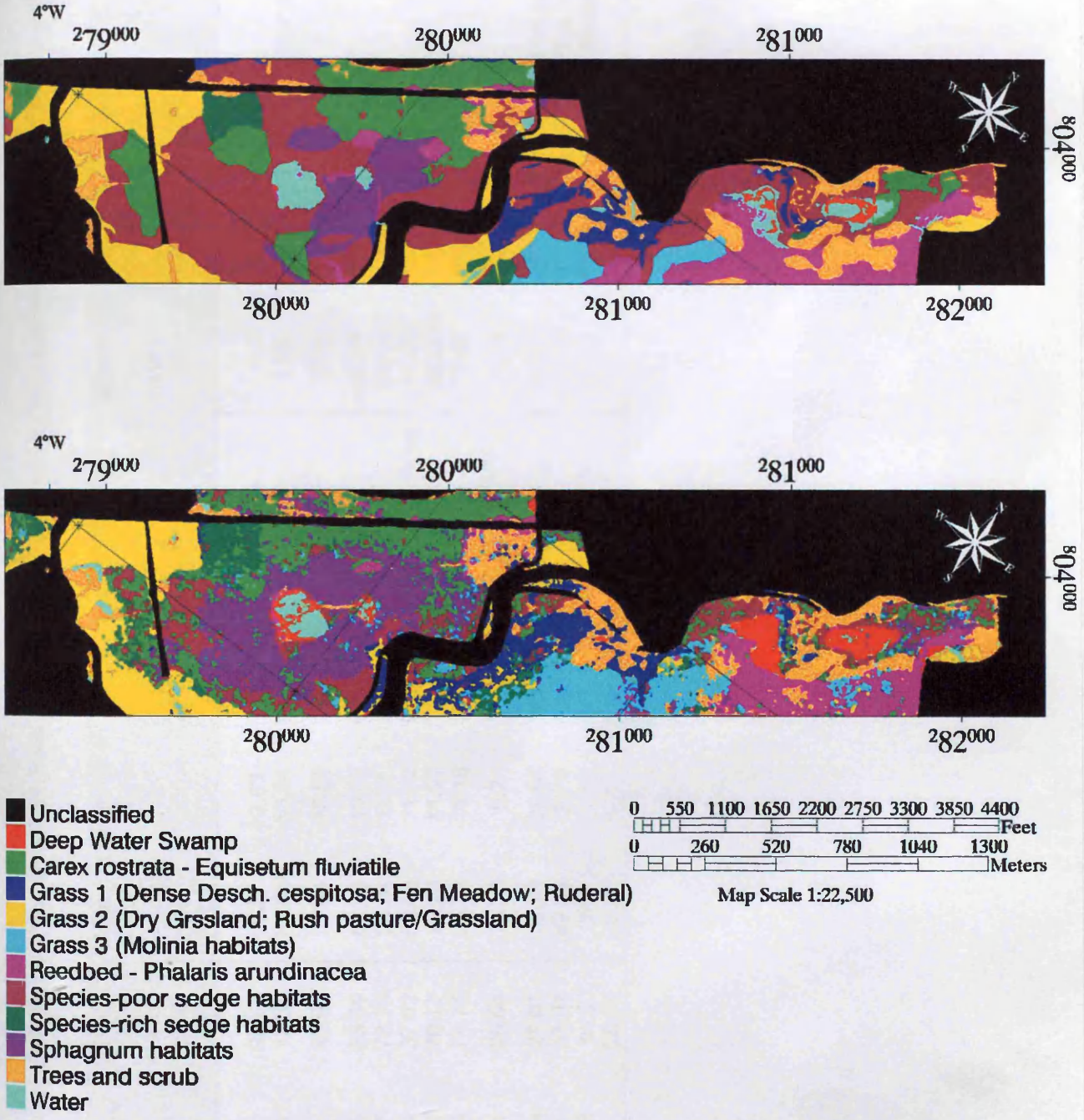

Figure 6:26 CASI 91: Supervised Classification - Grouped Habitat Types (x11) (Equalized Random Training samples (Overall Accuracy: 72.2%))

Table 6:15 Information extracted from confusion matrix produced from most successful supervised classification on CASI 91 (Grouped habitat types)

Habitat	Producer Accuracy (%)	User Accuracy (%)	Error of Commission (%)			Error of Omission (%)		
			Overall (%)	Greatest indiv. Habitat (%)	Habitat	Overall (%)	Greatest indiv. Habitat (%)	Habitat
Unclassified	100	98.63	1.37	2.83	Trees/scrub	0	0	-
Deep Water Swamp	92.41	18.32	81.68	53.54	Water	7.59	3.1	Reedbed – *Phal. arundinacea*
Carex rostrata – Equisetum fluviatile swamp	49.1	48.96	51.04	16.82	Species-poor sedge	50.9	22.16	*Sphagnum*
Grass 1	52.49	38.61	61.39	10.92	Grass 2	47.51	21.1	Trees/scrub
Grass 2	71.87	73.78	26.22	6.57	Species-poor sedge	28.13	10.92	Grass 1
Grass 3	88.54	37.92	62.08	11.72	Reedbed – *Phal. arundinacea*	11.46	5.16	Trees/scrub
Reedbed – *Phal. arundinacea*	57.34	70.77	29.23	11.97	Trees/scrub	42.66	11.72	Grass 3
Species-poor sedge	26.54	74.71	25.29	11.18	*Sphagnum*	73.46	24.66	*Sphagnum*
Species-rich sedge	73.21	26.64	73.36	9.2	*Carex rostrata – Equisetum fluviatile* swamp	26.79	10.7	Grass 3
Sphagnum	73.49	27.01	72.99	24.66	Species-poor sedge	26.51	11.18	Species-poor sedge
Trees/scrub	66.1	57.97	42.03	21.1	Grass 1	33.9	11.97	Reedbed – *Phal. arundinacea*
Water	29.88	61.2	38.8	1.94	Grass 2	70.12	53.54	Deep Water Swamp
Unclassified	100	98.63	1.37	2.83	Trees/scrub	0	0	-

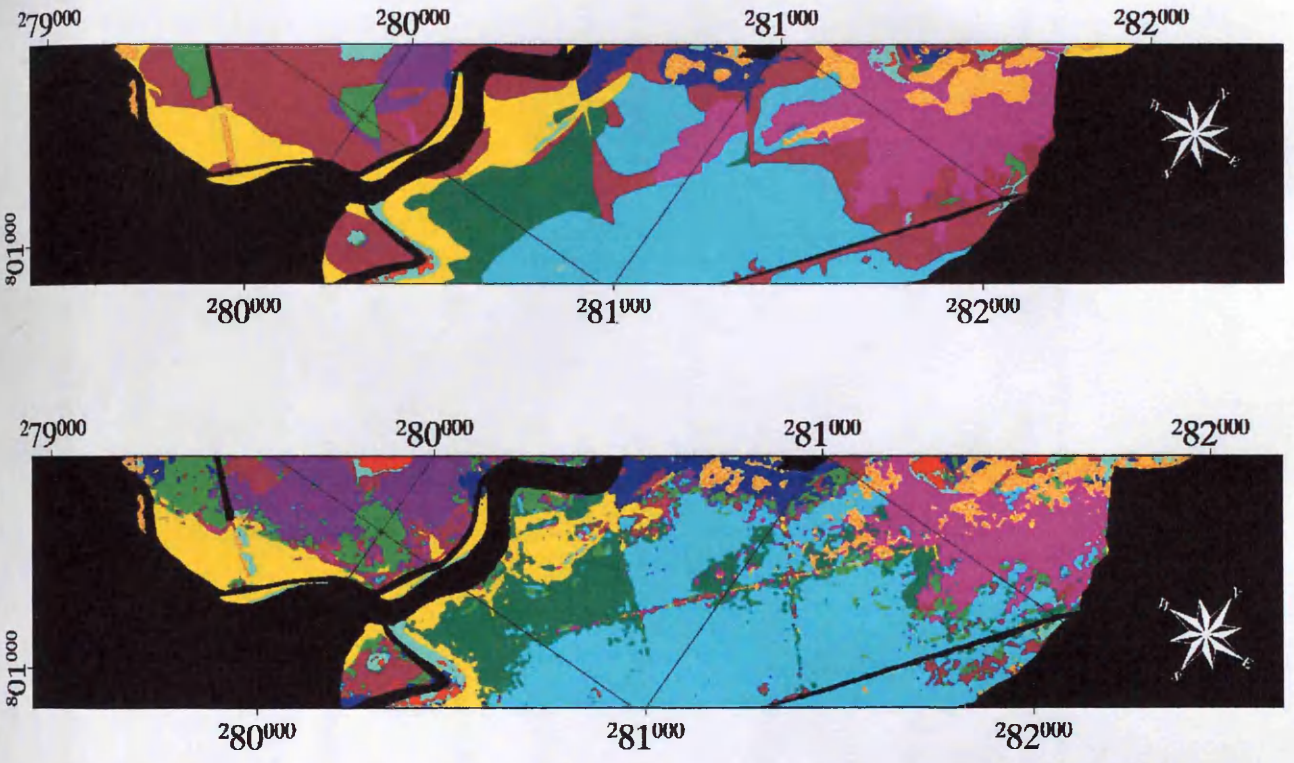

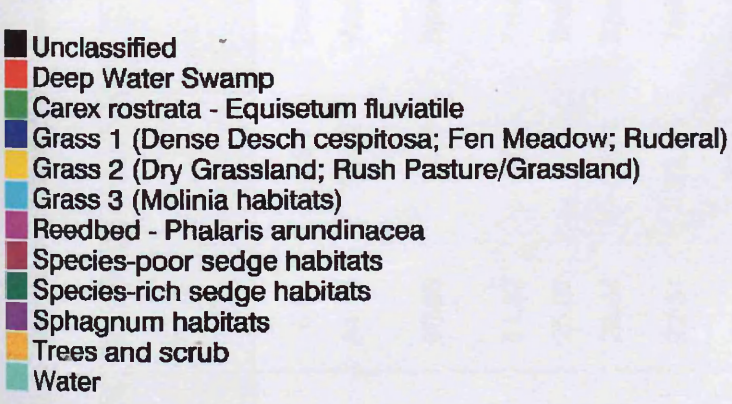

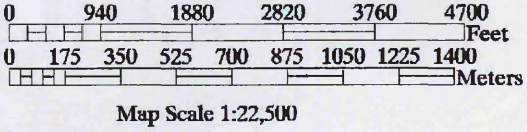

Figure 6:27 CASI 101: Supervised Classification - Grouped Habitat Types (x11) (Stratified Random Training samples (Overall Accuracy: 76.7%))

Table 6:16 Information extracted from confusion matrix produced from most successful supervised classification on CASI 101 (Grouped habitat types)

Habitat	Producer Accuracy (%)	User Accuracy (%)	Error of Commission (%)			Error of Omission (%)		
			Overall (%)	Greatest indiv. Habitat (%)	Habitat	Overall (%)	Greatest indiv. Habitat (%)	Habitat
Unclassified	100	99.2	0.8	4.91	Deep Water Swamp	0	0	-
Deep Water Swamp	58.74	15.86	84.14	34.82	Water	41.26	20.11	Water
Carex rostrata – Equisetum fluviatile swamp	70.91	19.04	80.96	14.68	Species-poor sedge	29.09	13.97	*Sphagnum*
Grass 1	65.98	48.68	51.32	5.63	Trees/scrub	34.02	14.41	Trees/scrub
Grass 2	67.7	74.98	25.02	5.24	Water	32.3	12.96	Species-rich sedge
Grass 3	90.96	71.16	28.84	20.74	Species-poor sedge	9.04	3.16	Species-rich sedge
Reedbed – *Phal. arundinacea*	54.64	77.46	22.54	22.95	Trees/scrub	45.36	15.27	Species-rich sedge
Species-poor sedge	19.4	77.21	22.79	9.49	Deep Water Swamp	80.6	22.39	*Sphagnum*
Species-rich sedge	74.31	49.95	50.05	15.27	Reedbed – *Phal. arundinacea*	25.69	15.1	Grass 3
Sphagnum	76.65	22.73	77.27	22.39	Species-poor sedge	23.35	10.92	Carex rostrata – Equisetum fluviatile swamp
Trees/scrub	57.53	49.4	50.6	14.41	Grass 1	42.47	22.95	Reedbed – *Phal. arundinacea*
Water	38.06	33.93	66.07	20.11	Deep Water Swamp	61.94	34.82	Deep Water Swamp

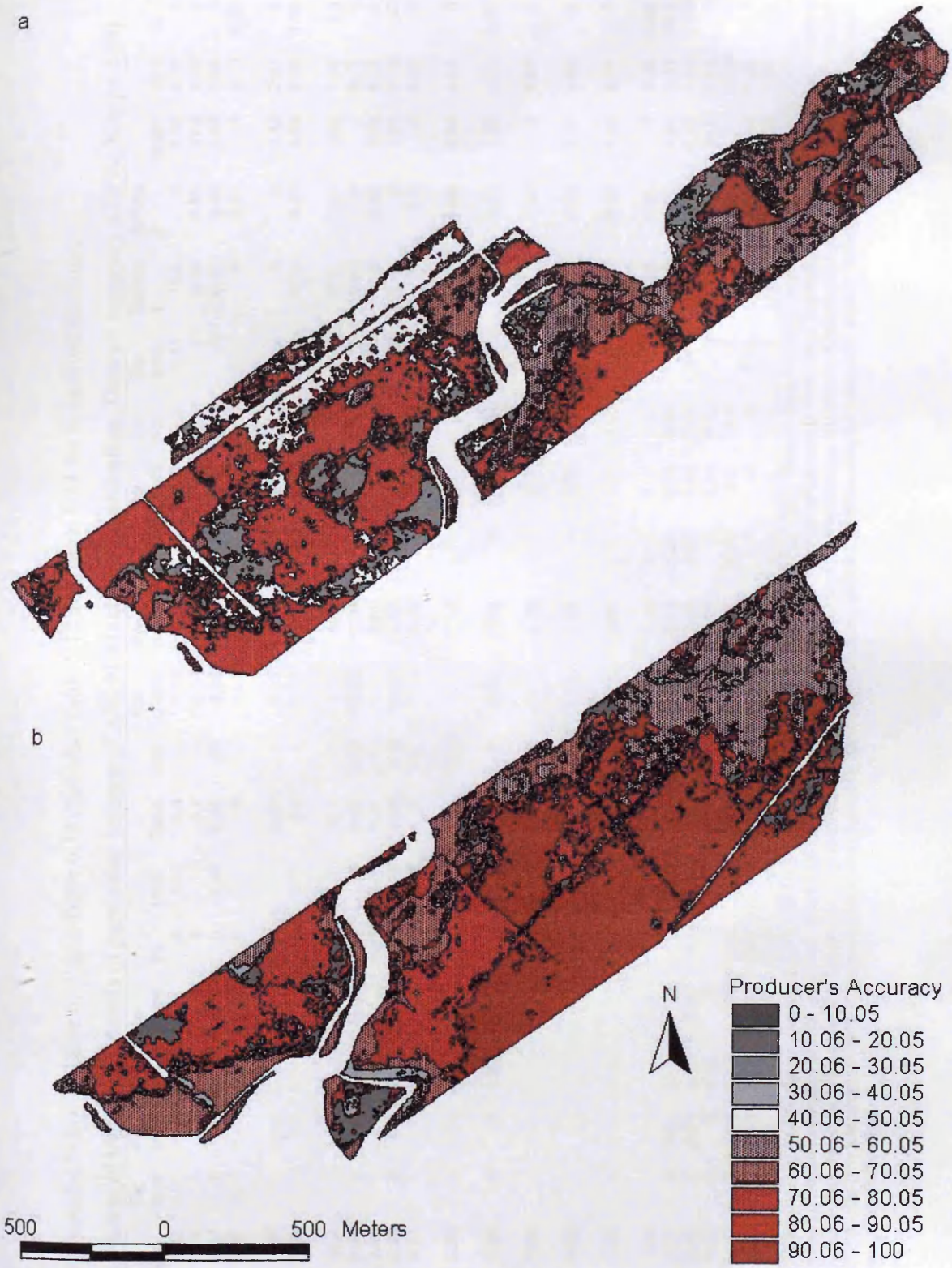

Figure 6:28 CASI91 (a) and CASI101 (b) Uncertainty maps showing producer's accuracy (%) of classes produced by Maximum Likelihood Classifications using all 22 a priori habitat types

Confusion matrices are presented below in Table 6:17 and Table 6:18 (See also Table 6:12 and Table 6:13 for associated statistics).

Table 6:17 Confusion Matrix to highlight habitats of particular interest (CASI 91 MaxLike Classification: Overall accuracy-67.5%; Kappa 0.58)

	Uncl	DWS	DDc	Dg' land	Fen med	MS	Mc-sedge	Pa	Pine	Reed	Rud	Rp/ g'land	Sp-poor1	Sp-poor2	Sp-poor3	Sp-rich1	Sp-rich2	Sphag 1	Sphag 2	Water	W/s	Cl	Cr-Ef
Uncl.	100	0	**0.63**	5.01	1.88	0.86	0	**0**	0.44	**0.4**	4.33	2.04	**1.86**	0.09	0	0	0.11	**0.3**	**0**	**0.89**	**3.25**	**0**	1.07
DWS	0	82.4	**0**	0	0	0.09	0	**0**	0	**3.2**	0	0.62	**1.58**	0	0	0	0	**0.33**	**0.85**	**57.5**	**0.03**	**0**	0.25
DDc	**0**	**0**	**55.4**	**0**	**0**	**0.41**	**0.01**	**0**	**0.06**	**0.26**	**43**	**6.54**	**7.17**	**0**	**0**	**0.48**	**0**	**0.03**	**0.06**	**0.92**	**3.55**	**0**	**0.06**
Dg'land	0	0	**0.07**	90.7	0.84	1.30	0	**0**	0.32	**0**	0	15.6	**0.29**	0	0	0	0.62	**0**	**0.01**	**0**	**0.13**	**0.22**	0.14
Fen med	0	0	**0.1**	0	71.1	4.44	0.01	**0**	0	**0.26**	0	0.03	**0.23**	0	0.54	0	0	**0**	**0**	**0.12**	**2.07**	**0**	2.14
MS	0	0	**0.38**	0.65	4.6	21.6	0.05	**2.01**	0.61	**0.2**	0	0.05	**11.3**	4.56	12.9	0	0	**4.14**	**4.36**	**0.53**	**0.39**	**1.26**	4.63
Mc-sedge	0	0	**10.4**	0	0.42	1.91	82.9	**2.35**	0	**10.1**	0	1.76	**10.8**	0.8	0	11.3	0	**2.39**	**1.61**	**0.45**	**7.29**	**2.9**	1.39
Pa	**0**	**0**	**0.44**	**0**	**0.31**	**0.45**	**0.06**	**32.1**	**0**	**0.02**	**1.33**	**0.05**	**1.38**	**0.28**	**0**	**0.69**	**0**	**0.19**	**0.9**	**0**	**0.17**	**0**	**0.5**
Pine	0	0	**3.25**	0	0	0.26	0	**1.68**	93.06	**0.27**	7.67	4.79	**0.96**	2.82	6.3	0	0	**0**	**0.08**	**0.39**	**5.13**	**0**	0.03
Reed	**0**	**0.8**	**0.05**	**0**	**0.1**	**0.28**	**0**	**0.34**	**0**	**53.6**	**0**	**0.07**	**0.63**	**0**	**0.27**	**0.16**	**0**	**0.64**	**0**	**1.69**	**11.5**	**0**	**0.34**
Rud	0	0	**0.97**	0	0	0	0	**0.67**	0	**0**	7.17	0.06	**0.03**	0	0	0	0	**0**	**0.2**	**0**	**0.03**	**0**	0
Rp/ g'land	0	0	**2.98**	2.34	2.93	1	0.01	**27.4**	2.45	**0.48**	18.5	44.4	**4**	5.03	7.77	0	0	**0.07**	**1.66**	**0.34**	**0.69**	**0**	0.37
Sp-poor1	**0**	**1.98**	**1.98**	**0**	**0**	**1.52**	**0**	**5.2**	**0.03**	**0.18**	**0**	**0.94**	**13.4**	**0**	**2.41**	**1.54**	**0**	**1.22**	**1.43**	**1.54**	**0.86**	**0.27**	**0.85**
Sp-poor2	0	0	**0.93**	0	0.64	3.29	0	**0.34**	0.15	**0**	0	11.8	**2.82**	73.6	3.89	0.16	0	**0**	**0.06**	**0**	**0.01**	**0**	3.85
Sp-poor3	0	0	**0.95**	0	0.1	0.87	0.06	**1.34**	0	**0.42**	0	0.03	**2.62**	1.74	30.8	2.07	0	**0.26**	**0.29**	**0.21**	**0.55**	**0**	0.85
Sp-rich1	0	0	**4.59**	0	0.23	0.99	11	**4.36**	0	**3.31**	0	5.08	**3.94**	0.05	1.07	65.2	0	**0.41**	**0.45**	**1.34**	**0.74**	**0**	0.23
Sp-rich2	0	0	**0.6**	0	0	5.8	0.31	**0**	0.09	**0.05**	0	1.08	**1.35**	6.11	4.29	0.42	97.21	**0.32**	**1.31**	**0**	**1.36**	**0.38**	9.22
Sphag1	**0**	**0**	**0.32**	**0**	**0.31**	**21.7**	**0**	**0**	**0**	**4.87**	**0**	**0.07**	**6.62**	**1.27**	**0.13**	**0.26**	**0**	**67.1**	**18.7**	**0.04**	**0.33**	**14.7**	**20.1**
Sphag2	**0**	**0**	**0.49**	**0**	**0.21**	**3.17**	**0.28**	**15.6**	**0**	**6.53**	**7.5**	**0.63**	**7.48**	**0.99**	**0.94**	**2.86**	**0.13**	**9.27**	**58.8**	**0.37**	**0.64**	**0.66**	**3.75**
Water	**0**	**13.7**	**0.17**	**0**	**0**	**0.31**	**0**	**0**	**1.11**	**1.09**	**0**	**1.49**	**2.27**	**0**	**1.34**	**0.11**	**0**	**0.15**	**1.53**	**30.6**	**0.43**	**0**	**0.61**
W/s	**0**	**0.16**	**14. 3**	**0**	**8.89**	**1.72**	**4.43**	**2.35**	**1.66**	**8.59**	**10.5**	**3.24**	**8.65**	**0.09**	**19.8**	**10.6**	**0**	**0.73**	**1.21**	**2.4**	**58.8**	**0**	**3.36**
Cl	**0**	**0**	**0.03**	**0**	**0.73**	**16.5**	**0.48**	**3.02**	**0**	**0.57**	**0**	**0**	**3.24**	**0.7**	**0**	**0**	**0.04**	**8.66**	**6.12**	**0.05**	**0.06**	**75.1**	**9.68**
Cr-Ef	0	0.91	**1.12**	1.31	5.86	12.1	0.41	**1.34**	0.03	**5.38**	0	0.21	**7.36**	1.88	7.51	4.19	1.9	**3.76**	**0.34**	**0.59**	**1.99**	**4.55**	36.6

Uncl.- Unclassified; Cl- *Carex lasiocarpa*; Cr-Ef- *Carex rostrata-Equisetum fluviatile* swamp; DWS- Deep Water Swamp; DDc- Dense *Deschampsia cespitosa*; Dg'land- Dry grassland; Fen med- Fen meadow; MS- Mixed sedge; Mc-Mg- *Molinia caerulea-Myrica gale* mire; Mc-sedge- *Molinia caerulea*-sedge mire; Pa- *Phalaris arundinacea*; Pine- Pine plantation; Reed- Reedbed; Rud- Ruderal; Rp/g'land- Rush pasture/Grassland; Sp-poor1- Species-poor tall sedge (*Car aquatilis*); Sp-poor2- Species-poor tall sedge (C. aqua)/Mixed sedge; Sp-poor3- Species-poor tall sedge (*C. vesicaria*); Sp-rich1- Species-rich low sedge mire; Sp-rich2- Species-rich low sedge mire/Rush pasture/grassland; Sp-rich3- Species-rich low sedge mire/Species-poor tall sedge (*C. vesic.*); Sphag1- *Sphagnum lawn*; Sphag2- *Sphagnum lawn*/Mixed sedge swamp; W/s- Woodland/scrub

Table 6:18 Confusion Matrix to highlight habitats of particular interest (CASI 101 MaxLike Classification: Overall accuracy-74.1%; Kappa 0.66)

	Uncl.	DWS	DDc	MS	Mc-Mg	Mc-sedge	Pa	Pine	Reed	Rud	Sp-poor1	Sp-poor2	Sp-poor3	Sp-rich1	Sp-rich2	Sp-rich3	Sphag 1	Sphag 2	Water	W/s	Cl	Cr-Ef	Rp/gind
Uncl.	100	7.08	**0.31**	1.67	0.25	0.21	**2.75**	2.25	**0.19**	4.33	**2.25**	0.06	3.2	0	0	0	**0**	**0**	**1.78**	**0.71**	**0.53**	0.8	2.05
DWS	0	42.29	**0.03**	0.15	0	0.02	**0**	0	**0.56**	0	**0.21**	0	0	0.01	0	0	**0.12**	**0**	**10.29**	**0.15**	**0.1**	0.12	0.13
DDc	**0**	**0.34**	**42.72**	**0.11**	**0.19**	**0.01**	**4.59**	**5.23**	**0.17**	**32.45**	**5.54**	**2.12**	**0**	**0.04**	**0.1**	**0**	**0.14**	**3.13**	**1.77**	**3.37**	**0**	**0.56**	**1.97**
MS	0	0	**0.17**	52.21	0.22	0.37	**5.24**	0	**0.58**	0	**4.05**	0	0.48	0.38	0	0.32	**0.53**	**0**	**0.47**	**0.02**	**1.12**	1.32	0.27
Mc-Mg	0	0	**0**	3.17	95.39	1.25	**0**	0	**0**	0	**0**	0	0.11	0.01	0	0.14	**0**	**0**	**0.25**	**0**	**8.76**	0	0.02
Mc-sedge	0	1.03	**0.48**	19.22	0.17	87.97	**9.17**	0	**14.31**	0	**6.45**	0	1.48	16.97	7.29	1.13	**5.2**	**0**	**2.38**	**3.91**	**8.2**	1.7	1.3
Pa	**0**	**0.46**	**1.76**	**0.48**	**0**	**0.37**	**10.35**	**0**	**0.52**	**3.49**	**2.64**	**0**	**0**	**1.42**	**0**	**0**	**0**	**0.08**	**0.77**	**0.71**	**0.23**	**0**	**1.5**
Pine	0	0	**0.7**	0.08	0	0	**0**	69.18	**0.04**	0	**0.05**	1.29	0.46	0.01	0	0.05	**0**	**0**	**0.09**	**1.18**	**0**	0	2.11
Reed	**0**	**0**	**0**	**1.6**	**0**	**0.31**	**0.26**	**0**	**52.82**	**0**	**0.76**	**0**	**2.97**	**0.5**	**0**	**0**	**0.1**	**0**	**3.8**	**24.02**	**0**	**4.69**	**0.39**
Rud	0	0	**3.61**	0	0.06	0	**0**	0	**0.02**	33.61	**0.14**	0	0	0	0	0	**0.12**	**0**	**0.03**	**0.86**	**0**	0	0.04
Sp-poor1	**0**	**6.06**	**8.06**	**2.61**	**0.19**	**1.25**	**10.62**	**0.08**	**0.29**	**7.49**	**18.62**	**0.29**	**3.54**	**0.45**	**0**	**0**	**2.09**	**0.89**	**2.18**	**2.9**	**0.13**	**3.04**	**1.00**
Sp-poor2	0	0.69	**13.04**	0.96	0.03	0.01	**0**	0	**0.27**	0.17	**4.34**	78.61	1.03	0.2	0	0	**0.26**	**1.12**	**0.92**	**0.35**	**0.07**	3.18	3.65
Sp-poor3	0	0	**0**	1.17	0.09	0.17	**2.36**	0	**0.7**	0	**1.33**	0	20.21	0.41	0	0.25	**0.31**	**0**	**0.3**	**1.75**	**0**	0.12	0.73
Sp-rich1	0	0	**0**	8.15	0	3.82	**3.93**	0	**9.64**	0	**1.61**	0	0.57	48.48	0	13.89	**1.2**	**0**	**0.88**	**1.55**	**1.35**	0.73	5.09
Sp-rich2	0	0.11	**0**	0.08	0.09	0.13	**0**	0	**0.04**	0	**0.03**	1.41	0	0.72	74.09	2.86	**0**	**0**	**0.08**	**0.03**	**0.53**	0	0.32
Sp-rich3	0	0	**0**	1.3	0	0.09	**1.83**	0	**4.87**	0	**0.01**	0	0	24.31	10.46	78.13	**0.05**	**0**	**0.09**	**0.29**	**0.43**	0	11.9
Sphag1	**0**	**0**	**0.03**	**16.3**	**0**	**0.42**	**1.83**	**2.25**	**0.4**	**0**	**21.51**	**0.18**	**5.02**	**0.55**	**0**	**0**	**62.4**	**3.96**	**0.47**	**0**	**1.85**	**10.8**	**0.35**
Sphag2	**0**	**0**	**5.89**	**8.34**	**0**	**0.08**	**3.28**	**0**	**0.09**	**0**	**7.08**	**0.06**	**1.37**	**0.01**	**0**	**0**	**11.49**	**88.84**	**0.25**	**1.15**	**12.62**	**7.48**	**0.03**
Water	**0**	**38.63**	**0.7**	**2.12**	**0**	**0.11**	**4.33**	**1.05**	**1.28**	**0**	**2.02**	**0**	**0.57**	**0.25**	**0**	**0**	**1.39**	**0**	**64.16**	**0.49**	**1.16**	**1.69**	**6.08**
W/s	**0**	**0**	**16.09**	**2.08**	**0.32**	**1.49**	**0.66**	**9.02**	**6.28**	**17.97**	**4.06**	**2.23**	**28.42**	**1.68**	**0**	**0**	**0.36**	**0**	**2.97**	**53.54**	**0.4**	**0.16**	**2.24**
Cl	**0**	**2.86**	**0.33**	**5.3**	**2.34**	**0.91**	**2.36**	**0**	**0.65**	**0**	**1.17**	**0**	**0.23**	**0.47**	**0.1**	**0**	**1.18**	**0.06**	**0.7**	**0.07**	**60.08**	**0.14**	**0.38**
Cr-Ef	0	0	**3.89**	11.01	0	0.71	**5.11**	0	**5.63**	0.5	**10.15**	11.58	13.58	1.31	0	0.74	**13.07**	**1.93**	**1.94**	**2.27**	**2.45**	69.5	0.62
Rp/g'land	0	0.48	**2.2**	1.77	0.16	0.41	**31.32**	10.95	**0.67**	0	**5.98**	2.76	18.78	1.95	7.97	2.5	**0**	**0**	**3.41**	**0.68**	**0**	0	57.7

Uncl.- Unclassified; Cl- Carex lasiocarpa; Cr-Ef- Carex rostrata-Equisetum fluviatile swamp; DWS- Deep Water Swamp; DDc- Dense Deschampsia cespitosa; Dg'land- Dry grassland; Fen med- Fen meadow; MS- Mixed sedge; Mc-Mg- Molinia caerulea-Myrica gale mire; Mc-sedge- Molinia caerulea-sedge mire; Pa- Phalaris arundinacea; Pine- Pine plantation; Reed- Reedbed; Rud- Ruderal; Rp/g'land- Rush pasture/Grassland; Sp-poor1- Species-poor tall sedge (Car aquatilis); Sp-poor2- Species-poor tall sedge (C. aqua)/Mixed sedge; Sp-poor3- Species-poor tall sedge (C. vesicaria); Sp-rich1- Species-rich low sedge mire; Sp-rich2- Species-rich low sedge mire/Rush pasture/grassland; Sp-rich3- Species-rich low sedge mire/Species-poor tall sedge (C. vesic.); Sphag1- Sphagnum lawn; Sphag2- Sphagnum lawn/Mixed sedge swamp; W/s- Woodland/scrub

Species-poor tall sedge (*Carex aquatilis*)

Carex lasiocarpa

Dense *Deschampsia cespitosa*

Phalaris arundinacea

Sphagnum lawn

Figure 6:29 Probability maps of sensitive habitats (CASI 91) (Dark pixels=Low probability; Lighter pixels=lower probabilities; red pixels=greatest probabilities

Sphagnum lawn/Mixed Sedge

Reedbed

Woodland/scrub

Water

Figure 6:29b Probability maps of sensitive habitats (CASI 91) (Dark pixels=Low probability; Lighter pixels=lower probabilities; red pixels=greatest probabilities)

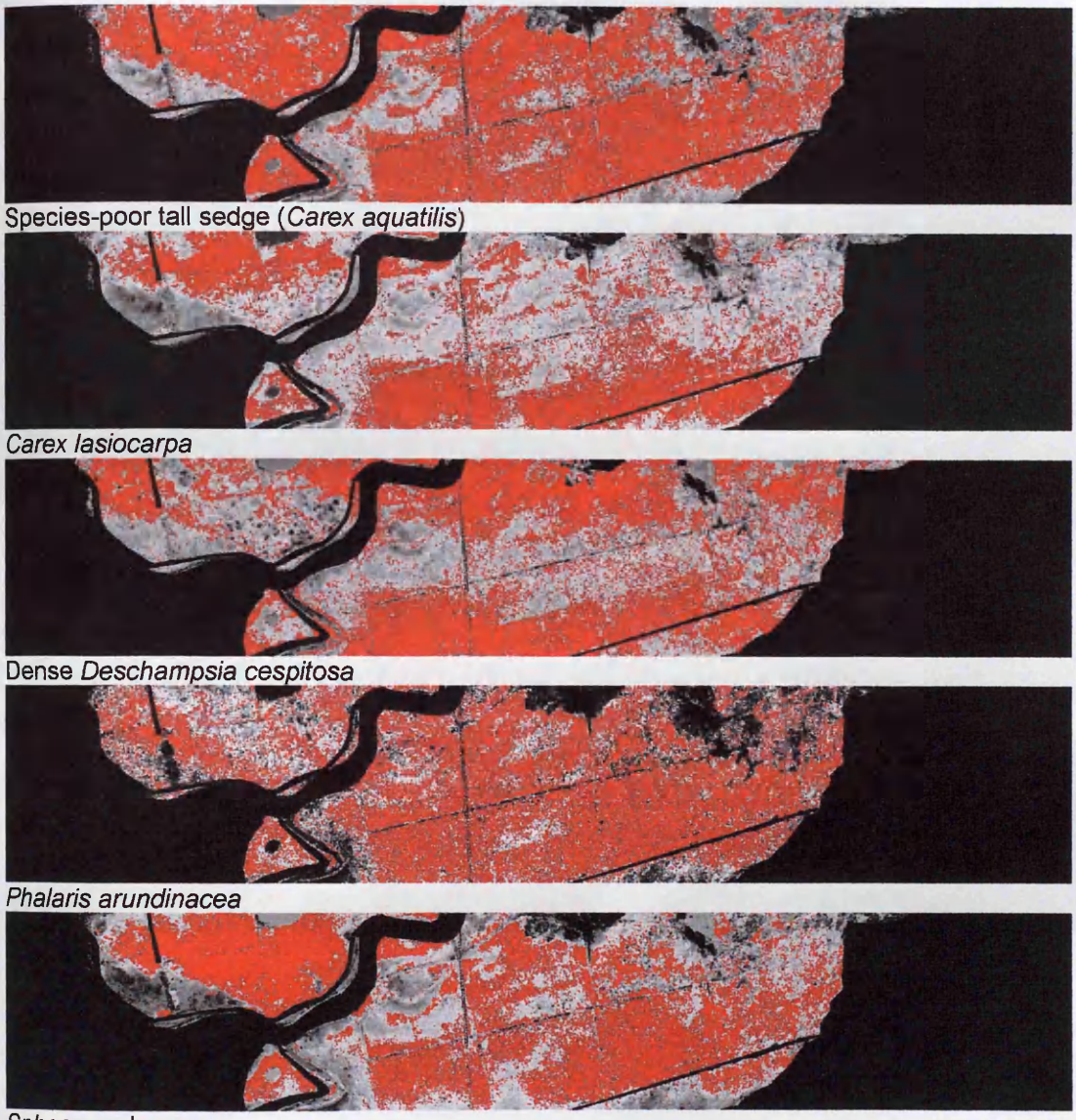

Figure 6:30a Probability maps of sensitive habitats (CASI 101) (Dark pixels=Low probability; Lighter pixels=lower probabilities; red pixels=greatest probabilities)

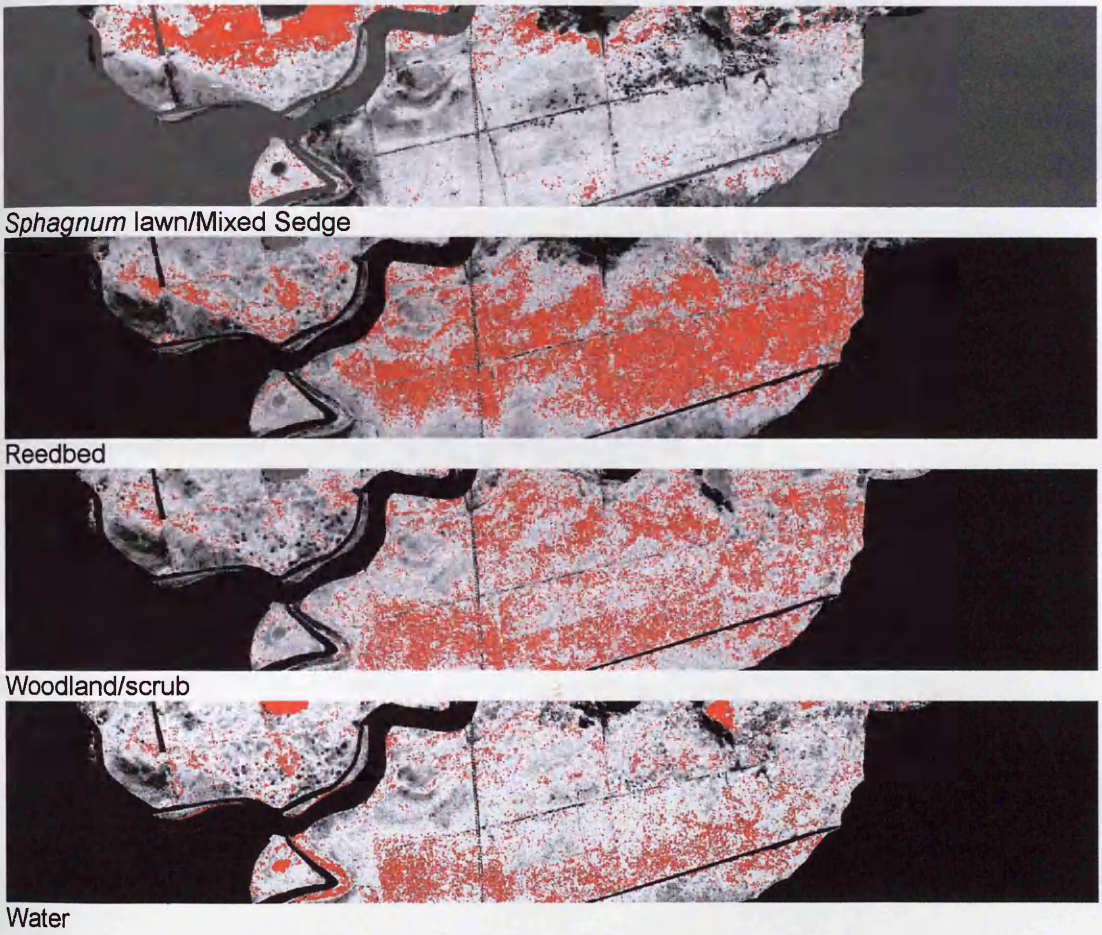

Figure 30b Probability maps of sensitive habitats (CASI 101) (Dark pixels=Low probability; Lighter pixels=lower probabilities; red pixels=greatest probabilities)

Spectral Feature Fitting

Spectral Feature Fitting was investigated as a method of discriminating between habitat types using differences between the size and shape of the absorption features present in the spectral response of pixels. Resultant classifications were compared with ground truth images using all habitats and the grouped habitats and results are presented below in Table 6:19. Results range from 51.64% to 58.58% and best results are attained from classifications involving the grouped habitats.

Table 6:19 CASI 91 and CASI 101-Overall Accuracy Results from Spectral Feature Fitting (Blue region absorption feature and red region absorption feature):-All Habitat Types (x22) and Grouped Habitat Types (x11) (using ground truth images as test data)

Image	Number of Habitat Classes	All 15 CASI bands Overall Accuracy	Kappa coefficient
CASI 91	11	58.58%	0.46
	22	51.64%	0.39
CASI 101	11	56.73%	0.44
	22	52.60%	0.39

6.3.4 Objective d) Variation across habitat boundaries

Explore the relationships between spectral variability derived from airborne imagery and detailed vegetation datasets along transects.

Results are presented in this section from Detrended Correspondence Analyses (DCAs) along each of the five transects described above. Small insets in Figure 6:31 to Figure 6:35 are provided which illustrate the location of habitat type change along each transect (habitat type labels along each transect can be referred to in Figure 6:8).

DCAs and Spectral Indices

The results of DCAs on the paired sample points of Transects 4.2 4.6, 8.3, 8.4 and 9.2 are presented here. DCAs using data at every pixel along each transect as well as derived NDVIs and REIPs were also calculated and presented here.

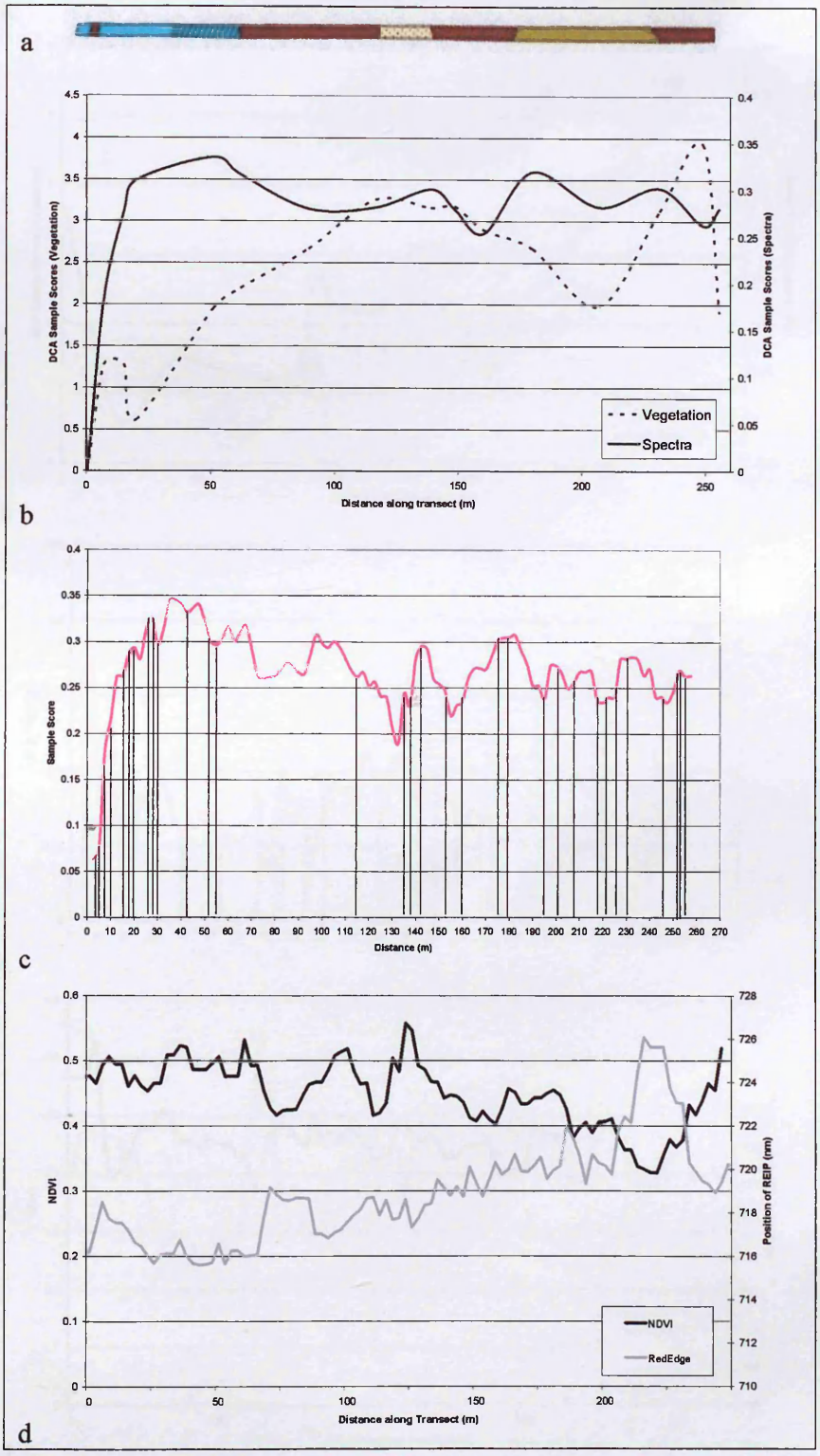

Figure 6:31 Analyses along Transect 4.2 (see Fig. 6:8): a) habitat type change along transect; b) DCA results showing sample scores at quadrat survey points along transect and DN values derived from imagery; c) illustrates the DCA Sample Scores at all pixels along the transect; recorded changes in vegetation cover are indicated by vertical bars; d) illustrates the patterns of NDVI and REIP values along the transect.

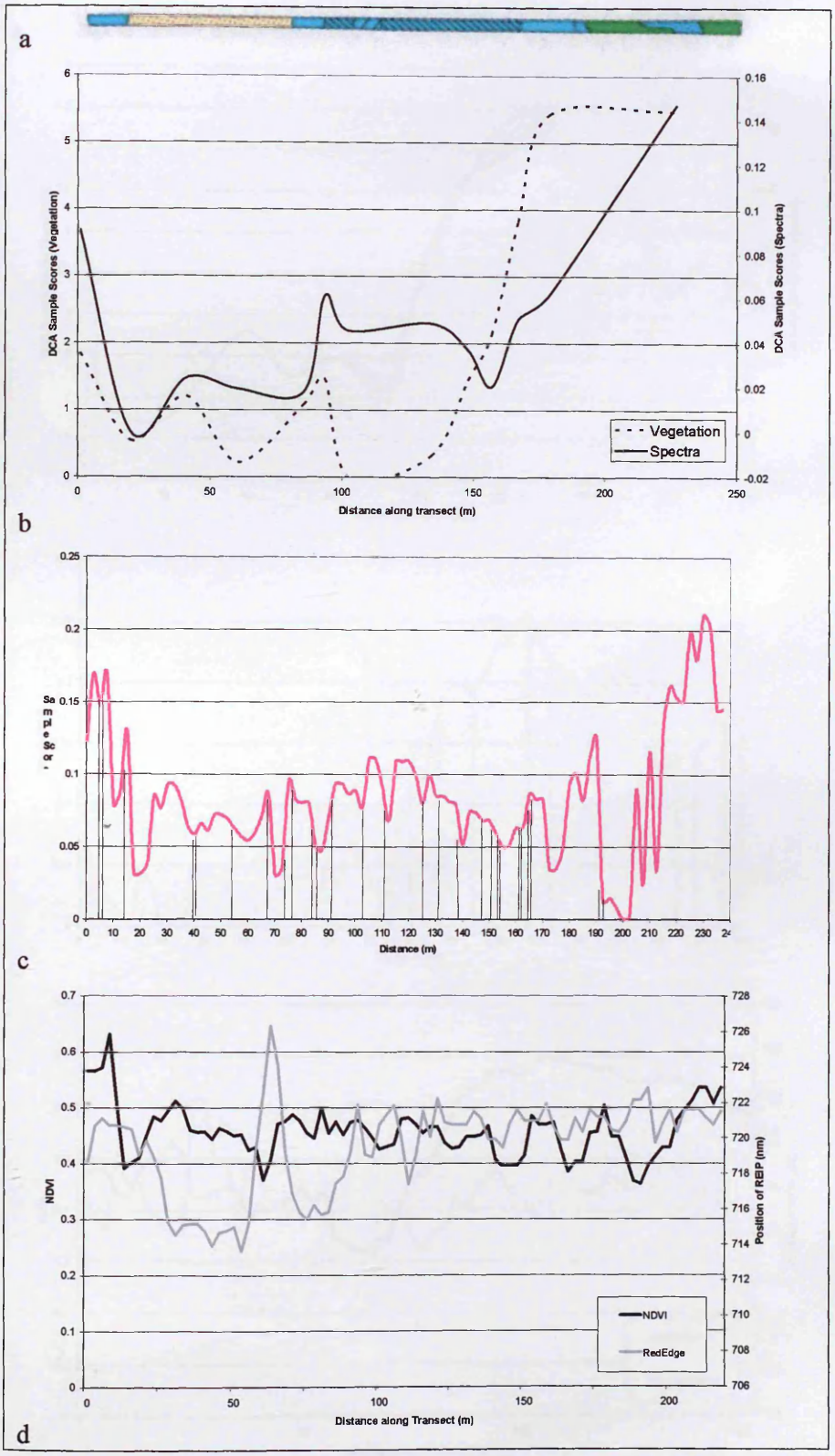

Figure 6:32 Analyses along Transect 4.6(see Fig. 6:8): a) habitat type change along transect; b) DCA results showing sample scores at quadrat survey points along transect and DN values derived from imagery; c) illustrates the DCA Sample Scores at all pixels along the transect; recorded changes in vegetation cover are indicated by vertical bars; d) illustrates the patterns of NDVI and REIP values along the transect .

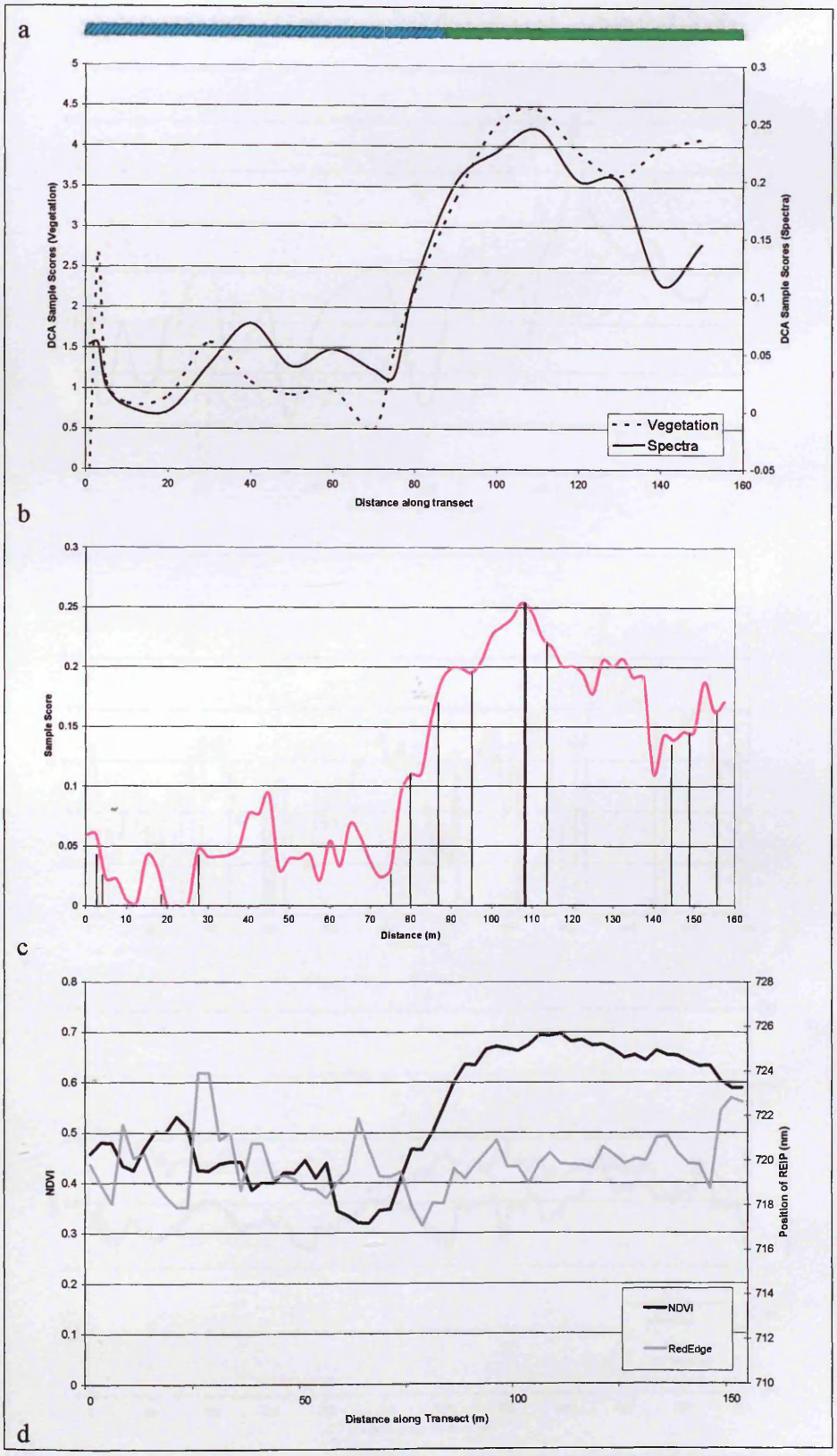

Figure 6:33 Analyses along Transect 8.3 (see Fig. 6:8): a) habitat type change along transect; b) DCA results showing sample scores at quadrat survey points along transect and DN values derived from imagery; c) illustrates the DCA Sample Scores at all pixels along the transect; recorded changes in vegetation cover are indicated by vertical bars; d) illustrates the patterns of NDVI and REIP values along the transect.

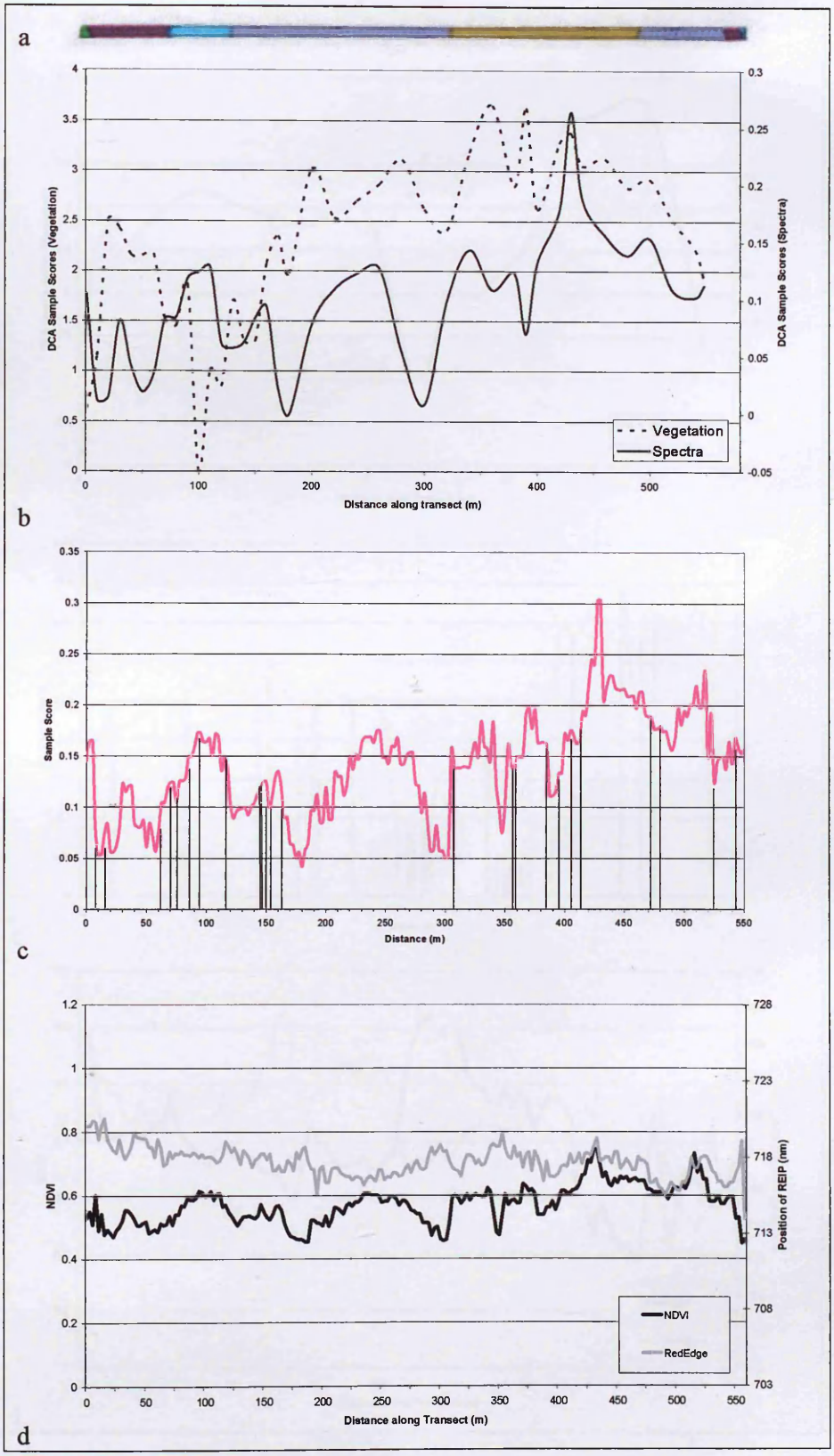

Figure 6:34 Analyses along Transect 8.4 (see Fig. 6:8): a) habitat type change along transect; b) DCA results showing sample scores at quadrat survey points along transect and DN values derived from imagery; c) illustrates the DCA Sample Scores at all pixels along the transect; recorded changes in vegetation cover are indicated by vertical bars; d) illustrates the patterns of NDVI and REIP values along the transect.

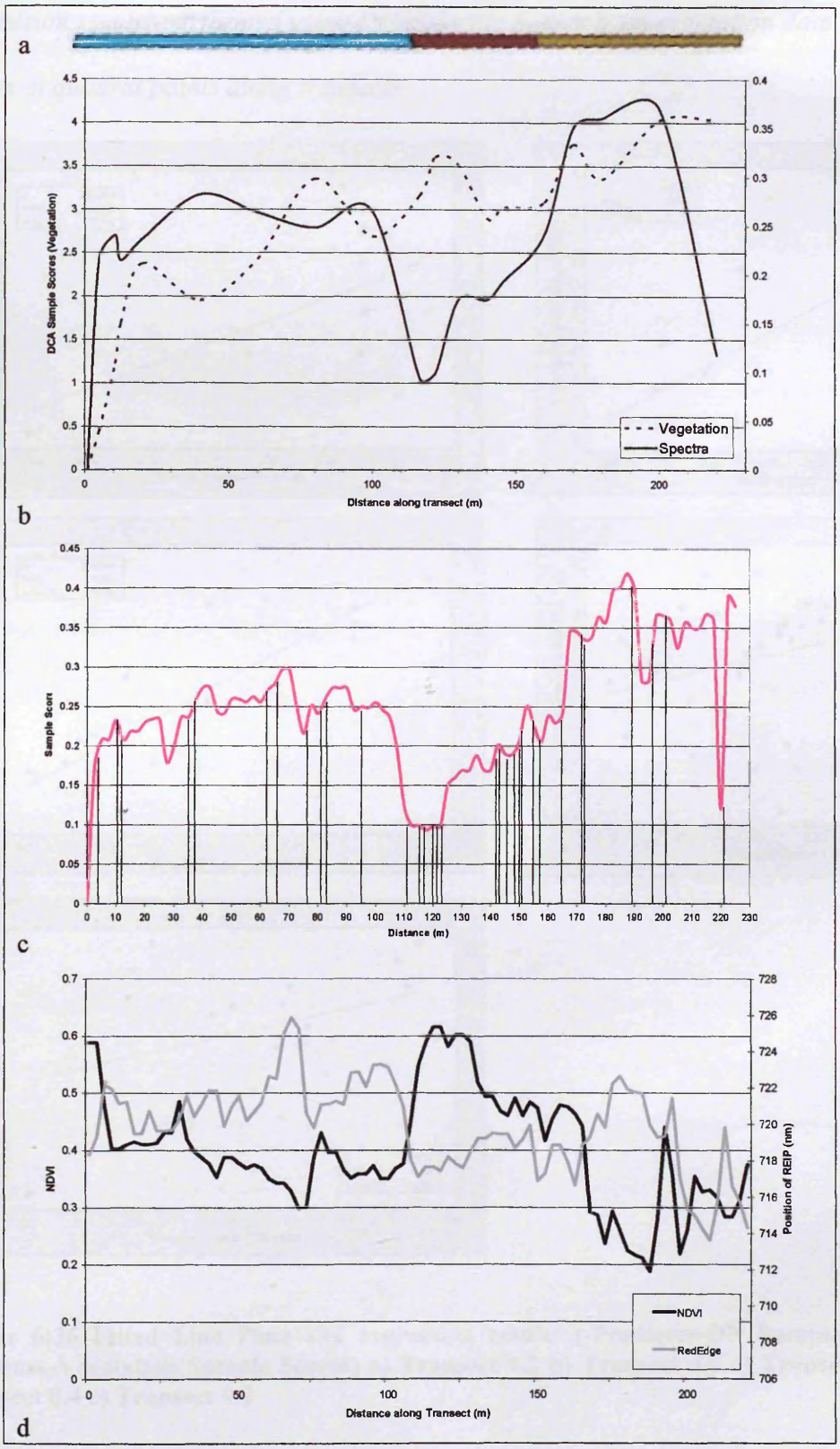

Figure 6:35 Analyses along Transect 9.2 (see Fig. 6:8): a) habitat type change along transect; b) DCA results showing sample scores at quadrat survey points along transect and DN values derived from imagery; c) illustrates the DCA Sample Scores at all pixels along the transect; recorded changes in vegetation cover are indicated by vertical bars; d) illustrates the patterns of NDVI and REIP values along the transect.

Regression results-performed using DCA Sample Scores from vegetation data and DN values at quadrat points along transects

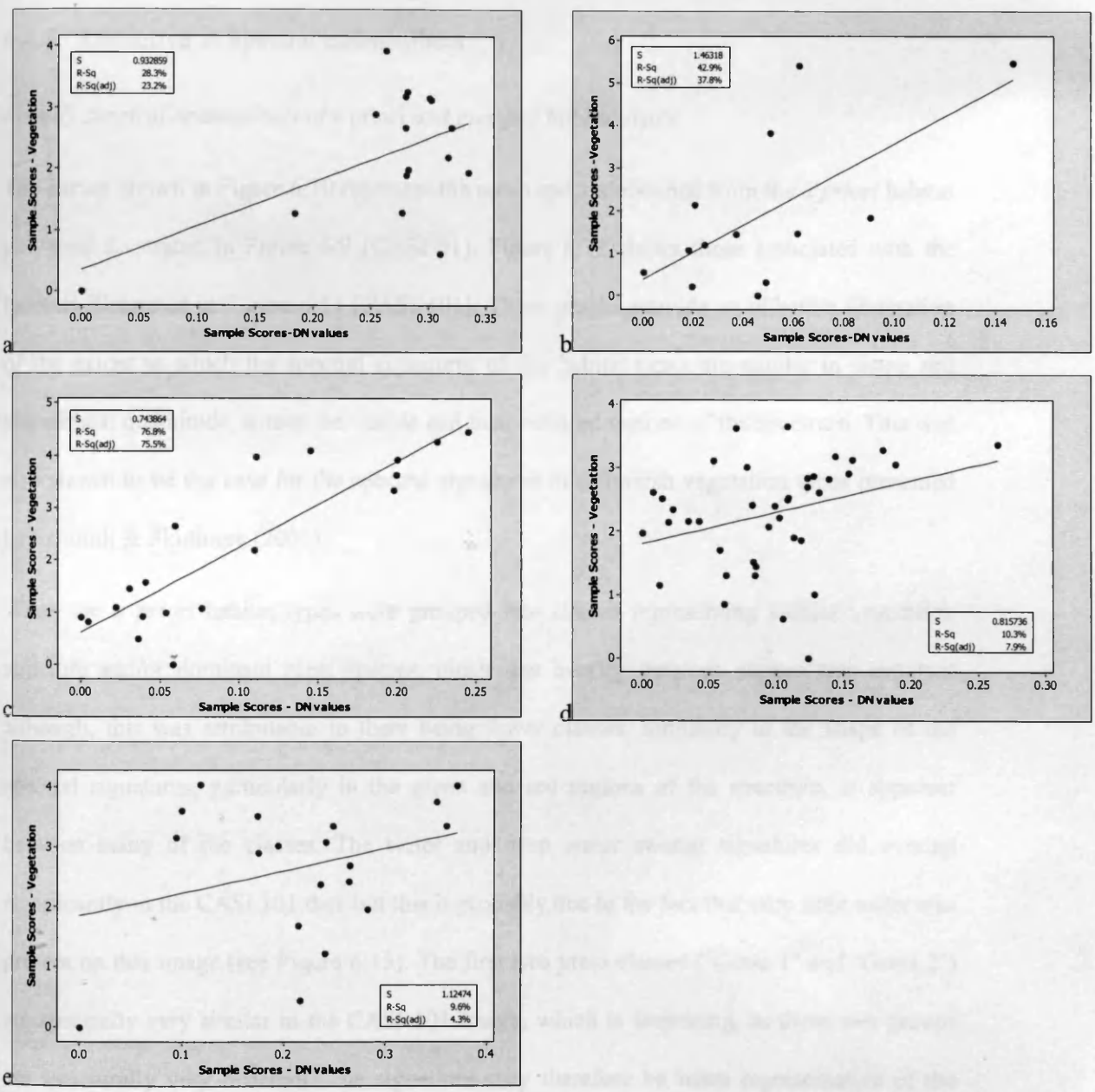

Figure 6:36 Fitted Line Plots and regression results (-Predictor-DN Sample Scores, Response-Vegetation Sample Scores) a) Transect 4.2 b) Transect 4.6 c) Transect 8.3 d) Transect 8.4 e) Transect 9.2

6.4 Discussion and Conclusions

6.4.1 Objective a) Spectral endmembers

Identify spectral endmembers of a priori *and grouped habitat types.*

The curves shown in Figure 6:10 represent the mean spectra obtained from the *a priori* habitat polygons illustrated in Figure 6:9 (CASI 91). Figure 6:12 shows those associated with the habitats illustrated in Figure 6:11 (CASI 101). These graphs provide an effective illustration of the extent to which the spectral signatures of the habitat types are similar in shape and sometimes, magnitude, across the visible and near-infrared regions of the spectrum. This was also shown to be the case for the spectral signatures of saltmarsh vegetation types presented by Schmidt & Skidmore (2003).

When the *a priori* habitat types were grouped into classes representing similar vegetation structure and/or dominant plant species, much less overlap between classes was apparent although, this was attributable to there being fewer classes. Similarity in the shape of the spectral signatures, particularly in the green and red regions of the spectrum, is apparent between many of the classes. The water and deep water swamp signatures did overlap significantly in the CASI 101 data but this is probably due to the fact that very little water was present on this image (see Figure 6:15). The first two grass classes ('Grass 1' and 'Grass 2') are spectrally very similar in the CASI 101 image, which is surprising, as these two groups are structurally very different. The signatures may therefore be more representative of the biophysical variables associated with the groups and, not necessarily the inherent species composition or structure, as this would be relatively high for both of these groups. The order of the magnitudes of reflectance in the NIR region does seem to relate to a productivity gradient between grass and trees at one extreme and, *Sphagnum* and *Carex rostrata-Equisetum fluviatile* swamp at the other. Moisture content also has a degree of influence on

the magnitude of reflectance in the NIR regions of the spectrum. Table 6:20 lists the habitats by reflectance in the NIR (as illustrated in Figure 6:10 and Figure 6:12).

Table 6:20 Habitat ordering in the NIR (Band 9) for both images (highest to lowest values of reflectance)

CASI 91	CASI 101
Dry grassland	Ruderal
Ruderal	Rush pasture/grassland
Rush pasture/grassland	Dense *Deschampsia cespitosa*
Dense *Deschampsia cespitosa*	Woodland/scrub
Woodland/scrub	Pine plantation
Species-poor tall sedge (*Carex aquatilis*)-Mixed sedge	*Phalaris arundinacea*
Molinia caerulea-sedge mire	*Molinia caerulea-Myrica gale* mire
Pine plantation	Species-rich low sedge mire-Species-poor tall sedge (*C. vesicaria*)
Phalaris arundinacea	*Molinia caerulea*-sedge mire
Species-rich low sedge mire-Rush pasture/grassland	Species-poor tall sedge (*Carex aquatilis*)-Mixed sedge
Species-poor tall sedge (*Carex aquatilis*)	Species-rich low sedge mire-Rush pasture/grassland
Species-rich low sedge mire	Species-rich low sedge mire
Reedbed	Reedbed
Fen Meadow	Species-poor tall sedge (*Carex aquatilis*)
Carex lasiocarpa	Species-poor tall sedge (*Carex vesicaria*)
Sphagnum lawn-Mixed sedge swamp	*Carex lasiocarpa*
Carex rostrata-Equisetum fluviatile swamp	*Sphagnum* lawn-Mixed sedge swamp
Mixed sedge swamp	Mixed sedge swamp
Sphagnum lawn	*Sphagnum* lawn
Species-poor tall sedge (*Carex vesicaria*)	*Carex rostrata-Equisetum fluviatile* swamp
Deep Water Swamp	Deep Water Swamp
Water	Water

6.4.2 Objective b) Unsupervised Classification

Explore the spectral variation within the available imagery using unsupervised classifications and various spectral indices.

K-Means classification using over and above the known number of classes was performed on each of the images and, the distribution of the *a priori* habitat types in each of the resultant cluster classes was assessed (Table 6:9 and Table 6:10). From these results it was shown that only two classes were consistently spectrally distinct (water and rush pasture/grassland); the rest of the habitat types were distributed between the remaining 33 clusters. The resultant maps shown in Figure 6:17 and Figure 6:18 (using fewer clusters for clarity) illustrate the heterogeneity of the clusters in terms of the *a priori* habitats that they contain. Given the

information available it is not possible to confirm whether this is due to spectral overlap between the *a priori* habitat types or to a degree of heterogeneity within the habitats themselves.

The results of the unsupervised classifications were surprising given the differences between some habitat types that were apparent from the spectra graphs discussed above. Unsupervised methods are demonstrated to be effective methods of vegetation classification in the literature (Mackey 1990; Cihlar 2000; Bachmann 2002). However, the results presented here indicate that K-Means is not an effective method to discriminate between wetland habitat types. There is further work that could be pursued involving the masking out of the pixels that can be interpreted, such as the water and grassland areas and, then running the classification again. There does appear to be some cluster patterning that is associated with the *Sphagnum* habitats and the mixed sedge habitats.

Imagery illustrating REIPs and NDVI values are presented in Figure 6:19 and Figure 6:20 (NDVI) and Figure 6:21 and Figure 6:22 (REIP). K-Means was used to create classes so that visual comparisons with the *a priori* habitat boundaries overlaid on the image could be easily made. NDVI has been found to be representative of biomass, productivity and chlorophyll content, though without extensive fieldwork, it is difficult to fully interpret the patterns illustrated here. There does appear to be some relationship between a number of the habitat boundaries and the indices, though the nature of the relationship is not explored in detail here (Engstrom *et al.* 2002).

The relatively low NDVI values associated with the *Sphagnum* and reedbed habitats and, high values associated with species-rich sedge habitats and the rush pasture habitats, suggest that perhaps these are maps best associated with biomass. The REIP maps pick out the vegetation along the marsh ditches very well, as well as habitats associated with relatively high productivity such as the *Molinia caerulea-Myrica gale* habitat on the eastern side of the marsh. Even though there is a great deal of within-habitat heterogeneity, the ecological information represented by these indices may still be of value in terms of informed

management at these sites and further work using these indices should be pursued (Ssegawa *et al.* 2004; Southall *et al.* 2003).

The potential benefit of NDVI datasets for the purposes of vegetation classification have been demonstrated in the literature (Boles *et al.* 2004; Schmidt & Karnieli 2002) and is only illustrated in principle here. Similarly, REIP images can also be used although there remain some limitations with the way in which this is calculated for multispectral images, in that, a singular peak in the first derivative of the spectra is assumed (Llewellyn & Curran 2005). It is acknowledged that further applications of such maps should be accompanied by a significant amount of fieldwork to identify the nature of the relationship of NDVI and REIP with wetland vegetation and habitat types, whether it is productivity, biomass or species richness. It is also necessary to determine the extent to which differing management between compartments affects the nature of the vegetation. Images such as those in Figure 6:19 and Figure 6:20 as well as Figure 6:21 and Figure 6:22 should then be validated before using them as additional bands in classification algorithms. Indices such as this can provide an invaluable source of ecological information across large areas that can then be utilised in management decisions and archived for future vegetation change studies.

6.4.3 Objective c) Supervised Classification

Assess the potential for supervised classification to correctly classify habitat types derived from field based a priori *habitat maps.*

Results from the supervised classifications using the Maximum Likelihood algorithm were promising. Kappa scores and overall accuracies were high for both images with the latter being in the range of around 70%, which compares favourably with similar vegetation studies (Bachmann *et al.* 2002). When the habitats were grouped into classes containing two or more habitat types, in an attempt to find a classification system consisting of classes that would discriminate spectrally more readily than perhaps the original *a priori* dataset, results did not significantly improve (Brook & Kenkel 2002; Davis *et al.* 1994; Cingolani *et al.* 2004). It is

considered, therefore, to be more beneficial to utilise all of the 22 habitat types in each image for training as this retains the greatest amount of ecological information at a minimal loss of overall classification accuracy.

Results from analyses that utilise only four bands of data (blue, red, green and NIR) are highest for the grouped habitat types (65-68%). This provides some evidence that the use of high spatial and low spectral resolution satellite datasets could provide data that can be interpreted in terms of habitat type at scales that are useful to ecologists and environmental managers. This may only be the case where classes are grouped into slightly broader class types. However, this may be a worthwhile compromise as satellite imagery such as IKONOS becomes less expensive, more readily available and reliably repeatable (Mehner *et al.* 2004; Goward *et al.* 2003). Temporal datasets of a low spectral resolution have been reported in the literature frequently, as a valuable means of classifying vegetation and, are therefore, an area worthy of future consideration in terms of resources for wetland habitat mapping (Key *et al.* 2001).

Despite the good results reported here the overall accuracies do fall below the 80% level considered as an acceptable classification accuracy vegetation mapping (Basham May 1997; Skidmore 2002; Kerr & Ostrovsky 2003). This will have much to do with the nature of the ground truth dataset used and the inaccuracies associated with that, as well as the nature of intergrading habitats in semi-natural environments. Some habitat types are mapped with a greater degree of success than others with some even achieving producer accuracy rates as low as 20% with user accuracies often falling below 50%. Particularly successful habitat types included Rush pasture/grassland, water, woodland/scrub, pine plantation, the *Molinia caerulea* habitats and reedbed. This fits with observations already made from the unsupervised classifications whereby a lot of the spectral overlap is evident between the sedge and *Sphagnum* habitat types. The Regions of Interest (ROIs) used within the class image to train the Maximum Likelihood algorithm should be homogenous or spectrally distinct, and this was examined using ENVI's n-D Visualiser. The distribution of the points within the n-D

Visualiser should be such that points from separate ROIs cluster tightly together and do not overlap in feature space. However, this was not the case with the training classes used here.

The overlap inherent in the training data was attributable to the method used to obtain the training samples. Random points within the polygons of the *a priori* habitat map were identified and homogeneity within the polygons was assumed when this may not have been the case. This is a problem that cannot be avoided in semi-natural environments where habitats grade into one another and as a result there is overlap in species composition and physical characteristics between classes of ecological interest (Townsend & Walsh 2001; Trodd 1993; Foody 1996b). Given the nature of the relationship between spectra and vegetation composition and structure, as demonstrated in previous chapters, spectral overlap in feature space is therefore unavoidable. For resultant classification maps to retain any sort of ecological meaning though, it remains fitting that a workable compromise be achieved between the type of information that ecologists require and can work with and, the methods by which remote sensing can provide that information.

MLC and Probability Mapping

The confusion matrix results for seven habitat types (includes two types of *Sphagnum* habitat) are highlighted in Table 6:17 and Table 6:18. These are habitats that have been identified as ecologically sensitive as they either contain rare or invasive species and as such, their distribution over the marshes is key information that concerns the effective conservation of the area. The confusion matrices show producer accuracies which indicate how much of the habitat area, as identified on the *a priori* habitat maps, were classified as the same habitat type through the classification procedure. This presupposes that the *a priori* map is 'true to life' and is an exact representation of the nature of the vegetation on the ground as defined by habitat type. The extent to which this is true has not been qualified here. In addition, there may have been changes in the extent of habitat area between the production of the *a priori* map and the airborne data collected for this study. Other inaccuracies are expected due to the RMSE calculated for the imagery which is around 2 pixels in any direction. Furthermore,

information regarding the positional accuracy of the *a priori* habitat map was not available. Misclassifications, are therefore, highly likely at the borders of habitats or around the edges of features in the marsh and, again, the proportion of errors due to the misalignment between the images has not been qualified.

Given the degree of expected error using the resources available, the producer accuracies were often above 60% for some of the sensitive habitats and, on one occasion, as high as 88%. The most successfully mapped habitat types were the *Sphagnum* classes which showed the greatest degree of association between the *a priori* habitat map and that produced by MLC. Producer accuracies for these habitat types ranged from 58.79% to 88.84%. *Carex lasiocarpa* habitat type achieved high producer accuracies (75.07% and 60.08% for CASI 91 and CASI 101 respectively). This is a structurally distinctive habitat type that is largely homogenous and, as such, it is likely that this habitat type exhibits a distinct spectral signature. These high producer accuracy results, are however, also likely to be due to some extent to the relatively small size of the habitat type and to a lesser degree of intra-habitat variation compared with other habitat types. Water performed well in only one of the images (CASI 101-64.16%) and for the other, a large proportion of the water class (57.51%) was misclassified as deep water swamp. This is considered to be, at least partly, due to inter-annual variation in the water surface vegetation of the deep water swamp vegetation. This would result in a shift in the spectral signature away from a response associated with vegetation to one more associated with water.

Producer accuracies for woodland/scrub habitat were over 50% for both images although a significant portion of this was misclassified as reedbed. The scrub areas on the marsh are in close proximity to the reedbed habitat and a degree of misclassification due to misalignment issues as discussed above can be expected. In addition, this may be indicative of a change in the spatial extent of scrub in this area of the marsh which was subject to intense scrub removal management practices between the data collection periods. Around half of the area of the reedbed and dense *Deschampsia* habitats were correctly classified using MLC. Although

there was a widespread of habitat types which these pixels were misclassified to, the majority were to woodland/scrub and species poor sedge habitats respectively. Habitats that did not achieve high producer accuracies were *Phalaris arundinacea* and species-poor tall sedge (*Carex aquatilis*). As the *Phalaris* habitat covers such a small area relative to all other habitats, misalignment between images as well as the proportion of pixels that are habitat boundary pixels is expected to be high and is, therefore, a source of error.

The probability maps show the areas that are most likely to be associated with these particularly sensitive habitat types. These maps should be interpreted in light of the associated producer accuracy results for each of the habitat types, although they do demonstrate the potential usefulness of the MLC technique in addition to the production of a hard classification habitat map. Probability maps could be consulted prior to a range of habitat management decisions that would benefit from the knowledge of the likelihood of locating certain species within certain areas of the marsh. This type of mapping, where each pixel is assigned a membership grade per class ('fuzzy classification'), is an attractive alternative to the hard classification output and its potential as an ecological tool is greatly underutilised (Foody 1992; Foody 1996a; Foody 1996b; Townsend 2000).

Continuum Removal/Spectral Feature Fitting

The success of Schmidt & Skidmore (2003) at discriminating between vegetation types in a saltmarsh demonstrates the potential of continuum removal for habitat discrimination and, thus, further work in this area is required. The use of the continuum removed bands alone in a supervised classification (applying Spectral Feature Fitting techniques) produced results in the present study that were lower than those achieved using the four-band spectral subsets (Table 6:19) and were in the range of 55% overall accuracies. As the resultant classes were tested against the class image from which the spectral feature datasets were constructed, these results are superficially high and, in fact, when randomly selected Regions of Interest (ROIs) were tested, the overall accuracies were much lower. The difficulty with this method may lie with the way in which the spectral feature datasets were constructed. A spectral library was

created from each habitat polygon and in doing so, spectral homogeneity per habitat class was assumed.There is little evidence from these results to suggest that the use of spectral features alone enhances habitat classification as information loss occurs in the process.

6.4.4 Objective d) Variation across habitat boundaries

Explore the relationships between spectral variability derived from airborne imagery and detailed vegetation datasets along transects.

The relationship between the two datasets compared using DCA scores was affected by the length of time between data collection and the positional inaccuracies associated with image and field-based georeferencing. Four out of the five transects considered here do not exhibit high correlations between the datasets although the vertical bars indicating points of significant ecological information are often associated with distinct peaks and troughs of the spectra DCA and a more comprehensive examination of this relationship is therefore warranted. These transects are composed of a number of habitat types rather than a transition between two and this may have compounded the effect that the assumed misalignment between the datasets had on the association between the datasets.

Despite the limitations expected, a strong correlation was apparent between the DCA scores of the vegetation dataset and the spectra obtained from the imagery along one of the five transects investigated. Transect 8.3 illustrates the close association between the beta diversity apparent in the vegetation dataset collected in the field, and that of the spectra of the pixels associated with the quadrat locations along the transect (Figure 6:33). The vertical bars in Figure 6:33c indicate the points at which the field worker identified notable changes or characteristics in the vegetation along the transect (Appendix D) and these are often closely aligned with significant changes in the DCA scores of the spectra obtained from the imagery. REIP values along the transect appear to fluctuate around a mean value however the pattern in NDVI values along the transects mirrors that of the DCA scores. These results provide strong

evidence that spectral information can be used to characterise the nature of transitional areas between semi-natural wetland habitat types.

6.5 Summary

In this section, the main conclusions drawn from this work are listed in relation to each objective and further work is also noted and recommended where applicable.

a) *Identify spectral endmembers of* a priori *and grouped habitat types.*

- Spectral signatures of wetland habitat types are similar in overall shape although variations in magnitude of reflectance are apparent between habitat types. Significant differences between habitat types are observed in the NIR and the habitats appear to be ordered in terms of varying moisture content and productivity.
- Grouping the habitat types into broader class categories produces classes that are significantly different in terms of magnitude of reflectance in the NIR although a large degree of similarity between these classes is evident in the red and green regions of the spectrum.

b) *Explore the spectral variation within the available imagery using unsupervised classifications and various spectral indices.*

- Unsupervised K-Means Classification effectively identifies very wet areas of the marsh (water and deep water swamp habitats) and very dry areas of the marsh (rush pasture/grassland). The next most promising class that can be interpreted using this method is *Sphagnum* habitats. This method could be developed further using expert knowledge and extensive fieldwork to validate findings.
- Classes of NDVI and REIP values derived using K-Means Classification were not clearly associated with most habitat boundaries. Some evidence of a relationship

between some of the habitat boundaries and these indices was apparent and further work should explore the full extent to which this is the case.

c) *Assess the potential for supervised classification to correctly classify habitat types derived from field based* a priori *habitat maps.*

- MLC performs well as a method of producing ecologically meaningful classes with overall accuracy ranging from around 65% to 75%. However, success varies between habitat types however: *Sphagnum* habitats, water, deep water swamp, dry grassland, *Molinia caerulea*-sedge mire and *Molinia caerulea-Myrica gale* mire are consistently associated with high producer accuracies.

- The use of a spectral subset resulted in overall accuracy results that were around 10% less than those obtained in equivalent analyses using all 15 CASI bands. Satellite data with high spatial resolution but few spectral bands may still achieve ecologically meaningful classifications in wetland environments and this is an area that warrants further research.

- The overall accuracies associated with the grouped habitat types were only slightly greater when compared with analyses using all *a priori* habitat types. Depending on end-user requirements, it may not be preferable to group the habitat types as some information is lost. Other class groupings could be explored in further work using the spectral endmembers illustrated above.

- Probability mapping is a useful addition to MLC output and can be exploited for use in management decisions. This should be limited to habitat types where associated producer accuracies are high or, at least, above 50%. In this respect, *Sphagnum* habitats, *C. lasiocarpa*, water and reedbed habitats performed well.

- The similarity between habitat classes in terms of reflectance in the red and green regions of the spectrum has contributed to the poor performance of spectral feature fitting as a method of habitat classification using MLC.

d) *Explore the relationships between spectral variability derived from airborne imagery and detailed vegetation datasets along transects.*

- DCA is a valuable method by which to explore the beta diversity of spectral datasets derived from imagery analysis and the associated relationships with vegetation datasets collected on the ground. A strong relationship was established using data collected along a transect spanning mixed sedge and rush pasture/grassland habitats.
- Further work is warranted to explore in more detail the changes in the beta diversity of spectra across habitat boundaries using data derived from remote sensing imagery and, how this is associated with ecological information obtained through field survey.

7 CONCLUSIONS

7.1 Introduction

Since the establishment of Ramsar Sites, the hydrological, ecological and economic values of wetlands all over the world have received growing levels of recognition. Interest in these sites is not only from conservationists but also academic institutions and the political sector. Public awareness of the need to protect semi-natural environments and enhance or at least maintain biodiversity has reached a level at which it has become a major driver of political and, consequently, research agendas. For this and other reasons, it has become necessary for the scientific community to contribute to the understanding of the environmental processes at work within wetlands and to establish firm links with those who manage wetland sites. Maintaining accurate and definable maps of vegetation type and condition is an important management goal in these areas. This research has taken important steps towards understanding the relationship between spectral data and vegetation characteristics on the ground and on the exploration of the role of remote sensing as a tool for environmental monitoring. The main scientific contributions to this area of research are summarized in this chapter.

7.2 Spectral Discrimination of Habitat Types using Field Data

7.2.1 Field Spectrometry

Six different habitat types were sampled intensively over the summer 2003. A good deal of overlap in the spectral signatures of the sample plot means was observed as well as relatively significant differences between sample plots within the same habitat types. The results presented from this study highlight the difficulties involved with using spectral signatures to characterise wetland habitat type as within-habitat variation, including differences caused by different management practices, can significantly alter the spectral response in the optical region. Despite the apparent difficulties in associating distinct spectral signatures with habitat type, Multiple Discriminant Analysis proved effective at predicting habitat type based on the spectral datasets collected (~80 – 85%). These results demonstrated that there was potential in using spectral data to discriminate between wetland habitat types and important wavebands are as follows: 380 – 394 nm, 443 – 457 nm, 459 – 473 nm, 711 – 725 nm and 758 – 773 nm.

Further analyses were carried out that focussed on determining which parts of the spectrum and which times over the summer period were most effective to use for identifying differences between habitat types. The results showed that different parts of the spectrum were significant predictors at different times. Timing of data collection for habitat discrimination is critical and August was identified as the best time over the summer period to discriminate between the six habitats in this study. This was seen to apply with the hyperspectral dataset and was less important when using the ten-band CASI dataset. Wavebands from this dataset were mostly all significant predictors over the sampling periods.

7.2.2 Multivariate analyses

Data from three transects were analysed to determine the vegetation-spectral relationship across habitat boundaries and results showed that spectra do relate to vegetation across

boundaries and, therefore, can be used as a way in which to characterize habitat boundaries. Once again phenological variation between sampling suggested that time of data collection affects the degree to which the spectra are related to the vegetation datasets. Detrended Correspondence Analysis is demonstrated here to be a good method of determining the significance of this relationship although no detailed information regarding how the spectra are changing at individual wavebands can be derived using this method.

Canonical Correspondence Analysis is an effective method of analyzing large multivariate datasets and is currently underutilised in the area of field spectrometry. This study demonstrates the wealth of information that this form of analysis can provide regarding the relationship between two multivariate datasets. The CCA results from July and September illustrate a similar pattern in the ordination of the vegetation datasets in terms of species-environment relationships, though clear distinctions between habitat types were not seen here. Significant relationships were established between the predictors and the ordination axes and a good degree of the variation in the vegetation datasets was explained (almost 50% in the case of the AVS1-42 dataset). The results were similar to those from published work on vegetation in the British uplands in that reflectance in the green and NIR regions of the spectrum were strongly correlated with the resultant ordination axes (Armitage *et al* 2004). The trend in the vegetation ordination has been reported in the literature as being related with biomass (Armitage *et al.* 2004); empirical data on sample biomass were not collected in this study, though species richness was considered and many of the structural variables that were measured could be considered as surrogates for biomass. As a result, significant correlations between sample species richness and axis I sample scores were established though canopy structure and soil moisture contents within samples are also variables that need to be investigated in further work.

7.2.3 Future Work

The results of the Principal Components Analyses illustrated differences in the axis I and II component scores between spectra collected at study plots within the same habitat type. This indicates a degree of variation in the spectral response of vegetation within a habitat that was not accounted for in the field method applied here. In order to investigate this further a stratified random method of sampling should be applied to each habitat type with samples divided into management categories. If there is no need to return to sample points over time, a random method of point sampling to collect a minimum of thirty sample points would be sufficient to then compare spectral response within a habitat and between different management regimes. However, this would be labour intensive and care should be taken to ensure that samples cover a sufficiently representative area of the habitat. In this respect, more than thirty samples or a predetermined proportion of area per habitat type would be desirable.

There has been a lack of attention in the literature to the representation of boundary characteristics and the issues relating to this in vegetation mapping (Adams 1999; Mucina 1997). This is due to the intergrading nature between areas that are otherwise different enough in nature to classify as separate units although there is often no clearly defined division between them (Arnot *et al.* 2004). The relationship between spectra and vegetation datasets across habitat boundaries warrants further research as this is an area largely under explored in the literature. Field studies designed to investigate the relationship between biophysical parameters and spectral response along transects should be repeated a number of times at points along the same boundary in order to establish the significance of the relationship. Conducting this across a number of different habitat types is a labour intensive and time consuming process and this is a major limitation of field spectrometry in this research area.

7.3.1 Determining Ecological Meaningful Classes

The ability to accurately map vegetation composition and structure in detail is an important goal in spatial ecology. The need to understand the relationship between vegetation structure, development and spatial distribution with environmental variables and anthropogenic influences will always remain a key research and management challenge. In relation to this, is the need to understand vegetation change through time whether it be natural or induced through management routines (Schmidt & Skidmore 2003; Bregt *et al.* 2002). Remote sensing as an objective method of vegetation classification and mapping at scales amenable to ecological studies and research objectives is an important ecological tool that is still largely underutilised. In order to establish the potential of remote sensing in this area, the direct nature of the relationship between what are deemed ecologically meaningful habitat classes and remote sensing data itself has been explored in this study.

Both supervised and unsupervised classifications were applied in this study and both are subject to criticisms. Supervised classification largely ignores the dynamic nature and vaguely defined boundaries of vegetation communities (Kent *et al.* 1997) and unsupervised classification produces classes determined by computed cluster analyses, described by labels or qualitative terms, which are rarely characterized by any botanically or ecologically accepted criteria (Lewis 1994). In this study a habitat map from an *a priori* ecological survey of Insh Marshes was provided for reference and related to airborne imagery of the area; supervised classification accuracies at and above ~70% were achieved. To use such datasets in this manner is a limitation as they are acknowledged as being simplifications of what is actually on the ground although at the same time, a level of generalization is required if vegetation is to be represented in a meaningful and readily interpretable way (Brook & Kenkel 2002). The way in which remote sensing data relates to vegetation data at various

scales of generalization is not explored in this study but is an area that warrants further research (Foody & Curran 1994; Goodchild & Quattrochi 1997). Fuzzy set theory and plant functional types, for example, are methods of vegetation classification that may relate to remote sensing data in a more effective manner than classification based on floristics alone (Pillar 1999; Mascarilla 1997; Mucina 1997; Wang *et al.* 2004).

7.3.2 Airborne Remote Sensing as a Management Tool

Although airborne remote sensing will never replace the need for detailed vegetation surveys on the ground, the wealth of information that it may provide is of great significance to wetland managers as illustrated by the probability maps produced in this study. Much of the work that is carried out under the auspices of routine field sampling can, in addition, be utilised for the training of remote sensing data, although certain adaptations to the sampling strategy may be necessary. This is a point that should be discussed in detail between ecologists and vegetation scientists and those skilled in remote sensing applications. The use of soft classification techniques as an insight into the probability distribution of species or vegetation assemblages is underutilised by wetland managers and is a relatively straightforward aspect of image analysis. More complex predictive modeling is an area of great potential, particularly where additional ancillary or remote sensing datasets are utilised. As the relationship between management and the spatial distribution of vegetation and the associated spectral response is better understood, this will feature increasingly in the ecological literature.

7.3.3 Future Work

Imaging radar and Light Detection And Ranging (LiDAR) data are considered of great potential in ecologically-oriented remote sensing studies due to their immunity to cloud cover and atmospheric conditions (Ozesmi & Bauer 2002; Steven *et al.* 1995). Given the fine spatial resolution offered by airborne LiDAR missions this is a method that has much to offer in

ecological studies (Paris 1990; Turner *et al.* 2003; Toyra & Pietronito 2005). Similar to remote sensing data in the optical region, LIDAR datasets would require a good deal of fieldwork to determine the nature of the relationship between the vegetation on the ground and the LiDAR imagery. However, the combination of LiDAR with optical data may prove very beneficial in the identification of wetland habitat classes, as demonstrated recently in a study on wetland vegetation characterisation in Alberta, Canada (Toyra & Pietronito 2005; Hill & Thomson 2005). The LiDAR data proved to be sufficiently detailed to detect the subtle topographic patterns in this relatively flat region and accurate information regarding vegetation structure can prove hugely beneficial to wetland managers. This is certain to be an area that will be explored in the literature imminently and one that warrants further research (Mertes 2002).

Multi-temporal approaches to vegetation mapping have generally proven more accurate than single date approaches (Townshend & Justice 1986; Lloyd 1990; Millington *et al.* 1994; Stone *et al.* 1994). Results presented from this study show how the spectral response of vegetation can change over just three months. The nature of the vegetation change within and between habitat types, and how this relates to spectral response is an area in which questions still remain. Reed *et al.* (1994) demonstrated the utility of remotely sensed data as input data for vegetation mapping by showing a distinct phenology of several land cover types (Mucher *et al.* 2000). If this was better resolved at finer scales, such as the habitat scale considered in the present study and, temporal datasets were also available, the potential for accurate wetland habitat and vegetation characterisation using remote sensing data is great.

It has been demonstrated here that airborne imagery can be interpreted in terms of habitat type using classes predefined by ecological survey. The concept of spectral libraries is an area that was not explored in this study due to the nature of the dataset although their use should be explored in future work. For this to be plausible, an image collected at the same time of year should be used where the spatial and spectral resolutions are comparable. Images should then be atmospherically corrected and normalised to each other and then a spectral library derived

from one image can be applied and tested on another. A good degree of confidence in the relationship between the samples used to derive the spectral library should be validated by work on the ground.

7.4 Main Contributions

7.4.1 Contributions to the Remote Sensing of Wetlands

There is very little literature concerning the spectral signatures of inland wetland habitat types and this study serves as an important contribution to this area of research. A good deal of overlap was identified between habitats although reflectance in the NIR illustrated a trend in habitat type that could be related with degrees of wetness. Multivariate analyses provide a good insight into the detailed relationships between spectral variation and vegetation datasets and results here serve as the first of their kind in wetland environments. Further work is necessary to fully understand the trends in this evidently complex relationship. However, it is believed that the work presented here will serve as a good reference for future work in this area. The results of the supervised classifications prove that wetlands can be effectively mapped into ecologically meaningful classes at the habitat scale which few previous studies have attempted to achieve.

7.4.2 Contributions to Wetland Ecology and Management

This work demonstrates the relationship between spectra and vegetation datasets across habitat boundaries and the use of spectral data in the characterisation of habitat boundaries. Multivariate analyses that are well understood in the vegetation sciences are demonstrated here as being an effective method by which to assess the nature of the relationship between spectral and vegetation datasets. Species richness is a well used parameter in vegetation studies and results from this study illustrate a significant relationship between this and spectra. Although additional field work is required to determine the full nature of this

relationship the benefits that extensive information on species richness offers to wetland managers is great. Remote sensing offers an objective and repeatable method of data collection and this study illustrates that the relationship between ecologically meaningful classes at the habitat scale and spectra collected by airborne imagery is significant enough to be utilised as a tool in the understanding of the spatial and temporal dynamics of wetland vegetation.

7.5 Final Conclusions and Recommendations

Most traditional vegetation mapping techniques have been developed by ecologists and biogeographers (Millington & Alexander 2000) and not by remote sensing specialists. However it is often the ecologists and biogeographers who are the 'end-users' and as technology advances and remotely sensed imagery is increasingly exploited, a perceivable knowledge and communication gap between ecologists and remote sensing specialists has become apparent (Roughgarden 1991). Lewis (1994) writes that, as well as changes in ecological paradigms and improved dialogue between disciplines, attention must be brought to the gap between conventional remote sensing classification methodologies and the more traditional approaches to ground-based vegetation mapping. Work over the last decade has seen a bridging of this relationship, although it is widely acknowledged that our ecological understanding of the remote sensing-vegetation relationship is largely underdeveloped at many scales and in many ecosystems, not least, the wetland environment. This study provides a much needed basis for research in this area by utilising ecological analyses and ecologically defined datasets in conjunction with remote sensing data and methods of analysis.

There were a number of general limitations encountered during this research. The major limitations are listed below:

- Long lasting clear-weather windows are uncommon in Scotland even during the summer months. As such, field spectrometry presents many practical limitations

regarding the extent to which a seasonal and widespread sampling is possible in practice.

- The sensitivity of the wetland habitats under study and, the associated timing of the breeding and nesting season for wetland birds, caused there to be limited access at certain times thereby shortening the length of time available for sampling prior to the start of the growing season.
- Semi-natural wetland vegetation and habitat types are made up of mixed species vegetation assemblages and therefore there will always be spectral overlap between habitat types that are composed of similar species.
- Neither metadata nor any information regarding data quality were provided with the *a priori* habitat data for this study and used as a 'ground-truth' dataset in this research. As a result, it was not possible to ascertain the degree to which geometrical accuracy, boundary definitions and classification methods may have affected the success of the classifications carried out.
- The results presented in this study have not been validated at the site using data from further sampling in proceeding years. In addition to this, the transferability of the methods used were not investigated in other wetland sites. These are areas of research where further work is recommended.

The objectives set out at the front of this thesis are listed below along with the important conclusions and any recommendations that are associated with them.

1. Determine the extent to which wetland habitats are spectrally distinct.

- It is possible to distinguish between wetland habitat types as defined by *a priori* vegetation surveys using spectral data in the visible and NIR wavebands using Multiple Discriminant Analysis.
- Hyperspectral datasets do not necessarily perform better than smaller multispectral datasets, such as those collected using CASI.

- Using Canonical Correspondence Analysis a significant proportion of the variation present in detailed wetland vegetation datasets can be predicted using spectral data.
- Spectra can be used as an effective surrogate for beta diversity within vegetation datasets across habitat boundaries.

3. Assess the potential of high spatial resolution multispectral airborne imagery for classifying and characterising wetland habitats.

- Airborne imagery can be interpreted using ecologically meaningful classes and acceptable classification accuracies can be achieved using supervised classification methodologies.
- Remote sensing data obtained from airborne imagery can be related to vegetation datasets collected along transects on the ground and a good relationship can be established which can aid in the characterisation of habitat boundaries.

REFERENCE LIST

Adams, J.M. (1999) A suggestion for an improved vegetation scheme for local and global mapping and monitoring. *Environmental Management* **23**, 1-13.

Agostinho, A.A., Thomaz, S.M. and Gomes, L.C. (2005) Conservation of the biodiversity of Brazil's inland waters. *Conservation Biology* **19**, 646-652.

Anderson, J.E. and Perry, J.E. (1996) Characterization of Wetland Plant Stress using Spectral Reflectance: Implications for Wetland Remote Sensing. *Wetlands* **16**, 477-487.

Andrefouet, S., Payri, C., Hochberg, E.J., Hu, C.M., Atkinson, M.J. and Muller-Karger, F.E. (2004) Use of in-situ and airborne reflectance for scaling-up spectral discrimination of coral reef macroalgae from species to communities. *Marine Ecology-Progress Series* **283**, 161-177.

Aplin, P. (2005) Remote Sensing: Ecology. *Progress in Physical Geography* **29**, 104-113.

Armitage, R.P., Kent, M. and Weaver, R.E. (2004) Identification of the spectral characteristics of British semi-natural upland vegetation using direct ordination: a case study from Dartmoor, UK. *International Journal of Remote Sensing* **25**, 3369-3388.

Armitage, R.P., Weaver, R.E. and Kent, M. (2000) Remote Sensing of Semi-Natural Upland Vegetation: the Relationship between Species Composition and Spectral Respone. In: Alexander, R.W. and Millington, A.C., (Eds.) *Vegetation mapping: From Patch to Planet*, Chichester: John Wiley & Sons

Arnot, C., Fisher, P.F., Wadsworth, R. and Wellens, J. (2004) Landscape metrics with ecotones: pattern under uncertainty. *Landscape Ecology* **19**, 181-195.

ARSF (2005) Website. Url: http://www.nerc.ac.uk/arsf/pages/aircraft/aircraftmain.htm, accessed 21-03-05.

ASD (2001) Website: Field Spectrometry: Techniques and Instrumentation. Url: http:// www.asdi.com, accessed 28-09-04.

Atkinson, P.M. (1993) The effect of spatial-resolution on the experimental variogram of airborne mss imagery. *International Journal of Remote Sensing* **14**, 1005-1011.

Atkinson, P.M. and Curran, P.J. (1995) Defining an optimal size of support for remote-sensing investigations. *IEEE Transactions on Geoscience and Remote Sensing* **33**, 768-776.

Atkinson, P.M. and Curran, P.J. (1997) Choosing an Appropriate Spatial Resolution for Remote Sensing Investigations. *Photogrammetric Engineering & Remote Sensing* **63**, 1345-1351.

Atkinson, P.M. and Emery, D.R. (1999) Exploring the Relation between Spatial Structure and Wavelength: Implications for Sampling Reflectance in the Field. *International Journal of Remote Sensing* **20**, 2663-2678.

Atkinson, P.M. and Lewis, P. (2000) Geostatistical classification for remote sensing: an introduction. *Computers & Geosciences* **26**, 361-371.

Bachmann, C.M., Donato, T.F., Lamela, G.M., Rhea, W.J., Bettenhausen, M.H., Fusina, R.A., Du Bois, K.R., Porter, J.H. and Truitt, B.R. (2002) Automatic classification of land cover on Smith Island,VA, using hymap imagery. *IEEE Transactions on Geoscience and Remote Sensing* **40**, 2313-2330.

Baines, M. (1992) A beetle survey of the Insh Marshes RSPB Reserve. Unpublished report for the RSPB.

Baranoski, G.V.G. and Rokne, J.G. (2005) A practical approach for estimating the red edge position of plant leaf reflectance. *International Journal of Remote Sensing* **26**, 503-521.

Bartlett, D.S. and Klemas, V. (1980) Quantitative assessment of tidal wetlands using remote-sensing. *Environmental Management* **4**, 337-345.

Basham May, M.A., Pinder, J.E.I. and Kroh, G.C. (1997) A Comparison of Landsat Thematic Mapper and SPOT Multi-spectral Imagery for the Classification of Shrub and Meadow Vegetation in Northern California, U.S.A. *International Journal of Remote Sensing* **18**, 3719-3728.

Becker, B.L., Lusch, D.P. and Qi, J. (2005) Identifying optimal spectral bands from in situ measurements of Great Lakes coastal wetlands using second-derivative analysis . *Remote Sensing of Environment* **97**, 238-248.

Beaumont, D., Prescott, T., Rout, F., Street, L. and Fraser, P. (1998) The first twenty-five years of the Insh Marshes, RSPB Nature Reserve, Inverness-shire. *RSPB Conservation Review* **12**, 102-110.

Becker, B.L., Lusch, D.P. and Qi, J. (2005) Identifying optimal spectral bands from in-situ measurements of Great Lakes coastal wetlands using second-derivative analysis . *Remote Sensing of Environment* **97**, 238-248.

Bell, I.E. and Baranoski, G.V.G. (2004) Reducing the dimensionality of plant spectral databases. *IEEE Transactions on Geoscience and Remote Sensing* **42**, 570-576.

Bhattarai, K.R., Vetaas, O.R. and Grytnes, J.A. (2004) Relationship between plant species richness and biomass in an arid sub-alpine grassland of the Central Himalayas, Nepal. *Folia Geobotanica* **39**, 57-71.

Biondi, E., Feoli, E. and Zuccarello, V. (2004) Modelling environmental responses of plant associations: a review of some critical concepts in vegetation study. *Critical Reviews in Plant Sciences* **23**, 149-156.

Blackburn, G.A. (1999) Relationships between spectral reflectance and pigment concentrations in stacks of deciduous broadleaves. *Remote Sensing of Environment* **70**, 224-237.

Blackburn, G.A. and Milton, E.J. (1995) Seasonal-variations in the spectral reflectance of deciduous tree canopies. *International Journal of Remote Sensing* **16**, 709-720.

Blackburn, G.A. and Steele, C.M. (1999) Towards the remote sensing of matorral vegetation physiology: relationships between spectral reflectance, pigment, and biophysical characteristics of semi-arid bushland canopies. *Remote Sensing of Environment* **70**, 278-292.

Boles, S.H., Xiao, X., Liu, J., Zhang, Q., Munkhtuya, S., Chen, S. and Ojima, D. (2004) Land cover characterization of temperate East Asia using multi-temporal VEGETATION sensor data. *Remote Sensing of Environment* **90**, 477-489.

Boochs, F., Kupfer, G., Dockter, K. and Kuhbauch, W. (1990) Shape of the red edge as vitality indicator for plants. *International Journal of Remote Sensing* **11**, 1741-1753.

Bragazza, L. and Gerdol, R. (1999) Hydrology, groundwater chemistry and peat chemistry in relation to habitat conditions in a mire on the south-eastern alps of Italy. *Plant Ecology* **144**, 243-256.

Bregt, A.K., Skidmore, A.K. and Nieuwenhuis, G. (2002) Environmental modelling: issues and discussion. In: Skidmore, A., (Ed.) *Environmental Modelling with GIS and Remote Sensing*, pp. 252-259. London: Taylor & Francis

Brook, R.K. and Kenkel, N.C. (2002) A Multivariate Approach to Vegetation Mapping of Manitoba's Hudson Bay Lowlands. *International Journal of Remote Sensing* **23**, 4761-4776.

Campbell, J.B. (2002) *Introduction to Remote Sensing*, 3rd Edition. Taylor & Francis, London.

Carpenter, G.A., Gopal, S., Macomber, S., Martens, S. and Woodcock, C.E. (1999a) A neural network method for mixture estimation for vegetation mapping. *Remote Sensing of Environment* **70**, 138-152.

Carpenter, G.A., Gopal, S., Macomber, S., Martens, S., Woodcock, C.E. and Franklin, J. (1999b) A neural network method for efficient vegetation mapping. *Remote Sensing of Environment* **70**, 326-338.

Carter, G.A. (1993) Responses of leaf spectral reflectance to plant stress. *American Journal of Botany* **80**, 239-243.

Carter, G.A., Knapp, A.K., Anderson, J.E., Hoch, G.A. and Smith, M.D. (2005) Indicators of plant species richness in AVIRIS spectra of a mesic grassland. *Remote Sensing of Environment* **98**, 304-316.

Cherrill, A. and Mcclean, C. (1995) An investigation of uncertainty in-field habitat mapping and the implications for detecting land-cover change. *Landscape Ecology* **10**, 5-21.

Cherrill, A.J., Mcclean, C., Lane, A. and Fuller, R.M. (1995) A comparison of land-cover types in an ecological field survey in northern England and a remotely-sensed land-cover map of Great-Britain. *Biological Conservation* **71**, 313-323.

Choesin, D. and Boerner, R.E.J. (2002) Vegetation boundary detection: a comparison of two approaches applied to field data. *Plant Ecology* **158**, 85-96.

Christensen, S. and Goudriaan, J. (1993) Deriving light interception and biomass from spectral reflectance ratio. *Remote Sensing of Environment* **43**, 87-95.

Chust, G., Ducrot, D., Riera, J.L.L. and Pretus, J.L.L. (1999) Characterising human-modelled landscapes at a stationary state: a case study of Minorca, Spain. *Environmental Conservation* **26**, 322-331.

Cihlar, J. (2000) Land cover mapping of large areas from satellites: Status and research priorities. *International Journal of Remote Sensing* **21**, 1093-1114.

Cingolani, A.M., Renison, D., Zak, M.R. and Cabido, M.R. (2004) Mapping vegetation in a heterogeneous mountain rangeland using Landsat data: an alternative method to define and classify land-cover units. *Remote Sensing of Environment* **92**, 84-97.

Clark, R.N. and Roush, T.L. (1984) Reflectance spectroscopy: Quantitative analysis techniques or remote sensing applications. *Journal of Geophysical Research* **10**, 6329-6340.

Clevers, J.G.P.W., de Jong, S.M., Epema, G.F., van der Meer, F., Bakker, W.H., Skidmore, A.K. and Addink, E.A. (2001) MERIS and the red-edge position. *Journal of Applied Geography* **3**, 313-320.

Clevers, J.G.P.W.D.L.S.M.E.G.F., Van Der Meer, B., Bakker, W.H., Skidmore, A.K. and Scholte, K.H. (2002) Derivation of the red edge index using the MERIS standard band setting. *International Journal of Remote Sensing* **23**, 3169-3184.

Cliff, A.D. and Ord, J.K. (1973) *Spatial autocorrelation*, Pion, London.

Cochrane, M.A. (2000) Using vegetation reflectance variability for species level classification of hyperspectral data. *International Journal of Remote Sensing* **21**, 2075-2087.

Comber, A., Fisher, P. and Wadsworth, R. (2004) Integrating land-cover data with different ontologies: Identifying change from inconsistency. *International Journal of Geographical Information Science* **18**, 691-708.

Coops, N.C., Stone, C., Culvenor, D.S., Chisholm, L.A. and Merton, R.N. (2003) Chlorophyll content in Eucalypt vegetation at the leaf and canopy scales as derived from high resolution spectral data. *Tree Physiology* **23**, 23-31.

Cortes, C. and Vapnik, V. (1995) Support-vector networks. *Machine Learning* **20**, 273-297.

Curran, P.J. (1980) Multispectral Remote Sensing of vegetation amount. *Progress in Physical Geography* **4**, 315-341.

Curran, P.J. (1981) Problems in the remote sensing of vegetation canopies for biomass estimation. In: Fuller, R.M. (Ed.) Ecological Mapping from ground, air and space. pp. 84-100

Curran, P.J. (1983) Multispectral remote-sensing for the estimation of green leaf- area index. *Philosophical Transactions of the Royal Society of London Series a-Mathematical Physical and Engineering Sciences* **309**, 257-270.

Curran, P.J. (1988) The semivariogram in remote-sensing - an introduction. *Remote Sensing of Environment* **24**, 493-507.

Curran, P.J., Dungan, J.L. and Gholz, H.L. (1992a) Seasonal LAI in slash pine estimated with Landsat TM. *Remote Sensing of Environment* **39**, 3-13.

Curran, P.J., Dungan, J.L., Macler, B.A., Plummer, S.E. and Peterson, D.L. (1992b) Reflectance spectroscopy of fresh whole leaves for the estimation of chemical concentration. *Remote Sensing of Environment* **39**, 153-166.

Curran, P.J., Dungan, J.L. and Peterson, D.L. (2001) Estimating the foliar biochemical concentration of leaves with reflectance spectrometry testing the Kokaly and Clark methodologies. *Remote Sensing of Environment* **76**, 349-359.

Curran, P.J., Windham, W.R. and Gholz, H.L. (1995) Exploring the relationship between reflectance red edge and chlorophyll concentration in slash pine leaves. *Tree Physiology* **15**, 203-206.

Danson F.M. (1995) Developments in the Remote Sensing of Forest Canopy Structure. In: Danson, F.M. and S.E. Plummer, (Eds.) *Advances in Environmental Remote Sensing*, pp. 53-69. John Wiley & Sons, Chichester.

Dash, J. and Curran, P.J. (2004) The meris terrestrial chlorophyll index. *International Journal of Remote Sensing* **25**, 5403-5413.

Davids, C. and Tyler, A.N. (2003) Detecting contamination-induced trees within the Chernobyl exclusion zone. *Remote Sensing of Environment* **85**, 1, 30-38.

Davis, F.W., Stine, P.A. and Stoms, D.M. (1994) Distribution and conservation status of coastal sage scrub in southwestern California. *Journal of Vegetation Science* **5**, 743-756.

Dawson, T.P. and Curran, P.J. (1998) A new technique for intepolating the reflectance red edge position. International Journal of Remote Sensing 19, 2133-2139.

Dawson, T.P., Curran, P.J. and Plummer, S.E. (1998) Liberty - Modeling the effects of leaf biochemical concentration on reflectance spectra. *Remote Sensing of Environment* **65**, 50-60.

Dechka, J.A., Franklin, S.E., Watmough, M.D., Bennett, R.P. and Ingstrup, D.W. (2002) Classification of wetland habitat and vegetation communities using multi-temporal IKONOS imagery in southern Saskatchewan. *Canadian Journal of Remote Sensing* **28**, 679-685.

Defries, R.S. and Townshend, J.R.G. (1994) NDVI-derived land-cover classifications at a global-scale. *International Journal of Remote Sensing* **15**, 3567-3586.

Dejong, S.M. and Burrough, P.A. (1995) A fractal approach to the classification of Mediterranean vegetation types in remotely-sensed images. *Photogrammetric Engineering and Remote Sensing* **61**, 1041-1053.

Dobrowski, S.Z., Pushnik, J.C., Zarco-Tejada, P.J. and Ustin, S.L. (2005) Simple reflectance indices track heat and water stress-induced changes in steady-state chlorophyll fluorescence at the canopy scale. *Remote Sensing of Environment* **97**, 403-414.

Doren, R.F., Rutchey, K. and Welch, R. (1999a) The everglades: A perspective on the requirements and applications for vegetation map and database products. *Photogrammetric Engineering and Remote Sensing* **65**, 155-161.

Doren, R.F., Rutchey, K. and Welch, R. (1999b) The Everglades: A perspective on the requirements and applications for vegetation map and database products. *Photogrammetric Engineering and Remote Sensing* **65**, 155-161.

Duncan, J., Stow, D., Franklin, J. and Hope, A. (1993) Assessing the relationship between spectral vegetation indexes and shrub cover in the Jornada basin, New-Mexico. *International Journal of Remote Sensing* **14**, 3395-3416.

Ekebom, J. and Erkkila, A. (2003) Using aerial photography for identification of marine and coastal habitats under the EU's habitats directive. *Aquatic Conservation-Marine and Freshwater Ecosystems* **13**, 287-304.

Elvidge, C.D. and Chen, Z.K. (1995) Comparison of broad-band and narrow-band red and near-infrared vegetation indexes. *Remote Sensing of Environment* **54**, 38-48.

Engstrom, R.N., Hope, A.S., Stow, D.A., Vourlitis, G.L. and Oechel, W.C. (2002) Priestley-Taylor alpha coefficient:variability and relationship to NDVI in Arctic tundra landscapes. *Journal of the American Water Resources Association* **38**, 1647-1659.

ENVI (2003) *ENVI User's Guide*, Research Systems Inc., United States of America.

Fensham, R.J. and Fairfax, R.J. (2002) Aerial photography for assessing vegetation change: A review of applications and the relevance of findings for Australian vegetation history. *Australian Journal of Botany* **50**, 415-429.

Filella, I. and Penuelas, J. (1994) The red edge position and shape as indicators of plant chlorophyll content, biomass and hydric status. *International Journal of Remote Sensing* **15**, 1459-1470.

Fisher, J. and Acreman, M.C. (2004) Wetland nutrient removal: A review of the evidence. *Hydrology and Earth System Sciences* **8**, 673-685.

Fitzgerald, R.W. and Lees, B.G. (1994) Assessing the classification accuracy of multisource remote- sensing data. *Remote Sensing of Environment* **47**, 362-368.

Fojt, W., Kirby, K., McLean, I., Palmer, M. and Pienkowski, M. (1987) The national importance of the Insh Marshes, Scotland. Chief Scientist's Directorate, Peterborough: NCC.

Foody, G.M. (1992) A fuzzy-sets approach to the representation of vegetation continua from remotely sensed data - an example from lowland heath. *Photogrammetric Engineering and Remote Sensing* **58**, 221-225.

Foody, G.M. (1996a) Fuzzy modelling of vegetation from remotely sensed imagery. *Ecological Modelling* **85**, 3-12.

Foody, G.M. (1996b) Approaches for the production and evaluation of fuzzy land cover classifications from remotely-sensed data. *International Journal of Remote Sensing* **17**, 1317-1340.

Foody, G.M. and Curran, P.J. (1994) Scale and Environmental Remote Sensing. In: Foody, G.M. and Curran, P.J., (Eds.) *Environmental Remote Sensing from Regional to Global Scales*, pp. 223-232. Chichester: Wiley

Foody, G.M. and Cutler, M.E.J. (2003) Tree biodiversity in protected and logged bornean tropical rain forests and its measurement by satellite remote sensing. *Journal of Biogeography* **30**, 1053-1066.

Fortin, M.J., Drapeau, P. and Legendre, P. (1989) Spatial auto-correlation and sampling design in plant ecology. *Vegetatio* **83**, 209-222.

Fortin, M.-J., Olson, R.J., Ferson, S., Iverson, L., Hunsaker, C., Edwards, G., Levine, D., Butera, K. and Klemas, V. (2000) Issues related to the detection of boundaries. *Landscape Ecology* **15**, 453-466.

Franklin, J. (1995) Predictive Vegetation Mapping: Geographic Modelling of Biospatial Patterns in relation to Environmental Gradients. *Progress in Physical Geography* **19**, 474-499.

Franklin, S.E., Gillespie, R.T., Titus, B.D. and Pike, D.B. (1994) Aerial and satellite sensor detection of *Kalmia-angustifolia* at forest regeneration sites in Central Newfoundland. *International Journal of Remote Sensing* **15**, 2553-2557.

Frederiksen, P. and Lawesson, J.E. (1992) Vegetation types and patterns in Senegal based on multivariate analysis of field and NOAA-AVHRR satellite data. *Journal of Vegetation Science* **3**, 535-544.

Gamon, J.A., Field, C.B., Goulden, M.L., Griffin, K.L., Hartley, A.E., Joel, G., Penuelas, J. and Valentini, R. (1995) Relationships between ndvi, canopy structure, and photosynthesis in 3 californian vegetation types. *Ecological Applications* **5**, 28-41.

Gamon, J.A., Huemmrich, K.F., Peddle, D.R., Chen, J., Fuentes, D., Hall, F.G., Kimball, J.S., Goetz, S., Gu, J., Mcdonald, K.C., Miller, J.R., Moghaddam, M., Rahman, A.F., Roujean, J.L., Smith, E.A., Walthall, C.L., Zarco-Tejada, P., Hu, B., Fernandes, R. and Cihlar, J. (2004) Remote sensing in boreas: Lessons leamed. *Remote Sensing of Environment* **89**, 139-162.

Gilvear, D.J. and Bradley, C. (2000) Hydrological monitoring and surveillance for wetland conservation and management; a UK perspective. *Phys. Chem. Earth (B)* **25**, 571-588.

Gilvear, D.J. and Watson, A. (1995) The Use of Remotely Sensed Imagery for Mapping Wetland Water Table Depths: Insh Marshes, Scotland. In: Hughes, J.M.R. and Heathwaite, A.L., (Eds.) *Hydrology and Hydrochemistry of British Wetlands*, pp. 419-430. John Wiley & Sons, Chichester, England.

Gleason, H.A. (1926) The individualistic concept of the plant association. *Bulletin of the Torrey Botanical Club* **53**, 7-26.

Gleason, H.A. (1939) The individualistic concept of the plant association. *American Midland Naturalist* **21**, 92-110.

Goel, N.S. (1988) Models of Vegetation Canopy Reflectance and their Use in Estimation of Biophysical Parameters from Reflectance Data. *Remote Sensing Reviews* **4**, 1-212.

Goel, N.S. and Qin, W. (1994) Influences of canopy architecture on relationships between various vegetation indices and LAI and FPAR: A computer simulation. *Remote Sensing Reviews* **10**, 309-347.

Goodchild, M.F. (1994) Integrating GIS and Remote Sensing for Vegetation Analysis and Modelling: Methodological Issues. *Journal of Vegetation Science* **5**, 615-626.

Goodchild, M.F. and Quattrochi, D.A. (1997) Scale, Multiscaling, Remote Sensing and GIS. In: Quattrochi, D.A. and Goodchild, M.F., (Eds.) *Scale in Remote Sensing and GIS*, pp. 1-11. Lewis Publishers, USA.

Goodwin, N., Turner, R. and Merton, R. (2005) Classifying Eucalyptus forests with high spatial and spectral resolution imagery: an investigation of individual species and vegetation communities. *Australian Journal of Botany* **53**, 337-345.

Gough, L., Grace, J.B. and Taylor, K.L. (1994) The relationship between species richness and community biomass - the importance of environmental variables. *Oikos* **70**, 271-279.

Gourmelon, F. (2002) Classification of digital orthophotographs for large-scale mapping of terrestrial plants. *Canadian Journal of Remote Sensing* **28**, 168-174.

Goward, S.N., Davis, P.E., Fleming, D., Miller, L. and Townshend, J.R. (2003) Empirical comparison of Landsat 7 and ikonos multispectral measurements for selected earth observation system (eos) validation sites. *Remote Sensing of Environment* **88**, 80-99.

Green, D.R., Cummins, R., Wright, R. and Miles, J. (1993) A methodology for acquiring information on vegetation succession from remotely sensed imagery. In: Haines-Young, R. , Green, D.R. and Cousins, S., (Eds.) *Landscape Ecology and Geographic Systems*, pp. 111-128. London: Taylor & Francis]

Grieve, I.C., Gilvear, D.J. and Bryant, R.G. (1995) Hydrochemical and Water Source Variations across a Floodplain Mire, Insh Marshes, Scotland. *Hydrological Processes* **9**, 99-110.

Griffiths, G.H., Lee, J. and Eversham, B.C. (2000) Landscape pattern and species richness; regional scale analysis from remote sensing. *International Journal of Remote Sensing* **21**, 2685-2704.

Grime, J.P. (1973) Competitive exclusion in herbaceous vegetation. *Nature* **242**, 344-347.

Gross, M.F., Hardisky, M.A. and Klema, V. (1988) Effects of Solar Angle on Reflectance from Wetland Vegetation. *Remote Sensing of Environment* **26**, 195-212.

Gross, M.F., Hardisky, M.A., Wolf, P.L. and Klemas, V. (1993) Relationships among *Typha* biomass, pore water methane, and reflectance in a Delaware (USA) brackish marsh. *Journal of Coastal Research* **9**, 339-355.

Guisan, A. and Zimmermann, N.E. (2000) Predictive habitat distribution models in ecology. *Ecological Modelling* **135**, 147-186.

Haack, B. (1996) Monitoring wetland changes with remote sensing: an East African example. *Environmental Management* **20**, 411-419.

Haboudane, D., Miller, J.R., Patty, E., Zarco-Tejada, P.J. and Strachan, I.B. (2004) Hyperspectral vegetation indices and novel algorithms for predicting green LAI of crop canopies: Modelling and validation in the context of precision agriculture. *Remote Sensing of Environment* **90**, 337-352.

Hansen, P.M. and Schjoerring, J.K. (2003) Reflectance measurement of canopy biomass and nitrogen status in wheat crops using normalized difference vegetation indices and partial least squares regression. *Remote Sensing of Environment* **86**, 542-553.

Harvey, K.R. and Hill, G.J.E. (2001) Vegetation mapping of a tropical freshwater swamp in the Northern Territory, Australia: A comparison of aerial photography, Landsat TM and spot satellite imagery. *International Journal of Remote Sensing* **22**, 2911-2925.

Heathwaite, A.L. (1995) Overview of the Hydrology of British Wetlands. In: Hughes, J.M.R. and Heathwaite, A.L., (Eds.) *Hydrology and Hydrochemistry of British Wetlands*, pp. 11-20. John Wiley & Sons Ltd., England.

Heathwaite, A.L., Eggelsmann, R. and Göttlich, K.H. (1993) Ecohydrology, mire drainage and mire conservation. In: Heathwaite, A.L. and Göttlich, K.H., (Eds.) *Mires: Process, Exploitations Conservation*, pp. 417-484. John Wiley & Sons, Chichester.

Hill, M.O. (1974) Correspondence Analysis - neglected multivariate method. *Journal of the Royal Statistical Society Series C-Applied Statistics* **23**, 340-354.

Hill, M.O. (1979) *TWINSPAN-a FORTRAN for arranging multi-variate data in an ordered two-way table by classification of the individuals and attributes.*, New York: Cornell University, Ithaca.

Hill, M.O., Bunce, R.G.H. and Shaw, M.W. (1975) Indicator species analysis, a divisive polythetic method of classification, and its application to a survey of native pinewoods in Scotland. *Journal of Ecology* **63**, 597-613.

Hill, M.O. and Gauch, H.G.Jr. (1980) Detrended Correspondence Analysis: an improved ordination technique. *Vegetatio* **42**, 47-58.

Hill, R.A. and Thomson, A.G. (2005) Mapping woodland species composition and structure using airborne spectral and LiDAR data. *International Journal of Remote Sensing* **26** (17), 3763-3779.

Hillbricht-Ilkowska, A. (2002) Links between landscape, catchment basin, wetland, and lake: the Jorka river-lake system (masurian lakeland, Poland) as the study object. *Polish Journal of Ecology* **50**, 411-425.

Hirata, M., Koga, N., Shinjo, H., Fujita, H., Gintzburger, G. and Miyazaki, A. (2001) Vegetation Classification by Satellite Image Processing in a dry area of North-Eastern Syria. *International Journal of Remote Sensing* **22**, 507-516.

Hobbs, R.J. (1990) Remote Sensing of Spatial and Temporal Dynamics of Vegetation. In: Hobbs, R.J. and Mooney, H.A., (Eds.) *Remote Sensing of Biosphere Functioning*, pp. 203-219. New York: Springer-Verlag]

Hodge, J.G.W. (1993) Scrub encroachment at Insh Marshes Nature Reserve Unpublished report: RSPB, Edinburgh.

Horler, D.N.H., Dockray, M. and Barber, J. (1983) The red edge of plant leaf reflectance. *International Journal of Remote Sensing* **4**, 273-288.

Huang, Z., Turner, B.J., Dury, S.J., Wallis, I.R. and Foley, W.J. (2004) Estimating foliage nitrogen concentration from hymap data using continuum removal analysis. *Remote Sensing of Environment* **93**, 18-29.

Hughes, J.M.R. and Heathwaite, A.L. (1995) *Hydrology and Hydrochemistry of British Wetlands*, John Wiley & Sons, England.

Hughes, J.M.R. and Johnes, P.J. (1995) Overview of the Ecology and Management of British Wetlands. In: Hughes, J.M.R. and Heathwaite, A.L., (Eds.) *Hydrology and Hydrochemistry of British Wetlands*, pp. 317-324. John Wiley & Sons, England.

Hurcom, S.J. and Harrison, A.R. (1998) The ndvi and spectral decomposition for semi-arid vegetation abundance estimation. *International Journal of Remote Sensing* **19**, 3109-3125.

Irons, J.R., Markham, B.L., Nelson, R.F., Toll, D.L., Williams, D.L., Latty, R.S. and Stauffer, M.L. (1985) The effects of spatial-resolution on the classification of Thematic Mapper data. *International Journal of Remote Sensing* **6**, 1385-1403.

Jacquemond, S., Baret, F., Andrieu, B., Danson, F.M. and Jaggard, K. (1995) Extraction of Vegetation Biophysical parameters by Inversion of the PROSPECT + SAIL Models on Sugar Beet Canopy Reflectance Data. Application to TM and AVIRIS Sensors. *Remote Sensing of Environment* **52**, 163-172.

Janssen, R., Goosen, H., Verhoeven, M.L., Verhoeven, J.T.A., Omtzigt, A.Q.A. and Maltby, E. (2005) Decision support for integrated wetland management. *Environmental Modelling & Software* **20**, 215-229.

Jensen, A. (1980) Seasonal-changes in near-infrared reflectance ratio and standing crop biomass in a salt-marsh community dominated by halimione-portulacoides (l) aellen. *New Phytologist* **86**, 57-67.

Jensen, J.R., Christensen, E.J. and Sharitz, R. (1984) Nontidal wetland mapping in South-Carolina using airborne Multispectral Scanner data. *Remote Sensing of Environment* **16**, 1-12.

Jensen, J.R., Hodgson, M.E., Christensen, E., Mackey, H.E., Tinney, L.R. and Sharitz, R. (1986) Remote-sensing inland wetlands - A multispectral approach. *Photogrammetric Engineering and Remote Sensing* **52**, 87-100.

Johnson, L.F., Hlavka, C.A. and Peterson, D.L. (1994) Multivariate-analysis of AVIRIS data for canopy biochemical estimation along the Oregon transect. *Remote Sensing of Environment* **47**, 216-230.

Johnston, R.M. and Barson, M.M. (1993) Remote-sensing of australian wetlands - an evaluation of landsat tm data for inventory and classification. *Australian Journal of Marine and Freshwater Research* **44**, 235-252.

Justice, C.O., Townshend, J.R.G., Holben, B.N. and Tucker, C.J. (1985) Analysis of the Phenology of Global Vegetation using Meteorological Satellite Data. *International Journal of Remote Sensing* **6**, 1271-1318.

Kao, J.T., Titus, J.E. and Zhu, W.X. (2003) Differential nitrogen and phosphorus retention by five wetland plant species. *Wetlands* **23**, 979-987.

Kawata, S. and Minami, S. (1984) Adaptive smoothing of spectroscopic data by a linear mean- square estimation. *Applied Spectroscopy* **38**, 49-58.

Keddy, P.A. (2000) *Wetland Ecology Principles and Conservation*, Cambridge, United Kingdom: Cambridge University Press.

Kent, M. and Coker, P. (1992) *Vegetation Description and Analysis-A Practical Approach*, John Wiley & Sons, UK.

Kent, M., Gill, W.J., Weaver, R.E. and Armitage, R.P. (1997) Landscape and Plant Community Boundaries in Biogeography. *Progress in Physical Geography* **21**, 315-353.

Kerr, J.T. and Ostrovsky, M. (2003) From space to species: Ecological applications for remote sensing. *Trends in Ecology & Evolution* **18**, 299-305.

Key, T., Warner, T.A., McGraw, J.B. and Fajvan, M.A. (2001) A comparison of multispectral and multitemporal information in high spatial resolution imagery for classification of individual tree species in a temperate hardwood forest. *Remote Sensing of Environment* **75**, 100-112.

Klemas, V.V. (2001) Remote Sensing of Landscape-Level Coastal Environmental Indicators. *Environmental Management* **27**, 47-57.

Kokaly, R.F. and Clark, J.A. (1999) Spectroscopic Determination of Leaf Biochemistry Using Band-Depth Analysis of Absorption Features and Stepwise Multiple Linear Regression. *Remote Sensing of Environment* 67, 267-287.

Kokaly, R.F., Clark, R.N., Despain, D.G. and Livo, K.E. (2001) The effects of temporal sampling and changing spatial scales on the mapping of forest cover in Yellowstone National Park using imaging spectroscopy. *Proceedings from 10th JPL Airborne Earth Science Workshop Volume 2*, JPL Publications.

Kokaly, R.F., Despain, D.G., Clark, R.N. and Livo, K.E. (2003) Mapping vegetation in Yellowstone national Park using spectral feature analysis of AVIRIS data. *Remote Sensing of Environment* **84**, 437-456.

Koskiaho, J. and Pustinen, M. (2005) Function and potential of constructed wetlands for the control of N and P transport from agriculture and peat production in boreal climate. *Journal of Environmental Science and Health Part a- Toxic/Hazardous Substances & Environmental Engineering* **40**, 1265-1279.

Kumar, L and Skidmore, A.K. (1998) Use of derivative spectroscopy to identify regions of differences between some Australian Eucalypt species. *Proceedings from 9th Australasian Remote Sensing and Photogrammetry conference*, Sydney, Australia.

Laba, S., Smith, S.D. and Degloria, S.D. (1997) Landsat-based land cover mapping in the lower Yuna River watershed in the Dominican Republic. *International Journal of Remote Sensing* **18**, 3011-3025.

Lamb, D.W., Steyn-Ross, M., Schaares, P., Hanna, M.M., Silvester, W. and Steyn-Ross, A. (2002) Estimating leaf nitrogen concentration in ryegrass (*Lolium* spp.) pasture using the chlorophyll red-edge: Theoretical modelling and experimental observations. *International Journal of Remote Sensing* **23**, 3619-3648.

Lark, R.M. (1996) Geostatistical description of texture on an aerial photograph for discriminating classes of land cover. *International Journal of Remote Sensing* **17**, 2115-2133.

Lee, J.K., Park, R.A. and Mausel, P.W. (1992) Application of geoprocessing and simulation modelling to estimate impacts of sea-level rise on the northeast coast of Florida. *Photogrammetric Engineering and Remote Sensing* **58**, 1579-1586.

Lee, K.H. and Lunetta, R.S. (1995) Wetlands Detection Methods. In: Lyon, J.G., (Ed.) *Wetland and Environmental Applications of GIS*, CRC Press Inc., United States of America.

Lee, P.Y. and Rotenberry, J.T. (2005) Relationships between bird species and tree species assemblages in forested habitats of eastern North America. *Journal of Biogeography* **32**, 1139-1150.

Le Maire, G., Francois, C. and Dufrene, E. (2004) Towards universal broad leaf chlorophyll indices using PROSPECT simulated database and hyperspectral reflectance measurements. *Remote Sensing of Environment* **89**, 1-28.

Levin, S.A. (1992) The problem of pattern and scale in ecology: The Robert H. MacArthur Award. *Ecology* **73**, 1943-1967.

Lewis, M.M. (1994) Species Composition related to Spectral Classification in an Australian Spinifex Hummock Grassland. *International Journal of Remote Sensing* **15**, 3223-3239.

Lewis, M.M. (1998) Numeric classification as an aid to spectral mapping of vegetation communities. *Plant Ecology* **136**, 133-149.

Lichtenthaler, H.K. and Miehe, J.A. (1997) Fluorescence imaging as a diagnostic tool for plant stress. *Trends in Plant Science* **2**, 316-320.

Liu, L., Wang, J., Huang, W., Zhao, C., Zhnag, B. and Tong, Q. (2004) Estimating winter wheat plant water content using red edge parameters. *International Journal of Remote Sensing* **25**, 3331-3342.

Liu, L.Y., Zhang, Y.J., Wang, J.H. and Zhao, C.J. (2005) Detecting solar-induced chlorophyll fluorescence from field radiance spectra based on the fraunhofer line principle. *IEEE Transactions on Geoscience and Remote Sensing* **43**, 827-832.

Llewellyn, G.M. and Curran,P.J. 2005 The truth about the red edge. *Proceedings from RSPSoc Annual Conference-Mapping and Monitoring a Hazardous World 2005*, Portsmouth, United Kingdom.

Lloyd, D. (1990) A phenological classification of terrestrial vegetation cover using shortwave vegetation index imagery. *International Journal of Remote Sensing* **11**, 2269-2279.

Lord, D., Desjardins, R.L. and Dube, P.A. (1985) Influence of wind on crop canopy reflectance measurements. *Remote Sensing of Environment* **18**, 113-123.

Lorenzen, B. and Jensen, A. (1988) Reflectance of blue, green, red and near-infrared radiation from wetland vegetation used in a model discriminating live and dead above ground biomass. *New Phytologist* **108**, 345-355.

Lunetta, R.S. and Balogh, M.E. (1999) Application of multi-temporal Landsat 5 TM imagery for wetland identification. *Photogrammetric Engineering and Remote Sensing* **65**, 1303-1310.

Mackey 1990 Monitoring seasonal and annual wetland changes in a freshwater marsh with SPOT HRV data. *Proceedings from ACSM-ASPRS Annual Convention*, Technical Papers 4, pp. 283-292 Denver, USA

Maier, R. and Cowie, N.R. (2002) Long-term vegetation monitoring of the Insh Marshes RSPB reserve-Baseline Survey. Unpublished report for the RSPB.

Malcolm, R. and Soulsby, C. (2001) Hydrogeochemistry of groundwater in coastal wetlands: implications for coastal conservation in Scotland. *Science of the Total Environment* **265**, 269-280.

Matson, P., Johnson, L., Billow, C., Miller, J. and Pu, R.L. (1994) Seasonal patterns and remote spectral estimation of canopy chemistry across the Oregon transect. *Ecological Applications* **4**, 280-298.

Mehner, H., Cutler, M., Fairbairn, D. and Thompson, G. (2004) Remote sensing of upland vegetation: the potential of high spatial resolution satellite sensors. *Global Ecology and Biogeography* **13**, 359-369.

Mertes, L.A.K. (2002) Remote sensing of riverine landscapes. *Freshwater Biology* **47**, 799-816.

Metzger, J.P. and Muller, E. (1996) Characterizing the Complexity of Landscape Boundaries by Remote Sensing. *Landscape Ecology* **11**, 65-77.

Millington, A.C. and Alexander, R.W. (2000) Vegetation Mapping in the Last Three Decades of the Twentieth Century. In: Millington, A.C. and Alexander, R.W., (Eds.) *Vegetation mapping: From Patch to Planet*, pp. 322-331. Chichester: John Wiley & Sons]

Millington, A.C., Wellens, J., Settle, J.J. and Saull, R.J. (1994) Explaining and Monitoring Land Cover Dynamics in Drylands Using Multi-Temporal Analysis of NOAA AVHRR Imagery. In: G.M.Foody and Curran, P.J., (Eds.) *Scale & Environmental Remote Sensing*, pp. 16-43. Chichester: Wiley]

Milton, E.J. (1987) Principles of Field Spectroscopy. *International Journal of Remote Sensing* **8**, 1807-1827.

Mitsch, W.J., Day, J.W., Zhang, L. and Lane, R.R. (2005) Nitrate-nitrogen retention in wetlands in the Mississippi river basin. *Ecological Engineering* **24**, 267-278.

Mitsch, W.J. and Gosselink, J.G. (2000a) The values of wetlands: importance of scale and landscape setting. *Ecological Economics* **35**, 25-33.

Mitsch, W.J. and Gosselink, J.G. (2000b) *Wetlands*, 3rd edn. Van Nostrand Reinhold, New York.

Mittelbach, G.G., Steiner, C.F., Scheiner, S.M., Gross, K.L., Reynolds, H.L., Waide, R.B., Willig, M.R., Dodson, S.I. and Gough, L. (2001) What is the observed relationship between species richness and productivity? *Ecology* **82**, 2381-2396.

Miyamoto, M., Yoshino, K., Nagano, T., Ishida, T. and Sato, Y. (2004) Use of balloon aerial photography for classification of Kushiro wetland vegetation, northeastern Japan. *Wetlands* **24**, 701-710.

Moody, A. and Strahler, A.H. (1994) Characteristics of composited AVHRR data and problems in their classification. *International Journal of Remote Sensing* **15**, 3473-3491.

Mooney, H.A., Hobbs, R.J., Gorham, J. and Williams, K. (1986) Biomass accumulation and resource utilization in co-occurring grassland annuals. *Oecologia* **70**, 555-558.

Moore, P.D. (2002) The future of cool temperate bogs. *Environmental Conservation* **29**, 3-20.

Mucher, C.A., Steinnocher, K.T., Kressler, K.P. and Heunks, C. (2000) Land Cover Characterization and Change Detection for Environmental Monitoring of Pan-Europe. *International Journal of Remote Sensing* **21**, 1159-1181.

Mucina, L. (1997) Classification of vegetation: Past, present and future. *Journal of Vegetation Science* **8**, 751-760.

Muller, E. (1997) Mapping Riparian Vegetation Along Rivers: Old Concepts and New Methods. *Aquatic Botany* **58**, 411-437.

Munden, R., Curran, P.J. and Catt, J.A. (1994) The relationship between red edge and chlorophyll concentration in the broadbalk winter-wheat experiment at Rothamsted. *International Journal of Remote Sensing* **15**, 705-709.

Munyati, C. (2000) Wetland change detection on the Kafue Flats, Zambia, by classification of a multitemporal remote sensing image dataset. *International Journal of Remote Sensing* **21**, 1787-1806.

Murphy, R.J., Tolhurst, T.J., Chapman, M.G. and Underwood, A.J. (2004) Estimation of surface chlorophyll on an exposed mudflat using digital colour-infrared (cir) photography. *Estuarine Coastal and Shelf Science* **59**, 625-638.

Murphy, R.J., Tolhurst, T.J., Chapman, M.G. and Underwood, A.J. (2005) Estimation of surface chlorophyll-*a* on an emersed mudflat using field spectrometry: accuracy of ratios and derivative-based approaches. *International Journal of Remote Sensing* **26**, 1835-1859.

Mutanga, O. and Skidmore, A.K (2003) Continuum-removed absorption features estimate tropical savanna grass quality in situ. *Proceedings from 3rd EARSEL Workshop on Imaging Spectroscopy*, Herrsching.

Mutanga, O. and Skidmore, A.K. (2004a) Integrating imaging spectroscopy and neural networks to map grass quality in the Kruger National Park, South Africa. *Remote Sensing of Environment* **90**, 104-115.

Mutanga, O. and Skidmore, A.K. (2004b) Narrow band vegetation indices overcome the saturation problem in biomass estimation. *International Journal of Remote Sensing* **25**, 3999-4014.

Mutanga, O., Skidmore, A.K. and Prins, H.H.T. (2004) Predicting in situ pasture quality in the Kruger National Park, South Africa, using continuum-removed absorption features. *Remote Sensing of Environment* **89**, 393-408.

Naiman, R.J. and Décamps, H. (1990) *The Ecology and Management of Aquatic Terestrial Ecosystems*, New Jersey: UNESCO, Paris and Parthenon.

Oindo, B.O., Skidmore, A.K. and De Salvo, P. (2003) Mapping habitat and biological diversity in the Maasai Mara ecosystem. *International Journal of Remote Sensing* **24**, 1053-1069.

Othman, J., Bennett, J. and Blamey, R. (2004) Environmental values and resource management options: a choice modelling experience in Malaysia. *Environment and Development Economics* **9**, 803-824.

Ozesmi, S.L. and Bauer, M.E. (2002) Satellite remote sensing of wetlands. *Wetlands, Ecology and Management* **10**, 381-402.

Pando, M., Lange, R.T. and Sparrow, A.D. (1992) Relationships between reflectance in Landsat wavelengths and floristic composition of Australian chenopod shrublands. *International Journal of Remote Sensing* **13**, 1861-1867.

Parmuchi, M.G., Karszenbaum, H. and Kandus, P. (2002) Mapping wetlands using multi-temporal radarsat-1 data and a decision-based classifier. *Canadian Journal of Remote Sensing* **28**, 175-186.

Pavri, F. and Aber, J.S. (2004) Characterizing wetland landscapes: a spatiotemporal analysis of remotely sensed data at Cheyenne Bottoms, Kansas. *Physical Geography* **25**, 86-104.

Penuelas, J., Filella, I., Gamon, J.A. and Field, C. (1997) Assessing photosynthetic radiation-use efficiency of emergent aquatic vegetation from spectral reflectance. *Aquatic Botany* **58**, 307-315.

Penuelas, J., Gamon, J.A., Griffin, K.L. and Field, C.B. (1993) Assessing Community Type, Plant Biomass, Pigment Composition, and Photosynthetic Efficiency of Aquatic Vegetation from Spectral Reflectance. *Remote Sensing of Environment* **46**, 110-118.

Phillips, R.L., Beeri, O. and Dekeyser, E.S. (2005) Remote wetland assessment for Missouri coteau prairie glacial basins. *Wetlands* **25**, 335-349.

Phinn, S., Franklin, J., Hope, A., Stow, D. and Huenneke, L. (1996) Biomass distribution mapping using airborne digital video imagery and spatial statistics in a semi-arid environment. *Journal of Environmental Management* **47**, 139-164.

Phinn, S.R., Stow, D.A. and van Mouwerik, D. (1999) Remotely Sensed Estimates of Vegetation Structural Charateristics in Restored Wetlands, Southern California. *Photogrammetric Engineering & Remote Sensing* **65**, 485-493.

Pignatti, S., Oberdorfer, E., Schaminee, J.H.J. and Westhoff, V. (1995) On the concept of vegetation class in phytosociology. *Journal of Vegetation Science* **6**, 143-152.

Pinar, A. and Curran, P.J. (1996) Grass chlorophyll and the reflectance red edge. *International Journal of Remote Sensing* **17**, 351-357.

Posse, G. and Cingolani, A.M. (2004) A test of the use of NDVI data to predict secondary productivity. *Applied Vegetation Science* **7**, 201-208.

Pitt, D.G., Wagner, R.G., Hall, R.J., King, D.J., Leckie, D.G. and Runesson, U. (1997) Use of remote sensing for forest vegetation management: A problem analysis. *Forestry Chronicle* **73**, 459-477.

Price, J.C. (1994) How Unique are Spectral Signatures? *Remote Sensing of Environment* **49**, 181-186.

Qi, J., Chehbouni, A., Huete, A.R., Kerr, Y.H. and Sorooshian, S. (1994) A modified soil adjusted vegetation index. *Remote Sensing of Environment* **48**, 119-126.

Ramsey, E.W. and Jensen, J.R. (1996) Remote sensing of mangrove wetlands: Relating canopy spectra to site-specific data. *Photogrammetric Engineering and Remote Sensing* **62**, 939-948.

Ramsey, R.D., Falconer, A. and Jensen, J.R. (1995) The relationship between NOAA-AVHRR NDVI and ecoregions in Utah. *Remote Sensing of Environment* **53**, 188-198.

Reed, B.C., Brown, J.F., VanderZee, D., Loveland, T.R., Merchant, J.W. and Ohlen, D.O. (1994) Measuring phenological variability from satellite imagery. *Journal of Vegetation Science* **5**, 703-714.

Revenga, C., Campbell, I., Abell, R., De Villiers, P. and Bryer, M. (2005) Prospects for monitoring freshwater ecosystems towards the 2010 targets. *Philosophical Transactions of the Royal Society B-Biological Sciences* **360**, 397-413.

Ricotta, C. (2004) Evaluating the classification accuracy of fuzzy thematic maps with a simple parametric measure. *International Journal of Remote Sensing* **25**, 2169-2176.

Rock, B.N., Vogelmann, J.E., Williams, D.L., Vogelmann, A.F. and Hoshizaki, T. (1986) Remote detection of forest damage. *Bioscience* **36**, 439-445.

Rodwell, J. S., ed. 1991. British Plant Communities. Volume 1. Woodlands and scrub. Cambridge University Press, Cambridge.

Rodwell, J. S., ed. 1991. British Plant Communities. Volume 2. Mires and heath. Cambridge, Cambridge University Press.Rodwell, J. S., ed. 1992. British Plant Communities. Volume 3. Grassland and montane communities. Cambridge University Press, Cambridge.

Rodwell, J. S., ed. 1993. British Plant Communities. Volume 4. Grasslands and montane communities. Cambridge University Press, Cambridge.

Rodwell, J. S., ed. 1995. British Plant Communities. Volume 4. Aquatic communities, swamps and tall-herb fens. Cambridge University Press, Cambridge.

Rodwell, J. S., ed. 2000. British plant communities. Volume 5. Maritime communities and vegetation of open habitats. Cambridge University Press, Cambridge.

Ross, S.M. (1995) Overview of the Hydrochemistry and Solute Processes in British Wetlands. In: Hughes, J.M.R. and Heathwaite, A.L., (Eds.) *Hydrology and Hydrochemistry of British Wetlands*, pp. 133-182. John Wiley & Sons, England.

Roughgarden, J., Running, S.W. and Mason, P.A. (1991) What Does Remote Sensing do for Ecology? *Ecology* **72**, 1918-1922.

Rouse, J.W., Haas, R.H., Deering, D.W. and Schell, J.A. (1974) Monitoring the vernel advancement and retrogradation (Green Wave Effect) of natural vegetation. Texas Remote Sensing Centre, Texas A&M University, College Station, 348pp.: Final Report 1974-8.

RSPB (2000) Insh Marshes Nature Reserve Management Plan: April 2000-March 2005. Unpublished Report for RSPB.

Rundquist, D., Perk, R., Leavitt, B., Keydan, G. and Gitelson, A. (2004) Collecting spectral data over cropland vegetation using machine positioning of the sensor. *Computers and Electronics in Agriculture* **43**, 173-178.

Rutchey, K. and Vilchek, L. (1999) Air photointerpretation and satellite imagery analysis techniques for mapping cattail coverage in a northern everglades impoundment. *Photogrammetric Engineering and Remote Sensing* **65**, 185-191.

Sampson, P.H., Zarco-Tejada, P.J., Mohammed, G.H., Miller, J.R. and Noland, T.L. (2003) Hyperspectral remote sensing of forest condition: Estimating chlorophyll content in tolerant hardwoods. *Forest Science* **49**, 381-391.

Savitzky, A. and Golay, M.J.E. (1964) Smoothing and Differentiation of Data by Simplified Least Squares Procedures. *Analytical Chemistry* **36**, 1627-1639.

Sawaya, K.E., Olmanson, L.G., Heinert, N.J., Brezonik, P.L. and Bauer, M.E. (2003) Extending satellite remote sensing to local scales: Land and water resource monitoring using high-resolution imagery. *Remote Sensing of Environment* **88**, 144-156.(Abstract)

Schaffers, A.P. (2002) Soil, biomass, and management of semi-natural vegetation - Part ii. Factors controlling species diversity. *Plant Ecology* **158**, 247-268.

Schmidt, H. and Karnieli, A. (2002) Analysis of the Temporal and Spatial Vegetation Patterns in a Semi-Arid Environment Observed by NOAA AVHRR Imagery and Spectral Ground Measurements. *International Journal of Remote Sensing* **23**, 3971-3990.

Schmidt, K.S. and Skidmore, A.K. (2003) Spectral discrimination of vegetation types in a coastal wetland. *Remote Sensing of Environment* **85**, 92-108.

Schmidt, K.S. and Skidmore, A.K. (2004) Smoothing vegetation spectra with wavelets. *International Journal of Remote Sensing* **25**, 1167-1184.

Schmidt, K.S., Skidmore, A.K., Kloosterman, E.H., Van Oosten, H., Kumar, L. and Janssen, J.A.M. (2004) Mapping coastal vegetation using an expert system and hyperspectral imagery. *Photogrammetric Engineering and Remote Sensing* **70**, 703-715.

Schmidtlein, S. and Sassin, J. (2004) Mapping of continuous floristic gradients in grasslands using hyperspectral imagery. *Remote Sensing of Environment* **92**, 126-138.

Skidmore, A. (2002) Vegetation Mapping and Monitoring. In: Skidmore, A., (Ed.) *Environmental Monitoring with GIS and Remote Sensing*, pp. -120(?) London: Taylor & Francis]

Schweik, C.M. and Thomas, C.W. (2002) Using remote sensing to evaluate environmental institutional designs: A habitat conservation planning example. *Social Science Quarterly* **83**, 244-262.

Seto, K.C., Fleishman, E., Fay, J.P. and Betrus, C.J. (2004) Linking spatial patterns of bird and butterfly species richness with Landsat TM derived NDVI. *International Journal of Remote Sensing* **25**, 4309-4324.

Shanmugam, S., Lucas, N., Phipps, P., Richards, A. and Barnsley, M. (2003) Assessment of remote sensing techniques for habitat mapping in coastal dune ecosystems. *Journal of Coastal Research* **19**, 64-75.

Shuman, C.S. and Ambrose, R.F. (2003) A comparison of remote sensing and ground-based methods for monitoring wetland restoration success. *Restoration Ecology* **11**, 325-333.

Silvestri, S., Marani, M., Settle, J., Benvenuto, F. and Marani, A. (2002) Salt marsh vegetation radiometry - data analysis and scaling. *Remote Sensing of Environment* **80**, 473-482.

Sims, D.A. and Gamon, J.A. (2002a) Relationships between leaf pigment content and spectral reflectance across a wide range of species, leaf structures and developmental stages. *Remote Sensing of Environment* **81**, 337-354.

Sims, D.A. and Gamon, J.A. (2002b) Relationships between leaf pigment content and spectral reflectance across a wide range of species, leaf structures and developmental stages. *Remote Sensing of Environment* **81**, 337-354.

Skidmore, A. (2002) Vegetation Mapping and Monitoring. In: Skidmore, A., (Ed.) *Environmental Monitoring with GIS and Remote Sensing*, pp. -120(?) London: Taylor & Francis]

Smith, E.M. and Smith, R.W.J. (1994) Odonata at Insh Marshes. Unpublished report: RSPB.

Smith, K.L., Steven, M.D. and Colls, J.J. (2004) Use of hyperspectral derivative ratios in the red-edge region to identify plant stress responses to gas leaks. *Remote Sensing of Environment* **92**, 207-217.

Song, C., Woodcock, C.E., Seto, K.C., Lenney, M.P. and Macomber, S.A. (2001) Classification and change detection using Landsat TM data: When and how to correct atmospheric effects? *Remote Sensing of Environment* **75**, 230-244.

Soukupova, J., Rock, B.N. and Albrechtova, J. (2002) Spectral characteristics of lignin and soluble phenolics in the near infrared - a comparative study. *International Journal of Remote Sensing* **23**, 3039-3055.

Southall, E.J., Dale, M.P. and Kent, M. (2003) Spatial and temporal analysis of vegetation mosaics for conservation: poor fen communities in a Cornish valley mire. *Journal of Biogeography* **30**, 1427-1443.

Spanglet, H.J., Ustin, S.L. and Rejmankova, E. (1998) Spectral Reflectance Characteristics of California Subalpine Marsh Plant Communities. *Wetlands* **18**, 307-319.

Ssegawa, P., Kakudidi, E., uasya, M. and Kalema, J. (2004) Diversity and distribution of sedges on multivariate environmental gradients. *Afrian Journal of Ecology* **42**, 21-33.

St-Onge, B.A. and Cavayas, F. (1997) Automated Forest Structure Mapping from High Resolution Imagery Based on Directional Semivariogram Estimates. *Remote Sensing of Environment* **61**, 82-95.

Steven, M.D. (1987) Ground Truth: An Underview. *International Journal of Remote Sensing* **8**, 1033-1038.

Steven, M.D., Malthus, T.J. and Clark, J.A. (1995) Achievements and unresolved problems in vegetation monitoring . In: Danson, F.M. and Plummer, S.E., (Eds.) *Advances in Environmental Remote Sensing*, pp. 133-145. John Wiley, Chichester.

Stevens, J.P., Blackstock, T.H., Howe, E.A. and Stevens, D.P. (2004) Repeatability of Phase 1 Habitat Survey. *Journal of Environmental Management* **73**, 53-59.

Stone, T.A., Schlesinger, P., Houghton, R.A. and Woodwell, G.M. (1994) A Map of Vegetation of South America based on Satellite Imagery. *Photogrammetric Engineering & Remote Sensing* **60**, 541-551.

Story, M. and Congalton, R.G. (1986) Accuracy assessment - a users perspective. *Photogrammetric Engineering and Remote Sensing* **52**, 397-399.

Ter Braak, C.J.F. (1994) Canonical community ordination. Part I: basic theory and linear methods. *Ecoscience* **1**, 127-140.

Ter Braak, C.J.F. and Šmilauer, P. (2002) CANOCO Reference Manual and CanoDraw for Windows User's Guide: Software for Canonical Community Ordination (version 4.5). Ithaca, NY: Microcomputer Power, 500 pp.

Thenkabail, P.S., Enclona, E.A., Ashton, M.S. and Van Der Meer, B. (2004) Accuracy assessments of hyperspectral waveband performance for vegetation analysis applications. *Remote Sensing of Environment* **91**, 354-376.

Thenkabail, P.S., Smith, R.B. and De Pauw, E. (2000) Hyperspectral vegetation indices and their relationships with agricultural crop characteristics. *Remote Sensing of Environment* **71**, 158-182.

Thomas, V., Treitz, P., Jelinski, D., Miller, J., Lafleur, P. and Mccaughey, J.H. (2002) Image classification of a northern peatland complex using spectral and plant community data. *Remote Sensing of Environment* **84**, 83-99.

Thomson, A.G., Fuller, R.M., Yates, M.G., Brown, S.L., Cox, R. and Wadsworth, R.A. (2003) The use of airborne remote sensing for extensive mapping of intertidal sediments and saltmarshes in eastern England. *International Journal of Remote Sensing* **24**, 2717-2737.

Townsend, P.A. (2000) A Quantitative Fuzzy Approach to Assess mapped Vegetation Classifications for Ecological Applications. *Remote Sensing of Environment* **72**, 253-267.

Townsend, P.A. and Walsh, S.J. (2001) Remote sensing of forested wetlands; an application of multitemporal and multispectral satellite imagery to determine plant community composition and structure in southeastern USA. *Plant Ecology* **157**, 129-149.

Townshend, J.R.G. and Justice, C.O. (1986) Analysis of the Dynamics if African Vegetation using the Normalized Difference of Vegetation Index. *International Journal of Remote Sensing* **7**, 1435-1445.

Townshend, J.R.G. and Tucker, C.J. (1984) Objective Assessment of Advanced Very High Resolution Radiometer Data for Land Cover Mapping. *International Journal of Remote Sensing* **5**, 497-504.

Toyra, J. and Pietronito, A. (2005) Towards operational monitoring of a northern wetland using geomatics-based techniques. *Remote Sensing of Environment* **97**, 174-191.

Tremolieres, M., Sanchez-Perez, J.M., Schnitzler, A. and Schmitt, D. (1998) Impact of river management history on the community structure, species composition and nutrient status in the Rhine alluvial hardwood forest. *Plant Ecology* **135**, 59-78.

Trisurat, Y., Eiumnoh, A., Murai, S., Hussain, M.Z. and Shrestha, R.P. (2000) Improvement of tropical vegetation mapping using a remote sensing technique: a case of Khao Yai National Park, Thailand. *International Journal of Remote Sensing* **21**, 2031-2042.

Trodd, N.M. (1990) Characterising Semi-Natural Vegetation: Continua and Ecotones *In Proceedings of the 19th Annual Conference of Remote Sensing Society*, Hilton, K., (Ed.).

Trodd, N.M. (1996) Analysis and representation of heathland vegetation from near- ground level remotely-sensed data. *Global Ecology and Biogeography Letters* **5**, 206-216.

Tsai, F. and Philpot, W. (1998) Derivative Analysis of Hyperspectral Data. *Remote Sensing of Environment* **66**, 41-51.

Tsuyuzaki, S., Haraguchi, A. and Kanda, F. (2004) Effects of scale-dependent factors on herbaceous vegetation patterns in a wetland, northern Japan. *Ecological Research* **19**, 349-355.

Tucker, C.J. (1979) Red and photographic infrared linear combinations for monitoring vegetation. *Remote Sensing of Environment* **8**, 127-150.

Tucker, C.J., Townshend, J.R.G. and Goff, T.E. (1985a) African Land-Cover Classification Using Satellite Data. *Science* **227**, 369-374.

Tucker, C.J., van Praet, C.L., Sharman, M.J. and van Ittersum, G. (1985b) Satellite Remote Sensing of Total Herbaceous Biomass Production in the Senegalese Sahel: 1980-1984. *Remote Sensing of Environment* **17**, 233-249.

Turner, D.P., Ollinger, S.V. and Kimball, J.S. (2004) Integrating remote sensing and ecosystem process models for landscape- to regional-scale analysis of the carbon cycle. *Bioscience* **54**, 573-584.

Turner, W., Spector, S., Gardiner, N., Fladeland, M., Sterling, E. and Steininger, M. (2003) Remote sensing for biodiversity science and conservation. *Trends in Ecology & Evolution* **18**, 306-314.

Turner, W., Sterling, E.J. and Janetos, A.C. (2001) Special section: contributions of remote sensing to biodiversity conservation: a NASA approach. *Conservation Biology* **15**, 832-834.

Underwood, E., Ustin, S. and Di Pietro, D. (2003) Mapping non-native plants using hyperspectral imagery. *Remote Sensing of Environment* **86**, 150-161.

Van der Maarel, E. (1990) Ecotones and ecoclines are different. *Journal of Vegetation Science* **1**, 135-138.

Van Wagtendonk, J.W. and Root, R.R. (2003) The use of multi-temporal Landsat normalized difference vegetation index (NDVI) data for mapping fuel models in Yosemite national park, usa. *International Journal of Remote Sensing* **24**, 1639-1651.

Verhoef, W. (1985) Earth observation modeling based on layer scattering matrices. *Remote Sensing of Environment* **17**, 165-178.

Vogelmann, J.E., Sohl, T.L., Campbell, P.V. and Shaw, D.M. (1998) Regional land cover characterization using Landsat Thematic Mapper data and ancillary data sources. *Environmental Monitoring and Assessment* **51**, 415-428.

Walker, D.A. (1999) An integrated vegetation mapping approach for northern Alaska (1 : 4 m scale). *International Journal of Remote Sensing* **20**, 2895-2920.

Wallace, C.S.A., Watts, J.M. and Yool, S.R. (2000) Characterizing the Spatial Structure of Vegetation Communities in the Mojave Desert using Geostatistical Techniques. *Computers & Geosciences* **26**, 397-410.

Wang, G., Gertner, G., Xiao, X. and Anderson, A.B. (2001) Appropriate plot size and spatial resolution for mapping multiple vegetation types. *Photogrammetric Engineering and Remtoe Sensing* **67**, 575-584.

Wang, S.Q., Tian, H.Q., Liu, J.Y. and Pan, S.F. (2003) Pattern and change of soil organic carbon storage in china: 1960s-1980s. *Tellus Series B-Chemical and Physical Meteorology* **55**, 416-427.

Warren, P.L. and Hutchinson, C.F. (1984) Indicators of rangeland change and their potential for remote sensing. *Journal of Arid Environments* **7**, 107-126.

Weiher, E., Forbes, S., Schauwecker, T. and Grace, J.B. (2004) Multivariate control of plant species richness and community biomass in blackland prairie. *Oikos* **106**, 151-157.

Welch, R., Madden, M., Doren, R.F. and Rutchey, K. (1999) A brief synopsis on mapping the Everglades - foreword. *Photogrammetric Engineering and Remote Sensing* **65**, 153-154.

Wheeler, B.D. and Giller, K.E. (1982) Species richness of herbaceous fen vegetation in Broadland, Norfolk in relation to the quantity of above-ground plant- material. *Journal of Ecology* **70**, 179-200.

Wheeler, B.D. and Shaw, S.C. (1991) Aboveground crop mass and species richness of the principal types of herbaceous rich-fen vegetation of lowland England and Wales. *Journal of Ecology* **79**, 285-301.

Whigham, D.F. and Jordan, T.E. (2003) Isolated wetlands and water quality. *Wetlands* **23**, 541-549.

Whittaker, R.H. (1962) Classification of natural communities. *Botanical Review* **28**, 1-239.

Willby, N.J., Murphy, K.J., Gilvear, D.J., Grieve, I.C. and Pulford, I.D. (1997) Hydrochemical-Vegetation Interactions on a Scottish Floodplain Mire. *British Hydrological Society* 40-52.

Williams, B.K. (1996) Assessment of accuracy in the mapping of vertebrate biodiversity. *Journal of Environmental Management* **47**, 269-282.

Witte, J.P.M. (2002) The descriptive capacity of ecological plant species groups. *Plant Ecology* **162**, 199-213.

Witte, J.P.M. and Van Der Meijden, R. (2000) Mapping ecosystem types by means of ecological species groups. *Ecological Engineering* **16**, 143-152.

Wood, D. (1989) A vegetation survey of Insh Marshes RSPB Reserve. Unpublished report: RSPB.

Wood, T.F. and Foody, G.M. (1989) Analysis and representation of vegetation continua from Landsat Thematic Mapper data for lowland heaths. *International Journal of Remote Sensing* **10**, 181-191.

Wulder, M., Niemann K.O. and Goodenough, D.G. (2000) Local Maximum Filtering for the Extraction of Tree Locations and Basal Area from High Spatial Resolution Imagery. *Remote Sensing of Environment* **73**, 103-114.

Wulder, M.A., Franklin, S.E., White, J.C., Cranny, M.M. and Dechka, J.A. (2004a) Inclusion of topographic variables in an unsupervised classification of satellite imagery. *Canadian Journal of Remote Sensing* **30**, 137-149.

Wulder, M.A., Hall, R.J., Coops, N.C. and Franklin, S.E. (2004b) High spatial resolution remotely sensed data for ecosystem characterization. *Bioscience* **54**, 511-521.

Yates, H., Strong, A., McGinnis, D. and Tarpley, D.Jr. (1986) Terrestrial Observations from NOAA Operational Satellites. *Science* **231**, 463-470.

Zarco-Tejada, P.J. and Miller, J.R. (1999) Land cover mapping at boreas using red edge spectral parameters from CASI imagery. *Journal of Geophysical Research-Atmospheres* **104**, 27921-27933.

Zarco-Tejada, P.J., Miller, J.R., Mohammed, G.H. and Noland, T.L. (2000a) Chlorophyll Fluorescence Effects on Vegetation Apparent Reflectance: I. Leaf-Level Measurements and Model Simulation. *Remote Sensing of Environment* **74**, 582-595.

Zarco-Tejada, P.J., Miller, J.R., Mohammed, G.H. , Noland, T.L. and Sampson, P.H. (2000b) Chlorophyll Fluorescence Effects on Vegetation Apparent Reflectance: II. Laboratory and Airborne Canopy-Level Measurements with Hyperspectral Data. *Remote Sensing of Environment* **74**, 596-608.

Zarco-Tejada, P.J., Miller, J.R., Mohammed, G.H. , Noland, T.L. and Sampson, P.H. (2002) Vegetation stress detection through chlorophyll *a+b* estimation and fluorescence effects on hyperspectral imagery. *Journal of Environmental Quality* **31**, 1433-1441.

Zarco-Tejada, P.J., Pushnik, J.C., Dobrowski, S. and Ustin, S.L. (2003) Steady-state chlorophyll *a* fluorescence detection from canopy derivative reflectance and double-peak red-edge effects. *Remote Sensing of Environment* **84**, 283-294.

Zarco-Tejada, P.J., Ustin, S.L. and Whiting, M.L. (2005) Temporal and spatial relationships between within-field yield variability in cotton and high-spatial hyperspectral remote sensing imagery. *Agronomy Journal* **97**, 641-653.

Zhang, M., Ustin, S.L., Rejmankova, E. and Sanderson, E.W. (1997) Monitoring Pacific coast salt marshes using remote sensing. *Ecological Applications* **7**, 1039-1053.

A. Appendix

RMSE

Table A:1 CASI 91-Ground Control Points and associated RMS error

GCP	Map x	Map y	Image x	Image y	Predict x	Predict y	Error x	Error y	RMSE
1	279888	802063	590	1434.25	583.36	1433.26	-6.64	-0.99	6.71
2	279728	801925	522.75	1495	520.5	1489.38	-2.25	-5.62	6.06
3	279375	801350	393	1735.5	397.71	1737.32	4.71	1.82	5.05
4	279100	801438	271.75	1679.75	270.35	1683.7	-1.4	3.95	4.19
5	278963	802013	174.75	1407	175.62	1413.13	0.87	6.13	6.19
6	279175	802200	256.5	1344	258.72	1337.09	2.22	-6.91	7.26
7	279731	802563	486.75	1193	484.05	1195.62	-2.7	2.62	3.76
8	279838	802438	544	1256.5	538.94	1258.11	-5.06	1.61	5.31
9	279963	802550	590.5	1214	587.78	1212.2	-2.72	-1.8	3.26
10	278838	801788	133.25	1515.25	133.36	1510.56	0.11	-4.69	4.7
11	279088	802263	213.25	1303	216.38	1304.11	3.13	1.11	3.32
12	278963	802175	166.5	1337.5	166.08	1338.74	-0.42	1.24	1.31
13	280350	803025	727	1009.25	731.28	1010.49	4.28	1.24	4.46
14	280563	802463	856	1275	859.24	1279.81	3.24	4.81	5.79
15	280600	802903	852	1072.25	849.45	1078.08	-2.55	5.83	6.36
16	280413	802938	762.75	1051	764.41	1053.5	1.66	2.5	3
17	280263	803150	680	949.75	685.26	948.89	5.26	-0.86	5.33
18	281463	802970	1220.5	1086	1228.3	1085.8	7.8	-0.2	7.81
19	280425	802550	791.25	1235	792.81	1233.29	1.56	-1.71	2.32
20	281150	803713	1050.5	725.75	1045.03	727.47	-5.47	1.72	5.73
21	281200	803675	1072	748.5	1069.47	747.25	-2.53	-1.25	2.83
22	281713	803255	1321.25	964.75	1322.1	964.63	0.85	-0.12	0.86
23	281505	803575	1210.5	805.25	1210.68	806.92	0.18	1.67	1.68
24	281825	803850	1336.25	697.5	1336.04	693.1	-0.21	-4.4	4.4
25	281500	803970	1188	628	1184.79	623.39	-3.21	-4.61	5.61
26	282313	804425	1514.5	440.75	1517.7	446.42	3.2	5.67	6.51
27	282250	803575	1544	842.5	1540.99	839.45	-3.01	-3.05	4.28
28	282063	804425	1407.25	437	1406.94	435.91	-0.31	-1.09	1.13
29	280725	803300	878.25	898.75	881.24	900.06	2.99	1.31	3.26
30	279950	802113	612.5	1414.5	607.93	1413.1	-4.57	-1.4	4.78
31	279338	802288	322	1306	325.88	1304.16	3.88	-1.84	4.3
32	279655	802288	469.5	1321.5	466.6	1318.79	-2.9	-2.71	3.97

A:2 CASI 101- Ground Control Pointss and associated RMS error

GCP	Map x	Map y	Image x	Image y	Predict x	Predict y	Error x	Error y	RMSE
1	279888	802063	445.25	1275.75	441.83	1271.12	-3.42	-4.63	5.76
2	279375	801350	255	1580.5	257.25	1578.44	2.25	-2.06	3.06
3	279100	801438	134	1524	134.24	1525.03	0.24	1.03	1.05
4	279488	801088	320.75	1706.25	319.44	1705.15	-1.31	-1.1	1.71
5	279913	801180	502	1681.75	497.55	1681.97	-4.45	0.22	4.45
6	280050	801463	540	1556	542.17	1556.94	2.17	0.94	2.36
7	280118	801295	579	1633	579.95	1638.01	0.95	5.01	5.1
8	280013	801225	537.25	1661	538.3	1665.68	1.05	4.68	4.79
9	280263	801388	636	1603	637.69	1601.5	1.69	-1.5	2.26
10	280358	802045	648.67	1299.67	645.7	1300.92	-2.97	1.25	3.22
11	280583	801575	763.33	1526	766.21	1529.35	2.88	3.35	4.42
12	280743	801683	827.33	1487.67	829.83	1486.54	2.5	-1.13	2.75
13	281113	802000	974	1360.33	973.93	1356.26	-0.07	-4.07	4.07
14	281455	802965	1071	919.67	1075.18	923.67	4.18	4	5.79
15	281688	802725	1185	1044	1187.62	1045.72	2.62	1.72	3.14
16	281883	802990	1261.67	928	1259.53	931.47	-2.14	3.47	4.07
17	282250	803575	1388.33	668.33	1391.36	676.27	3.03	7.94	8.5
18	282238	803443	1383.67	730	1392.3	737.07	8.63	7.07	11.15
19	282108	802888	1366.33	993	1361.87	989.06	-4.46	-3.94	5.95
20	282675	803263	1599.33	848.33	1590.38	840.49	-8.95	-7.84	11.9
21	283200	803588	1804.33	719	1803.64	713.14	-0.69	-5.86	5.9
22	279975	802395	467.67	1125	462.54	1121.04	-5.13	-3.96	6.48
23	279950	802113	464.67	1255.33	466.06	1250.75	1.39	-4.58	4.79

Meteorological Data

Table A:3 Meteorological data and solar altitude and azimuth at paired sampling points -July 2003

Plot	Quad	Alt	Azi	Wind Direction	Wind Speed	Cld	Temp	RH	Prsr	Rain	Rad
EF1	1	51	201.7	220	5	8	15.3	85.5	1005.9	0.0	1698.23
	2	51	201.7	220	5	8	15.3	85.5	1005.9	0.0	1698.23
	3	50.5	205.3	220	5	8	15.3	85.5	1005.9	0.0	1653.32
	4	50.5	205.3	220	5	8	15.3	85.5	1005.9	0.0	1653.32
	5	50.5	205.3	220	5	8	15.3	85.5	1005.3	0.0	1917.93
	6	50.5	205.3	220	5	8	15.3	85.5	1005.3	0.0	1917.93
	7	49.2	212.3	220	5	8	15.3	85.5	1005.3	0.0	1828.54
	8	49.2	212.3	220	5	8	15.3	85.5	1005.3	0.0	1828.54
	9	48.4	215.7	220	5	8	15.3	85.5	1005.3	0.0	1784.06
	10	48.4	215.7	220	5	8	15.3	85.5	1005.3	0.0	1784.06
LS1	1	48.6	219.7	130	9	6	24.7	60.8	1011.4	0.0	1285
	2	48.6	219.7	130	9	6	24.7	60.8	1011.4	0.0	1285
	3	47.7	222.9	130	9	6	24.7	60.8	1011.4	0.0	1285
	4	47.7	222.9	130	9	6	24.7	60.8	1011.4	0.0	1285
	5	47.7	222.9	130	9	6	24.7	60.8	1011.4	0.0	1285
	6	47.7	222.9	130	9	6	24.7	60.8	1011.4	0.0	1285
	7	47.7	222.9	130	9	6	24.7	60.8	1011.4	0.0	1285
	8	47.7	222.9	130	9	6	24.7	60.8	1011.4	0.0	1285
	9	46.8	226.1	130	9	6	24.7	60.8	1011.4	0.0	1285
	10	46.8	226.1	130	9	6	24.7	60.8	1011.4	0.0	1285
LS2	1	43.7	235	130	9	6	26.8	56.6	1011.6	0.0	1671
	2	43.7	235	130	9	6	26.8	56.6	1011.6	0.0	1671
	3	42.6	237.8	130	9	6	26.8	56.6	1011.6	0.0	1671
	4	42.6	237.8	130	9	6	26.8	56.6	1011.6	0.0	1671
	5	42.6	237.8	130	9	6	26.8	56.6	1011.6	0.0	1671
	6	42.6	237.8	130	9	6	26.8	56.6	1011.6	0.0	1671
	7	42.6	237.8	130	9	6	26.8	56.6	1011.6	0.0	1671
	8	42.6	237.8	130	9	6	26.8	56.6	1011.6	0.0	1671
	9	42.6	237.8	130	9	6	26.8	56.6	1011.6	0.0	1671
	10	42.6	237.8	130	9	6	26.8	56.6	1011.6	0.0	1671
LS3	1	53.4	179.2	70	6	8	22.6	68.0	1012.0	0.0	860
	2	53.4	179.2	70	6	8	22.6	68.0	1012.0	0.0	860
	3	53.4	179.2	70	6	8	22.6	68.0	1012.0	0.0	860
	4	53.4	179.2	70	6	8	22.6	68.0	1012.0	0.0	860
	5	53.4	179.2	70	6	8	22.6	68.0	1012.0	0.0	860
	6	53.4	179.2	70	6	8	22.6	68.0	1012.0	0.0	860
	7	45.7	229	90	8	4	25.0	69.8	1010.3	0.0	2016
	8	45.7	229	90	8	4	25.0	69.8	1010.3	0.0	2016
	9	44.6	232	90	8	4	25.0	69.8	1010.3	0.0	2016
	10	44.6	232	90	8	4	25.0	69.8	1010.3	0.0	2016
MC1	1	50.3	149.2	40	3	8	16.9	93.8	1011.0	0.0	473
	2	50.3	149.2	40	3	8	16.9	93.8	1011.0	0.0	473
	3	50.3	149.2	40	3	8	16.9	93.8	1011.0	0.0	473
	4	50.3	149.2	40	3	8	16.9	93.8	1011.0	0.0	473
	5	50.9	152.7	40	3	8	16.9	93.8	1011.0	0.0	473
	6	50.9	152.7	40	3	8	16.9	93.8	1011.0	0.0	473

Table A: 3 Continued

	7	50.9	152.7	40	3	8	16.9	93.8	1011.0	0.0	473
	8	50.9	152.7	40	3	8	16.9	93.8	1011.0	0.0	473
	9	50.9	152.7	40	3	8	16.9	93.8	1011.0	0.0	473
	10	51.5	156.3	40	3	8	16.9	93.8	1011.0	0.0	473
MC2	1	54.1	171.5	230	10	8	14.3	78.9	1011.8	0.2	1550
	2	54.2	175.5	230	10	8	14.3	78.9	1011.8	0.2	1550
	3	54.2	175.5	230	10	8	14.3	78.9	1011.8	0.2	1550
	4	54.2	175.5	230	10	8	14.3	78.9	1011.8	0.2	1550
	5	54.2	175.5	230	10	8	14.3	78.9	1011.8	0.2	1550
	6	54.2	175.5	230	10	8	14.3	78.9	1011.8	0.2	1550
	7	54.2	175.5	230	10	8	14.3	78.9	1011.8	0.2	1550
	8	54.2	175.5	230	10	8	14.3	78.9	1011.8	0.2	1550
MC3	1	47.5	226.8	230	14	6	18.4	63.2	1008.1	0.0	2089
	2	47.5	226.8	230	14	6	18.4	63.2	1008.1	0.0	2089
	3	46.5	229.9	230	14	6	18.4	63.2	1008.1	0.0	2089
	4	46.5	229.9	230	14	6	18.4	63.2	1008.1	0.0	2089
	5	46.5	229.9	230	14	6	18.4	63.2	1008.1	0.0	2089
	6	46.5	229.9	230	14	6	18.4	63.2	1008.1	0.0	2089
	7	46.5	229.9	230	14	6	18.4	63.2	1008.1	0.0	2089
	8	46.5	229.9	230	14	6	18.4	63.2	1008.1	0.0	2089
	9	46.5	229.9	230	14	6	18.4	63.2	1008.1	0.0	2089
	10	46.5	229.9	230	14	6	18.4	63.2	1008.1	0.0	2089
MC4	1	53.1	175.3	40	3	8	18.4	81.5	1010.5	0.0	1262
	2	53.1	175.3	40	3	8	18.4	81.5	1010.5	0.0	1262
	3	53.2	179.1	40	3	8	18.4	81.5	1010.5	0.0	1262
	4	53.2	179.1	40	3	8	18.4	81.5	1010.5	0.0	1262
	5	53.2	179.1	40	3	8	18.4	81.5	1010.5	0.0	1262
	6	53.2	179.1	40	3	8	18.4	81.5	1010.5	0.0	1262
	7	53.2	179.1	40	3	8	18.4	81.5	1010.5	0.0	1262
	8	53.2	179.1	40	3	8	18.4	81.5	1010.5	0.0	1262
	9	53.2	179.1	40	3	8	18.4	81.5	1010.5	0.0	1262
	10	53.2	179.1	40	3	8	18.4	81.5	1010.5	0.0	1262
MG1	1	48	219.2	190	8	7	20.5	71.2	1007.0	0.0	1815
	2	48	219.2	190	8	7	20.5	71.2	1007.0	0.0	1815
	3	47.1	222.4	190	8	7	20.5	71.2	1007.0	0.0	1815
	4	47.1	222.4	190	8	7	20.5	71.2	1007.0	0.0	1815
	5	47.1	222.4	190	8	7	20.5	71.2	1007.0	0.0	1815
	6	46.2	225.6	190	8	7	20.5	71.2	1007.0	0.0	1815
	7	46.2	225.6	190	8	7	20.5	71.2	1007.0	0.0	1815
	8	46.2	225.6	190	8	7	20.5	71.2	1007.0	0.0	1815
	9	46.2	225.6	200	9	6	18.2	78.5	1007.4	0.0	1194
	10	46.2	225.6	200	9	6	18.2	78.5	1007.4	0.0	1194
MG2	1	49	145.9	200	5	7	16.2	77.2	1005.6	0.0	3131.73
	2	49	145.9	200	5	7	16.2	77.2	1005.6	0.0	3131.73
	3	49	145.9	200	5	7	16.2	77.2	1005.6	0.0	3131.73
	4	49	145.9	200	5	7	16.2	77.2	1005.6	0.0	3131.73
	5	49	145.9	200	5	7	16.2	77.2	1005.6	0.0	3131.73
	6	49.7	149.4	200	5	7	16.2	77.2	1005.6	0.0	3095.54
	7	49.7	149.4	200	5	7	16.2	77.2	1005.6	0.0	3095.54
	8	49.7	149.4	200	5	7	16.2	77.2	1005.6	0.0	3095.54
	9	49.7	149.4	200	5	7	16.2	77.2	1005.6	0.0	3095.54
	10	49.7	149.4	200	5	7	16.2	77.2	1005.6	0.0	3095.54

Table A: 3 Continued

MS1	1	46.9	226.2	160	6	1	25.0	46.0	1011.8	0.0	2114
	2	46.9	226.2	160	6	1	25.0	46.0	1011.8	0.0	2114
	3	46.9	226.2	160	6	1	25.0	46.0	1011.8	0.0	2114
	4	46.9	226.2	160	6	1	25.0	46.0	1011.8	0.0	2114
	5	45.9	229.3	160	6	1	25.0	46.0	1011.8	0.0	2114
	6	45.9	229.3	160	6	1	25.0	46.0	1011.8	0.0	2114
	7	45.9	229.3	160	6	1	25.0	46.0	1011.8	0.0	2114
	8	45.9	229.3	160	6	1	25.0	46.0	1011.8	0.0	2114
	9	45.9	229.3	160	6	1	25.0	46.0	1011.8	0.0	2114
	10	45.9	229.3	160	6	1	25.0	46.0	1011.8	0.0	2114
MS2	1	52.5	159.9	190	4	5	24.2	44.9	1012.5	0.0	1844
	2	52.5	159.9	190	4	5	24.2	44.9	1012.5	0.0	1844
	3	52.5	159.9	200	4	3	25.5	44.7	1012.3	0.0	2487
	4	52.5	159.9	200	4	3	25.5	44.7	1012.3	0.0	2487
	5	52.9	163.7	200	4	3	25.5	44.7	1012.3	0.0	2487
	6	52.9	163.7	200	4	3	25.5	44.7	1012.3	0.0	2487
	7	52.9	163.7	200	4	3	25.5	44.7	1012.3	0.0	2487
	8	52.9	163.7	200	4	3	25.5	44.7	1012.3	0.0	2487
	9	47.9	223.1	160	6	1	25.0	46.0	1011.8	0.0	2114
	10	47.9	223.1	160	6	1	25.0	46.0	1011.8	0.0	2114
MS3	1	51.7	156.3	50	5	8	21.5	73.6	1012.5	0.0	701
	2	51.7	156.3	50	5	8	21.5	73.6	1012.5	0.0	701
	3	51.7	156.3	50	5	8	21.5	73.6	1012.5	0.0	701
	4	51.7	156.3	50	5	8	21.5	73.6	1012.5	0.0	701
	5	51.7	156.3	50	5	8	21.5	73.6	1012.5	0.0	701
	6	51.7	156.3	50	5	8	21.5	73.6	1012.5	0.0	701
	7	52.6	163.7	70	6	8	22.6	68.0	1012.0	0.0	860
	8	52.6	163.7	70	6	8	22.6	68.0	1012.0	0.0	860
	9	52.6	163.7	70	6	8	22.6	68.0	1012.0	0.0	860
	10	52.6	163.7	70	6	8	22.6	68.0	1012.0	0.0	860
RP1	1	49.3	142.2	190	4	5	24.2	44.9	1012.5	0.0	1844
	2	49.3	142.2	190	4	5	24.2	44.9	1012.5	0.0	1844
	3	49.3	142.2	190	4	5	24.2	44.9	1012.5	0.0	1844
	4	49.3	142.2	190	4	5	24.2	44.9	1012.5	0.0	1844
	5	49.3	142.2	190	4	5	24.2	44.9	1012.5	0.0	1844
	6	49.3	142.2	190	4	5	24.2	44.9	1012.5	0.0	1844
	7	53.2	145.6	190	4	5	24.2	44.9	1012.5	0.0	1844
	8	53.2	145.6	190	4	5	24.2	44.9	1012.5	0.0	1844
	9	53.2	145.6	190	4	5	24.2	44.9	1012.5	0.0	1844
	10	53.2	145.6	190	4	5	24.2	44.9	1012.5	0.0	1844
RP2	1	50.8	149	190	4	5	24.2	44.9	1012.5	0.0	1844
	2	50.8	149	190	4	5	24.2	44.9	1012.5	0.0	1844
	3	51.4	152.6	190	4	5	24.2	44.9	1012.5	0.0	1844
	4	51.4	152.6	190	4	5	24.2	44.9	1012.5	0.0	1844
	5	51.4	152.6	190	4	5	24.2	44.9	1012.5	0.0	1844
	6	51.4	152.6	190	4	5	24.2	44.9	1012.5	0.0	1844
	7	52	156.2	190	4	5	24.2	44.9	1012.5	0.0	1844
	8	52	156.2	190	4	5	24.2	44.9	1012.5	0.0	1844
	9	52	156.2	190	4	5	24.2	44.9	1012.5	0.0	1844
	10	52	156.2	190	4	5	24.2	44.9	1012.5	0.0	1844
RP3	1	52.7	163.7	140	8	5	27.0	51.7	1011.0	0.0	2913
	2	52.7	163.7	140	8	5	27.0	51.7	1011.0	0.0	2913

Table A: 3 Continued

3	52.7	163.7	140	8	5	27.0	51.7	1011.0	0.0	2913
4	53.1	167.5	140	8	5	27.0	51.7	1011.0	0.0	2913
5	53.1	167.5	140	8	5	27.0	51.7	1011.0	0.0	2913
6	53.1	167.5	140	8	5	27.0	51.7	1011.0	0.0	2913
7	53.1	167.5	140	8	5	27.0	51.7	1011.0	0.0	2913
8	53.1	167.5	140	8	5	27.0	51.7	1011.0	0.0	2913
9	53.3	171.4	140	8	5	27.0	51.7	1011.0	0.0	2913
10	53.3	171.4	140	8	5	27.0	51.7	1011.0	0.0	2913

Table A:4 Meteorological data and solar altitude and azimuth at paired sampling points -Sept 2003

Plot	Quad	Alt	Azi	Wind Direction	Wind Speed	Cld	Temp	RH	Prsr	Rain	Rad
EF1	1	26.5	214.6	210	12	7	13.5	58.9	1016.1	0.0	691
	2	26.5	214.6	210	12	7	13.5	58.9	1016.1	0.0	691
	3	26.5	214.6	210	12	7	13.5	58.9	1016.1	0.0	691
	4	26.5	214.6	210	12	7	13.5	58.9	1016.1	0.0	691
	5	26.5	214.6	210	12	7	13.5	58.9	1016.1	0.0	691
	6	25.7	217.2	210	12	7	13.5	58.9	1016.1	0.0	691
	7	25.7	217.2	210	12	7	13.5	58.9	1016.1	0.0	691
	8	25.7	217.2	210	12	7	13.5	58.9	1016.1	0.0	691
	9	25.7	217.2	210	12	7	13.5	58.9	1016.1	0.0	691
	10	25.7	217.2	210	12	7	13.5	58.9	1016.1	0.0	691
LS1	1	27.6	212	220	11	7	12.2	84.2	1022.3	0.0	596
	2	27.6	212	220	11	7	12.2	84.2	1022.3	0.0	596
	3	27.6	212	220	11	7	12.2	84.2	1022.3	0.0	596
	4	27.6	212	220	11	7	12.2	84.2	1022.3	0.0	596
	5	26.9	214.6	220	11	7	12.2	84.2	1022.3	0.0	596
	6	26.9	214.6	220	11	7	12.2	84.2	1022.3	0.0	596
	7	26.9	214.6	220	11	7	12.2	84.2	1022.3	0.0	596
	8	26.9	214.6	220	11	7	12.2	84.2	1022.3	0.0	596
	9	26.1	217.3	220	11	7	12.2	84.2	1022.3	0.0	596
	10	26.1	217.3	220	11	7	12.2	84.2	1022.3	0.0	596
LS2	1	28.9	206.5	220	11	7	12.2	84.2	1022.3	0.0	596
	2	28.9	206.5	220	11	7	12.2	84.2	1022.3	0.0	596
	3	28.9	206.5	220	11	7	12.2	84.2	1022.3	0.0	596
	4	28.9	206.5	220	11	7	12.2	84.2	1022.3	0.0	596
	5	28.9	206.5	220	11	7	12.2	84.2	1022.3	0.0	596
	6	28.9	206.5	220	11	7	12.2	84.2	1022.3	0.0	596
	7	28.3	209.2	220	11	7	12.2	84.2	1022.3	0.0	596
	8	28.3	209.2	220	11	7	12.2	84.2	1022.3	0.0	596
	9	28.3	209.2	220	11	7	12.2	84.2	1022.3	0.0	596
	10	28.3	209.2	220	11	7	12.2	84.2	1022.3	0.0	596
LS3	1	25.3	219.9	220	11	7	12.2	84.2	1022.3	0.0	596
	2	25.3	219.9	220	11	7	12.2	84.2	1022.3	0.0	596
	3	25.3	219.9	220	11	7	12.2	84.2	1022.3	0.0	596
	4	25.3	219.9	220	11	7	12.2	84.2	1022.3	0.0	596
	5	25.3	219.9	220	11	7	12.2	84.2	1022.3	0.0	596
	6	25.3	219.9	220	11	7	12.2	84.2	1022.3	0.0	596
	7	25.3	219.9	220	13	2	12.8	75.5	1021.8	0.0	731
	8	25.3	219.9	220	13	2	12.8	75.5	1021.8	0.0	731

Table A: 4 Continued

	9	25.3	219.9	220	13	2	12.8	75.5	1021.8	0.0	731
	10	25.3	219.9	220	13	2	12.8	75.5	1021.8	0.0	731
MC1	1	31.3	183.6	220	8	7	12.4	63.9	1017.9	0.0	210
	2	31.3	183.6	220	8	7	12.4	63.9	1017.9	0.0	210
	3	31.3	183.6	220	8	7	12.4	63.9	1017.9	0.0	210
	4	31.3	183.6	220	8	7	12.4	63.9	1017.9	0.0	210
	5	31.2	186.5	220	8	7	12.4	63.9	1017.9	0.0	210
	6	31.2	186.5	220	8	7	12.4	63.9	1017.9	0.0	210
	7	31.2	186.5	220	10	8	12.7	65.4	1016.8	0.0	272
	8	31.2	186.5	220	10	8	12.7	65.4	1016.8	0.0	272
	9	31.2	186.5	220	10	8	12.7	65.4	1016.8	0.0	272
	10	31.2	186.5	220	10	8	12.7	65.4	1016.8	0.0	272
MC2	1	31.3	177.7	220	8	7	12.4	63.9	1017.9	0.0	210
	2	31.3	177.7	220	8	7	12.4	63.9	1017.9	0.0	210
	3	31.3	177.7	220	8	7	12.4	63.9	1017.9	0.0	210
	4	31.3	177.7	220	8	7	12.4	63.9	1017.9	0.0	210
	5	31.3	177.7	220	8	7	12.4	63.9	1017.9	0.0	210
	6	31.3	177.7	220	8	7	12.4	63.9	1017.9	0.0	210
	7	31.3	177.7	220	8	7	12.4	63.9	1017.9	0.0	210
	8	31.3	177.7	220	8	7	12.4	63.9	1017.9	0.0	210
	8	31.4	180.6	220	8	7	12.4	63.9	1017.9	0.0	210
	8	31.4	180.6	220	8	7	12.4	63.9	1017.9	0.0	210
MC3	1	30.9	169	230	8	8	12.2	66.9	1018.1	0.0	149
	2	30.9	169	220	8	7	12.4	63.9	1017.9	0.0	210
	3	30.9	169	220	8	7	12.4	63.9	1017.9	0.0	210
	4	30.9	169	220	8	7	12.4	63.9	1017.9	0.0	210
	5	30.9	169	220	8	7	12.4	63.9	1017.9	0.0	210
	6	30.9	169	220	8	7	12.4	63.9	1017.9	0.0	210
	7	31.1	171.9	220	8	7	12.4	63.9	1017.9	0.0	210
	8	31.1	171.9	220	8	7	12.4	63.9	1017.9	0.0	210
	9	31.1	171.9	220	8	7	12.4	63.9	1017.9	0.0	210
	10	31.1	171.9	220	8	7	12.4	63.9	1017.9	0.0	210
MC4	1	30.2	163.2	230	8	8	12.2	66.9	1018.1	0.0	149
	2	30.2	163.2	230	8	8	12.2	66.9	1018.1	0.0	149
	3	30.2	163.2	230	8	8	12.2	66.9	1018.1	0.0	149
	4	30.2	163.2	230	8	8	12.2	66.9	1018.1	0.0	149
	5	30.2	163.2	230	8	8	12.2	66.9	1018.1	0.0	149
	6	30.2	163.2	230	8	8	12.2	66.9	1018.1	0.0	149
	7	30.2	163.2	230	8	8	12.2	66.9	1018.1	0.0	149
	8	30.2	163.2	230	8	8	12.2	66.9	1018.1	0.0	149
	9	30.6	166.1	230	8	8	12.2	66.9	1018.1	0.0	149
	10	30.6	166.1	230	8	8	12.2	66.9	1018.1	0.0	149
MG1	1	31.3	168.8	220	14	8	12.6	73.0	1021.9	0.0	891
	2	31.3	168.8	220	14	8	12.6	73.0	1021.9	0.0	891
	3	31.3	168.8	220	14	8	12.6	73.0	1021.9	0.0	891
	4	31.3	168.8	220	14	8	12.6	73.0	1021.9	0.0	891
	5	29.2	154.6	220	14	8	12.6	73.0	1021.9	0.0	891
	6	29.2	154.6	220	14	8	12.6	73.0	1021.9	0.0	891
	7	29.2	154.6	220	14	8	12.6	73.0	1021.9	0.0	891
	8	29.2	154.6	220	14	8	12.6	73.0	1021.9	0.0	891
	9	29.2	154.6	220	14	8	12.6	73.0	1021.9	0.0	891
	10	29.2	154.6	220	14	8	12.6	73.0	1021.9	0.0	891

Table A: 4 Continued

MG2	1	31.6	174.7	220	14	8	12.6	73.0	1021.9	0.0	891
	2	31.6	174.7	220	14	8	12.6	73.0	1021.9	0.0	891
	3	31.6	174.7	220	14	8	12.6	73.0	1021.9	0.0	891
	4	31.6	174.7	220	14	8	12.6	73.0	1021.9	0.0	891
	5	31.6	174.7	220	14	8	12.6	73.0	1021.9	0.0	891
	6	31.6	174.7	220	14	8	12.6	73.0	1021.9	0.0	891
	7	31.7	177.6	220	14	8	12.6	73.0	1021.9	0.0	891
	8	31.7	177.6	220	14	8	12.6	73.0	1021.9	0.0	891
	9	31.7	177.6	220	14	8	12.6	73.0	1021.9	0.0	891
	10	31.7	177.6	220	14	8	12.6	73.0	1021.9	0.0	891
MS1	1	32.8	165.1	230	3	0	14.8	53.9	1010.9	0.0	1335
	2	32.8	165.1	230	3	0	14.8	53.9	1010.9	0.0	1335
	3	32.8	165.1	230	3	0	14.8	53.9	1010.9	0.0	1335
	4	33.1	168.1	230	3	0	14.8	53.9	1010.9	0.0	1335
	5	33.1	168.1	230	3	0	14.8	53.9	1010.9	0.0	1335
	6	33.1	168.1	230	3	0	14.8	53.9	1010.9	0.0	1335
	7	33.1	168.1	230	3	0	14.8	53.9	1010.9	0.0	1335
	8	33.1	168.1	230	7	5	13.7	60.3	1012.3	0.0	1266
	9	33.4	171	230	7	5	13.7	60.3	1012.3	0.0	1266
	10	33.4	171	230	7	5	13.7	60.3	1012.3	0.0	1266
MS2	1	33.7	177	230	7	5	13.7	60.3	1012.3	0.0	1266
	2	33.7	177	230	7	5	13.7	60.3	1012.3	0.0	1266
	3	33.7	177	230	7	5	13.7	60.3	1012.3	0.0	1266
	4	33.7	177	230	7	5	13.7	60.3	1012.3	0.0	1266
	5	33.7	177	230	7	5	13.7	60.3	1012.3	0.0	1266
	6	33.7	180	230	7	5	13.7	60.3	1012.3	0.0	1266
	7	33.7	180	230	7	5	13.7	60.3	1012.3	0.0	1266
	8	33.7	180	230	7	5	13.7	60.3	1012.3	0.0	1266
	9	33.7	180	230	7	5	13.7	60.3	1012.3	0.0	1266
	10	33.7	180	230	7	5	13.7	60.3	1012.3	0.0	1266
MS3	1	27.3	220.2	220	8	3	14.5	51.3	1012.9	0.0	1805
	2	27.3	220.2	250	5	3	14.1	54.7	1013.6	0.0	763
	3	27.3	220.2	250	5	3	14.1	54.7	1013.6	0.0	763
	4	27.3	220.2	250	5	3	14.1	54.7	1013.6	0.0	763
	5	26.4	222.8	250	5	3	14.1	54.7	1013.6	0.0	763
	6	26.4	222.8	250	5	3	14.1	54.7	1013.6	0.0	763
	7	26.4	222.8	250	5	3	14.1	54.7	1013.6	0.0	763
	8	26.4	222.8	250	5	3	14.1	54.7	1013.6	0.0	763
	9	25.4	225.4	250	5	3	14.1	54.7	1013.6	0.0	763
	10	25.4	225.4	250	5	3	14.1	54.7	1013.6	0.0	763
RP1	1	33.8	170.9	210	5	5	16.3	58.9	1006.9	0.0	1315
	2	33.8	170.9	210	5	5	16.3	58.9	1006.9	0.0	1315
	3	33.8	170.9	210	5	5	16.3	58.9	1006.9	0.0	1315
	4	33.8	170.9	210	5	5	16.3	58.9	1006.9	0.0	1315
	5	33.8	170.9	210	5	5	16.3	58.9	1006.9	0.0	1315
	6	33.9	173.9	210	5	5	16.3	58.9	1006.9	0.0	1315
	7	33.9	173.9	210	5	5	16.3	58.9	1006.9	0.0	1315
	8	33.9	173.9	210	5	5	16.3	58.9	1006.9	0.0	1315
	9	33.9	173.9	210	5	5	16.3	58.9	1006.9	0.0	1315
	10	33.9	173.9	210	5	5	16.3	58.9	1006.9	0.0	1315
RP2	1	34.1	179.9	210	5	5	16.3	58.9	1006.9	0.0	1315
	2	34.1	179.9	210	5	5	16.3	58.9	1006.9	0.0	1315

Table A: 4 Continued

	3	34.1	179.9	210	5	5	16.3	58.9	1006.9	0.0	1315
	4	34.1	179.9	210	5	5	16.3	58.9	1006.9	0.0	1315
	5	34.1	179.9	210	5	5	16.3	58.9	1006.9	0.0	1315
	6	34.1	179.9	210	5	5	16.3	58.9	1006.9	0.0	1315
	7	34	182.9	210	5	5	16.3	58.9	1006.9	0.0	1315
	8	34	182.9	210	5	5	16.3	58.9	1006.9	0.0	1315
	9	34	182.9	210	5	5	16.3	58.9	1006.9	0.0	1315
	10	34	182.9	210	5	5	16.3	58.9	1006.9	0.0	1315
RP3	1	33.8	188.9	210	4	7	15.8	64.0	1006.9	0.0	1050
	2	33.8	188.9	210	4	7	15.8	64.0	1006.9	0.0	1050
	3	33.8	188.9	210	4	7	15.8	64.0	1006.9	0.0	1050
	4	33.8	188.9	210	4	7	15.8	64.0	1006.9	0.0	1050
	5	33.8	188.9	210	4	7	15.8	64.0	1006.9	0.0	1050
	6	33.5	191.9	210	4	7	15.8	64.0	1006.9	0.0	1050
	7	33.5	191.9	210	4	7	15.8	64.0	1006.9	0.0	1050
	8	33.5	191.9	210	4	7	15.8	64.0	1006.9	0.0	1050
	9	33.5	191.9	210	4	7	15.8	64.0	1006.9	0.0	1050
	10	33.5	191.9	210	4	7	15.8	64.0	1006.9	0.0	1050

Table A:5 Daily meteorological averages for July 2003 (sampling days highlighted)

DAY	MAX TEMP (Deg C)	MIN TEMP (Deg C)	RAIN (mm)	SUN (hours)	GRASS MIN (Deg C)	WIND SPEED (knots)	WIND DIRECTION (degrees)	GUST (knots)	WEATHER (key-chpt 3)
1	16.4	12.0	0.8	1.0	9.1	6	40	20	
2	17.1	10.3	0.2	2.3	9.9	3	360	15	
3	18.9	7.2	0.0	1.9	2.5	3	20	12	
4	20.5	10.1	0.0	9.7	6.9	4	50	15	
5	16.4	10.6	0.0	0.1	10.4	3	180	10	
6	17.3	10.8	0.6	0.6	10.6	6	230	23	
7	17.5	11.2	4.0	2.3	10.1	5	170	19	
8	19.7	10.8	0.0	2.7	7.6	5	200	14	
9	24.6	5.8	0.2	3.4	0.0	5	190	22	
10	22.2	15.4	0.2	3.0	13.7	11	200	31	
11	19.0	10.0	0.4	4.1	7.9	9	210	29	
12	18.6	10.3	0.0	1.5	8.7	7	200	23	
13	24.5	7.4	1.2	14.0	2.8	8	230	32	
14	27.5	13.3	0.0	8.5	11.3	---	50	16	
15	27.5	10.2	0.0	12.8	4.7	---	230	20	
16	27.9	8.6	0.0	11.3	4.4	5	120	20	
17	26.4	15.9	0.0	5.1	11.3	5	50	18	
18	21.9	16.2	4.6	0.7	13.6	---	40	19	
19	22.4	10.7	0.4	3.8	6.2	5	110	20	
20	20.7	12.2	4.0	5.4	8.3	6	200	22	
21	19.3	12.1	2.9	2.0	10.3	4	220	---	
22	17.5	---	0.0	3.0	---	5	---	---	---
23	18.3	---	0.6	0.3	---	6	210	26	
24	19.8	13.1	0.0	9.8	12.0	9	220	26	
25	21.6	13.3	0.2	2.4	11.3	5	230	19	
26	18.2	8.4	0.8	4.1	4.9	4	210	17	
27	19.0	6.3	0.0	10.9	2.2	6	210	22	
28	20.1	7.0	1.8	3.3	2.0	6	210	20	
29	20.0	10.8	2.8	1.2	8.8	4	210	17	
30	17.7	12.3	---	1.5	12.4	2	30	11	
31	18.7	12.8	3.0	2.3	11.7	---	210	29	

Table A:6 Daily meteorological averages for August 2003 (sampling days highlighted)

DAY	MAX TEMP (Deg C)	MIN TEMP (Deg C)	RAIN (mm)	SUN (hours)	GRASS MIN (Deg C)	WIND SPEED (knots)	WIND DIRECTION (degrees)	GUST (knots)	WEATHER (key-chpt 3)
1	18.6	11.5	0.6	9.9	8.4	9	210	26	
2	18.7	9.5	0.0	5.5	6.0	8	220	28	
3	20.2	8.9	0.0	9.4	3.2	7	210	23	
4	24.3	12.5	0.0	5.2	10.6	3	170	15	
5	27.1	8.0	1.4	4.1	4.5	3	100	21	
6	29.1	15.5	0.0	10.3	15.2	3	90	13	
7	29.0	12.2	0.0	12.3	8.9	3	130	14	
8	30.6	11.9	0.0	12.6	8.2	4	130	19	
9	28.8	13.0	2.0	6.1	7.6	8	230	27	
10	20.2	15.9	0.4	2.9	16.1	3	60	11	
11	23.1	12.1	0.0	5.6	9.0	3	130	12	
12	22.0	10.5	0.0	2.6	7.6	---	160	13	
13	18.9	11.4	1.4	8.8	9.1	7	230	25	
14	18.7	10.6	0.0	3.6	6.1	4	310	17	
15	19.7	7.4	0.0	3.3	2.6	2	310	12	
16	21.8	2.8	0.0	9.2	-1.6	2	140	12	
17	22.2	7.8	1.2	3.0	5.1	6	220	23	
18	18.9	10.1	3.0	5.7	6.8	8	220	31	
19	17.6	9.9	0.4	4.9	5.0	9	210	28	
20	19.0	10.5	2.8	2.7	8.7	8	210	23	
21	16.8	12.5	3.8	0.5	11.1	10	220	31	
22	18.9	10.8	0.0	4.5	8.4	9	230	27	
23	21.1	7.5	0.0	8.4	2.4	3	160	13	
24	22.1	4.5	0.0	10.5	0.0	3	100	13	
25	18.2	7.9	0.6	6.3	2.1	3	50	13	
26	16.9	10.0	0.0	5.4	4.9	3	30	13	
27	16.6	5.7	1.4	1.6	0.3	3	220	14	
28	13.7	6.2	9.6	2.6	1.9	4	30	22	
29	13.8	8.2	3.0	4.1	4.5	5	20	17	
30	13.4	7.5	4.6	2.8	3.8	4	340	---	
31	14.6	7.5	0.0	2.5	3.1	---	330	---	

Table A:7 Daily meteorological averages for September 2003 (sampling days highlighted)

DAY	MAX TEMP (Deg C)	MIN TEMP (Deg C)	RAIN (mm)	SUN (hours)	GRASS MIN (Deg C)	WIND SPEED (knots)	WIND DIRECTION (degrees)	GUST (knots)	WEATHER (key-chpt 3)
1	16.1	7.9	0.4	0.1	3.1	3	---	---	
2	---	7.9	0.0	0.1	3.1	3	250	---	
3	19.4	---	0.0	2.6	0.9	5	210	---	---
4	20.9	9.8	0.0	5.3	6.4	6	210	26	
5	18.2	10.1	0.4	1.3	4.7	7	220	24	
6	17.6	4.4	2.0	6.0	-1.1	3	170	13	
7	17.6	3.3	4.2	7.3	-1.3	5	170	22	
8	17.7	7.9	0.0	7.3	5.2	---	200	18	
9	16.9	8.2	2.6	3.5	4.4	5	190	17	
10	17.7	6.0	0.2	8.8	2.1	2	140	12	
11	16.6	0.4	1.0	1.1	-3.0	8	210	34	
12	17.7	7.0	4.4	7.4	1.6	8	200	33	
13	19.6	9.9	1.0	2.5	8.9	16	210	42	
14	18.0	14.0	0.6	1.0	14.3	8	230	25	
15	20.0	7.1	0.0	4.2	3.5	5	130	23	
16	18.0	7.3	0.0	0.7	2.2	6	120	23	
17	22.2	11.8	0.0	6.1	12.2	15	220	35	
18	17.9	12.4	0.0	3.0	10.0	---	---	---	
19	16.4	7.1	0.0	5.3	0.4	4	---	---	
20	16.7	6.0	0.2	4.6	2.6	2	210	10	
21	15.9	2.9	1.8	3.5	-2.2	7	220	29	
22	10.7	6.6	13.4	3.8	5.7	4	290	21	
23	9.7	0.8	0.0	6.6	-3.3	4	230	30	
24	13.6	0.0	0.2	0.9	-4.5	11	210	31	
25	14.1	9.6	7.2	0.1	8.7	9	220	27	
26	12.3	5.5	0.2	3.0	0.3	3	---	---	
27	13.2	2.6	0.8	3.0	-1.5	2	160	12	
28	14.0	4.4	0.0	6.4	2.3	3	160	15	
29	12.5	5.7	1.8	0.1	0.7	5	210	21	
30	15.3	0.3	0.0	7.4	-3.4	2	130	8	f

B. Appendix

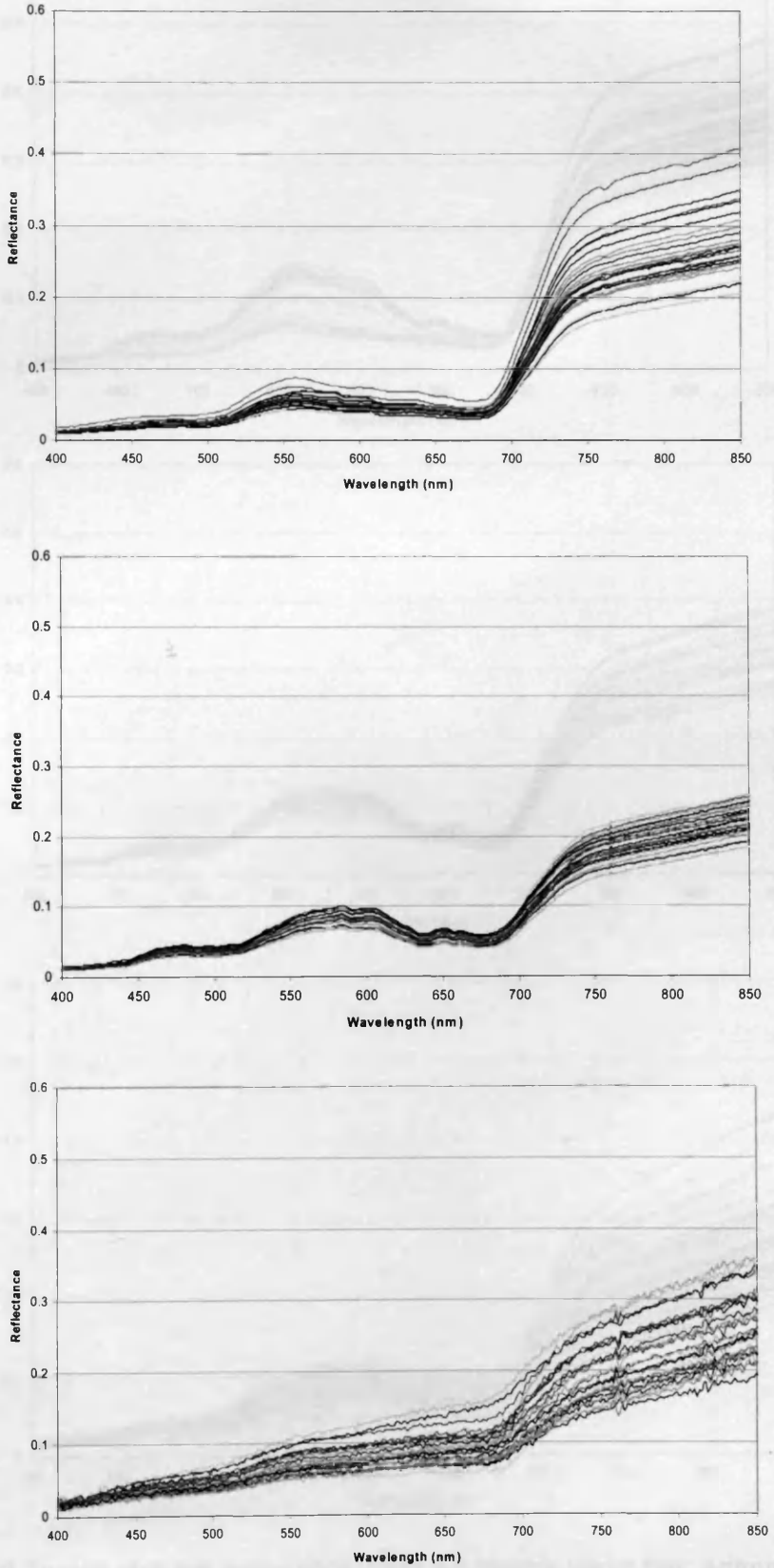

Figure B:1 *Equisetum fluviatile* (EF1) All spectra (July: top; August: middle; Sept: bottom)

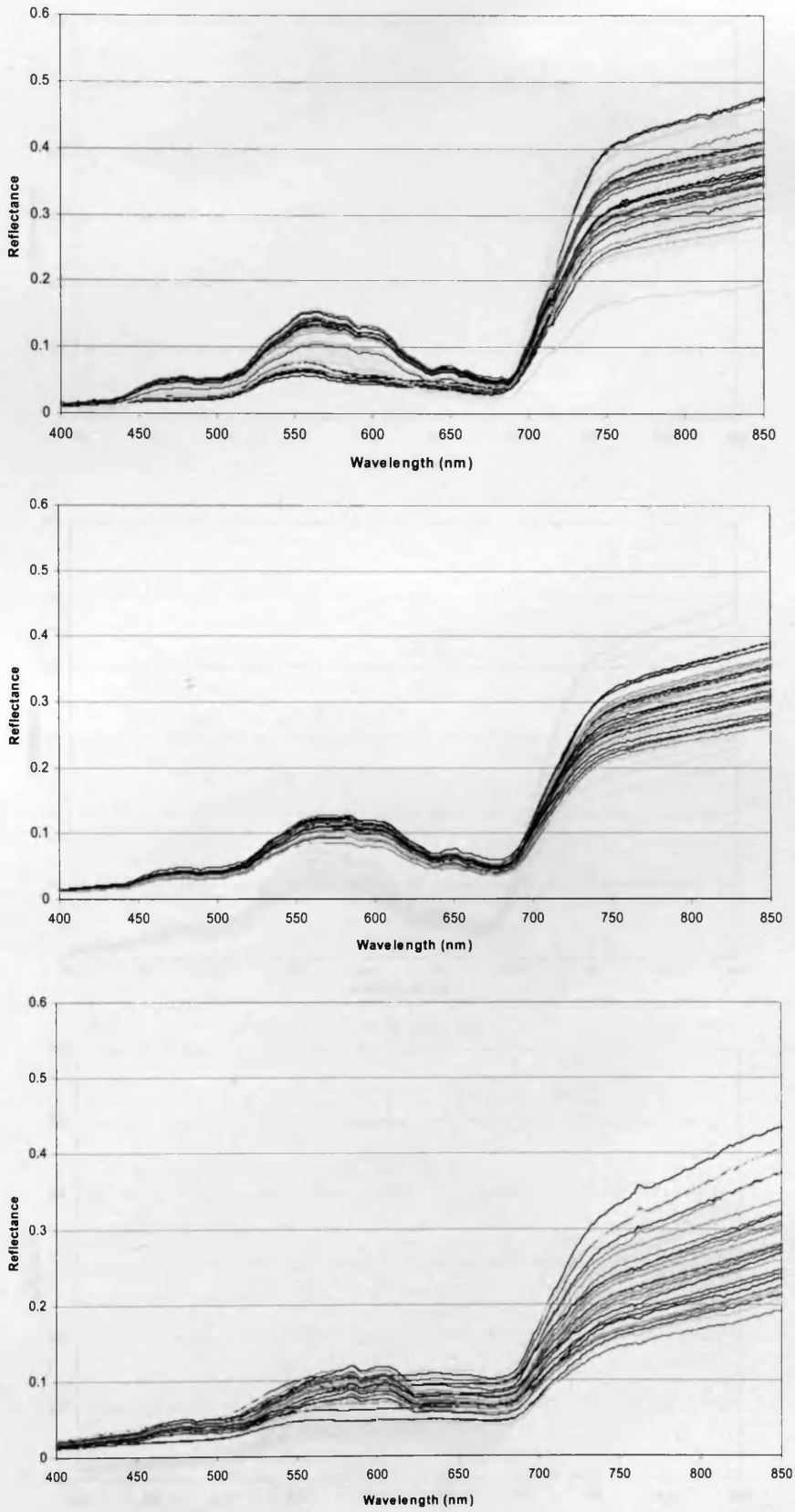

Figure B:2 Species rich low sedge mire (LS1) All spectra (July: top; August: middle; Sept: bottom)

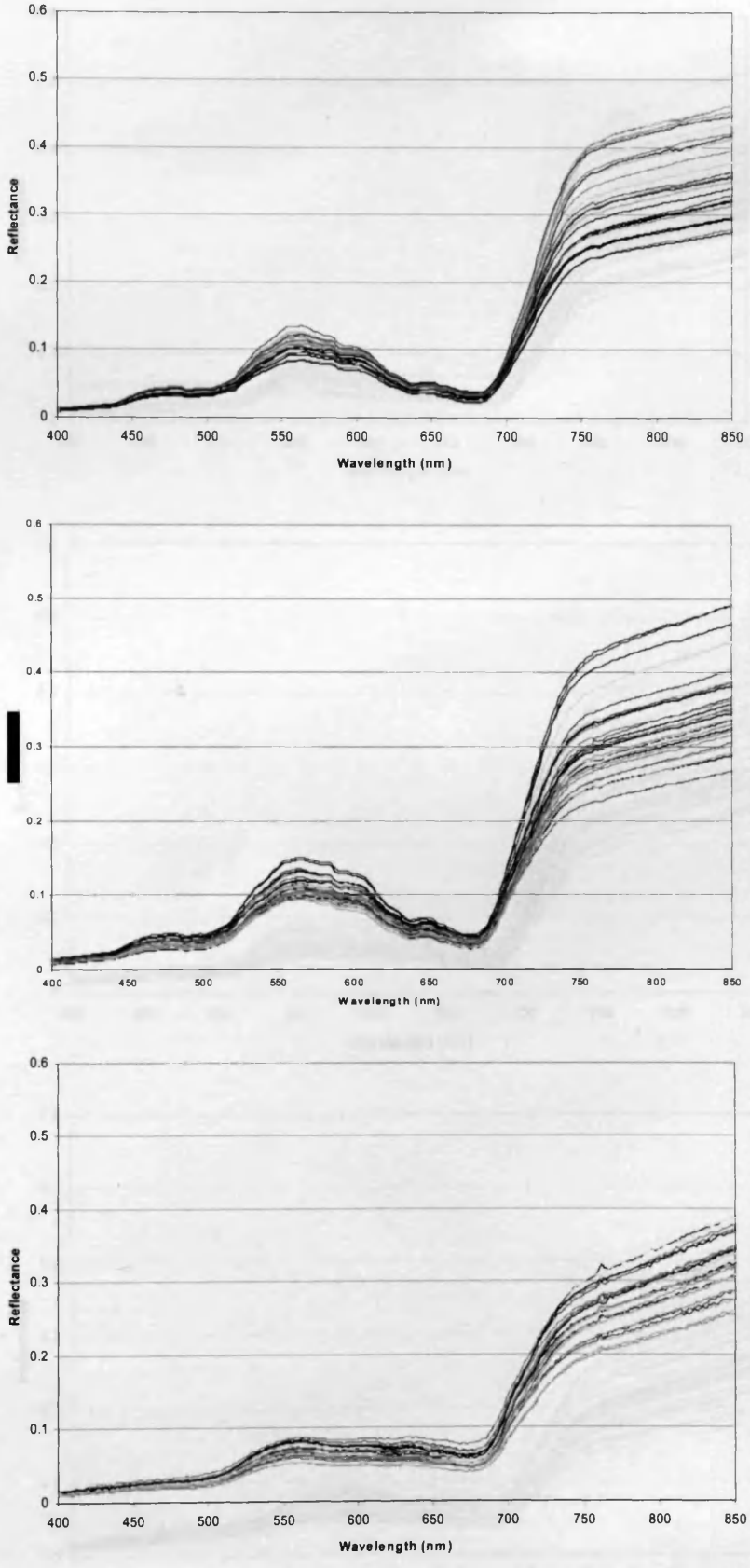

Figure B:3 Species rich low sedge mire (LS2) All spectra (July: top; August: middle; Sept: bottom)

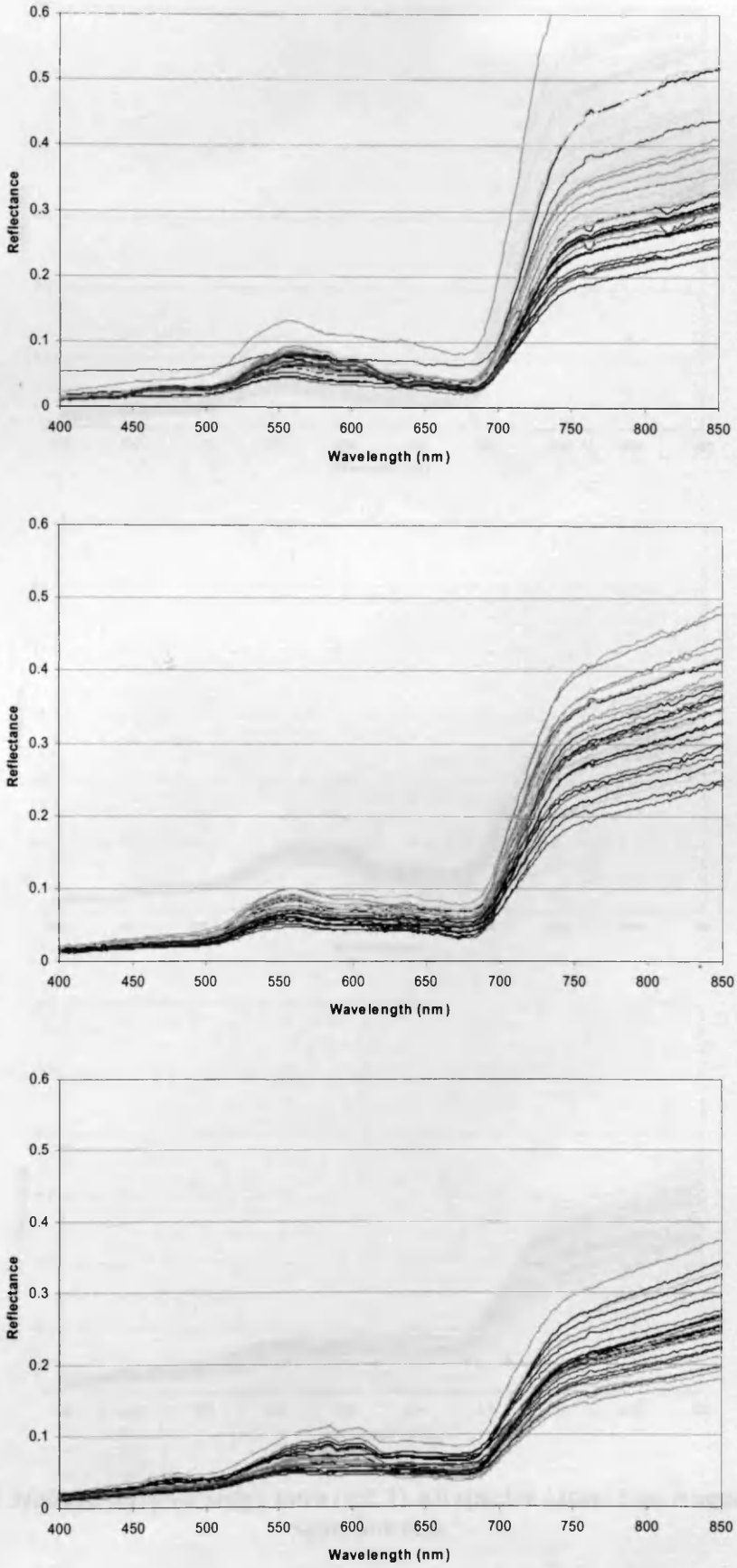

Figure B:4 Species rich low sedge mire (LS3) All spectra (July: top; August: middle; Sept: bottom)

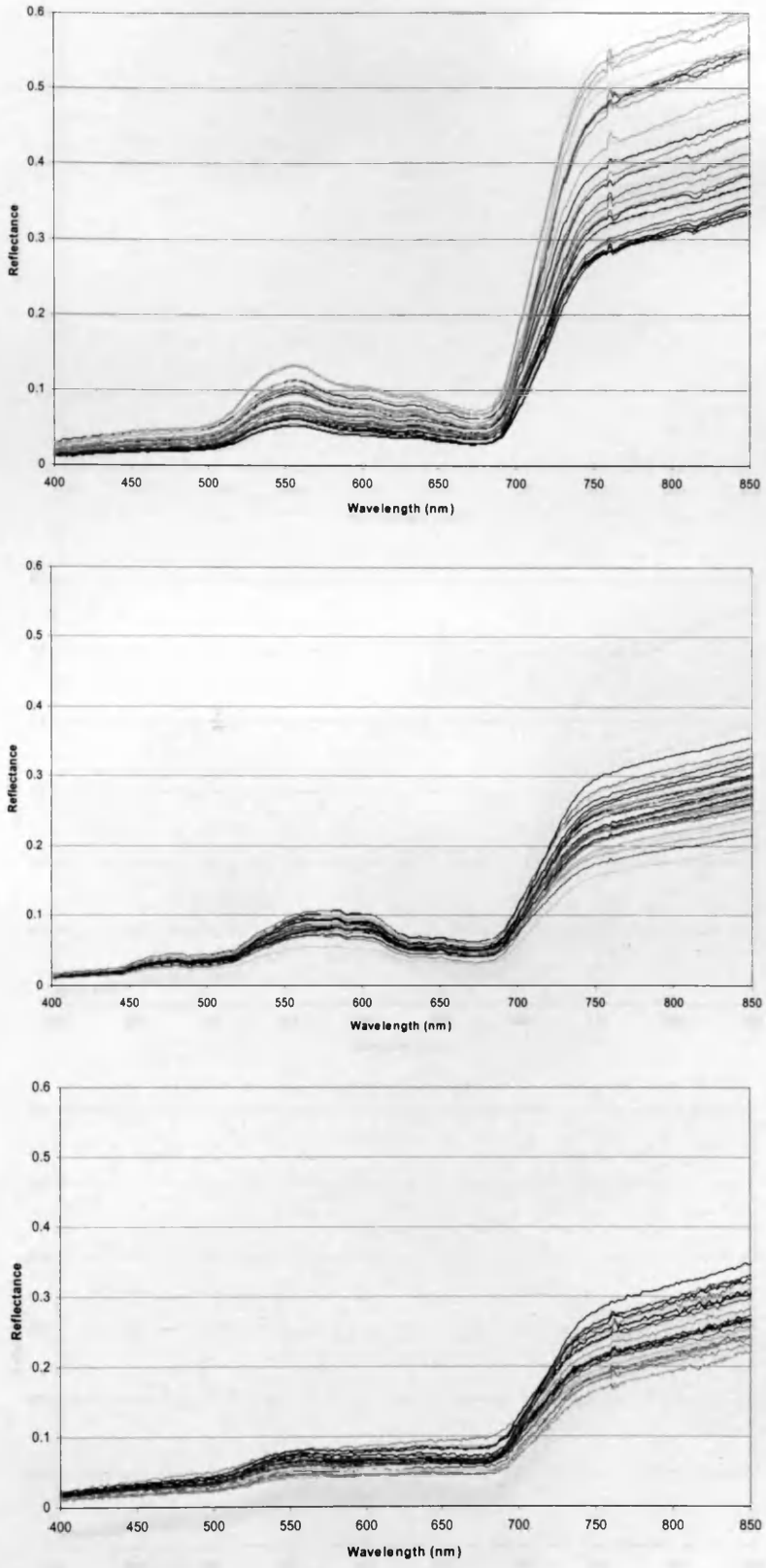

Figure B:5 *Molinia caerulea*-sedge mire (MC1) All spectra (July: top; August: middle; Sept: bottom)

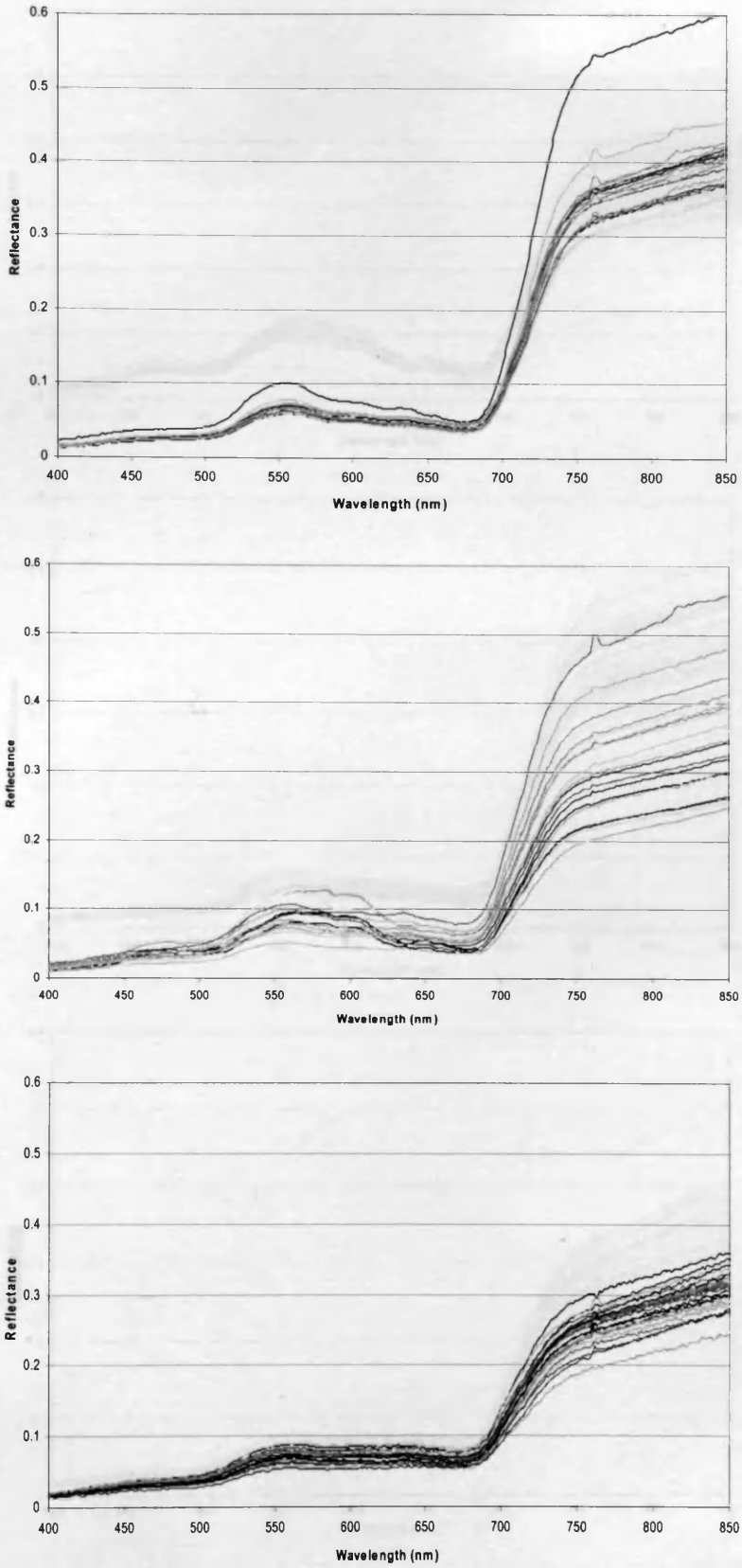

Figure B:6 *Molinia caerulea*-sedge mire (MC2) All spectra (July: top; August: middle; Sept: bottom)

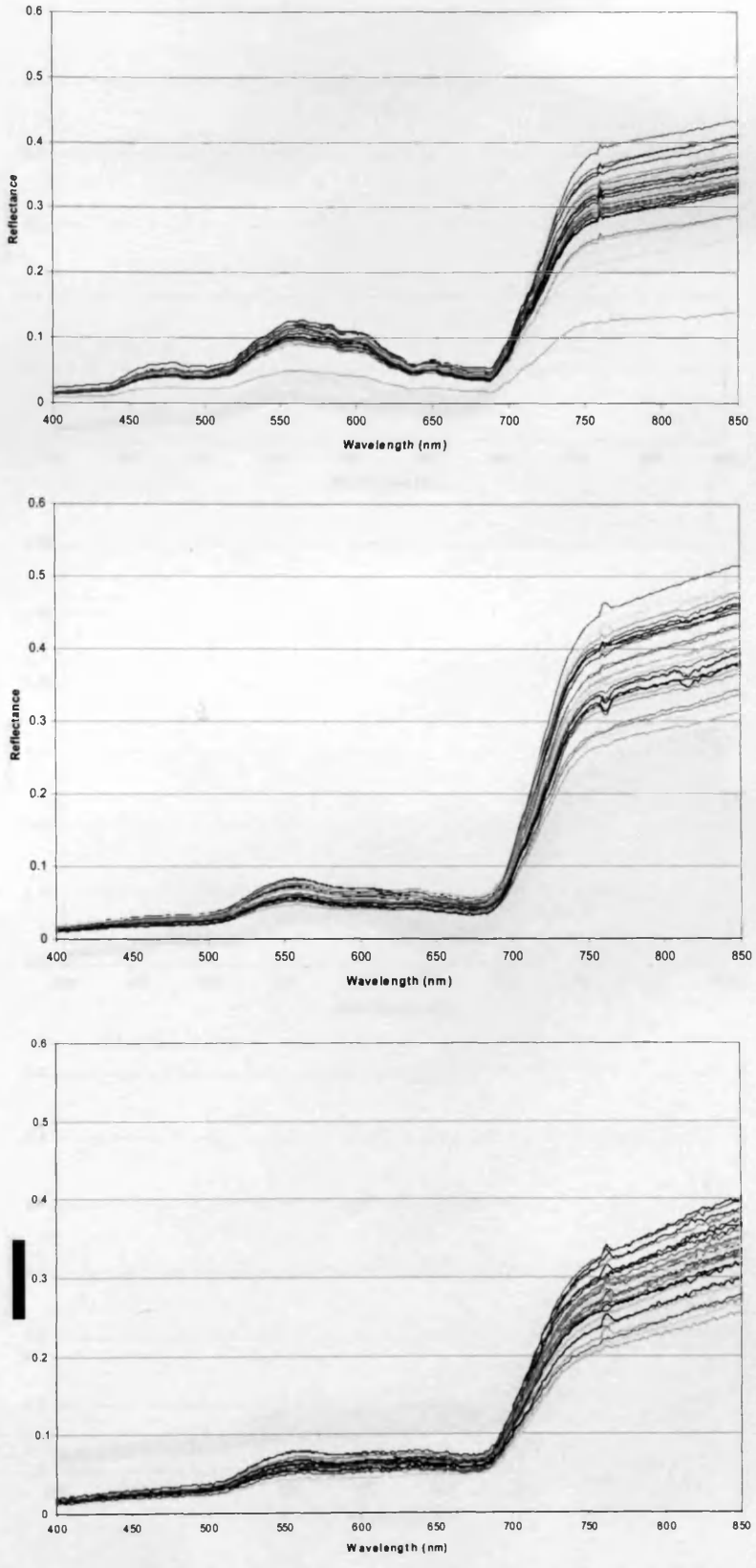

Figure B:7 *Molinia caerulea*-sedge mire (MC3) All spectra (July: top; August: middle; Sept: bottom)

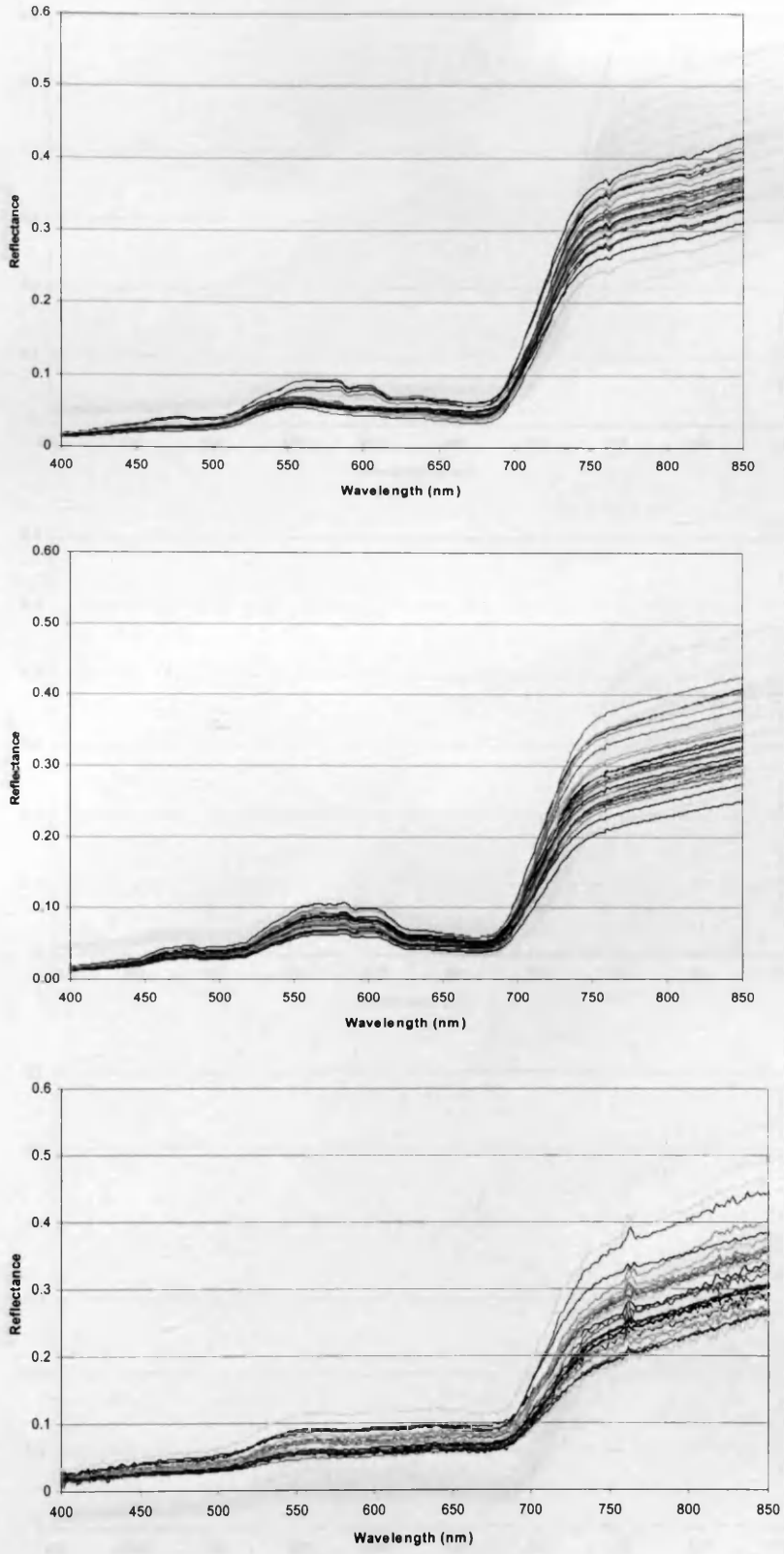

Figure B:8 *Molinia caerulea*-sedge mire (MC4) All spectra (July: top; August: middle; Sept: bottom)

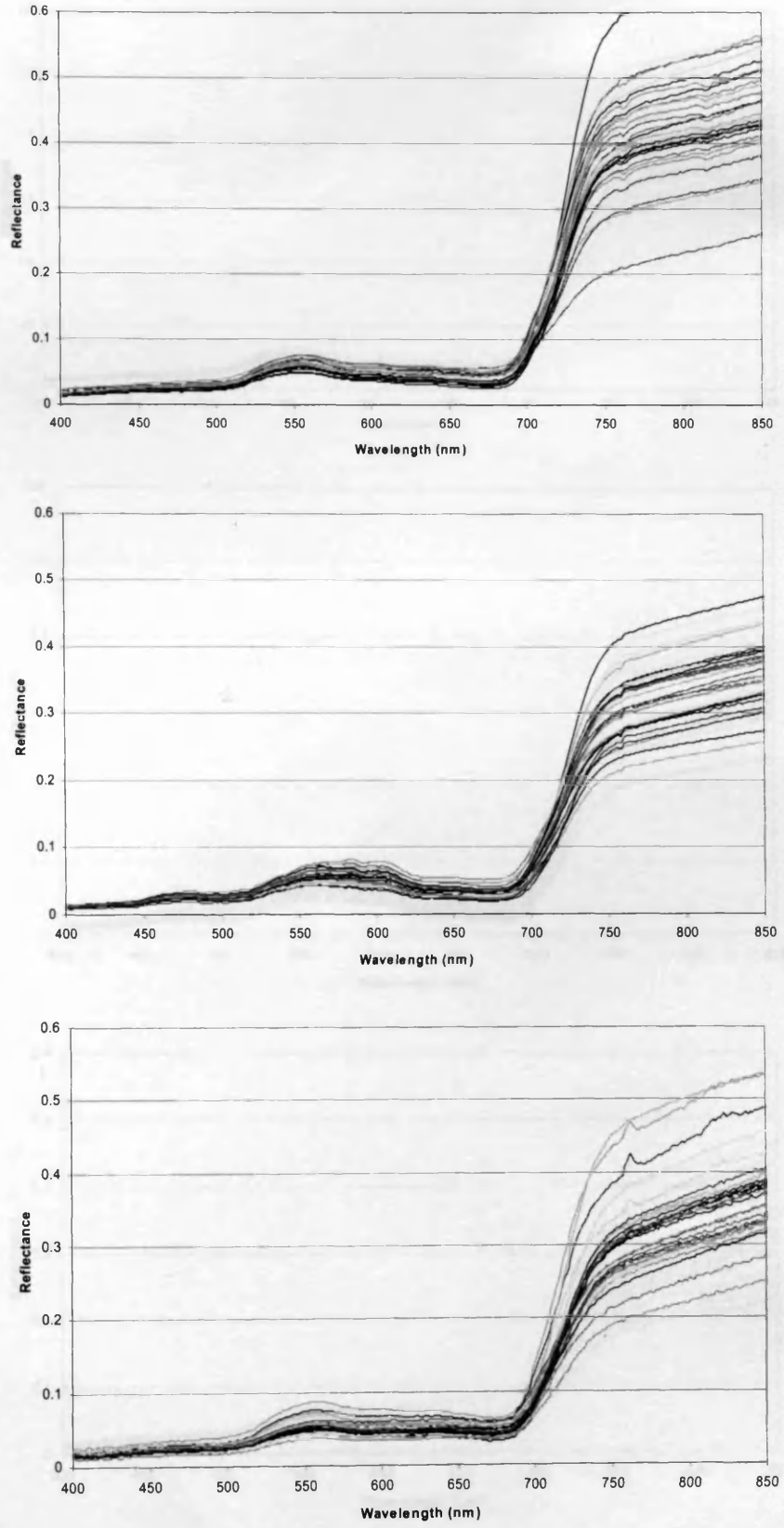

Figure B:9 *Myrica gale-Molinia caerulea*-sedge mire (MG1) All spectra (July: top; August: middle; Sept: bottom)

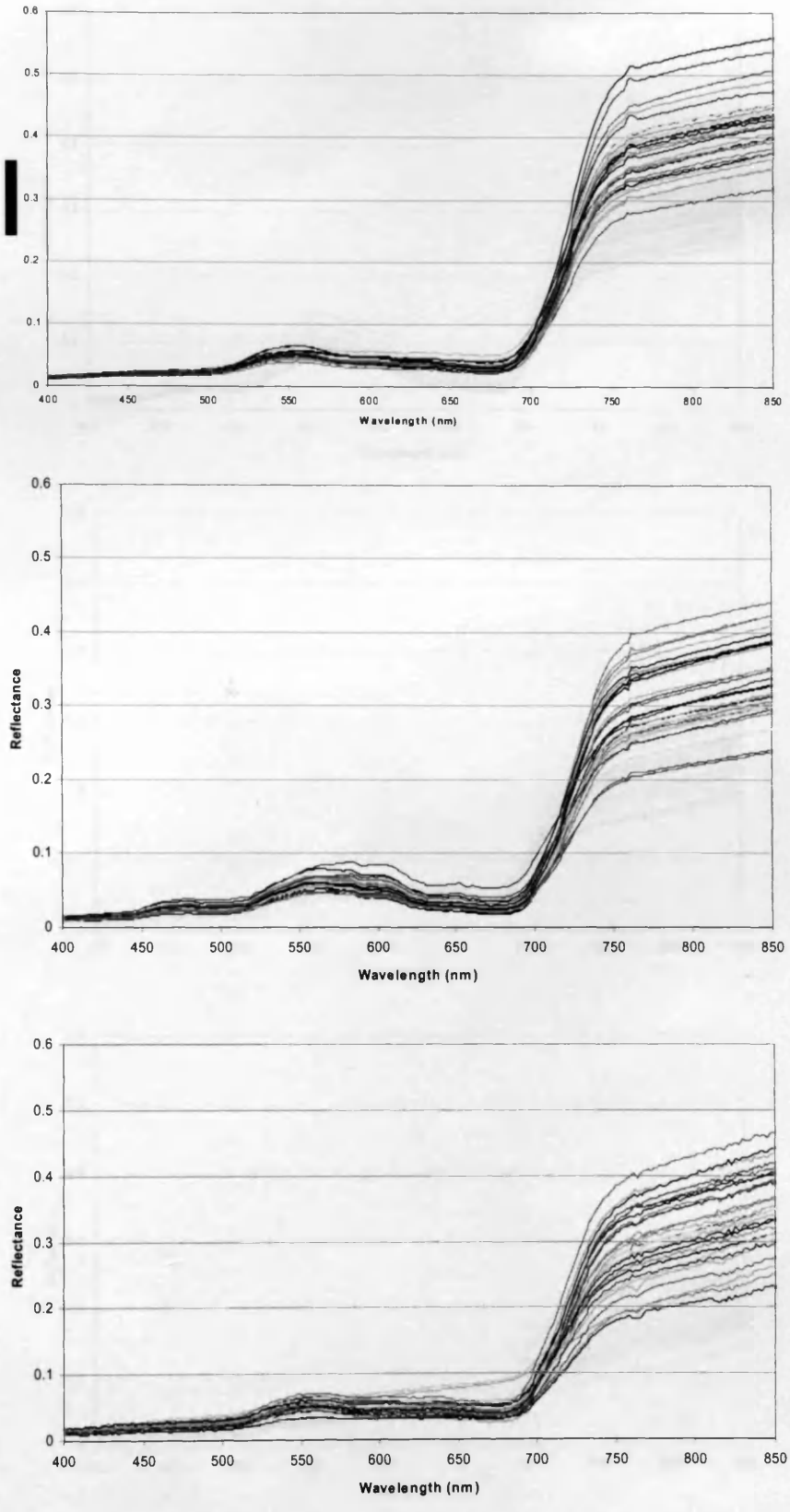

Figure B:10 ***Myrica gale-Molinia caerulea*****-sedge mire (MG2) All spectra (July: top; August: middle; Sept: bottom)**

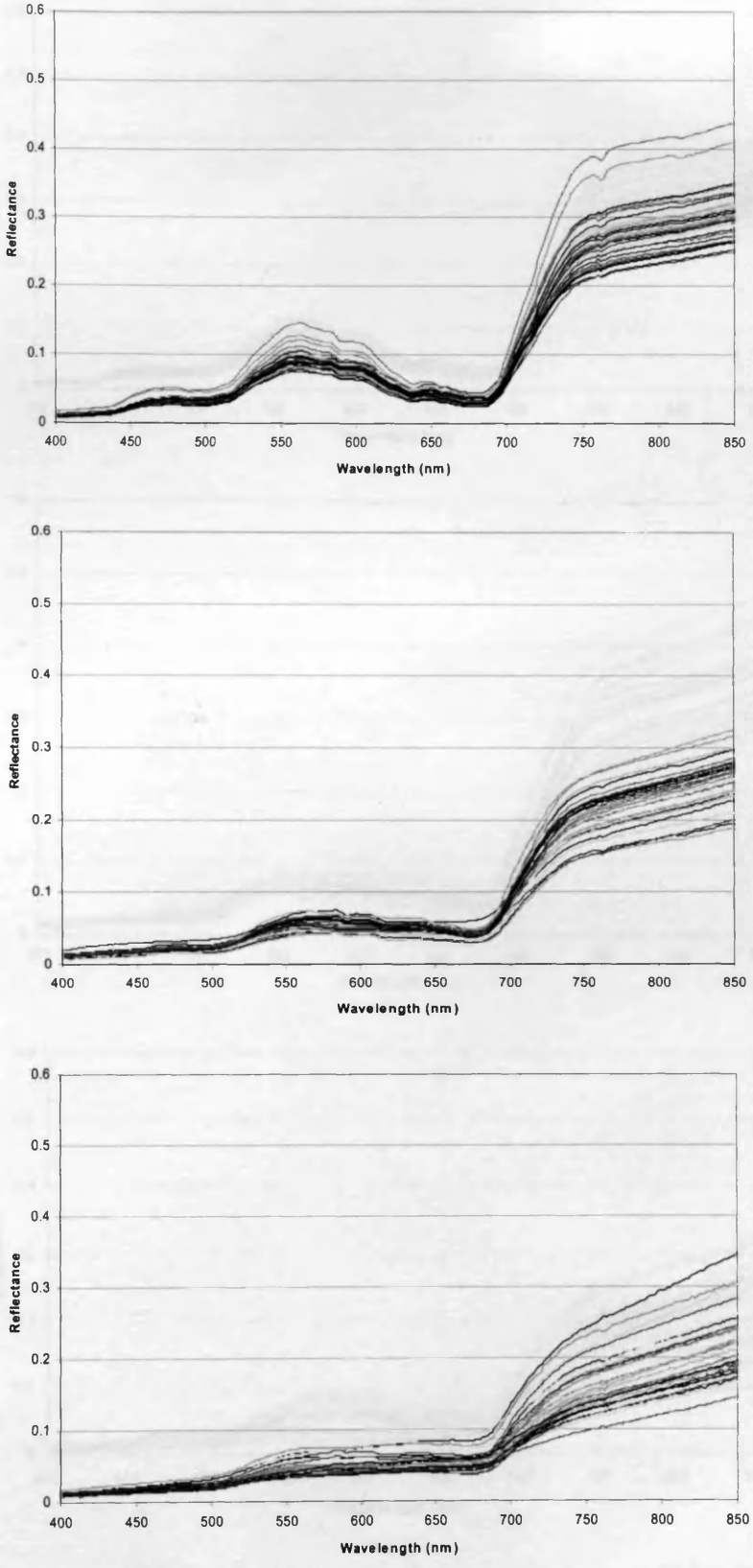

Figure B:11 Mixed sedge (MS1) All spectra (July: top; August: middle; Sept: bottom)

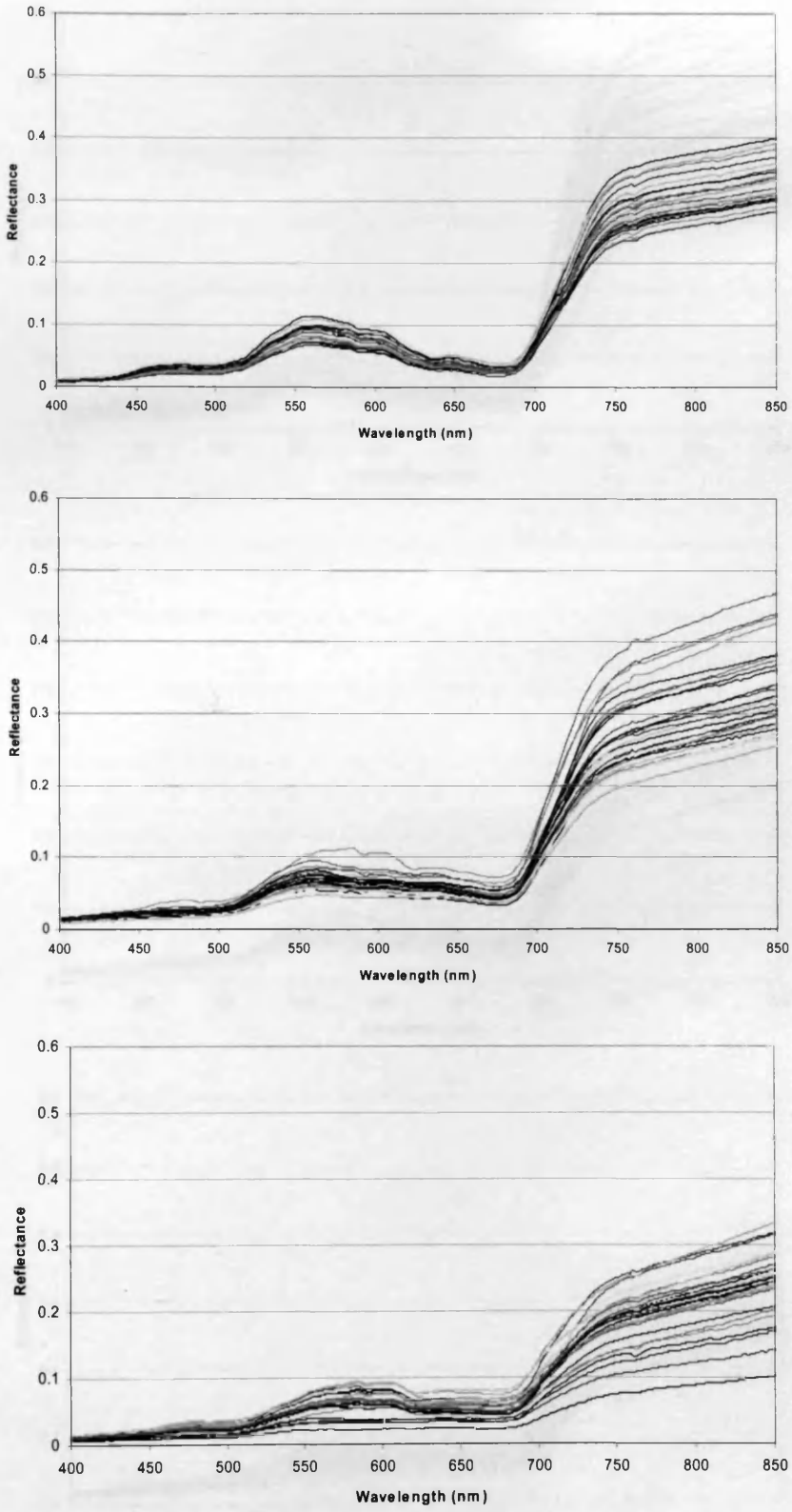

Figure B:12 Mixed sedge (MS2) All spectra (July: top; August: middle; Sept: bottom)

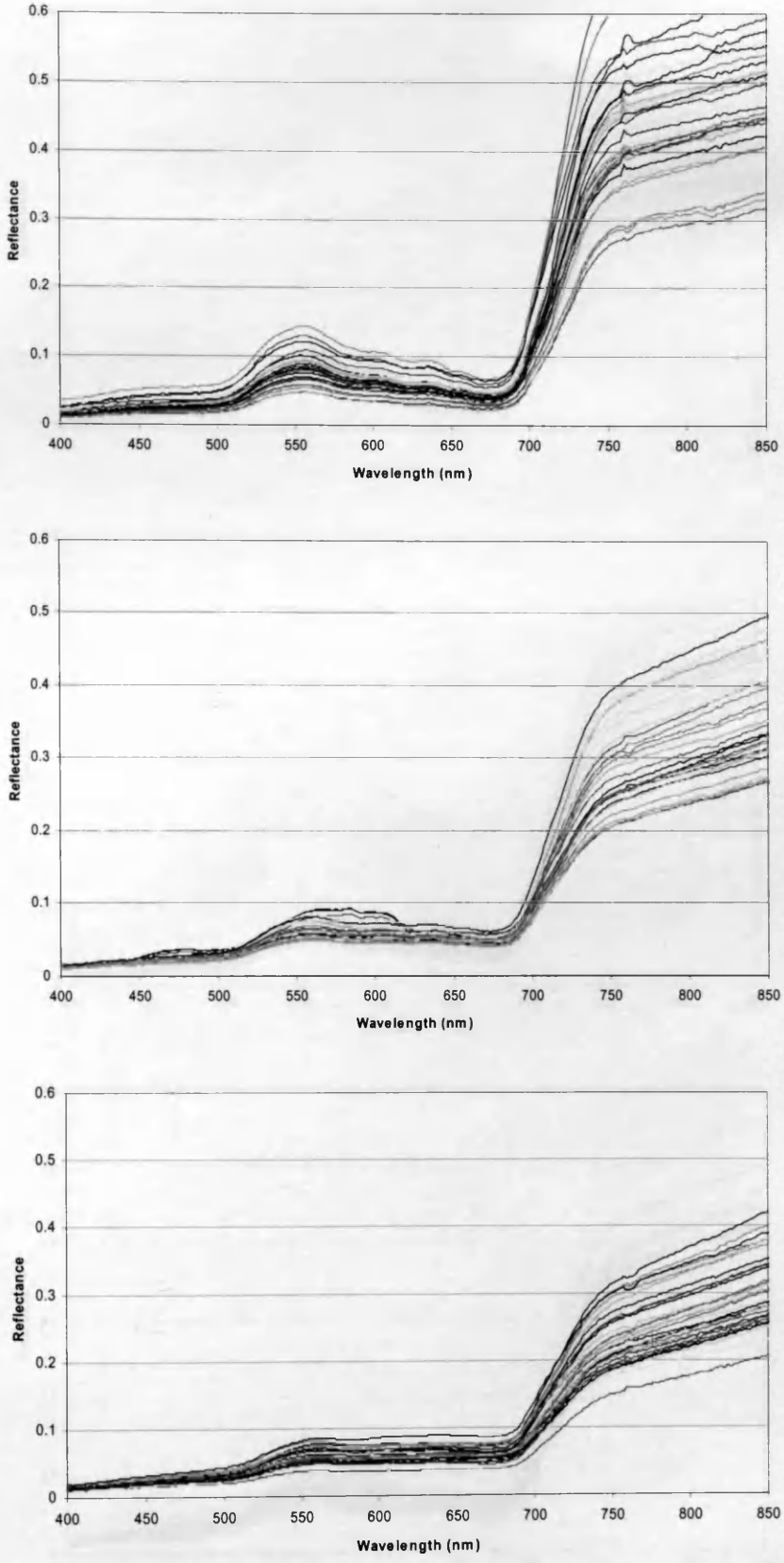

Figure B:13 Mixed sedge (MS3) All spectra (July: top; August: middle; Sept: bottom)

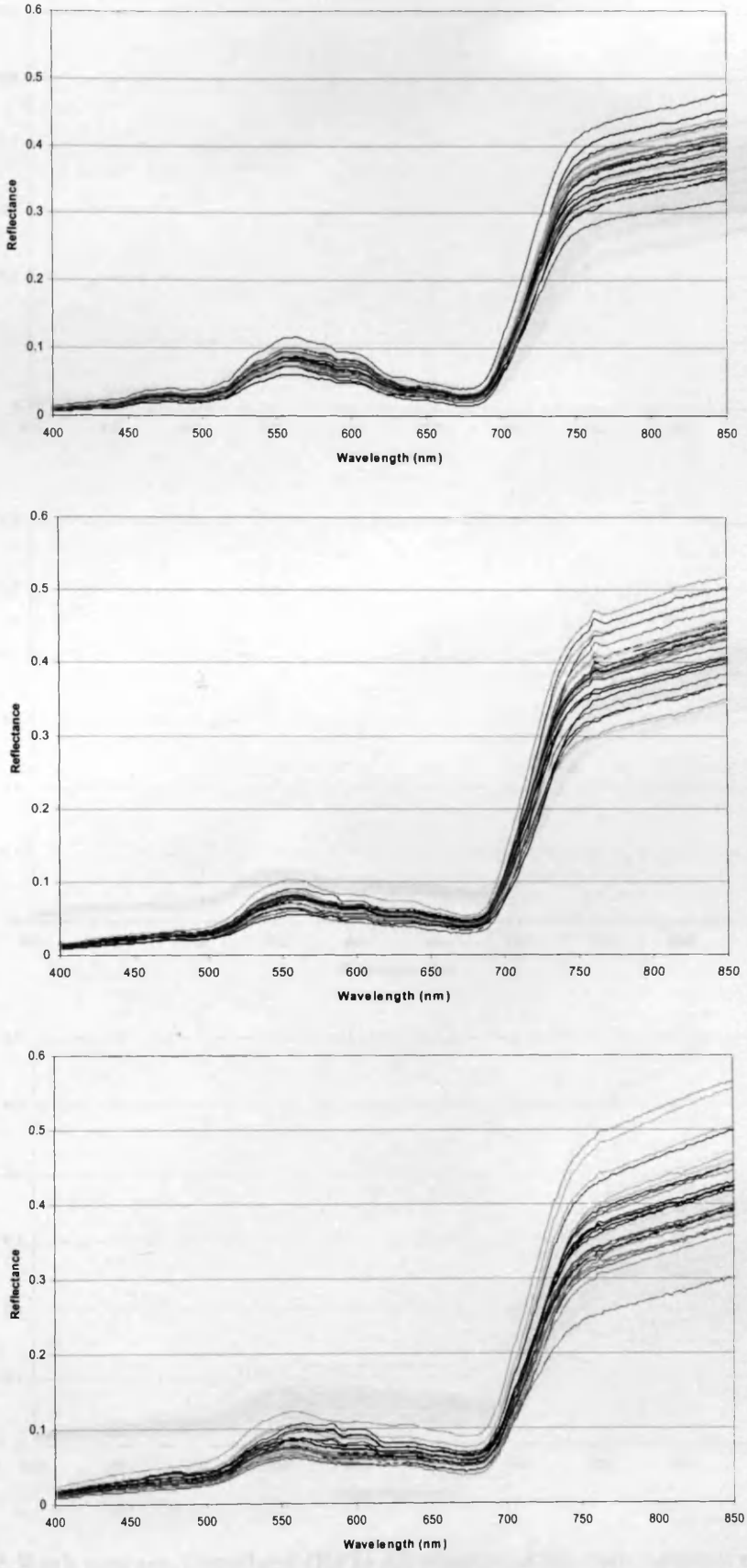

Figure B:14 Rush pasture/Grassland (RP1) All spectra (July: top; August: middle; Sept: bottom)

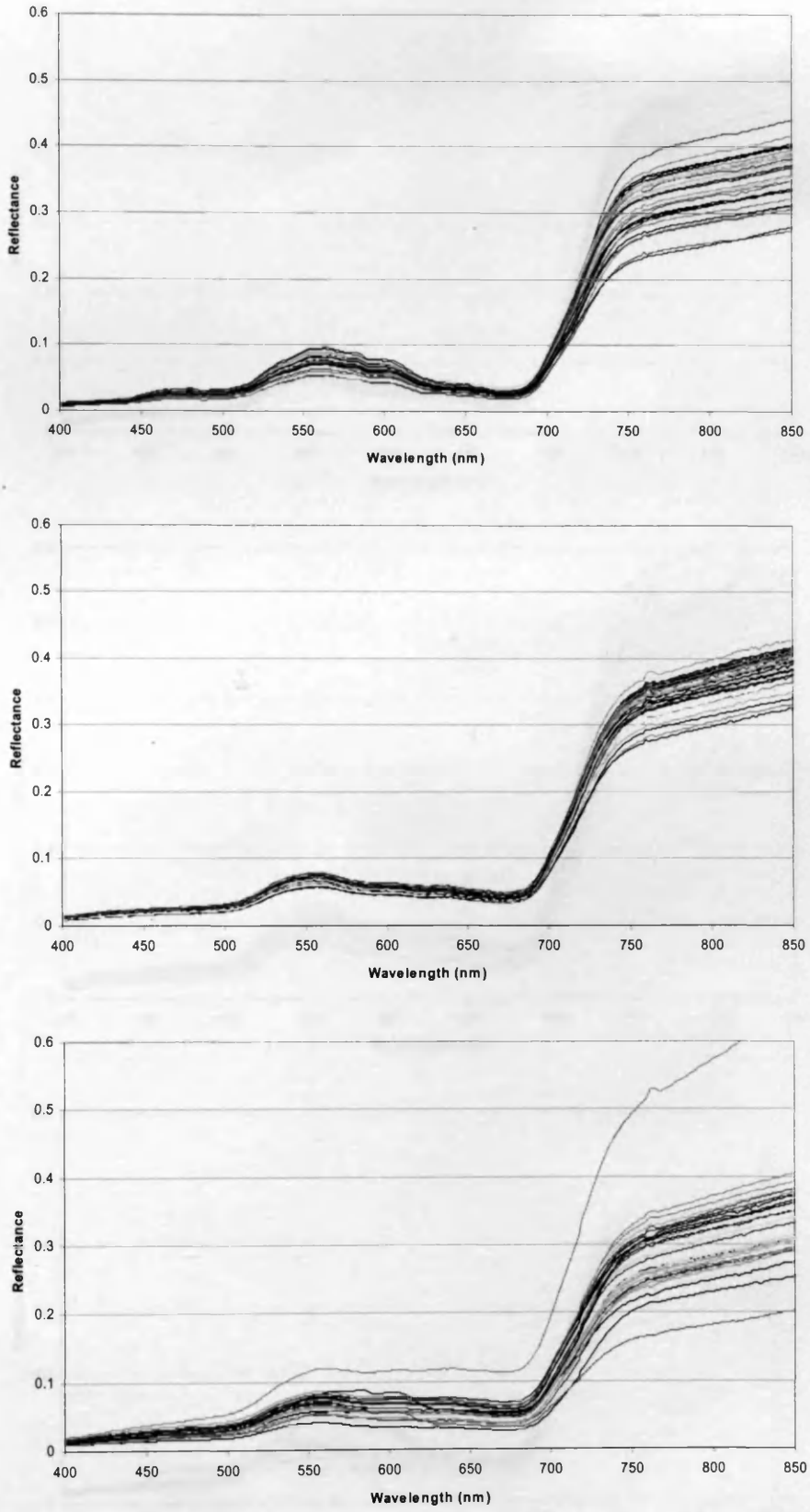

Figure B:15 Rush pasture/Grassland (RP2) All spectra (July: top; August: middle; Sept: bottom)

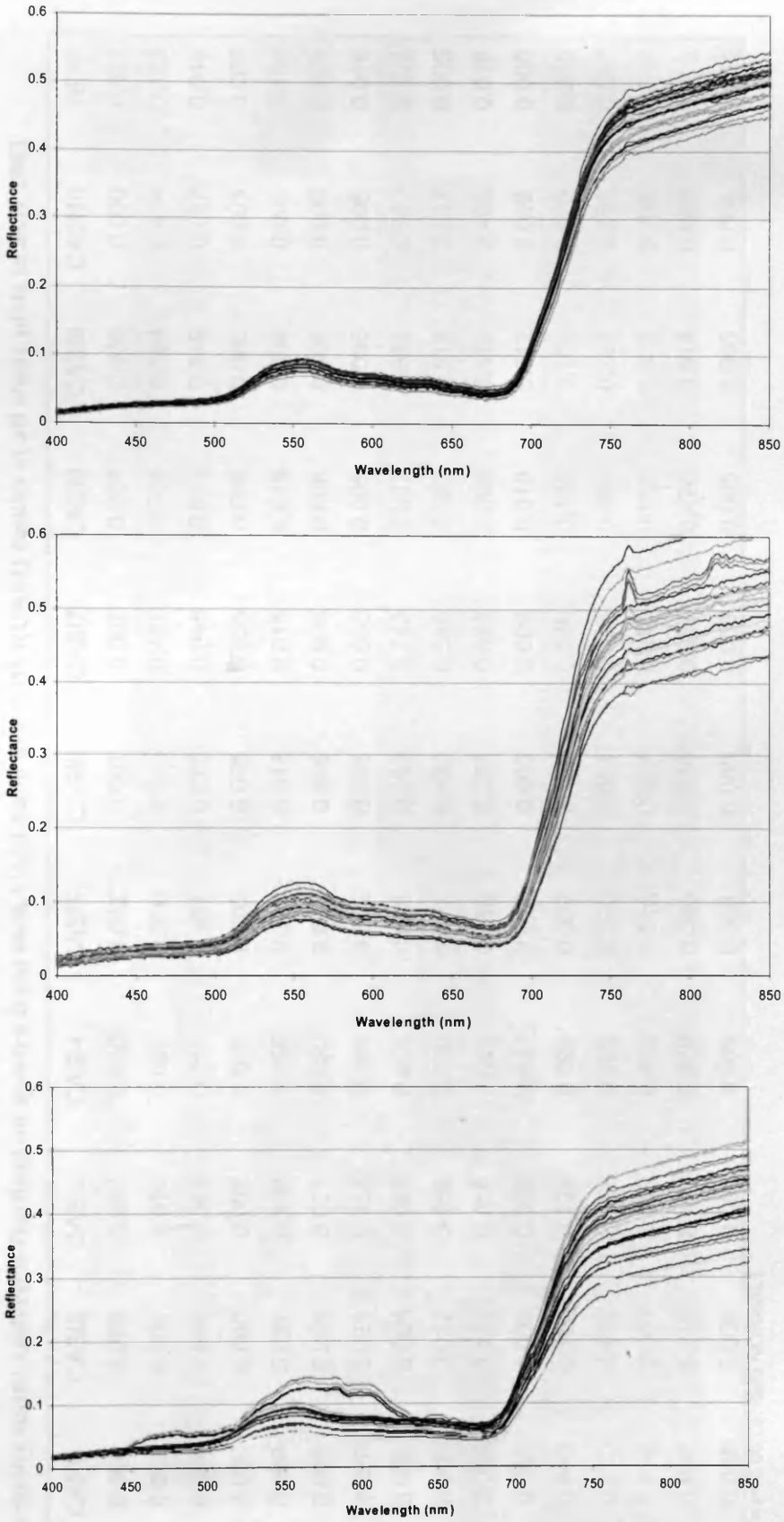

Figure B:16 Rush pasture/Grassland (RP3) All spectra (July: top; August: middle; Sept: bottom)

Normality test on all simulated CASI data

Table B:1 Normality tests (Anderson-Darling) on spectra from each CASI band and NDVI(CASI) results at all study plots in July 2003

	CASI1	CASI2	CASI3	CASI4	CASI5	CASI6	CASI7	CASI8	CASI9	CASI10	NDVI
EF1	0.009	0.009	0.237	0.440	0.012	0.007	0.007	0.007	0.009	0.006	0.461
LS1	0.005	0.005	0.016	0.005	0.016	0.430	0.487	0.508	0.504	0.414	0.122
LS2	0.054	0.898	0.549	0.756	0.981	0.076	0.048	0.051	0.049	0.097	0.049
LS3	0.005	0.040	0.001	0.005	0.005	0.005	0.005	0.005	0.005	0.005	0.005
MC1	0.008	0.022	0.186	0.066	0.026	0.013	0.015	0.015	0.008	0.009	0.483
MC2	0.005	0.005	0.021	0.082	0.013	0.005	0.005	0.005	0.005	0.005	0.103
MC3	0.020	0.031	0.151	0.005	0.005	0.005	0.005	0.005	0.005	0.005	0.016
MC4	0.005	0.005	0.067	0.005	0.028	0.893	0.742	0.667	0.885	0.843	0.108
MG1	0.005	0.022	0.008	0.330	0.487	0.482	0.346	0.383	0.517	0.597	0.005
MG2	0.068	0.118	0.016	0.068	0.318	0.397	0.471	0.508	0.415	0.453	0.019
MS1	0.005	0.005	0.269	0.117	0.012	0.005	0.009	0.010	0.012	0.008	0.005
MS2	0.905	0.109	0.124	0.005	0.009	0.122	0.149	0.138	0.105	0.070	0.515
MS3	0.220	0.439	0.198	0.096	0.225	0.611	0.564	0.449	0.283	0.252	0.567
RP1	0.658	0.680	0.119	0.493	0.513	0.927	0.894	0.850	0.923	0.756	0.847
RP2	0.687	0.249	0.497	0.339	0.086	0.174	0.324	0.470	0.514	0.585	0.226
RP3	0.005	0.008	0.005	0.005	0.005	0.005	0.005	0.005	0.005	0.005	0.624

(Highlighted cells = P>0.05 i.e. data NORMAL)

Table B:2 Normality tests (Anderson-Darling) on spectra from each CASI band and NDVI(CASI) results at all study plots in August 2003

	CASI1	CASI2	CASI3	CASI4	CASI5	CASI6	CASI7	CASI8	CASI9	CASI10	NDVI
EF1	0.658	0.457	0.119	0.022	0.178	0.788	0.793	0.792	0.828	0.850	0.991
LS1	0.555	0.044	0.941	0.255	0.534	0.887	0.893	0.826	0.768	0.704	0.454
LS2	0.555	0.044	0.941	0.255	0.534	0.887	0.893	0.826	0.768	0.704	0.454
LS3	0.081	0.826	0.405	0.734	0.875	0.929	0.901	0.912	0.898	0.906	0.337
MC1	0.529	0.310	0.278	0.772	0.705	0.962	0.949	0.985	0.997	0.982	0.052
MC2	0.572	0.580	0.361	0.285	0.396	0.664	0.693	0.728	0.648	0.692	0.564
MC3	0.625	0.097	0.693	0.165	0.117	0.441	0.524	0.657	0.678	0.869	0.629
MC4	0.623	0.524	0.445	0.718	0.533	0.188	0.157	0.174	0.205	0.196	0.565
MG1	0.382	0.680	0.082	0.423	0.862	0.792	0.669	0.649	0.764	0.774	0.025
MG2	0.072	0.588	0.006	0.191	0.522	0.301	0.301	0.276	0.251	0.255	0.020
MS1	0.005	0.839	0.133	0.370	0.858	0.885	0.852	0.762	0.719	0.642	0.008
MS2	0.005	0.005	0.005	0.005	0.005	0.012	0.020	0.021	0.013	0.011	0.005
MS3	0.607	0.305	0.184	0.145	0.142	0.103	0.111	0.111	0.077	0.114	0.571
RP1	0.424	0.625	0.720	0.214	0.211	0.106	0.298	0.337	0.229	0.326	0.259
RP2	0.130	0.069	0.330	0.457	0.247	0.036	0.022	0.016	0.023	0.012	0.680
RP3	0.005	0.005	0.005	0.005	0.021	0.373	0.326	0.384	0.703	0.388	0.005

(Highlighted cells = P>0.05 i.e. data NORMAL)

Table B:3 Normality tests (Anderson-Darling) on spectra from each CASI band and NDVI(CASI) results at all study plots in September 2003

	CASI1	CASI2	CASI3	CASI4	CASI5	CASI6	CASI7	CASI8	CASI9	CASI10	NDVI
EF1	0.385	0.292	0.119	0.215	0.204	0.290	0.377	0.363	0.351	0.427	0.090
LS1	0.908	0.161	0.540	0.552	0.516	0.273	0.251	0.217	0.122	0.105	0.209
LS2	0.792	0.875	0.369	0.788	0.827	0.755	0.785	0.735	0.829	0.790	0.107
LS3	0.051	0.122	0.330	0.142	0.085	0.108	0.113	0.125	0.207	0.225	0.214
MC1	0.100	0.835	0.053	0.362	0.725	0.404	0.365	0.287	0.238	0.168	0.575
MC2	0.738	0.970	0.372	0.941	0.940	0.131	0.147	0.242	0.543	0.920	0.518
MC3	0.505	0.735	0.355	0.713	0.743	0.821	0.870	0.847	0.909	0.834	0.675
MC4	0.005	0.005	0.005	0.005	0.005	0.005	0.005	0.005	0.005	0.005	0.005
MG1	0.005	0.005	0.036	0.090	0.013	0.010	0.015	0.016	0.006	0.010	0.056
MG2	0.474	0.404	0.005	0.159	0.494	0.760	0.674	0.679	0.796	0.840	0.005
MS1	0.008	0.006	0.025	0.005	0.005	0.025	0.029	0.024	0.021	0.026	0.766
MS2	0.005	0.005	0.005	0.005	0.005	0.005	0.005	0.005	0.005	0.005	0.005
MS3	0.882	0.503	0.949	0.572	0.542	0.226	0.206	0.265	0.313	0.340	0.553
RP1	0.316	0.225	0.200	0.053	0.031	0.123	0.208	0.167	0.082	0.070	0.903
RP2	0.690	0.090	0.005	0.005	0.009	0.009	0.007	0.005	0.005	0.005	0.961
RP3	0.032	0.005	0.005	0.005	0.005	0.187	0.261	0.271	0.224	0.135	0.973

(Highlighted cells = P>0.05 i.e. data NORMAL)

Table B:4 Kruskal Wallis H test results: LS habitat, July

Plots	LS1	LS2	LS3
N	30	30	30
DF	2		

	CASI-1			CASI-2			CASI-3			CASI-4			CASI-5		
	LS1	LS2	LS3	LS1	LS2	LS3	LS1	LS2	LS3	LS1	LS2	LS3	LS1	LS2	LS3
Median	0.034	0.030	0.022	0.123	0.108	0.073	0.046	0.032	0.032	0.087	63.9	4.72	0.141	0.118	0.101
Ave Rank	56.3	54.9	25.3	56	57.1	23.3	63.5	37.7	35.3	0.073	39.7	-1.48	62.5	42.7	31.3
Z	2.77	2.41	-5.18	2.7	2.99	-5.69	4.63	-2.01	-2.62	0.063	32.9	-3.24	4.37	-0.73	-3.65
H	26.86			32.42			21.56			23.27			21.97		
P	0.000			0.000			0.000			0.000			0.000		

	CASI-6			CASI-7			CASI-8			CASI-9			CASI-10		
	LS1	LS2	LS3	LS1	LS2	LS3	LS1	LS2	LS3	LS1	LS2	LS3	LS1	LS2	LS3
Median	0.282	0.279	0.233	0.304	0.301	0.251	0.330	0.326	0.274	0.350	0.346	0.292	0.374	0.368	0.316
Ave Rank	52.4	51	33.1	52	51	33.6	51.9	50.6	34	52.1	50.6	33.8	51.7	50	34.8
Z	1.76	1.41	-3.18	1.66	1.4	-3.06	1.65	1.31	-2.96	1.69	1.32	-3	1.59	1.15	-2.74
H	10.12			9.41			8.81			9.07			7.57		
P	0.006			0.009			0.012			0.011			0.023		

Table B:5 Kruskal Wallis H test results: MC habitat, July

Plots	MC1	MC2	MC3	MC4
N	30	21	30	32
DF	3			

	CASI-1				CASI-2				CASI-3				CASI-4			
	MC1	MC2	MC3	MC4	MC1	MC2	MC3	MC4	MC1	MC2	MC3	MC4	MC1	MC2	MC3	MC4
Median	0.02621	0.02373	0.0338	0.02373	0.08045	0.06671	0.101	0.06434	0.04637	0.03789	0.0435	0.04449	0.09902	0.08142	0.0724	0.08302
Ave Rank	52.8	43.6	87.1	41.5	63.8	41.4	86.7	33	62.7	38.6	57.5	63.3	78.5	59.3	30.7	60
Z	-0.83	-2.07	5.88	-3.16	1.32	-2.41	5.79	-4.89	1.11	-2.86	0.09	1.29	4.19	0.36	-5.14	0.61
H	36.54				47.8				8.75				32.67			
P	0.000				0.000				0.033				0.000			

	CASI-5				CASI-6				CASI-7				CASI-8			
	MC1	MC2	MC3	MC4	MC1	MC2	MC3	MC4	MC1	MC2	MC3	MC4	MC1	MC2	MC3	MC4
Median	0.1525	0.1292	0.1152	0.1248	0.3359	0.3051	0.269	0.2763	0.3616	0.3322	0.2905	0.2971	0.3919	0.3615	0.3141	0.3222
Ave Rank	79	61.2	36.7	52.6	75.8	71.4	39.4	46.4	75.5	71.2	40.2	46.1	75.9	72.1	39.4	45.8
Z	4.29	0.65	-3.95	-0.89	3.67	2.23	-3.44	-2.15	3.6	2.2	-3.27	-2.22	3.69	2.35	-3.43	-2.28
H	25.92				25.97				24.87				26.83			
P	0.000				0.000				0.000				0.000			

	CASI-9				CASI-10			
	MC1	MC2	MC3	MC4	MC1	MC2	MC3	MC4
Median	0.4118	0.3856	0.3317	0.3412	0.4459	0.4081	0.3521	0.3683
Ave Rank	76.3	75.9	38.2	44.2	78.3	74.9	35	45.9
Z	3.76	2.92	-3.66	-2.62	4.15	2.78	-4.3	-2.26
H	32.09				36.16			
P	0.000				0.000			

Table B:6 Kruskal Wallis H test results: MG habitat, July

Plots	MG1	MG2
N	31	30
DF	1	

	CASI-1		CASI-2		CASI-3		CASI-4		CASI-5	
	MG1	MG2	MG1	MG2	MG1	MG2	MG1	MG2	MG1	MG2
Median	0.02448	0.01806	0.06264	0.04993	0.03722	0.02777	0.07612	0.05988	0.1237	0.1031
Ave Rank	43.5	18.1	42.3	19.4	41.1	20.5	41.6	20	41.2	20.5
Z	5.58	-5.58	5.03	-5.03	4.53	-4.53	4.75	-4.75	4.56	-4.56
H	31.17		25.35		20.52		22.53		20.78	
P	0.000		0.000		0.000		0.000		0.000	

	CASI-6		CASI-7		CASI-8		CASI-9		CASI-10	
	MG1	MG2	MG1	MG2	MG1	MG2	MG1	MG2	MG1	MG2
Median	0.343	0.3146	0.3783	0.3501	0.4175	0.386	0.4392	0.4063	0.4699	0.4266
Ave Rank	37.8	23.9	37.1	24.7	36.5	25.3	35.8	26	36.4	25.4
Z	3.06	-3.06	2.74	-2.74	2.47	-2.47	2.16	-2.16	2.41	-2.41
H	9.35		7.51		6.09		4.68		5.8	
P	0.002		0.006		0.014		0.030		0.016	

Table B:7 Kruskal Wallis H test results: MS habitat, July

Plots	MS1	MS2	MS3
N	32	29	30
DF	2		

	CASI-1			CASI-2			CASI-3			CASI-4			CASI-5		
	MS1	MS2	MS3	MS1	MS2	MS3	MS1	MS2	MS3	MS1	MS2	MS3	MS1	MS2	MS3
Median	0.024	0.021	0.026	0.088	0.079	0.081	0.032	0.028	0.041	0.064	0.060	0.094	0.103	0.101	0.151
Ave Rank	49.5	31.7	56.1	55.2	41.8	40.3	45.3	26.4	65.7	37.1	31.2	69.9	35.2	33.7	69.5
Z	0.93	-3.53	2.56	2.45	-1.05	-1.45	-0.19	-4.83	4.98	-2.38	-3.66	6.04	-2.88	-3.05	5.95
H	13.46			6.06			32.55			37.3			35.48		
P	0.001			0.048			0.000			0.000			0.000		

	CASI-6			CASI-7			CASI-8			CASI-9			CASI-10		
	MS1	MS2	MS3	MS1	MS2	MS3	MS1	MS2	MS3	MS1	MS2	MS3	MS1	MS2	MS3
Median	0.228	0.247	0.379	0.248	0.268	0.414	0.270	0.292	0.448	0.283	0.306	0.464	0.302	0.326	0.488
Ave Rank	27.5	38.2	73.3	27	38.4	73.5	26.5	38.8	73.8	26.2	39.3	73.6	25.6	39.5	74
Z	-4.93	-1.92	6.91	-5.05	-1.87	6.97	-5.19	-1.79	7.05	-5.26	-1.66	6.99	-5.42	-1.6	7.09
H	50.22			51.47			52.99			52.58			54.5		
P	0.000			0.000			0.000			0.000			0.000		

Table B:8 Kruskal Wallis H test results: RP habitat, July

Plots	RP1	RP2	RP3
N	30	31	30
DF	2		

	CASI-1			CASI-2			CASI-3			CASI-4			CASI-5		
	RP1	RP2	RP3	RP1	RP2	RP3	RP1	RP2	RP3	RP1	RP2	RP3	RP1	RP2	RP3
Median	0.022	0.020	0.028	0.085	0.072	0.088	0.029	0.028	0.047	0.073	0.068	0.104	0.119	0.114	0.166
Ave Rank	37.7	27.5	73.4	51.9	27.5	59.2	32.3	30	76.2	35.3	27.3	76.1	36.6	26	76
Z	-2.09	-4.81	6.94	1.5	-4.81	3.34	-3.47	-4.15	7.65	-2.72	-4.86	7.62	-2.37	-5.19	7.61
H	50.46			24.24			58.62			59.38			60.33		
P	0.000			0.000			0.000			0.000			0.000		

	CASI-6			CASI-7			CASI-8			CASI-9			CASI-10		
	RP1	RP2	RP3	RP1	RP2	RP3	RP1	RP2	RP3	RP1	RP2	RP3	RP1	RP2	RP3
Median	0.308	0.284	0.394	0.340	0.309	0.426	0.371	0.335	0.463	0.390	0.353	0.492	0.410	0.375	0.518
Ave Rank	39.4	23.2	76.2	40	22.5	76.2	40.1	22.4	76.3	39.9	22.5	76.3	39.3	23.1	76.4
Z	-1.68	-5.92	7.65	-1.51	-6.09	7.65	-1.49	-6.12	7.67	-1.54	-6.09	7.68	-1.69	-5.95	7.69
H	64.22			65.19			65.6			65.6			64.94		
P	0.000			0.000			0.000			0.000			0.000		

Table B:9 Kruskal Wallis H test results: LS habitat, August

Plots	LS1	LS2	LS3
N	30	30	30
DF	2		

	CASI-1			CASI-2			CASI-3			CASI-4			CASI-5		
	LS1	LS2	LS3	LS1	LS2	LS3	LS1	LS2	LS3	LS1	LS2	LS3	LS1	LS2	LS3
Median	0.028	0.028	0.023	0.105	0.105	0.070	0.047	0.047	0.049	0.097	0.097	0.099	0.141	0.141	0.145
Ave Rank	52.7	52.7	31.2	59.2	59.2	18.1	42.9	42.9	50.6	44.2	44.2	48.1	43.9	43.9	48.6
Z	1.84	1.84	-3.68	3.52	3.52	-7.04	-0.66	-0.66	1.32	-0.33	-0.33	0.67	-0.4	-0.4	0.8
H	13.55			49.51			1.74			0.45			0.65		
P	0.001			0.000			0.419			0.800			0.723		

	CASI-6			CASI-7			CASI-8			CASI-9			CASI-10		
	LS1	LS2	LS3	LS1	LS2	LS3	LS1	LS2	LS3	LS1	LS2	LS3	LS1	LS2	LS3
Median	0.251	0.251	0.271	0.265	0.265	0.288	0.288	0.288	0.314	0.311	0.311	0.345	0.336	0.336	0.378
Ave Rank	41	41	54.4	40.8	40.8	54.9	40.6	40.6	55.2	40.5	40.5	55.4	39.9	39.9	56.6
Z	-1.15	-1.15	2.29	-1.21	-1.21	2.41	-1.25	-1.25	2.5	-1.28	-1.28	2.55	-1.43	-1.43	2.86
H	5.26			5.83			6.25			6.51			8.17		
P	0.072			0.054			0.044			0.039			0.017		

Table B:10 Kruskal Wallis H test results: MC habitat, August

Plots	MC1	MC2	MC3	MC4
N	30	20	27	30
DF	3			

	CASI-1				CASI-2				CASI-3				CASI-4			
	MC1	MC2	MC3	MC4	MC1	MC2	MC3	MC4	MC1	MC2	MC3	MC4	MC1	MC2	MC3	MC4
Median	0.02448	0.03006	0.02364	0.02544	0.0775	0.08848	0.06076	0.07205	0.04775	0.05038	0.04433	0.04399	0.08432	0.09786	0.08961	0.08113
Ave Rank	48.8	82	40.4	52.8	63.5	78.6	29.4	50.2	58.5	67	49.9	44.6	49	62.4	65	43.4
Z	-1.07	4.47	-2.64	-0.26	1.98	3.93	-4.76	-0.78	0.94	2.08	-0.8	-1.96	-1.03	1.34	2.14	-2.2
H	22.37				32.78				7.4				9.13			
P	0.000				0.000				0.060				0.028			

	CASI-5															
Median	MC1	MC2	MC3	MC4	CASI-6				CASI-7				CASI-8			
Ave Rank	0.1185	0.14	0.1394	0.1189	MC1	MC2	MC3	MC4	MC1	MC2	MC3	MC4	MC1	MC2	MC3	MC4
Z	40.2	62.3	72.7	45.5	0.2087	0.2692	0.3185	0.2439	0.2216	0.2866	0.3431	0.261	0.2429	0.3109	0.3729	0.2842
H	-2.88	1.32	3.61	-1.76	27.1	60.6	84.3	49.2	26.5	60.6	84.8	49.4	26	60.3	85.2	49.7
P	19.38				-5.6	1.05	5.87	-0.99	-5.72	1.05	5.97	-0.96	-5.82	1	6.05	-0.89
Median	0.000				49.89				51.73				53.08			
					0.000				0.000				0.000			

	CASI 9				CASI-10			
Median	MC1	MC2	MC3	MC4	MC1	MC2	MC3	MC4
Ave Rank	0.2661	0.3348	0.3942	0.3048	0.291	0.363	0.422	0.3258
Z	26.3	60.6	84.5	49.9	26.4	60.7	84.9	49.4
H	-5.76	1.05	5.91	-0.86	-5.75	1.07	5.97	-0.96
P	51.44				52.07			
	0.000				0.000			

Table B:11 Kruskal Wallis H test results: MG habitat, August

Plots	MG1	MG2
N	30	30
DF	1	

	CASI-1		CASI-2		CASI-3		CASI-4		CASI-5	
	MG1	MG2	MG1	MG2	MG1	MG2	MG1	MG2	MG1	MG2
Median	0.02015	0.01909	0.05886	0.05791	0.03089	0.02514	0.06329	0.05377	0.10033	0.09445
Ave Rank	33.1	27.9	31.8	29.2	34.4	26.6	34.7	26.3	35.3	25.7
Z	1.15	-1.15	0.58	-0.58	1.71	-1.71	1.86	-1.86	2.13	-2.13
H	1.33		0.33		2.94		3.47		4.53	
P	0.249		0.564		0.086		0.062		0.033	

	CASI-6		CASI-7		CASI-8		CASI-9		CASI-10	
	MG1	MG2	MG1	MG2	MG1	MG2	MG1	MG2	MG1	MG2
Median	0.2637	0.2443	0.2891	0.2671	0.3184	0.2957	0.3397	0.318	0.3606	0.3412
Ave Rank	33.2	27.8	32.7	28.3	32.5	28.5	32.6	28.4	32.8	28.2
Z	1.2	-1.2	0.96	-0.96	0.9	-0.9	0.92	-0.92	1.02	-1.02
H	1.43		0.92		0.81		0.84		1.04	
P	0.231		0.337		0.367		0.359		0.308	

Table B:12 Kruskal Wallis H test results: MS habitat, August

Plots	MS1	MS2	MS3
N	30	31	25
DF	2		

	CASI-1			CASI-2			CASI-3			CASI-4			CASI-5		
	MS1	MS2	MS3	MS1	MS2	MS3	MS1	MS2	MS3	MS1	MS2	MS3	MS1	MS2	MS3
Median	0.017	0.020	0.021	0.053	0.067	0.062	0.042	0.045	0.048	0.082	0.092	0.090	0.113	0.131	0.125
Ave Rank	26.2	51.6	54.2	26.6	56.1	48.1	32.3	46.4	53.4	29.7	54.3	46.6	27.2	55.6	48
Z	-4.7	2.25	2.55	-4.58	3.51	1.1	-3.05	0.8	2.35	-3.74	3.01	0.75	-4.43	3.39	1.07
H	22.27			22.43			10.42			15.3			20.93		
P	0.000			0.000			0.005			0.000			0.000		

	CASI-6			CASI-7			CASI-8			CASI-9			CASI-10		
	MS1	MS2	MS3	MS1	MS2	MS3	MS1	MS2	MS3	MS1	MS2	MS3	MS1	MS2	MS3
Median	0.192	0.249	0.238	0.203	0.263	0.255	0.223	0.281	0.283	0.245	0.302	0.312	0.271	0.332	0.346
Ave Rank	22.2	54.6	55.3	21.9	54.3	56	21.5	54	56.9	21.2	53.4	58	20.7	52.5	59.7
Z	-5.79	3.1	2.8	-5.86	3.02	2.96	-5.98	2.93	3.18	-6.06	2.77	3.44	-6.2	2.5	3.86
H	33.53			34.43			35.95			37.2			39.57		
P	0.000			0.000			0.000			0.000			0.000		

Table B:13 Kruskal Wallis H test results: RP habitat, August

Plots	RP1	RP2	RP3
N	30	30	22
DF	2		

	CASI-1			CASI-2			CASI-3			CASI-4			CASI-5		
	RP1	RP2	RP3	RP1	RP2	RP3	RP1	RP2	RP3	RP1	RP2	RP3	RP1	RP2	RP3
Median	0.022	0.020	0.031	0.078	0.067	0.096	0.041	0.039	0.054	0.093	0.084	0.114	0.149	0.130	0.176
Ave Rank	37	25.6	69.3	42.4	21.4	67.7	36.5	28.4	66.2	41.2	23.7	66.2	42.7	21.9	66.6
Z	-1.3	-4.59	6.4	0.25	-5.8	6.03	-1.43	-3.79	5.68	-0.09	-5.14	5.68	0.34	-5.65	5.78
H	44.46			47.93			34.06			40.39			44.74		
P	0.000			0.000			0.000			0.000			0.000		

	CASI-6			CASI-7			CASI-8			CASI-9			CASI-10		
	RP1	RP2	RP3	RP1	RP2	RP3	RP1	RP2	RP3	RP1	RP2	RP3	RP1	RP2	RP3
Median	0.341	0.293	0.416	0.367	0.317	0.449	0.397	0.347	0.483	0.424	0.372	0.510	0.447	0.394	0.530
Ave Rank	42.8	19.8	69.3	43	19.6	69.4	43.1	19.6	69.3	42.9	20.1	68.8	42.6	20.3	68.9
Z	0.39	-6.27	6.39	0.43	-6.33	6.42	0.45	-6.33	6.39	0.39	-6.17	6.28	0.32	-6.12	6.31
H	54.92			55.68			55.49			53.1			52.98		
P	0.000			0.000			0.000			0.000			0.000		

Table B:14 Kruskal Wallis H test results: LS habitat, September

Plots	LS1	LS2	LS3
N	30	25	30
DF	2		

	CASI-1			CASI-2			CASI-3			CASI-4			CASI-5		
	LS1	LS2	LS3	LS1	LS2	LS3	LS1	LS2	LS3	LS1	LS2	LS3	LS1	LS2	LS3
Median	0.029	0.022	0.023	0.082	0.069	0.061	0.068	0.057	0.051	0.110	0.104	0.083	0.136	0.144	0.109
Ave Rank	59.4	29.2	38.1	56	42.2	30.7	59.6	35.3	32.9	53.4	50	26.8	49.5	54.2	27.2
Z	4.53	-3.33	-1.36	3.6	-0.2	-3.4	4.57	-1.86	-2.8	2.87	1.68	-4.47	1.78	2.69	-4.35
H	22.31			15.89			21.02			20.24			19.41		
P	0.000			0.000			0.000			0.000			0.000		

	CASI-6			CASI-7			CASI-8			CASI-9			CASI-10		
	LS1	LS2	LS3	LS1	LS2	LS3	LS1	LS2	LS3	LS1	LS2	LS3	LS1	LS2	LS3
Median	0.201	0.235	0.186	0.210	0.248	0.196	0.231	0.272	0.214	0.256	0.301	0.236	0.286	0.337	0.259
Ave Rank	41.5	59.6	30.6	41.2	59.8	30.8	41.1	60.4	30.5	41.4	60.8	29.7	41.8	61.3	28.9
Z	-0.4	4.01	-3.42	-0.49	4.05	-3.37	-0.53	4.19	-3.46	-0.44	4.3	-3.66	-0.33	4.42	-3.88
H	19.04			19.11			20.29			21.86			23.59		
P	0.000			0.000			0.000			0.000			0.000		

Table B:15 Kruskal Wallis H test results: MC habitat, September

Plots	MC1	MC2	MC3	MC4
N	30	30	30	31
DF	3			

	CASI-1				CASI-2				CASI-3				CASI-4			
	MC1	MC2	MC3	MC4	MC1	MC2	MC3	MC4	MC1	MC2	MC3	MC4	MC1	MC2	MC3	MC4
Median	0.025	0.030	0.024	0.029	0.063	0.070	0.061	0.062	0.064	0.065	0.062	0.068	0.097	0.106	0.106	0.106
Ave Rank	49.6	84.4	34.1	75.4	53	81.4	47.9	61.7	56.2	62.7	47.3	77.2	42.8	64.8	63.7	72.3
Z	-2.05	4.22	-4.85	2.65	-1.45	3.68	-2.36	0.13	-0.86	0.31	-2.47	2.99	-3.27	0.68	0.49	2.07
H	39.49				15.97				11.85				11.78			
P	0.000				0.001				0.008				0.008			

	CASI-5				CASI-6				CASI-7				CASI-8			
	MC1	MC2	MC3	MC4	MC1	MC2	MC3	MC4	MC1	MC2	MC3	MC4	MC1	MC2	MC3	MC4
Median	0.121	0.140	0.141	0.138	0.199	0.236	0.247	0.232	0.211	0.249	0.261	0.247	0.231	0.271	0.285	0.274
Ave Rank	39.1	66.2	68.6	69.9	34.6	63	78.4	67.7	34.6	62.8	78.8	67.6	33.8	62	79.1	68.8
Z	-3.95	0.94	1.36	1.63	-4.76	0.37	3.14	1.24	-4.76	0.32	3.21	1.22	-4.9	0.19	3.26	1.44
H	15.77				25.7				25.97				27.65			
P	0.001				0.000				0.000				0.000			

	CASI-9				CASI-10			
	MC1	MC2	MC3	MC4	MC1	MC2	MC3	MC4
Median	0.252	0.297	0.317	0.303	0.278	0.322	0.342	0.333
Ave Rank	32.1	60.6	79.8	71.2	31.6	60.2	78.7	73.1
Z	-5.2	-0.07	3.39	1.87	-5.3	-0.14	3.19	2.23
H	31.59				32.47			
P	0.000				0.000			

Table B:16 Kruskal Wallis H test results: MG habitat, September

Plots	MG1	MG2
N	30	30
DF	1	

	CASI-1		CASI-2		CASI-3		CASI-4		CASI-5	
	MG1	MG2	MG1	MG2	MG1	MG2	MG1	MG2	MG1	MG2
Median	0.02079	0.01953	0.05294	0.05002	0.04337	0.0397	0.08371	0.07755	0.1265	0.1147
Ave Rank	33.3	27.7	33.1	27.9	34.5	26.5	35.7	25.3	35.3	25.7
Z	1.23	-1.23	1.17	-1.17	1.77	-1.77	2.29	-2.29	2.11	-2.11
H	1.51		1.36		3.15		5.25		4.47	
P	0.22		0.243		0.076		0.022		0.035	

	CASI-6		CASI-7		CASI-8		CASI-9		CASI-10	
	MG1	MG2	MG1	MG2	MG1	MG2	MG1	MG2	MG1	MG2
Median	0.2717	0.2539	0.2926	0.2782	0.3253	0.3081	0.3543	0.3292	0.3858	0.3575
Ave Rank	31.9	29.1	31.5	29.5	31.6	29.4	32.2	28.8	32	29
Z	0.62	-0.62	0.46	-0.46	0.47	-0.47	0.75	-0.75	0.65	-0.65
H	0.39		0.21		0.22		0.57		0.42	
P	0.535		0.647		0.636		0.451		0.515	

Table B:17 Kruskal Wallis H test results: MS habitat, September

Plots	MS1	MS2	MS3
N	30	31	30
DF	2		

	CASI-1			CASI-2			CASI-3			CASI-4			CASI-5		
	MS1	MS2	MS3	MS1	MS2	MS3	MS1	MS2	MS3	MS1	MS2	MS3	MS1	MS2	MS3
Median	0.017	0.020	0.023	0.041	0.058	0.057	0.054	0.050	0.060	0.080	0.084	0.094	0.095	0.110	0.123
Ave Rank	28.2	45	64.8	27.4	54.2	56.1	44.7	36.9	56.7	37.3	42	58.8	32.9	44.7	60.4
Z	-4.5	-0.26	4.76	-4.7	2.12	2.57	-0.33	-2.35	2.7	-2.2	-1.03	3.24	-3.31	-0.33	3.65
H	28.82			22.2			8.62			11			16.33		
P	0.000			0.000			0.013			0.004			0.000		

	CASI-6			CASI-7			CASI-8			CASI-9			CASI-10		
	MS1	MS2	MS3	MS1	MS2	MS3	MS1	MS2	MS3	MS1	MS2	MS3	MS1	MS2	MS3
Median	0.135	0.181	0.21	0.142	0.192	0.224	0.158	0.212	0.248	0.182	0.233	0.278	0.212	0.258	0.316
Ave Rank	26.7	45.3	66.1	26.5	45.2	66.3	26.8	44.7	66.5	27.9	43.5	66.7	28.1	42.8	67.3
Z	-4.9	-0.19	5.09	-4.93	-0.2	5.13	-4.85	-0.33	5.18	-4.58	-0.66	5.25	-4.54	-0.84	5.39
H	33.47			33.98			33.88			32.86			33.74		
P	0.000			0.000			0.000			0.000			0.000		

Table B:18 Kruskal Wallis H test results: RP habitat, September

Plots	RP1	RP2	RP3
N	30	30	30
DF	2		

	CASI-1			CASI-2			CASI-3			CASI-4			CASI-5		
	RP1	RP2	RP3	RP1	RP2	RP3	RP1	RP2	RP3	RP1	RP2	RP3	RP1	RP2	RP3
Median	0.027	0.023	0.032	0.081	0.064	0.0912	0.055	0.049	0.061	0.104	0.087	0.113	0.151	0.125	0.165
Ave Rank	44.8	28.4	63.3	48.6	25.2	62.7	45.5	34.9	56.1	50	29.5	57	51.2	26.2	59.1
Z	-0.17	-4.39	4.56	0.8	-5.22	4.42	0	-2.73	2.73	1.16	-4.11	2.95	1.47	-4.96	3.48
H	26.75			31.61			9.94			17.96			25.91		
P	0.000			0.000			0.007			0.000			0.000		

	CASI-6			CASI-7			CASI-8			CASI-9			CASI-10		
	RP1	RP2	RP3	RP1	RP2	RP3	RP1	RP2	RP3	RP1	RP2	RP3	RP1	RP2	RP3
Median	0.320	0.252	0.346	0.343	0.268	0.372	0.372	0.292	0.403	0.397	0.315	0.426	0.422	0.34	0.452
Ave Rank	53.7	21.3	61.5	54	21.1	61.5	54.1	21.2	61.1	54.3	21.6	60.6	54.5	22.3	59.8
Z	2.1	-6.21	4.12	2.17	-6.27	4.1	2.22	-6.23	4.01	2.27	-6.15	3.88	2.3	-5.97	3.66
H	39.97			40.6			39.9			38.63			36.21		
P	0.000			0.000			0.000			0.000			0.000		

Table B:19 MDA stepwise model output (groups by habitat type-See Chapter 4 for Group labels) July-AVS1-42

Classification Results[b,c]

			Predicted Group Membership						
		groups	1.00	2.00	3.00	4.00	5.00	6.00	Total
Original	Count	1.00	30	0	0	0	0	0	30
		2.00	0	78	6	0	3	0	87
		3.00	8	11	86	0	5	0	110
		4.00	3	0	3	53	1	0	60
		5.00	3	1	8	1	78	0	91
		6.00	0	0	2	0	0	88	90
	%	1.00	100.0	.0	.0	.0	.0	.0	100.0
		2.00	.0	89.7	6.9	.0	3.4	.0	100.0
		3.00	7.3	10.0	78.2	.0	4.5	.0	100.0
		4.00	5.0	.0	5.0	88.3	1.7	.0	100.0
		5.00	3.3	1.1	8.8	1.1	85.7	.0	100.0
		6.00	.0	.0	2.2	.0	.0	97.8	100.0
Cross-validated[a]	Count	1.00	29	0	1	0	0	0	30
		2.00	0	76	8	0	3	0	87
		3.00	10	13	80	0	7	0	110
		4.00	3	0	4	52	1	0	60
		5.00	3	2	11	1	74	0	91
		6.00	0	0	2	0	0	88	90
	%	1.00	96.7	.0	3.3	.0	.0	.0	100.0
		2.00	.0	87.4	9.2	.0	3.4	.0	100.0
		3.00	9.1	11.8	72.7	.0	6.4	.0	100.0
		4.00	5.0	.0	6.7	86.7	1.7	.0	100.0
		5.00	3.3	2.2	12.1	1.1	81.3	.0	100.0
		6.00	.0	.0	2.2	.0	.0	97.8	100.0

a. Cross validation is done only for those cases in the analysis. In cross validation, each case is classified by the functions derived from all cases other than that case.

b. 88.2% of original grouped cases correctly classified.

c. 85.3% of cross-validated grouped cases correctly classified.

Table B:20 MDA stepwise model output (groups by habitat type-See Chapter 4 for Group labels) July-CASI

Classification Results[b,c]

			Predicted Group Membership						
		group	1.00	2.00	3.00	4.00	5.00	6.00	Total
Original	Count	1.00	30	0	0	0	0	0	30
		2.00	0	67	9	0	7	4	87
		3.00	4	11	90	1	3	1	110
		4.00	1	0	6	53	0	0	60
		5.00	1	12	13	3	51	11	91
		6.00	0	6	1	0	12	71	90
	%	1.00	100.0	.0	.0	.0	.0	.0	100.0
		2.00	.0	77.0	10.3	.0	8.0	4.6	100.0
		3.00	3.6	10.0	81.8	.9	2.7	.9	100.0
		4.00	1.7	.0	10.0	88.3	.0	.0	100.0
		5.00	1.1	13.2	14.3	3.3	56.0	12.1	100.0
		6.00	.0	6.7	1.1	.0	13.3	78.9	100.0
Cross-validated[a]	Count	1.00	29	0	1	0	0	0	30
		2.00	0	63	10	0	10	4	87
		3.00	6	14	85	1	3	1	110
		4.00	1	0	6	52	1	0	60
		5.00	1	12	16	3	47	12	91
		6.00	0	6	1	0	12	71	90
	%	1.00	96.7	.0	3.3	.0	.0	.0	100.0
		2.00	.0	72.4	11.5	.0	11.5	4.6	100.0
		3.00	5.5	12.7	77.3	.9	2.7	.9	100.0
		4.00	1.7	.0	10.0	86.7	1.7	.0	100.0
		5.00	1.1	13.2	17.6	3.3	51.6	13.2	100.0
		6.00	.0	6.7	1.1	.0	13.3	78.9	100.0

a. Cross validation is done only for those cases in the analysis. In cross validation, each case is classified by the functions derived from all cases other than that case.

b. 77.4% of original grouped cases correctly classified.

c. 74.1% of cross-validated grouped cases correctly classified.

Table B:21 MDA stepwise model output (groups by habitat type-See Chapter 4 for Group labels) Aug-AVS1-42

Classification Results[b,c]

			Predicted Group Membership						
		group	1.00	2.00	3.00	4.00	5.00	6.00	Total
Original	Count	1.00	30	0	0	0	0	0	30
		2.00	0	86	1	0	3	0	90
		3.00	0	2	105	0	0	0	107
		4.00	2	0	2	56	0	0	60
		5.00	0	2	0	0	81	0	83
		6.00	0	0	0	0	0	81	81
	%	1.00	100.0	.0	.0	.0	.0	.0	100.0
		2.00	.0	95.6	1.1	.0	3.3	.0	100.0
		3.00	.0	1.9	98.1	.0	.0	.0	100.0
		4.00	3.3	.0	3.3	93.3	.0	.0	100.0
		5.00	.0	2.4	.0	.0	97.6	.0	100.0
		6.00	.0	.0	.0	.0	.0	100.0	100.0
Cross-validated[a]	Count	1.00	29	0	1	0	0	0	30
		2.00	0	85	1	0	4	0	90
		3.00	2	3	101	0	1	0	107
		4.00	2	0	3	55	0	0	60
		5.00	0	3	0	0	80	0	83
		6.00	0	0	0	0	0	81	81
	%	1.00	96.7	.0	3.3	.0	.0	.0	100.0
		2.00	.0	94.4	1.1	.0	4.4	.0	100.0
		3.00	1.9	2.8	94.4	.0	.9	.0	100.0
		4.00	3.3	.0	5.0	91.7	.0	.0	100.0
		5.00	.0	3.6	.0	.0	96.4	.0	100.0
		6.00	.0	.0	.0	.0	.0	100.0	100.0

a. Cross validation is done only for those cases in the analysis. In cross validation, each case is classified by the functions derived from all cases other than that case.

b. 97.3% of original grouped cases correctly classified.

c. 95.6% of cross-validated grouped cases correctly classified.

Table B:22 MDA stepwise model output (groups by habitat type-See Chapter 4 for Group labels) Aug-CASI

Classification Results[b,c]

			Predicted Group Membership						
		group	1.00	2.00	3.00	4.00	5.00	6.00	Total
Original	Count	1.00	30	0	0	0	0	0	30
		2.00	0	60	3	0	24	3	90
		3.00	13	11	71	0	0	12	107
		4.00	0	0	7	53	0	0	60
		5.00	0	0	3	0	78	3	84
		6.00	0	0	5	2	0	75	82
	%	1.00	100.0	.0	.0	.0	.0	.0	100.0
		2.00	.0	66.7	3.3	.0	26.7	3.3	100.0
		3.00	12.1	10.3	66.4	.0	.0	11.2	100.0
		4.00	.0	.0	11.7	88.3	.0	.0	100.0
		5.00	.0	.0	3.6	.0	92.9	3.6	100.0
		6.00	.0	.0	6.1	2.4	.0	91.5	100.0
Cross-validated[a]	Count	1.00	30	0	0	0	0	0	30
		2.00	0	60	3	0	24	3	90
		3.00	13	11	69	0	1	13	107
		4.00	0	0	7	53	0	0	60
		5.00	0	0	4	0	77	3	84
		6.00	0	0	5	2	0	75	82
	%	1.00	100.0	.0	.0	.0	.0	.0	100.0
		2.00	.0	66.7	3.3	.0	26.7	3.3	100.0
		3.00	12.1	10.3	64.5	.0	.9	12.1	100.0
		4.00	.0	.0	11.7	88.3	.0	.0	100.0
		5.00	.0	.0	4.8	.0	91.7	3.6	100.0
		6.00	.0	.0	6.1	2.4	.0	91.5	100.0

a. Cross validation is done only for those cases in the analysis. In cross validation, each case is classified by the functions derived from all cases other than that case.

b. 81.0% of original grouped cases correctly classified.

c. 80.4% of cross-validated grouped cases correctly classified.

Table B:23 MDA stepwise model output (groups by habitat type-See Chapter 4 for Group labels) Sept-AVS1-42

Classification Results[b,c]

			Predicted Group Membership						
		group	1.00	2.00	3.00	4.00	5.00	6.00	Total
Original	Count	1.00	26	1	1	0	2	0	30
		2.00	0	66	4	0	15	0	85
		3.00	1	1	105	2	8	2	119
		4.00	2	0	5	53	0	0	60
		5.00	0	11	5	1	73	0	90
		6.00	0	2	3	0	1	83	89
	%	1.00	86.7	3.3	3.3	.0	6.7	.0	100.0
		2.00	.0	77.6	4.7	.0	17.6	.0	100.0
		3.00	.8	.8	88.2	1.7	6.7	1.7	100.0
		4.00	3.3	.0	8.3	88.3	.0	.0	100.0
		5.00	.0	12.2	5.6	1.1	81.1	.0	100.0
		6.00	.0	2.2	3.4	.0	1.1	93.3	100.0
Cross-validated[a]	Count	1.00	25	1	1	0	3	0	30
		2.00	0	65	4	0	16	0	85
		3.00	1	2	103	2	9	2	119
		4.00	2	0	5	53	0	0	60
		5.00	0	13	6	1	70	0	90
		6.00	0	3	3	0	1	82	89
	%	1.00	83.3	3.3	3.3	.0	10.0	.0	100.0
		2.00	.0	76.5	4.7	.0	18.8	.0	100.0
		3.00	.8	1.7	86.6	1.7	7.6	1.7	100.0
		4.00	3.3	.0	8.3	88.3	.0	.0	100.0
		5.00	.0	14.4	6.7	1.1	77.8	.0	100.0
		6.00	.0	3.4	3.4	.0	1.1	92.1	100.0

a. Cross validation is done only for those cases in the analysis. In cross validation, each case is classified by the functions derived from all cases other than that case.

b. 85.8% of original grouped cases correctly classified.

c. 84.1% of cross-validated grouped cases correctly classified.

Table B:24 MDA stepwise model output (groups by habitat type-See Chapter 4 for Group labels) Sept-CASI

Classification Results[b,c]

			Predicted Group Membership						
		group	1.00	2.00	3.00	4.00	5.00	6.00	Total
Original	Count	1.00	27	0	3	0	0	0	30
		2.00	0	65	8	0	12	0	85
		3.00	2	0	108	1	9	0	120
		4.00	2	0	3	54	1	0	60
		5.00	0	18	6	0	66	0	90
		6.00	0	2	5	0	3	79	89
	%	1.00	90.0	.0	10.0	.0	.0	.0	100.0
		2.00	.0	76.5	9.4	.0	14.1	.0	100.0
		3.00	1.7	.0	90.0	.8	7.5	.0	100.0
		4.00	3.3	.0	5.0	90.0	1.7	.0	100.0
		5.00	.0	20.0	6.7	.0	73.3	.0	100.0
		6.00	.0	2.2	5.6	.0	3.4	88.8	100.0
Cross-validated[a]	Count	1.00	27	0	3	0	0	0	30
		2.00	0	63	8	0	14	0	85
		3.00	2	0	106	2	9	1	120
		4.00	2	0	3	54	1	0	60
		5.00	0	18	6	1	65	0	90
		6.00	0	2	5	0	3	79	89
	%	1.00	90.0	.0	10.0	.0	.0	.0	100.0
		2.00	.0	74.1	9.4	.0	16.5	.0	100.0
		3.00	1.7	.0	88.3	1.7	7.5	.8	100.0
		4.00	3.3	.0	5.0	90.0	1.7	.0	100.0
		5.00	.0	20.0	6.7	1.1	72.2	.0	100.0
		6.00	.0	2.2	5.6	.0	3.4	88.8	100.0

a. Cross validation is done only for those cases in the analysis. In cross validation, each case is classified by the functions derived from all cases other than that case.

b. 84.2% of original grouped cases correctly classified.

c. 83.1% of cross-validated grouped cases correctly classified.

NDVI: Kruskal Wallis Results (July, August and September 2003)

Table B:25 All results from Kruskal Wallis analyses on CASI derived NDVI values (greyed out cells=statistically significant at P<0.05)

July				
	LS1	LS2	LS3	
Median	0.7585	0.8002	0.7998	
Ave Rank	31.3	56.7	48.5	
Z	-3.64	2.88	0.76	
H	14.72			
P	0.001			
	MC1	MC2	MC3	MC4
Median	0.787	0.8068	0.7536	0.7574
Ave Rank	74.8	85.1	37.8	39.8
Z	3.48	4.36	-3.75	-3.5
H	43.49			
P	0.000			
	MG1	MG2		
Median	0.8361	0.8662		
Ave Rank	24.9	37.3		
Z	-2.74	2.74		
H	7.51			
P	0.000			
	MS1	MS2	MS3	
Median	0.7997	0.818	0.8284	
Ave Rank	27	54.3	58.3	
Z	-5.05	2.04	3.11	
H	25.88			
P	0.000			
	RP1	RP2	RP3	
Median	0.8564	0.8359	0.8177	
Ave Rank	63.1	50.8	24	
Z	4.33	1.24	-5.58	
H	34.46			
P	0.000			

Aug				
	LS1	LS2	LS3	
Median	0.7269	0.7269	0.7245	
Ave Rank	44.9	44.9	46.7	
Z	-0.15	-0.15	0.31	
H	0.09			
P	0.954			
	MC1	MC2	MC3	MC4
Median	0.6697	0.7208	0.783	0.7355
Ave Rank	22.9	46.7	89.6	58
Z	-6.47	-1.17	6.89	0.83
H	67.17			
P	0.000			
	MG1	MG2		
Median	0.8243	0.8473		
Ave Rank	28.4	32.6		
Z	-0.95	0.95		
H	0.9			
P	0.344			
	MS1	MS2	MS3	
Median	0.6867	0.7144	0.7187	
Ave Rank	28.6	49.8	53.6	
Z	-4.05	1.76	2.39	
H	16.72			
P	0.000			
	RP1	RP2	RP3	
Median	0.8091	0.7922	0.7944	
Ave Rank	51.3	33.9	38.5	
Z	2.82	-2.19	-0.68	
H	8.44			
P	0.015			

Sept				
	LS1	LS2	LS3	
Median	0.5484	0.6681	0.6108	
Ave Rank	19.9	69.4	44.1	
Z	-6.38	6.38	0.3	
H	55.1			
P	0.000			
	MC1	MC2	MC3	MC4
Median	0.5773	0.6063	0.6426	0.5836
Ave Rank	40.8	60.8	95.8	47
Z	-3.64	-0.03	6.27	-2.58
H	44.48			
P	0.000			
	MG1	MG2		
Median	0.7589	0.7761		
Ave Rank	27.7	33.3		
Z	-1.24	1.24		
H	1.54			
P	0.214			
	MS1	MS2	MS3	
Median	0.5217	0.5895	0.6198	
Ave Rank	23.3	51.9	62.6	
Z	-5.76	1.54	4.2	
H	35.64			
P	0.000			
	RP1	RP2	RP3	
Median	0.7408	0.7027	0.7414	
Ave Rank	54	27.5	55	
Z	2.18	-4.61	2.43	
H	21.3			
P	0.000			

Frequency tables compiled using 1st derivative analyses to derive REIP at each sampling stage

Table B:26 Frequency table to show REIP at each study plot using spectra collected in July 2003

Wavelength (nm)	All	EF1	LS1	LS2	LS3	MC1	MC2	MC3	MC4	MG1	MG2	MS1	MS2	MS3	RP1	RP2	RP3	Total
690	0	0	0	0	0	0	0	0	0	0	0	0	0	0	0	0	0	0
692	0	0	0	0	0	0	0	0	0	0	0	0	0	0	0	0	0	0
694	0	0	0	0	0	0	0	0	0	0	0	0	0	0	0	0	0	0
696	0	0	0	0	0	0	0	0	0	0	0	0	0	0	0	0	0	0
698	0	0	0	0	0	0	0	0	0	0	0	0	0	0	0	0	0	0
700	2	0	0	0	0	1	0	0	0	0	0	1	0	0	0	0	0	2
702	0	0	0	0	0	0	0	0	0	0	0	0	0	0	0	0	0	0
704	23	0	17	0	0	1	0	0	0	0	0	3	2	0	0	0	0	23
706	1	1	0	0	0	0	0	0	0	0	0	0	0	0	0	0	0	1
708	0	0	0	0	0	0	0	0	0	0	0	0	0	0	0	0	0	0
710	0	0	0	0	0	0	0	0	0	0	0	0	0	0	0	0	0	0
712	0	0	0	0	0	0	0	0	0	0	0	0	0	0	0	0	0	0
714	16	3	0	0	2	5	3	3	0	0	0	0	0	0	0	0	0	16
716	9	6	1	1	1	0	0	0	0	0	0	0	0	0	0	0	0	9
718	142	14	5	11	6	14	8	8	17	2	0	15	2	18	4	8	10	142
720	206	6	7	16	19	8	8	8	13	18	6	11	24	7	19	21	15	206
722	4	0	0	0	0	0	1	1	0	0	1	0	1	0	0	0	0	4
724	2	0	0	0	0	0	0	0	0	0	0	0	0	1	0	1	0	2
726	53	0	0	2	1	1	1	1	0	10	23	0	0	2	7	1	4	53
728	3	0	0	0	1	0	0	0	0	0	0	0	0	2	0	0	0	3
730	0	0	0	0	0	0	0	0	0	0	0	0	0	0	0	0	0	0
Total	461	30	30	30	30	30	21	21	30	30	30	30	29	30	30	31	29	461

Table B:27 Frequency table to show REIP at each study plot using spectra collected in August 2003

Wavelength (nm)	All	EF1	LS1	LS2	LS3	MC1	MC2	MC3	MC4	MG1	MG2	MS1	MS2	MS3	RP1	RP2	RP3	Total
690	0	0	0	0	0	0	0	0	0	0	0	0	0	0	0	0	0	0
692	0	0	0	0	0	0	0	0	0	0	0	0	0	0	0	0	0	0
694	0	0	0	0	0	0	0	0	0	0	0	0	0	0	0	0	0	0
696	4	0	0	0	0	0	0	0	0	0	0	2	2	0	0	0	0	4
698	33	0	8	4	3	2	0	0	0	0	0	14	2	0	0	0	0	33
700	74	6	21	3	1	12	0	0	0	0	0	12	18	1	0	0	0	74
702	59	19	0	10	7	8	4	0	1	0	0	0	6	4	0	0	0	59
704	10	5	0	0	2	1	0	0	1	0	0	0	0	1	0	0	0	10
706	0	0	0	0	0	0	0	0	0	0	0	0	0	0	0	0	0	0
708	0	0	0	0	0	0	0	0	0	0	0	0	0	0	0	0	0	0
710	1	0	0	0	1	0	0	0	0	0	0	0	0	0	0	0	0	1
712	2	0	0	0	1	0	0	0	0	0	0	0	0	1	0	0	0	2
714	11	0	0	0	1	0	0	0	6	0	0	0	0	0	0	0	4	11
716	22	0	0	1	0	1	6	1	7	1	0	0	0	2	3	0	0	22
718	84	0	0	7	9	4	7	14	9	6	0	1	0	4	8	12	3	84
720	117	0	1	5	3	1	3	9	6	13	20	0	1	10	15	16	14	117
722	7	0	0	0	2	0	0	2	0	0	0	0	0	2	0	1	0	7
724	0	0	0	0	0	0	0	0	0	0	0	0	0	0	0	0	0	0
726	26	0	0	0	0	0	0	0	0	10	10	0	0	0	4	1	1	26
728	0	0	0	0	0	0	0	0	0	0	0	0	0	0	0	0	0	0
730	1	0	0	0	0	0	0	1	0	0	0	0	0	0	0	0	0	1
Total	451	30	30	30	30	29	20	27	30	30	30	29	29	25	30	30	22	451

Table B:28 Frequency table to show REIP at each study plot using spectra collected in September 2003

Wavelength (nm)	All	EF1	LS1	LS2	LS3	MC1	MC2	MC3	MC4	MG1	MG2	MS1	MS2	MS3	RP1	RP2	RP3	Total
690	2	2	0	0	0	0	0	0	0	0	0	0	0	0	0	0	0	2
692	0	0	0	0	0	0	0	0	0	0	0	0	0	0	0	0	0	0
694	5	4	0	0	0	0	1	0	0	0	0	0	0	0	0	0	0	5
696	72	5	14	13	3	5	2	4	2	0	0	16	8	0	0	0	0	72
698	78	1	11	8	4	2	12	4	1	0	0	11	14	9	0	1	0	78
700	38	1	5	3	14	1	2	0	2	0	0	2	6	0	0	2	0	38
702	27	0	0	1	6	4	1	1	1	0	0	0	1	9	1	2	0	27
704	8	3	0	0	0	1	3	0	1	0	0	0	0	0	0	0	0	8
706	1	0	0	0	0	0	0	0	0	0	1	0	0	0	0	0	0	1
708	3	1	0	0	0	0	1	0	1	0	0	0	0	0	0	0	0	3
710	5	2	0	0	0	0	0	0	2	0	0	0	0	1	0	0	0	5
712	4	0	0	0	0	0	0	1	0	1	1	0	0	1	0	0	0	4
714	29	0	0	0	0	0	4	7	11	5	1	0	0	1	0	0	0	29
716	34	1	0	0	2	6	1	11	4	3	1	0	0	0	2	3	0	34
718	61	5	0	0	1	5	1	1	1	8	2	0	0	7	11	10	9	61
720	79	2	0	0	0	1	2	1	0	12	13	0	1	1	16	11	19	79
722	21	2	0	0	0	5	0	0	3	1	7	1	0	1	0	0	1	21
724	2	0	0	0	0	0	0	0	1	0	1	0	0	0	0	0	0	2
726	5	1	0	0	0	0	0	0	0	0	3	0	0	0	0	1	0	5
728	1	0	0	0	0	0	0	0	0	0	0	0	0	0	0	1	0	1
730	0	0	0	0	0	0	0	0	0	0	0	0	0	0	0	0	0	0
Total	475	30	30	25	30	30	30	30	30	30	30	30	30	30	30	31	29	475

C. Appendix

Table C:1 July-AVS1-42 spectra grouped using *a priori* habitat types

Classification Results[b,c]

			Predicted Group Membership						
		HabType	1.00	2.00	3.00	4.00	5.00	6.00	Total
Original	Count	1.00	9	1	0	0	0	0	10
		2.00	1	20	0	0	4	3	28
		3.00	0	0	36	2	0	0	38
		4.00	0	0	7	8	3	2	20
		5.00	0	3	0	1	23	3	30
		6.00	0	2	0	0	5	23	30
	%	1.00	90.0	10.0	.0	.0	.0	.0	100.0
		2.00	3.6	71.4	.0	.0	14.3	10.7	100.0
		3.00	.0	.0	94.7	5.3	.0	.0	100.0
		4.00	.0	.0	35.0	40.0	15.0	10.0	100.0
		5.00	.0	10.0	.0	3.3	76.7	10.0	100.0
		6.00	.0	6.7	.0	.0	16.7	76.7	100.0
Cross-validated[a]	Count	1.00	9	1	0	0	0	0	10
		2.00	1	20	0	0	4	3	28
		3.00	0	0	35	3	0	0	38
		4.00	0	0	7	6	3	4	20
		5.00	0	3	0	1	23	3	30
		6.00	0	2	0	1	6	21	30
	%	1.00	90.0	10.0	.0	.0	.0	.0	100.0
		2.00	3.6	71.4	.0	.0	14.3	10.7	100.0
		3.00	.0	.0	92.1	7.9	.0	.0	100.0
		4.00	.0	.0	35.0	30.0	15.0	20.0	100.0
		5.00	.0	10.0	.0	3.3	76.7	10.0	100.0
		6.00	.0	6.7	.0	3.3	20.0	70.0	100.0

a. Cross validation is done only for those cases in the analysis. In cross validation, each case is classified by the functions derived from all cases other than that case.

b. 76.3% of original grouped cases correctly classified.

c. 73.1% of cross-validated grouped cases correctly classified.

Table C:2 July-CASI spectra grouped using *a priori* habitat types

Classification Results[b,c]

			Predicted Group Membership						
		HabType	1.00	2.00	3.00	4.00	5.00	6.00	Total
Original	Count	1.00	10	0	0	0	0	0	10
		2.00	2	22	0	0	0	4	28
		3.00	6	3	27	0	1	1	38
		4.00	1	0	1	18	0	0	20
		5.00	0	2	2	1	20	5	30
		6.00	0	2	1	0	9	18	30
	%	1.00	100.0	.0	.0	.0	.0	.0	100.0
		2.00	7.1	78.6	.0	.0	.0	14.3	100.0
		3.00	15.8	7.9	71.1	.0	2.6	2.6	100.0
		4.00	5.0	.0	5.0	90.0	.0	.0	100.0
		5.00	.0	6.7	6.7	3.3	66.7	16.7	100.0
		6.00	.0	6.7	3.3	.0	30.0	60.0	100.0
Cross-validated[a]	Count	1.00	10	0	0	0	0	0	10
		2.00	3	21	0	0	0	4	28
		3.00	8	3	25	0	1	1	38
		4.00	1	0	1	18	0	0	20
		5.00	0	3	2	2	18	5	30
		6.00	0	3	1	0	9	17	30
	%	1.00	100.0	.0	.0	.0	.0	.0	100.0
		2.00	10.7	75.0	.0	.0	.0	14.3	100.0
		3.00	21.1	7.9	65.8	.0	2.6	2.6	100.0
		4.00	5.0	.0	5.0	90.0	.0	.0	100.0
		5.00	.0	10.0	6.7	6.7	60.0	16.7	100.0
		6.00	.0	10.0	3.3	.0	30.0	56.7	100.0

a. Cross validation is done only for those cases in the analysis. In cross validation, each case is classified by the functions derived from all cases other than that case.

b. 73.7% of original grouped cases correctly classified.

c. 69.9% of cross-validated grouped cases correctly classified.

Table C:3 September-AVS1-42 spectra grouped using *a priori* habitat types

Classification Results[b,c]

			Predicted Group Membership						
		HabType	1.00	2.00	3.00	4.00	5.00	6.00	Total
Original	Count	1.00	9	0	0	0	1	0	10
		2.00	0	25	0	0	5	0	30
		3.00	0	0	38	1	1	0	40
		4.00	0	0	2	18	0	0	20
		5.00	0	3	2	0	25	0	30
		6.00	0	0	1	0	2	27	30
	%	1.00	90.0	.0	.0	.0	10.0	.0	100.0
		2.00	.0	83.3	.0	.0	16.7	.0	100.0
		3.00	.0	.0	95.0	2.5	2.5	.0	100.0
		4.00	.0	.0	10.0	90.0	.0	.0	100.0
		5.00	.0	10.0	6.7	.0	83.3	.0	100.0
		6.00	.0	.0	3.3	.0	6.7	90.0	100.0
Cross-validated[a]	Count	1.00	9	0	0	0	1	0	10
		2.00	0	23	0	0	7	0	30
		3.00	0	2	36	1	1	0	40
		4.00	0	0	2	18	0	0	20
		5.00	0	4	2	0	24	0	30
		6.00	0	0	2	0	2	26	30
	%	1.00	90.0	.0	.0	.0	10.0	.0	100.0
		2.00	.0	76.7	.0	.0	23.3	.0	100.0
		3.00	.0	5.0	90.0	2.5	2.5	.0	100.0
		4.00	.0	.0	10.0	90.0	.0	.0	100.0
		5.00	.0	13.3	6.7	.0	80.0	.0	100.0
		6.00	.0	.0	6.7	.0	6.7	86.7	100.0

a. Cross validation is done only for those cases in the analysis. In cross validation, each case is classified by the functions derived from all cases other than that case.

b. 88.8% of original grouped cases correctly classified.

c. 85.0% of cross-validated grouped cases correctly classified.

Table C:4 Sept-CASI spectra grouped using *a priori* habitat types

Classification Results[b,c]

			Predicted Group Membership						
		HabType	1.00	2.00	3.00	4.00	5.00	6.00	Total
Original	Count	1.00	9	0	1	0	0	0	10
		2.00	0	23	1	0	6	0	30
		3.00	1	0	35	1	3	0	40
		4.00	0	0	0	19	1	0	20
		5.00	0	5	2	0	23	0	30
		6.00	0	0	1	0	2	27	30
	%	1.00	90.0	.0	10.0	.0	.0	.0	100.0
		2.00	.0	76.7	3.3	.0	20.0	.0	100.0
		3.00	2.5	.0	87.5	2.5	7.5	.0	100.0
		4.00	.0	.0	.0	95.0	5.0	.0	100.0
		5.00	.0	16.7	6.7	.0	76.7	.0	100.0
		6.00	.0	.0	3.3	.0	6.7	90.0	100.0
Cross-validated[a]	Count	1.00	8	0	2	0	0	0	10
		2.00	0	22	1	0	7	0	30
		3.00	2	0	34	1	3	0	40
		4.00	0	0	0	18	2	0	20
		5.00	0	5	2	1	22	0	30
		6.00	0	0	1	0	2	27	30
	%	1.00	80.0	.0	20.0	.0	.0	.0	100.0
		2.00	.0	73.3	3.3	.0	23.3	.0	100.0
		3.00	5.0	.0	85.0	2.5	7.5	.0	100.0
		4.00	.0	.0	.0	90.0	10.0	.0	100.0
		5.00	.0	16.7	6.7	3.3	73.3	.0	100.0
		6.00	.0	.0	3.3	.0	6.7	90.0	100.0

a. Cross validation is done only for those cases in the analysis. In cross validation, each case is classified by the functions derived from all cases other than that case.

b. 85.0% of original grouped cases correctly classified.

c. 81.9% of cross-validated grouped cases correctly classified.

Table C:5 July-AVS1-42 spectra grouped using TWINSPAN cluster groups (species composition datasets only)

Classification Results[b,c]

			Predicted Group Membership							
		groups	1.00	2.00	3.00	4.00	5.00	6.00	7.00	Total
Original	Count	1.00	11	0	0	0	0	12	0	23
		2.00	0	13	1	0	0	4	0	18
		3.00	0	4	3	2	1	3	15	28
		4.00	3	3	1	4	10	6	1	28
		5.00	2	1	0	1	36	2	0	42
		6.00	2	1	1	0	1	2	1	8
		7.00	0	0	2	0	1	0	8	11
	%	1.00	47.8	.0	.0	.0	.0	52.2	.0	100.0
		2.00	.0	72.2	5.6	.0	.0	22.2	.0	100.0
		3.00	.0	14.3	10.7	7.1	3.6	10.7	53.6	100.0
		4.00	10.7	10.7	3.6	14.3	35.7	21.4	3.6	100.0
		5.00	4.8	2.4	.0	2.4	85.7	4.8	.0	100.0
		6.00	25.0	12.5	12.5	.0	12.5	25.0	12.5	100.0
		7.00	.0	.0	18.2	.0	9.1	.0	72.7	100.0
Cross-validated[a]	Count	1.00	11	0	0	0	0	12	0	23
		2.00	0	13	1	0	0	4	0	18
		3.00	0	4	3	2	1	3	15	28
		4.00	3	3	1	4	10	6	1	28
		5.00	2	2	0	1	35	2	0	42
		6.00	2	1	1	0	1	2	1	8
		7.00	0	0	2	0	1	0	8	11
	%	1.00	47.8	.0	.0	.0	.0	52.2	.0	100.0
		2.00	.0	72.2	5.6	.0	.0	22.2	.0	100.0
		3.00	.0	14.3	10.7	7.1	3.6	10.7	53.6	100.0
		4.00	10.7	10.7	3.6	14.3	35.7	21.4	3.6	100.0
		5.00	4.8	4.8	.0	2.4	83.3	4.8	.0	100.0
		6.00	25.0	12.5	12.5	.0	12.5	25.0	12.5	100.0
		7.00	.0	.0	18.2	.0	9.1	.0	72.7	100.0

a. Cross validation is done only for those cases in the analysis. In cross validation, each case is classified by the functions derived from all cases other than that case.

b. 48.7% of original grouped cases correctly classified.

c. 48.1% of cross-validated grouped cases correctly classified.

Table C:6 July-CASI spectra grouped using TWINSPAN cluster groups (species composition datasets only)

Classification Results[b,c]

			Predicted Group Membership							
		group	1.00	2.00	3.00	4.00	5.00	6.00	7.00	Total
Original	Count	1.00	14	3	0	6	0	0	0	23
		2.00	1	11	5	0	1	0	0	18
		3.00	3	8	13	3	0	1	0	28
		4.00	7	3	2	14	1	1	0	28
		5.00	0	0	0	4	20	8	10	42
		6.00	0	0	0	0	0	8	0	8
		7.00	0	0	0	0	0	1	10	11
	%	1.00	60.9	13.0	.0	26.1	.0	.0	.0	100.0
		2.00	5.6	61.1	27.8	.0	5.6	.0	.0	100.0
		3.00	10.7	28.6	46.4	10.7	.0	3.6	.0	100.0
		4.00	25.0	10.7	7.1	50.0	3.6	3.6	.0	100.0
		5.00	.0	.0	.0	9.5	47.6	19.0	23.8	100.0
		6.00	.0	.0	.0	.0	.0	100.0	.0	100.0
		7.00	.0	.0	.0	.0	.0	9.1	90.9	100.0
Cross-validated[a]	Count	1.00	12	3	1	6	0	0	1	23
		2.00	1	11	5	0	1	0	0	18
		3.00	3	8	13	3	0	1	0	28
		4.00	8	3	2	13	1	1	0	28
		5.00	0	0	0	5	18	8	11	42
		6.00	0	0	0	0	0	7	1	8
		7.00	0	0	0	0	0	1	10	11
	%	1.00	52.2	13.0	4.3	26.1	.0	.0	4.3	100.0
		2.00	5.6	61.1	27.8	.0	5.6	.0	.0	100.0
		3.00	10.7	28.6	46.4	10.7	.0	3.6	.0	100.0
		4.00	28.6	10.7	7.1	46.4	3.6	3.6	.0	100.0
		5.00	.0	.0	.0	11.9	42.9	19.0	26.2	100.0
		6.00	.0	.0	.0	.0	.0	87.5	12.5	100.0
		7.00	.0	.0	.0	.0	.0	9.1	90.9	100.0

a. Cross validation is done only for those cases in the analysis. In cross validation, each case is classified by the functions derived from all cases other than that case.

b. 57.0% of original grouped cases correctly classified.

c. 53.2% of cross-validated grouped cases correctly classified.

Table C:7 Sept-AVS1-42 spectra grouped using TWINSPAN cluster groups (species composition datasets only)

Classification Results[b,c]

			Predicted Group Membership						
		group	1.00	2.00	3.00	4.00	5.00	6.00	Total
Original	Count	1.00	7	0	0	0	0	0	7
		2.00	2	13	4	0	0	0	19
		3.00	0	5	23	2	3	0	33
		4.00	0	2	5	44	5	0	56
		5.00	0	4	5	0	15	4	28
		6.00	0	0	1	0	3	13	17
	%	1.00	100.0	.0	.0	.0	.0	.0	100.0
		2.00	10.5	68.4	21.1	.0	.0	.0	100.0
		3.00	.0	15.2	69.7	6.1	9.1	.0	100.0
		4.00	.0	3.6	8.9	78.6	8.9	.0	100.0
		5.00	.0	14.3	17.9	.0	53.6	14.3	100.0
		6.00	.0	.0	5.9	.0	17.6	76.5	100.0
Cross-validated[a]	Count	1.00	6	0	1	0	0	0	7
		2.00	2	12	5	0	0	0	19
		3.00	0	5	23	2	3	0	33
		4.00	0	3	4	41	8	0	56
		5.00	0	5	6	0	11	6	28
		6.00	0	0	1	0	3	13	17
	%	1.00	85.7	.0	14.3	.0	.0	.0	100.0
		2.00	10.5	63.2	26.3	.0	.0	.0	100.0
		3.00	.0	15.2	69.7	6.1	9.1	.0	100.0
		4.00	.0	5.4	7.1	73.2	14.3	.0	100.0
		5.00	.0	17.9	21.4	.0	39.3	21.4	100.0
		6.00	.0	.0	5.9	.0	17.6	76.5	100.0

a. Cross validation is done only for those cases in the analysis. In cross validation, each case is classified by the functions derived from all cases other than that case.

b. 71.9% of original grouped cases correctly classified.

c. 66.3% of cross-validated grouped cases correctly classified.

TableC:8 Sept-CASI spectra grouped using TWINSPAN cluster groups (species composition datasets only)

Classification Results[b,c]

			Predicted Group Membership						
		group	1.00	2.00	3.00	4.00	5.00	6.00	Total
Original	Count	1.00	7	0	0	0	0	0	7
		2.00	2	11	3	0	3	0	19
		3.00	2	4	19	3	4	1	33
		4.00	0	7	6	34	9	0	56
		5.00	0	5	4	5	8	6	28
		6.00	0	0	1	2	2	12	17
	%	1.00	100.0	.0	.0	.0	.0	.0	100.0
		2.00	10.5	57.9	15.8	.0	15.8	.0	100.0
		3.00	6.1	12.1	57.6	9.1	12.1	3.0	100.0
		4.00	.0	12.5	10.7	60.7	16.1	.0	100.0
		5.00	.0	17.9	14.3	17.9	28.6	21.4	100.0
		6.00	.0	.0	5.9	11.8	11.8	70.6	100.0
Cross-validated[a]	Count	1.00	6	0	1	0	0	0	7
		2.00	2	9	4	0	4	0	19
		3.00	2	4	19	3	4	1	33
		4.00	0	8	8	31	9	0	56
		5.00	0	5	5	6	6	6	28
		6.00	0	0	1	2	2	12	17
	%	1.00	85.7	.0	14.3	.0	.0	.0	100.0
		2.00	10.5	47.4	21.1	.0	21.1	.0	100.0
		3.00	6.1	12.1	57.6	9.1	12.1	3.0	100.0
		4.00	.0	14.3	14.3	55.4	16.1	.0	100.0
		5.00	.0	17.9	17.9	21.4	21.4	21.4	100.0
		6.00	.0	.0	5.9	11.8	11.8	70.6	100.0

a. Cross validation is done only for those cases in the analysis. In cross validation, each case is classified by the functions derived from all cases other than that case.

b. 56.9% of original grouped cases correctly classified.

c. 51.9% of cross-validated grouped cases correctly classified.

TableC:9 July AVS1-42 spectra grouped using TWINSPAN cluster groups (species with structure and environmental variables datasets only)

Classification Results[b,c]

			Predicted Group Membership							
		group	1.00	2.00	3.00	4.00	5.00	6.00	7.00	Total
Original	Count	1.00	14	1	3	1	0	0	1	20
		2.00	7	26	10	0	2	6	1	52
		3.00	7	5	26	7	1	1	2	49
		4.00	1	0	0	8	0	1	0	10
		5.00	0	0	0	0	4	2	1	7
		6.00	0	0	0	0	4	5	1	10
		7.00	0	1	0	0	3	2	4	10
	%	1.00	70.0	5.0	15.0	5.0	.0	.0	5.0	100.0
		2.00	13.5	50.0	19.2	.0	3.8	11.5	1.9	100.0
		3.00	14.3	10.2	53.1	14.3	2.0	2.0	4.1	100.0
		4.00	10.0	.0	.0	80.0	.0	10.0	.0	100.0
		5.00	.0	.0	.0	.0	57.1	28.6	14.3	100.0
		6.00	.0	.0	.0	.0	40.0	50.0	10.0	100.0
		7.00	.0	10.0	.0	.0	30.0	20.0	40.0	100.0
Cross-validated[a]	Count	1.00	14	1	3	1	0	0	1	20
		2.00	7	25	11	0	2	6	1	52
		3.00	7	6	25	7	1	1	2	49
		4.00	2	0	0	7	0	1	0	10
		5.00	0	0	0	0	4	2	1	7
		6.00	0	0	0	0	4	4	2	10
		7.00	0	1	0	0	3	2	4	10
	%	1.00	70.0	5.0	15.0	5.0	.0	.0	5.0	100.0
		2.00	13.5	48.1	21.2	.0	3.8	11.5	1.9	100.0
		3.00	14.3	12.2	51.0	14.3	2.0	2.0	4.1	100.0
		4.00	20.0	.0	.0	70.0	.0	10.0	.0	100.0
		5.00	.0	.0	.0	.0	57.1	28.6	14.3	100.0
		6.00	.0	.0	.0	.0	40.0	40.0	20.0	100.0
		7.00	.0	10.0	.0	.0	30.0	20.0	40.0	100.0

a. Cross validation is done only for those cases in the analysis. In cross validation, each case is classified by the functions derived from all cases other than that case.

b. 55.1% of original grouped cases correctly classified.

c. 52.5% of cross-validated grouped cases correctly classified.

Table C:10 CASI spectra grouped using TWINSPAN cluster groups (species with structure and environmental variables datasets only)

Classification Results[b,c]

			Predicted Group Membership							
		group	1.00	2.00	3.00	4.00	5.00	6.00	7.00	Total
Original	Count	1.00	16	4	0	0	0	0	0	20
		2.00	9	36	1	0	3	3	0	52
		3.00	4	2	31	8	1	0	3	49
		4.00	1	0	1	6	0	0	2	10
		5.00	0	1	0	0	5	1	0	7
		6.00	1	1	0	0	5	3	0	10
		7.00	0	0	0	0	0	0	10	10
	%	1.00	80.0	20.0	.0	.0	.0	.0	.0	100.0
		2.00	17.3	69.2	1.9	.0	5.8	5.8	.0	100.0
		3.00	8.2	4.1	63.3	16.3	2.0	.0	6.1	100.0
		4.00	10.0	.0	10.0	60.0	.0	.0	20.0	100.0
		5.00	.0	14.3	.0	.0	71.4	14.3	.0	100.0
		6.00	10.0	10.0	.0	.0	50.0	30.0	.0	100.0
		7.00	.0	.0	.0	.0	.0	.0	100.0	100.0
Cross-validated[a]	Count	1.00	16	4	0	0	0	0	0	20
		2.00	9	34	1	0	3	5	0	52
		3.00	5	2	30	8	1	0	3	49
		4.00	1	0	2	5	0	0	2	10
		5.00	0	1	0	0	3	3	0	7
		6.00	1	1	0	0	5	3	0	10
		7.00	0	0	0	1	0	0	9	10
	%	1.00	80.0	20.0	.0	.0	.0	.0	.0	100.0
		2.00	17.3	65.4	1.9	.0	5.8	9.6	.0	100.0
		3.00	10.2	4.1	61.2	16.3	2.0	.0	6.1	100.0
		4.00	10.0	.0	20.0	50.0	.0	.0	20.0	100.0
		5.00	.0	14.3	.0	.0	42.9	42.9	.0	100.0
		6.00	10.0	10.0	.0	.0	50.0	30.0	.0	100.0
		7.00	.0	.0	.0	10.0	.0	.0	90.0	100.0

a. Cross validation is done only for those cases in the analysis. In cross validation, each case is classified by the functions derived from all cases other than that case.

b. 67.7% of original grouped cases correctly classified.

c. 63.3% of cross-validated grouped cases correctly classified.

Table C:11 Sept AVS1-42 spectra grouped using TWINSPAN cluster groups (species with structure and environmental variables datasets only)

Classification Results[b,c]

			Predicted Group Membership						
		group	1.00	2.00	3.00	4.00	5.00	6.00	Total
Original	Count	1.00	9	3	0	3	0	0	15
		2.00	0	32	1	9	0	0	42
		3.00	1	8	46	6	0	0	61
		4.00	0	3	0	8	0	0	11
		5.00	0	0	0	1	11	2	14
		6.00	0	0	0	0	7	10	17
	%	1.00	60.0	20.0	.0	20.0	.0	.0	100.0
		2.00	.0	76.2	2.4	21.4	.0	.0	100.0
		3.00	1.6	13.1	75.4	9.8	.0	.0	100.0
		4.00	.0	27.3	.0	72.7	.0	.0	100.0
		5.00	.0	.0	.0	7.1	78.6	14.3	100.0
		6.00	.0	.0	.0	.0	41.2	58.8	100.0
Cross-validated[a]	Count	1.00	8	3	1	3	0	0	15
		2.00	0	29	1	12	0	0	42
		3.00	1	9	44	7	0	0	61
		4.00	0	4	0	7	0	0	11
		5.00	0	0	0	1	11	2	14
		6.00	0	0	0	0	7	10	17
	%	1.00	53.3	20.0	6.7	20.0	.0	.0	100.0
		2.00	.0	69.0	2.4	28.6	.0	.0	100.0
		3.00	1.6	14.8	72.1	11.5	.0	.0	100.0
		4.00	.0	36.4	.0	63.6	.0	.0	100.0
		5.00	.0	.0	.0	7.1	78.6	14.3	100.0
		6.00	.0	.0	.0	.0	41.2	58.8	100.0

a. Cross validation is done only for those cases in the analysis. In cross validation, each case is classified by the functions derived from all cases other than that case.

b. 72.5% of original grouped cases correctly classified.

c. 68.1% of cross-validated grouped cases correctly classified.

Table C:12 July CASI spectra grouped using TWINSPAN cluster groups (species with structure and environmental variables datasets only)

Classification Results[b,c]

			Predicted Group Membership						
		group	1.00	2.00	3.00	4.00	5.00	6.00	Total
Original	Count	1.00	11	3	0	1	0	0	15
		2.00	4	22	6	10	0	0	42
		3.00	2	11	29	12	7	0	61
		4.00	0	4	1	6	0	0	11
		5.00	0	0	2	0	9	3	14
		6.00	0	1	0	0	6	10	17
	%	1.00	73.3	20.0	.0	6.7	.0	.0	100.0
		2.00	9.5	52.4	14.3	23.8	.0	.0	100.0
		3.00	3.3	18.0	47.5	19.7	11.5	.0	100.0
		4.00	.0	36.4	9.1	54.5	.0	.0	100.0
		5.00	.0	.0	14.3	.0	64.3	21.4	100.0
		6.00	.0	5.9	.0	.0	35.3	58.8	100.0
Cross-validated[a]	Count	1.00	10	3	0	2	0	0	15
		2.00	4	22	6	10	0	0	42
		3.00	2	11	29	12	7	0	61
		4.00	1	4	1	5	0	0	11
		5.00	0	0	2	0	8	4	14
		6.00	0	1	0	0	7	9	17
	%	1.00	66.7	20.0	.0	13.3	.0	.0	100.0
		2.00	9.5	52.4	14.3	23.8	.0	.0	100.0
		3.00	3.3	18.0	47.5	19.7	11.5	.0	100.0
		4.00	9.1	36.4	9.1	45.5	.0	.0	100.0
		5.00	.0	.0	14.3	.0	57.1	28.6	100.0
		6.00	.0	5.9	.0	.0	41.2	52.9	100.0

a. Cross validation is done only for those cases in the analysis. In cross validation, each case is classified by the functions derived from all cases other than that case.

b. 54.4% of original grouped cases correctly classified.

c. 51.9% of cross-validated grouped cases correctly classified.

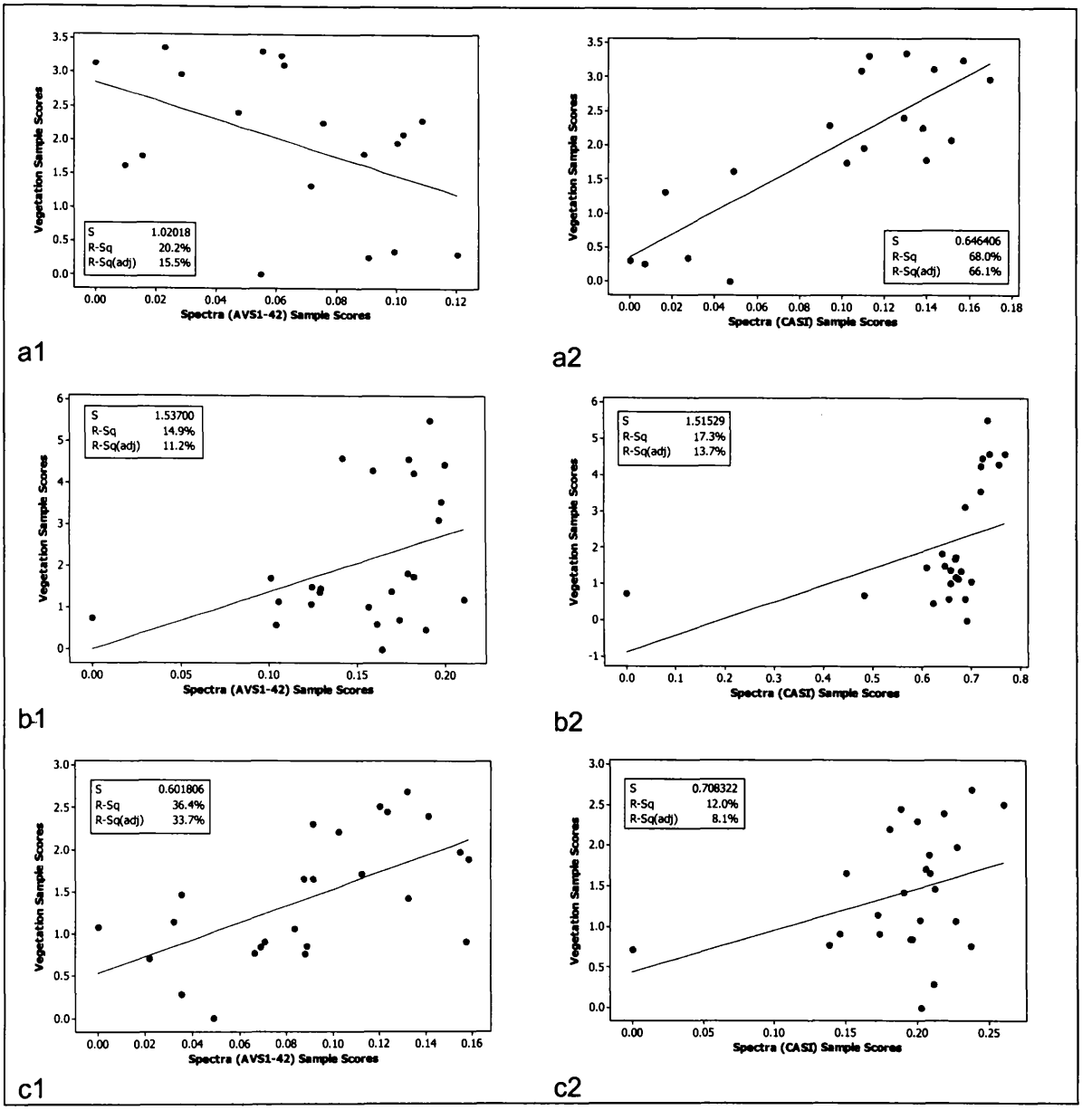

Figure C:1 Regression results on vegetation and spectra (AVS1-42- '1' and CASI- '2' datasets) sample scores from data collected at Transects a-c in July

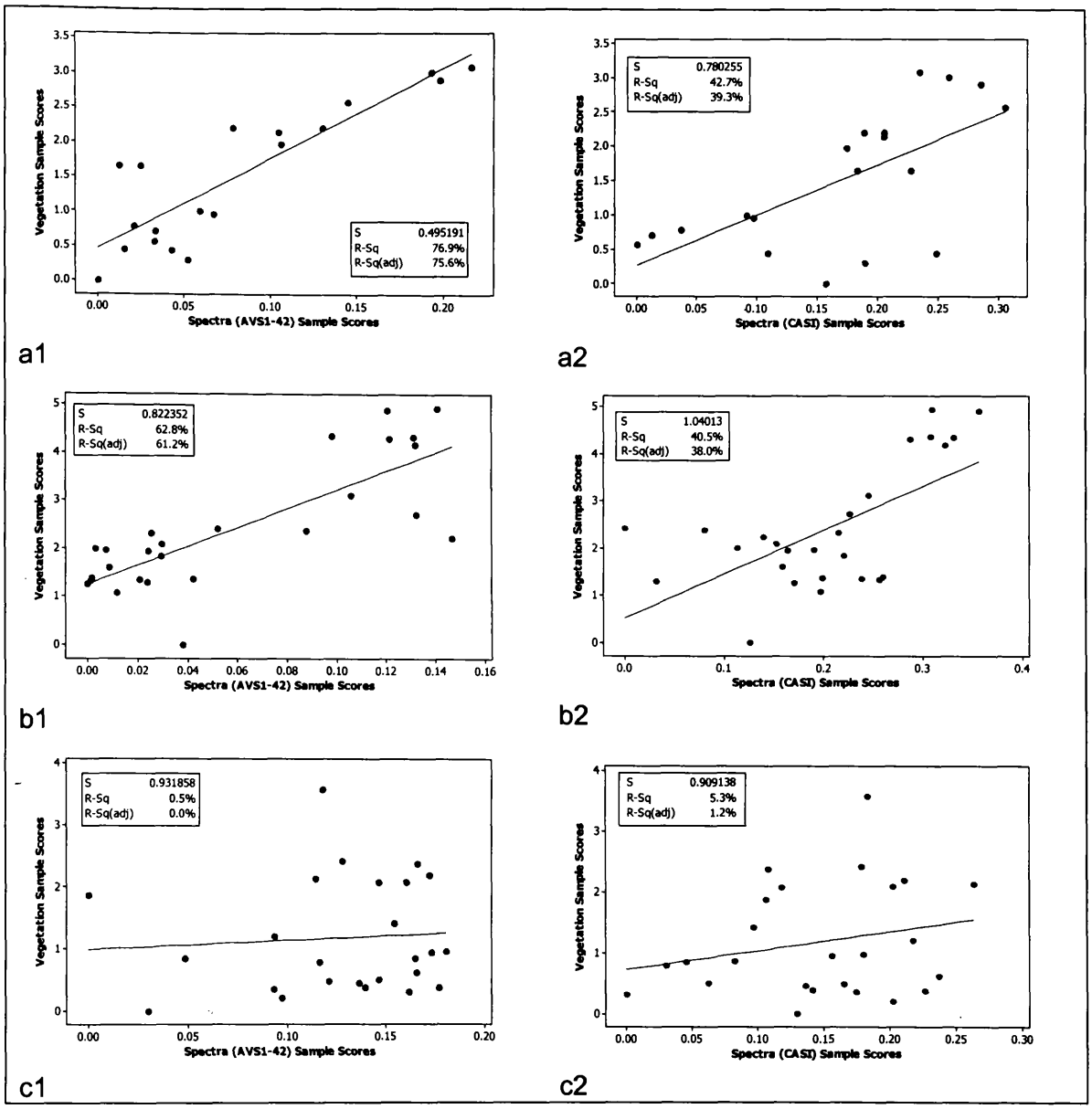

Figure C:2 Regression results on vegetation and spectra (AVS1-42- '1' and CASI- '2' datasets) sample scores from data collected at Transects a-c in September

Marginal Effects: CCAs July and September

Table C:13 Marginal effects results from CCA with AVS1-42 spectral dataset (predictors) and both vegetation datasets (independents)-July

Species composition dataset			Species composition and structure dataset		
Band	Var. N	LambdaA	Variable	Var. N	LambdaA
AV14	14	0.26	AV26	26	0.1
AV13	13	0.26	AV25	25	0.1
AV15	15	0.26	AV27	27	0.1
AV12	12	0.26	AV28	28	0.1
AV16	16	0.25	AV24	24	0.1
AV26	26	0.24	AV29	29	0.1
AV27	27	0.24	AV32	32	0.1
AV28	28	0.24	AV33	33	0.09
AV29	29	0.23	AV30	30	0.09
AV8	8	0.23	AV31	31	0.09
AV32	32	0.23	AV34	34	0.09
AV33	33	0.23	AV15	15	0.09
AV11	11	0.23	AV23	23	0.09
AV34	34	0.23	AV6	6	0.09
AV9	9	0.23	AV35	35	0.09
AV25	25	0.23	AV14	14	0.09
AV30	30	0.23	AV5	5	0.09
AV31	31	0.23	AV16	16	0.09
AV17	17	0.23	AV36	36	0.09
AV35	35	0.23	AV22	22	0.09
AV10	10	0.22	AV13	13	0.09
AV36	36	0.22	AV37	37	0.08
AV24	24	0.22	AV41	41	0.08
AV37	37	0.22	AV42	42	0.08
AV41	41	0.21	AV12	12	0.08
AV42	42	0.21	AV4	4	0.08
AV40	40	0.21	AV8	8	0.08
AV23	23	0.2	AV17	17	0.08
AV7	7	0.2	AV40	40	0.08
AV39	39	0.2	AV9	9	0.08
AV38	38	0.2	AV3	3	0.08
AV6	6	0.18	AV11	11	0.07
AV5	5	0.18	AV38	38	0.07
AV18	18	0.17	AV39	39	0.07
AV22	22	0.17	AV10	10	0.07
AV1	1	0.17	AV2	2	0.07
AV4	4	0.17	AV1	1	0.07
AV19	19	0.16	AV19	19	0.07
AV3	3	0.16	AV7	7	0.06
AV2	2	0.15	AV21	21	0.06
AV20	20	0.14	AV18	18	0.05
AV21	21	0.13	AV20	20	0.05

Table C:14 Marginal effects results from CCA with CASI spectral dataset (predictors) and both vegetation datasets (independents)-July

Species composition dataset			Species composition and structure dataset		
Band	Var. N	LambdaA	Variable	Var. N	LambdaA
CASI 8	8	0.22	CASI 8	8	0.09
CASI 9	9	0.22	CASI 9	9	0.09
CASI 10	10	0.22	CASI 7	7	0.09
CASI 7	7	0.21	CASI 10	10	0.09
CASI 2	2	0.21	CASI 6	6	0.08
CASI 6	6	0.21	CASI 2	2	0.07
CASI 5	5	0.16	CASI 5	5	0.06
CASI 4	4	0.15	CASI 4	4	0.05
CASI 3	3	0.15	CASI 3	3	0.05
CASI 1	1	0.14	CASI 1	1	0.04

Table C:15 Marginal effects results from CCA with AVS1-42 spectral dataset (predictors) and both vegetation datasets (independents)-Sept

Species composition dataset			Species composition and structure dataset		
Variable	Var. N	LambdaA	Variable	Var. N	LambdaA
AV-21	21	0.31	AV-26	26	0.11
AV-22	22	0.28	AV-27	27	0.11
AV-20	20	0.28	AV-28	28	0.1
AV-27	27	0.27	AV-29	29	0.1
AV-26	26	0.27	AV-30	30	0.1
AV-28	28	0.27	AV-25	25	0.1
AV-29	29	0.26	AV-12	12	0.09
AV-30	30	0.25	AV-31	31	0.09
AV-19	19	0.25	AV-32	32	0.09
AV-31	31	0.24	AV-13	13	0.09
AV-32	32	0.24	AV-21	21	0.09
AV-25	25	0.24	AV-33	33	0.09
AV-18	18	0.23	AV-34	34	0.09
AV-33	33	0.23	AV-35	35	0.08
AV-34	34	0.23	AV-36	36	0.08
AV-10	10	0.22	AV-22	22	0.08
AV-11	11	0.22	AV-20	20	0.08
AV-12	12	0.22	AV-11	11	0.08
AV-13	13	0.22	AV-14	14	0.08
AV-35	35	0.22	AV-37	37	0.08
AV-7	7	0.21	AV-19	19	0.07
AV-36	36	0.21	AV-24	24	0.07
AV-9	9	0.21	AV-10	10	0.07
AV-14	14	0.2	AV-18	18	0.07
AV-17	17	0.2	AV-39	39	0.07
AV-37	37	0.2	AV-7	7	0.06
AV-16	16	0.19	AV-40	40	0.06
AV-8	8	0.19	AV-38	38	0.06
AV-15	15	0.19	AV-9	9	0.06
AV-39	39	0.18	AV-15	15	0.06
AV-6	6	0.17	AV-41	41	0.06
AV-40	40	0.17	AV-42	42	0.06
AV-38	38	0.17	AV-8	8	0.06
AV-41	41	0.17	AV-16	16	0.06
AV-42	42	0.17	AV-17	17	0.06
AV-24	24	0.16	AV-6	6	0.05
AV-23	23	0.14	AV-23	23	0.04
AV-5	5	0.12	AV-5	5	0.04
AV-3	3	0.1	AV-4	4	0.02
AV-2	2	0.09	AV-3	3	0.02
AV-4	4	0.09	AV-2	2	0.02
AV-1	1	0.07	AV-1	1	0.02

Table C:16 Marginal effects results from CCA with CASI spectral dataset (predictor) and both vegetation datasets (independents)-Sept

Species composition dataset			Species composition and structure dataset		
Band	Var. N	LambdaA	Variable	Var. N	LambdaA
CASI-3	3	0.29	CASI-7	7	0.1
CASI-7	7	0.27	CASI-8	8	0.1
CASI-8	8	0.26	CASI-6	6	0.1
CASI-6	6	0.25	CASI-9	9	0.09
CASI-9	9	0.24	CASI-3	3	0.08
CASI-10	10	0.23	CASI-10	10	0.08
CASI-2	2	0.2	CASI-2	2	0.08
CASI-1	1	0.19	CASI-1	1	0.06
CASI-4	4	0.17	CASI-4	4	0.05
CASI-5	5	0.12	CASI-5	5	0.04

Marginal Effects: RDAs July and September

Table C:17 Marginal effects results from RDA with AVS1-42 spectral dataset (independent) and both vegetation datasets (predictors)-July

Species composition dataset			Species composition and structure dataset		
Variable	Var. N	LambdaA	Variable	Var. N	LambdaA
Poa pra	33	0.11	Poa pra	33	0.11
Des ces	17	0.1	Des ces	17	0.1
Cal pal	4	0.09	Cal pal	4	0.09
Car cur	7	0.09	Car cur	7	0.09
Car hos	10	0.09	Car hos	10	0.09
Pot pal	36	0.05	gr-top	49	0.08
Equ pal	20	0.05	Pot pal	36	0.05
Vio pal	42	0.05	drops	53	0.05
Car ros	15	0.05	Equ pal	20	0.05
Pot ere	35	0.05	Vio pal	42	0.05
Mol cae	28	0.04	Car ros	15	0.05
Equ flu	19	0.04	st dens	48	0.05
Tri rep	40	0.03	Pot ere	35	0.05
Car pra	5	0.03	Mol cae	28	0.04
Car ova	12	0.02	Equ flu	19	0.04
Moss	44	0.02	mx ht	47	0.04
Agr sp	1	0.02	Tri rep	40	0.03
Car nig	11	0.02	POH	46	0.03
Nar str	30	0.02	wd stms	55	0.03
Car pau	14	0.01	Car pra	5	0.03
Gal pal	24	0.02	wt dep	51	0.03
Pota po	34	0.02	Car ova	12	0.02
Epi pal	18	0.01	bar pt	52	0.02
Ran fla	37	0.01	Moss	44	0.02
Car aqu	6	0.01	Agr sp	1	0.02
Jun eff	26	0.01	Car nig	11	0.02
Hol lan	25	0.01	Nar str	30	0.02
Car dem	8	0.01	Car pau	14	0.01
Car pan	13	0.01	Gal pal	24	0.02
Bet sp	3	0.01	Pota po	34	0.02
Ver scu	41	0.01	Epi pal	18	0.01
Car ves	16	0.01	Ran fla	37	0.01
Ant ode	2	0.01	Car aqu	6	0.01
Myr gal	29	0.01	Jun eff	26	0.01
Nar oss	31	0	Hol lan	25	0.01
Car ech	9	0	lf lit	54	0.01
Eri cin	21	0	Car dem	8	0.01
Eri ang	22	0	Car pan	13	0.01
Pha aru	32	0	Bet sp	3	0.01
Fil ulm	23	0	Ver scu	41	0.01
Blad	43	0	tuss	50	0.01
Ran rep	38	0	Car ves	16	0.01
Rum ace	39	0	Ant ode	2	0.01
Men tri	27	0	Myr gal	29	0.01

Table C:18 Marginal effects results from RDA with CASI spectral dataset (independent) and both vegetation datasets (predictors)-July

Species composition dataset			Species composition and structure dataset		
Variable	Var. N	LambdaA	Variable	Var. N	LambdaA
Ant ode	2	0.09	bar pt	52	0.12
Cal pal	4	0.08	st dens	48	0.1
Nar str	30	0.08	Ant ode	2	0.09
Car aqu	6	0.07	Cal pal	4	0.08
Equ flu	19	0.06	Nar str	30	0.08
Men tri	27	0.05	Car aqu	6	0.07
Car ros	15	0.05	Equ flu	19	0.06
Agr sp	1	0.05	Men tri	27	0.05
Pota po	34	0.04	Car ros	15	0.05
Pha aru	32	0.04	Agr sp	1	0.05
Car ves	16	0.04	Pota po	34	0.04
Ran fla	37	0.04	Pha aru	32	0.04
Blad	43	0.04	Car ves	16	0.04
Hol lan	25	0.04	Ran fla	37	0.04
Tri rep	40	0.03	Blad	43	0.04
Pot pal	36	0.02	mx ht	47	0.04
Myr gal	29	0.02	wt dep	51	0.04
Car nig	11	0.02	Hol lan	25	0.04
Poa pra	33	0.02	gr-top	49	0.03
Car dem	8	0.01	Tri rep	40	0.03
Vio pal	42	0.01	Pot pal	36	0.02
Bet sp	3	0.01	Myr gal	29	0.02
Car pan	13	0.01	Car nig	11	0.02
Epi pal	18	0.01	Poa pra	33	0.02
Rum ace	39	0.01	POH	46	0.01
Car cur	7	0.01	Car dem	8	0.01
Eri cin	21	0.01	Vio pal	42	0.01
Pot ere	35	0.01	Bet sp	3	0.01
Eri ang	22	0	lf lit	54	0.01
Car ech	9	0	Car pan	13	0.01
Mol cae	28	0	Epi pal	18	0.01
Ran rep	38	0	Rum ace	39	0.01
Ver scu	41	0	Car cur	7	0.01
Des ces	17	0	Eri cin	21	0.01
Car pra	5	0	Pot ere	35	0.01
Car hos	10	0	wd stms	55	0.01
Car ova	12	0	Eri ang	22	0
Car pau	14	0	TOH	45	0
Equ pal	20	0	drops	53	0
Fil ulm	23	0	Car ech	9	0
Gal pal	24	0	Mol cae	28	0
Jun eff	26	0	Ran rep	38	0
Nar oss	31	0	Ver scu	41	0
Moss	44	0	Des ces	17	0

Table C:19 Marginal effects results from RDA with AVS1-42 spectral dataset (independent) and both vegetation datasets (predictors)-Sept

Species composition dataset			Species composition and structure dataset		
Variable	Var. N	LambdaA	Variable	Var. N	LambdaA
Nar str	36	0.23	Nar str	47	0.23
Rum ace	45	0.15	Rum ace	56	0.15
Hol lan	27	0.14	Hol lan	38	0.14
Fil ulm	24	0.09	mx ht	3	0.1
Pha aru	37	0.07	gr-top	5	0.09
Moss	32	0.05	Fil ulm	35	0.09
Myr gal	34	0.05	drops	9	0.09
Car pan	13	0.05	lf lit	10	0.08
Car nig	11	0.05	Pha aru	48	0.07
Gal pal	25	0.03	p-o ht	2	0.05
Phr sp	38	0.03	Moss	43	0.05
Jun eff	29	0.03	Myr gal	45	0.05
Pot pal	41	0.02	Car pan	24	0.05
Sal sp	46	0.02	Car nig	22	0.05
Vio pal	49	0.02	Gal pal	36	0.03
Equ flu	20	0.02	Phr sp	49	0.03
Cal pal	5	0.02	Jun eff	40	0.03
Epi pal	19	0.02	Pot pal	52	0.02
Mol cae	31	0.01	bar pt	8	0.02
Pota po	42	0.01	wd stms	11	0.02
Tri rep	47	0.01	Sal sp	57	0.02
Car ech	9	0.01	Vio pal	60	0.02
Car ros	16	0.01	Equ flu	31	0.02
Pot ere	40	0.01	Cal pal	16	0.02
Car cur	7	0.01	t-o ht	1	0.02
Men tri	30	0.01	Epi pal	30	0.02
Car aqu	6	0.01	Mol cae	42	0.01
Des ces	18	0.01	Pota po	53	0.01
Gly flu	26	0.01	Tri rep	58	0.01
Car ova	12	0.01	Car ech	20	0.01
Eri cin	23	0	Car ros	27	0.01
Jun acu	28	0	Pot ere	51	0.01
Agr sp	1	0	Car cur	18	0.01
Car hos	10	0	Men tri	41	0.01
Equ pal	21	0	Car aqu	17	0.01
Bet sp	3	0	Des ces	29	0.01
Blad	4	0	Gly flu	37	0.01
Car dem	8	0	Car ova	23	0.01
Car pra	15	0	tuss	6	0.01
Car ves	17	0	Eri cin	34	0
Ran fla	43	0	Jun acu	39	0
Ant ode	2	0	Agr sp	12	0
Eri ang	22	0	Car hos	21	0
Poa pra	39	0	Equ pal	32	0

Table C:20 Marginal effects results from RDA with CASI spectral dataset (independent) and both vegetation datasets (predictors)-Sept

Species composition dataset			Species composition and structure dataset		
Variable	Var. N	LambdaA	Variable	Var. N	LambdaA
Nar str	36	0.24	Nar str	47	0.24
Rum ace	45	0.17	Rum ace	56	0.17
Hol lan	27	0.16	Hol lan	38	0.16
Fil ulm	24	0.1	gr-top	5	0.11
Pha aru	37	0.07	mx ht	3	0.1
Car nig	11	0.07	drops	9	0.1
Car pan	13	0.07	Fil ulm	35	0.1
Moss	32	0.05	lf lit	10	0.08
Myr gal	34	0.05	Pha aru	48	0.07
Gal pal	25	0.03	Car nig	22	0.07
Pot pal	41	0.03	Car pan	24	0.07
Phr sp	38	0.03	p-o ht	2	0.06
Equ flu	20	0.02	Moss	43	0.05
Jun eff	29	0.02	Myr gal	45	0.05
Vio pal	49	0.02	Gal pal	36	0.03
Sal sp	46	0.02	Pot pal	52	0.03
Epi pal	19	0.02	Phr sp	49	0.03
Cal pal	5	0.02	wd stms	11	0.03
Tri rep	47	0.02	bar pt	8	0.03
Pota po	42	0.02	Equ flu	31	0.02
Car ros	16	0.01	Jun eff	40	0.02
Car cur	7	0.01	Vio pal	60	0.02
Car ech	9	0.01	Sal sp	57	0.02
Des ces	18	0.01	t-o ht	1	0.02
Men tri	30	0.01	Epi pal	30	0.02
Mol cae	31	0.01	Cal pal	16	0.02
Pot ere	40	0.01	Tri rep	58	0.02
Car aqu	6	0.01	Pota po	53	0.02
Equ pal	21	0.01	Car ros	27	0.01
Agr sp	1	0.01	Car cur	18	0.01
Car ova	12	0.01	Car ech	20	0.01
Gly flu	26	0.01	Des ces	29	0.01
Car pra	15	0	Men tri	41	0.01
Eri cin	23	0	Mol cae	42	0.01
Jun acu	28	0	Pot ere	51	0.01
Bet sp	3	0	Car aqu	17	0.01
Car dem	8	0	Equ pal	32	0.01
Car hos	10	0	tuss	6	0.01
Ran fla	43	0	Agr sp	12	0.01
Blad	4	0	Car ova	23	0.01
Car ves	17	0	Gly flu	37	0.01
Eri ang	22	0	Car pra	26	0
Mush	33	0	Eri cin	34	0
Nar oss	35	0	Jun acu	39	0

Ordination diagrams: Predictors July and Sept

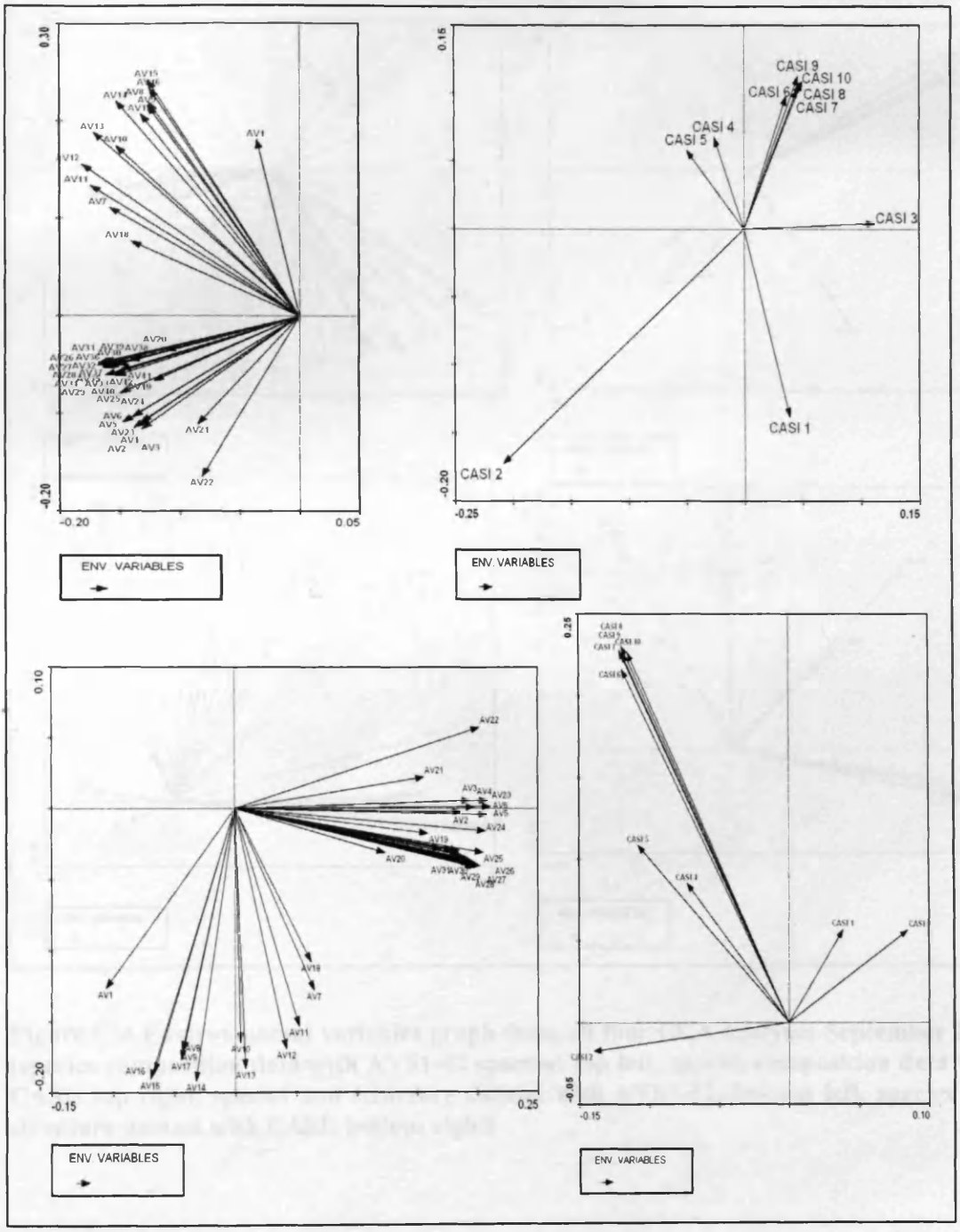

Figure C:3 Environmental variables graph from all four CCA analyses-July 2003 (species composition data with AVS1-42 spectra: top left, species composition data with CASI: top right, species and structure dataset with AVS1-42: bottom left, species and structure dataset with AVS1-42: bottom left, species and structure dataset with CASI: bottom right)

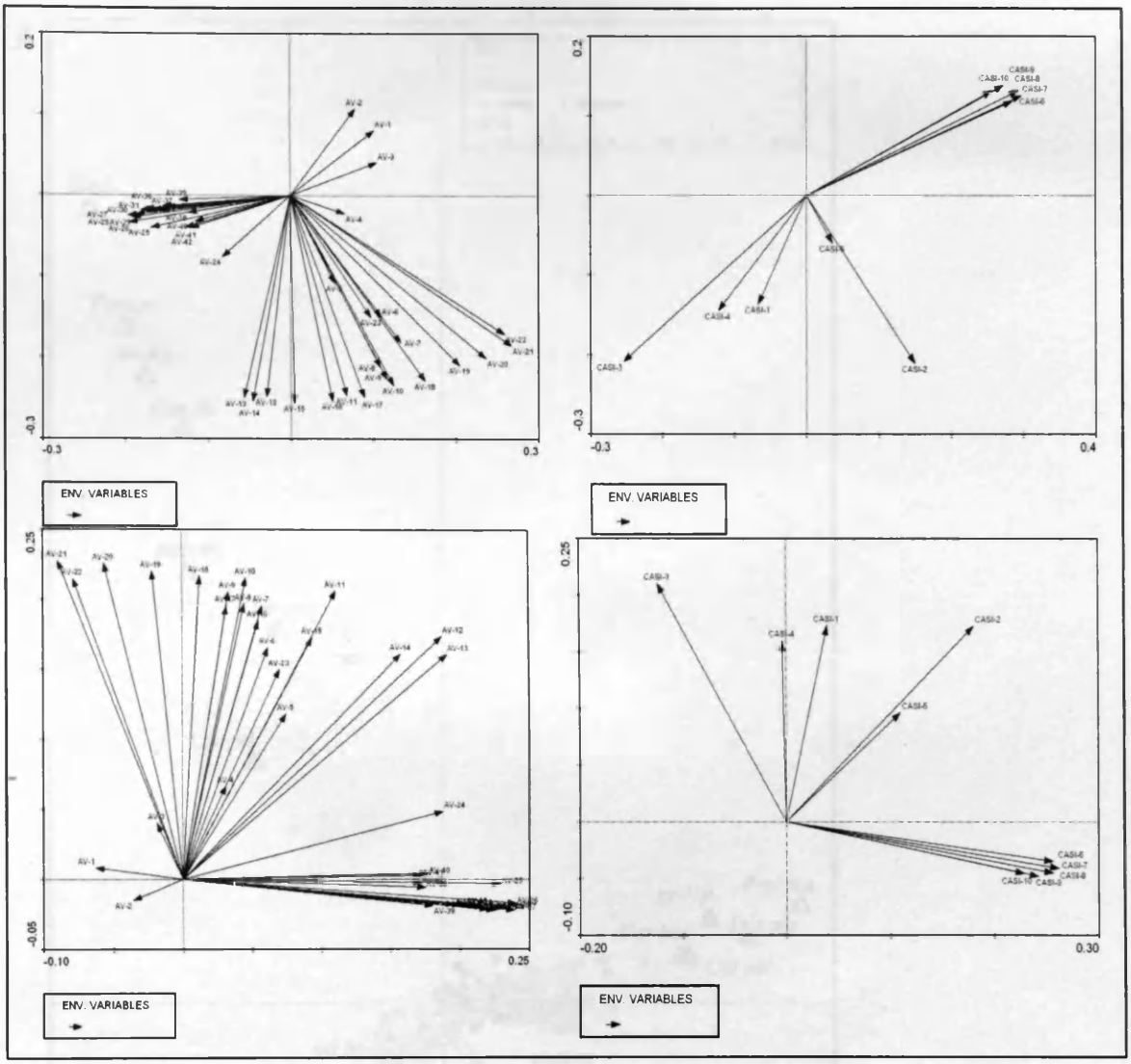

Figure C:4 Environmental variables graph from all four CCA analyses-September 2003 (species composition data with AVS1-42 spectra: top left, species composition data with CASI: top right, species and structure dataset with AVS1-42: bottom left, species and structure dataset with CASI: bottom right)

CCA triplots: July

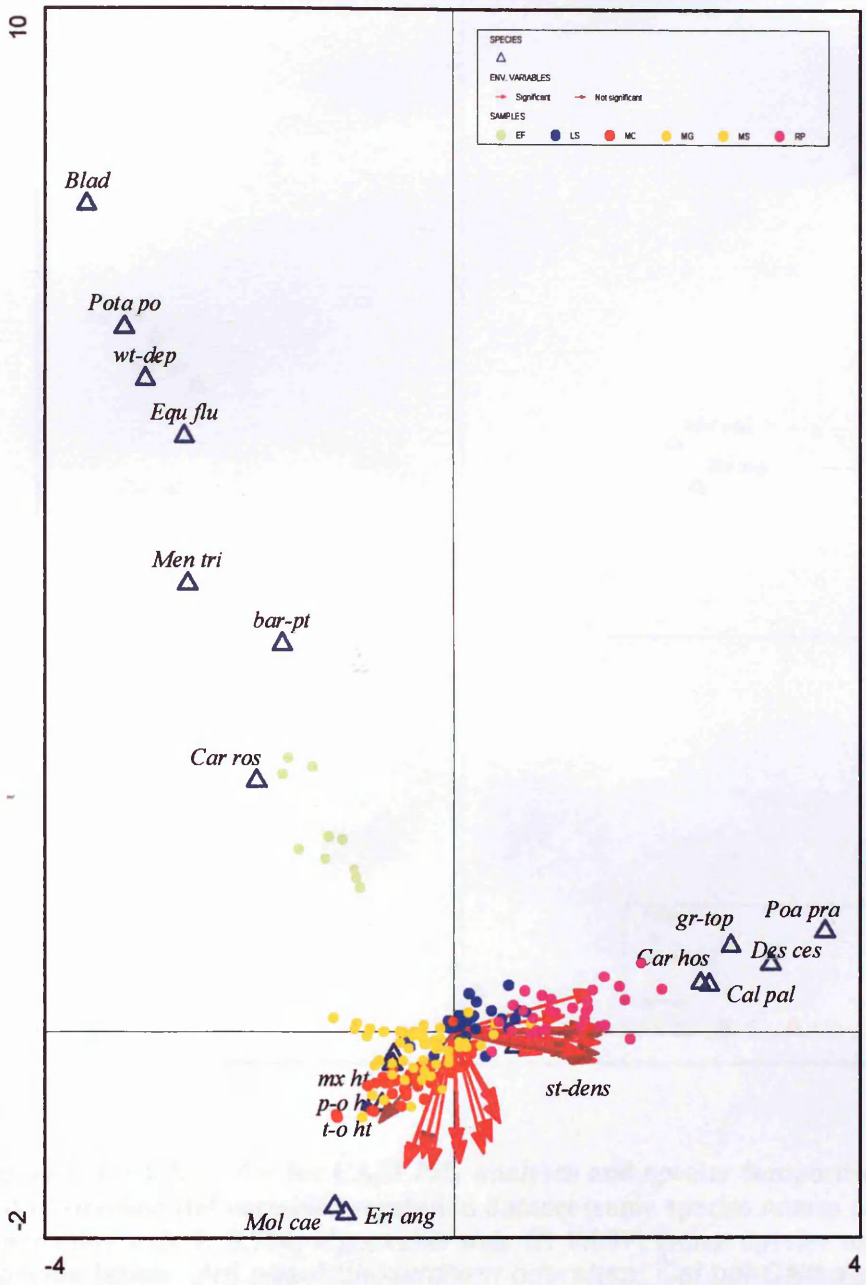

Figure C:5 CCA triplot for AVS1-42 July analyses and species composition with structural and environmental variables vegetation dataset (some species names omitted for clarity and only significant predictors labelled) (eigenvalue axis I: 0.874; eigenvalue axis II: 0.931) (see ordination diagrams above for predictor variables labels) (some species omitted for clarity) (species labels: *Blad-Utricularia intermedia agg; Cal pal-Caltha palustris; Car hos-Carex hostiana; Car ros-Carex rostrata; Des ces-Deschamsia cespitosa; Equ flu-Equisetum fluviatile; Eri ang-Eriophorum angustifolium; Men tri-Menyanthes trifoliata; Mol cae-Molinia caerulea; Poa pra-Poa pratensis; Pota po-Potamogeton polygonifolius;* Structural and environmental predictors: *t-o-ht-totally obscured height; p-o-ht-partially obscured height; mx ht-maximum height; st dems-stem density; gr-top-grazed/topped; wt dep-water depth; bar pt-bare peat*)

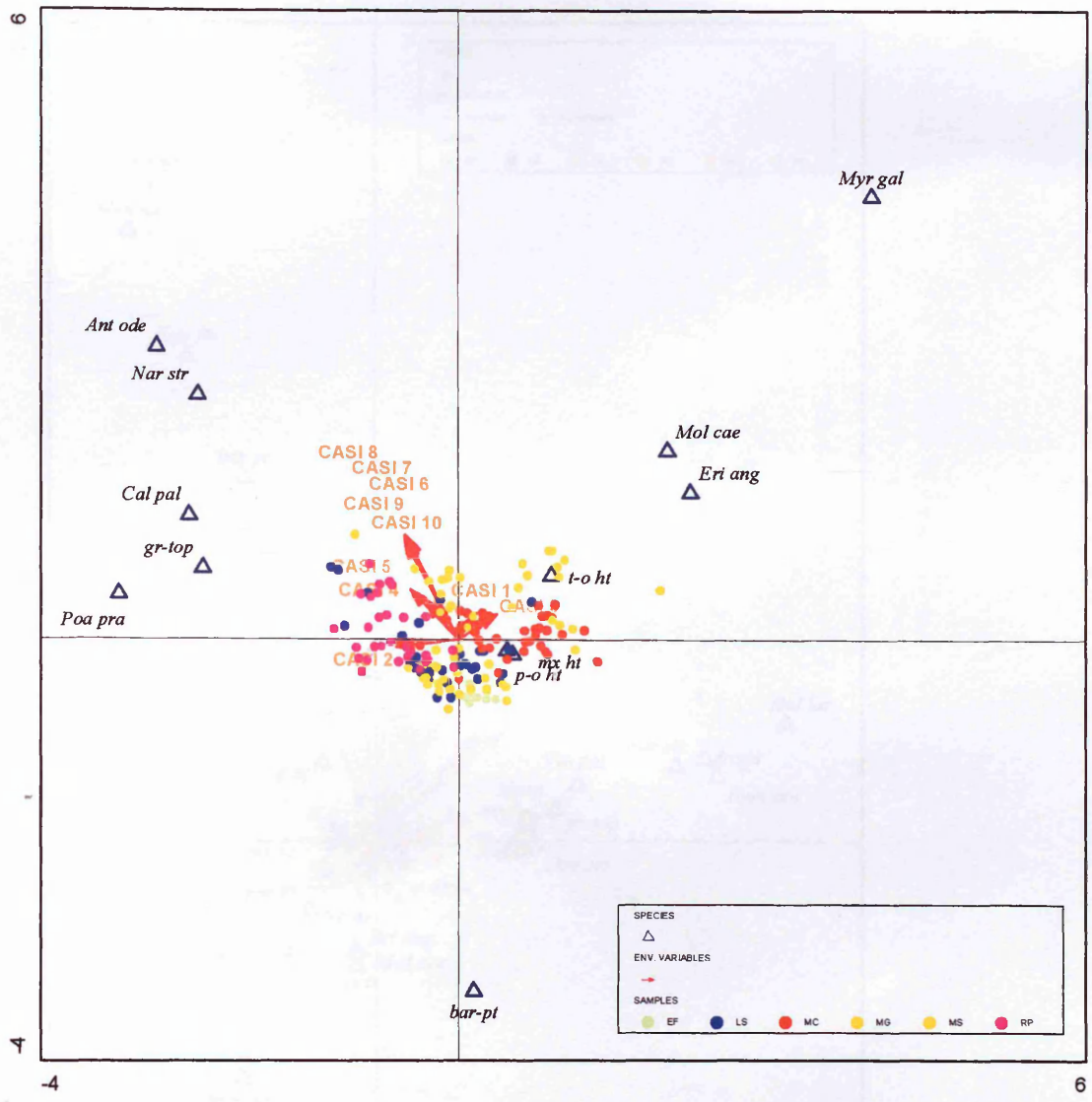

Figure C:6 CCA triplot for CASI July analyses and species composition with structural and environmental variables vegetation dataset (some species names omitted for clarity) (eigenvalue axis I: 0.764; eigenvalue axis II: 0.689) (some species omitted for clarity) (species labels: *Ant ode-Anthoxanthem oderatum; Cal pal-Caltha palustris; Eri ang-Eriophorum angustifolium; Mol cae-Molinia caerulea; Myr gal-Myrica gale; Nar str-Nardus stricta; Poa pra-Poa pratensis;* Structural and environmental predictors*: t-o-ht-totally obscured height; p-o-ht-partially obscured height; mx ht-maximum height; gr-top-grazed/topped; bar pt-bare peat*)

CCA triplots: September

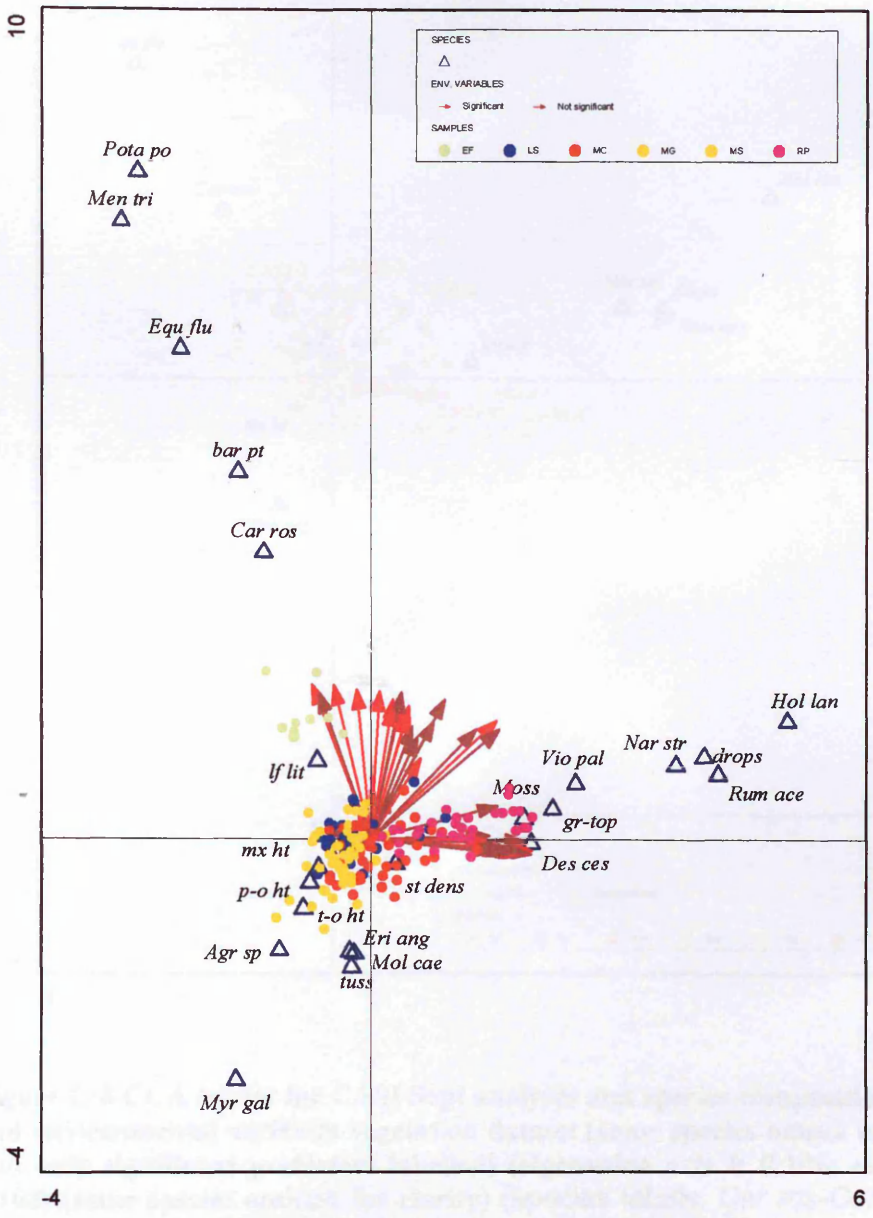

Figure C:7 CCA triplot for AVS1-42 Sept analyses and species composition with structural and environmental variables vegetation dataset (some species names omitted for clarity and only significant predictors labelled) (eigenvalue axis I:0.305; eigenvalue axis II: 0.193) (see ordination diagrams above for predictor variables labels) (some species omitted for clarity) (species labels: *Agr sp-Agrostis sp.; Car ros-Carex rostrata; Equ flu-Equisetum fluviatile; Eri ang-Eriophorum angustifolium; Hol lan-Holcus lanatus; Men tri-Menyanthes trifoliata; Mol cae-Molinia caerulea; Moss-Sphagnum sp.; Myr gal-Myrica gale; Nar str-Nardus stricta; Pota po-Potamogeton polygonifolius; Rum ace-Rumex acetosa; Vio pal-Viola palustris;* Structural and environmental predictors*: t-o-ht-totally obscured height; p-o-ht-partially obscured height; mx ht-maximum height; st dems-stem density; gr-top-grazed/topped; tuss-tussocks;; bar pt-bare peat; drops-droppings; lf lit-leaf litter*)

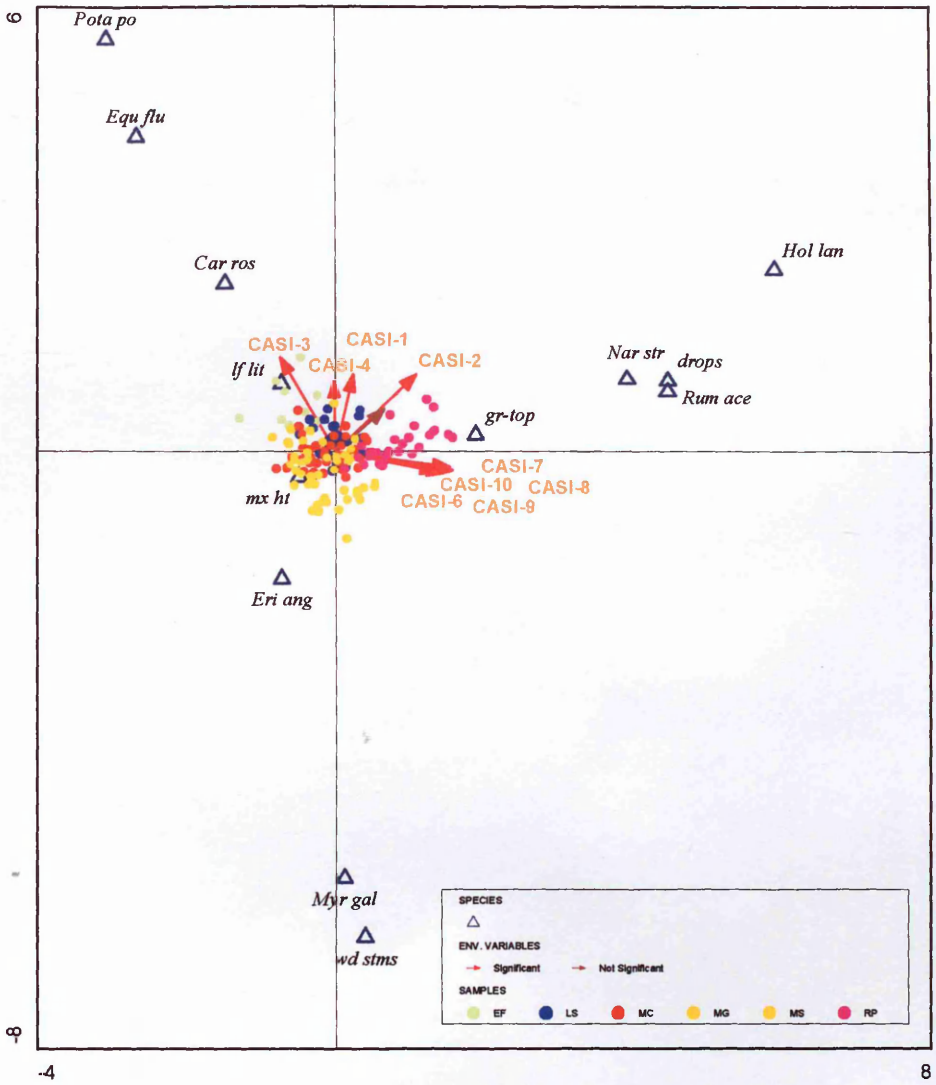

Figure C:8 CCA triplot for CASI Sept analyses and species composition with structural and environmental variables vegetation dataset (some species names omitted for clarity and only significant predictors labelled) (eigenvalue axis I: 0.196; eigenvalue axis II: 0.108) (some species omitted for clarity) (species labels: *Car ros-Carex rostrata; Equ flu-Equisetum fluviatile; Hol lan-Holcus lanatus; Myr gal-Myrica gale; Nar str-Nardus stricta; Pota po-Potamogeton polygonifolius; Rum ace-Rumex acetosa*; Structural and environmental predictors: *mx ht-maximum height; gr-top-grazed/topped; drops-droppings; lf lit-leaf litter; wd-stms-woody stems*)

D. Appendix

Habitat Areas

Table D:1 Habitat Areas (x22)-CASI 91

Habitat (CASI91)	Meters²	Hectares
Carex lasiocarpa	11,518.75	1.152
Carex rostrata-Equisetum fluviatile swamp	260,425.00	26.043
Deep Water Swamp	11,987.50	1.199
Dense Deschampsia cespitosa	68,112.50	6.811
Dry grassland	11,543.75	1.154
Fen meadow	6,068.75	0.606875
Mixed sedge swamp	344,937.50	34.494
Molinia caerulea - sedge mire	64,568.75	6.457
Phalaris arundinacea	3,750.00	0.375
Pine plantation	21,850.00	2.185
Reedbed	160,650.00	16.065
Ruderal	3,800.00	0.38
Rush pasture/grassland	240,162.50	24.016
Species-poor tall sedge (Carex aquatilis)	270,718.75	27.072
Species-poor tall sedge (Carex aquatilis)/mixed sedge	13,300.00	1.33
Species-poor tall sedge (Carex vesicaria)	4,775.00	0.4775
Species-rich low sedge mire	11,831.25	1.183
Species-rich low sedge mire/Rush pasture/grassland	29,350.00	2.935
Sphagnum lawn	67,400.00	6.74
Sphagnum lawn/Mixed sedge swamp	49,806.25	4.981
Water	66,912.50	6.691
Woodland/scrub	191,587.50	19.159

Table D:2 Habitat Areas (x22) –CASI 101

Habitat (CASI101)	Meters²	Hectares
Carex lasiocarpa	18,912.50	1.891
Carex rostrata-Equisetum fluviatile swamp	35,950.00	3.595
Deep Water Swamp	5,700.00	0.57
Dense Deschampsia cespitosa	48,893.75	4.889
Mixed sedge swamp	316,500.00	31.65
Molinia caerulea - Myrica gale mire	39,625.00	3.962
Molinia caerulea - sedge mire	447,943.75	44.794
Phalaris arundinacea	4,887.50	0.48875
Pine plantation	7,881.25	0.788125
Reedbed	282,362.50	28.236
Ruderal	3,812.50	0.38125
Rush pasture/grassland	211,118.75	21.112
Species-poor tall sedge (Carex aquatilis)	164,881.25	16.488
Species-poor tall sedge (Carex aquatilis)/mixed sedge	10,756.25	1.076
Species-poor tall sedge (Carex vesicaria)	5,600.00	0.56
Species-rich low sedge mire	121,150.00	12.115
Species-rich low sedge mire/Rush pasture/grassland	6,600.00	0.66
Species-rich low sedge mire/Species-poor tall sedge (Carex v	27,831.25	2.783
Sphagnum lawn	26,106.25	2.611
Sphagnum lawn/Mixed sedge swamp	22,393.75	2.239
Water	40,168.75	4.017
Woodland/scrub	91,993.75	9.199

Vegetation Datasets: Points of change along Transects 4.2, 4.6, 8.3, 8.4, 9.2.

Table D:3 Transect 4.2 (Balavil) –start NH 80261, 02445

Distance in m	*Description*	Simple habitat type
0	*Deschampsia cespitosa*, *Phalaris arundinacea* and *Juncus effusus* at edge of river bank.	Rush pasture/wet grassland
0.5	End of *Deschampsia cespitosa*. Increased *Juncus effusus* with *Carex aquatilis*	Tall species-poor sedge (*Carex aquatilis*)
0.7	End of *Phalaris arundinacea*	Tall species-poor sedge (*Carex aquatilis*)
4.3	Decrease in *Juncus effusus*	Tall species-poor sedge (*Carex aquatilis*)
5	*Equisetum fluviatile* with *Carex aquatilis* and *Sphagnum* lawns, mainly *S. squarrosum*	Floating *Sphagnum* lawn
8	End of *Juncus effusus*. Vegetation grassier with abundant *Agrostis canina*, *Eriophorum angustifolium* and *Carex nigra*. *Carex aquatilis* scarce. Semi-floating mat.	Floating *Sphagnum* lawn
10.3	*Carex aquatilis* more abundant again but mostly short-growing with *Carex nigra*. Decrease in *Sphagnum*	Non-floating *Sphagnum* lawn
15.4	End of *Equisetum fluviatile* and *Sphagnum*, *Carex aquatilis* becomes taller and more dense.	Tall species-poor sedge (*Carex aquatilis*)
17.7	Start of *Juncus effusus*, with *Carex aquatilis*	Tall species-poor sedge (*Carex aquatilis*)
19.7	End of *Juncus effusus*. Tall, dense *Carex aquatilis*	Tall species-poor sedge (*Carex aquatilis*)
26	Start of *Juncus effusus* with *Carex aquatilis*	Tall species-poor sedge (*Carex aquatilis*)
28	Start of *Carex vesicaria* with *Carex aquatilis* and *Juncus effusus*	Tall species-poor sedge (*Carex aquatilis*)
30.6	End of *Carex vesicaria* and *Juncus effusus*. Tall dense *Carex aquatilis* with scattered *Equisetum fluviatile*.	Tall species-poor sedge (*Carex aquatilis*)
42	With scattered *Juncus effusus*, *Potentilla palustris* and *Veronica scutellata*. Also some elongated *Carex nigra* and patches of *Agrostis canina*	Tall species-poor sedge (*Carex aquatilis*)
52.2	*Juncus effusus* dominant with *Agrostis canina*, *Carex aquatilis*, elongated *Carex nigra* and *Equisetum fluviatile*	Tall species-poor sedge (*Carex aquatilis*)
55.5	Abundant *Agrostis canina* and sedges (mainly *Carex nigra* and some *Carex rostrata*) with patchy *Sphagnum* (mainly *S. inundatum*, some *S. subsecundum*) and *Potentilla palustris*, *Galium palustre*, *Caltha palustris*, occasional *Menyanthes trifoliata*.	Non-floating *Sphagnum* lawn
116.2	End of *Agrostis canina* and *Sphagnum*. Abrupt boundary to wetter, open, *Menyanthes trifoliata* and *Carex rostrata* with *Equisetum fluviatile* scattered *Potentilla palustris*.	*Carex rostrata-Equisetum fluviatile* swamp
136	Increase in *Potentilla palustris*	*Carex rostrata-Equisetum fluviatile* swamp

Table D:3 Continued (Transect 4.2)

138	Start of *Agrostis canina* patches within *Carex rostrata-Menyanthes trifoliata* swamp. Also some *Carex curta* and *Sphagnum*.	Non-floating *Sphagnum* lawn
142	Several big *Carex curta* tussocks until 149	Non-floating *Sphagnum* lawn
153	Start of scattered short *Carex aquatilis* with *Equisetum fluviatile*, *Agrostis canina* and *Potentilla palustris*	*Carex rostrata-Equisetum fluviatile* swamp
160	Scattered *Carex lasiocarpa* with *Agrostis canina*, *Carex nigra*, *Potentilla palustris* and *Sphagnum*.	Non-floating *Sphagnum* lawn
175.2	First *Phragmites australis* just south of line.	Non-floating *Sphagnum* lawn
179	*Phragmites australis* more dense, with *Equisetum fluviatile*, *Potentilla palustris*, *Carex nigra* and *Agrostis canina*	Reedbed
195.6	*Molinia caerulea* tussock, 50cm wide. Ground hummocky but *Molinia caerulea* tussocks very scattered, dominated by *Agrostis canina*, *Carex nigra*, *Potentilla palustris* and *Sphagnum inundatum*.	Reedbed
201	Very dense *Phragmites australis* with *Carex nigra*, *Carex aquatilis*, *Agrostis canina* and *Equisetum fluviatile*. Very little *Sphagnum*.	Reedbed

Table D:4 Transect 4.6 (Balavil) –start NH 79538, 01801

Distance in m	*Description*	**Simple habitat type**
0	Edge of ditch with scattered scrub and dense *Carex aquatilis* with *Juncus effusus*, *Carex rostrata*, *Potentilla palustris* and *Equisetum fluviatile*, quite trampled	Tall species-poor sedge (*Carex aquatilis*)
4	*Salix cinerea*, 2.2m tall, 1.5m wide	Tall species-poor sedge (*Carex aquatilis*)
6	*Carex aquatilis* less dense, increase in *Carex rostrata*	*Carex rostrata-Equisetum fluviatile* swamp
13.4	End of *Carex aquatilis*, apart from a few scattered shoots within the *Carex rostrata* swamp	*Carex rostrata-Equisetum fluviatile* swamp
39.5	Increase in *Carex aquatilis*, small tufts of this species within *Carex rostrata* swamp	*Carex rostrata-Equisetum fluviatile* swamp
40.6	*Carex aquatilis* is dominant sedge, *Carex rostrata* still present in small quantities	*Carex rostrata-Equisetum fluviatile* swamp
53.6	*Carex rostrata* dominant, with some *Carex aquatilis* still present, also a few dense *Carex vesicaria* patches, eg. 60.3-60.6m	*Carex rostrata-Equisetum fluviatile* swamp
68	*Carex aquatilis* dominant	Tall species-poor sedge (*Carex aquatilis*)
73.5	*Carex aquatilis* decreases	Tall species-poor sedge (*Carex aquatilis*)
77	End of *Carex aquatilis* patch, apart from a few scattered shoots within *Carex rostrata* swamp	Mixed sedge swamp
83.2	Start of *Juncus effusus* in *Carex rostrata-Potentilla palustris* swamp	Mixed sedge swamp

Table D:4 Continued (Transect 4.6)

86.2	End of *Juncus effusus*	Mixed sedge swamp
90.9	Start of dense *Juncus effusus* with some *Potentilla palustris* with few other species apart from occasional small patches of *Carex rostrata* and *Carex vesicaria* inbetween *Juncus effusus* tussocks. Sedges are trampled	Tall species-poor sedge (*Carex vesicaria*)
102.2	End of *Juncus effusus*, abrupt boundary to *Carex vesicaria* with some *Carex rostrata*	Tall species-poor sedge (*Carex vesicaria*)
110.3	End of *Carex vesicaria*, start of *Carex rostrata-Potentilla palustris* swamp with just a few scattered shoots of *Carex vesicaria*	Mixed sedge swamp
125	Start of dense *Juncus effusus*	Mixed sedge swamp
131	End of dense *Juncus effusus*, back into *Carex rostrata* swamp with little *Potentilla palustris*	Mixed sedge swamp
139	Start of dense *Juncus effusus* with understorey of *Carex rostrata*	Mixed sedge swamp
148	Start of *Carex aquatilis* within dense *Juncus effusus*	Tall species-poor sedge (*Carex aquatilis*)
151	*Carex aquatilis* dominant understorey species	Tall species-poor sedge (*Carex aquatilis*)
153	*Juncus effusus* decreases, *Carex aquatilis* is dominant species	Tall species-poor sedge (*Carex aquatilis*)
154.8	End of *Juncus effusus*, start of pure dense *Carex aquatilis*	Tall species-poor sedge (*Carex aquatilis*)
161.6	Start of scattered *Juncus effusus* in *Carex aquatilis*	Tall species-poor sedge (*Carex aquatilis*)
162.5	Start of *Deschampsia cespitosa* with *Juncus effusus* and *Carex aquatilis*	Tall species-poor sedge (*Carex aquatilis*)
165	End of *Carex aquatilis*, pure dense *Juncus effusus*	Tall species-poor sedge (*Carex aquatilis*)
166.5	Dense *Deschampsia cespitosa* with some *Juncus effusus* and scattered grasses, mainly *Agrostis capillaris*, some *Carex nigra* and *Carex echinata*	Rush pasture/wet grassland
191	*Carex aquatilis* along eastern edge of transect line, western edge is *Juncus effusus –Deschampsia cespitosa*	Tall species-poor sedge (*Carex aquatilis*)
192.8	Dense *Carex vesicaria* with scattered *Juncus effusus*	Tall species-poor sedge (*Carex vesicaria*)
196	*Deschampsia cespitosa* and *Carex nigra*, some *Carex vesicaria*	Tall species-poor sedge (*Carex vesicaria*)
199	*Carex vesicaria*, *Carex nigra* and *Deschampsia cespitosa* with scattered *Carex aquatilis*	Tall species-poor sedge (*Carex vesicaria*)
200	Dense *Carex aquatilis* with scattered *Deschampsia cespitosa* west of transect line, *Carex vesicaria* east of line	Tall species-poor sedge (*Carex aquatilis*)
202.8	*Juncus effusus* with some *Deschampsia cespitosa* and *Carex vesicaria*	Tall species-poor sedge (*Carex vesicaria*)
213	Increase in *Deschampsia cespitosa*, decrease in *Juncus effusus*	Rush pasture/wet grassland
220	End of *Juncus effusus*, *Deschampsia cespitosa* tussocks open with other grasses including *Agrostis capillaris* and *Holcus lanatus* within and between tussocks	Rush pasture/wet grassland
231.3	End	

Table D:5 Transect 8.3 (Insh) –start NH 80300, 02389

Dist. in m	*Description*	Simple habitat type
0	*Carex vesicaria* with occasional *Deschampsia cespitosa*	Tall species-poor sedge (*Carex vesicaria)*
2.8	Some *Juncus effusus*, start of *Carex aquatilis*	Mixed sedge swamp
4.5	Increase in *Carex aquatilis*	Mixed sedge swamp
18.5	open and heavily grazed	Mixed sedge swamp
27	scattered tufts of *Juncus effusus*	Mixed sedge swamp
75	more species-rich with *Ranunculus flammula, Galium palustre, Potentilla palustris*	Mixed sedge swamp
80	Start of *Deschampsia cespitosa* and *Agrostis capillaris* with dense *Carex aquatilis*	Tall species-poor sedge (*Carex aquatilis)*
87	Grassier with only a few patches of *Carex nigra, Carex aquatilis* and abundant *Deschampsia cespitosa*	Rush pasture/wet grassland
94.8	Start of *Juncus acutiflorus*, end of sedges	Rush pasture/wet grassland
108.4	End of *Juncus acutiflorus*	Rush pasture/wet grassland
109	*Juncus effusus* and *Nardus stricta*	Rush pasture/wet grassland
113	Vegetation dominated by *Juncus effusus* and *Deschampsia cespitosa*	Rush pasture/wet grassland
144	Levee with tall *Deschampsia cespitosa* and few other species	Dense *Deschampsia cespitosa*
149	Dominated by *Deschampsia cespitosa* tussocks within short-grazed sward of other grasses	Rush pasture/wet grassland
157	End	

Table D:6 Transect 8.4 (Insh) –start NH 80604, 02428

Dist. in m	*Description*	Simple habitat type
0	*Deschampsia cespitosa* to 0.8m tall, open, short-grazed sward between tussocks, some *Juncus effusus* , *Urtica dioica, Ranunculus repens, Rumex acetosa.*	Dense *Deschampsia cespitosa*
9.5	*Deschampsia cespitosa* with sedges and grasses	Rush pasture/wet grassland
16	Small sedges and grasses, 20 cm tall, scattered *Juncus effusus, Deschampsia cespitosa*	Species-rich low sedge mire
61.5	1st *Juncus effusus* tussock on T line,	Species-rich low sedge mire
70	*Juncus effusus* more dense, boundary zone between small sedge and *Deschampsia cespitosa - Juncus effusus*	Species-rich low sedge mire
77	*Juncus effusus - Deschampsia cespitosa*	Species-rich low sedge mire
85.4	End of dense *Juncus effusus -Deschampsia cespitosa*, back to small sedge boundary	Species-rich low sedge mire
93	Start of tall sedge, mainly *Carex vesicaria* with *Deschampsia cespitosa, Juncus effusus*	Tall species-poor sedge (*Carex aquatilis)*
117.6	Dense *Carex aquatilis* with occasional *Juncus effusus* and *Carex rostrata*	Tall species-poor sedge (*Carex aquatilis)*
147	Start of *Carex vesicaria*	Tall species-poor sedge (*Carex aquatilis)*
148	Increase in *Juncus effusus*	Tall species-poor sedge (*Carex aquatilis)*

Table D:6 Continued (Transect 8.4)

150	Tall sedges but more species-rich and much *Carex nigra* – boundary zone with small sedge mire	Tall species-poor sedge (*Carex aquatilis*)/Species-rich low sedge mire
155.5	Start of *Eriophorum angustifolium*, still much *Juncus effusus*, *Deschampsia cespitosa*	Species-rich low sedge mire
162.6	Start of *Molinia caerulea*, very little *Juncus effusus* from here. *Molinia* mire with much sedge in the runnels between tussocks	*Molinia caerulea* – sedge mire
308.2	Start of scattered *Phragmites australis* (less than 10%) in the *Molinia* mire. *Molinia caerulea* tussocks to 40 cm high. Gradually getting wetter with patches of *Sphagnum* between tussocks.	*Molinia caerulea* – sedge mire
358	Ditch 2.5m wide (see Q28)	Reedbed
360	Back in *Molinia caerulea* mire with *Phragmites australis* more than 10%	Reedbed
384	Start of wet hollow with denser *Phragmites australis* (Q30). 384-386 with *Sphagnum* carpet.	Reedbed
395.5	Back to *Molinia caerulea* with sedges and *Phragmites australis*	Reedbed
406.5	*Salix cinerea* with fieldlayer open, mossy, with scattered *Molinia caerulea* and *Phragmites australis* (Q33)	Willow scrub
413	Back to *Molinia caerulea* with sedges and *Phragmites australis*	Reedbed
471	*Phragmites australis* consistently less than 10%	*Molinia caerulea* – sedge mire
480.5	Last *Phragmites australis* on T line, scattered *Deschampsia cespitosa*	*Molinia caerulea* – sedge mire
525	Track. *Deschampsia cespitosa* more abundant on far side.	*Molinia caerulea* – sedge mire
544	Last *Molinia caerulea*, small sedge mire to end	Species-rich low sedge mire
557	End	

Table D:7 Transect 9.2 (Coull) –start NH 80987, 03148

Distance in m	*Description*	**Simple habitat type**
0	*Deschampsia cespitosa* tussocks	Dense *Deschampsia cespitosa*
3.3	Start of *Juncus effusus*, *Carex vesicaria* and *Phalaris arundinacea*, *Deschampsia cespitosa* scattered	Tall species-poor sedge (*Carex vesicaria*)
10.5	Start of *Carex aquatilis* with *Carex vesicaria*, other species end	Mixed sedge swamp
12	Decrease in *Carex vesicaria*, only present in a few patches within *Carex aquatilis* (at 24m, 28m, 34m), *Carex aquatilis* is low-growing, open, with *Potentilla palustris*	Mixed sedge swamp
35	Start of standing water, 5cm deep	Mixed sedge swamp
38	Increase in *Carex vesicaria*, mixed with *Carex aquatilis*. Gradually getting drier with much leaflitter	Mixed sedge swamp
62.2	End of *Carex vesicaria*, dense *Carex aquatilis*	Tall species-poor sedge (*Carex aquatilis*)
67	*Carex vesicaria* patch, 1 m wide	Tall species-poor sedge (*Carex aquatilis*)

Table D:7 Continued (Transect 9.2)

77	More open and wetter, start of scattered *Carex rostrata, Phalaris arundinacea* and *Veronica scutellata* within *Carex aquatilis*	Mixed sedge swamp
81	*Carex rostrata* dominant with scattered *Carex aquatilis*	Mixed sedge swamp
83.4	*Carex aquatilis* dominant	Mixed sedge swamp
95	Dense, species-poor *Carex aquatilis*	Tall species-poor sedge (*Carex aquatilis*)
110.5	*Carex vesicaria* patch, 1.5m wide	Tall species-poor sedge (*Carex aquatilis*)
116	Start of floating mat	Mixed sedge swamp
117.8	Pond, 2m wide with scattered *Potentilla palustris, Menyanthes trifoliata* but mostly open water, end of *Carex aquatilis*	Mixed sedge swamp
119.9	Start of *Carex rostrata* with *Sphagnum squarrosum*, scattered *Molinia caerulea* tussocks and *Carex curta, Agrostis canina* and scattered other grasses and small sedges	Floating *Sphagnum* lawn
121.5	Start of *Carex aquatilis* in scattered tufts	Floating *Sphagnum* lawn
123	Increase in *Carex aquatilis* and *Carex rostrata* tufts, still with grasses/small sedges, *Sphagnum squarrosum*	Floating *Sphagnum* lawn
141.8	End of floating mat with *Sphagnum squarrosum* patches, only a few scattered individuals after this point	Mixed sedge swamp
143	Start of abundant *Potentilla palustris* and *Menyanthes trifoliata* with *Carex aquatilis* and some *Carex rostrata*	Mixed sedge swamp
146	Wetter, start of *Equisetum fluviatile, Carex aquatilis* dominant and only sedge present apart from very scattered *Carex rostrata*	*Carex rostrata-Equisetum fluviatile* swamp
149	Start of dead *Phragmites australis* in *Carex aquatilis*	*Carex rostrata-Equisetum fluviatile* swamp
150	*Carex aquatilis* with patches of *Agrostis canina* and *Potentilla palustris, Menyanthes trifoliata*, scattered *Phalaris arundinacea* and dead *Phragmites australis*	Mixed sedge swamp
151.5	Start of floating mat with much *Sphagnum squarrosum, Carex curta* and *Agrostis canina* with tall sedges	Floating *Sphagnum* lawn
156	End of floating mat	Mixed sedge swamp
158	Start of live *Phragmites australis*	Mixed sedge swamp
164.5	Start of open reedbed, to 1.2m tall with *Equisetum fluviatile* and *Carex rostrata* understorey, *Carex aquatilis* scattered	Reedbed
172	*Cicuta virosa* on transect line	Reedbed
173	Start of dense reedbed with understorey of *Carex aquatilis*	Reedbed
189.5	Dense reedbed, 1.8m tall with few other species, only *Galium palustre* frequent in understorey	Reedbed
197	Dense reed, 2m tall, 4m wide	Reedbed
201	Reed more open with understorey of *Carex rostrata*	Reedbed
221	End	Reedbed